

Department of Ocean Technology, Policy and Environment  
Graduate School of Frontier Sciences

2017

Master's Thesis

Study on Anthropogenic Carbon Uptake in the  
Ocean

(海洋中人為起源溶存炭素に関する研究)

Submitted January 23, 2017

Advisor: Visiting Professor Takeshi Kawano

Yida Li

## CONTENTS

1. Introduction.....	1
1.1. Background.....	1
1.2. Previous Studies on Anthropogenic Carbon in the Ocean from Observation ....	1
1.2.1. Measured Carbon Concentration by Gruber et al. (1996).....	2
1.2.2. Anthropogenic Carbon Increase in a Certain Period by Murata et al. (2007)	4
1.2.3. Extended Multiple Linear Regression of Observed Carbon by Sabine et al. (2008)	5
1.3. The Estimated State of the Global Ocean for Climate Research (ESTOC) Model and Dataset.....	7
2. Research Objectives.....	10
2.1. DIC Time Variation in Basin Scale .....	10
2.2. Evaluate the Contribution of Biogeochemical System to Carbon uptake .....	10
2.3. Difference between Approximation Method and Simulation Method .....	10
3. Decadal Variation of DIC Concentration and Relation between Air-sea CO <sub>2</sub> Exchange and the Biological Process in the Shallow Water in the ESTOC .....	12
3.1. Decadal Variation of DIC Concentration .....	12
3.2. CO <sub>2</sub> Exchange in the North Pacific in the ESTOC with NPDZC model.....	16
3.3. Summary.....	24
4. Indication of Biochemical System Contribution to the Carbon Uptake in the ESTOC	25
4.1. Indication of the Biochemical System Contribution to the Global Carbon Uptake in the ESTOC.....	25
4.2. The effect of El Niño on Carbon uptake and Biology Process Contribution ....	28
4.3. Summary.....	34
5. Anthropogenic Carbon Uptake Difference Calculated by Different Methods.....	35
5.1. Comparison between Simulation Method and Approximation Method .....	35
5.2. Spatial Difference in Carbon Uptake between the Simulation Method and the Approximation Method .....	38
5.2.1. Temporal and Spatial Difference between Methods in the North Pacific ..	39
5.2.2. Temporal and Spatial Difference between Methods in the South Pacific...	40
5.2.3. Temporal and Spatial Difference between Methods in the North Atlantic	42
5.2.4. Temporal and Spatial Difference between Methods in the South Atlantic	44
5.2.5. Temporal and Spatial Difference between Methods in the Southern Ocean	46

5.2.6. Temporal and Spatial Difference between Methods in the Indian Ocean..	48
6. Conclusion .....	51
6.1. CO <sub>2</sub> Gas Exchange in the North Pacific.....	51
6.2. Biogeochemical System Contribution to the Carbon Uptake in the ESTOC data	
51	
6.3. Difference between Methods for the Calculation of the Anthropogenic Carbon	
Increase .....	52
REFERENCES .....	53
AKNOWLEDGEMENT.....	55
APPENDIX.....	-1-

## FIGURE LIST

Figure 3.1 Monthly mean Concentration of DIC in the Pacific within the depth of 0-200m.....	13
Figure 3.2 East-west DIC Difference in the North Pacific.....	15
Figure 3.3 Averaged CO <sub>2</sub> Exchange at the Sea Surface between January 1991 and December 2010.....	16
Figure 3.4 Time Series CO <sub>2</sub> Exchange in the North Pacific.....	16
Figure 3.5 Distribution of K <sub>v</sub> , K <sub>h</sub> , and pCO <sub>2</sub> .....	19
Figure 3.6 Distribution of Alk and N.....	20
Figure 3.7 Contour maps of pCO <sub>2</sub> and CO <sub>2</sub> exchange.....	22
Figure 3.8 Time Series of CO <sub>2</sub> Exchange in the North Pacific without NPDZC model.....	22
Figure 4.1 Biogeochemical System Contribution to the Global Carbon Uptake in the layer between 0m-200m depth from January 1991 to December 2010, normalized to January 1991.....	27
Figure 4.2 Biogeochemical System Contribution to the Global-scale Carbon Uptake in the layer between 0m-200m from January 1971 to December 2010, normalized to January 1991.....	28
Figure 4.3 Biogeochemical System Contribution to the Global-scale Carbon Uptake in the layer between 0m-200m depth of winter (Dec., Jan. and Feb.) average of 20 years (1991-2010).....	29
Figure 4.4 SST Variation Comparing to JMA Observation Data.....	30
Figure 4.5 Correlation of Carbon Uptake and SST Variation of Every Winter in 1991-2010.....	31
Figure 4.6 Shallow (0-200m) Carbon Uptake Variation Contour, Normalized to the winter of 1991 (Average Dec.1990, Jan. 1991, Feb. 1991.....	33
Figure 5.1 Anthropogenic Carbon Uptake Increase (0-200m) by Approximation Method and Simulation Method from January, 1991 to December, 2010, Normalized to January, 1991.....	37
Figure 5.2 Anthropogenic Carbon Uptake (0-200m) in the North Pacific.....	39
Figure 5.3 20-year Averaged Difference Distribution of Anthropogenic Carbon Uptake (0-200m) in the North Pacific.....	40
Figure 5.4 Anthropogenic Carbon Uptake (0-200m) in the South Pacific.....	41
Figure 5.5 20-year Averaged Difference Distribution of Anthropogenic Carbon Uptake (0-200m) in the South Pacific.....	42
Figure 5.6 Anthropogenic Carbon Uptake (0-200m) in the South Pacific.....	43

Figure 5.7 20-year Averaged Difference Distribution of Anthropogenic Carbon Uptake (0-200m) in the North Atlantic. ....	44
Figure 5.8 Anthropogenic Carbon Uptake (0-200m) in the South Atlantic.The vertical axis is the year, the horizontal axis is the carbon uptake. ....	45
Figure 5.9 20-year Averaged Difference Distribution of Anthropogenic Carbon Uptake (0-200m) in the South Atlantic. ....	46
Figure 5.10 Anthropogenic Carbon Uptake (0-200m) in the Southern Ocean.The vertical axis is the year, the horizontal axis is the carbon uptake. ....	47
Figure 5.11 20-year Averaged Difference Distribution of Anthropogenic Carbon Uptake (0-200m) in the Southern Ocean.....	47
Figure 5.12 Anthropogenic Carbon Uptake (0-200m) in the Indian Ocean. ....	48
Figure 5.13 20-year Averaged Difference Distribution of Anthropogenic Carbon Uptake (0-200m) in the Indian Ocean. ....	49

## TABLE LIST

Table 1.1 Variables consisted in the ESTOC and information of output dataset .....	8
Table 1.2 Models Defined in the ESTOC Model .....	9
Table 3.1 Definition of the Basins in the Pacific Ocean.....	12
Table 3.2 Definitions of the east and west region in the North Pacific Ocean.....	15
Table 3.3 Constants for the Calculation of the Solubility of CO <sub>2</sub> in Molar and Gravimetric units. ....	17
Table 4.1 Carbon Portions of the Four Models .....	25
Table 4.2 Four Models Consistence of Carbon Portions .....	26
Table 4.3 Carbon Uptake Contribution by Biogeochemical System in ESTOC .....	27
Table 5.1 Definition of the Basins in this study .....	38

## 1. Introduction

### 1.1. Background

According to the Intergovernmental Panel on Climate Change (IPCC) 5<sup>th</sup> Assessment Report (AR5), Climate change is now apparent and it will amplify existing risks and create new risks for natural and human systems. Many aspects of climate change are irreversible, even if anthropogenic emissions of greenhouse gases are completely ceased. Therefore, difficulties are foreseeable when global warming is studied, if oceanic anthropogenic  $CO_2$  is uncertain. However, it is almost impossible to distinguish the anthropogenic  $CO_2$  emission apart from total  $CO_2$  in the natural system. Therefore, researchers usually estimate the anthropogenic  $CO_2$  indirectly, by assuming all of total  $CO_2$  increase after industrial revolution (18<sup>th</sup> century) is anthropogenic influence, in order to understand the associated climate change properly.

### 1.2. Previous Studies on Anthropogenic Carbon in the Ocean from Observation

In previous studies, researchers estimate the anthropogenic  $CO_2$  by repeated surveys of the carbon system that would reveal the concentration increase over time. In the later studies, it is pointed out that, anthropogenic  $CO_2$  in the ocean interior can be estimated by correcting the measured carbon concentration in a water sample for the changes incurred due to the remineralization of organic matter and the dissolution of carbonates since it lost contact with the surface and by subtracting the preformed preindustrial carbon [Brewer 1978, Chen and Millero 1979]. However, the Brewer (1978) and Chen/Millero (1979)'s approaches are regarded as containing too large uncertainty. The main points under discussion are the role of mixing of different water types with poorly known initial concentrations which can lead to nonlinear effects, the difficulty of choosing appropriate preindustrial end-member water types [Shiller 1981], and the large uncertainties in the assumptions relating to the constant stoichiometric ratios and the use of the apparent oxygen utilization (AOU) [Broecker et al., 1985a] for determining the contribution of the remineralization of organic matter. Above all, more improvements should be developed in order to optimize observation correcting method.

### 1.2.1. Measured Carbon Concentration by Gruber et al. (1996)

To eliminate the nonlinear effects due to mixing, Gruber et al. (1996) developed a new technique which applied to the North Atlantic where Transient Tracers in the Ocean observations are in good quality and they used water age estimates obtained by tracers.

Three main pumps control the dissolved inorganic carbon in the ocean which are air-sea gas exchange including the uptake of anthropogenic  $CO_2$  (solubility pump), the biological process of photosynthesis, respiration, and remineralization (soft-tissue pump), and the formation and dissolution of carbonate particles (carbonate pump) [Volk and Hoffert, 1985]. All these processes have been carefully established in this method. This method is looking forward to removing all pumps change of carbon in order to estimate anthropogenic carbon comparing to the preindustrial carbon distribution. Among the three processes discussed above, the dissolution of solid calcium carbonates also represents the main process of alkalinity (Alk). At the same time Alk is affected by soft-tissue pump too. On the other hand, biogeochemical oxygen cycling is entirely controlled by the soft-tissue pump only. Therefore, focusing on carbonate pump and soft-tissue pump, the continuity equation of C, Alk, and  $O_2$  in the interior of the ocean can be written as

$$\Gamma(C) = J_{soft}(C) + J_{carb}(C) \quad (1-1)$$

$$\Gamma(Alk) = J_{soft}(Alk) + J_{carb}(Alk) \quad (1-2)$$

$$\Gamma(O_2) = J_{soft}(O_2) \quad (1-3)$$

where  $J_{soft}$  denotes the source minus sink term due to the remineralization of organic matter and  $J_{carb}$  denotes the source minus sink term due to the dissolution of solid calcium carbonates. The operator  $\Gamma$  represents the transport and time rate of change:

$$\Gamma(T) = \frac{\partial T}{\partial t} + \mathbf{u} \cdot \nabla T - \nabla \cdot (D \cdot \nabla T) \quad (1-4)$$

where T represents any tracer concentration,  $\nabla$  represents the gradient operator in three dimensions,  $\mathbf{u}$  represents the velocity field, and D represents the eddy diffusivity tensor. It is assumed that C and  $O_2$  are influenced by soft-tissue pump with a stoichiometric ratio ( $\gamma_{C:O_2}$ ) and that the carbonate pump changes alkalinity twice as much as it changes C. The proton flux during the process of photosynthesis, respiration, and remineralization, which in turn is proportional to the change in  $O_2$  through the



constant stoichiometric ratio  $\gamma_{N:O_2}$ , thus

$$J_{soft}(C) = \gamma_{C:O_2} J_{soft}(O_2) \quad (1-5)$$

$$J_{carb}(C) = \frac{1}{2} \gamma_{C:O_2} J_{carb}(Alk) \quad (1-6)$$

$$J_{soft}(Alk) = -\gamma_{N:O_2} J_{soft}(O_2) \quad (1-7)$$

Combine the equation (1) and (2),

$$\Gamma(C) = \gamma_{C:O_2} J_{soft}(O_2) + \frac{1}{2} J_{carb}(Alk) \quad (1-8)$$

$$\Gamma(Alk) = -\gamma_{N:O_2} J_{soft}(O_2) + J_{carb}(Alk) \quad (1-9)$$

hereby,  $J_{soft}$  and  $J_{carb}$  term can be removed,

$$\Gamma(C) - \gamma_{C:O_2} \Gamma(O_2) - \frac{1}{2} (\Gamma(Alk) + \gamma_{N:O_2} \Gamma(O_2)) = 0 \quad (1-10)$$

since the stoichiometric ratio  $\gamma_{C:O_2}$  and  $\gamma_{N:O_2}$  is presumed constant, equation (10) is a linear relation among C, Alk, and  $O_2$ . Therefore, a new tracer is defined as

$$C^* = C - \gamma_{C:O_2} O_2 - \frac{1}{2} (Alk + \gamma_{N:O_2} O_2) \quad (1-11)$$

which obey conservative properties as well

$$\Gamma(C^*) = 0 \quad (1-12)$$

Since soft-tissue pump and carbonate pump has been subtract from DIC (C),  $C^*$  represents the information of sea-air gas exchange strongly. Consequently, it is influenced by the water parcel age which provides the time that the water parcel detached from the air-sea interface.

Therefore, if the age of a water parcel is known, the  $C^*$  and the preindustrial preformed  $C^{*0}$  can be calculated and the carbon uptake portion of anthropogenic and carbon contributed by dissolution can be calculated.

$$\Delta C^* = C - C_{eq}(S, T, Alk^0)_{fCO_2=280\mu atm} - \gamma_{C:O_2} (O_2 - O_2^{sat})$$

$$-\frac{1}{2}(Alk - Alk^0 + \gamma_{N:O_2}(O_2 - O_2^{sat})) \quad (1-13)$$

hereby, preformed  $O_2$  is estimated by its saturation concentration  $O_2^{sat}$  and preformed  $Alk$   $Alk^0$  by a multiple linear regression while neglecting the uncertainties introduced because of nonlinear effects on a given density surface.  $fCO_2 = 280\mu atm$  is considered to be the preformed fugacity of air-sea gas exchange.

Anthropogenic carbon  $\Delta C_{ant}$  can be calculated by subtracting the effect of air-sea disequilibrium on a certain density  $\rho$  surface.

$$\Delta C_{ant} = \Delta C^* - \Delta C_{dis eq(\rho)} \quad (1-14)$$

$$\Delta C_{ant} = C_{eq}(S, T, Alk^0, fCO_2(t_{sample} - \tau)) - C_{eq}(S, T, Alk^0, fCO_2)_{fCO_2=280\mu atm} \quad (1-15)$$

where  $\tau$  is the water age and calculated as

$$\tau = \lambda^{-1} \cdot (1 + \frac{H}{He}), \quad \lambda^{-1} = 1.77e - 9/s \quad (1-16)$$

in Gruber et al. (1996) specifically.

By the method above, anthropogenic carbon can be calculated by correcting the observed DIC data. However, either the age of the water parcel or limitation of a certain depth and basin is required. And both of them are difficult to be applied in any other basin than the North Atlantic. Furthermore, there are more uncertainties expected, since many variables are involved in the approach. Therefore, most of the following researchers improved this method to adapt to other specific oceans and developed many variations.

### 1.2.2. Anthropogenic Carbon Increase in a Certain Period by Murata et al. (2007)

To improve the approach in the Section 1.2.1 using oxygen ( $O_2$ ), the following studies including Murata et al. 2007 simplified it into dissolved oxygen (DO), and the  $\gamma_{C:O_2}$  into  $\gamma_{C:O}$  ratio, because DO is often used as an index to reveal decadal changes in the ocean [Matear et al., 2000, Garcia et al., 2005], which is helpful in interpreting spatial and temporal changes of anthropogenic carbon. The equation, therefore, is refined as:

$$C_{ant} = C - \gamma_{C:O} \times AOU - [0.5 \times (A_{TM} - A_{T0}) + C_{T0} + \Delta C_{Tdisseq}] \quad (1-17)$$

where  $C$  is the measured DIC and  $AOU$  represents apparent oxygen utilization, which is the difference between saturated dissolved oxygen and observed oxygen concentration.  $A_{T0}$  is the preindustrial alkalinity and  $C_{T0}$  is the preindustrial dissolved inorganic carbon concentration. Furthermore, if the same preindustrial condition is chosen to be applied to this approach, these terms can be canceled out by subtracting  $C_{ant}(t)$  from  $C_{ant}(t+\Delta t)$ , since the equation is considered as linear relation. Therefore, Murata et al. (2007) removed the preindustrial preformed data, considering the difficulty to obtain the age of water parcel and accurate preindustrial stoichiometric data.

$$\Delta C_{ant} = C_{ant}^{t1} - C_{ant}^{t2} \quad (1-18)$$

This study calculated the accumulation of anthropogenic carbon in a certain period of time rather than the whole accumulation in history. However the uncertainty caused by neglecting  $\Delta C_{Tdisseq}$  requires one of the following assumptions: (1) the air-sea difference of  $pCO_2$  in a water mass formation area does not change over time. (2) The formation areas for water masses found in the present study are fixed over time.  $A_{TM}$  cancels out under the assumption that there exists no change in  $A_{TM}$  over the observation periods. If both assumptions are satisfied or the uncertainties they contain are negligible, the  $C_{ant}$  can be simplified as

$$C_{ant} = C - \gamma_{C:O} \times AOU \quad (1-19)$$

Where  $C$  and  $AOU$  are the data observed at the same time.

By this approach, Murata et al. (2007) calculated the anthropogenic  $CO_2$  along P06 section (nominally  $32^\circ$  S) in the South Pacific of World Ocean Circulation Experiment (WOCE) and Blue Earth Global Expedition 2003 (BEAGLE), increased significantly by  $10.3 \pm 3.1$  and  $4.1 \pm 2.0$   $mmol\ kg^{-1}$  for Sub-Antarctic mode water (SAMW) and Antarctic intermediate water (AAIW), respectively. Furthermore, a small but important increase of approximately  $3.0$   $mmol\ kg^{-1}$  at longitude  $180^\circ$  -  $160^\circ$  W. A slight east-west difference of distribution was found in the South Pacific as well.

### 1.2.3. Extended Multiple Linear Regression of Observed Carbon by Sabine et al. (2008)

Calculating anthropogenic carbon in a certain period of time is a regular

approach when no age estimation of water parcel is available. However, since more assumptions are introduced into the approach, it is important to refrain from inaccuracy. The approach and its simplification are based on the linear relation between DIC and other stoichiometric parameters. From some aspects, the simplified method (1-19) is a linear regression function between DIC and DO. Sabine et al. (2008) followed the thought of simplification by multiple linear regression and improved the accuracy of observed DIC data by applying extended multiple linear regression which was first introduced by Wallace (1995) to the DIC measured data.

The observed DIC on one cruise is fit as a function of physical and biological parameters that are expected not to be impacted by increasing CO<sub>2</sub> in the atmosphere. In Sabine et al. 2008, the function is defined as

$$C_{meas,t1} = F_1(\sigma_\theta, \theta, S, Si, P) \quad (1-20)$$

$$= a_1 \cdot \sigma_\theta + b_1 \cdot \theta + c_1 \cdot S + d_1 \cdot Si + e_1 \cdot P + k_1 \quad (1-21)$$

where  $\sigma_\theta$  is the potential density.  $\theta$  is the potential temperature.  $S$  is the salinity.  $Si$  and  $P$  are parameters associated to biology which represent silicate and phosphate and  $a_1$ ,  $b_1$ ,  $c_1$ ,  $d_1$ ,  $e_1$ , and  $k_1$  are coefficients of the multiple linear regression against measured DIC. By applying function  $F_1$  to the other cruise observation data, predicted data on cruise two can be calculated as

$$C_{pred,t2} = a_1 \cdot \sigma_\theta' + b_1 \cdot \theta' + c_1 \cdot S' + d_1 \cdot Si' + e_1 \cdot P' + k_1 \quad (1-22)$$

The difference between actual observation and this prediction is presumed to be the anthropogenic CO<sub>2</sub> increase between the cruises.

$$\Delta C_{ant} = \Delta C_{t2-t1} = C_{meas,t2} - C_{pred,t2} \quad (1-23)$$

Comparing to the Multiple Linear Regression (MLR) fitting, eMLR is proposed by Firrs et al. (2005) which reduces the measurement errors that the independent parameters introduce to final calculation. In eMLR fitting, the same set of independent parameters is used to determine for both cruises. Consequently, the DIC change between the two cruises is calculated as

$$\Delta C_{t2-t1} = (a_2 - a_1) \cdot \sigma_\theta' + (b_1 - b_1) \cdot \theta' + (c_1 - c_1) \cdot S' + (d_2 - d_1) \cdot Si' + (e_2 - e_1) \cdot P' +$$

$$(k_1 - k_1) \tag{1-24}$$

Sabine et al. (2008) calculated the anthropogenic carbon increase along P02 (nominally 47° N in the Pacific) and P16 (nominally 150° W in the Pacific) sections between the cruises of 1994-2004 and 1991/1992 -2005/2006, respectively. The results are 0.43 mol m<sup>-2</sup>yr<sup>-1</sup> along the P02 within 1994-2004 and 0.25 mol m<sup>-2</sup>yr<sup>-1</sup> within 1991/1992 -2005/2006. However, this approach is inappropriate in the shallow sea water which is affected strongly by nonlinear mixing.

### 1.3. The Estimated State of the Global Ocean for Climate Research (ESTOC) Model and Dataset

The approach discussed above using observation data has its limits that require either age estimation or a proper location. Lacking one of those may cause lack of accuracy. Another possible approach to estimate anthropogenic carbon increase in the ocean is involving modeling and simulation of the oceanic carbon cycle.

A four-dimensional variational (4D-VAR) system for a quasi-global ocean general circulation model (OGCM), version 3 of the Modular Ocean Model (MOM3) of the US Geophysical Fluid Dynamics Laboratory [Pacanowski and Griffes, 1999] was developed under a collaborate program between the Japan Agency for Marine-Earth Science and Technology (JAMSTEC) and Kyoto University and proved to be successful in reproducing the seasonal state of the North Pacific [Masuda et al. 2003]. This model was first developed for the purpose of a long-term states estimation with a better representation of the deep ocean, which has been difficult to reproduce until then. The model is developed with data assimilation technique using careful compilation of observational data and installation of a unique method for assimilating anomalies. This approach was proven to be partially successful on the system of warming mechanism, while the resulting data was used to evaluate more accurately the global heat and mass budgets [Kouketsu et al. 2011]. These successes imply that the data set better represents the ocean state throughout the entire depth range, which makes the data set unique among long-term ocean state estimates and thus particularly useful for climate research. [Osafune et al. 2015].

Excluding the background dynamic ocean state, a biogeochemical model able to describe the dynamics state of oceanic CO<sub>2</sub> was introduced by [Doi et al. 2015]. This model contains six variables which represent the biomasses of phytoplankton (P), zooplankton (Z), nitrate (N), detritus (D), DIC (C) and alkalinity (A). This NPZDC Model

is a pelagic, lower-trophic-level ecosystem model based on nitrogen cycle and an additional function of carbon cycle [Doi et al. 2015]. The quality of reproducing carbon cycle and biogeochemical system has been proven by comparing with multiple observed datasets, including those that are not assimilated by the model.

Furthermore, a state of dissolved oxygen (DO) has been adapted to the model. Though, the accuracy of the dissolved oxygen has not been discussed, it is worth making attempt calculation based on dissolved oxygen as well, since the DO state is assimilated to the observed data.

Above all, variables and units contained in the ESTOC are summarized in the Table 1.1. The scale and the resolution of the model are 75°S-80°N and horizontal  $1^\circ \times 1^\circ$ , respectively. Depth range of the model is from the sea surface to the sea bottom and divided in to 46 layers. In this study, we use the 55 years (1957-2011), monthly mean output dataset.

**Table 1.1 Variables consisted in the ESTOC and information of output dataset**

Variable & Abbreviation	Potential Temperature [°C],	tmp
	Salinity [PSU],	sal
	Flow Rate [m/s] v[m/s],	vel
	Surface Heat Flux [cal/m <sup>2</sup> /s],	shf
	Surface Freshwater Flux [m/s],	sff
	Wind Shear Stress $\tau_x$ [N/m <sup>2</sup> ] $\tau_y$ [N/m <sup>2</sup> ],	tau
	Nitrogen [ $\mu$ mol/L],	no3
	Phytoplankton [ $\mu$ mol/L],	pht
	Detritus [ $\mu$ mol/L],	det
	Zooplankton [ $\mu$ mol/L],	zoo
	Dissolved Inorganic Carbon [ $\mu$ mol/kg],	dic
Dissolved Oxygen [ $\mu$ mol/L],	oxy	
Territory	Whole Sphere (75°S-80°N)	
Spatial Resolution	Horizontal $1^\circ \times 1^\circ$ , 46 Layers	
Period of Time	1957 -2011 (Ver. 02c)	

Additionally, excluding the model introduced above, other simulation models under

assumptions are developed as well. Were some of the models lacking of partial parameters state or a certain system are actually developed before the newest ESTOC model, for convenience, we define it as Model 1 to Model 4 in this study (Table 1.2) .

**Table 1.2 Models Defined in the ESTOC Model**

Models and Datasets	Biogeochemical System	Atmosphere CO2 Increasing
Model 1	○	○
Model 2	○	×
Model 3	×	○
Model 4	×	×

In our definition, Model 1 is the model we discussed in the first place. Model 2 is the model assuming no increase of CO<sub>2</sub> occurrence in the atmosphere. Model 3 is a model that simulated without NPDZC model introduced by [Doi et al. 2015]. Model 4 is the model under the assumption that CO<sub>2</sub> does not increase and no biogeochemical process exist in the ocean.

Osafune et al. (2014) compared the results from Model 3 and Model 4 to discuss the impact of anthropogenic carbon increase to the ocean mainly in the physical oceanographic aspect, and Doi et al., (2015) compare the results from Model 1 and Model 2 to know the impact of including biological processes.

## 2. Research Objectives

### 2.1. DIC Time Variation in Basin Scale

Doi et al. (2015) calculated the Basin Scale DIC increase and vertical DIC flux by using ESTOC model (Model 1 and 2 in Table 1.2). The vertical DIC flux is an obvious diffusive vertical flux rather than associated with the atmosphere CO<sub>2</sub> increase, since the vertical DIC flux is controlled by the biological process in the shallow water. Excluding the vertical DIC flux in the sea water, the presence of the biological contribution to the air-sea exchange and the mechanism of it, are worth discussing.

In this study, we discuss the biogeochemical system contribution to the air-sea exchange and indirectly to the carbon uptake, with the ESTOC model, qualitatively by choosing a specific basin.

### 2.2. Evaluate the Contribution of Biogeochemical System to Carbon uptake

An NPDZC model has been added to the ESTOC model. By using this biogeochemical system, Doi et al. (2015) calculated the decadal DIC increase in global scale. However, the contribution of this biogeochemical system to the DIC increase has not been discussed yet. Nor the biological process contribution to the carbon uptake or anthropogenic carbon has been estimated by any observation approach. Though the NPDZC model in the ESTOC is simple and contains only a few components, it is worth evaluating biological contribution.

In this study, we calculate the proportion of the biogeochemical system contributed carbon to the total carbon, in order to better understand the role of biological cycle in carbon uptake.

### 2.3. Difference between Approximation Method and Simulation Method

As discussed in chapter one, Brewer (1978) and Chen and Millero (1979) calculated anthropogenic carbon uptake from observation result by estimating equations under some assumptions (Approximation method, hereafter). Gruber et al. (1996) improved Approximation method by it still has some flaws that either the target water parcel is limited or the water age estimation is required. DO has been added to the ESTOC model recently, therefore approximation method, especially the approaches of Murata et al. (2007) and Sabine et al. (2008), excluding the correction of the observed data, can be



simulated by using the output data of the ESTOC. Assuming the output data of the ESTOC model are the true values of the state, the effect of biological cycle in anthropogenic carbon uptake can also be calculated as a difference between Model 1 and Model 3 (Simulation method, hereafter). Comparison of the results from both methods will show the bias that approximation method introduced. Furthermore, it is possible to estimate some of the anthropogenic carbon state in the regions that approximation method should not be applied or to correct some results that approximation method obtained in the regions that the bias and uncertainties are large.

Therefore, in this study, we compare the approximation method and simulation method by using the same ESTOC dataset, and discuss the spatial variation of the difference between two methods.

### 3. Decadal Variation of DIC Concentration and Relation between Air-sea CO<sub>2</sub> Exchange and the Biological Process in the Shallow Water in the ESTOC

#### 3.1. Decadal Variation of DIC Concentration

DIC increase in 55 years (1957-2011) has been calculated by Doi et al. (2015) using the ESTOC data from Model 1. Anthropogenic carbon increase considered as the difference between the Model 1 and Model 2 of the ESTOC model, and was calculated in Doi et.al (2015) as well. However, the decadal variation of the time-series has not been discussed. Therefore, by using the same dataset, I calculated the average DIC concentration in basin-scale in the Pacific, to examine how DIC in the shallow water is influenced by biological processes which is the NPDZC model in the ESTOC model. Murata et al. (2007) and Sabine et al (2008) have pointed out the importance of such influence but it was not clear because of the uncertainty caused by mixing. In this study, I assumed the layer from the surface to 200 meters as the photic layer. I focused on this layer because it is considered to contain most of the biological process, especially, the photosynthesis.

In order to investigate possible differences among basins, I divided the world oceans. The definition of the basins in the Pacific Ocean is summarized in Table. 3.1

**Table 3.1 Definition of the Basins in the Pacific Ocean**

Basin	Latitude	Longitude
North Pacific	130°E – 180° – 120°W	60N – 30°N
Tropic Pacific	130°E – 180° – 120°W	30°N – 30°S
South Pacific	150°E–180°–75°W	30°S – 55°S

We focus on the Model 1 and Model 2 of the ESTOC model, to compare the scenario with and without atmospheric CO<sub>2</sub> increase.

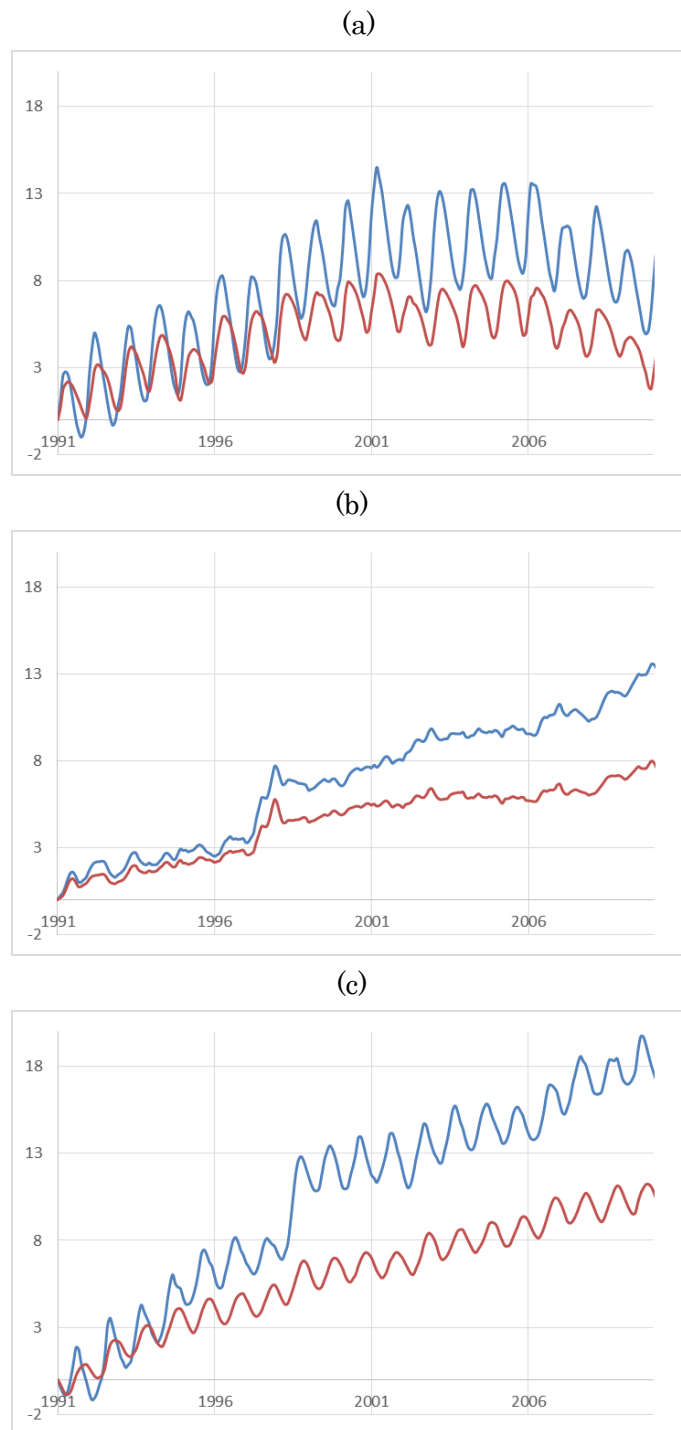
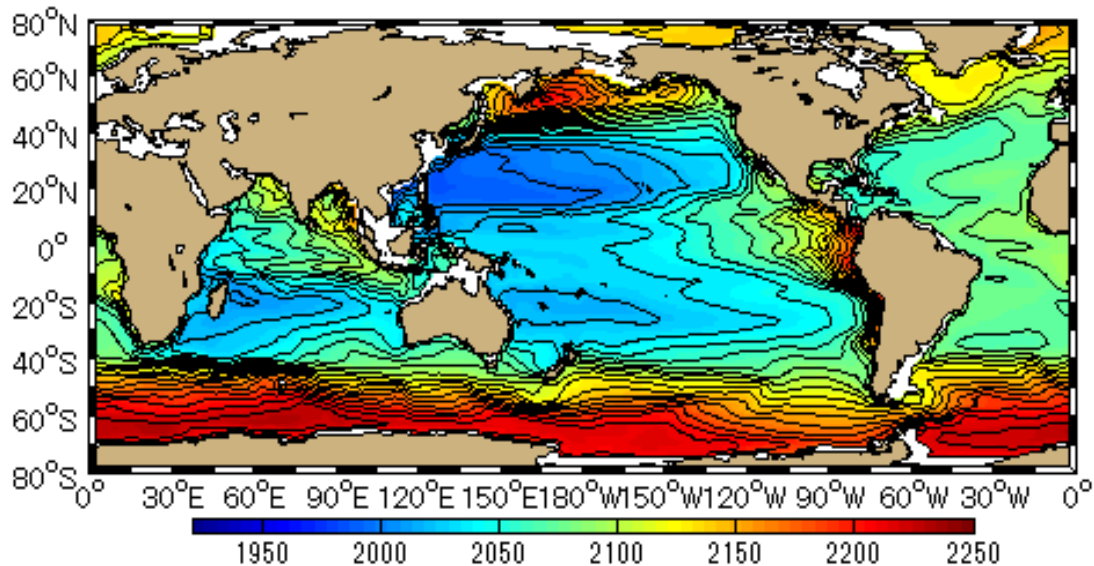


**Figure 3.1 Monthly mean Concentration of DIC in the Pacific within the depth of 0-200m. (a) the North Pacific (b) the Tropical Pacific (c) the South Pacific The vertical axis is the DIC concentration [ $\mu\text{mol kg}^{-1}$ ], normalized to January 1991, respectively. The horizontal axis is the years between January, 1991 and December, 2010. The blue curve is the result of Model 1 and the red curve is the result of the Model 3 which contains no biogeochemical system.**

From Figure. 3.1, it appears that in the North Pacific Ocean the difference between the carbon increase in Model 1 and Model 3 is small and getting closer. In the other two basins, the difference between the two models are growing larger. It is considered that, the contribution of biological process contributes to enlarge the carbon uptake, responding to the increased atmospheric CO<sub>2</sub>. However, the contribution of the biological process in the North Pacific is relatively small.

This result suggests that most of the carbon increase in the North Pacific is not contributed from the biogeochemical system in the basin. Murata et al. (2007) and Sabine et al. (2008) pointed out that the AOU change has been occurred in the late 1990s because of the climate change in the North Pacific Ocean. Non-increasing DIC shown in Figure 3.1. (a) could be a reflection of this change. In order to further investigate the phenomena, I drew the contour of the 20 years average DIC concentration (Figure 3.2. (a)). As shown in Figure 3.2.(a), there is a high concentration zone exists in the eastern North Pacific, near the east coast of Russia and Hokkaido, which is similar to the result by Murata et al. (2007) and the concentration decreased gradually to the east. Therefore, I examined the difference between the east and west sides of the north Pacific.

(a)



(b)

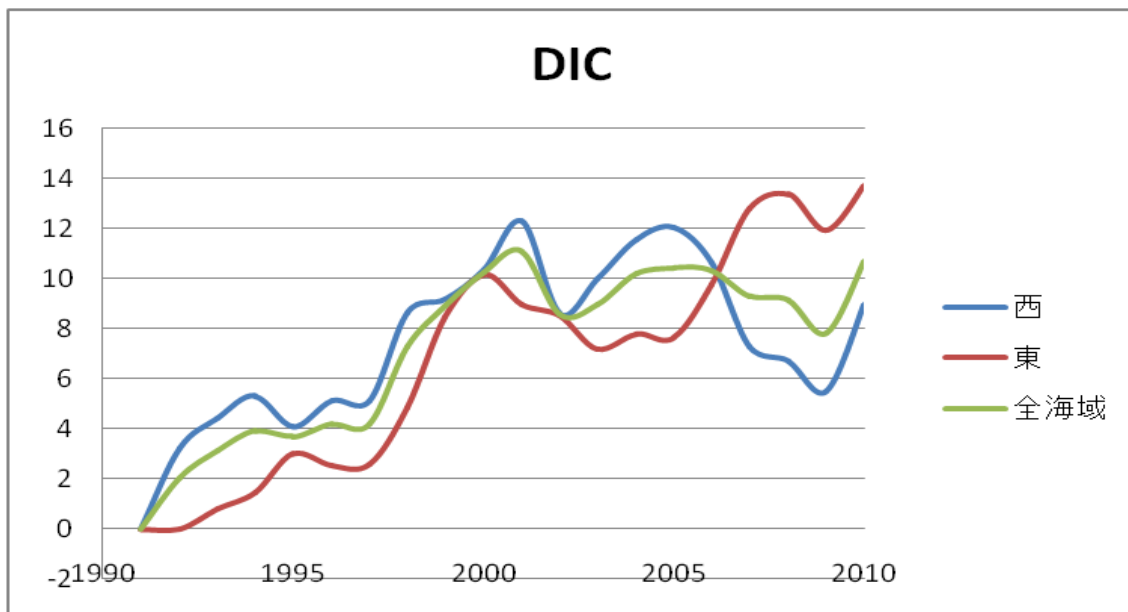


Figure 3.2 East-west DIC Difference in the North Pacific

(a) the contour map of the 20 years average of DIC concentration. (b) the DIC concentration variation in the east and west of the North Pacific Ocean. The regions we defined as east and west are tabulated in Table 3.2. The blue curve is the variation of DIC Concentration in the west and the red curve represents the east. The green curve is the entire North Pacific Ocean. DIC concentrations are all the anomaly from the DIC concentration in January, 1991 respectively.

Table 3.2 Definitions of the east and west region in the North Pacific Ocean

Region	Latitude	Longitude
East	130°E – 180° – 160°W	60N – 30°N
West	160°E – 120°W	60N – 30°N

Table 3.2 shows the definitions of the east and west region of the North Pacific Ocean. It should be noted that Figure 3.2. (b) shows the time-series of the DIC concentration in the east and west of the North Pacific Ocean. The time series shows that in the low concentration zone (the eastern side), the concentration has been increased constantly. On the other hand, the DIC concentration in the higher concentration zone (the western side) started decreasing since the year of 2000. Therefore, we speculate that the concentration distribution reached a new equilibrium in the North Pacific, so as the entire carbon uptake in the North Pacific Ocean keep roughly constant, since the late 1990s.

### 3.2. CO<sub>2</sub> Exchange in the North Pacific in the ESTOC with NPDZC model

To better understand the mechanism of the east-west difference, CO<sub>2</sub> gas exchange in the surface of the North Pacific was calculated.

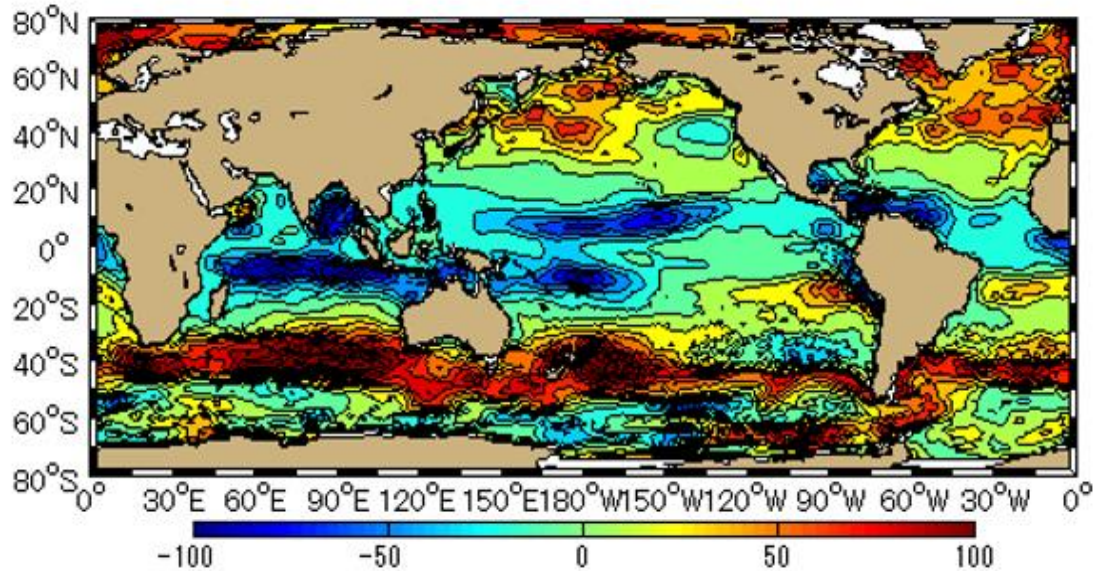


Figure 3.3 Averaged CO<sub>2</sub> Exchange at the Sea Surface between January 1991 and December 2010. The unit is [cm·mol/kg·h].

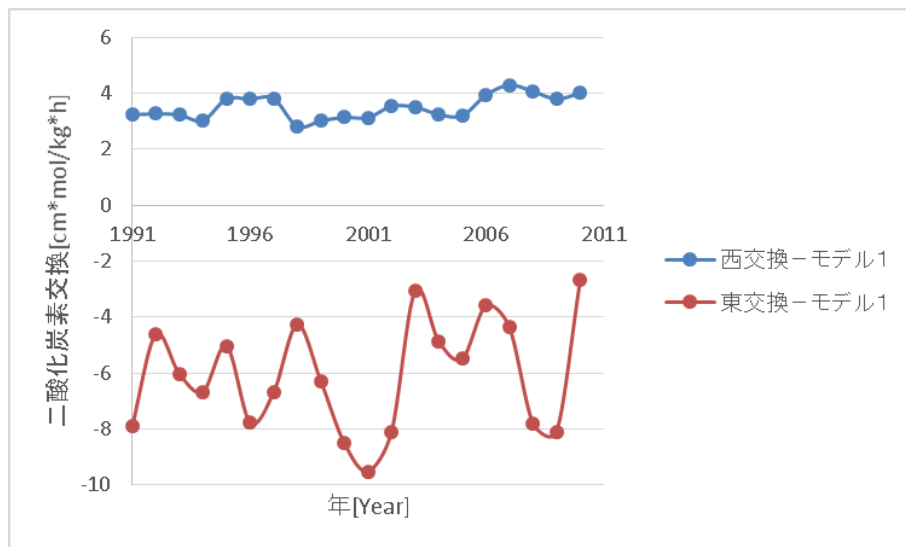


Figure 3.4 Time Series CO<sub>2</sub> Exchange in the North Pacific.

X axis shows exchange rate in cm·mol/kg·h, and Y-axis is year. The blue curve shows the CO<sub>2</sub> exchange in the west and red represents that in the west.

CO<sub>2</sub> Exchange at the Sea Surface averaged over the period from January 1991 and December 2010 is shown in Figure 3.3. From Figure 3.3, it should be noted that atmospheric CO<sub>2</sub> was absorbed in the west area of the North Pacific and atmospheric CO<sub>2</sub> was emitted from the east area of the North Pacific which are associated with the east-west difference of DIC concentration in the North Pacific. The Southern Ocean and the North Atlantic are the large resources of CO<sub>2</sub>, and there is a small emission region in the Sea of Okhotsk. This pattern is partially fit the observation results of Takahashi et al. (2002) Figure 3.4 shows time series CO<sub>2</sub> Exchange in the North Pacific. From Figure 3.4, I speculated there is an inter-annual vertical spatial change in the North Pacific, since the emission of the CO<sub>2</sub> in the eastern North Pacific, has a large variation and which suggest that the area of the CO<sub>2</sub> emission region changes inter-annually.

In the ESTOC simulation model, the CO<sub>2</sub> was calculated by

$$CO_2Exchange = K_v \cdot K_h \cdot \Delta pCO_2 \quad (3-1)$$

Where K<sub>h</sub> is the coefficient represents the gas exchange rate which is calculated by the wind speed at 10m above sea surface (U<sub>10</sub>) [Ho et al., 2006].

$$K_h = (0.266 \pm 0.019)U_{10}^2 \quad (3-2)$$

The U<sub>10</sub> data was taken from NCEP/NCAR reanalysis monthly mean data [Kalnay et al., 1996]. K<sub>v</sub> is the gas solubility in the sea surface [Weiss, 1997]

$$\ln(K_v) = A_1 + A_2(100/T) + A_3(T/100) + S[B_1 + B_2(T/100) + B_3(T/100)^2] \quad (3-3)$$

Hereby, T represents temperature and S stands for salinity. A<sub>1</sub>, A<sub>2</sub>, A<sub>3</sub>, B<sub>1</sub>, B<sub>2</sub>, B<sub>3</sub> are constants dependent on the expected unit, which are tabulated in Table 3.3.

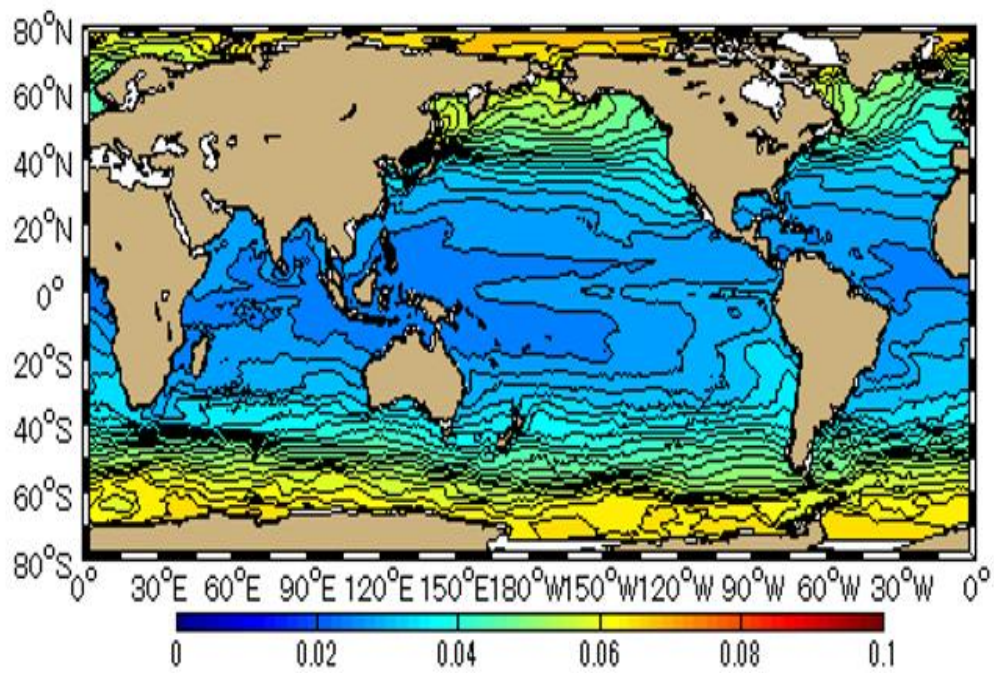
**Table 3.3 Constants for the Calculation of the Solubility of CO<sub>2</sub> in Molar and Gravimetric units.**

	Molar Units of K <sub>v</sub> [moles/l · atm]	Gravimetric Units of K <sub>v</sub> [moles/kg · atm]
A <sub>1</sub>	-58.0931	-60.2409
A <sub>2</sub>	90.5069	93.4517
A <sub>3</sub>	22.2940	23.3585
B <sub>1</sub>	0.027766	0.023517
B <sub>2</sub>	-0.025888	-0.023656
B <sub>3</sub>	0.0050578	0.0047036

Partial pressure of atmospheric CO<sub>2</sub>, obtained from monthly mean values observed at Mauna Loa (NOAA/ESRL data; US Department of Commerce [2013]), was used as the sea surface boundary condition. The formulations are those in the ESTOC model to

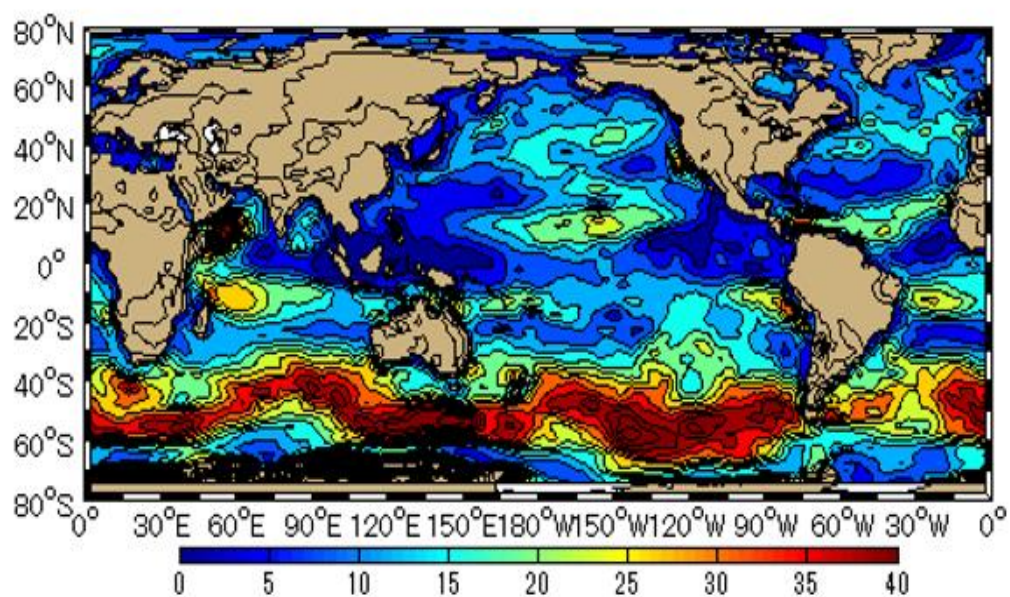
calculate the ocean  $p\text{CO}_2$  and  $\text{CO}_2$  solubility when the model was built [e.g., Lewis and Wallace, 1998]. Horizontal distributions of  $K_v, K_h, \Delta p\text{CO}_2$  are calculated (Figure 3.5) using the same dataset and formulations above, in order to show the procedure parameters that may cause the east-west difference of the  $\text{CO}_2$  exchange in the sea surface.

(a)





(b)



(c)

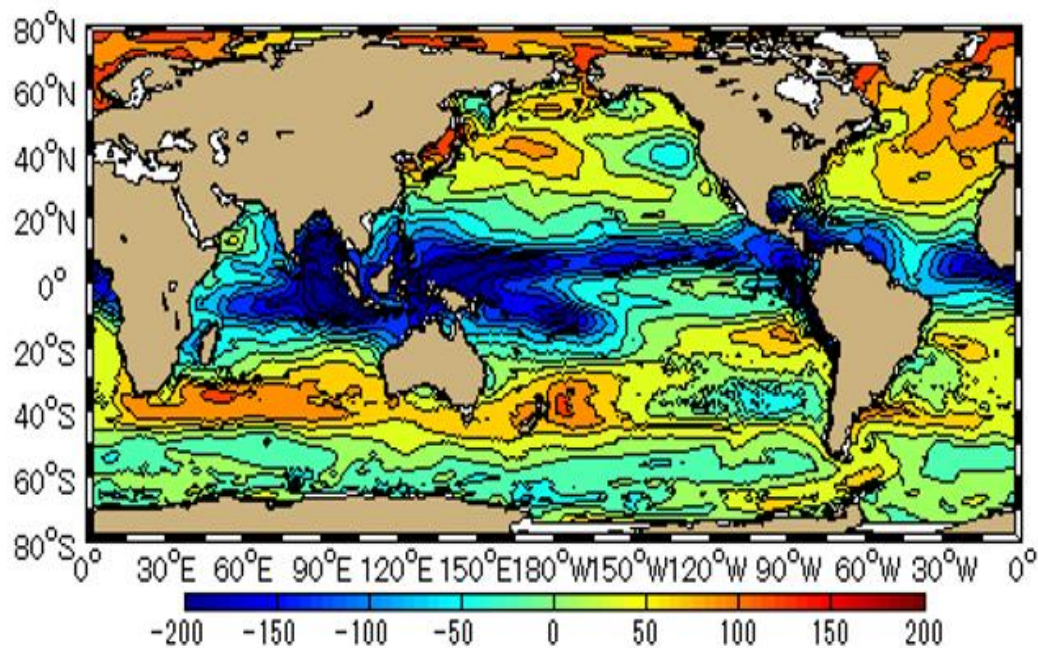


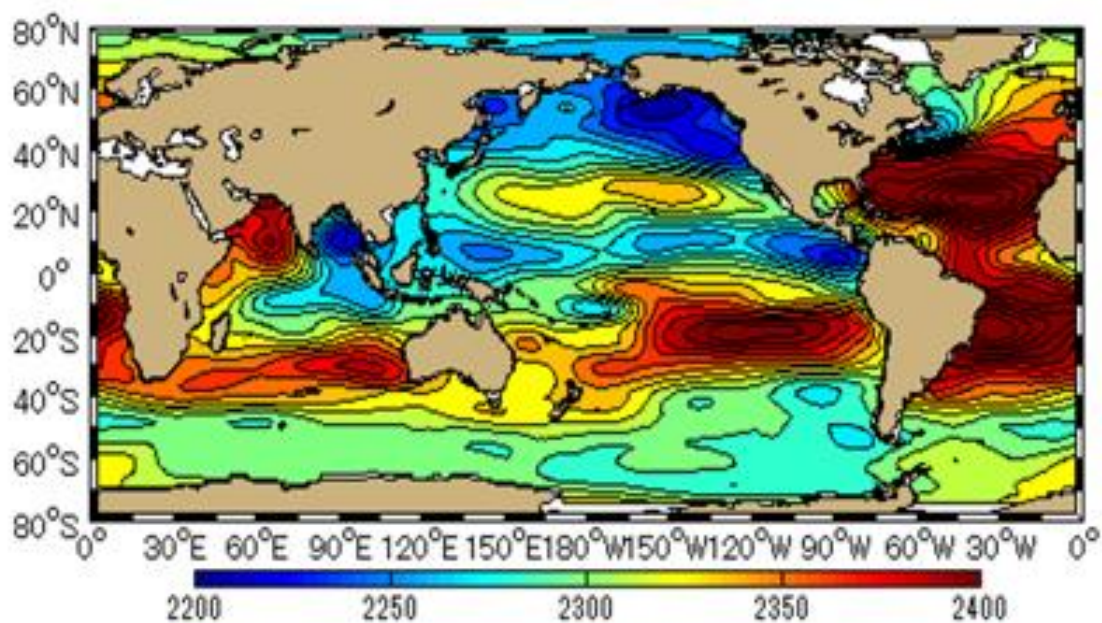
Figure 3.5 Distribution of  $K_v$ ,  $K_h$ , and  $pCO_2$

(a) the Solubility Coefficient  $K_v$ , (b) the Gas Exchange Rate Coefficient  $K_h$ , (c) the  $\Delta pCO_2 = pCO_{2,air} - pCO_{2,sea}$

A difference between east and west exists in the  $\Delta pCO_2$  distribution only as

shown in Figure 3.5. The calculation in the ESTOC requires values for alkalinity along with DIC. There is no direct process connection between the DIC and alkalinity. Therefore, only changes in the nitrate concentration can change the alkalinity [Doi et al., 2015].

(a)



(b)

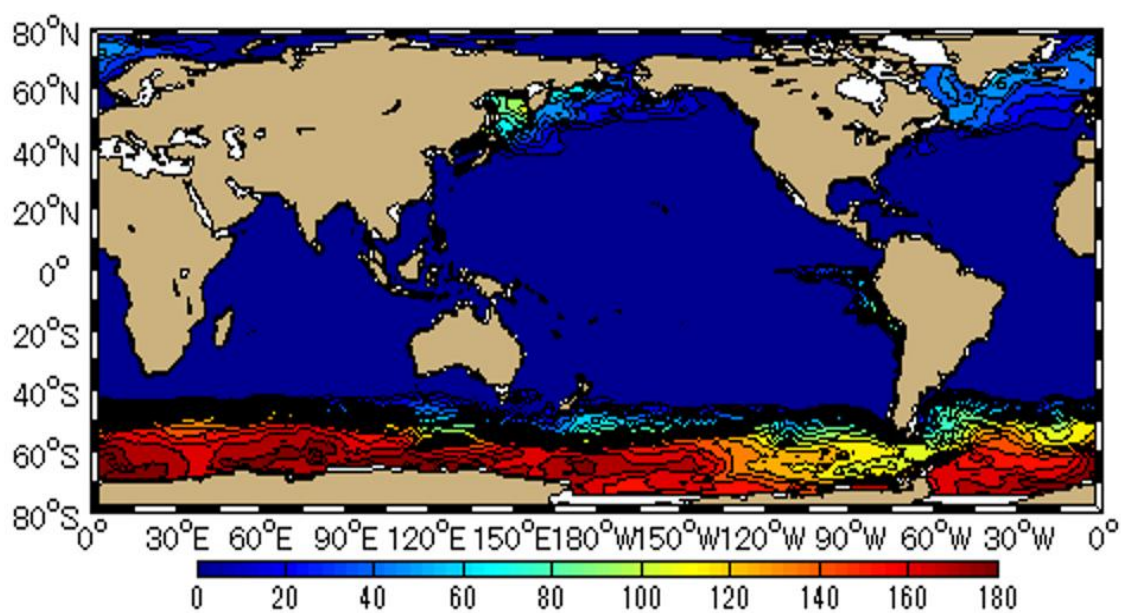
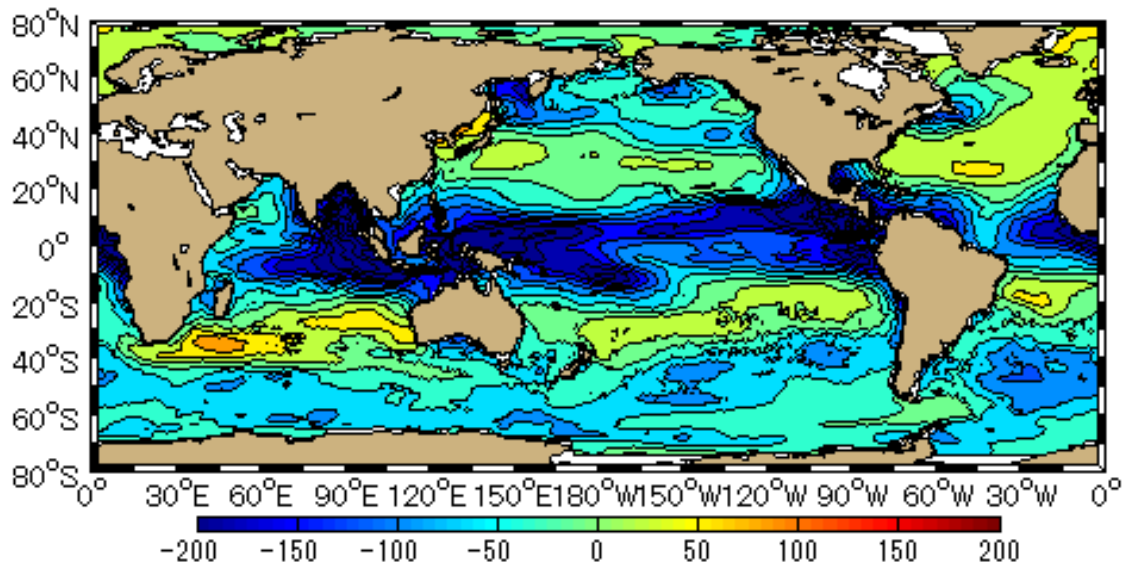


Figure 3.6 Distribution of Alk and N

(a) Horizontal Distribution of averaged Alkalinity [ $\mu\text{mol/kg}$ ]. (b) averaged Nitrate [ $\mu\text{mol/kg}$ ].

Figure 3.6 shows horizontal distributions of Alkalinity and Nitrate. Both alkalinity and nitrate distribution show an east-west difference in the North Pacific. Since the nitrate is the fundamental variable of the NPDZC model, it is possible that the biogeochemical system indirectly control the  $\text{CO}_2$  gas exchange through nitrate in the surface water. I used output data of the Model 3 that contains no NPDZC model to calculate the  $\Delta p\text{CO}_2$ , and  $\text{CO}_2$  gas exchange to confirm it (Fig3.8).

(a)



(b)

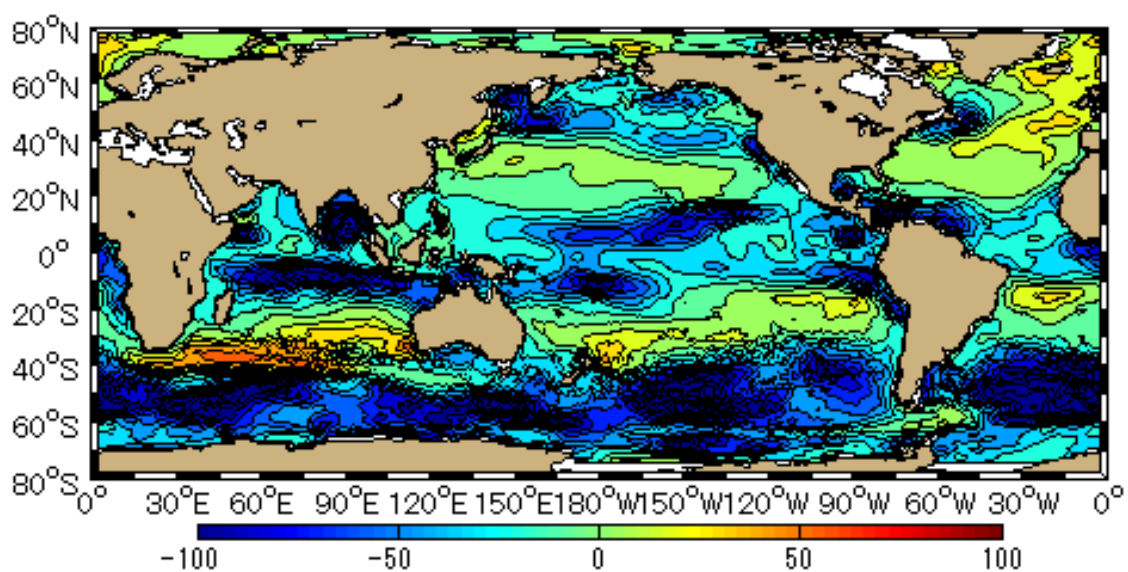


Figure 3.7 Contour maps of pCO<sub>2</sub> and CO<sub>2</sub> exchange  
(a) the  $\Delta pCO_2$ , and (b) the CO<sub>2</sub> gas exchange [cm·mol/kg·h].

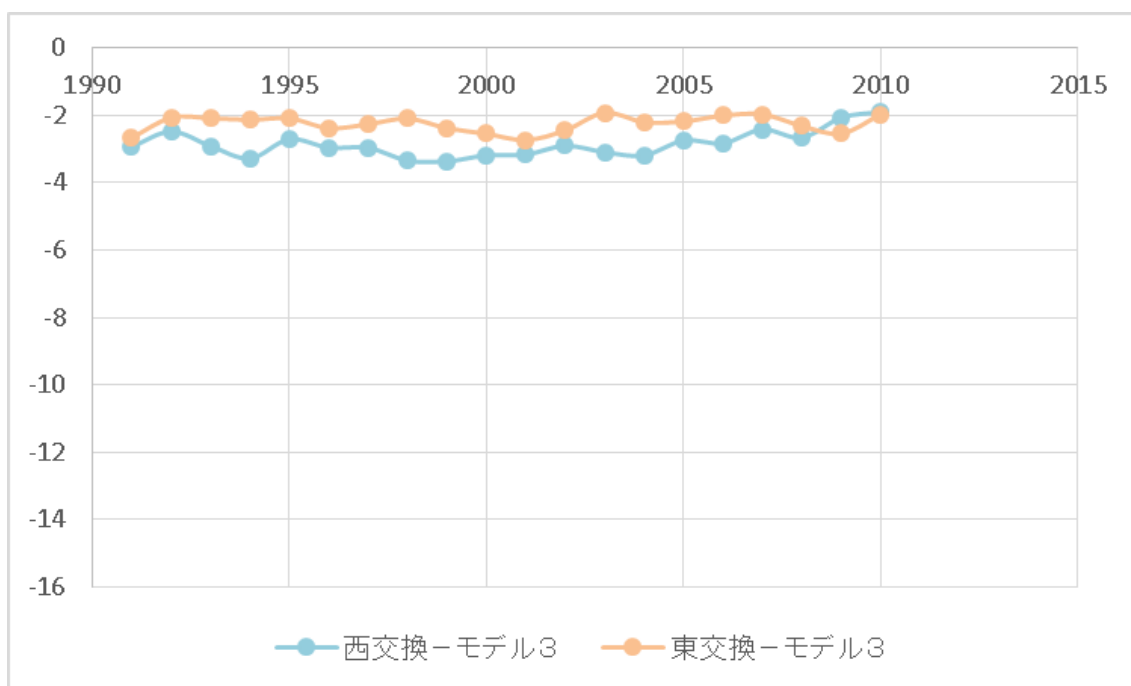


Figure 3.8 Time Series of CO<sub>2</sub> Exchange in the North Pacific without NPDZC model.  
The blue curve shows the CO<sub>2</sub> exchange in the west and red represents the east. The vertical axis is the difference of the CO<sub>2</sub> gas exchange [cm·mol/kg·h].

As shown in Figure 3.8, there is no apparent contrast of partial pressure of CO<sub>2</sub> or CO<sub>2</sub> gas exchange in the sea surface between the east and west of the North Pacific. It should also be noted that the difference between CO<sub>2</sub> exchange in the east and the west is close to zero.

### 3.3. Summary

In this chapter, from the carbon uptake calculated from ESTOC models (Figure 3.1), it was found that the increase of averaged DIC concentration stopped since the late 1990s in the North Pacific. The difference between Model 1 and Model 3 is small.

In the ESTOC model, there is a contrast of air-sea CO<sub>2</sub> exchange and DIC concentration between the east and the west of the North Pacific, which is partly consistent with the observation of Murata et al. (2007). The CO<sub>2</sub> gas exchange in the western North Pacific is an uptake area and the eastern North Pacific is not, along the 40°N. This partially fits the observation results calculation of Takahashi et al. 2002.

In the ESTOC model, it is figured out that nitrate distribution indirectly controls the CO<sub>2</sub> gas exchange in the sea surface by affecting the alkalinity distribution and partial pressure CO<sub>2</sub> in the sea surface water. Combining the results of averaged DIC concentration increase in the Figure 3.1, the values of DIC in the west and the east have negative correlations, the overall DIC contribution in the North Pacific comes to constant after the late 1990s.

Above all in the Chapter 3, it is suggested that biological process in is important for carbon cycle in the ESTOC model.

## 4. Indication of Biochemical System Contribution to the Carbon Uptake in the ESTOC

### 4.1. Indication of the Biochemical System Contribution to the Global Carbon Uptake in the ESTOC

The dissolved inorganic carbon (DIC) distribution in the ocean is controlled by air-sea gas exchange including the CO<sub>2</sub> uptake (solubility pump), the biological process of photosynthesis, respiration, and remineralization (soft-tissue pump), and the formation and dissolution of carbonate particles (carbonate pump) [Volk and Hoffert 1985]. The soft-tissue pump is very significant and it is the only pump that cannot be neglected by any assumptions or corrections on DIC, when calculating the anthropogenic carbon in the ocean. However, the contribution of the biological process to the inorganic carbon uptake has not been measured by any researcher previously. Especially, to calculate the anthropogenic carbon dissolved in the ocean, approximation method that developed by [Gruber 1996, Sabine 2004, etc.] has a bias that is usually neglected. To better understand the effect of biological process on the anthropogenic carbon uptake in the ocean and approximate the anthropogenic carbon dissolved in the ocean, it is important to calculate the contribution of the biological process to the carbon uptake in the ocean. The new biogeochemical model in the ESTOC can be used to roughly calculate the contribution to the carbon uptake of biological processes. We define the dissolved inorganic carbon in the ocean that it consists of four portions that are either belong to different carbon resources or dissolved due to different pumps.

**Table 4.1 Carbon Portions of the Four Models**

Cn	Dissolved natural carbon due to the physical dynamic variation
Ca	Dissolved anthropogenic carbon due to the physical dynamic variation
Bn	Dissolved natural carbon due to the biogeochemical dynamic variation
Ba	Dissolved anthropogenic carbon due to the biogeochemical dynamic variation

**Table 4.2 Four Models Consistence of Carbon Portions**

Model 1 DIC	$C_n + C_a + B_n + B_a$
Model 2 DIC	$C_n + B_n$
Model 3 DIC	$C_n + C_a$
Model 4 DIC	$C_n$

Consequently, we can separate the dissolved carbon due to the biogeochemical system in ESTOC and gain an estimation of the biogeochemical system contribution to the global-scale carbon uptake.

$$B_a + B_n = (C_a + C_n + B_a + B_n) - (C_a + C_n) \quad (4-1)$$

$$C_{Bio} = C_{Model 1} - C_{Model 3} \quad (4-2)$$

The biogeochemical system contribution to the anthropogenic carbon uptake can also be calculated by eliminating the  $B_n$  term from equation (1) and (2),

$$B_a = (C_a + C_n + B_a + B_n) - (C_a + C_n) - \{(C_n + B_n) - C_n\} \quad (4-3)$$

$$C_{Bio}^{ANT} = C_{Model 1} - C_{Model 3} - (C_{Model 2} - C_{Model 4}) \quad (4-4)$$

Since the ESTOC model is a model assimilated to the observed data, the quality and the quantity that the ESTOC data assimilated to, determine the accuracy of the ESTOC model. Therefore, the recent data from January, 1991 to December 2010 have been chosen, since they were assimilated to larger quantity and higher quality datasets. Consequently, all resulting data can be normalized to the stoichiometric state in the January, 1991. In this study, we focused on the biogeochemical system, therefore, I intended to calculate the dissolved carbon concentration in the photic layer which is simplified as the layer between sea surface and 200 meters depth on the global scale in the latest two decades (1991 – 2010).



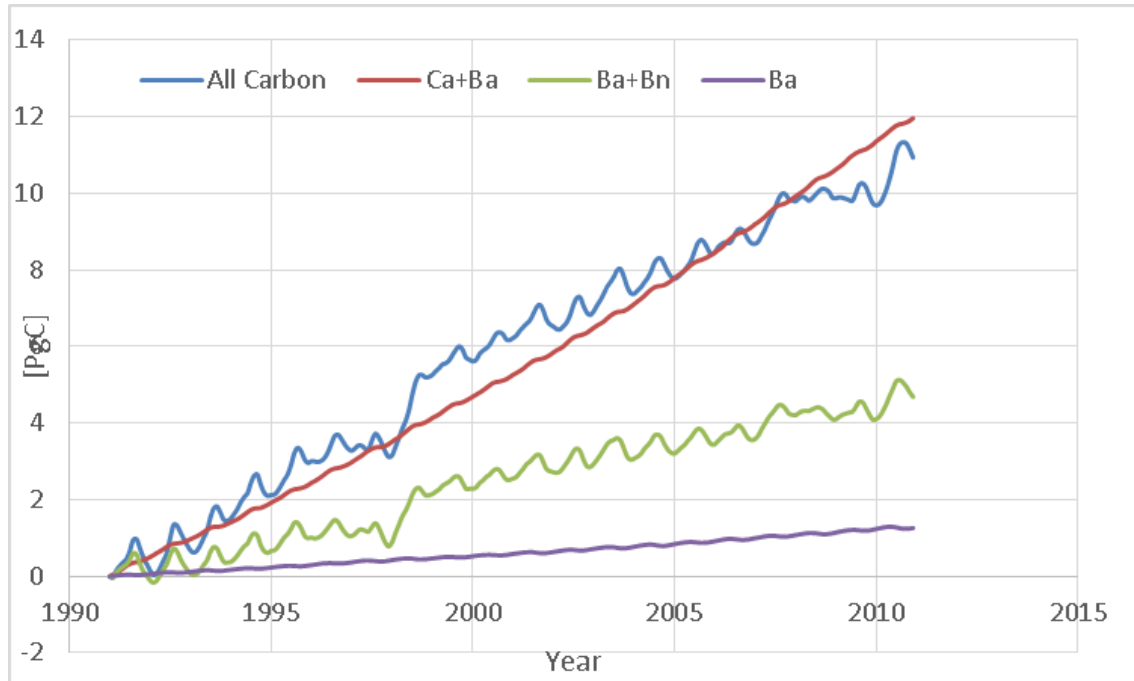


**Figure 4.1 Biogeochemical System Contribution to the Global Carbon Uptake in the layer between 0m-200m depth from January 1991 to December 2010, normalized to January 1991**

Hereby, all carbon stands for  $(C_n + C_a + B_n + B_a)$ , and  $(C_a + B_a)$  represents the total anthropogenic carbon,  $(B_a + B_n)$  is the total carbon dissolved due to the biological system.

From Figure 4.1, it is noted that biogeochemical system in the ESTOC model, contributes most of the seasonal variation to all carbon uptake. The all carbon uptake, in this 20 years, is 0.60 [PgC/yr]; the increase of the anthropogenic carbon  $(C_a + B_a)$ , is 0.56 [PgC/yr]. It is noted that over 92.4% of the increase in all carbon is anthropogenic. In the two decades, the carbon uptake contributed by biogeochemical system is summarized below.

**Table 4.3 Carbon Uptake Contribution by Biogeochemical System in ESTOC**

Carbon Uptake [PgC/yr]		Proportion	
Ba	0.06	$\frac{B_a}{B_a + C_a}$	11.5%
Ba + Bn	0.25	$\frac{B_a + B_n}{All\ Carbon}$	41.5%

It is shown that 41.5% of the shallow layer carbon uptake in the two decades is due to the biogeochemical system, and 11.5% of the all anthropogenic carbon dissolved is due to the biogeochemical system. Although, the accuracy requires further discussion and improvement, the outcome above is an important outset estimation of the biological process contribution to the carbon uptake in the entire ocean.

#### 4.2. The effect of El Niño on Carbon uptake and Biology Process Contribution

Except the knowledge we obtained in Chapter 4 Section 1, we also noticed that, in 1998, the carbon uptake decreased rapidly, and return to the ordinary level after 1999. It is necessary to exam the causes of the variation in 1998, since it concerns about the validity of the linear approximation we took above when we concluded the results of the biogeochemical process. Furthermore, it is possible to discover any possible force that affect biogeochemical process strongly and indirectly affect the shallow layer carbon uptake in a short period. We extend the carbon uptake calculation to 40-year (1971-2010) to compare with the Figure. 4.1.

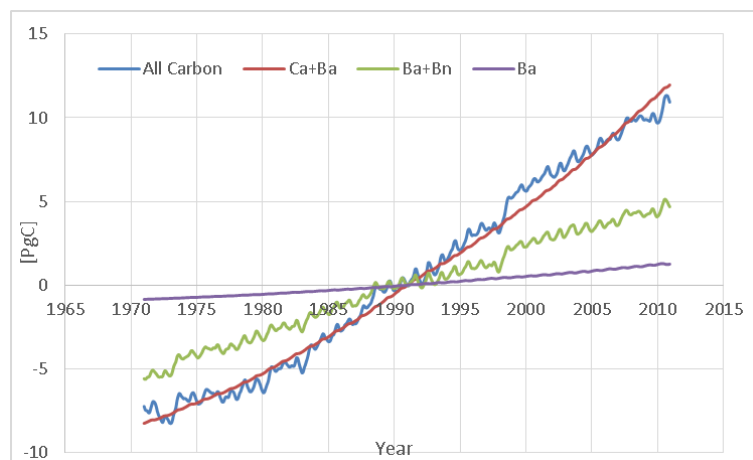


**Figure 4.2 Biogeochemical System Contribution to the Global-scale Carbon Uptake in the layer between 0m-200m from January 1971 to December 2010, normalized to January 1991**

It is confirmed that linear approximation is practicable in this case and slowing-down of carbon uptake increasing in 1998 is a peculiar case. Since the January is the minimum, we focus on three months (December, January, and February) average as winter variation of 20 years, so that we can eliminate the seasonal variation as well.

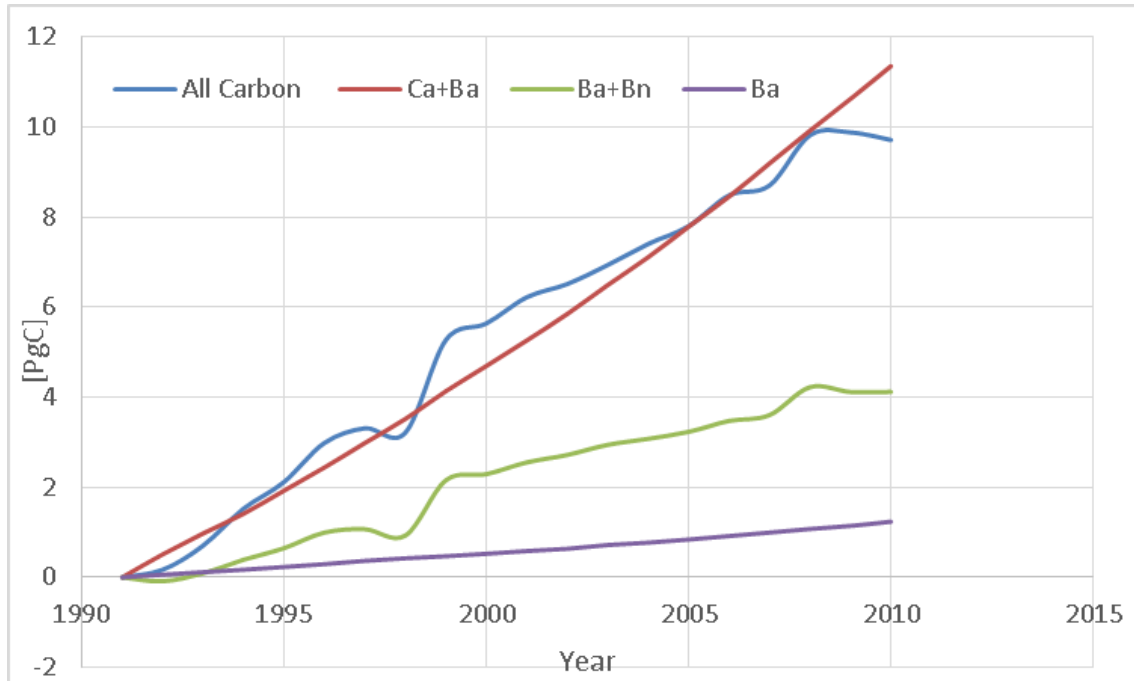


**Figure 4.3 Biogeochemical System Contribution to the Global-scale Carbon Uptake in the layer between 0m-200m depth of winter (Dec., Jan. and Feb.) average of 20 years (1991-2010)**

Not only a rapid variation occurred between 1997 and 1999, but also a reverse variation shows up in 2008 and possibly a similar variation in 2010 as well. This time series pattern is similar to the El Niño phenomenon in this two decades. To better understand a potential relation between short term climate change such as El Niño or La Niña phenomenon, and the biogeochemical system contribution to the anthropogenic carbon increasing in the ESTOC, the quality of short term climate change reproduction and it's correlation with the carbon increasing variation in the model should be discussed.

Firstly, we confirmed the sea surface temperature (SST) variation in 1991 to 2010 in the ESTOC reproduction by comparing the observed SST data with the Japanese Meteorological Agency (JMA).

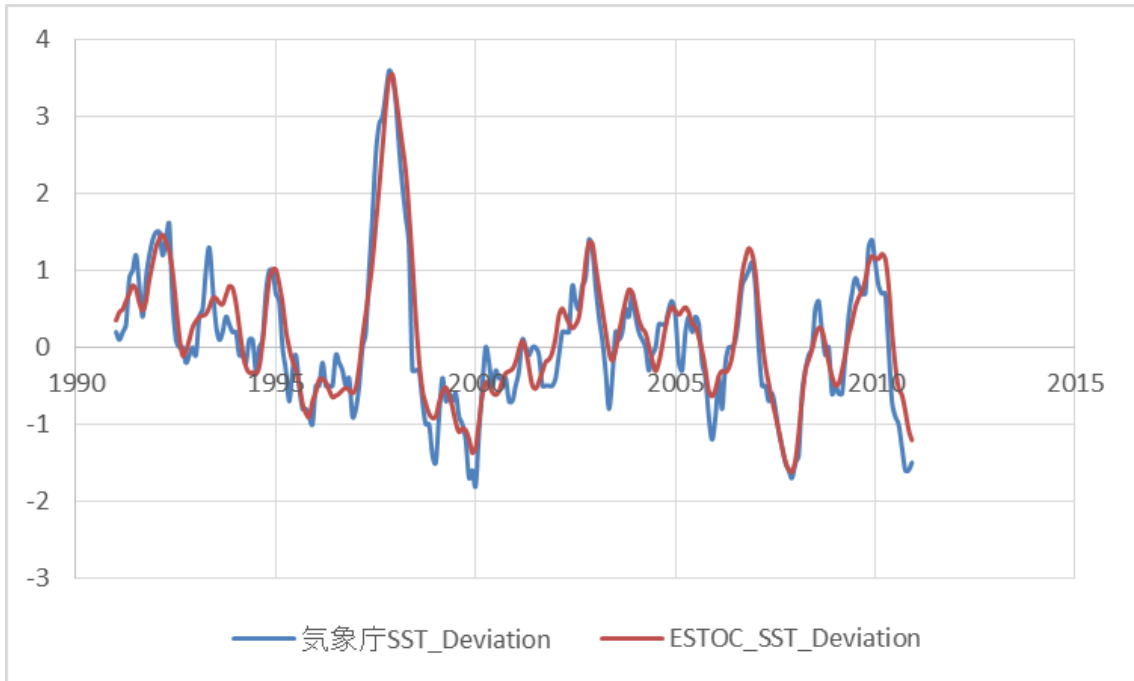


**Figure 4.4 SST Variation Comparing to JMA Observation Data**

The correlation of JMA observation and ESTOC data is 0.91. The SST variation is reproduced well in the model.

Secondly, the correlation of carbon uptake and SST variation of Niño. 3 area in the ESTOC was examined.

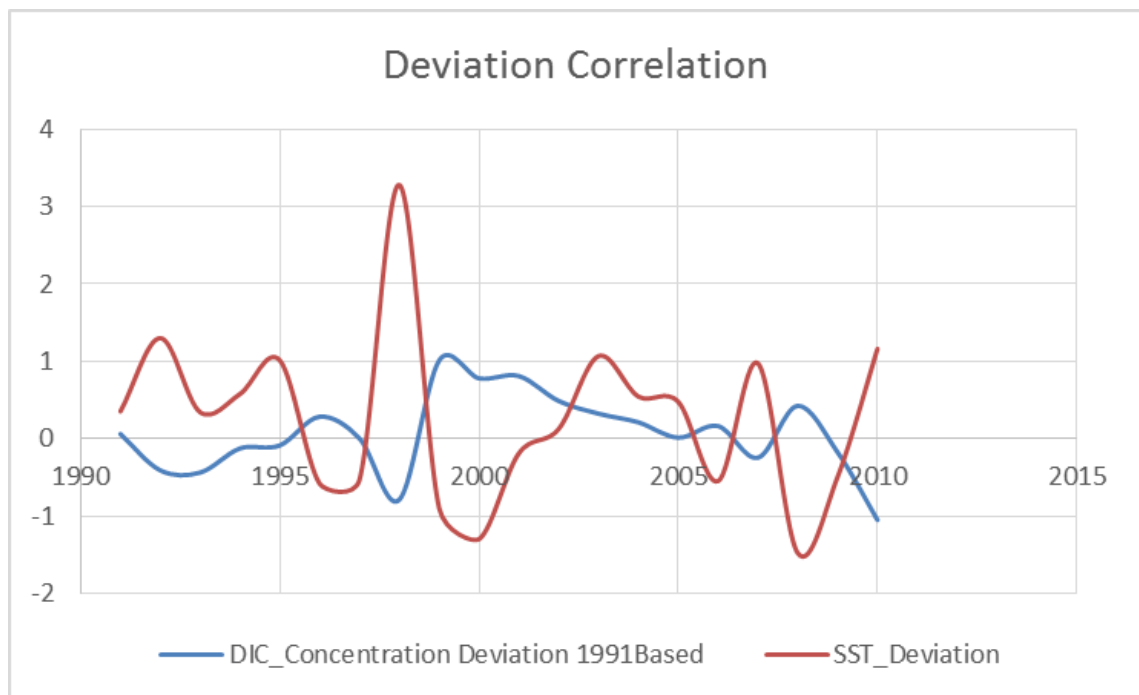
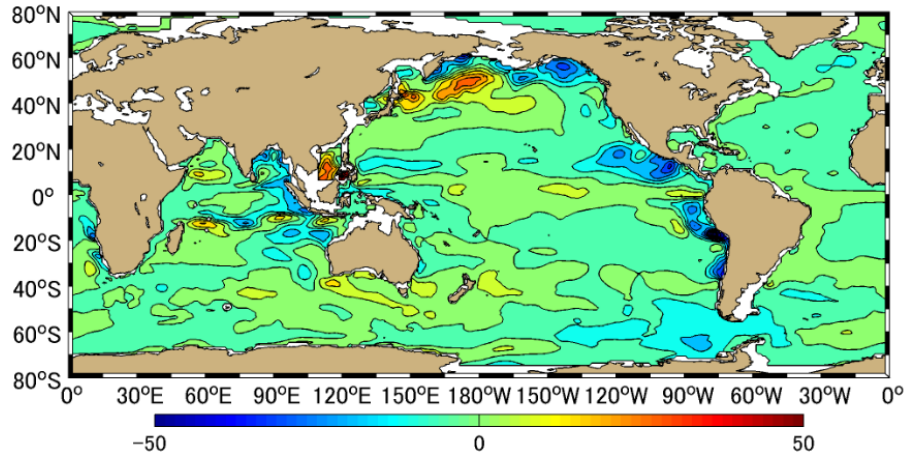


#### **Figure 4.5 Correlation of Carbon Uptake and SST Variation of Every Winter in 1991-2010**

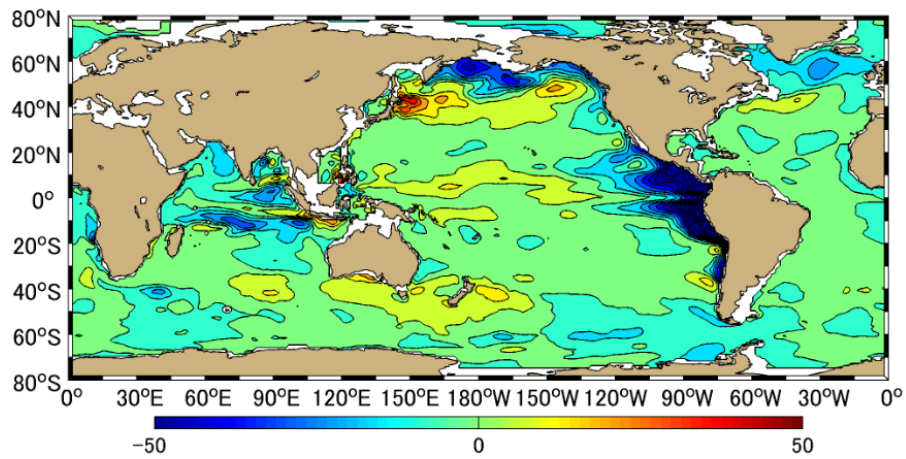
Figure 4.5 shows a relatively strong negative correlation of -0.74 between carbon uptake and SST variation of Niño. 3 area in this 20 years which means that when El Niño phenomenon occurs, the carbon uptake is relatively low in the global ocean and the carbon uptake is more than usual when La Niña phenomenon occurs. It is well known that not only the SST in Niño. 3 area is high in El Niño years, but also the global scale SST is higher than usual. Consequently, the carbon uptake is less than other years, since the solubility pump contribution decreases because of the high sea-water temperature. In such case, the biological pump contribution is presumed to be larger than normal years. However, carbon uptake proportion of biogeochemical process contribution to the total carbon is 39.9% which is slightly smaller than the 20years carbon uptake. Therefore, biogeochemical system contribution has decreased by nearly the same rate as the solubility pump did in El Niño years. To better understand the behavior of biogeochemical system contribution, we calculated the carbon distribution variation of 20 years. We focus on the winter of every year to reduce the impact of seasonal variation as we did above. We also reduced the accumulation of anthropogenic by removing linear approximation slope, so as to distinguish the variation of carbon uptake distribution. The all carbon distribution variation of 20 years are shown in Appendix, Figure A-1 and biological contribution are shown in Appendix, Figure A-2.

Ca + Cn + Ba + Bn [PgC]

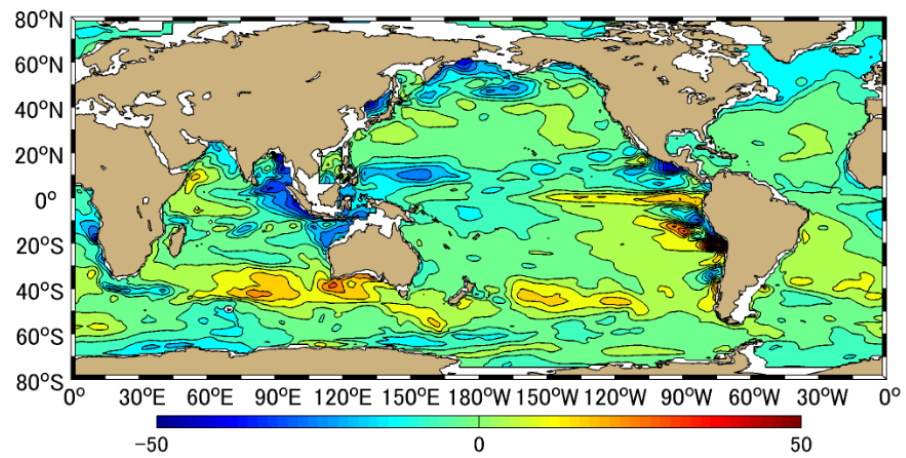
(a) Average of Dec. 1993, Jan. 1994, Feb. 1994



(b) Average of Dec. 1997, Jan. 1998, Feb. 1998

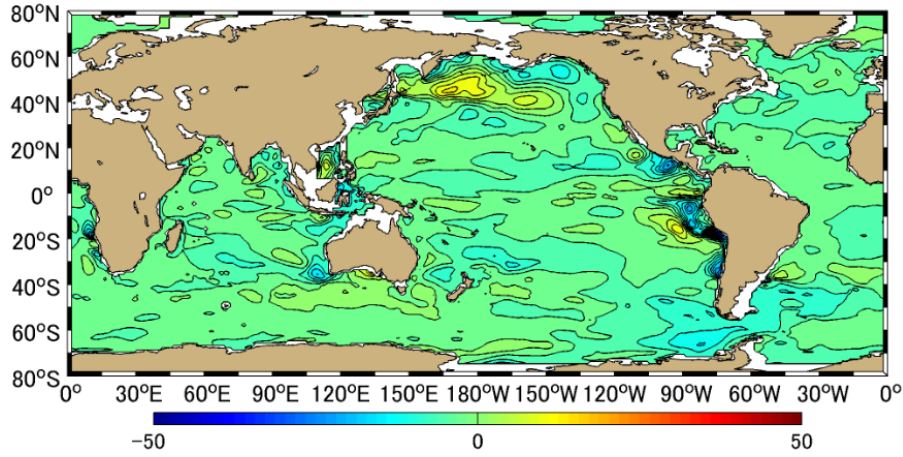


(c) Average of Dec. 2007, Jan. 2008, Feb. 2008

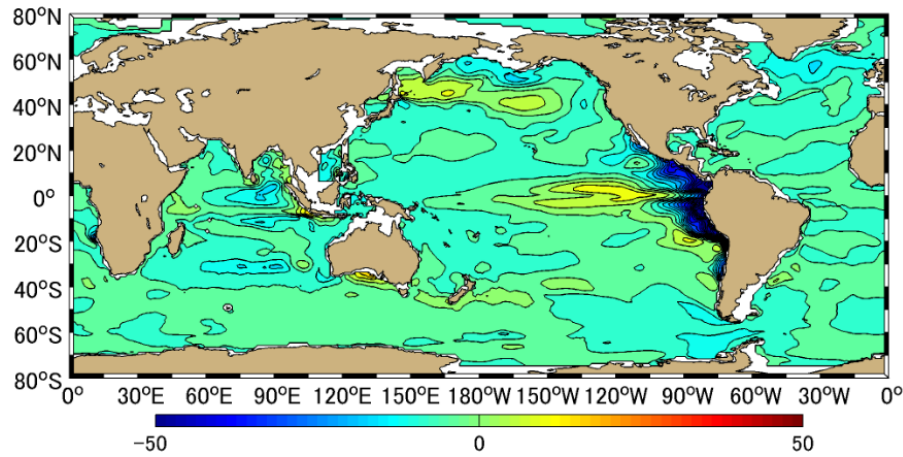


Ba+Bn [PgC]

(d) Average of Dec. 1993, Jan. 1994, Feb. 1994



(e) Average of Dec. 2007, Jan. 2008, Feb. 2008



(f) Average of Dec. 2007, Jan. 2008, Feb. 2008

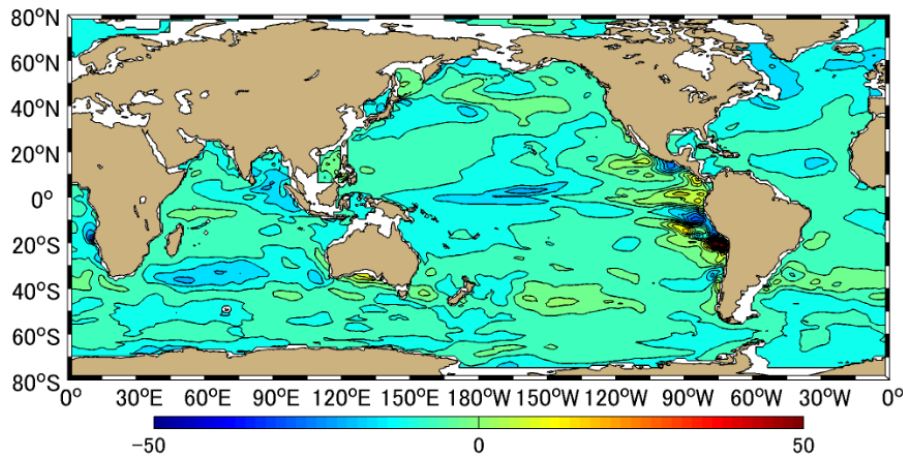


Figure 4.6 Shallow (0-200m) Carbon Uptake Variation Contour, Normalized to the winter of 1991 (Average Dec.1990, Jan. 1991, Feb. 1991.. (a) is the all carbon variation

distribution of 1994 (normal year) winter. (b) is the all carbon variation distribution of 1998 (El Niño year) winter. (c) is the all carbon variation distribution of 2008 (La Niña year) winter. (d) is the biogeochemical contribution variation distribution of 1994 winter. (e) is the biogeochemical contribution variation distribution of 1998 winter. (f) is the biogeochemical contribution variation distribution of 2008 winter.

In the winter of 1998, which we considered as the example of El Niño year, both all carbon uptake and biogeochemical contribution show that Niño. 3 area contains lower carbon uptake than other years. Except the solubility pump reason we discussed above, the cause of this distribution is considered that upwelling in the western Middle American coast was suppressed. Consequently, the deeper water which contains higher concentration of carbon is difficult to move to upper level. The same condition happens to the nutrients, therefore the carbon uptake contributed by biological process is suppressed as well. We also noticed that, there is a relatively high concentration area in the north-western Pacific Ocean. This difference between the eastern and western Pacific Ocean becomes unclear in the La Niña year.

#### 4.3. Summary

In this chapter, we discussed the biological process contribution to the carbon uptake, its move when short term climate change occurred and the spatial pattern in different basins, in the ESTOC. Although the NPDZC model in the ESTOC needs more careful discussion, such as the impact of lacking calcium carbon dynamics and iron in controlling primary production [Doi et al. 2015], we understand that the contribution of the biological process to the carbon uptake is unneglectable and the first guess the contribution and proportion of it that we calculated in Chapter 4 is worth being referred to.



## 5. Anthropogenic Carbon Uptake Difference Calculated by Different Methods

### 5.1. Comparison between Simulation Method and Approximation Method

Four models have been developed in the ESTOC (Table. 1.2). By calculating the difference of the DIC output data in different models, the state of a specific DIC uptake in the ESTOC can be calculated. Model 1 is the model with all the variables. Model 2 is the model without atmospheric CO<sub>2</sub> increase. The anthropogenic DIC in the ocean can be calculated in the ESTOC by the subtracting DIC in Model 2 from Model 1. Difference of the DIC between both methods within a certain period of time is considered to be the anthropogenic CO<sub>2</sub> increase in this period.

$$C_{ANT} = C_{Model\ 1} - C_{Model\ 2} \quad (5-1)$$

where  $C_{model\ 1}$  is the DIC concentration in the Model 1 ( $C_n + C_a + B_n + B_a$ ), and  $C_{model\ 2}$  is the DIC concentration in the Model 2 that contains no atmospheric CO<sub>2</sub> ( $C_n + B_n$ ), and  $C_{ANT}$  is considered to be the carbon variation caused by the missing of atmospheric CO<sub>2</sub> ( $C_a + B_a$ ). However, since both models are spun up separately with different boundary conditions such as atmospheric CO<sub>2</sub>, there may be an enormous difference in stoichiometric variables of the equilibrium state. Therefore, choosing a certain period of time and calculating the variation within the period can eliminate the uncertainty caused by separate simulation. In this study, the chosen period is January, 1991 to December, 2010 so as to focus on the decadal increase of DIC concentration. The quality of the later data in the 55 years (1971 – 2011) is considered to be higher than the earlier ones because the observation data that the model assimilated to, have better quality and larger quantity. Therefore, the anthropogenic DIC increase  $\Delta C_{ANT\ t2-t1}$  is calculated by the equation below.

$$\Delta C_{ANT\ t2-t1} = (C_{Model\ 1} - C_{Model\ 2})_{t2} - (C_{Model\ 1} - C_{Model\ 2})_{t1} \quad (5-2)$$

Since the period of time was set to be from January, 1991 to December, 2010, hereafter, the amount or the concentration of DIC we discuss, is normalized to the value of January, 1991. For instance, the normalized DIC concentration in time  $t$  is the difference of the DIC uptake between  $t$  and January, 1991.

$$nC_{MO}^{ANT,t} = (C_{Model\ 1} - C_{Model\ 2})_t - (C_{Model\ 1} - C_{Model\ 2})_{JAN.,1991} \quad (5-3)$$

As discussed in the Chapter one, Murata et al. (2007) simplified the approximation method. Only DIC and AOU are required in this method to calculate the anthropogenic carbon. (Chapter 1, Equation (1-18))

$$C_{ant} = C - \gamma_{C:O} \times AOU \quad (1-18)$$

The second one of the two assumptions that the formation areas for water masses found in the present study are fixed over time, is considered to be satisfied as the basic model was spun-up for 3000 years from initial motionless state [Osafune et al. 2014]. DIC(C) is contained in the ESTOC data, and the AOU, which is the difference between the observed DO concentration and its equilibrium saturation concentration in sea water with the same physical and chemical properties.

$$AOU = DO_{sat} - DO \quad (5-4)$$

$\gamma_{C:O}$  is the ratio of DIC to the DO, which is set to 0.69 referring to Murata et al. (2007). The approximation method improved by Murata et al. (2007) is also a calculation of the anthropogenic carbon increase, which is in a chosen period time. In the original study, this time is determined by the time of observed DIC and DO data. Hereby, it is set from January, 1991 to December, 2010, so that it can be compared with the simulation method. The Cant data of time t between January, 1991 and December, 2010 are also normalized to January, 1991.

$$nC_{DO}^{ANT,t} = (C_t - C_{JAN,1991}) - \gamma_{C:O} \times \{(DO_t - DO_{Jan,1991}) - \{(DO_{sat} t - DO_{sat} Jan,1991)\}\} \quad (5-5)$$

Since all values of variables are available in the ESTOC model, the formulations of both methods can be imputed by the same output dataset of ESTOC. In such case, the resulting data of the simulation method can be presumed to be the true value, and the difference between that and the results calculated by approximation method using the same dataset is considered to be the bias of approximation method. Consequently, the bias that approximation method introduced in the previous observational researches can be estimated. The bias in the approximation method is mostly because of too much simplified assumption in the approximation method, which could represent the change in AOU. To evaluate these bias in the previous researches, I focused on the shallow water, the layer from the sea surface to 200 meters depth, where is considered that mixing and dissolution occur most. Figure. 5.1 is the results of anthropogenic carbon uptake by different methods in the shallow layer from January, 1991 to December, 2010, and all results are normalized to January, 1991.

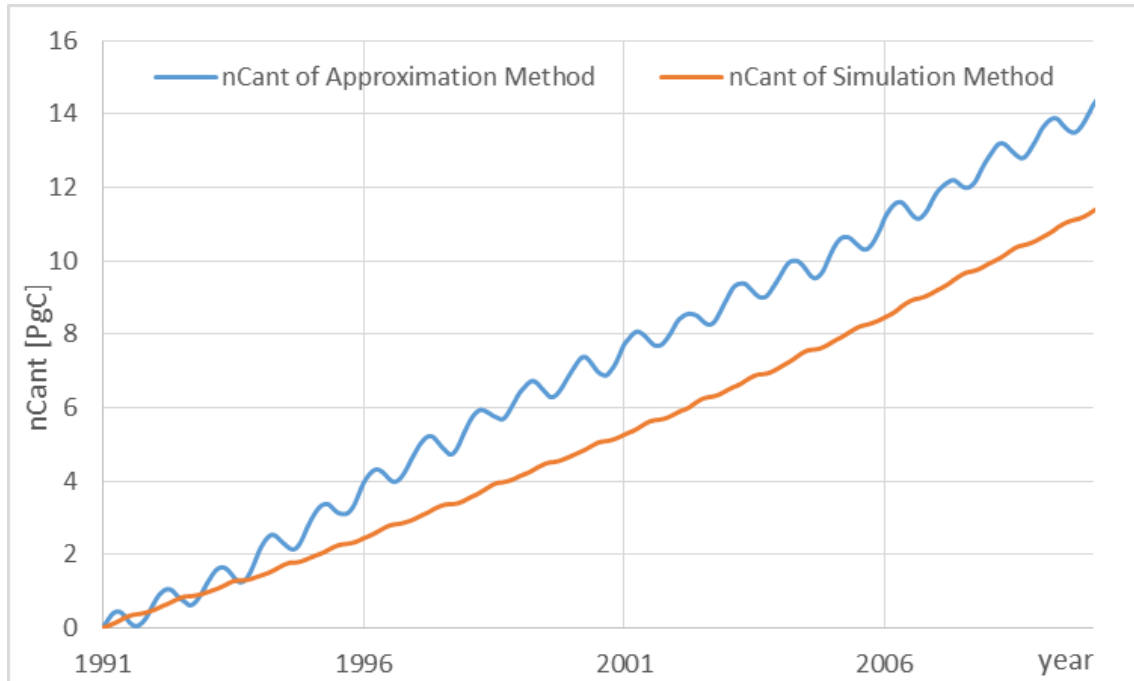


**Figure 5.1 Anthropogenic Carbon Uptake Increase (0-200m) by Approximation Method and Simulation Method from January, 1991 to December, 2010, Normalized to January, 1991. The blue curve is the result of approximation method; the red curve is the result of simulation method. The vertical axis is the carbon uptake [PgC], the horizontal axis is the year.**

The anthropogenic carbon uptake by approximation method has increased by  $0.74[\text{PgC}/\text{year}]$ , and the anthropogenic carbon uptake by simulation method increased by  $0.60[\text{PgC}/\text{year}]$ . It is noted that, assuming the simulation method as the true value, the approximation method overestimates the anthropogenic carbon uptake about  $2.86[\text{PgC}]$  in the two decades. And a seasonal variation in the approximation method, which is assumed due to formula bias.

## 5.2. Spatial Difference in Carbon Uptake between the Simulation Method and the Approximation Method

In Section 5.1, the difference in carbon uptake between the simulation method and the approximation method on a global scale has been discussed. Regional anthropogenic carbon uptake calculated by both methods could vary from the global scale results because the effect of climate change to ocean may be different in each basin. In order to understand how the results of the approximation method differ from those of the simulation method, in different basins, I calculated anthropogenic carbon uptake in each basin separately. Ocean has been divided into the basins below (Table 5.1).

**Table 5.1 Definition of the Basins in this study**

Ocean/Basin	Latitude	Longitude	Xdef	Ydef
North Pacific(NP)	120°E – 180° – 75°W	65°N – 0°	121-285	76-140
South Pacific(SP)	150°E – 180 – 75°W	0° – 55°S	151-285	21-75
North Atlantic(NA)	75°W – 0° – 20°E	65°N – 0°	296-360,1-20	76-140
South Atlantic(SA)	75°W – 0° – 20°E	0° – 55°S	296-360,1-20	21-75
Southern Ocean(SO)	All	55°S – 75°S	1-360	1-20
Indian Ocean(IO)	20°E – 110°E	30°N – 55°S	21-110	21-105

Hereby, Xdef and Ydef are the cell number of latitude and longitude in ESTOC output dataset, respectively.

The difference of DIC uptake results between two methods is calculated by subtracting the DIC uptake calculated by simulation method from the result of approximation method.

$$\text{Difference} = C_{DO}^{ANT} - C_{MO}^{ANT} \quad (5-6)$$

Since the results of both methods are normalized to the January, 1991, the difference normalized to January, 1991 is calculated, so as to reveal the temporal and spatial variation of the approximation method bias.

$$n\text{Difference} = nC_{DO}^{ANT,t} - nC_{MO}^{ANT,t} \quad (5-7)$$

By, using the formula discussed, the distribution of anthropogenic carbon difference between approximation method and simulation method are drawn into contour map in basin scale.

The increase of anthropogenic carbon uptake in all basins is proper to be applied

with linear approximation. I calculated distribution by removing the linear slope of the anthropogenic carbon uptake increase, in the basin, respectively, so that it is easy to capture the spatial variation of the resulting difference between two methods. These distributions can be checked from Figure. A-2 to Figure. A-7 in the Appendix. On the other hand, the decadal spatial pattern in a certain basin was calculated by taking average of monthly mean distribution in 20 years (January, 1991 – December, 2010). Averaged distributions of difference are revealed and discussed in the several sections below.

### 5.2.1. Temporal and Spatial Difference between Methods in the North Pacific

Figure 5.2 shows anthropogenic carbon uptake in the North Pacific calculated by the simulation method and approximation method.

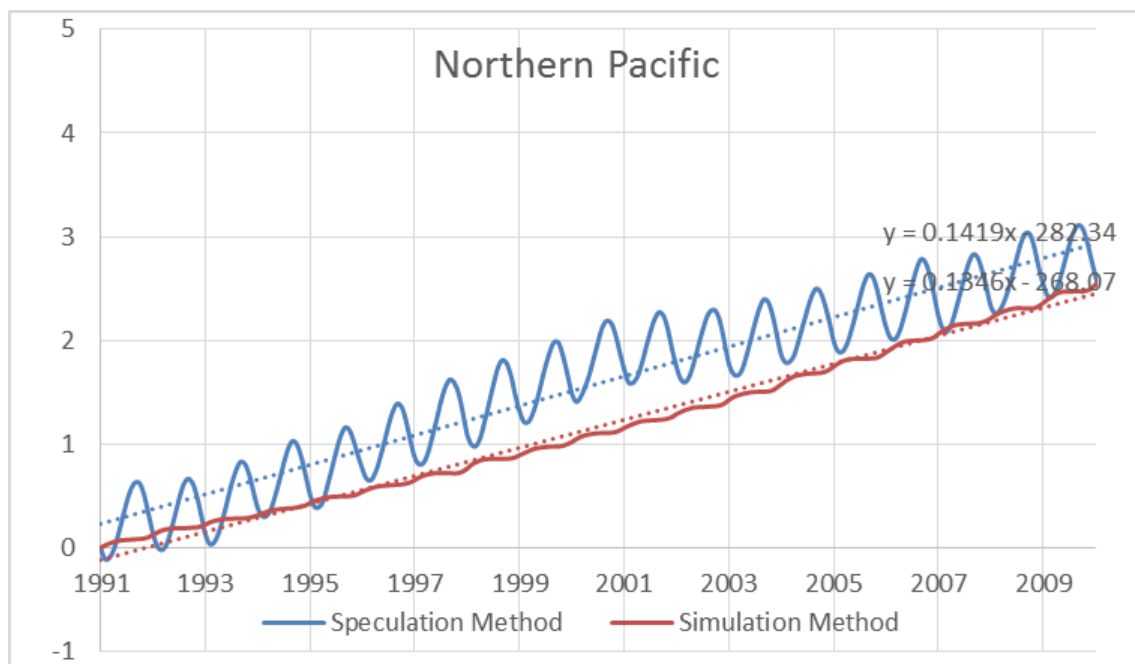


**Figure 5.2 Anthropogenic Carbon Uptake (0-200m) in the North Pacific. The vertical axis is the year, the horizontal axis is the carbon uptake [PgC]. The red curve is the simulation method result, and the blue curve is the result of approximation method.**

Anthropogenic carbon uptake rates by the simulation method is 0.135 [PgC/yr] and 0.142 [PgC/yr] by the approximation method. There is a 0.007 [PgC/yr] difference between the two methods. The approximation method overestimates by about 5.4% comparing to the simulation method.

Figure. 5.3 shows the difference distribution pattern of anthropogenic carbons between approximation method and simulation method in the North Pacific.

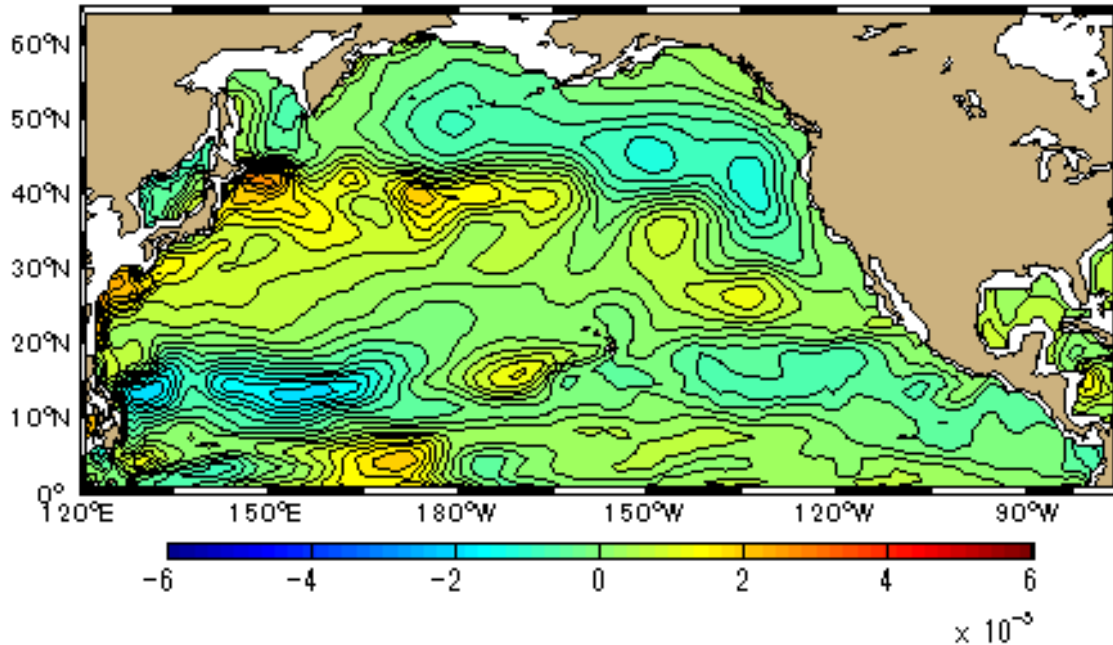
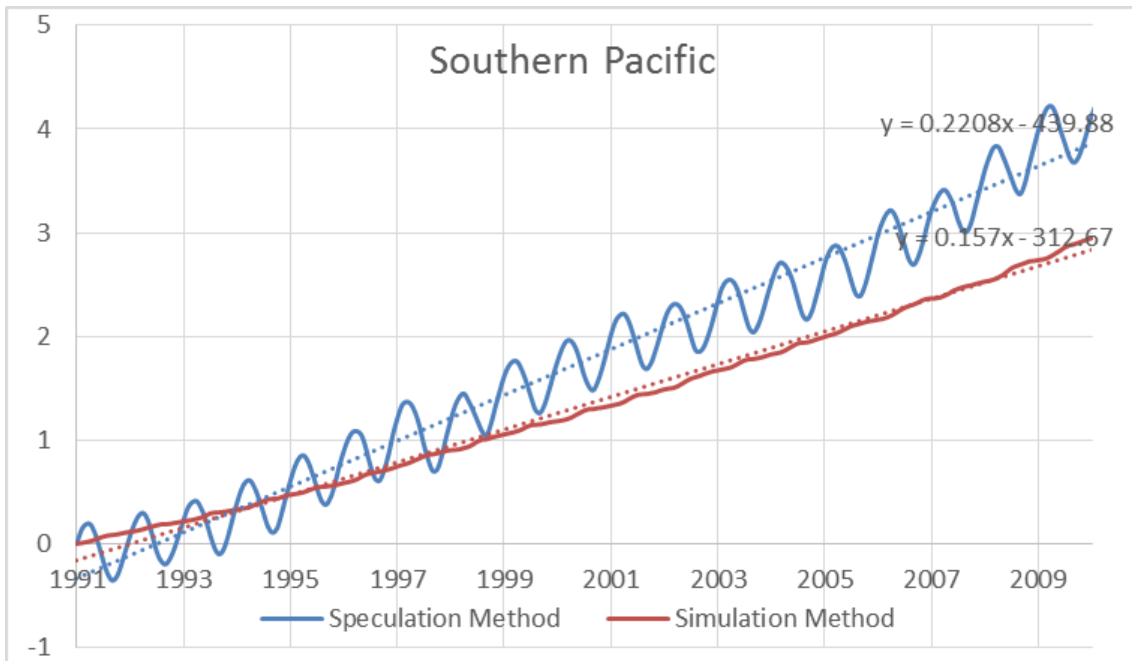


**Figure 5.3 20-year Averaged Difference Distribution of Anthropogenic Carbon Uptake (0-200m) in the North Pacific. [PgC]**

Figure 5.3 shows that the western part of the North Pacific from Japanese coast to the middle of the North Pacific around 40°N is overestimated more than other regions in the basin. On the other hand, the rest regions, especially the east part of the North Pacific from Berling Strait to the North America is an underestimation zone by the approximation method comparing to the simulation method. There is an apparent front along ca. 40°N in the west of the North Pacific as well, combining the other small-difference region in the tropical ocean from Philippines to 165°W, along 14°N, it is speculated that the contrast of high absolute difference regions is possibly controlled by the gyre, western boundary current and other local current in the North Pacific.

#### 5.2.2. Temporal and Spatial Difference between Methods in the South Pacific

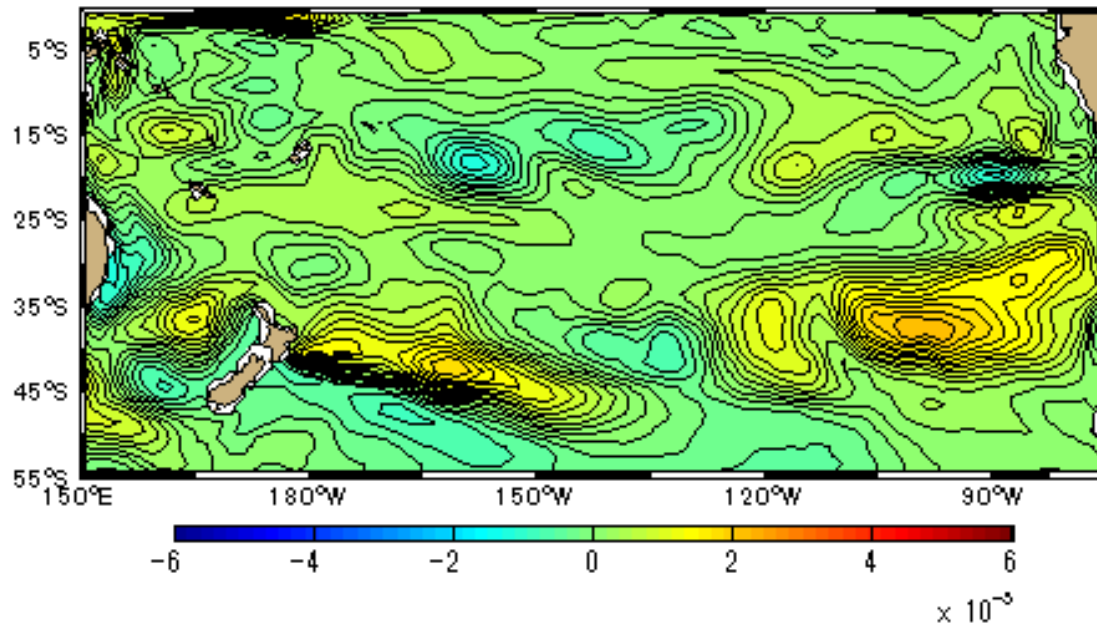
Figure 5.4 shows anthropogenic carbon uptake in the North Pacific calculated by the simulation method and approximation method.



**Figure 5.4 Anthropogenic Carbon Uptake (0-200m) in the South Pacific.**The vertical axis is the year, the horizontal axis is the carbon uptake [PgC]. The red curve is the simulation method result, and the blue curve is the result of approximation method.

Anthropogenic carbon uptake rates by the simulation method are 0.157 [PgC/yr] and 0.221 [PgC/yr] by the approximation method. There is a 0.064 [PgC/yr] difference between two methods. The approximation method overestimates by about 40.6% comparing to the simulation method. Comparing to the North Pacific, the overestimation is larger.

Figure. 5.5 shows the difference distribution pattern of anthropogenic carbons between approximation method and simulation method in the North Pacific.



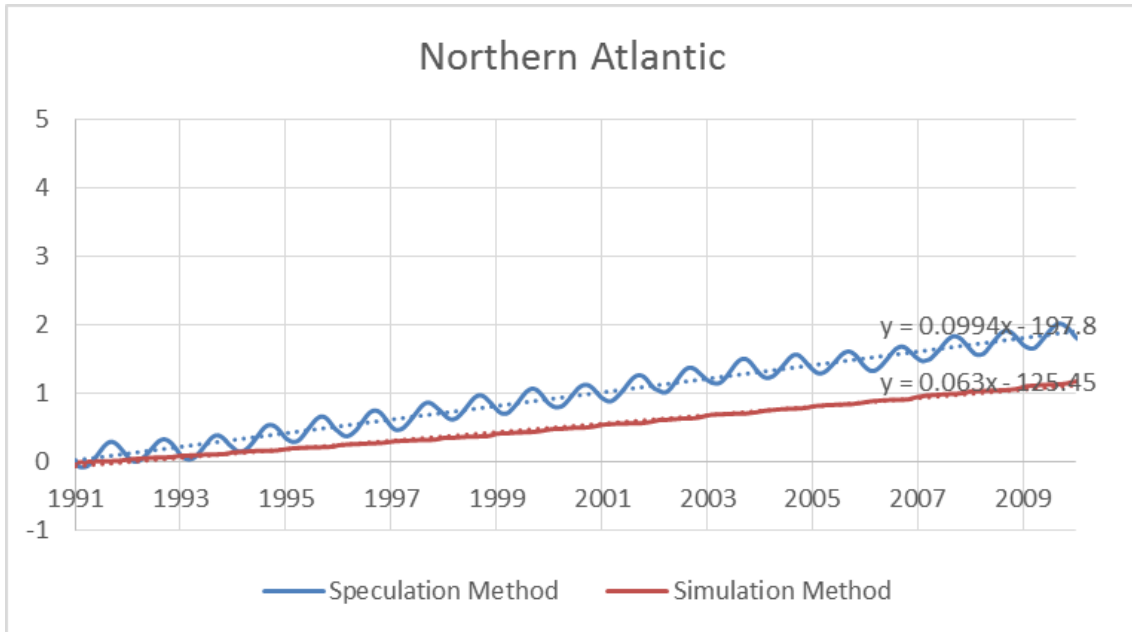
**Figure 5.5 20-year Averaged Difference Distribution of Anthropogenic Carbon Uptake (0-200m) in the South Pacific. [PgC]**

Figure 5.5 shows that there are two regions that the approximation method overestimated the anthropogenic carbon with a large bias. One is the North-east regions of Wellington, New Zealand and it appears radial to the east. The other region is near to the west coast of the South America. The extremal difference appears at (110°W, 40°S).

### 5.2.3. Temporal and Spatial Difference between Methods in the North Atlantic

Figure 5.6 shows anthropogenic carbon uptake in the North Atlantic calculated by the simulation method and approximation method.





**Figure 5.6 Anthropogenic Carbon Uptake (0-200m) in the South Pacific. The vertical axis is the year, the horizontal axis is the carbon uptake [PgC]. The red curve is the simulation method result, and the blue curve is the result of approximation method.**

Anthropogenic carbon uptake rates by the simulation method is 0.063 [PgC/yr] and 0.099 [PgC/yr] by the approximation method. There is a 0.063 [PgC/yr] difference between two methods. The approximation method overestimates by about 57.1% comparing to the simulation method. It is the region that the approximation method overestimates the most positive difference portion to the simulation method.

Figure. 5.7 shows the difference distribution pattern of anthropogenic carbons between approximation method and simulation method in the North Atlantic.

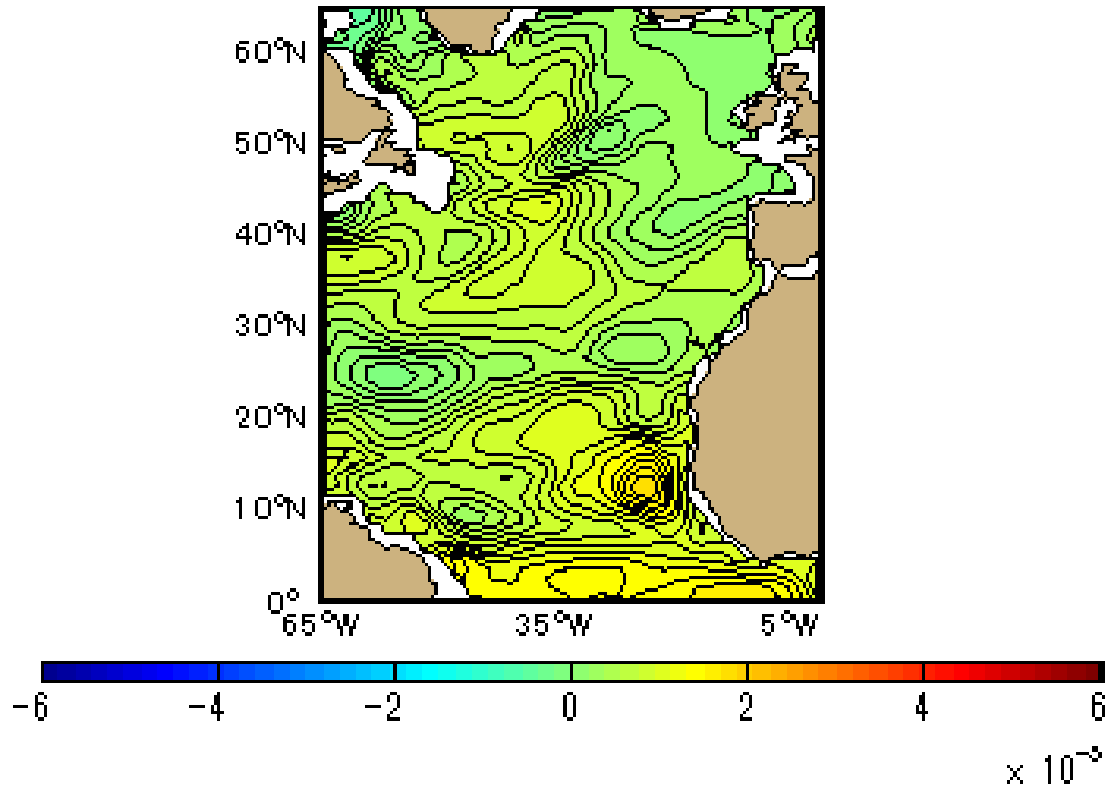


**Figure 5.7 20-year Averaged Difference Distribution of Anthropogenic Carbon Uptake (0-200m) in the North Atlantic. [PgC]**

There is no apparent negative anthropogenic carbon difference zone between two methods in the North Atlantic. The difference is higher in the tropical ocean, than the water in the subarctic ocean.

#### 5.2.4. Temporal and Spatial Difference between Methods in the South Atlantic

Figure 5.8 shows anthropogenic carbon uptake in the South Atlantic calculated by the simulation method and approximation method.

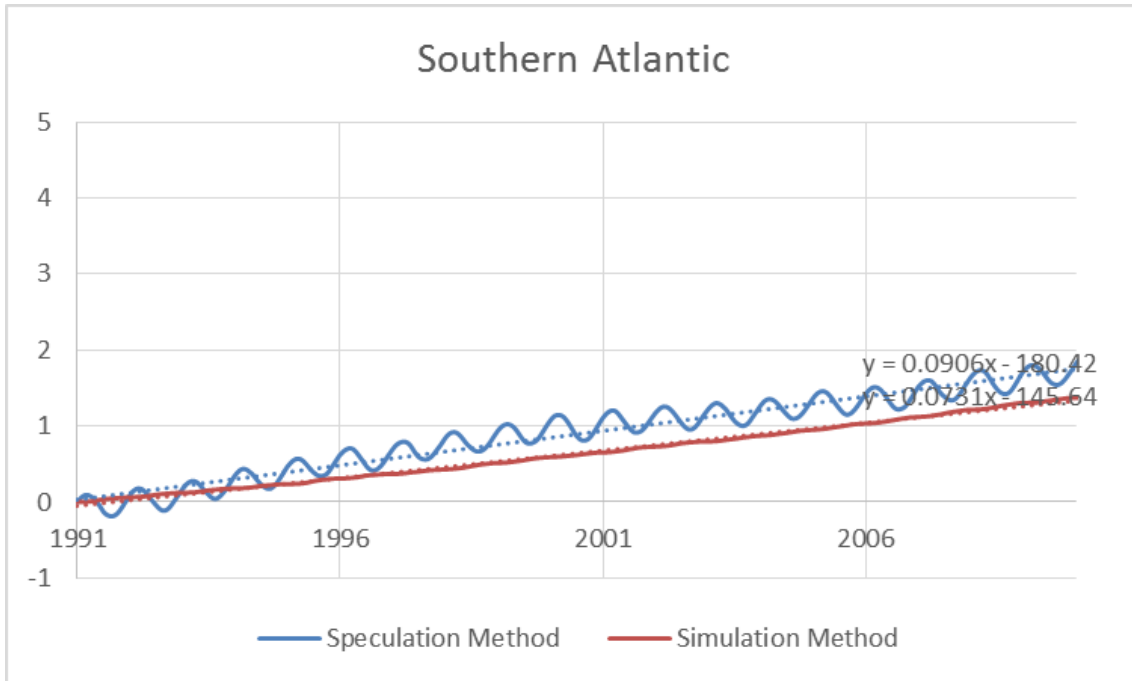


**Figure 5.8 Anthropogenic Carbon Uptake (0-200m) in the South Atlantic.**The vertical axis is the year, the horizontal axis is the carbon uptake [PgC]. The red curve is the simulation method result, and the blue curve is the result of approximation method.

Anthropogenic carbon uptake rates by the simulation method is 0.073 [PgC/yr] and 0.091 [PgC/yr] by the approximation method. There is a 0.018 [PgC/yr] difference between two methods. The approximation method overestimates by about 24.0% comparing to the simulation method.

Figure. 5.9 shows the difference distribution pattern of anthropogenic carbons between approximation method and simulation method in the South Atlantic.

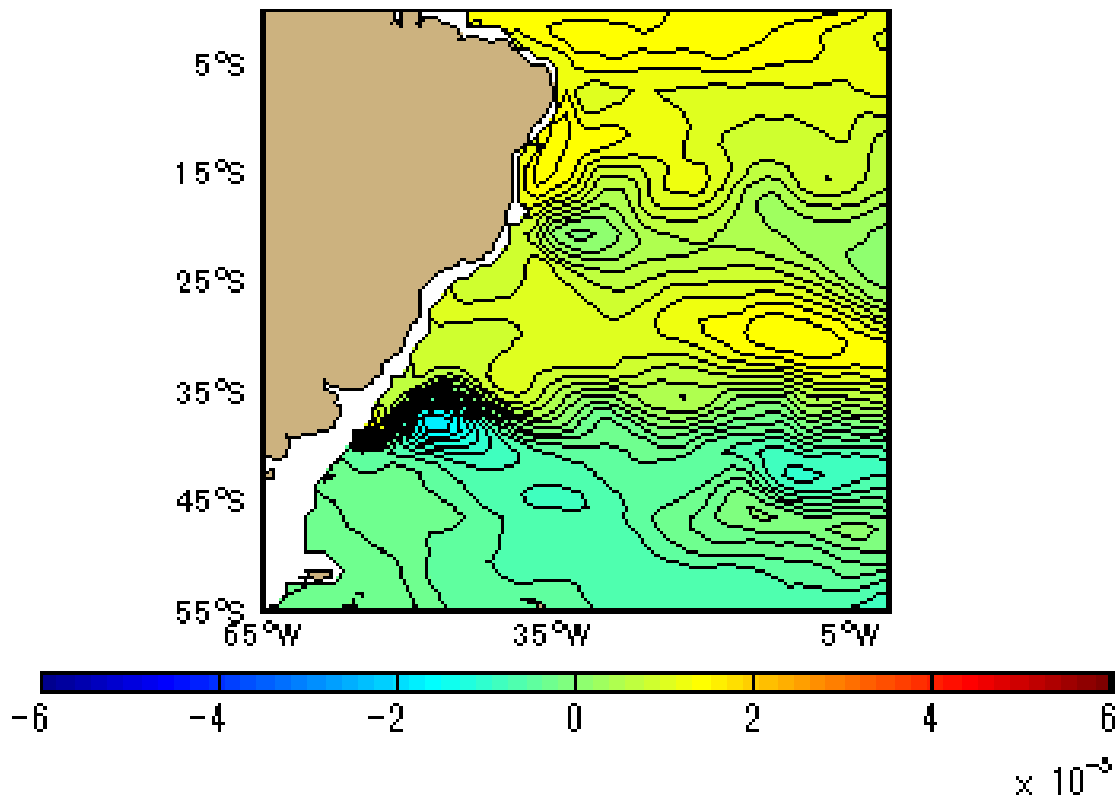


**Figure 5.9 20-year Averaged Difference Distribution of Anthropogenic Carbon Uptake (0-200m) in the South Atlantic. [PgC]**

There is an apparent border along 40°S, the north of the border is the region that estimation of approximation method is apparently larger than the estimation that approximation method makes in the south of the border. It is highly possible that this border is the Southern Ocean Front. Therefore the distribution of the difference of anthropogenic carbon increase combines both the characteristic of the Southern Ocean and the Atlantic.

#### 5.2.5. Temporal and Spatial Difference between Methods in the Southern Ocean

Figure 5.10 shows anthropogenic carbon uptake in the Southern Ocean calculated by the simulation method and approximation method.

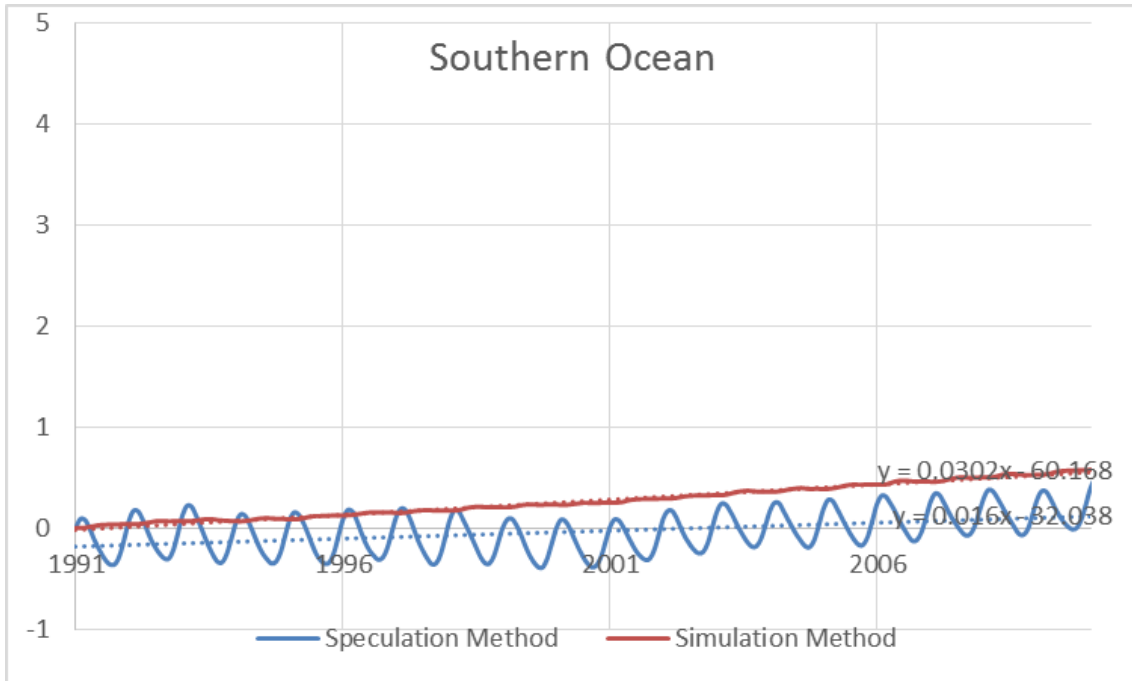


**Figure 5.10 Anthropogenic Carbon Uptake (0-200m) in the Southern Ocean.**The vertical axis is the year, the horizontal axis is the carbon uptake [PgC]. The red curve is the simulation method result, and the blue curve is the result of approximation method.

Anthropogenic carbon uptake rates by the simulation method is 0.016 [PgC/yr] and 0.030 [PgC/yr] by the approximation method. There is a -0.014 [PgC/yr] difference between the two methods. This is the only basin that the approximation method underestimates the anthropogenic carbon increase.

Figure. 5.11 shows the difference distribution pattern of anthropogenic carbons between approximation method and simulation method in the Southern Ocean.

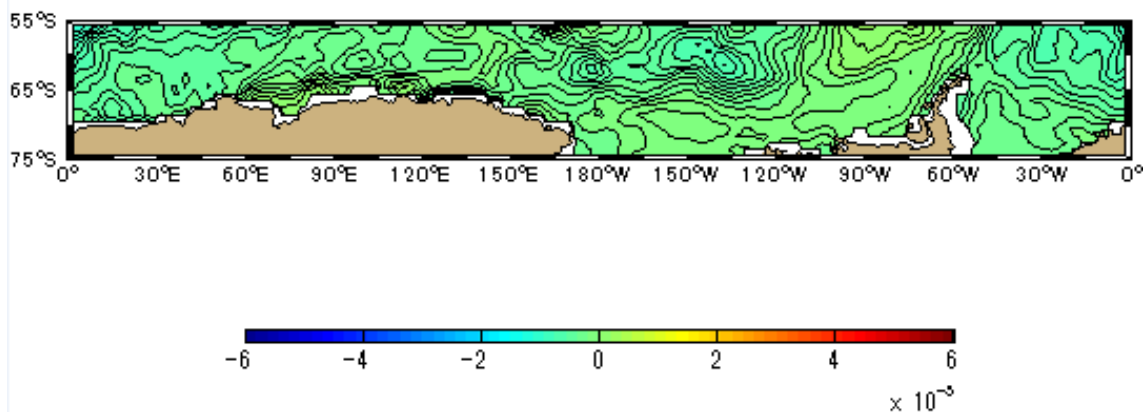


**Figure 5.11 20-year Averaged Difference Distribution of Anthropogenic Carbon Uptake**

### (0-200m) in the Southern Ocean.[PgC]

Difference between approximation method and simulation method in most of the Southern Ocean is close to zero. This differs from all the other basins. A few regions are slightly below zero and changes quickly without an apparent pattern. It fits the results in the region south of 40°S, South Atlantic.

#### 5.2.6. Temporal and Spatial Difference between Methods in the Indian Ocean

Figure 5.12 shows anthropogenic carbon uptake in the Indian Ocean calculated by the simulation method and approximation method.

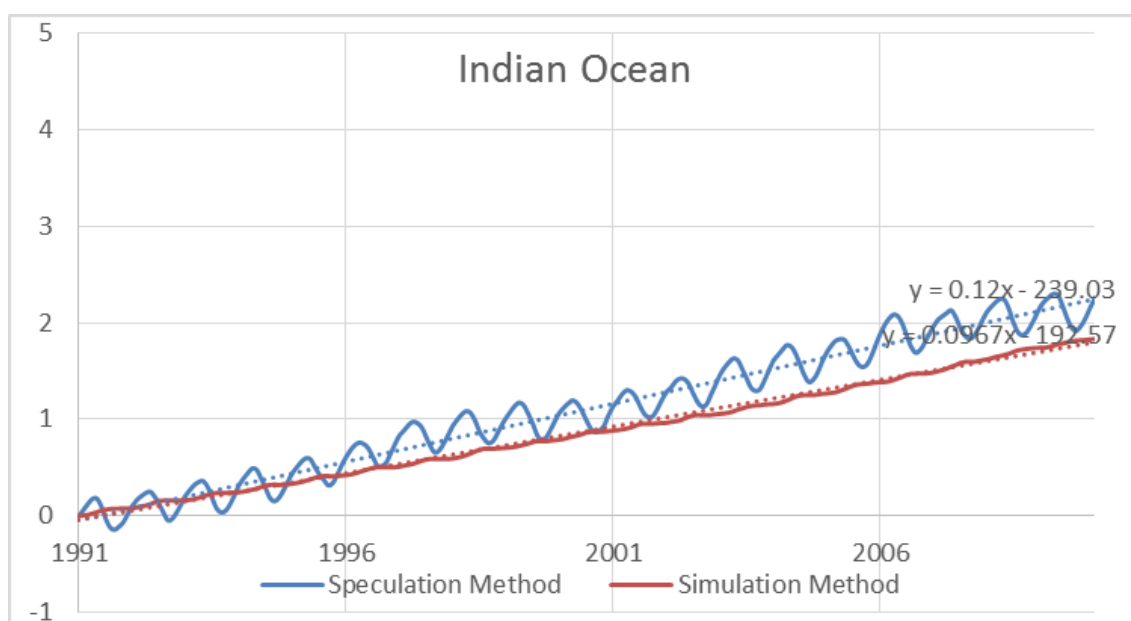


**Figure 5.12 Anthropogenic Carbon Uptake (0-200m) in the Indian Ocean. The vertical axis is the year, the horizontal axis is the carbon uptake [PgC]. The red curve is the simulation method result, and the blue curve is the result of approximation method.**

Anthropogenic carbon uptake rates by the simulation method is 0.097 [PgC/yr] and 0.12 [PgC/yr] by the approximation method. There is a 0.023 [PgC/yr] difference between the two methods. The approximation method overestimates by about 24.1% comparing to the simulation method.

Figure. 5.9 shows the difference distribution pattern of anthropogenic carbons between approximation method and simulation method in the South Atlantic.

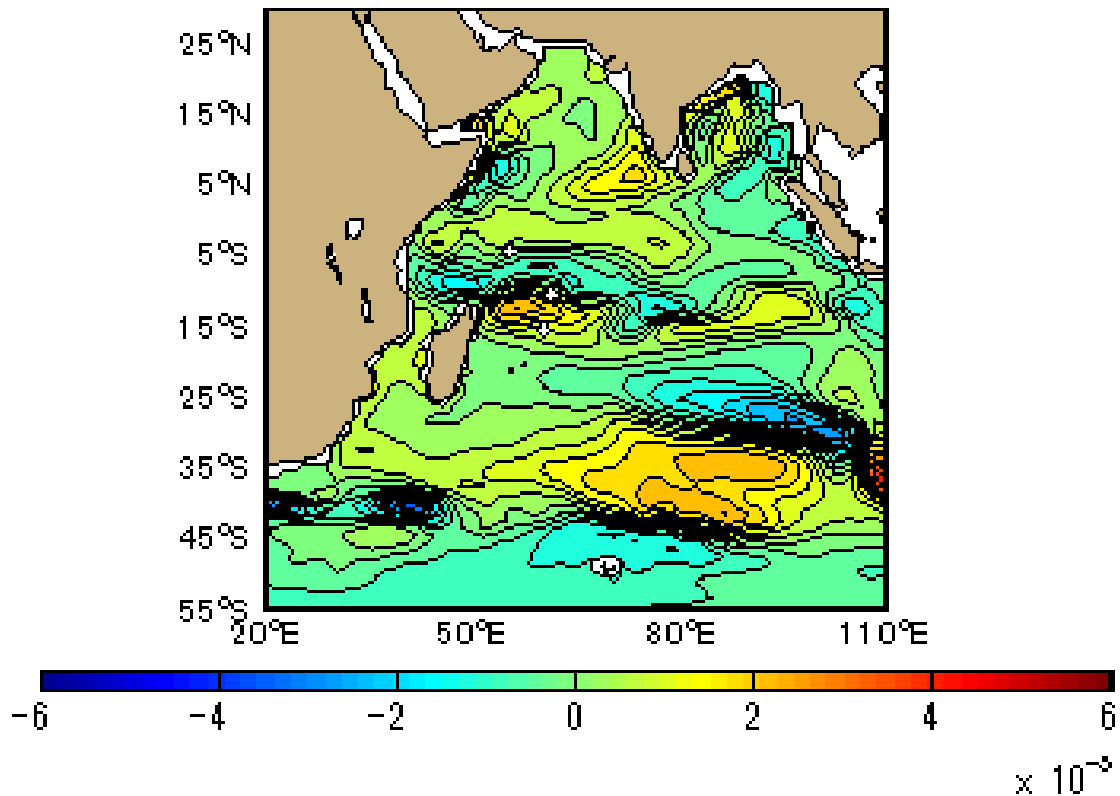


**Figure 5.13 20-year Averaged Difference Distribution of Anthropogenic Carbon Uptake (0-200m) in the Indian Ocean. [PgC]**

This is another region that contrasts are apparent, other than the North Pacific. There is a pattern that both positive difference and negative difference regions appear in pair. One pair is in the region of 20°S – 45°S, 65°E – 100°E. In this region the positive and negative difference region are divided by 30°S, and the positive difference region only appears in the southern part of the region and the negative difference region only appears in the northern part of the region. The other pair of the contrast is shown between 5°S – 15°S, 40°E – 80°E, which is the north-eastern ocean of the Sri Lanka. The positive difference region also appears in the southern part of this pair. The third pair of difference pattern in the Indian Ocean is in the Bay of Bengal. The positive difference region appears at the western area of the bay. The pattern in the Indian Ocean is assumed to be concerned with the complex current system which probably contains the West Australia Current, South Equatorial Current, Equatorial Counter Current and Monsoon Drift. The region that the south of the 45°S, appears to be the same as the pattern of the Southern Ocean Front.

From the results of Indian Ocean (Figure 5.12 & Figure 5.13) and the North Pacific (Figure 5.2 & Figure 5. 3), I speculated that the uncertainty of the approximation method is strongly controlled by the current in such basins.



## 6. Conclusion

### 6.1. CO<sub>2</sub> Gas Exchange in the North Pacific

According to Figure 3.1 differences in DIC concentration between Model 1 and Model 3 in the tropical Pacific and the South Pacific is relatively large, which indicate importance of biological process in the CO<sub>2</sub> uptake to the ocean. In the North Pacific, the difference between Model 1 and Model 3 is small. To investigate the reason, the horizontal distribution of CO<sub>2</sub> was calculated as Figure 3.3 for Model 1 and Figure 3.7 for Model 3.

In Model 1, shown in Figure 3.3, there is a strong east-west contrast in CO<sub>2</sub> gas exchange around 40°N in the North Pacific, and so, the CO<sub>2</sub> exchange is positive in the west and negative in the east. Figure 3.2 shows, DIC concentration in the east and west of the North Pacific as shown in this figure, the values of DIC in the west and east have negative correlation. So the overall DIC concentration in the North Pacific comes to constant after the late 1990s.

Such east-west contrast can be found in Model 3 (Figure 3.2), however, it is weaker than that obtained from Model 1, and most of all, the CO<sub>2</sub> exchange is negative in all of the North Pacific, although it is positive in Model 1 (Figure 3.2). This also suggests that biological process is important for carbon cycle, in the ESTOC.

### 6.2. Biogeochemical System Contribution to the Carbon Uptake in the ESTOC data

The biogeochemical system contribution to the carbon uptake and anthropogenic carbon uptake, in the decades from 1991 to 2010, was calculated. The contribution to the total carbon uptake is 0.25[PgC/yr] and is 41.5% to the total DIC; and the contribution to the anthropogenic carbon is 0.06[PgC/yr] and is the 11.5% to the dissolved anthropogenic carbon in the global scale shallow water (0-200m)

The anomalies of carbon uptake occurred in the year of 1998 and other years, such as 2008, were found in the ESTOC, and suggested to be associated with El Niño and La Niña phenomena. It is well known that the carbon uptake is supposed to decrease in the year of El Niño and increase in the year of La Niña, because the SST variation in such climate phenomena changes and affects the solubility pump. However, it is noted that in the ESTOC, the biological contribution to the carbon uptake varied in the El Niño and La Niña as well, and the carbon uptake, contributed by biological process during the El Niño phenomenon in 1998, occupied 39.9%, which is nearly the same proportion in the regular years. As shown in Figure 4.4, that the SST in the ESTOC model reproduced the SST variation relatively well, and it is able to reproduce some of the characteristic of El

Niño phenomena. By discussing the distribution of the biological contribution to the carbon uptake in the shallow water, it is noted that the change responding to the El Niño phenomenon is caused by the reduction in nutrients associated with suppressed upwelling..

### 6.3. Difference between Methods for the Calculation of the Anthropogenic Carbon Increase

According to the properties and the stoichiometric variables the ESTOC model contains, the anthropogenic carbon increase can be calculated by the Model 1 and the Model 2 which is the model under the assumption that atmospheric CO<sub>2</sub> does not increase constantly. Anthropogenic carbon increase is also calculated by another method, which is called approximation method, using the ESTOC data. The difference between the two approaches using the same input data, indicates the bias that the approximation method introduces. It appears that the approximation method overestimated anthropogenic carbon in the shallow water (0-200m) by 0.14[PgC/yr], in global scale. I also discussed the distribution of this difference in basin scale. In the North Pacific and Indian Ocean, the contrasts of the difference distribution are apparent and we speculate that the differences in such basins were affected by the gyre and local current. The overestimation of the approximation method appears to exist in the entire Atlantic Ocean, the slightly larger in the tropical latitudes than other regions. The Southern Ocean is the only basin where the approximation method underestimated the anthropogenic carbon and estimated the anthropogenic carbon better than other basins excluding the large seasonal variation.

## REFERENCES

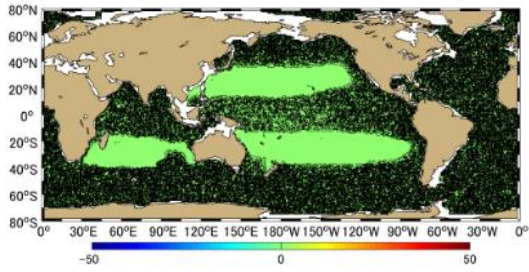
- Brewer, P, Direct Observation of oceanic CO<sub>2</sub> increase, *Geophys. Res. Lett.*, *5*(1978)997-1000
- Broecker, W., T. Takahashi, and T. Peng, Reconstruction of past atmospheric CO<sub>2</sub> from the chemistry of the contemporary ocean: An evaluation, *Tech. Rep. TRO 20*, U.S. Dep. Of Energy, Washinton, D.C. 1985a
- Chen, C and F. J. Millero (1979), Gradual increase of oceanic CO<sub>2</sub>, *Nature*, **277**,205-206.
- Doi, T, S. Osafune, N. Sugiura (2015), Multi-decadal change in the dissolved inorganic carbon in a long-term ocean state estimation, *J. Adv. Model Earth SY.* **7**, 1885-1900.
- Earth System Research Laboratory (ESRL),  
<https://www.esrl.noaa.gov/psd/data/gridded/data.ncep.reanalysis.pressure.html>
- Estimated State of global Ocean for Climate reasearch (ESTOC), <http://www.godac.jamstec.go.jp/estoc/e/top/>
- Friis, K., A. Kortzinger, J. Patsch, and D. Wallace (2005), On the temporal increase of anthropogenic CO<sub>2</sub> in the subpolar North Atlantic, *Deep Sea Res. I*, **52**,681-698.
- Garcia, N., J. L. Sarmiento, and T. F. Stocker (1996), An improved method for detecting anthropogenic CO<sub>2</sub> in the oceans, *Global Biogeochemical Cycles*, **10**,809-837.
- Ho, D., M. Smith, P. Schlosser et al. (2006), Measurements of air-sea gas exchange at high wind speeds in the Southern Ocean: Implications for global parameterizations, *Geophys. Res. Lett.*, **33**, L16611.
- Intergovernmental Panel on Climate Change, Fifth Assessment Report  
Japan Meteorological Agency, <http://www.jma.go.jp/jma/index.html>
- Kalnay et al.(1996), The NCEP/NCAR 40-year reanalysis project, *Bull. Amer. Meteor. Soc.*, **77**, 437-470.
- Kouketsu, S. et al.(2011), Deep Ocean heat content changes estimated from observation and reanalysis product and their influence on sea level change, *J. Geophys. Res.*, **116**(C3).
- Masuda, S., T. Awaji, N. Sugiura, et al. Improved estimates of the dynamical state of the North Pacific Ocean from a 4 dimensional variational data assimilation, *Geophys. Res. Letts.* **30**(16), 1868.
- Matear, R. J., A. Hirst, and B. McNeil (2000), Changes in dissolved oxygen in the Southern Ocean with climate change, *Geochem. Geophys. Geosyst. I.*
- Murata, A., Y. Kumamoto, S. Watanabe et al. (2007), Decadal increases of anthropogenic CO<sub>2</sub> in the South Pacific subtropical ocean and 32°S, *Geophys. Res. Lett.* , **42**, 4903-4911.
- Osafune, S., S. Masuda, N. Sugiura et al. (2015), Evaluation of the applicability of the Estimated State of the Global Ocean for Climate Research (ESTOC) dataset, *Geophys. Res. Lett.*, **42**, 4903-4911.
- Pacanowski, R. and S. Griffies (1999), The MOM 3 manual, report, 680 pp, Geophys. Fluid Dyn. Lab., Princeton, N. J.
- Sabine, C., R. Feely, F. Millero et al. (2008), Decadal changes in Pacific carbon, *J.*

- Geophys. Res.* **113**, C07021.
- Shiller, A. (1981), Calculating the oceanic CO<sub>2</sub> increase: A need for caution, *J. Geophys. Res.*, **86**(C11), 11083-11088
- Takahashi, T., S. Sutherland, C. Sweeney, et al. (2002), Global sea-air CO<sub>2</sub> flux based on climatological surface ocean pCO<sub>2</sub>, and seasonal biological and temperature effects, *Deep-Sea Res. II* **49**(2002)1601-1622
- Volk, T., and M. Hoffert (1985), Ocean carbon pumps: Analysis of relative strengths and efficiencies in ocean-driven atmospheric CO<sub>2</sub> changes, in *The Carbon Cycle and Atmospheric CO<sub>2</sub>: Natural Variations Archean to Present*, Geophys. Monogr. Ser., **32**, edited by E. Sundquist and W. Broecker, pp. 99-110, AGU, Washinton D.C.
- Wallace, D. (1995), monitoring global ocean carbon inventories, OOSDP Background Rep., 5, Ocean Obs. Syst. Dev. Panel, Texas A&M Univ., College Station, Texas.
- Weiss, R. (1974), Carbon dioxide in water and seawater: The solubility of non-ideal gas, *Mar. Chem.*, **2**, 203-215.

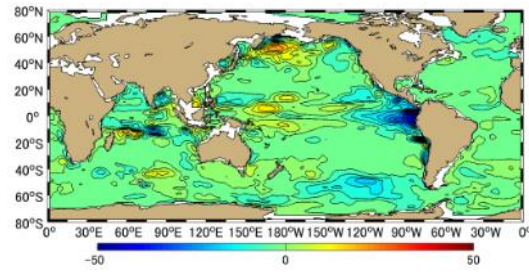
## **ACKNOWLEDGEMENT**

By the moment that I finish this thesis, memories of these two short years have been recalled. First of all, I am really grateful that Professor Kawano accepted me as his student in the first place, and enlighten me with his knowledge and encourage me on the research with his foresight. I also appreciate that Professor Sato gives me advice and help me sort my logic through, in every weekly meeting. I am grateful to Professor Tabeta who help me considering my own study from different aspect. Hereby, I am thankful to Dr. T. Doi who helped me to start the research about ESTOC, from zero and keep in touch to help me solve the difficulties that I encountered. I also want to thank Assistant Professor Georgios Fytianos, who helped me check the thesis and outcome many times, and also help me dealing with the unexpected condition. I am also grateful to Assistant Professor H. Oyama, who help me and my fellow students in the Sato Lab. with the daily problems, and advised us from multiple aspects. I also want to say thank you to all the members in the laboratory who help and study together with me for last two years. At last, but not least, I am grateful to my parents, girlfriend and friends who support me without a word of complaint.

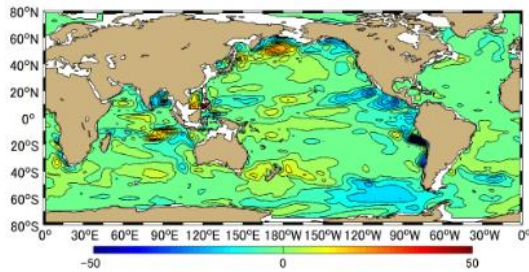
# Appendix



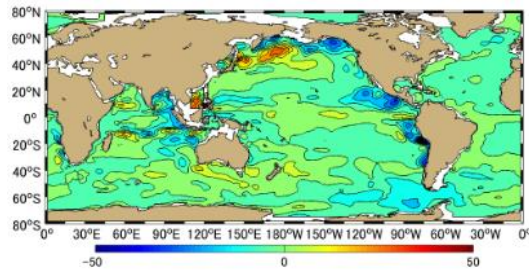
(a)



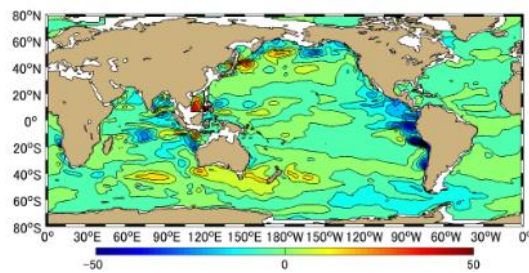
(b)



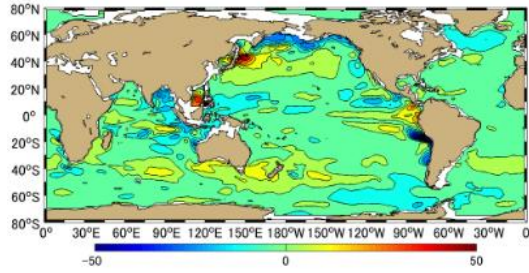
(c)



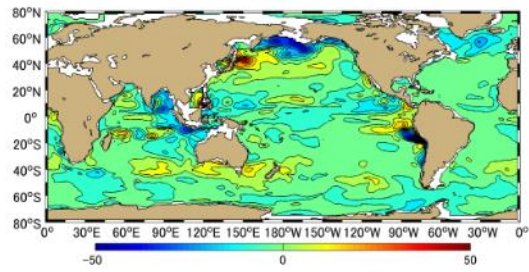
(d)



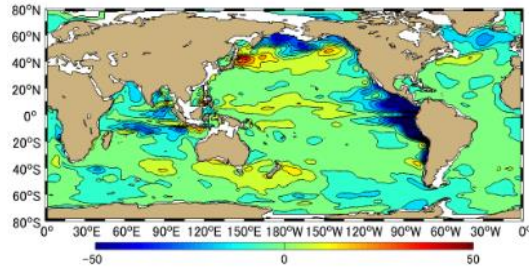
(e)



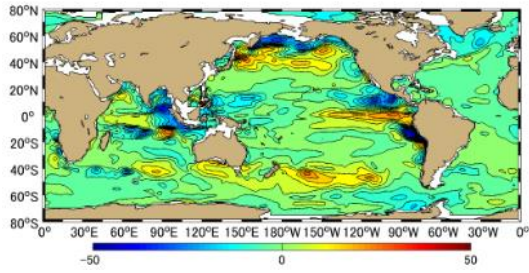
(f)



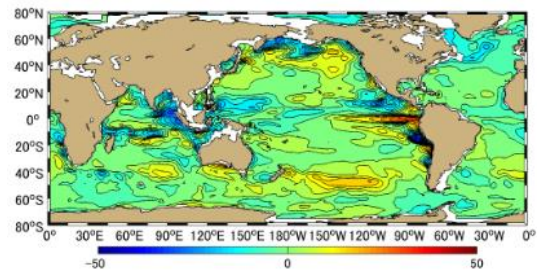
(g)



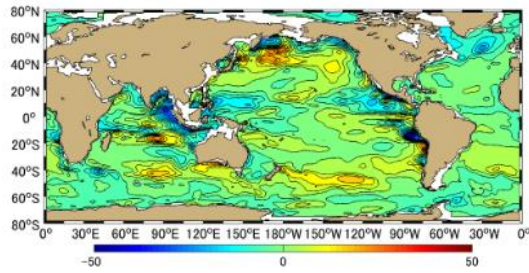
(h)



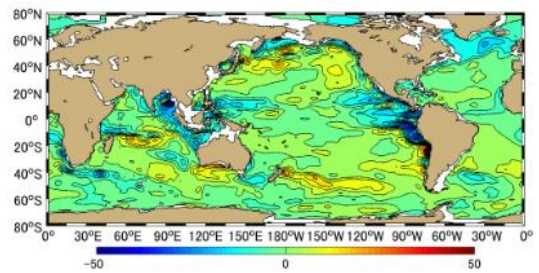
(i)



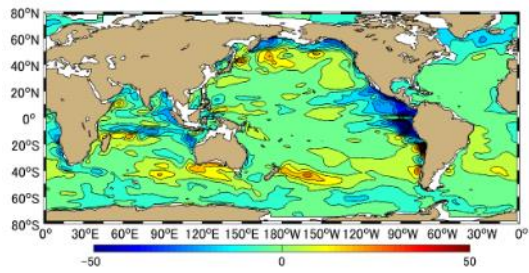
(j)



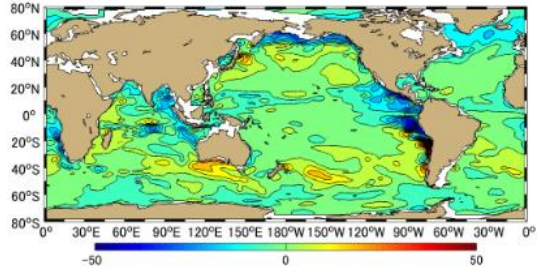
(k)



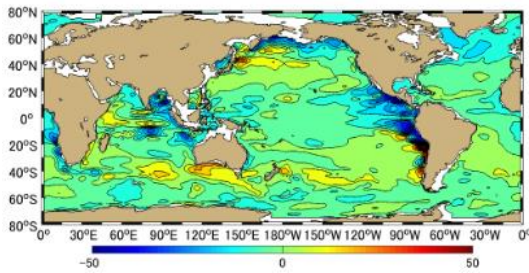
(l)



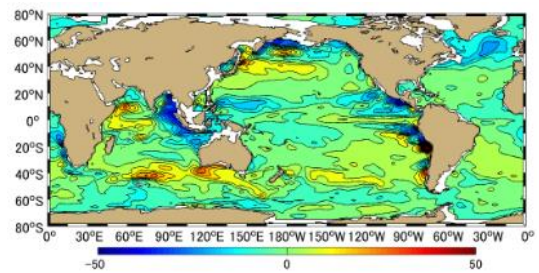
(m)



(n)



(o)



(p)

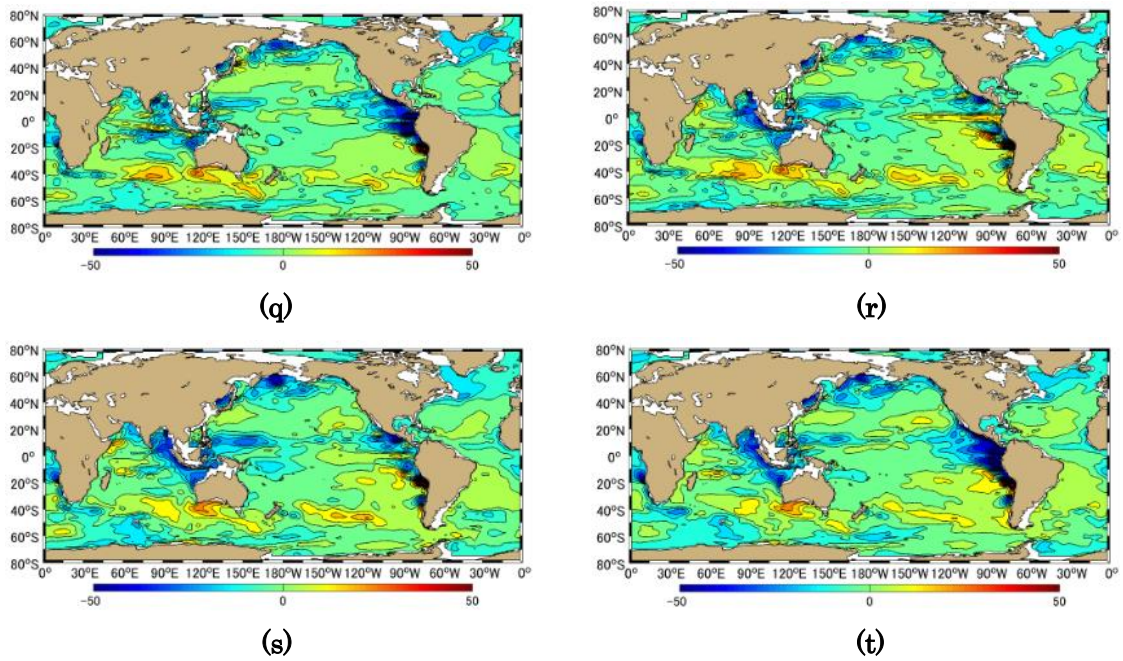
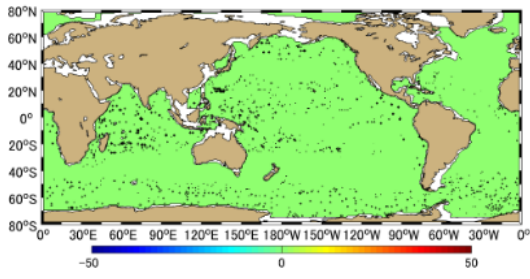
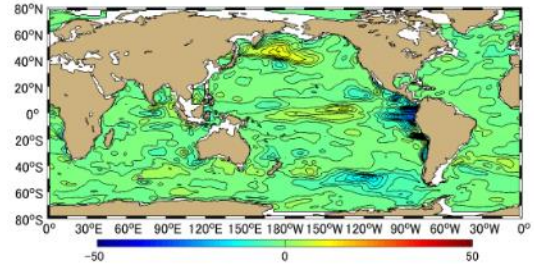


Figure.A-1 Winter Deviation (average of December of the former year, January, and February) of All Carbon Uptake in shallow sea water (Sea Surface-200m Depth) in 20years, (a)-(t) refers to 1991-2010. Based on the average of December 1990, January 1991 and February 1991. Slope of the carbon uptake increase has been removed.

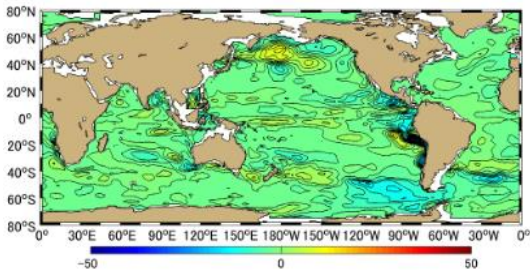




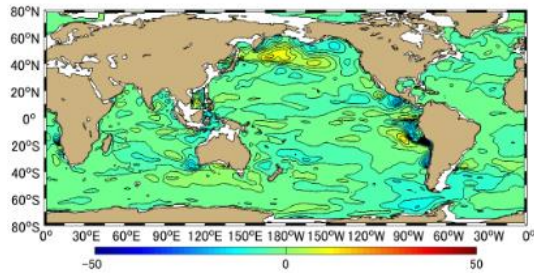
(a)



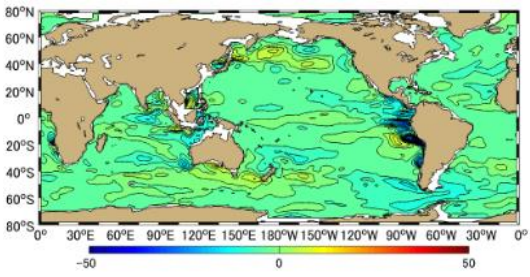
(b)



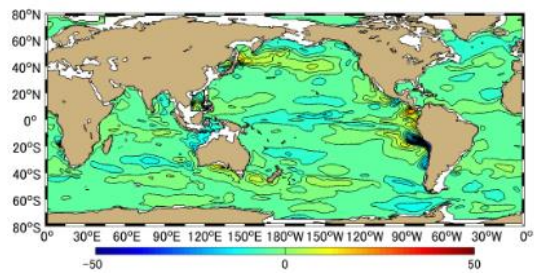
(c)



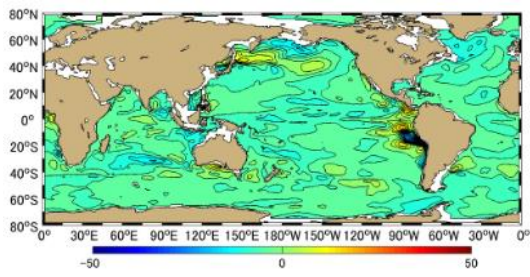
(d)



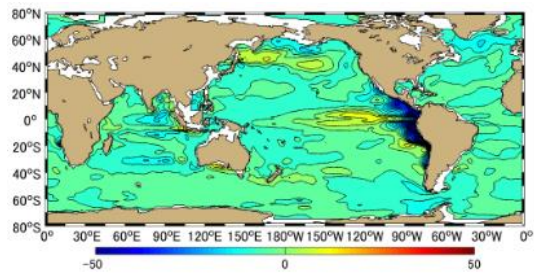
(e)



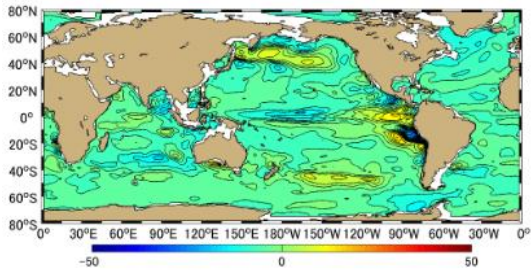
(f)



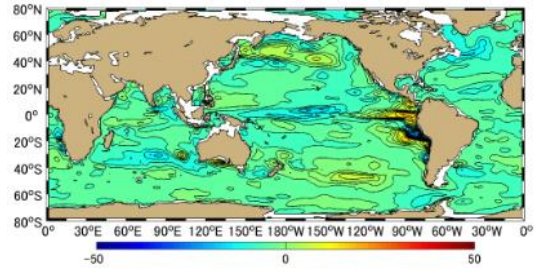
(g)



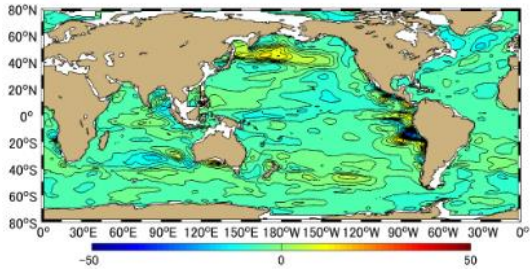
(h)



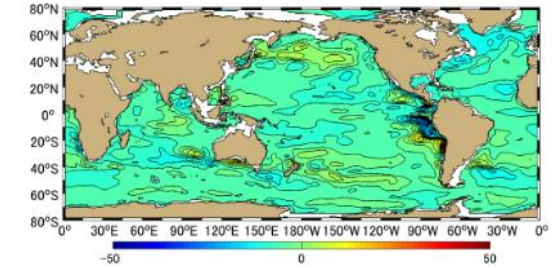
(i)



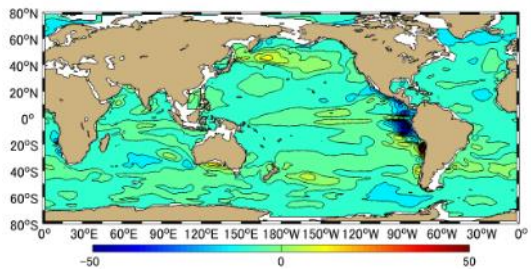
(j)



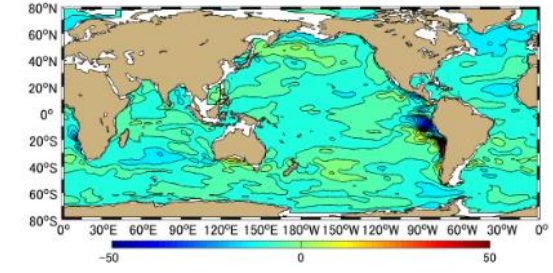
(k)



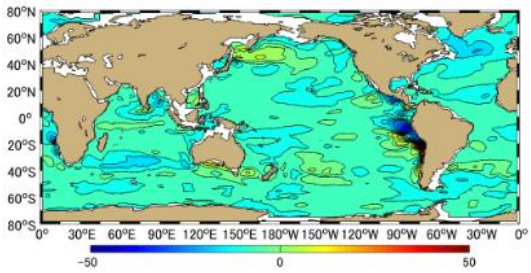
(l)



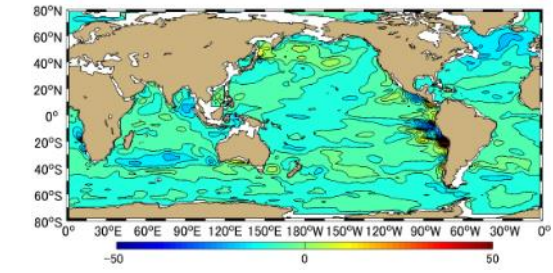
(m)



(n)



(o)



(p)

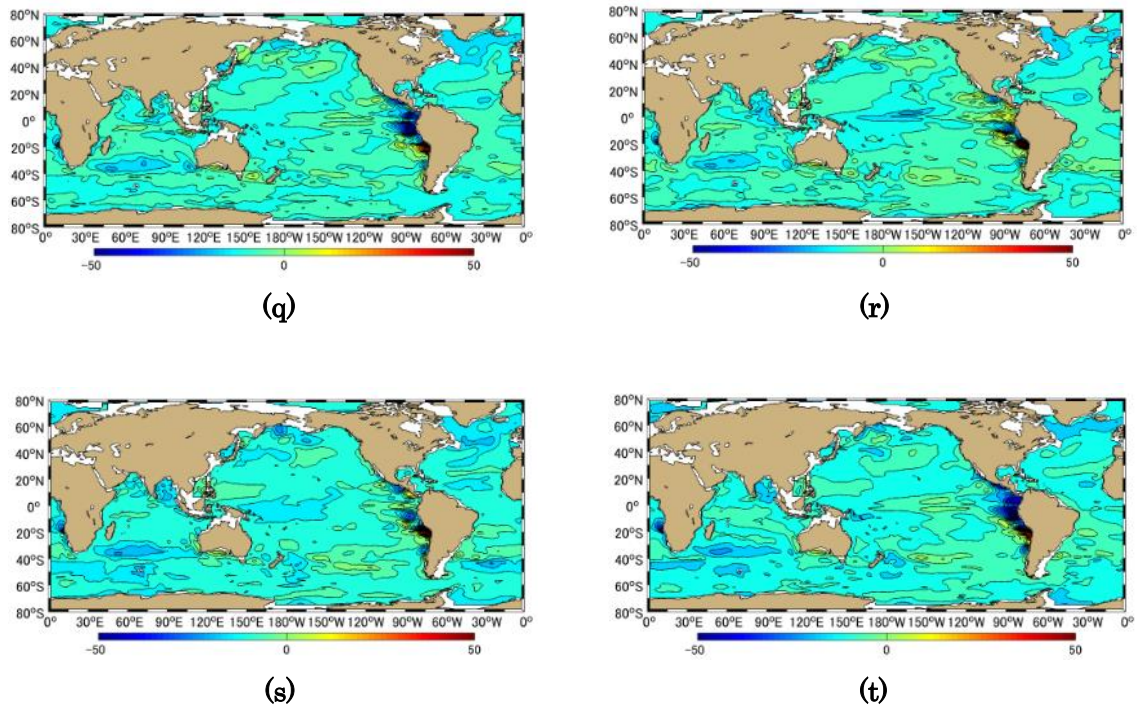
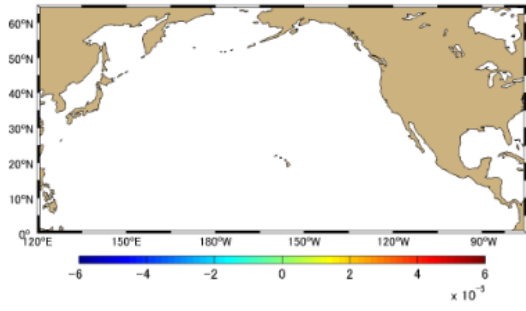
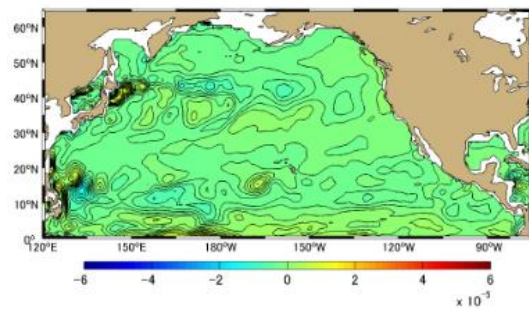


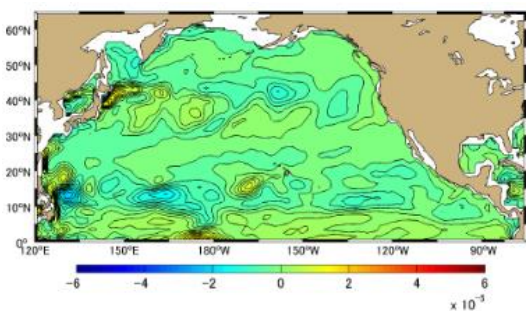
Figure.A-1 Winter Deviation (average of December of the former year, January, and February) of Biology System Contribution (Ba+Bn) in shallow sea water (Sea Surface-200m Depth) in 20years, (a)-(t) refers to 1991-2010. Based on the average of December 1990, January 1991 and February 1991. Slope of the carbon uptake increase has been removed.



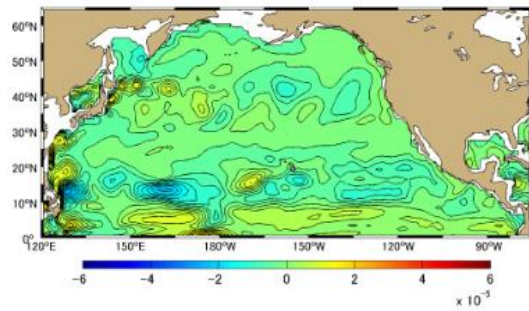
(a)



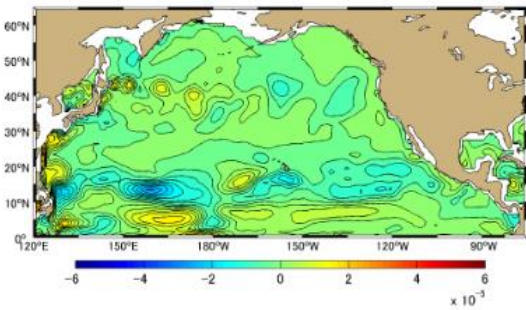
(b)



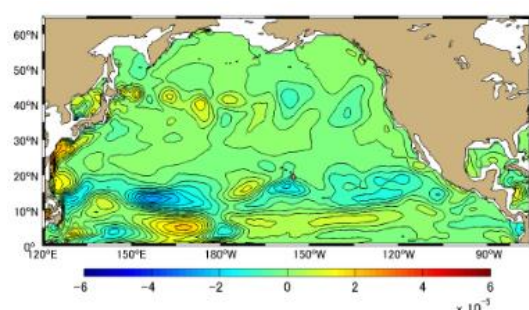
(c)



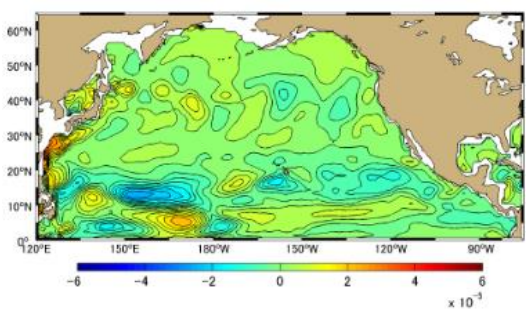
(d)



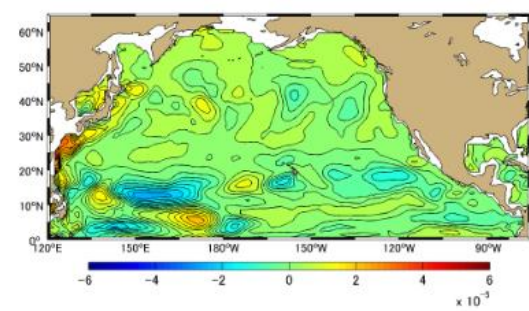
(e)



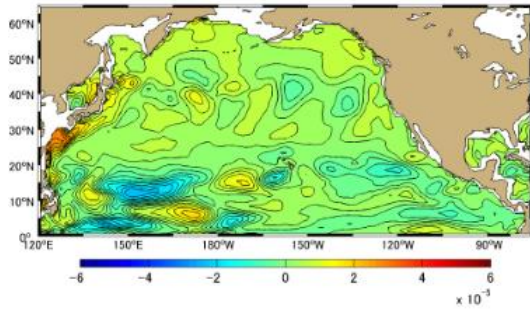
(f)



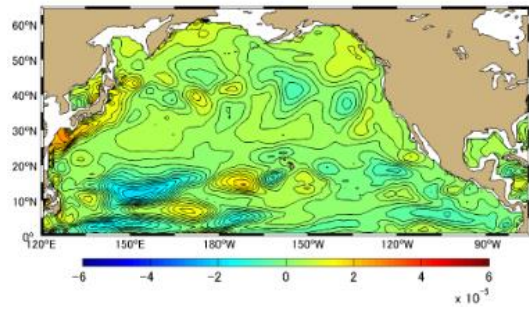
(g)



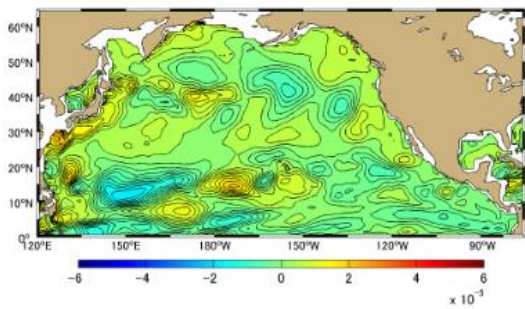
(h)



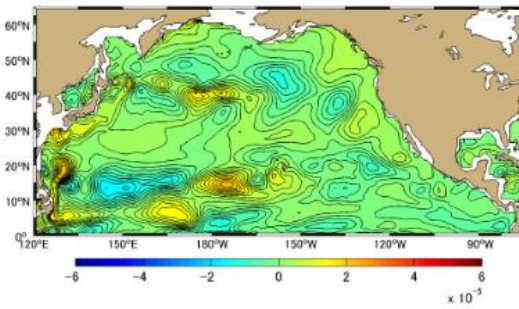
(i)



(j)

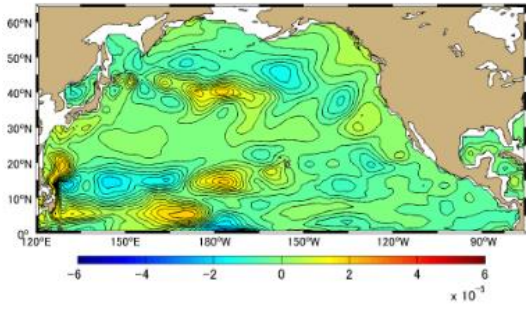


(k)

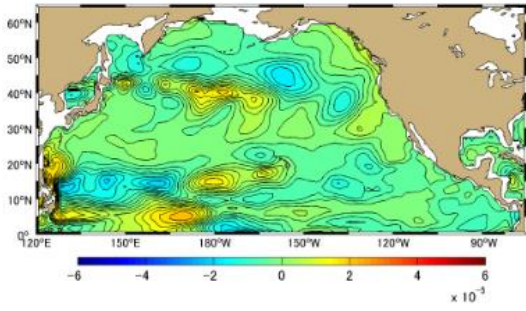


(l)

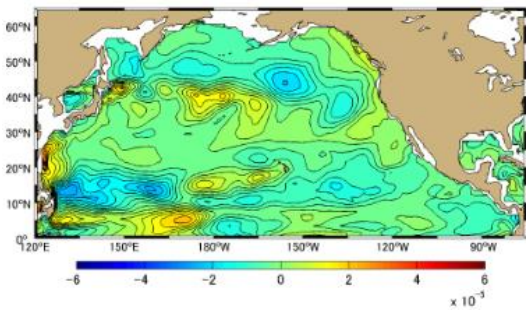
**Figure A-2.1 Difference [PgC] between Approximation Method and Simulation Method Monthly Mean in 1991, the North Pacific Ocean based on January 1991. (a)-(l) represents January-December.**



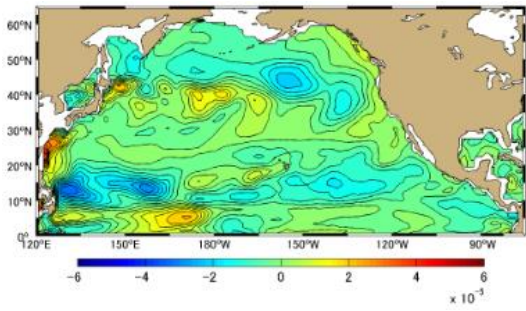
(a)



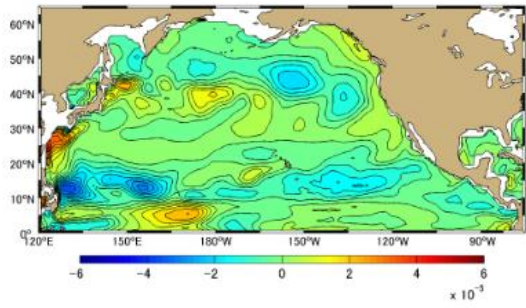
(b)



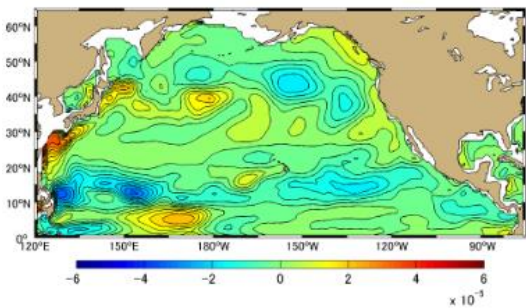
(c)



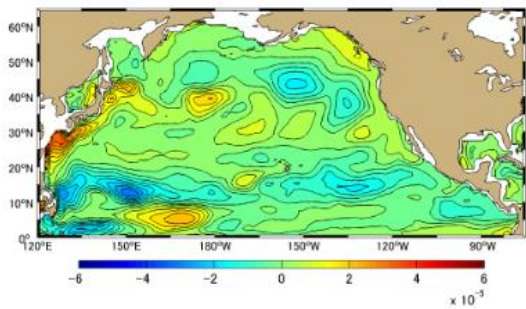
(d)



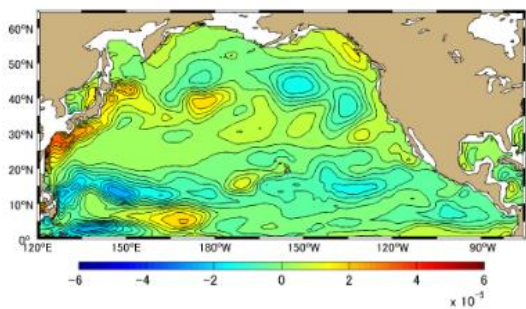
(e)



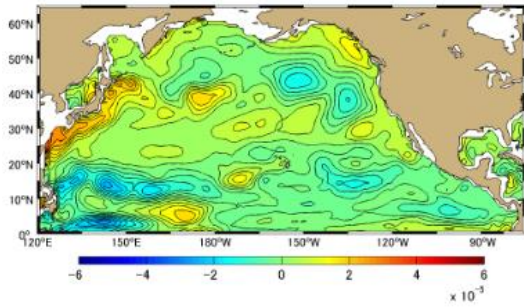
(f)



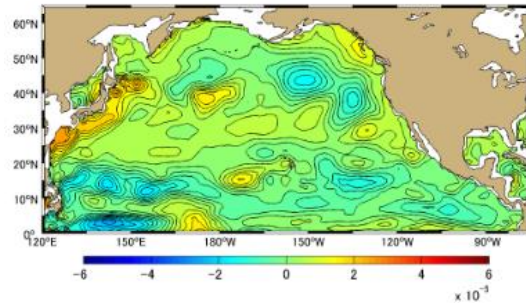
(g)



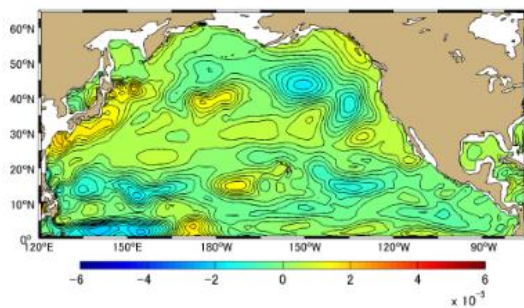
(h)



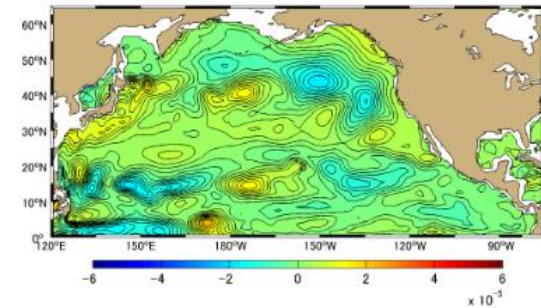
(i)



(j)

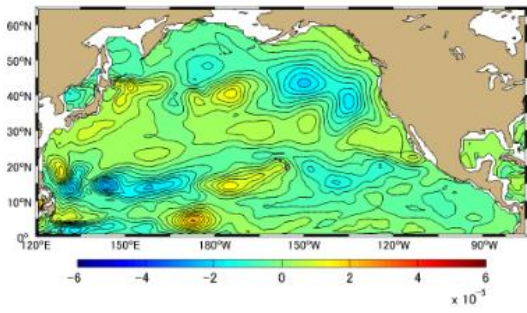


(k)

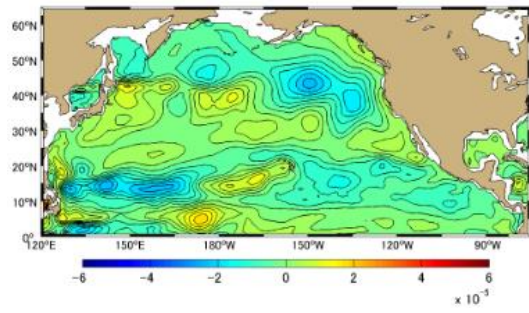


(l)

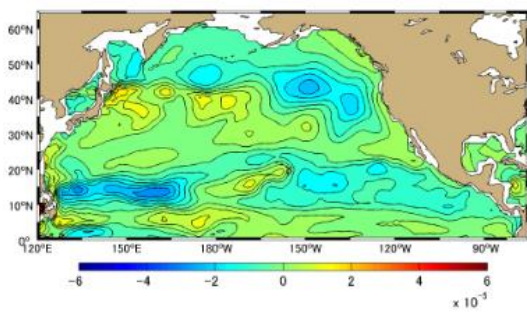
Figure A-2.2 Difference [PgC] between Approximation Method and Simulation Method Monthly Mean in 1992, the North Pacific Ocean based on January 1991. (a)-(l) represents January-December.



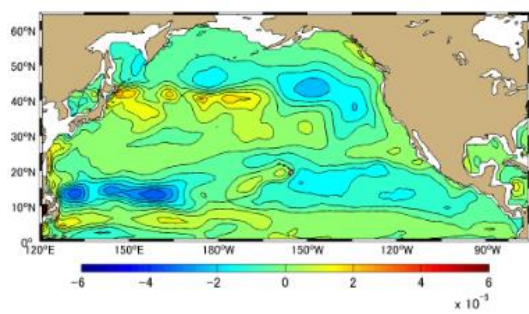
(a)



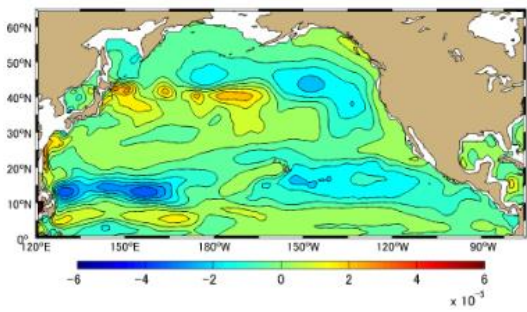
(b)



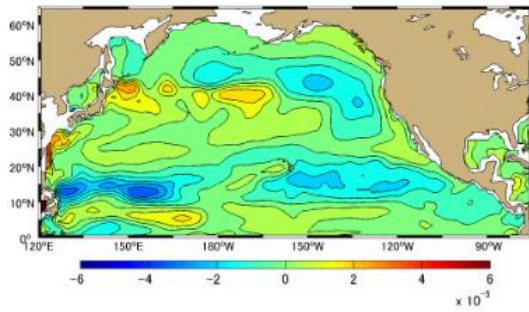
(c)



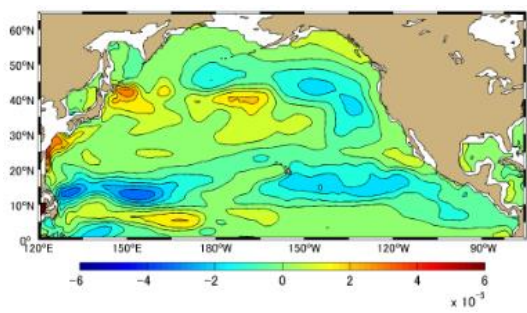
(d)



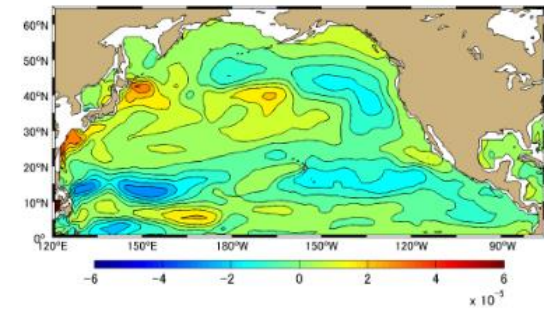
(e)



(f)



(g)



(h)



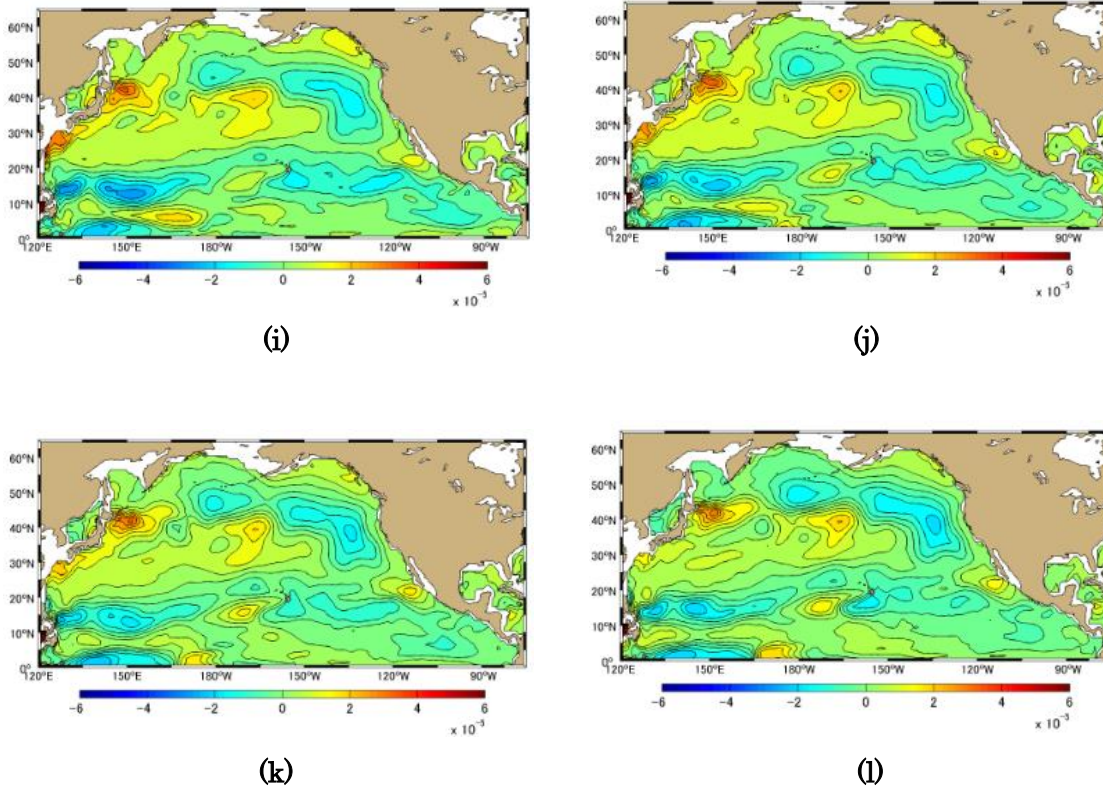
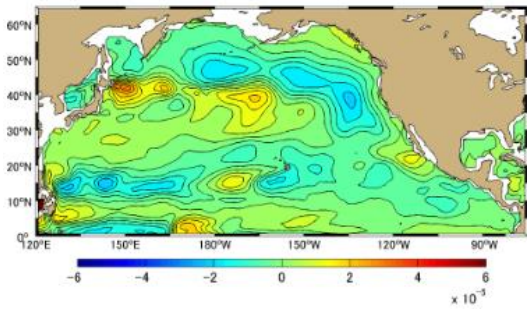
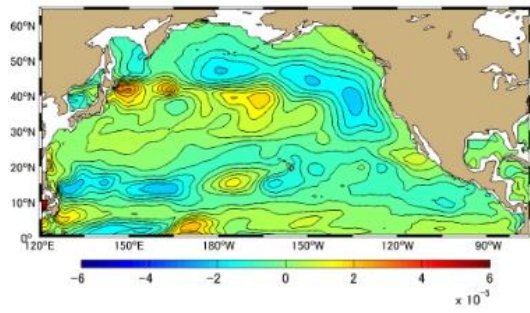


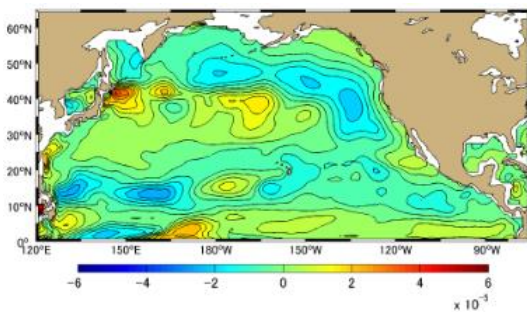
**Figure A-2.3 Difference [PgC] between Approximation Method and Simulation Method Monthly Mean in 1993, the North Pacific Ocean based on January 1991. (a)-(l) represents January-December.**



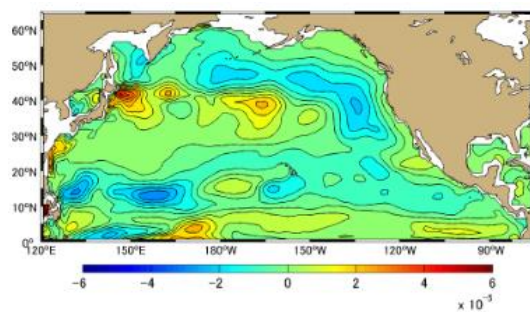
(a)



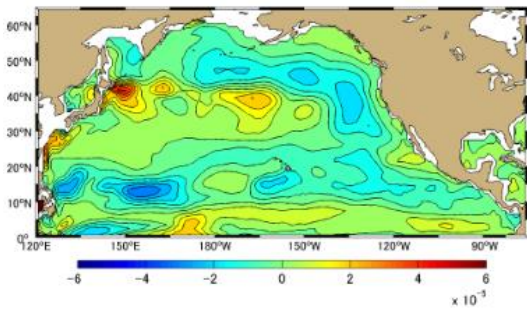
(b)



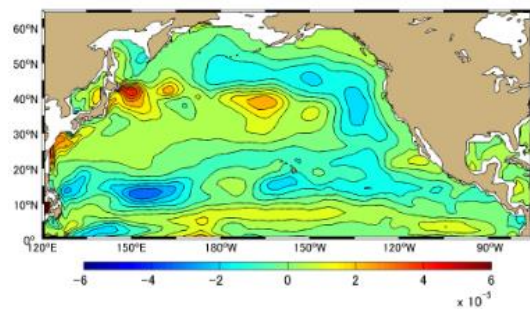
(c)



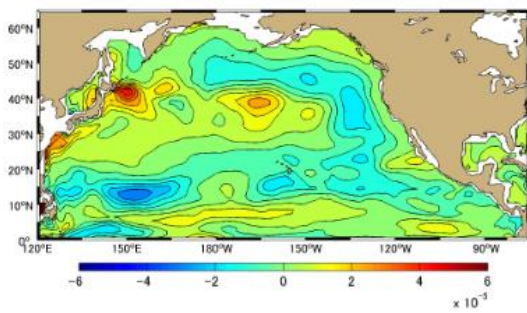
(d)



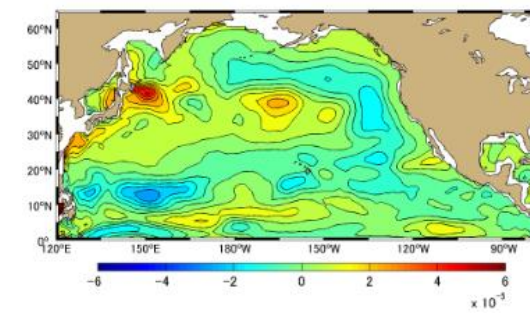
(e)



(f)



(g)



(h)

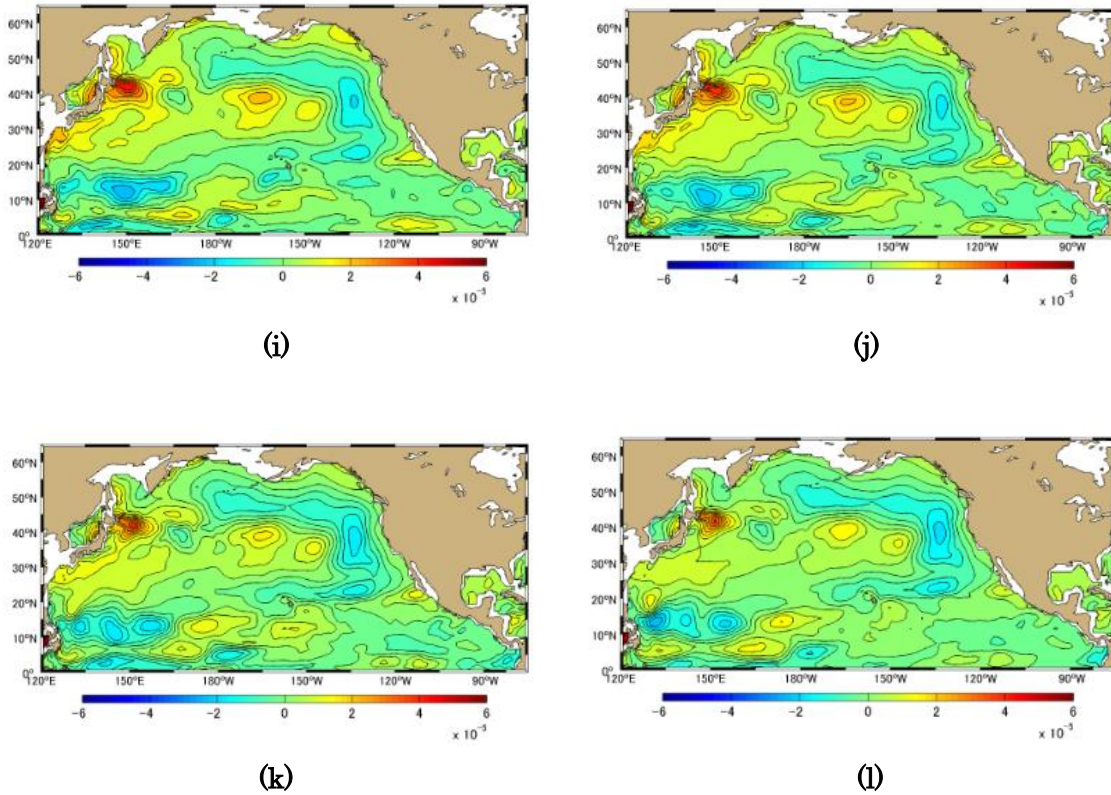
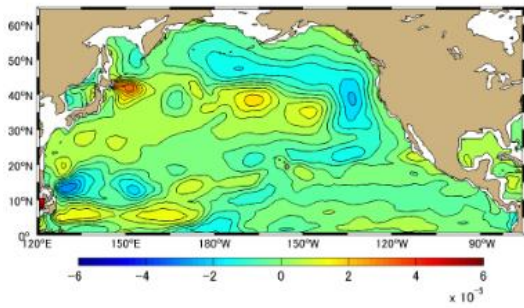
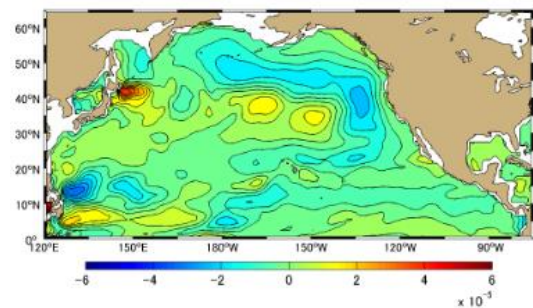


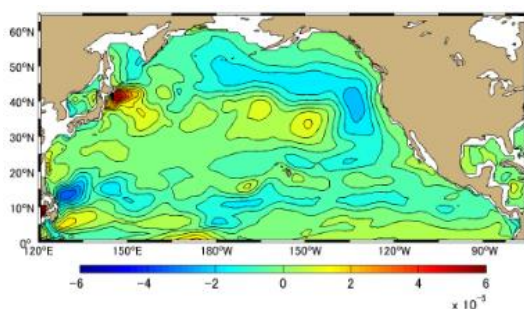
Figure A-2.4 Difference [PgC] between Approximation Method and Simulation Method Monthly Mean in 1994, the North Pacific Ocean based on January 1991. (a)-(l) represents January-December.



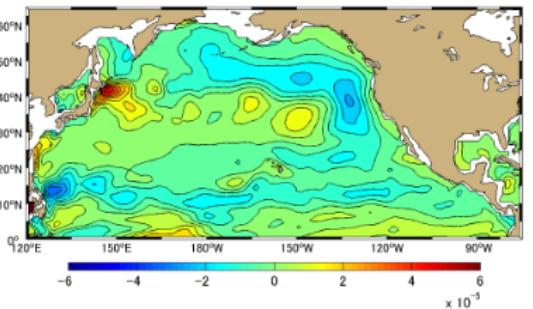
(a)



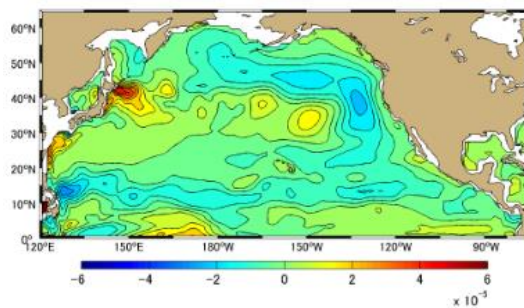
(b)



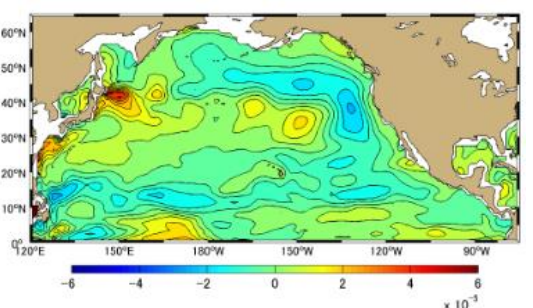
(c)



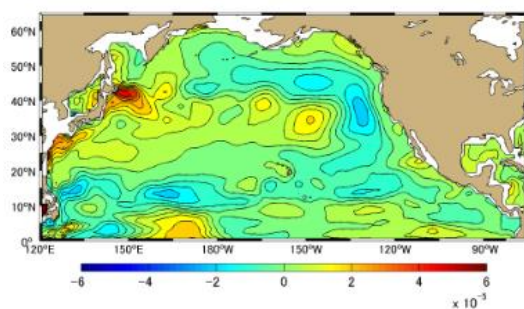
(d)



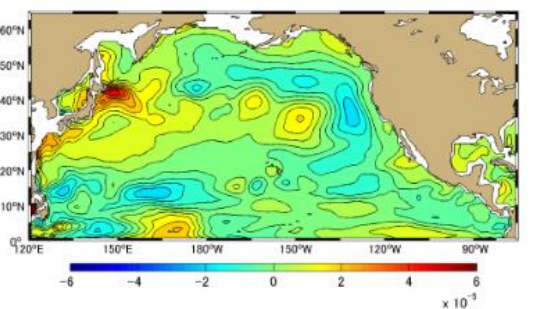
(e)



(f)



(g)



(h)

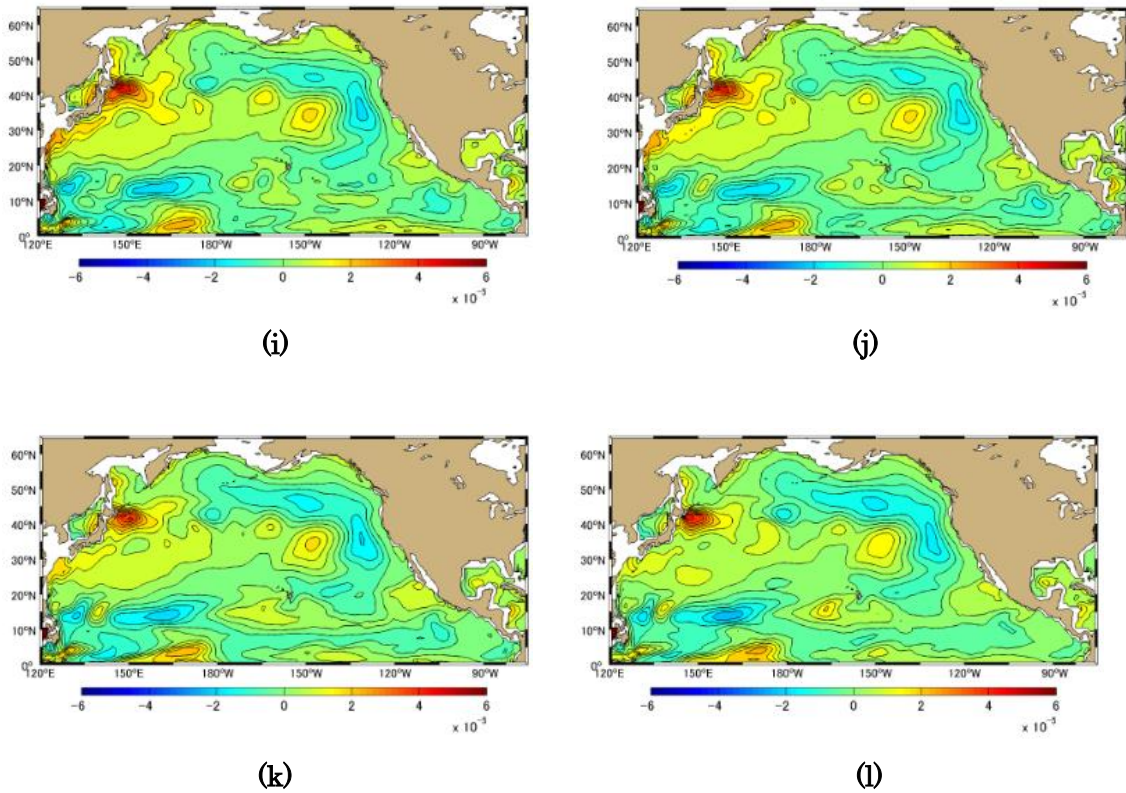
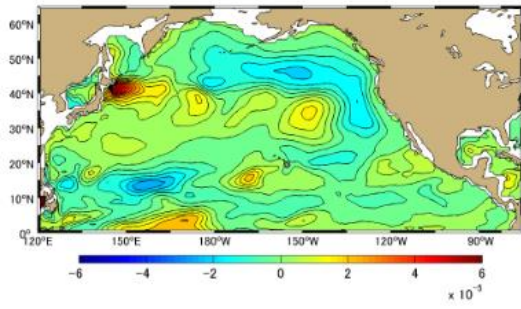
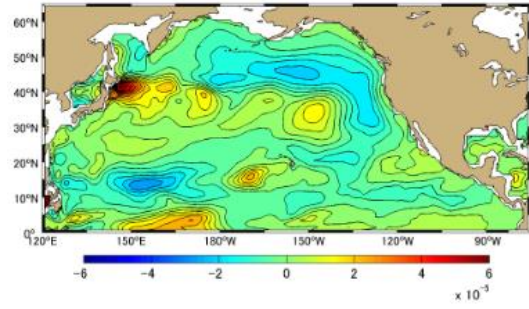


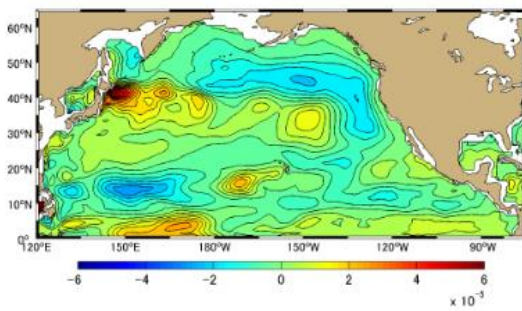
**Figure A-2.5 Difference [PgC] between Approximation Method and Simulation Method Monthly Mean in 1995, the North Pacific Ocean based on January 1991. (a)-(l) represents January-December**



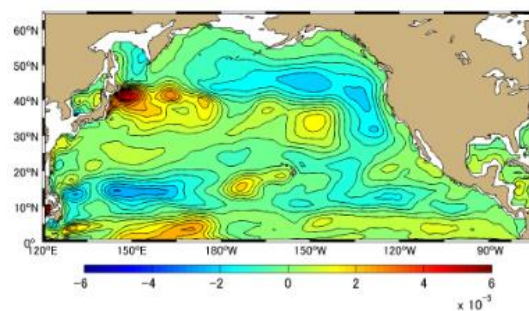
(a)



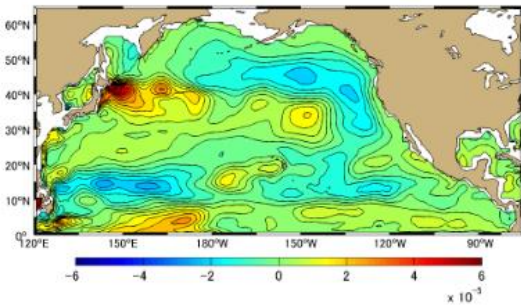
(b)



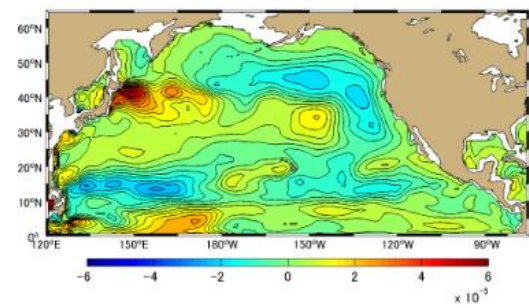
(c)



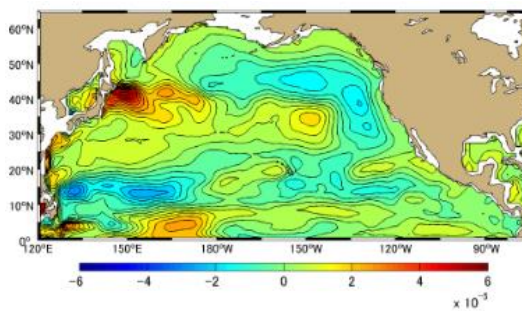
(d)



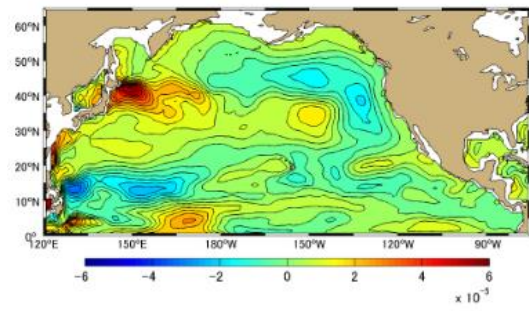
(e)



(f)



(g)



(h)

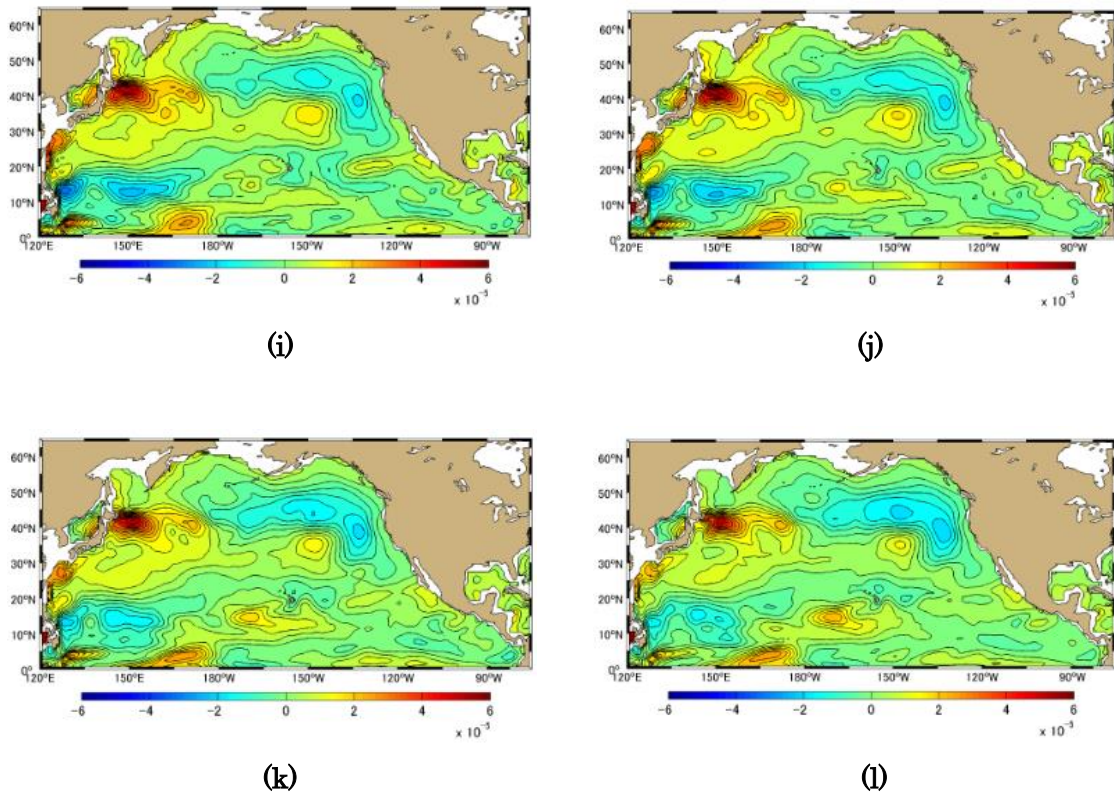
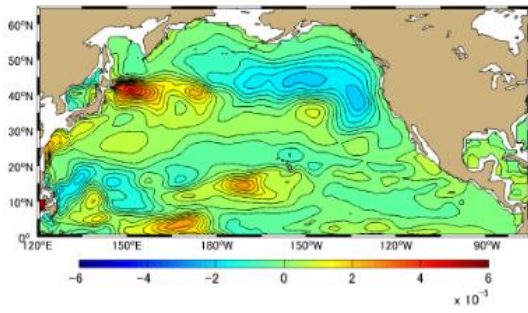
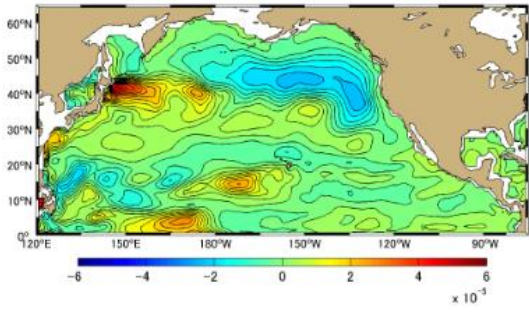


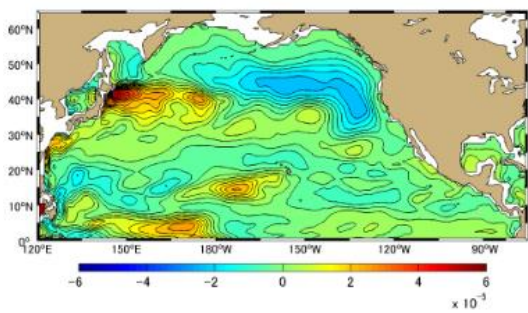
**Figure A-2.6 Difference [PgC] between Approximation Method and Simulation Method Monthly Mean in 1996, the North Pacific Ocean based on January 1991. (a)-(l) represents January-December**



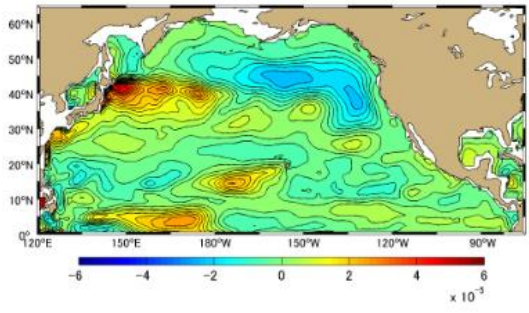
(a)



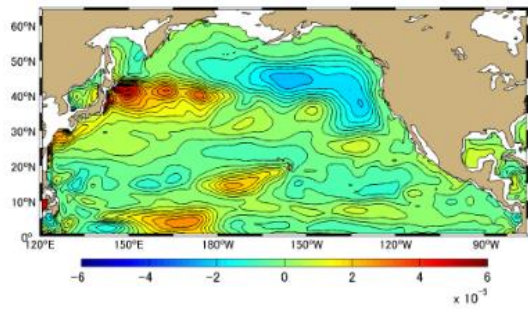
(b)



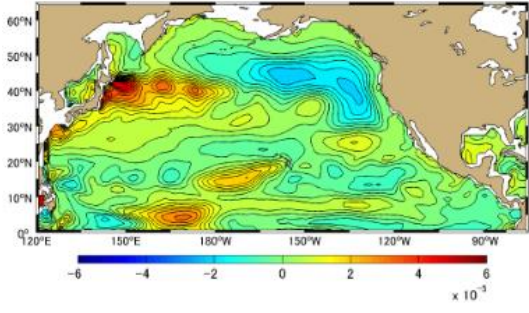
(c)



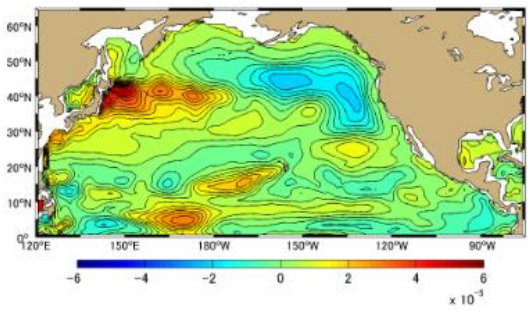
(d)



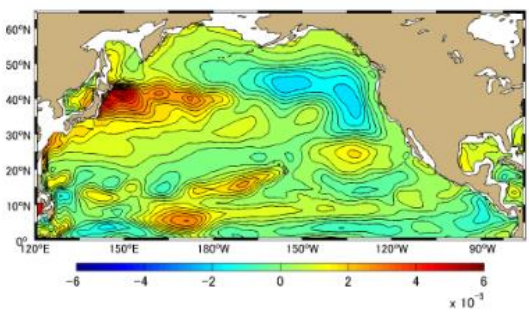
(e)



(f)

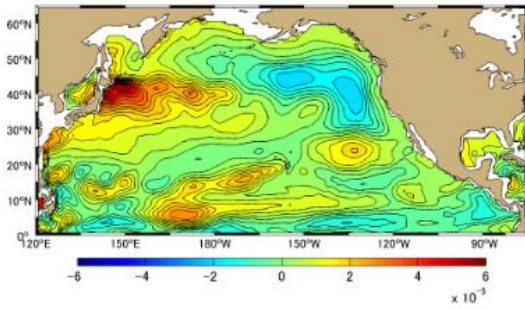


(g)

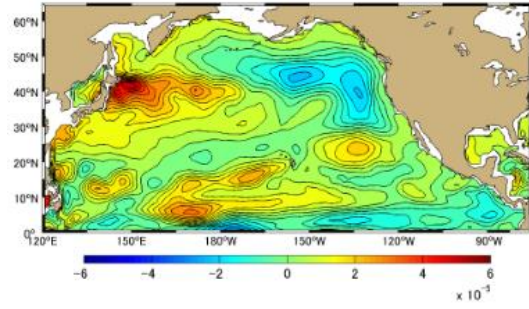


(h)

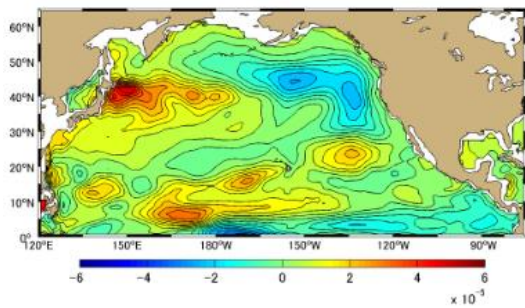




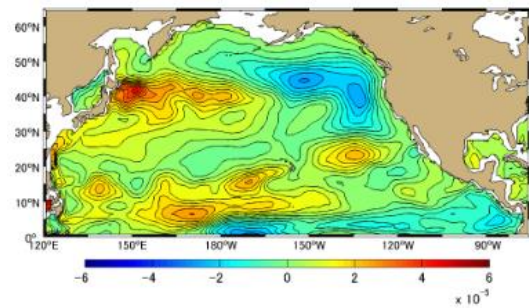
(i)



(j)

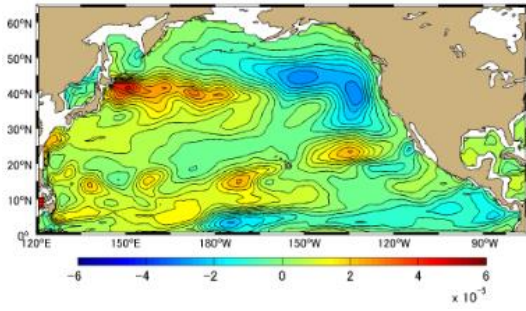


(k)

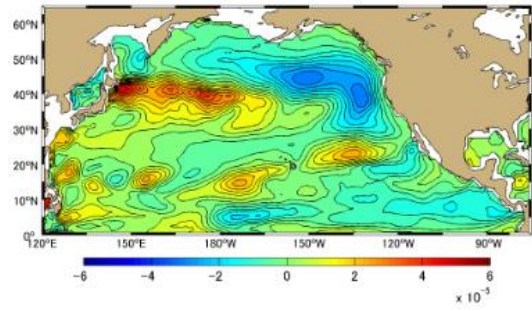


(l)

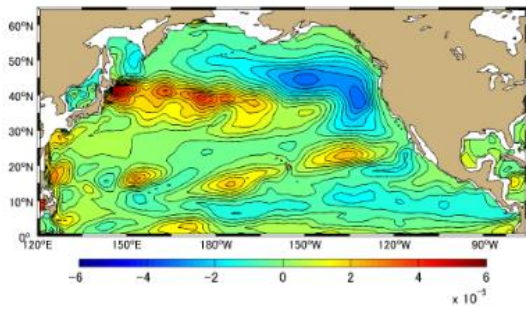
**Figure A-2.7 Difference [PgC] between Approximation Method and Simulation Method Monthly Mean in 1997, the North Pacific Ocean based on January 1991. (a)-(l) represents January-December**



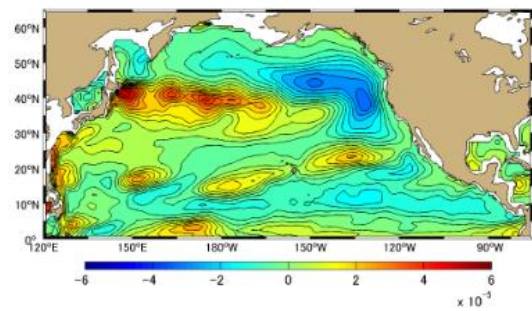
(a)



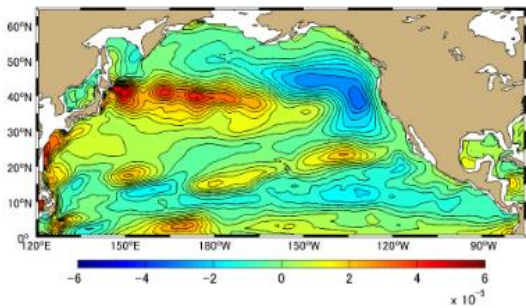
(b)



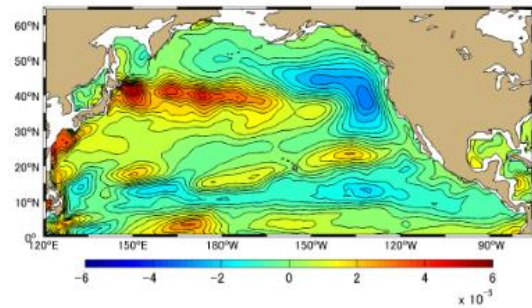
(c)



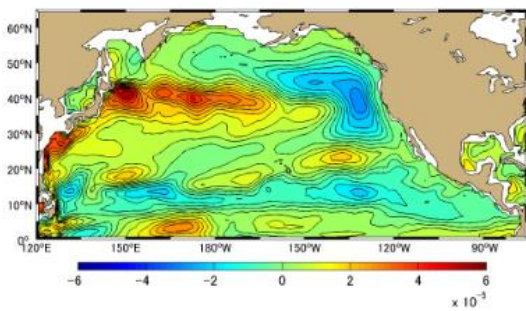
(d)



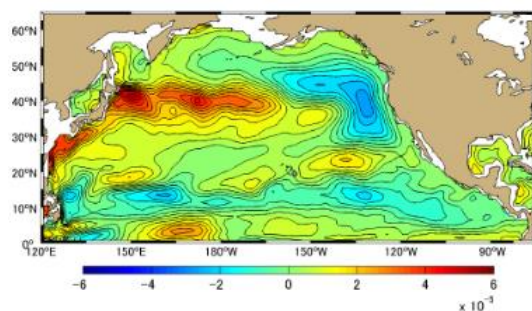
(e)



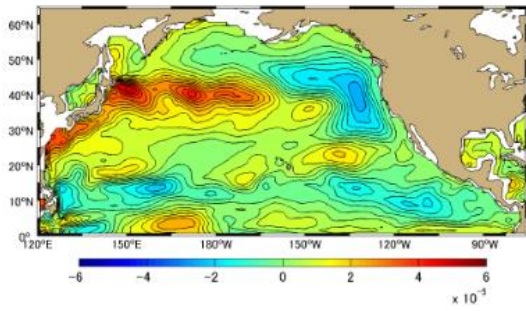
(f)



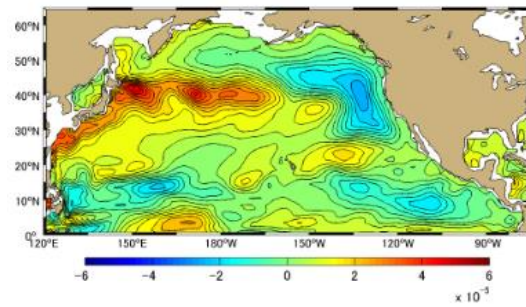
(g)



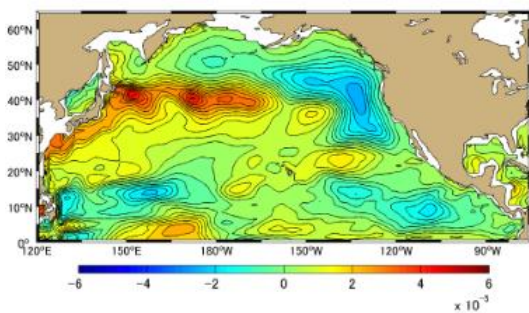
(h)



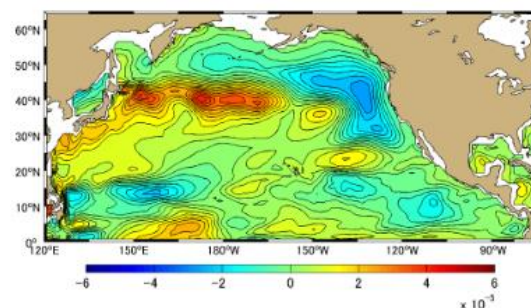
(i)



(j)

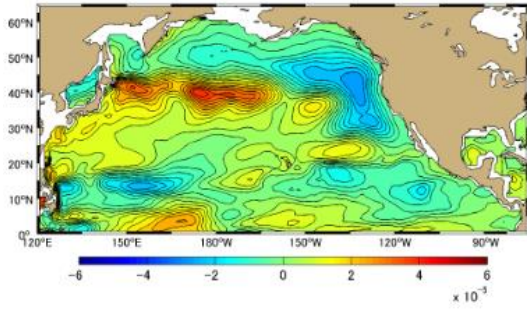


(k)

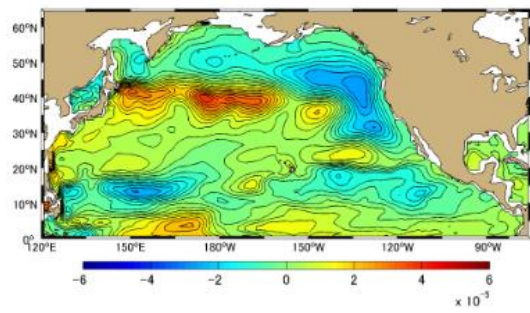


(l)

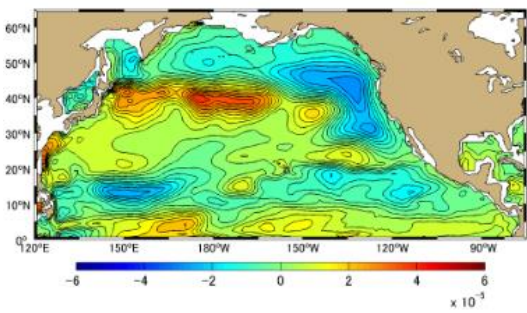
**Figure A-2.8 Difference [PgC] between Approximation Method and Simulation Method Monthly Mean in 1998, the North Pacific Ocean based on January 1991. (a)-(l) represents January-December**



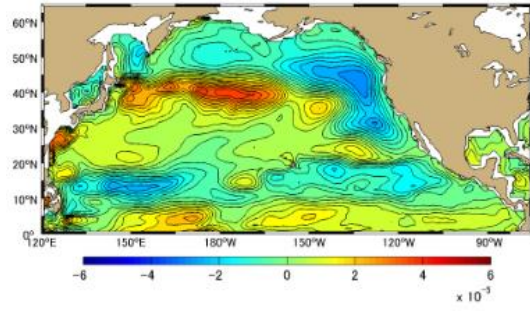
(a)



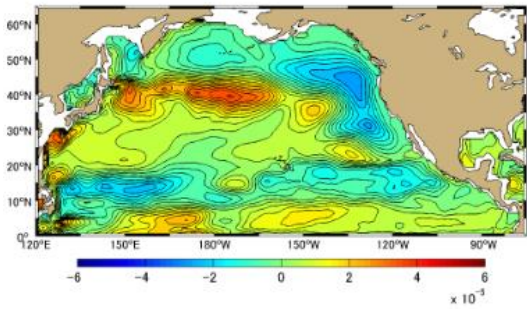
(b)



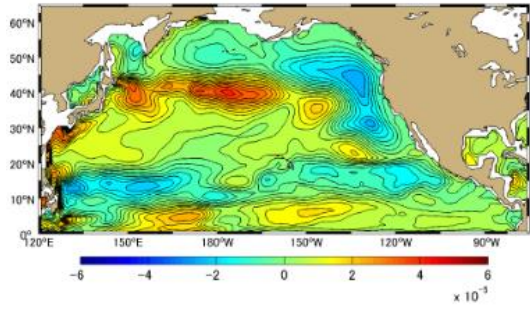
(c)



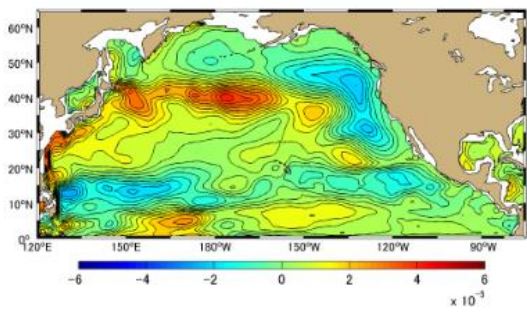
(d)



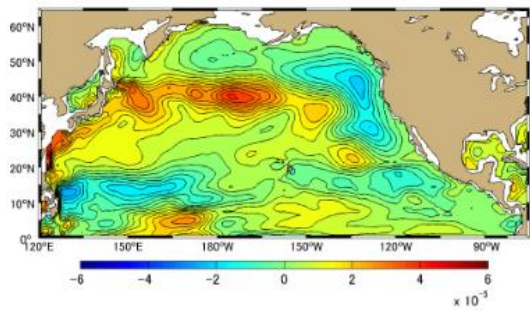
(e)



(f)



(g)



(h)

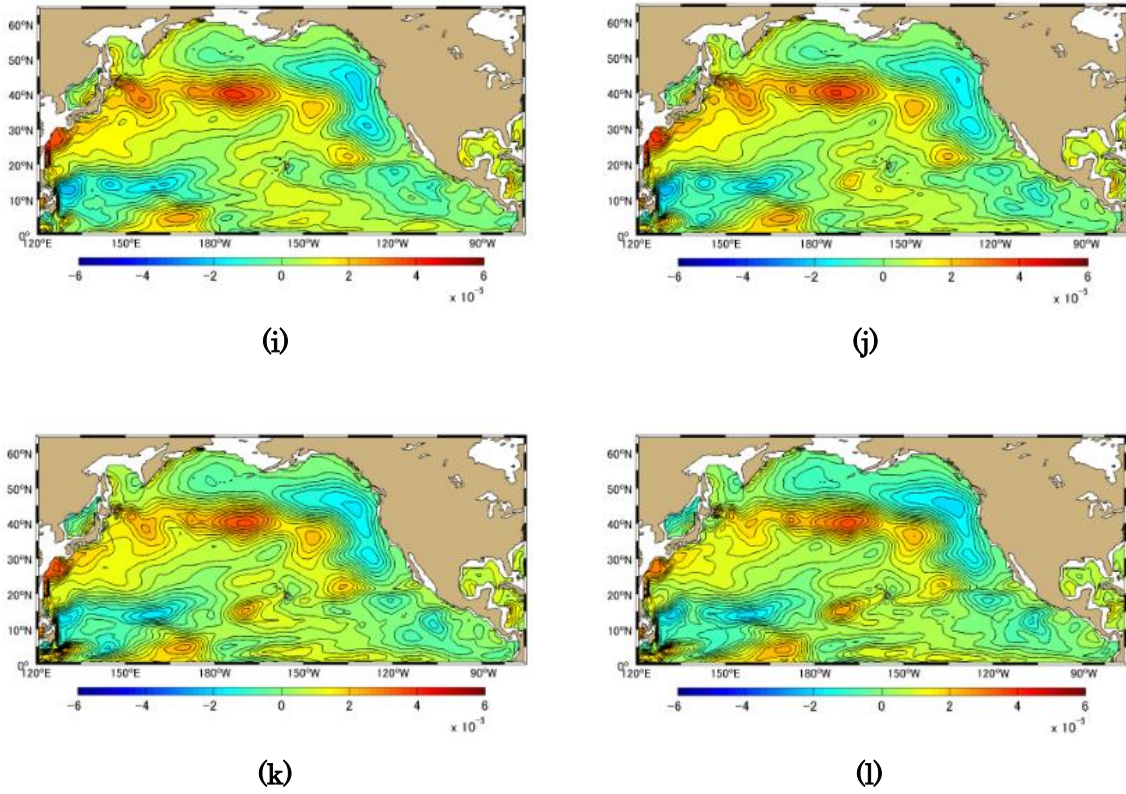
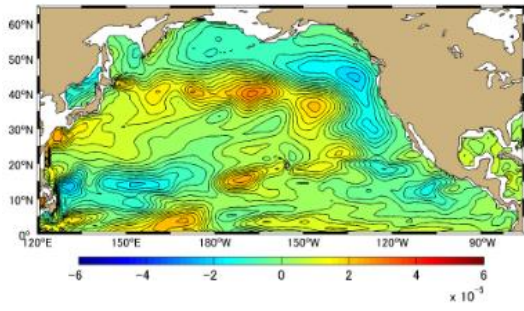
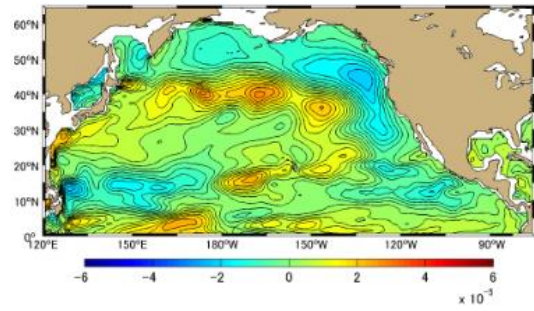


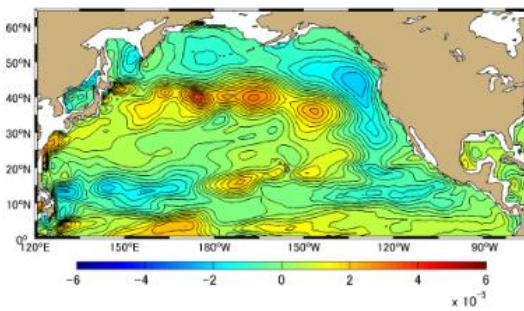
**Figure A-2.9** Difference [PgC] between Approximation Method and Simulation Method Monthly Mean in 1999, the North Pacific Ocean based on January 1991. (a)-(l) represents January-December



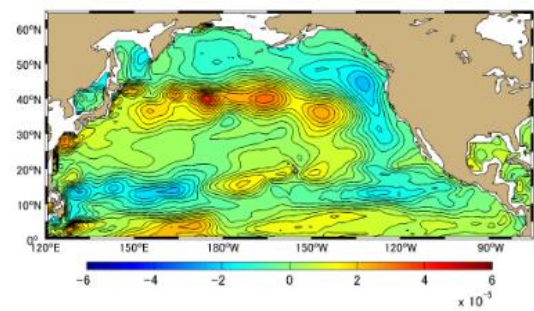
(a)



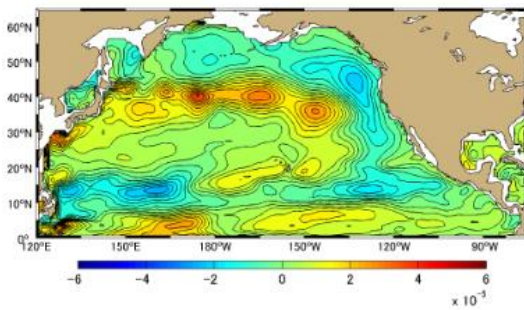
(b)



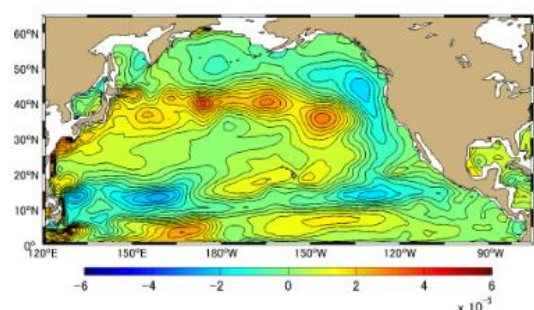
(c)



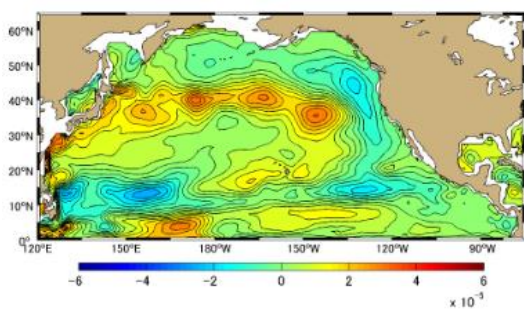
(d)



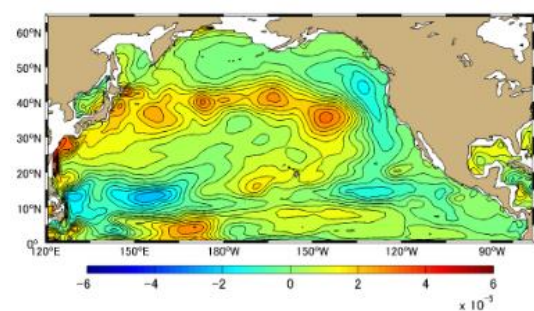
(e)



(f)



(g)



(h)

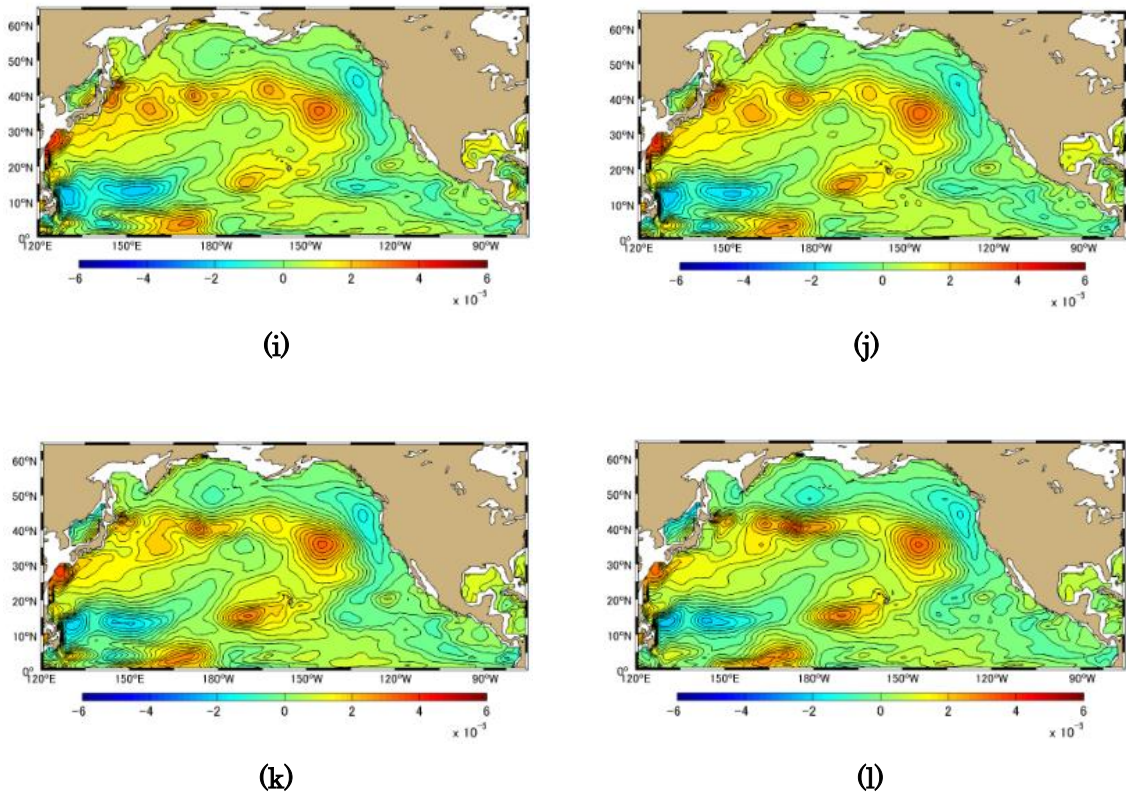
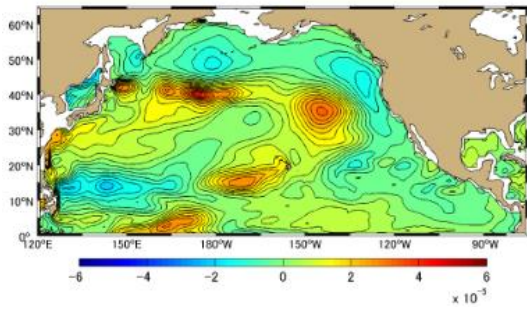
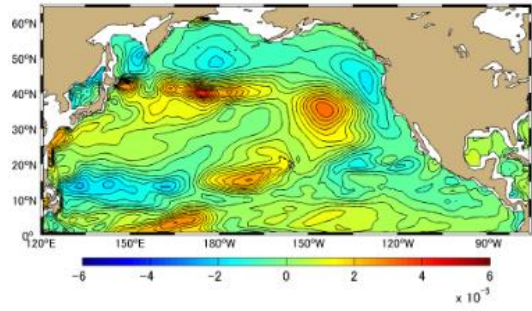


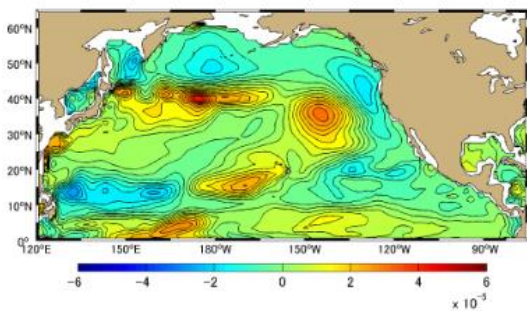
**Figure A-2.10 Difference [PgC] between Approximation Method and Simulation Method Monthly Mean in 2000, the North Pacific Ocean based on January 1991. (a)-(l) represents January-December**



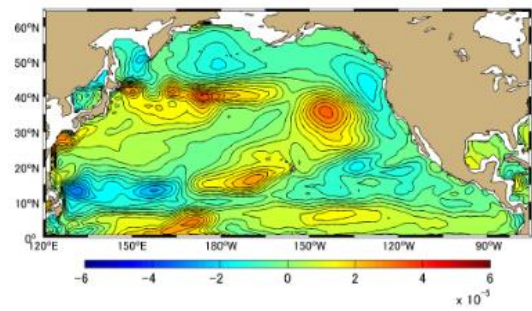
(a)



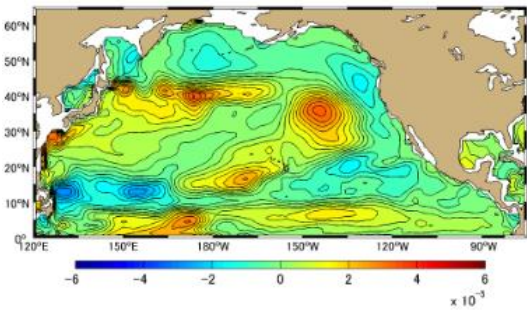
(b)



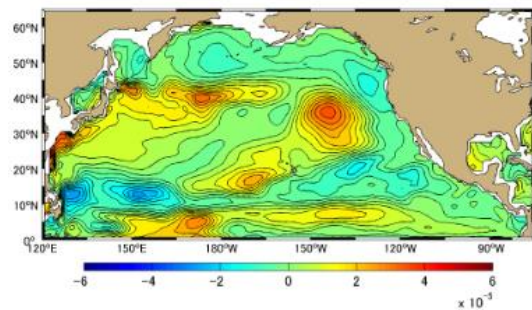
(c)



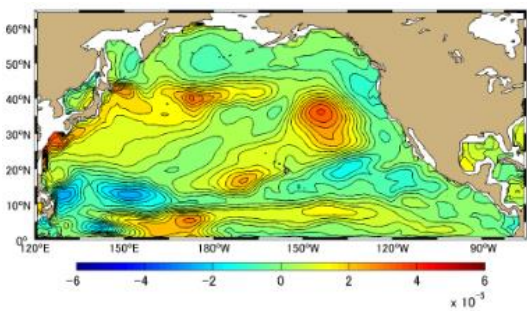
(d)



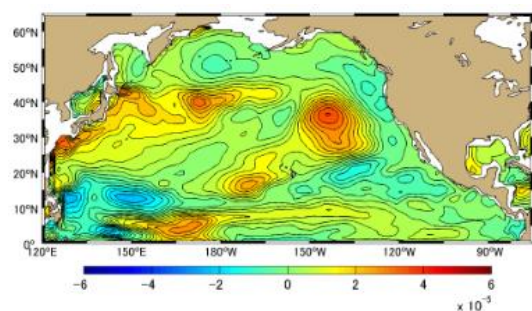
(e)



(f)



(g)



(h)



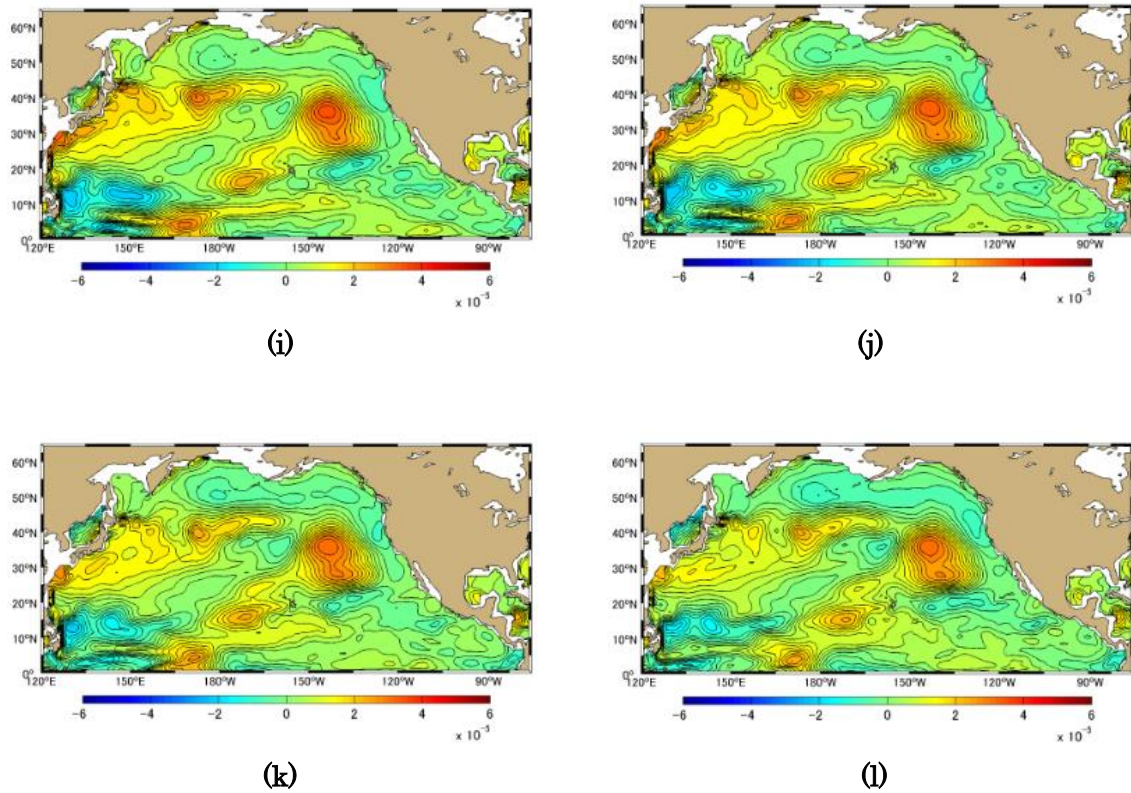
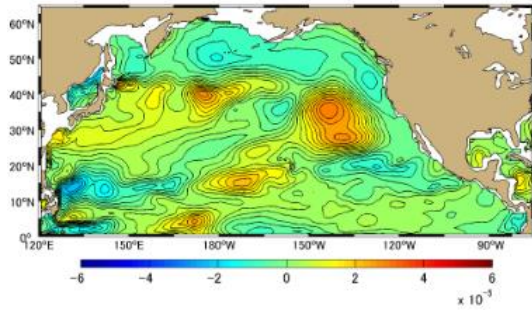
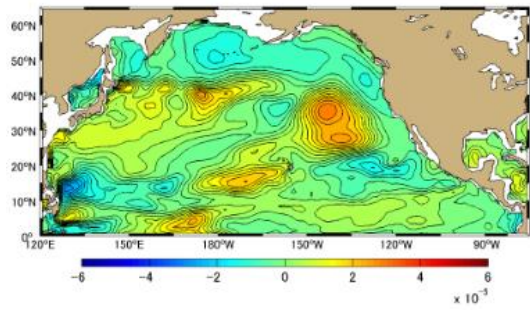


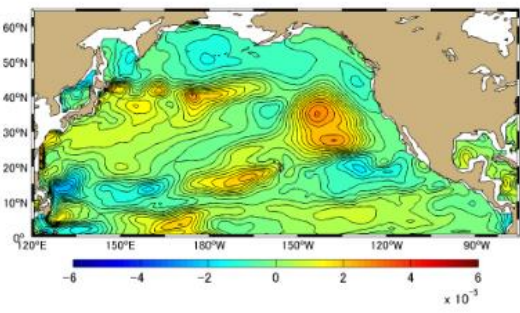
**Figure A-2.11 Difference [PgC] between Approximation Method and Simulation Method Monthly Mean in 2001, the North Pacific Ocean based on January 1991. (a)-(l) represents January-December**



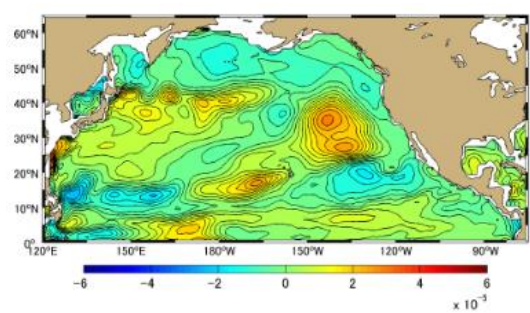
(a)



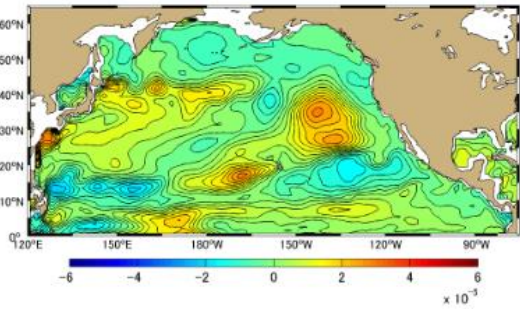
(b)



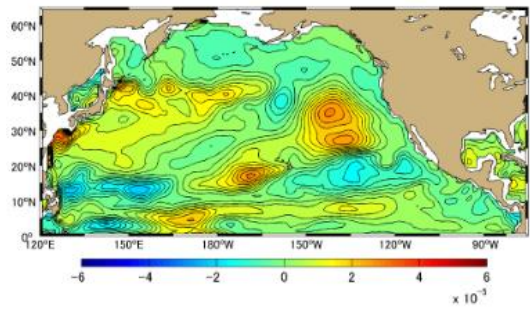
(c)



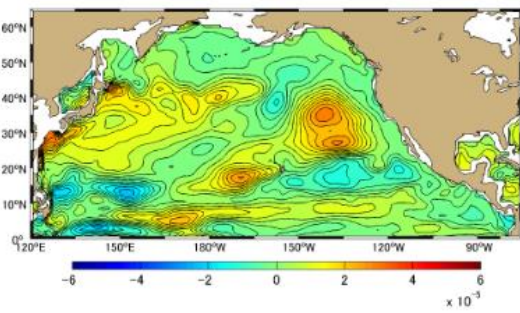
(d)



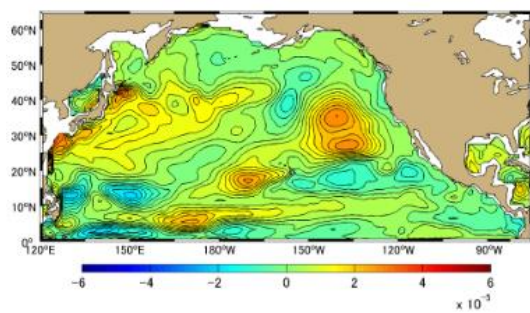
(e)



(f)



(g)



(h)

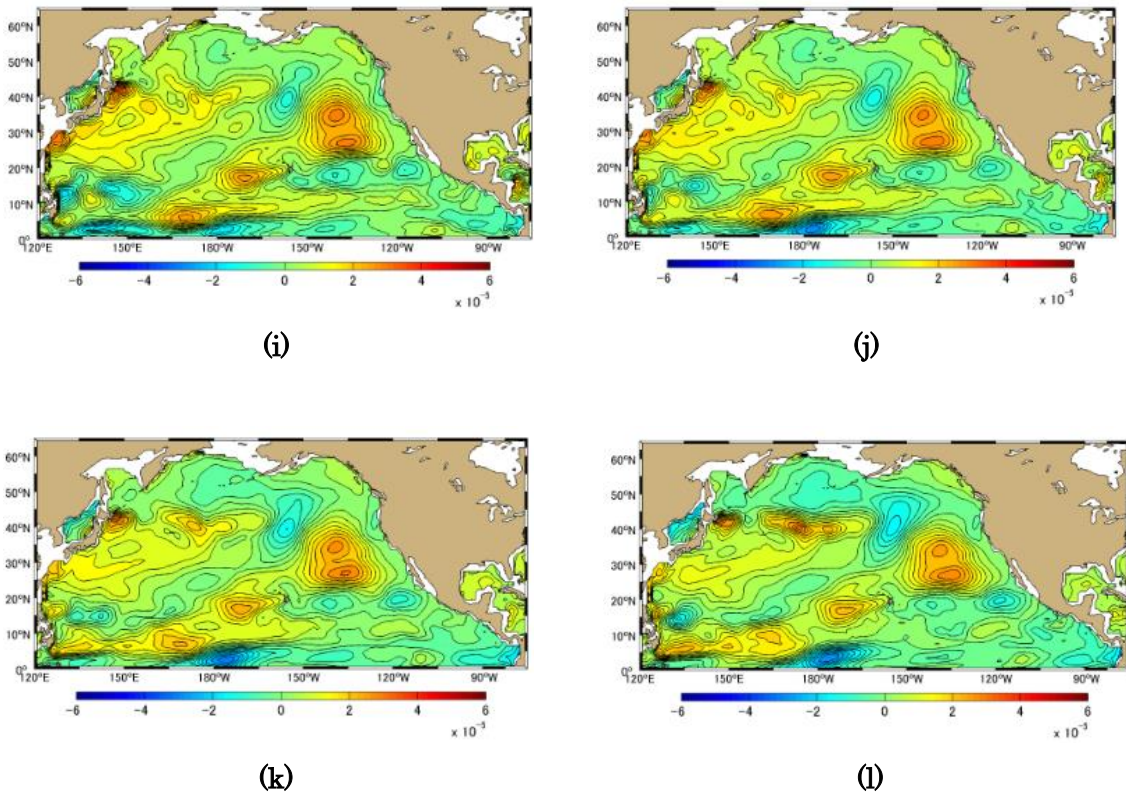
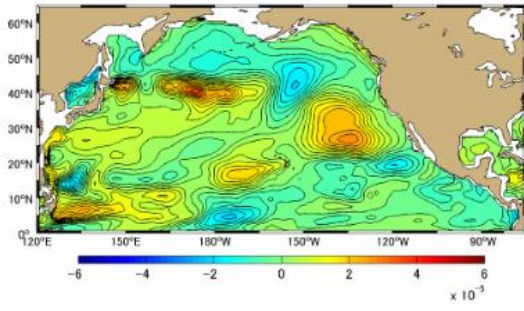
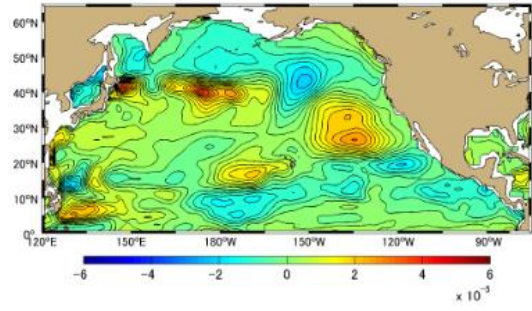


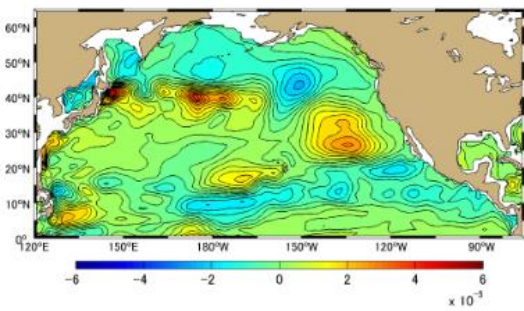
Figure A-2.12 Difference [PgC] between Approximation Method and Simulation Method Monthly Mean in 2002, the North Pacific Ocean based on January 1991. (a)-(l) represents January-December



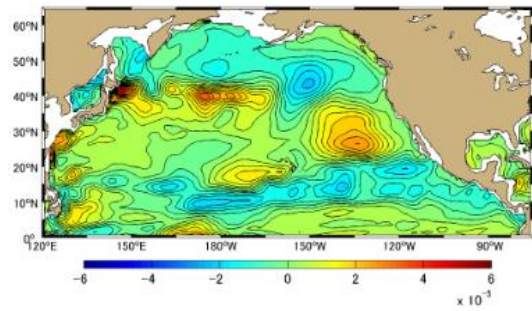
(a)



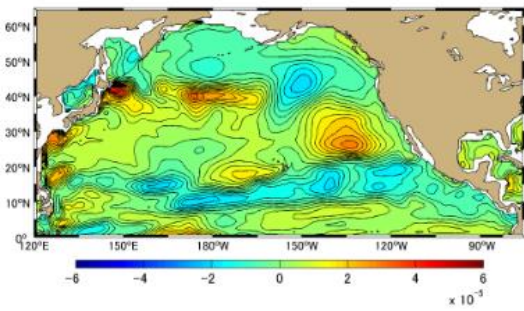
(b)



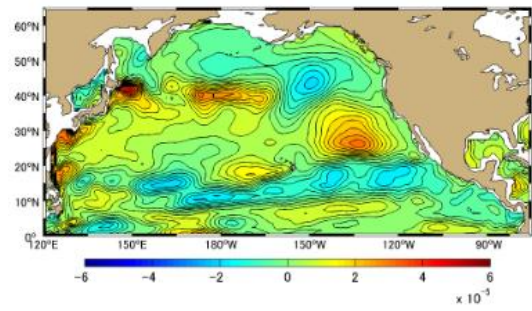
(c)



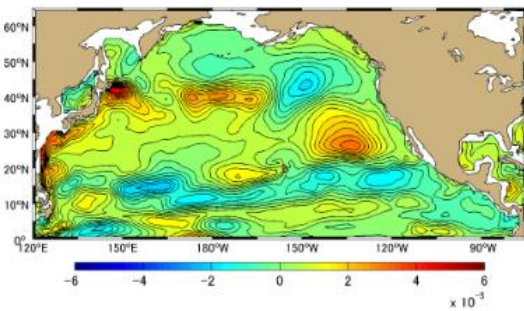
(d)



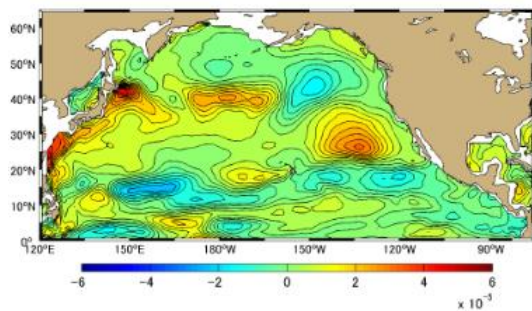
(e)



(f)



(g)



(h)

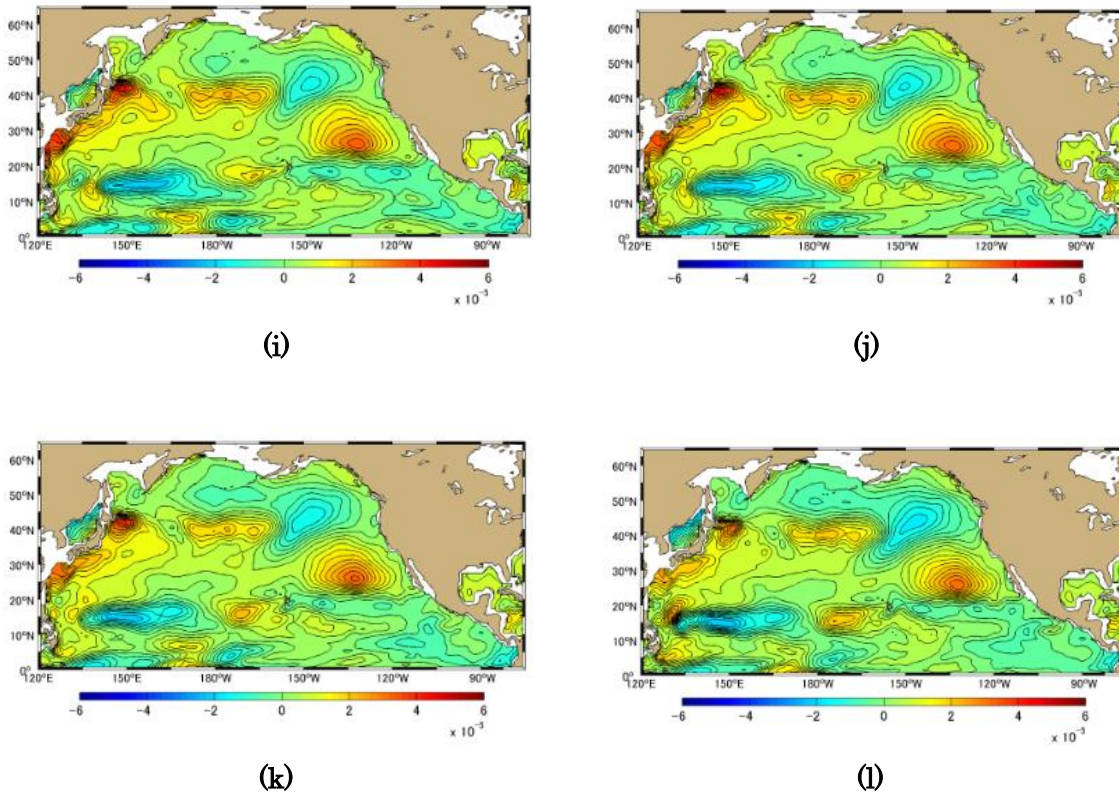
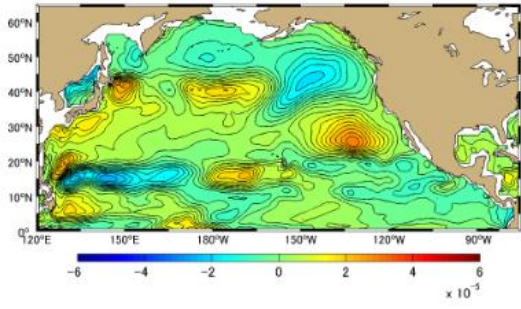
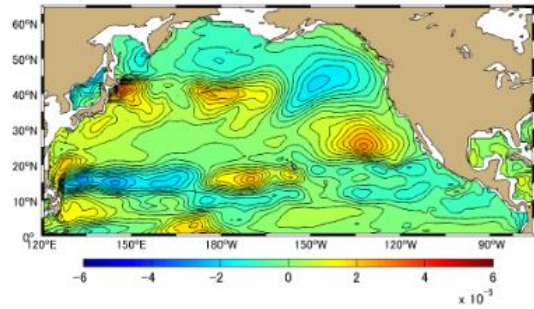


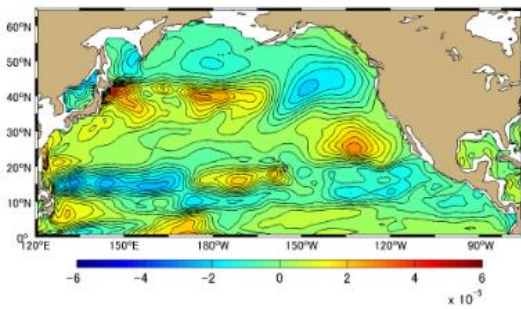
**Figure A-2.13** Difference [PgC] between Approximation Method and Simulation Method Monthly Mean in 2003 the North Pacific Ocean based on January 1991. (a)-(l) represents January-December



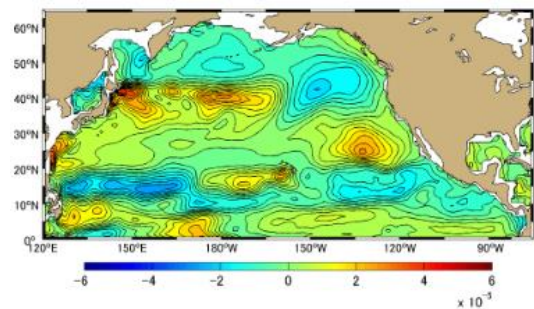
(a)



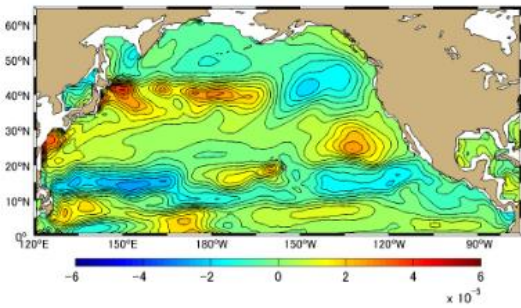
(b)



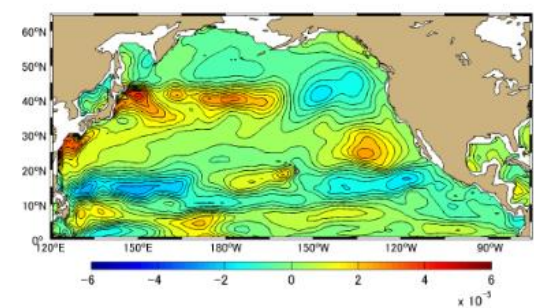
(c)



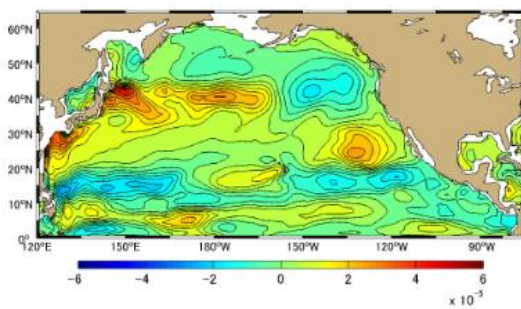
(d)



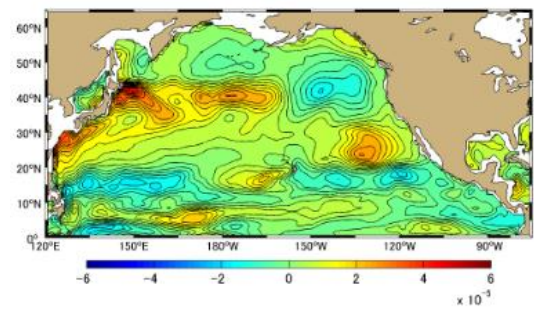
(e)



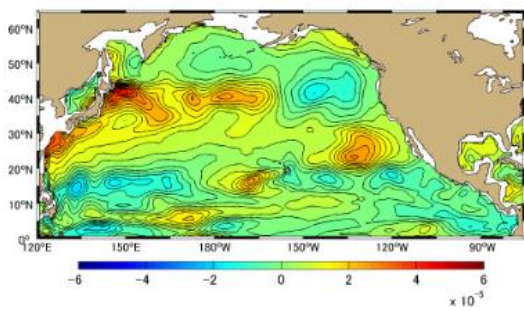
(f)



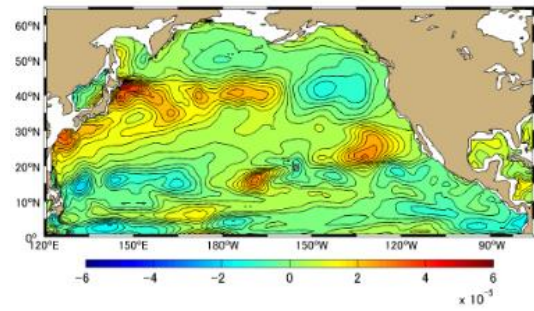
(g)



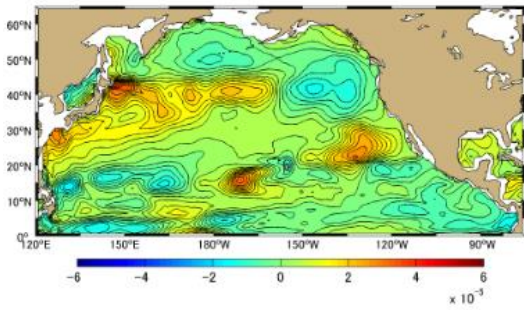
(h)



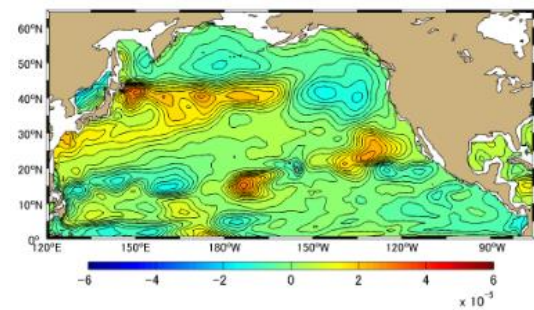
(i)



(j)

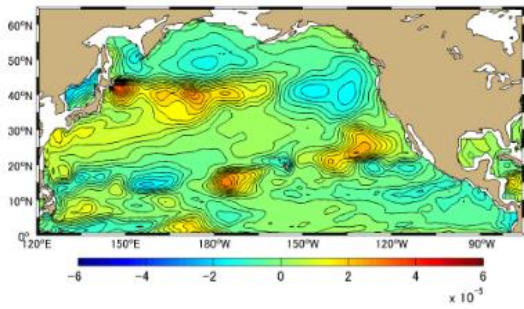


(k)

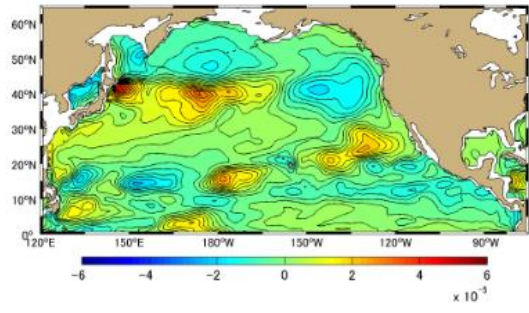


(l)

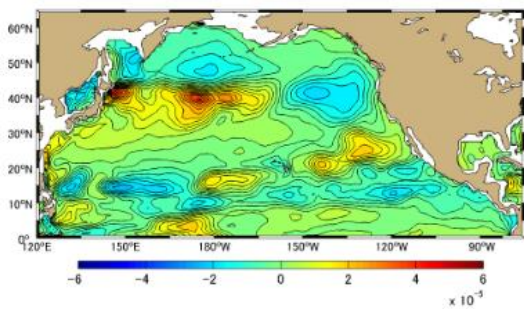
**Figure A-2.14 Difference [PgC] between Approximation Method and Simulation Method Monthly Mean in 2004, the North Pacific Ocean based on January 1991. (a)-(l) represents January-December**



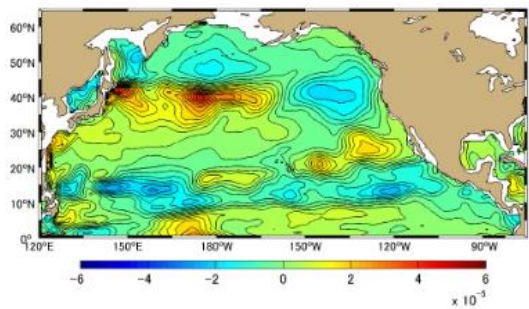
(a)



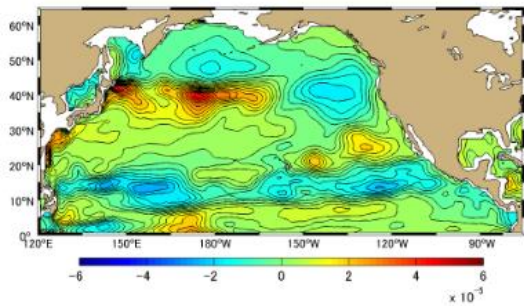
(b)



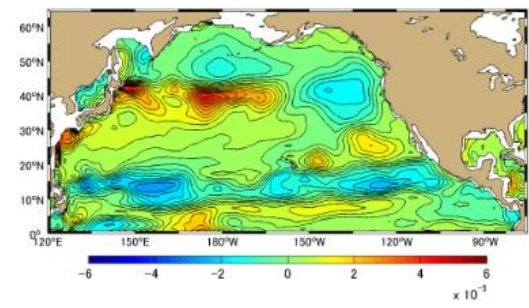
(c)



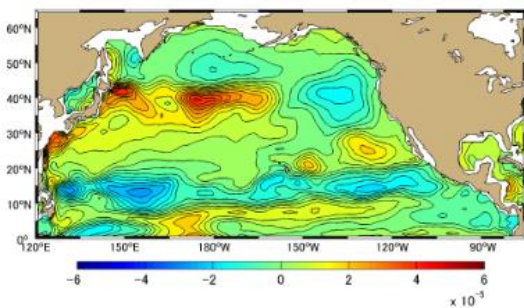
(d)



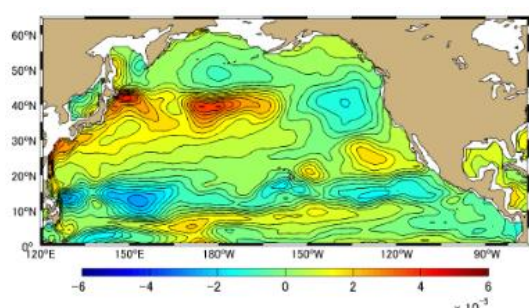
(e)



(f)

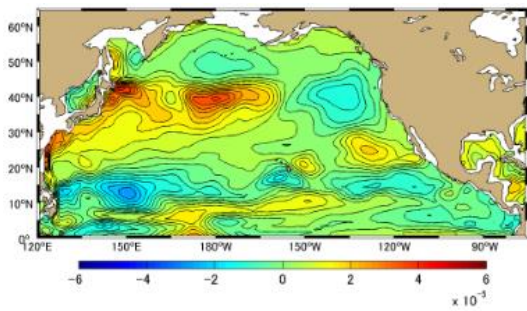


(g)

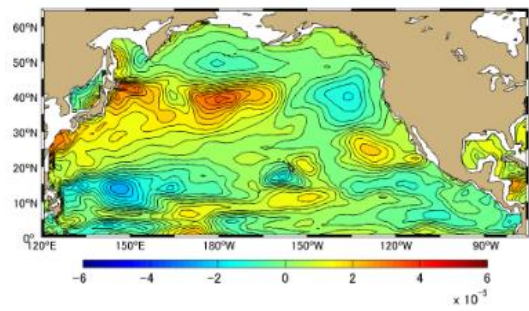


(h)

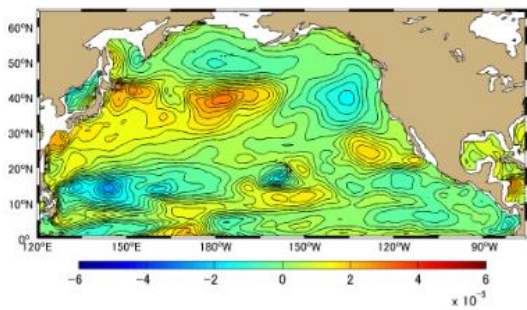




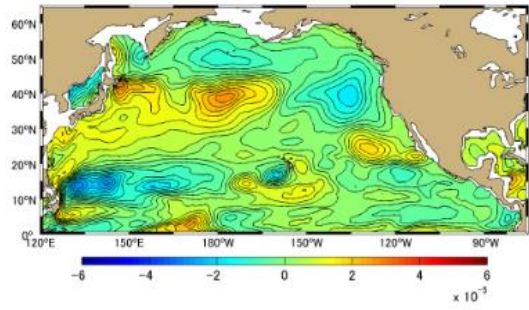
(i)



(j)

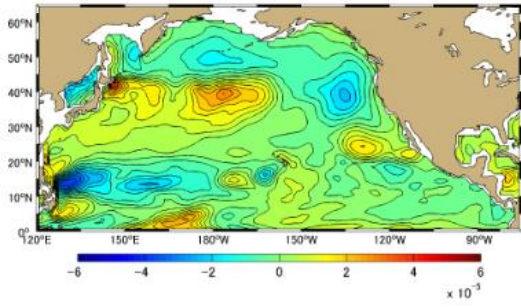


(k)

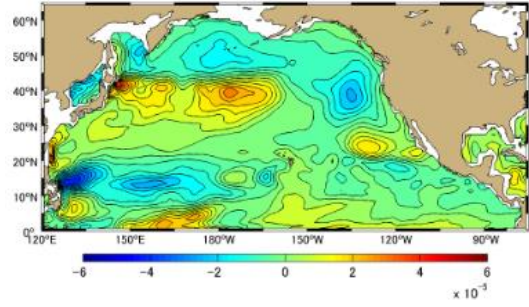


(l)

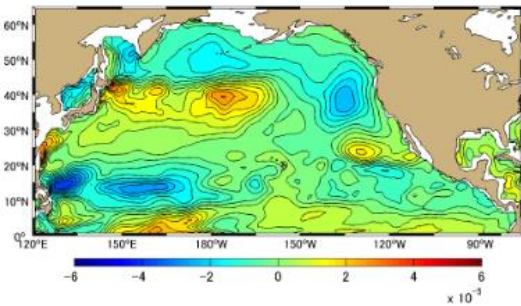
**Figure A-2.15 Difference [PgC] between Approximation Method and Simulation Method Monthly Mean in 2005, the North Pacific Ocean based on January 1991. (a)-(l) represents January-December**



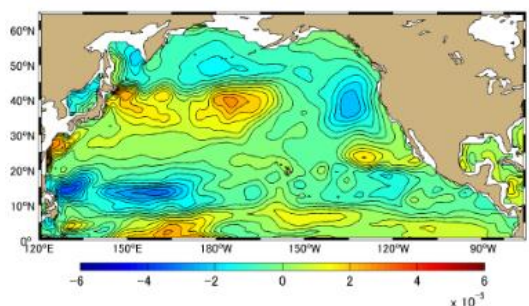
(a)



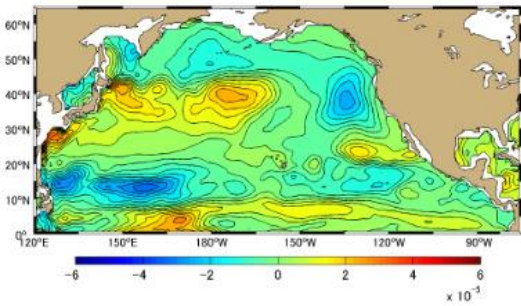
(b)



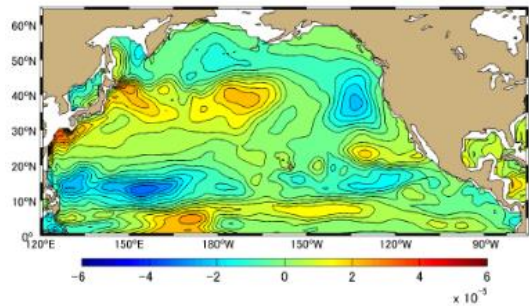
(c)



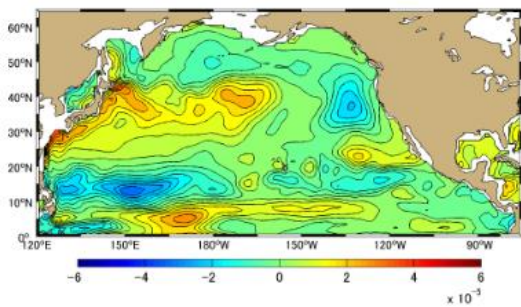
(d)



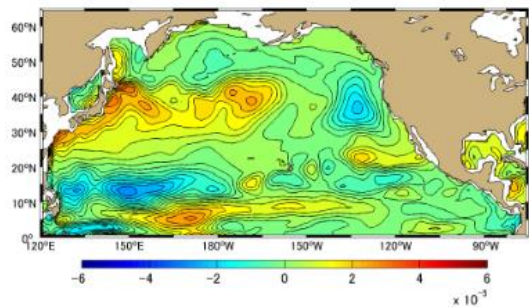
(e)



(f)



(g)



(h)

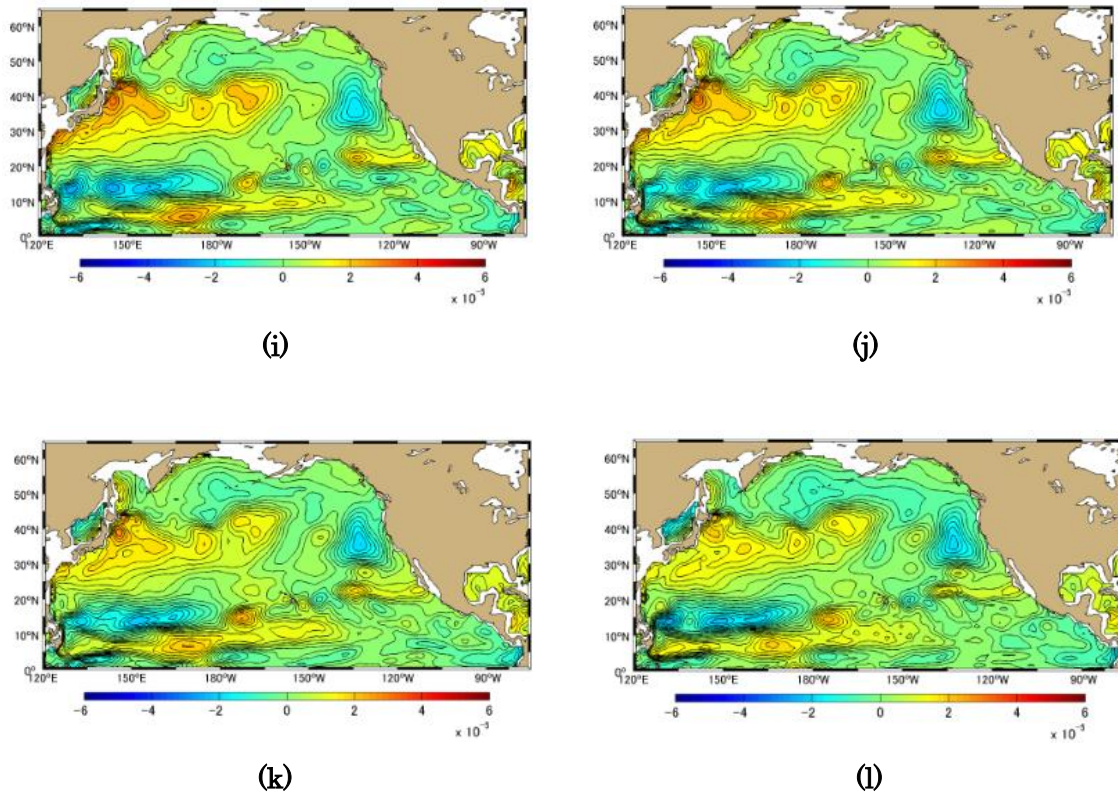
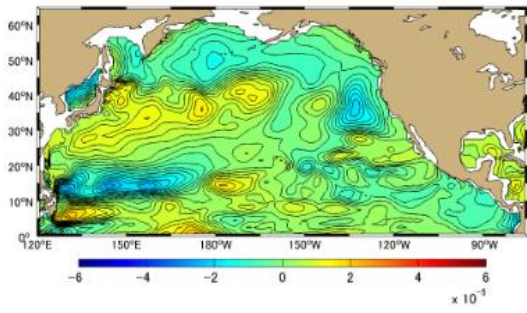
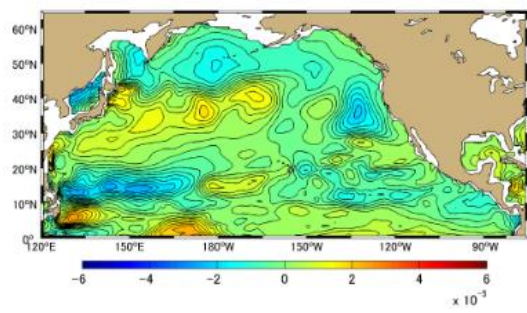


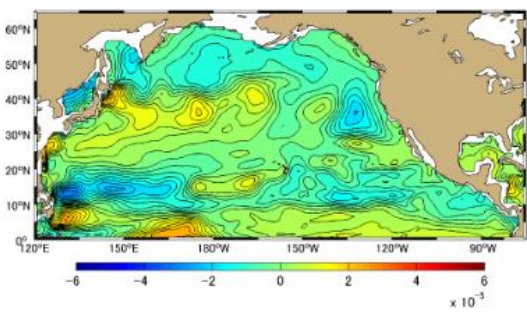
**Figure A-2.16 Difference [PgC] between Approximation Method and Simulation Method Monthly Mean in 2006, the North Pacific Ocean based on January 1991. (a)-(l) represents January-December**



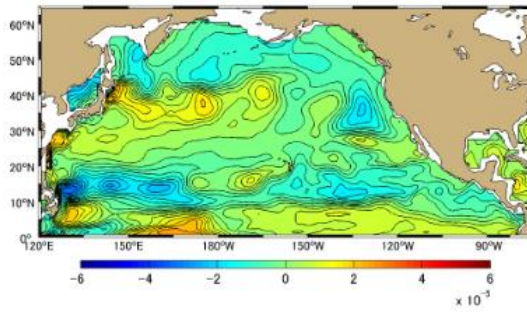
(a)



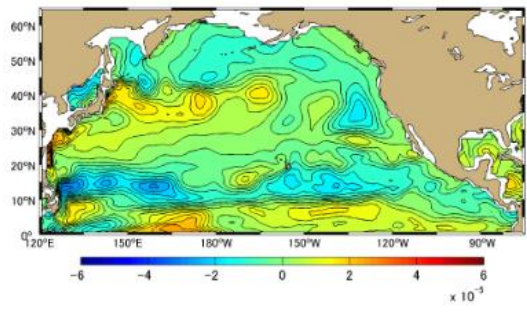
(b)



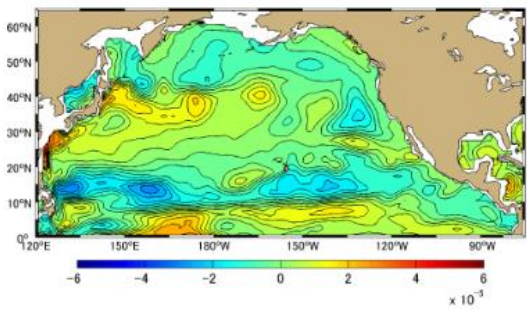
(c)



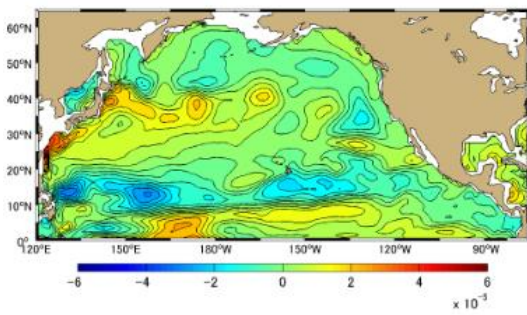
(d)



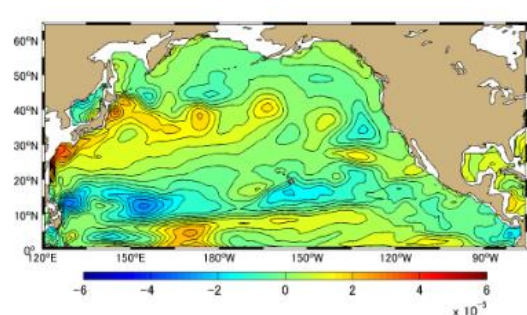
(e)



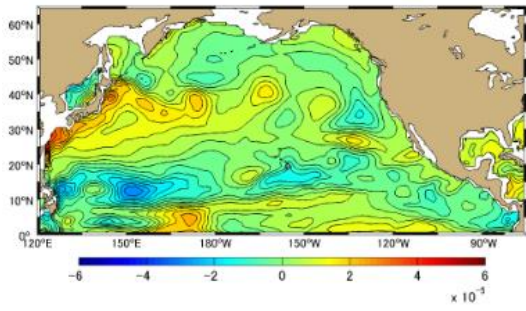
(f)



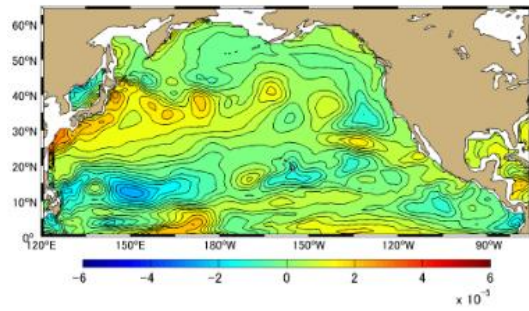
(g)



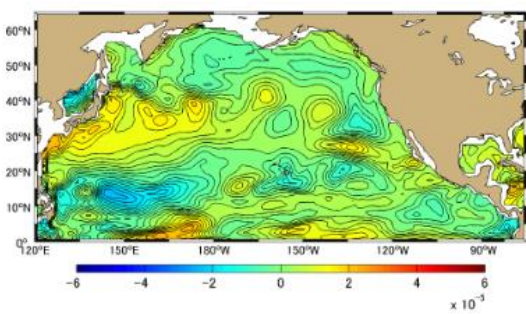
(h)



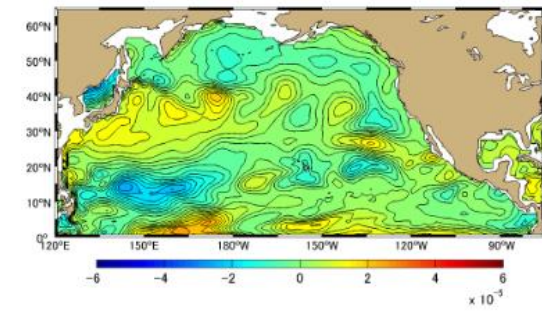
(i)



(j)

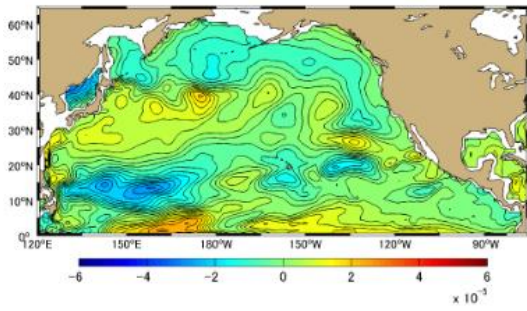


(k)

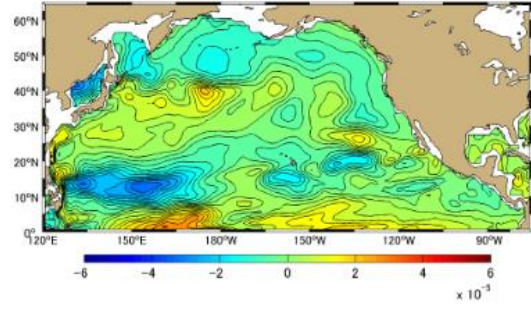


(l)

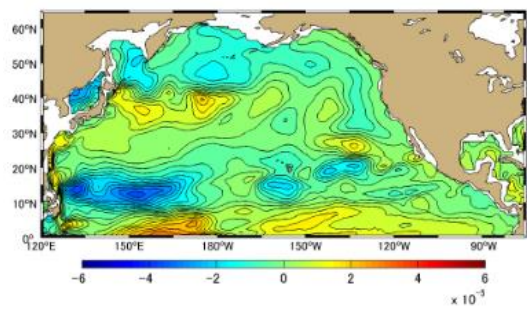
Figure A-2.17 Difference [PgC] between Approximation Method and Simulation Method Monthly Mean in 2007, the North Pacific Ocean based on January 1991. (a)-(l) represents January-December



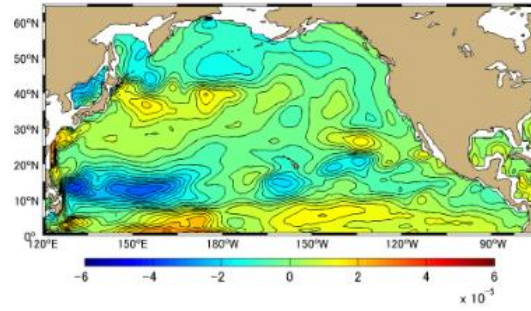
(a)



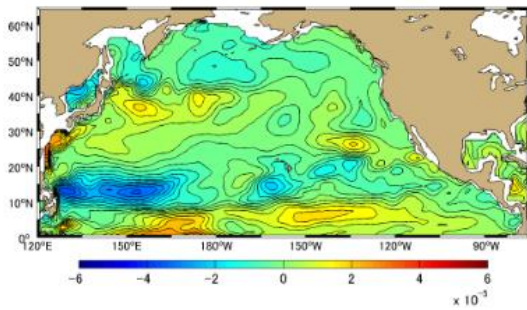
(b)



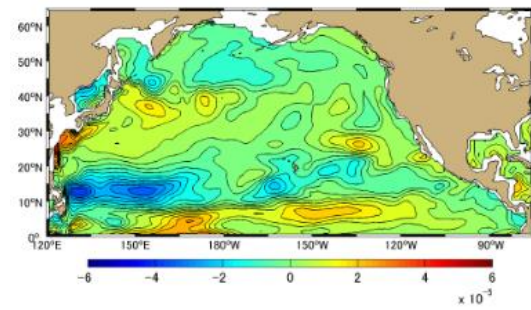
(c)



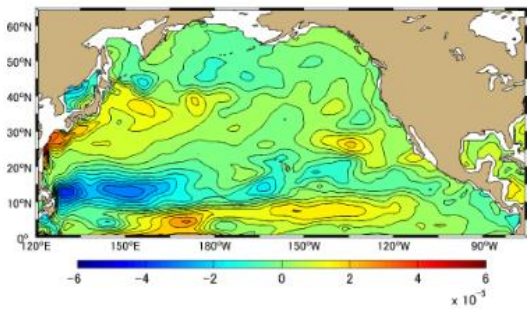
(d)



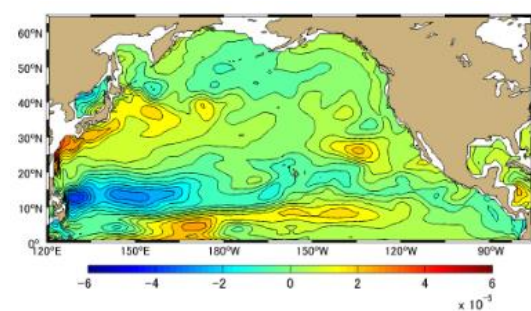
(e)



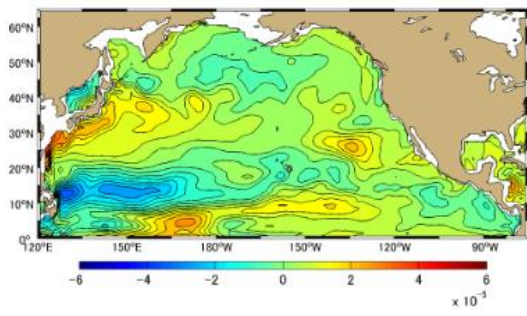
(f)



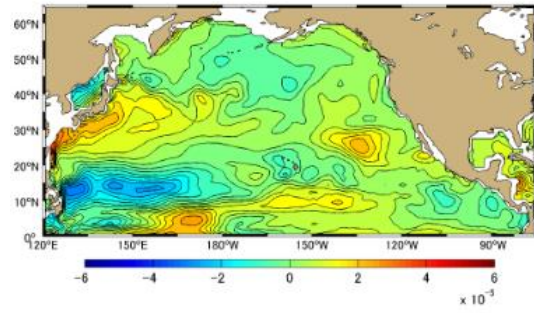
(g)



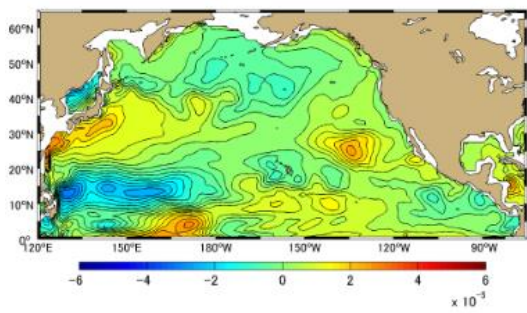
(h)



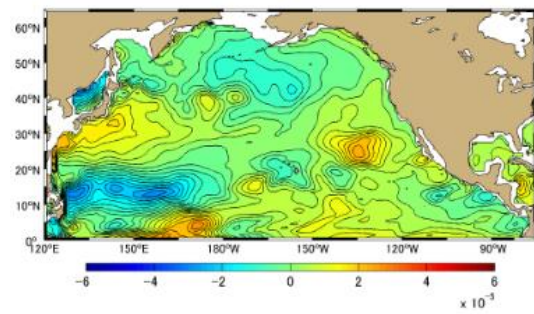
(i)



(j)

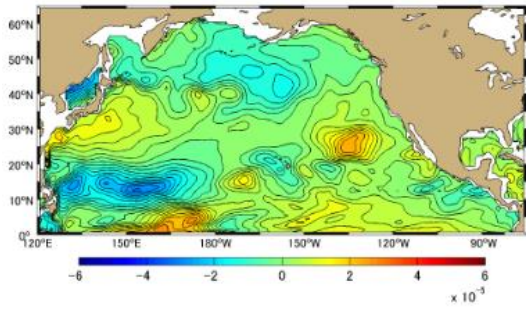


(k)

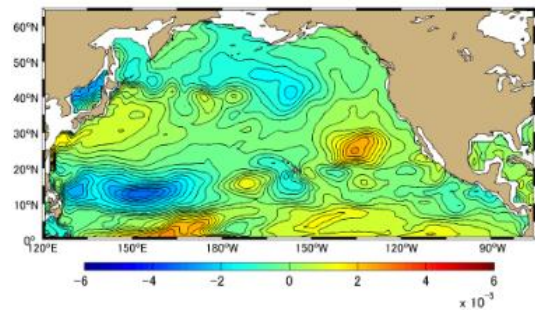


(l)

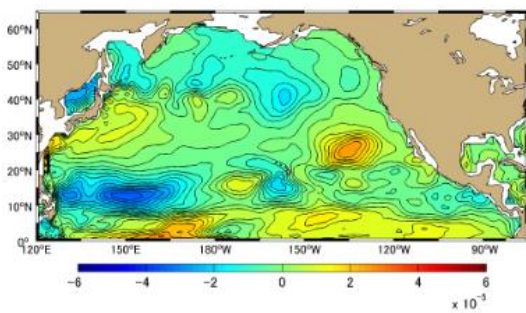
**Figure A-2.18 Difference [PgC] between Approximation Method and Simulation Method Monthly Mean in 2008, the North Pacific Ocean based on January 1991. (a)-(l) represents January-December**



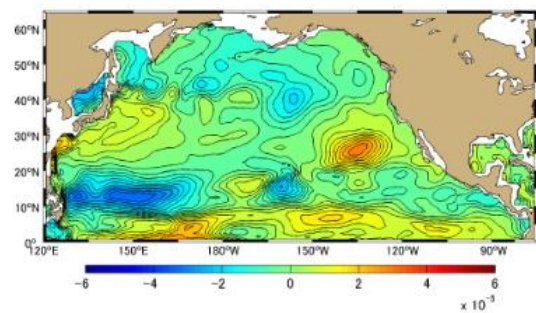
(a)



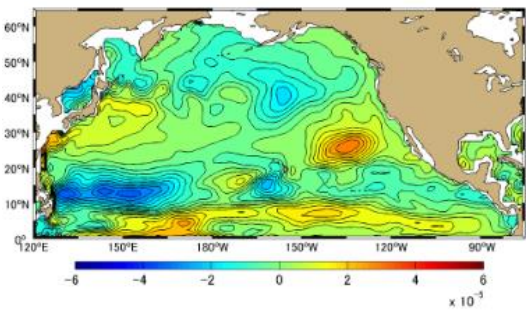
(b)



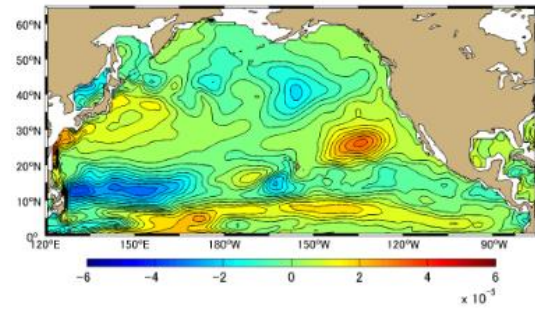
(c)



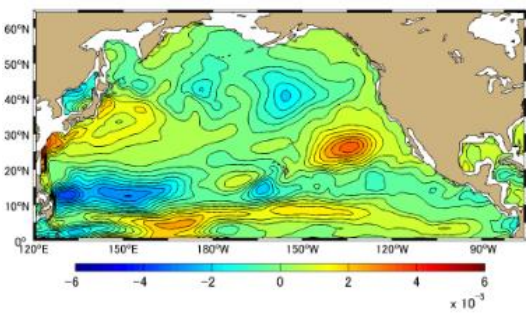
(d)



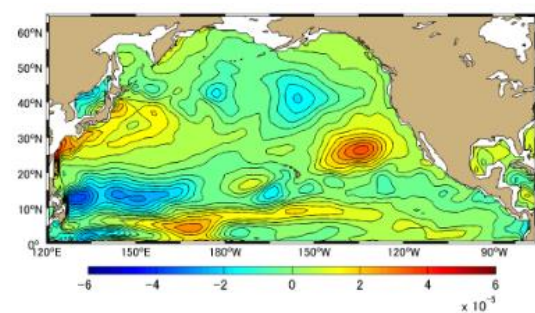
(e)



(f)



(g)



(h)



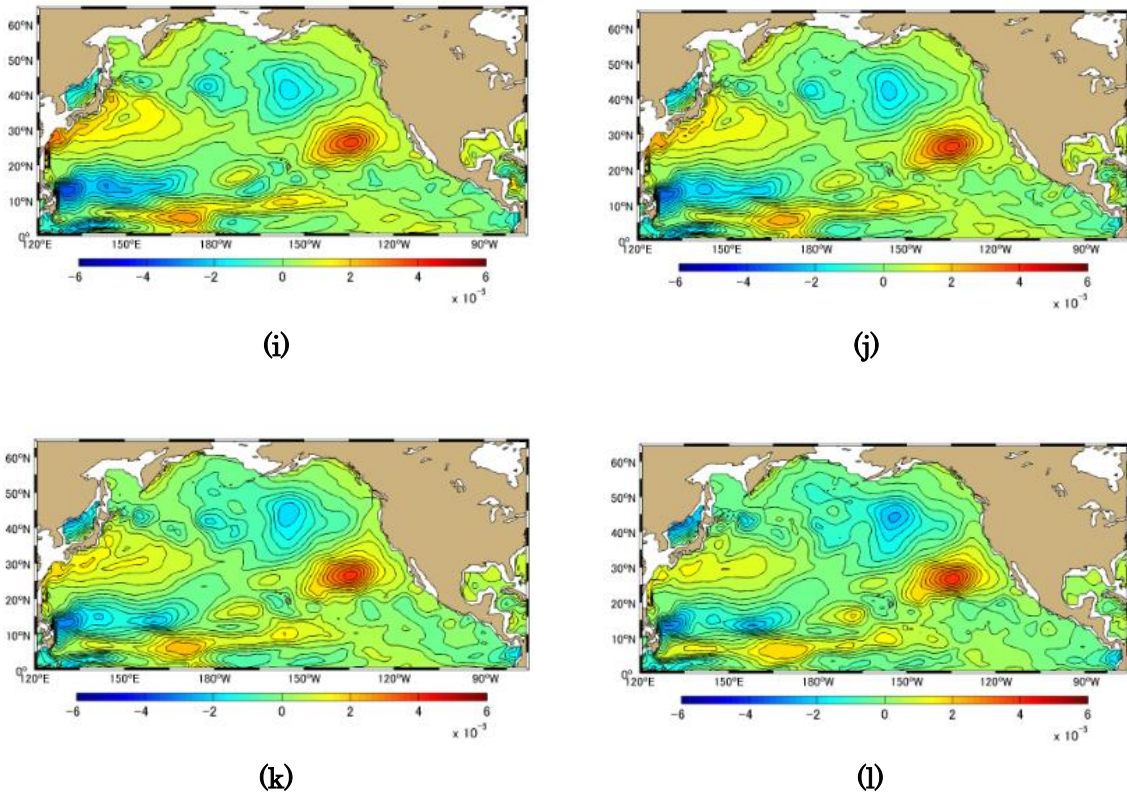
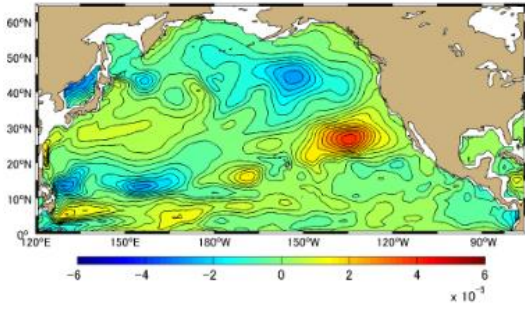
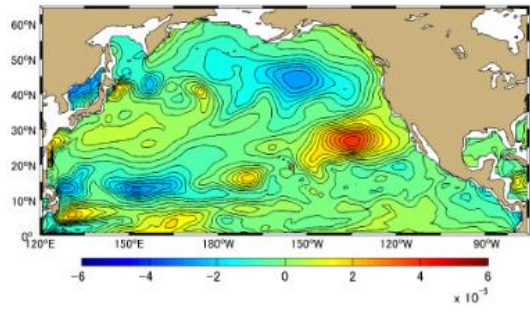


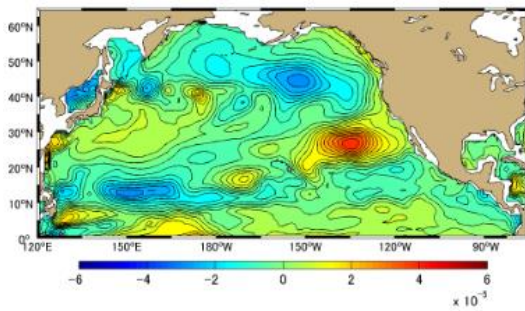
Figure A-2.19 Difference [PgC] between Approximation Method and Simulation Method Monthly Mean in 2009, the North Pacific Ocean based on January 1991. (a)-(l) represents January-December



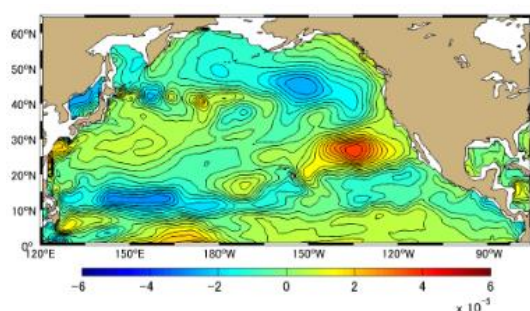
(a)



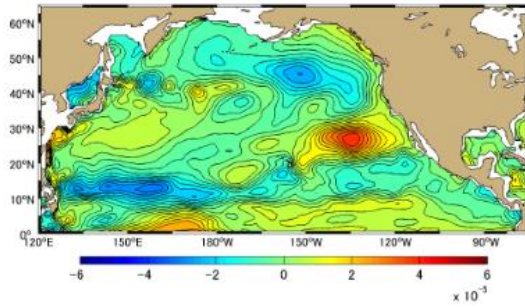
(b)



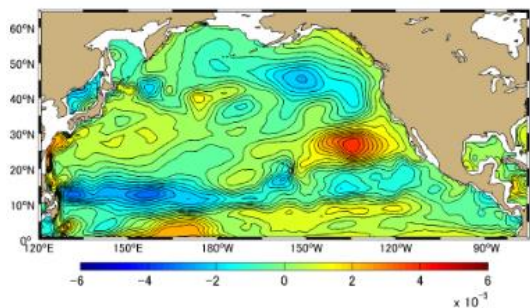
(c)



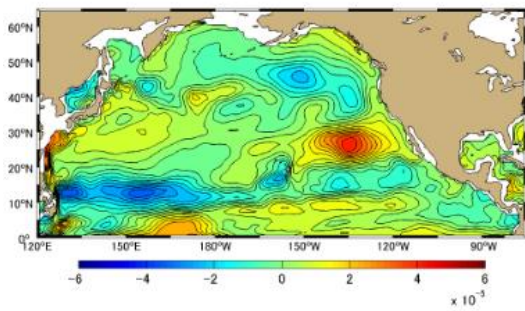
(d)



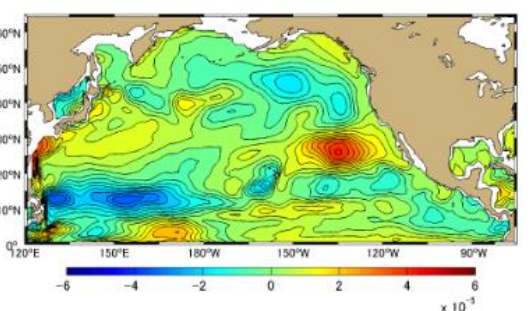
(e)



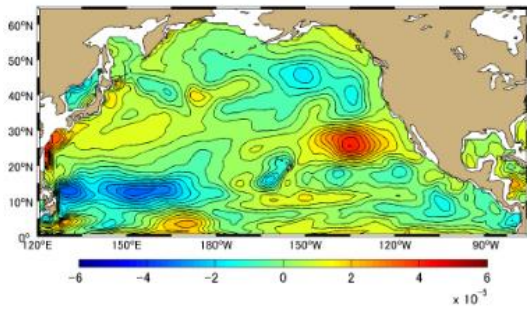
(f)



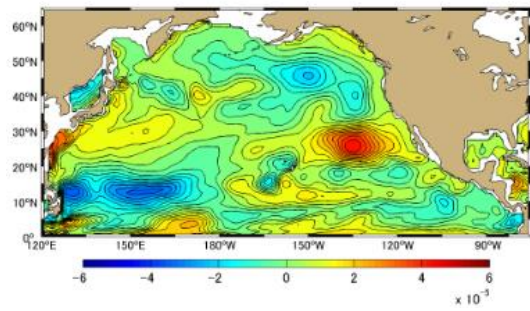
(g)



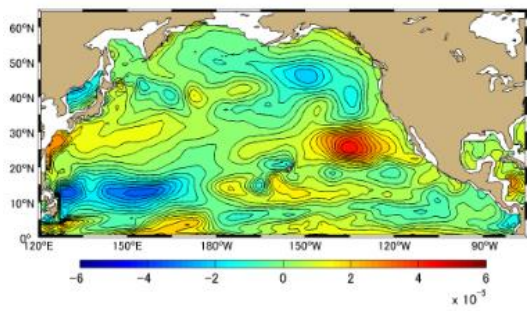
(h)



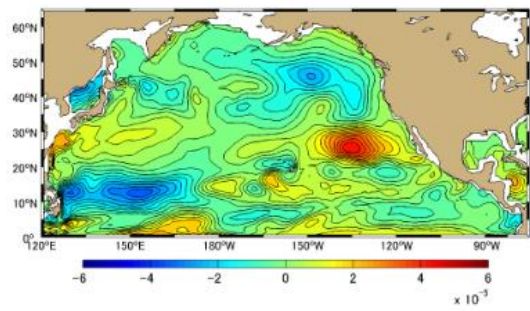
(i)



(j)

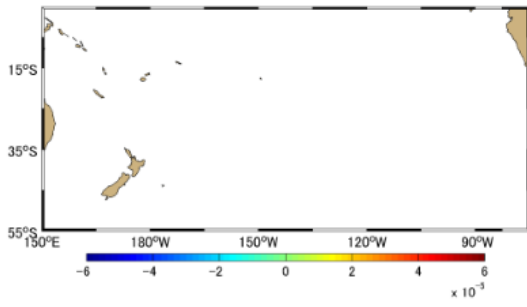


(k)

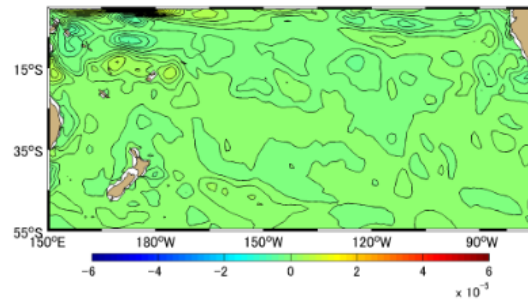


(l)

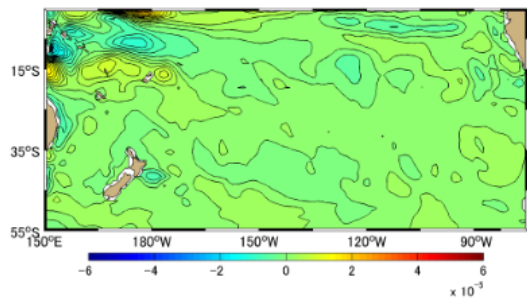
**Figure A-2.20 Difference [PgC] between Approximation Method and Simulation Method Monthly Mean in 2010, the North Pacific Ocean based on January 1991. (a)-(l) represents January-December**



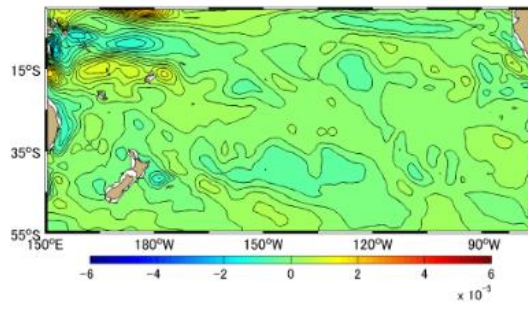
(a)



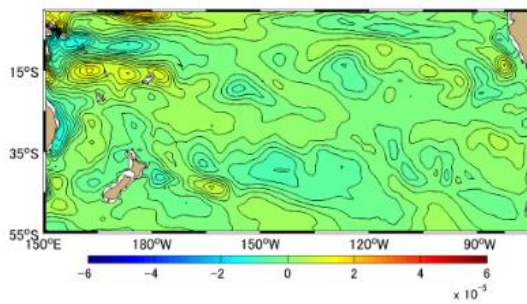
(b)



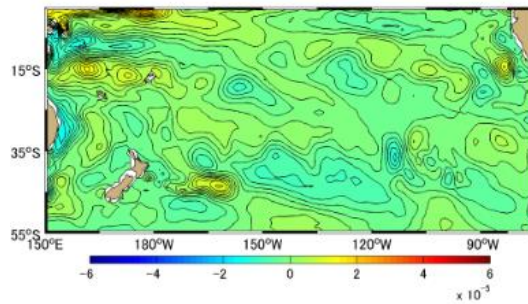
(c)



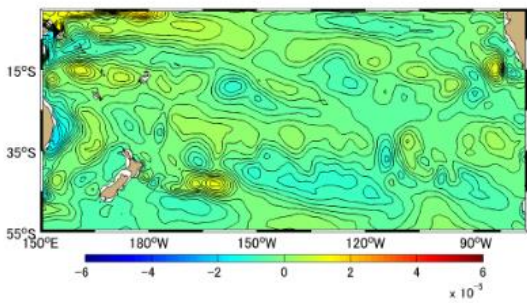
(d)



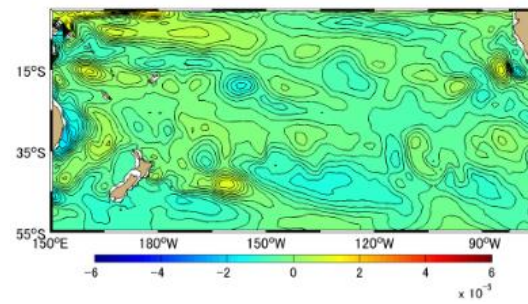
(e)



(f)



(g)



(h)

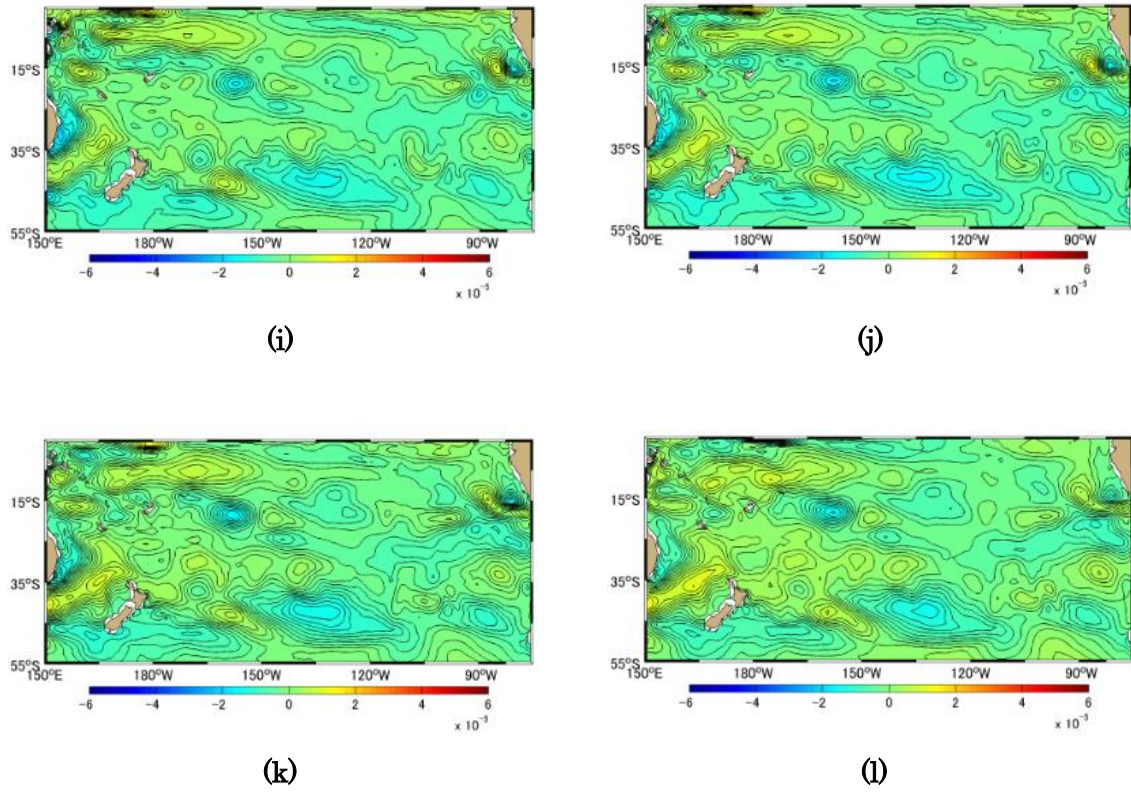
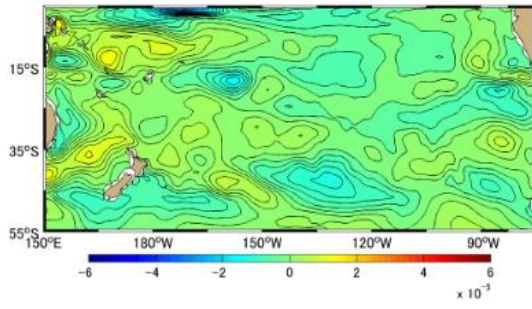
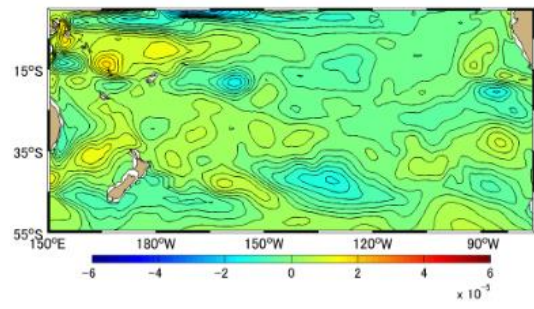


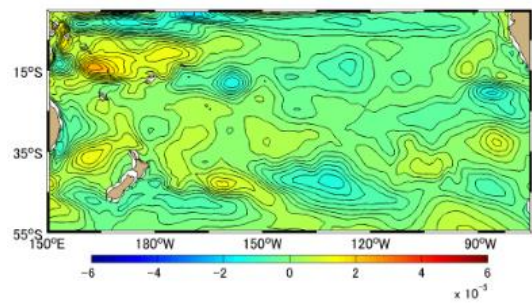
**Figure A-3.1 Difference [PgC] between Approximation Method and Simulation Method Monthly Mean in 1991, the South Pacific Ocean based on January 1991. (a)-(l) represents January-December**



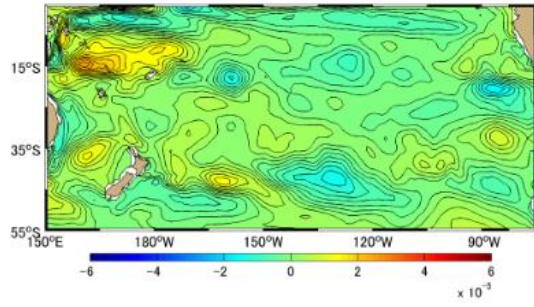
(a)



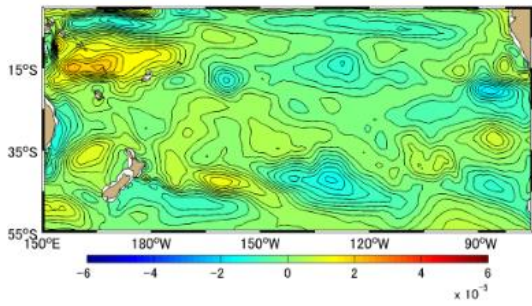
(b)



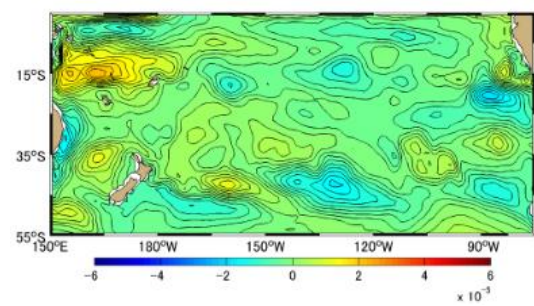
(c)



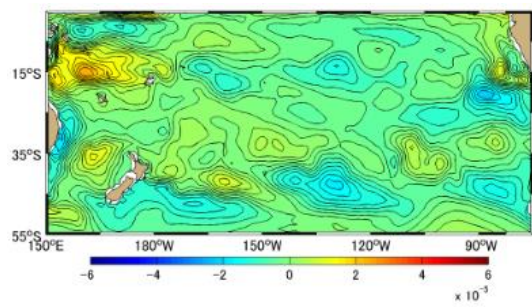
(d)



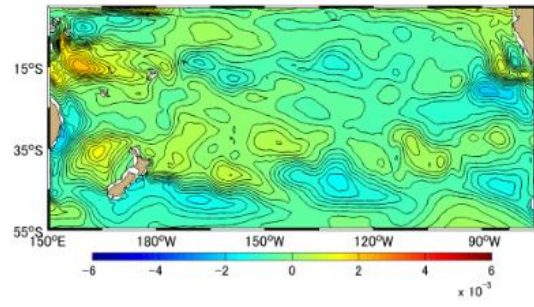
(e)



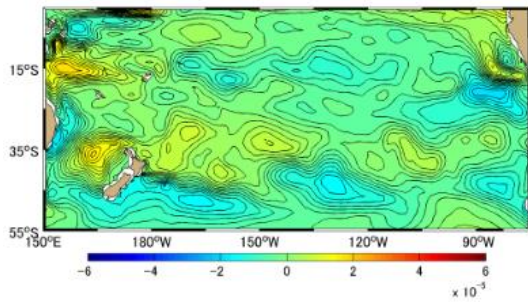
(f)



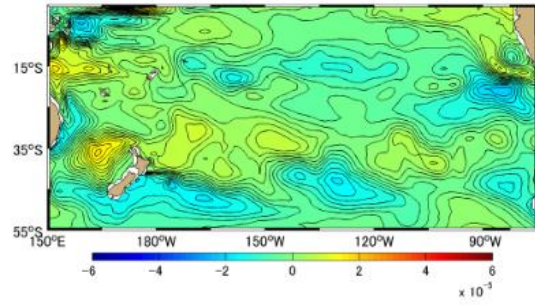
(g)



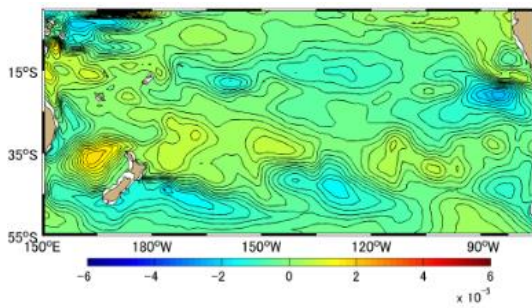
(h)



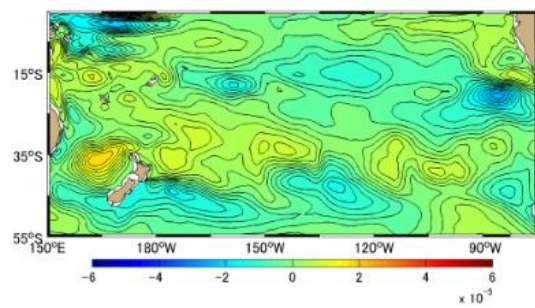
(i)



(j)

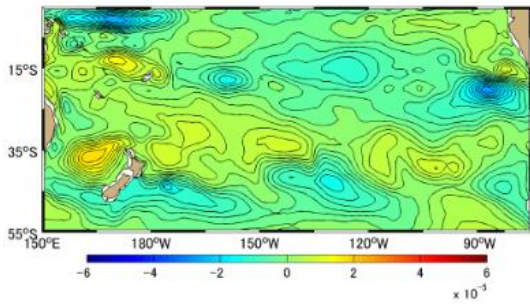


(k)

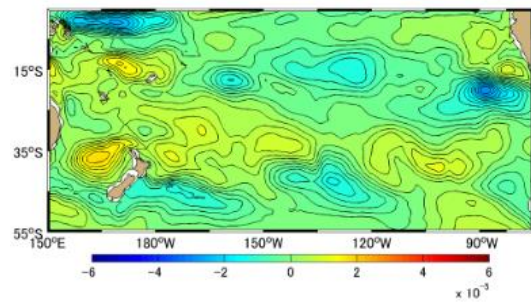


(l)

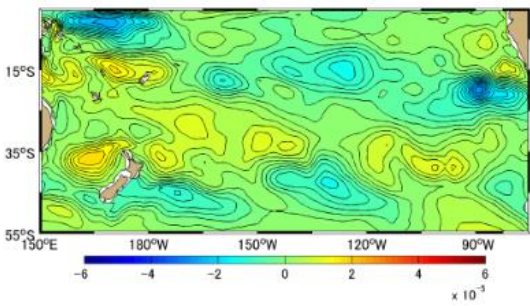
**Figure A-3.2 Difference [PgC] between Approximation Method and Simulation Method Monthly Mean in 1992, the South Pacific Ocean based on January 1991. (a)-(l) represents January-December**



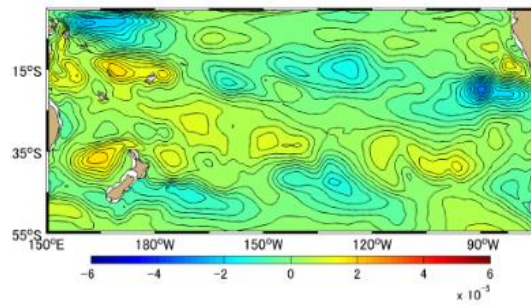
(a)



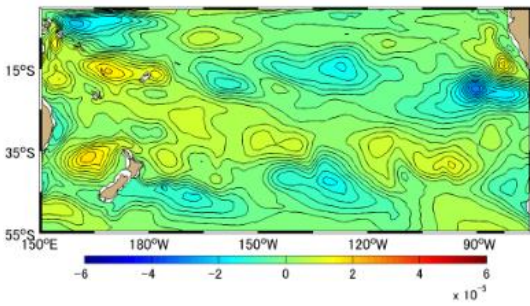
(b)



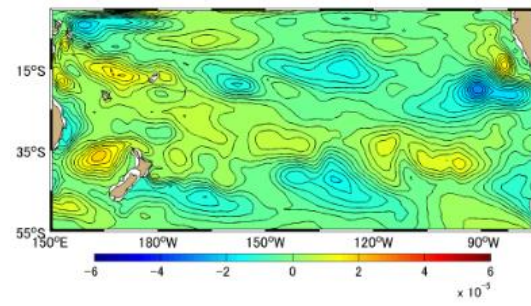
(c)



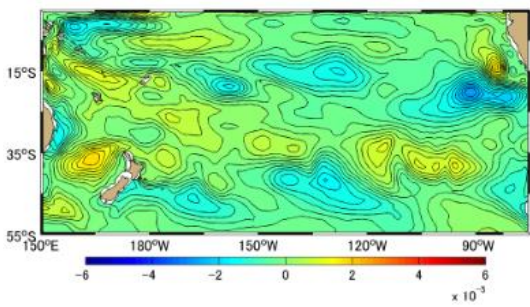
(d)



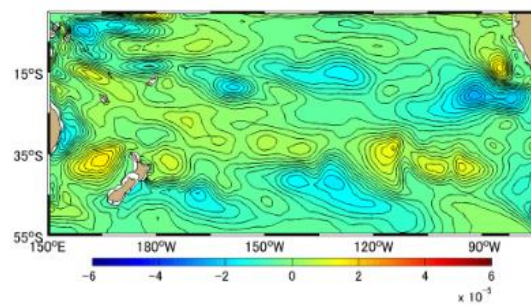
(e)



(f)



(g)



(h)



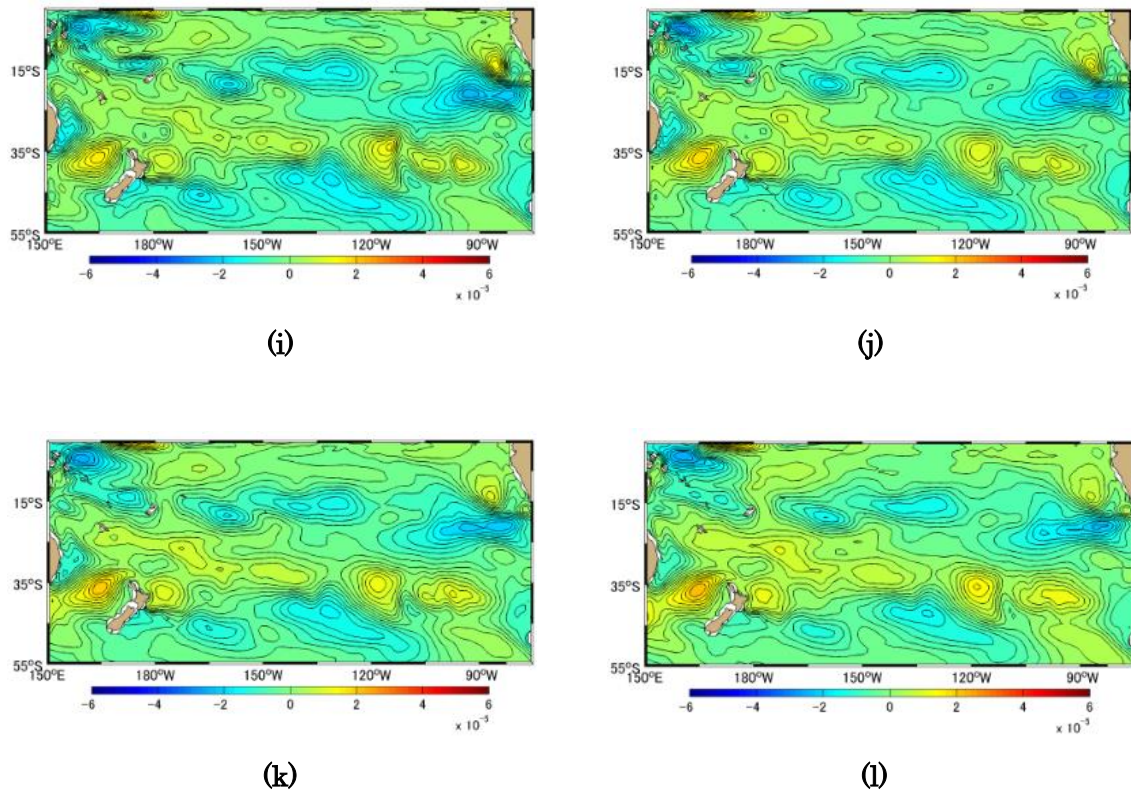
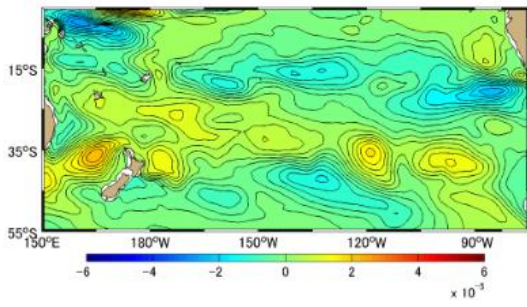
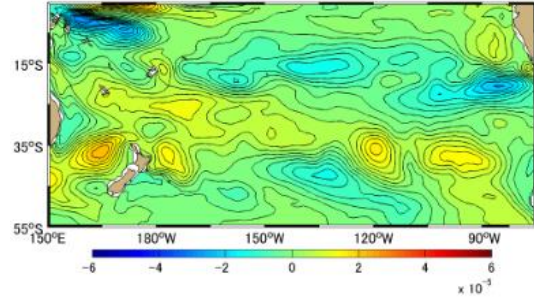


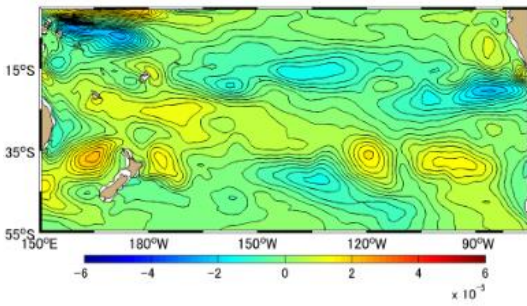
**Figure A-3.3** Difference [PgC] between Approximation Method and Simulation Method Monthly Mean in 1993, the South Pacific Ocean based on January 1991. (a)-(l) represents January-December



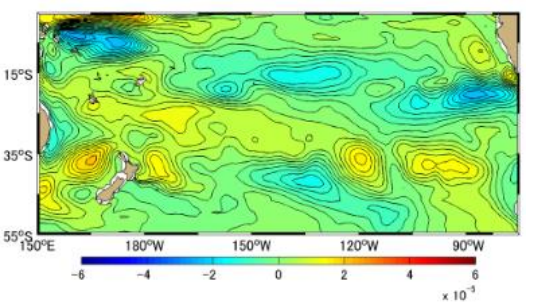
(a)



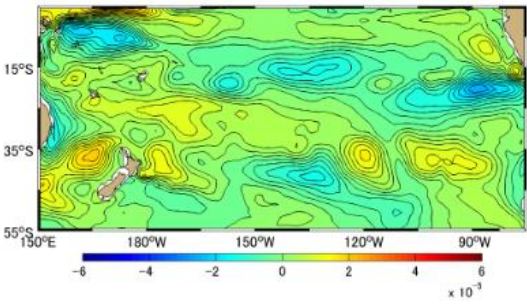
(b)



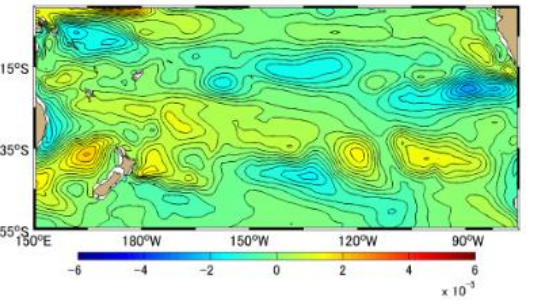
(c)



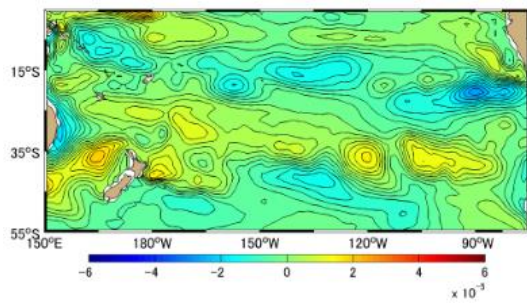
(d)



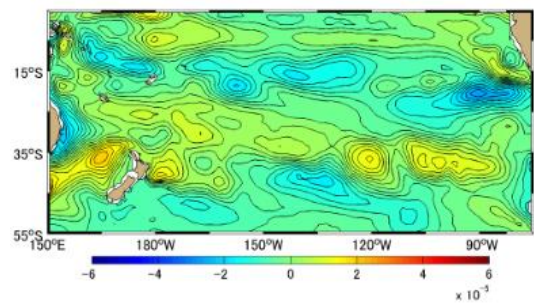
(e)



(f)



(g)



(h)

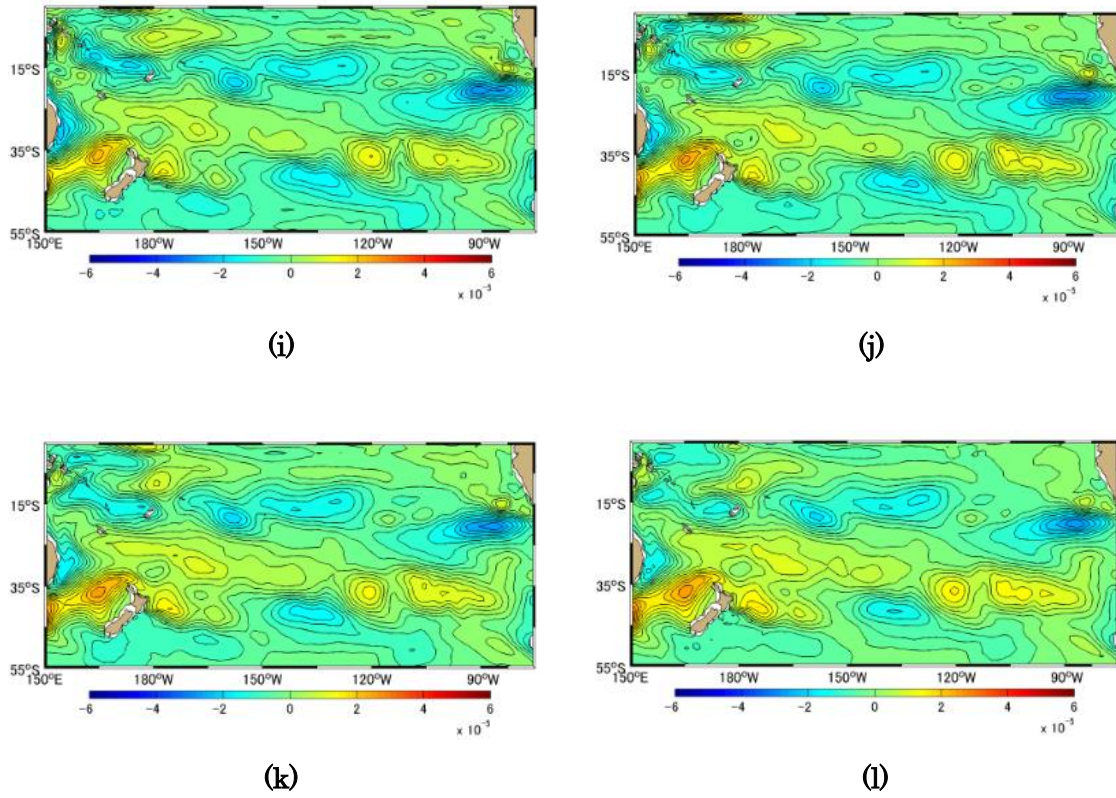
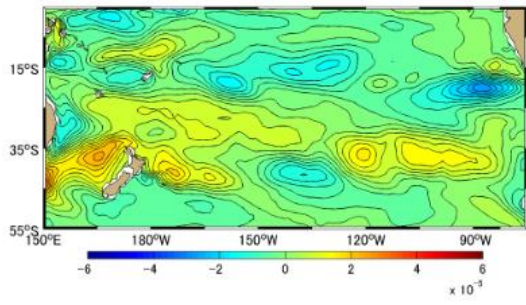
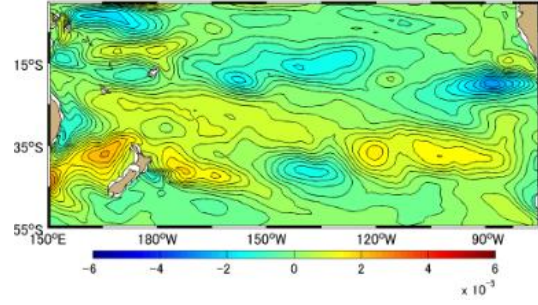


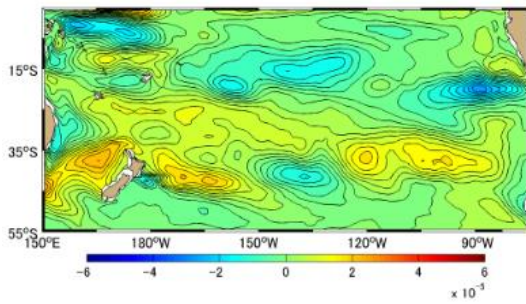
**Figure A-3.4** Difference [PgC] between Approximation Method and Simulation Method Monthly Mean in 1994, the South Pacific Ocean based on January 1991. (a)-(l) represents January-December



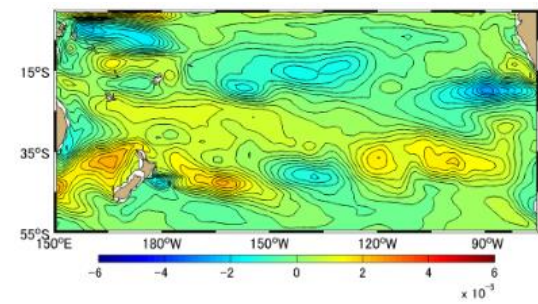
(a)



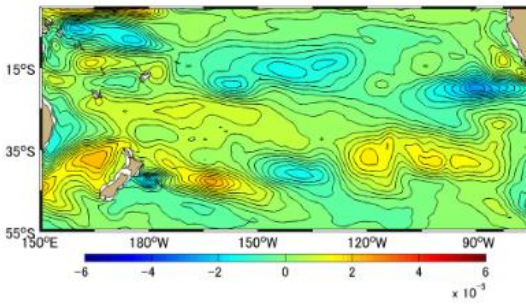
(b)



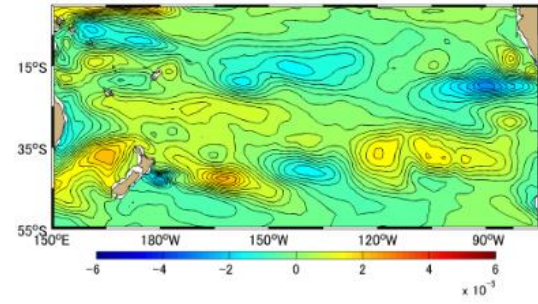
(c)



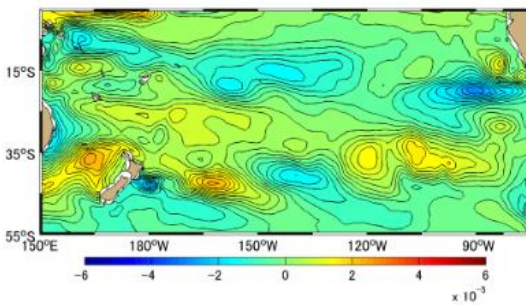
(d)



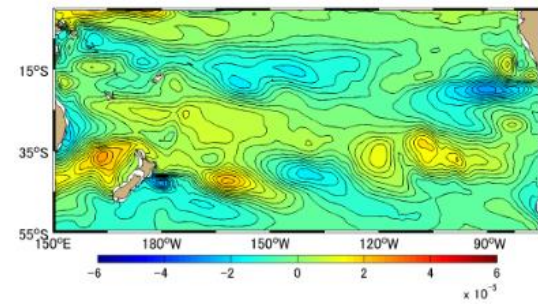
(e)



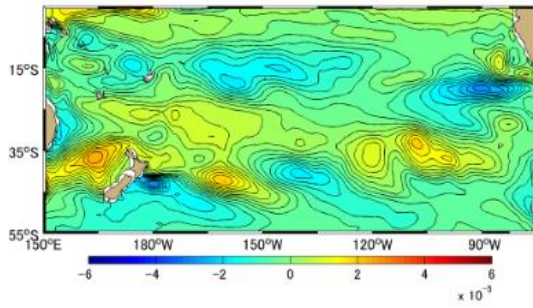
(f)



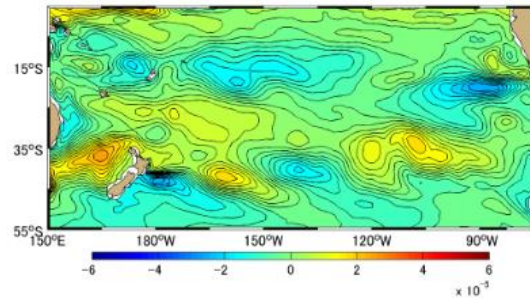
(g)



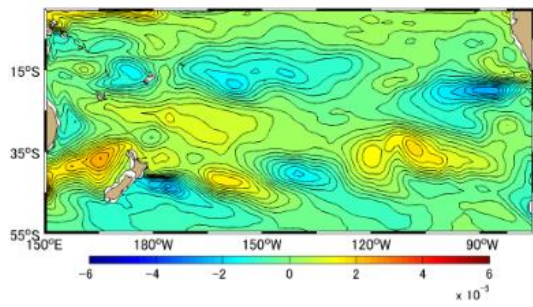
(h)



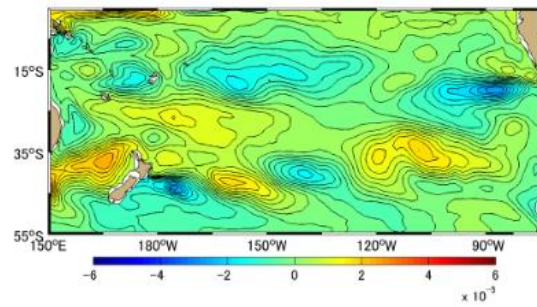
(i)



(j)

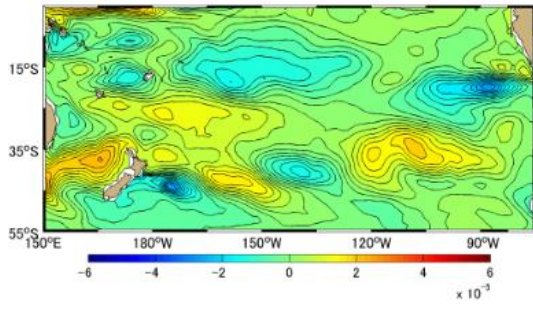


(k)

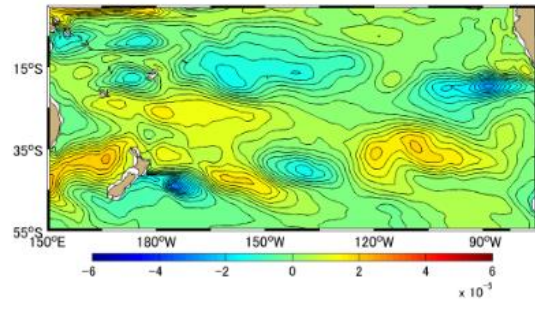


(l)

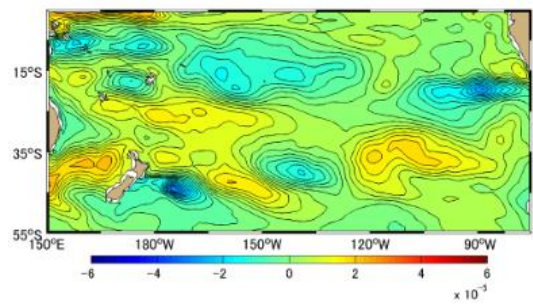
**Figure A-3.5 Difference [PgC] between Approximation Method and Simulation Method Monthly Mean in 1995, the South Pacific Ocean based on January 1991. (a)-(l) represents January-December**



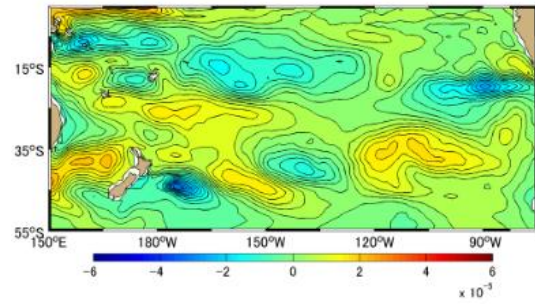
(a)



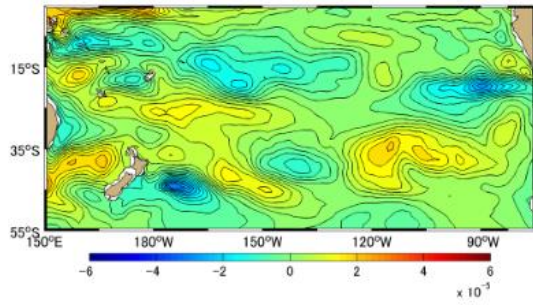
(b)



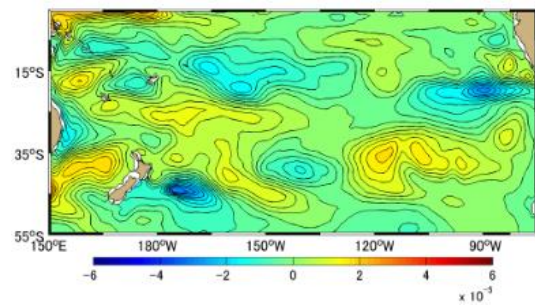
(c)



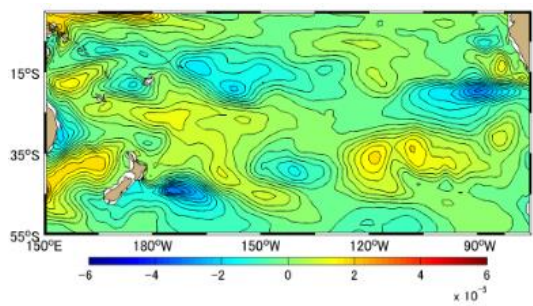
(d)



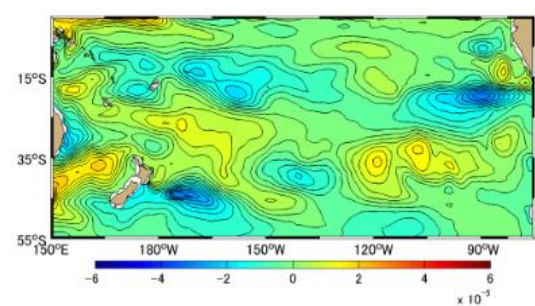
(e)



(f)



(g)



(h)

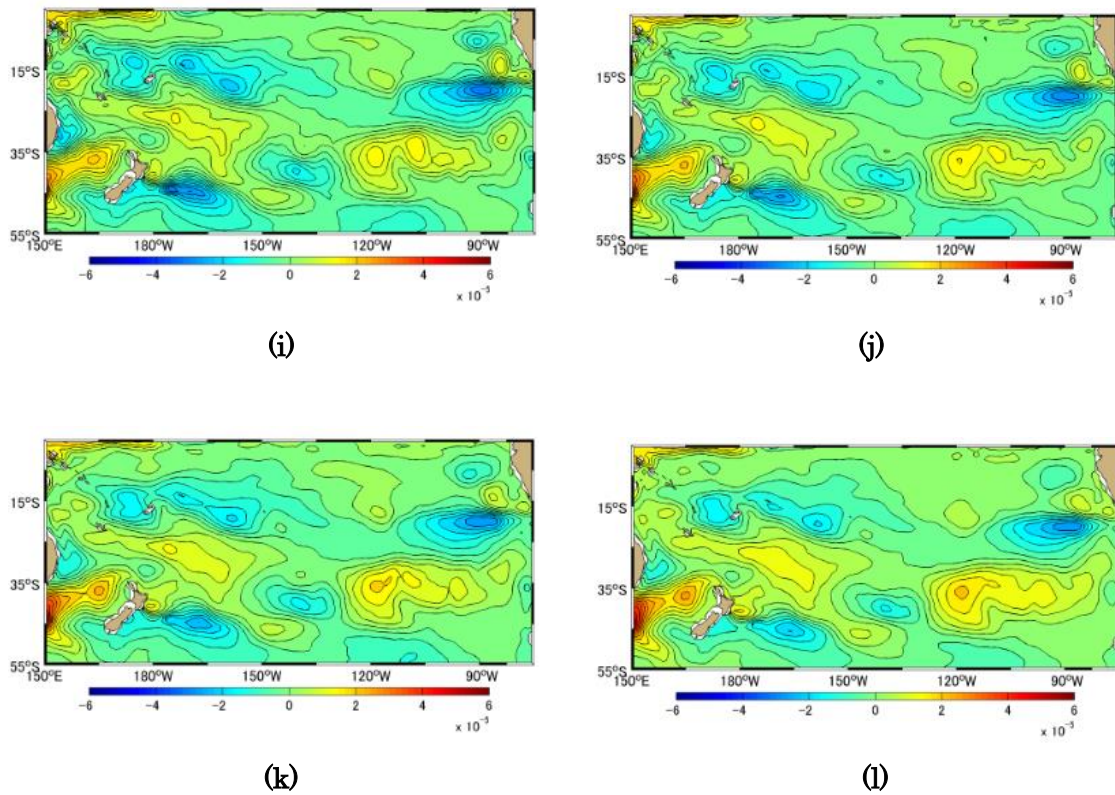
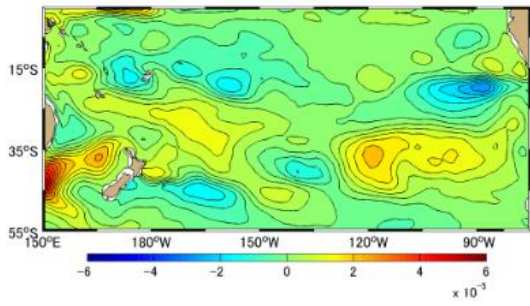
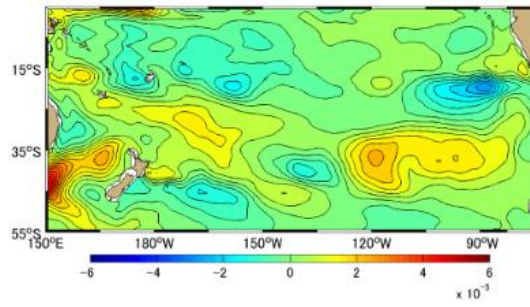


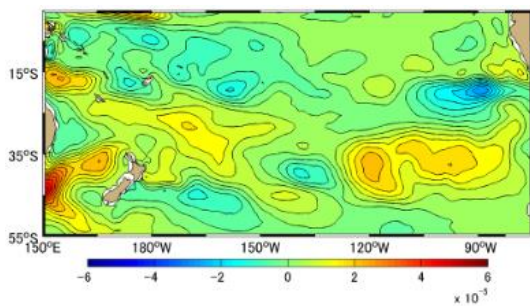
**Figure A-3.6** Difference [PgC] between Approximation Method and Simulation Method Monthly Mean in 1996, the South Pacific Ocean based on January 1991. (a)-(l) represents January-December



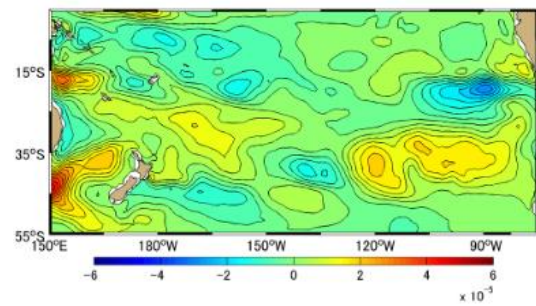
(a)



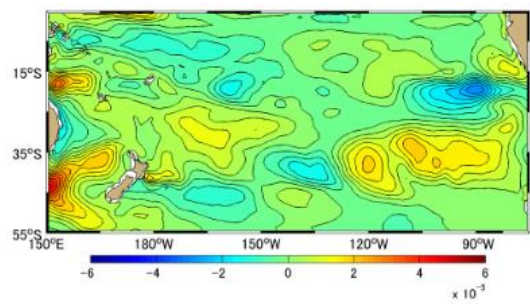
(b)



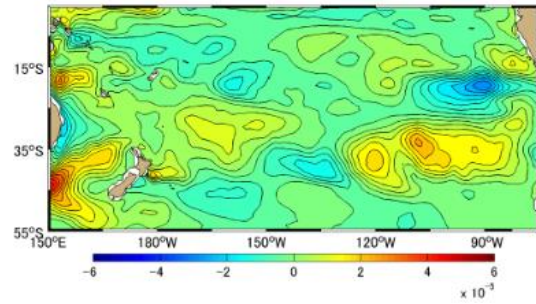
(c)



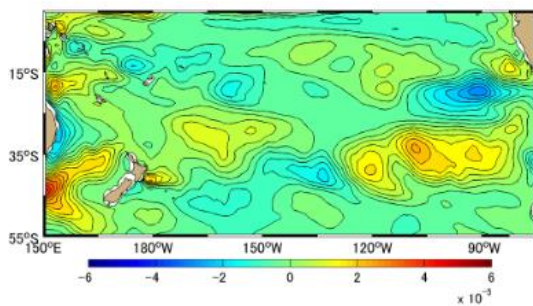
(d)



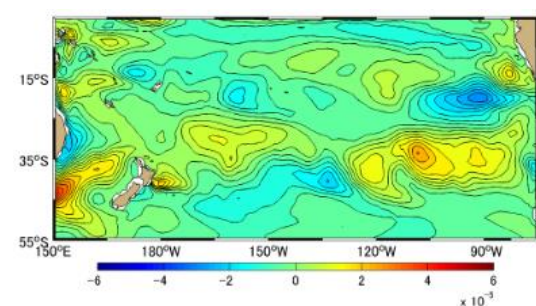
(e)



(f)



(g)



(h)



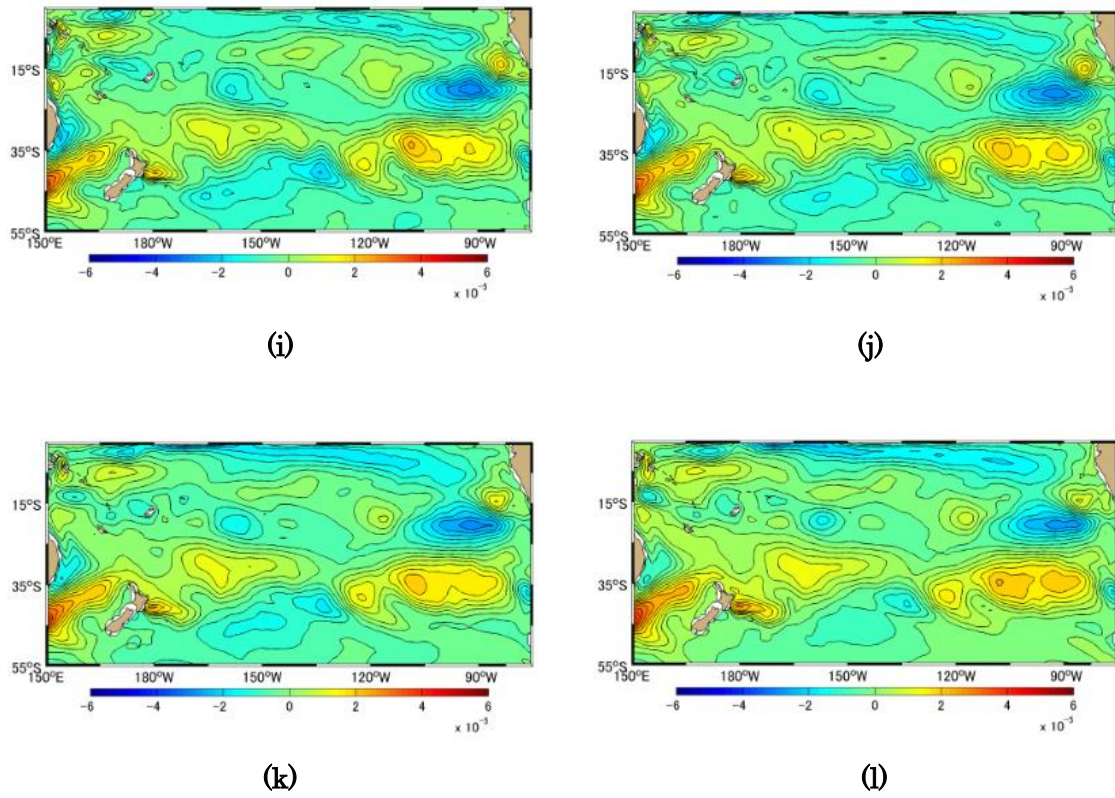
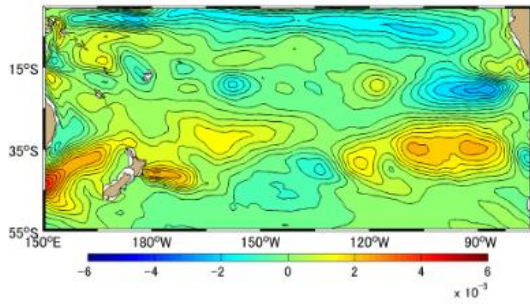
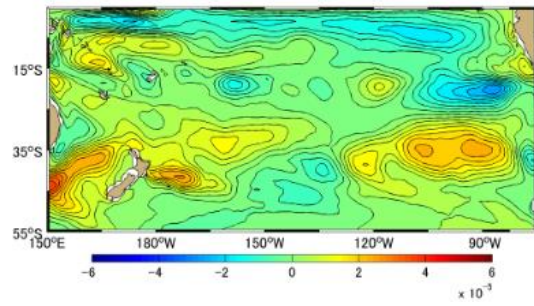


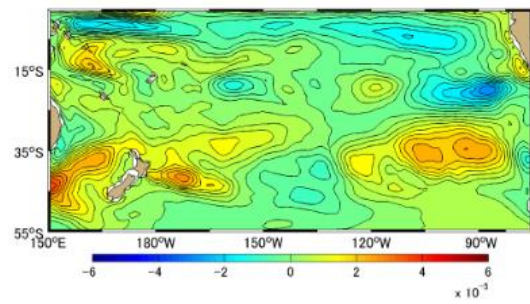
**Figure A-3.7** Difference [PgC] between Approximation Method and Simulation Method Monthly Mean in 1997, the South Pacific Ocean based on January 1991. (a)-(l) represents January-December



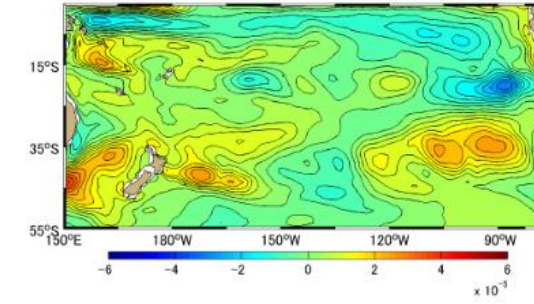
(a)



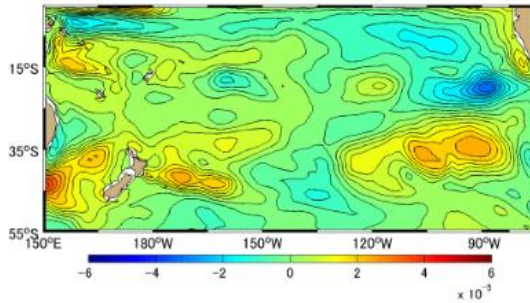
(b)



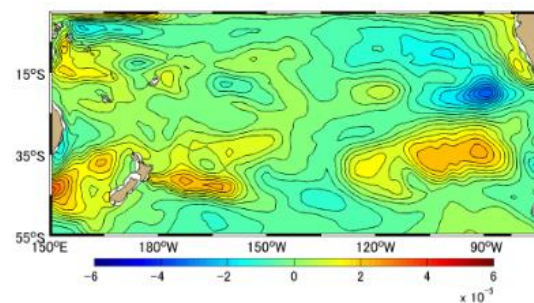
(c)



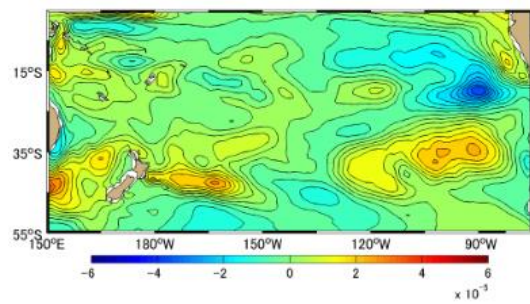
(d)



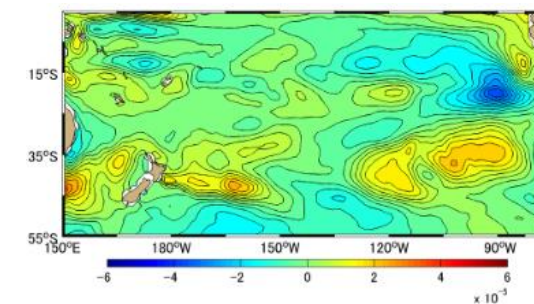
(e)



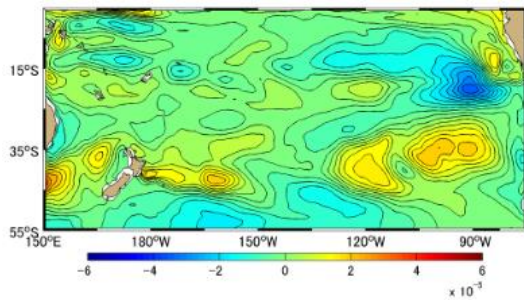
(f)



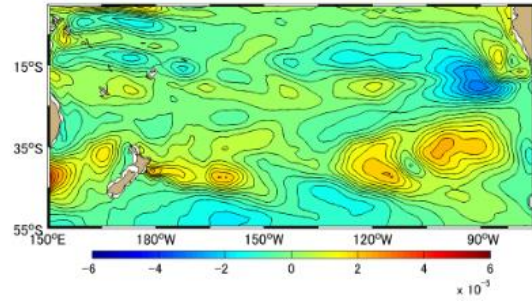
(g)



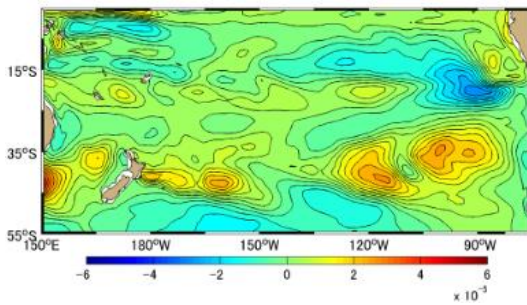
(h)



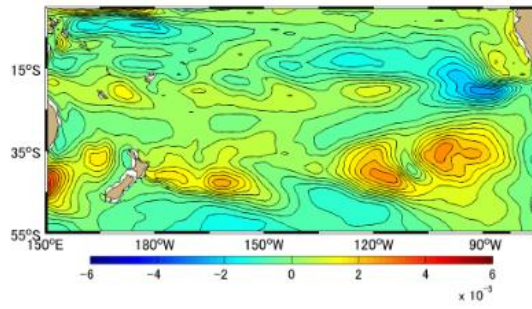
(i)



(j)

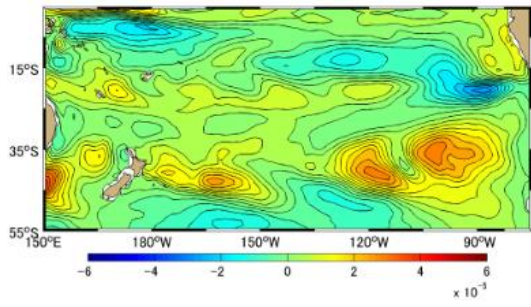


(k)

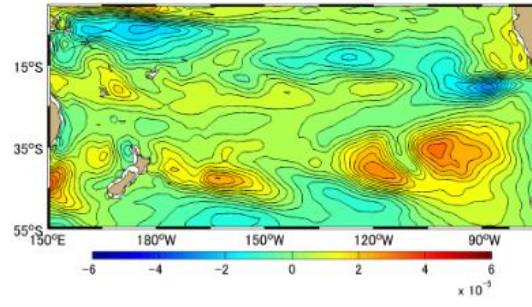


(l)

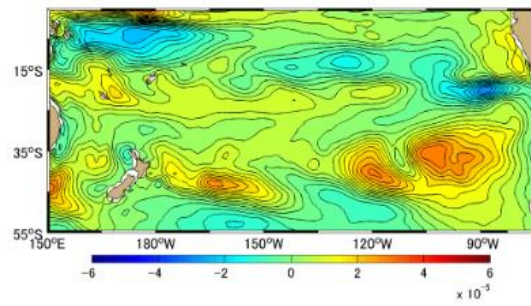
**Figure A-3.8 Difference [PgC] between Approximation Method and Simulation Method Monthly Mean in 1998, the South Pacific Ocean based on January 1991. (a)-(l) represents January-December**



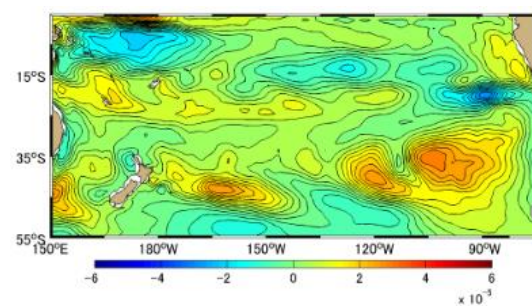
(a)



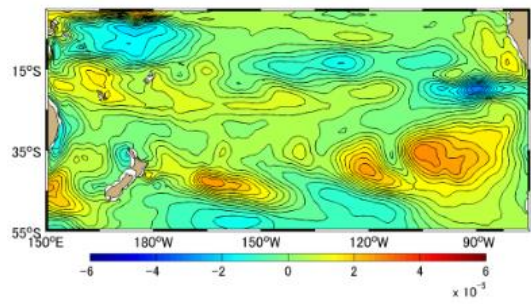
(b)



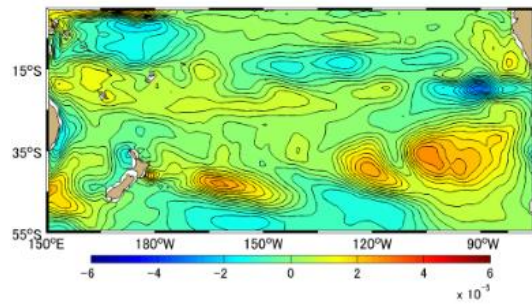
(c)



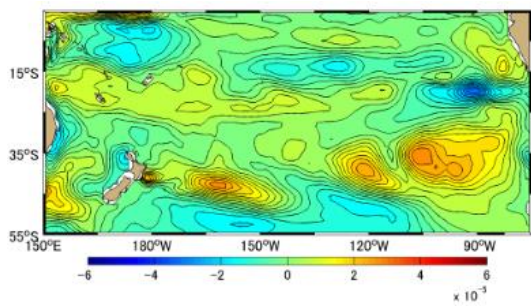
(d)



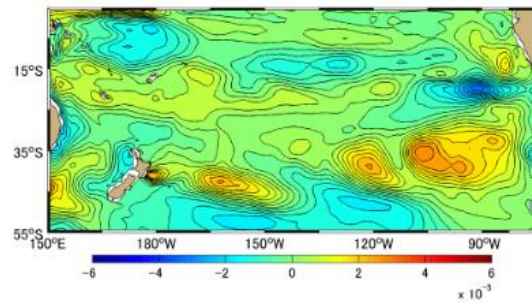
(e)



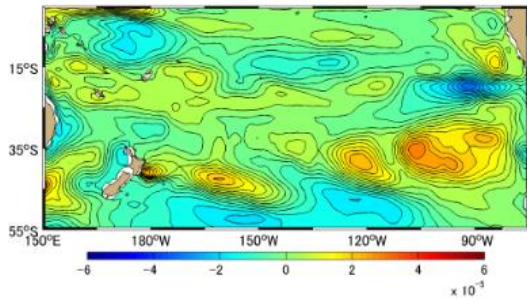
(f)



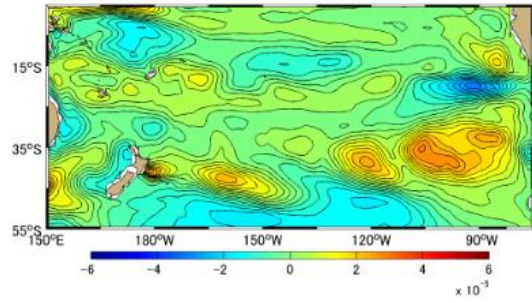
(g)



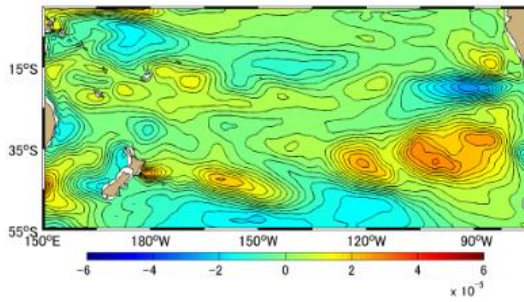
(h)



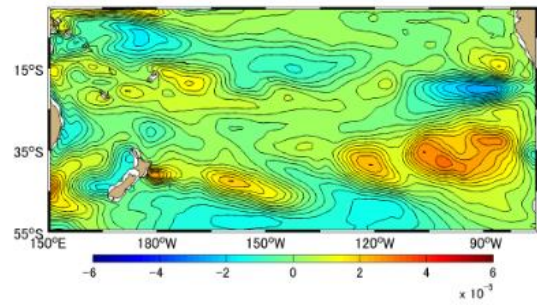
(i)



(j)

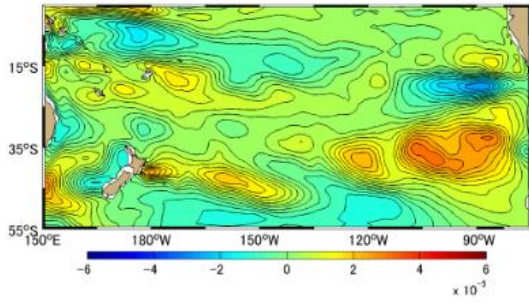


(k)

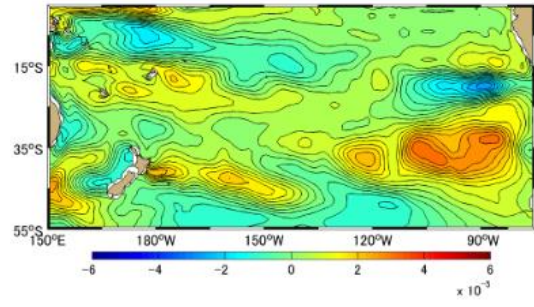


(l)

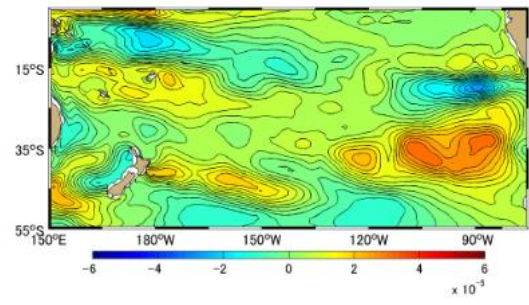
Figure A-3.9 Difference [PgC] between Approximation Method and Simulation Method Monthly Mean in 1999, the South Pacific Ocean based on January 1991. (a)-(l) represents January-December



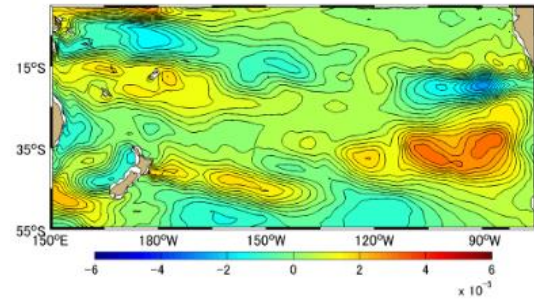
(a)



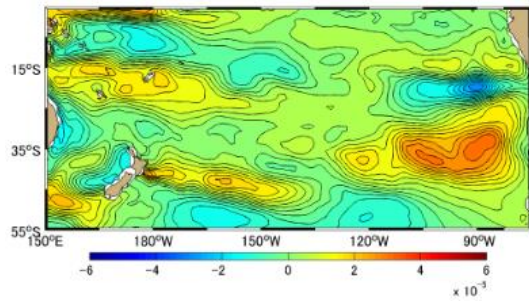
(b)



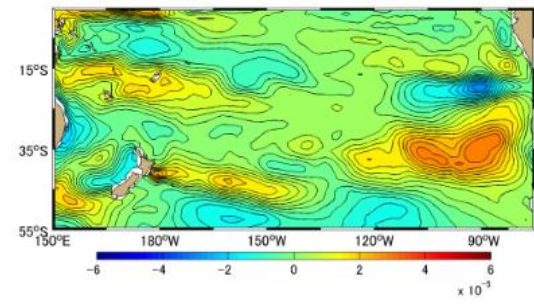
(c)



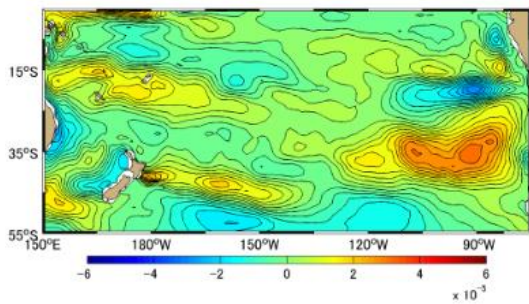
(d)



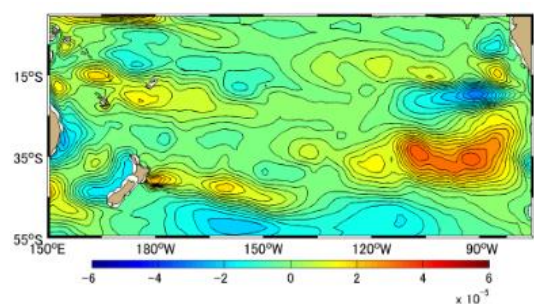
(e)



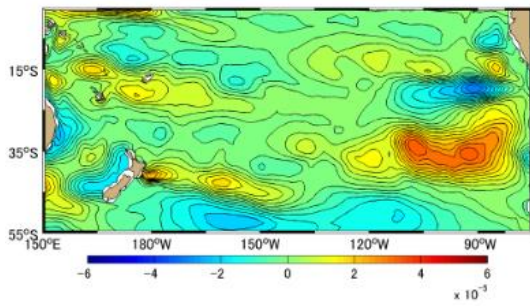
(f)



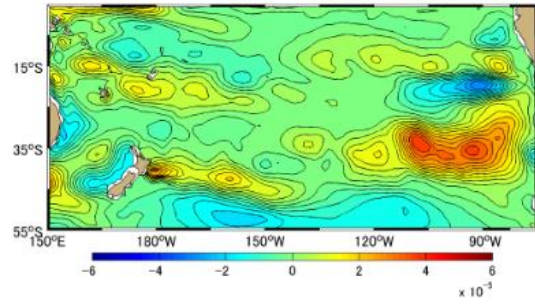
(g)



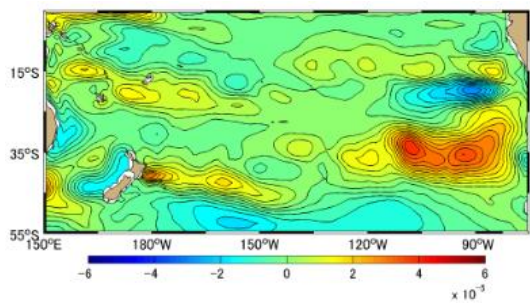
(h)



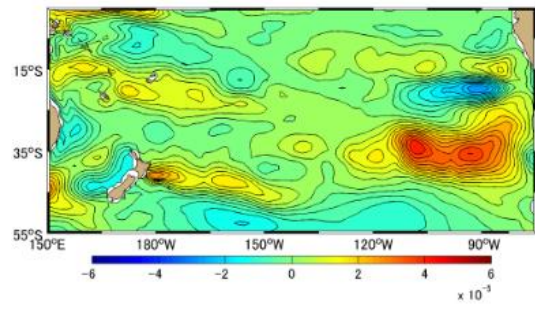
(i)



(j)

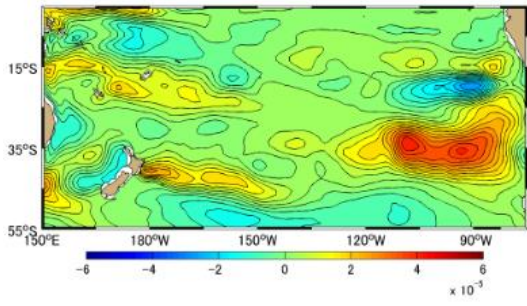


(k)

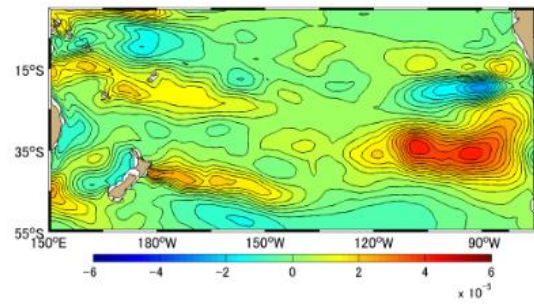


(l)

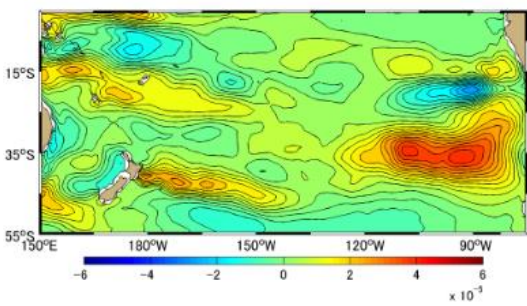
**Figure A-3.10 Difference [PgC] between Approximation Method and Simulation Method Monthly Mean in 2000, the South Pacific Ocean based on January 1991. (a)-(l) represents January-December**



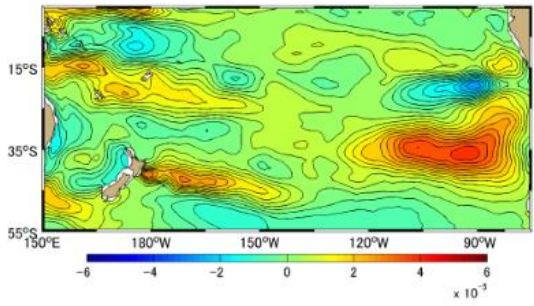
(a)



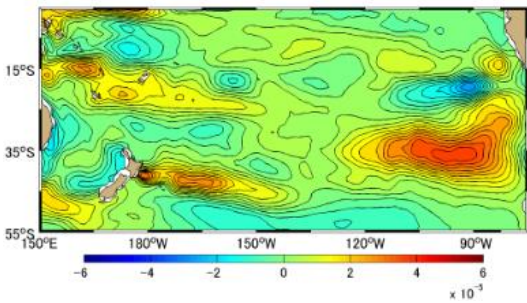
(b)



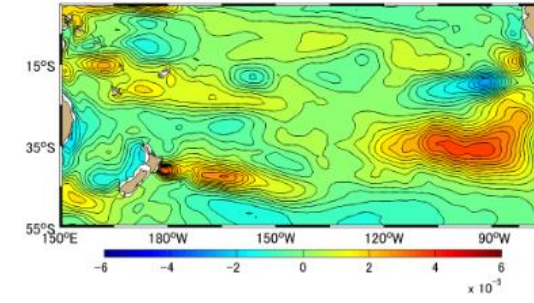
(c)



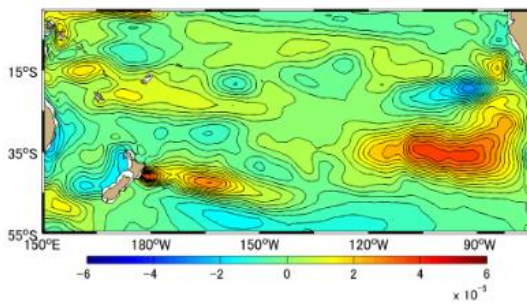
(d)



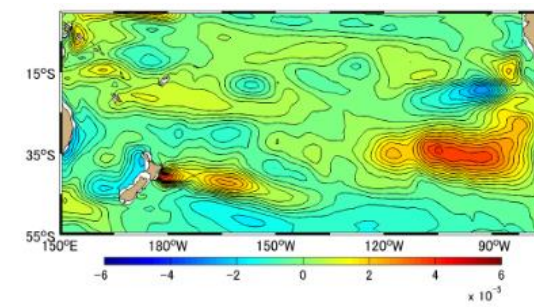
(e)



(f)



(g)



(h)



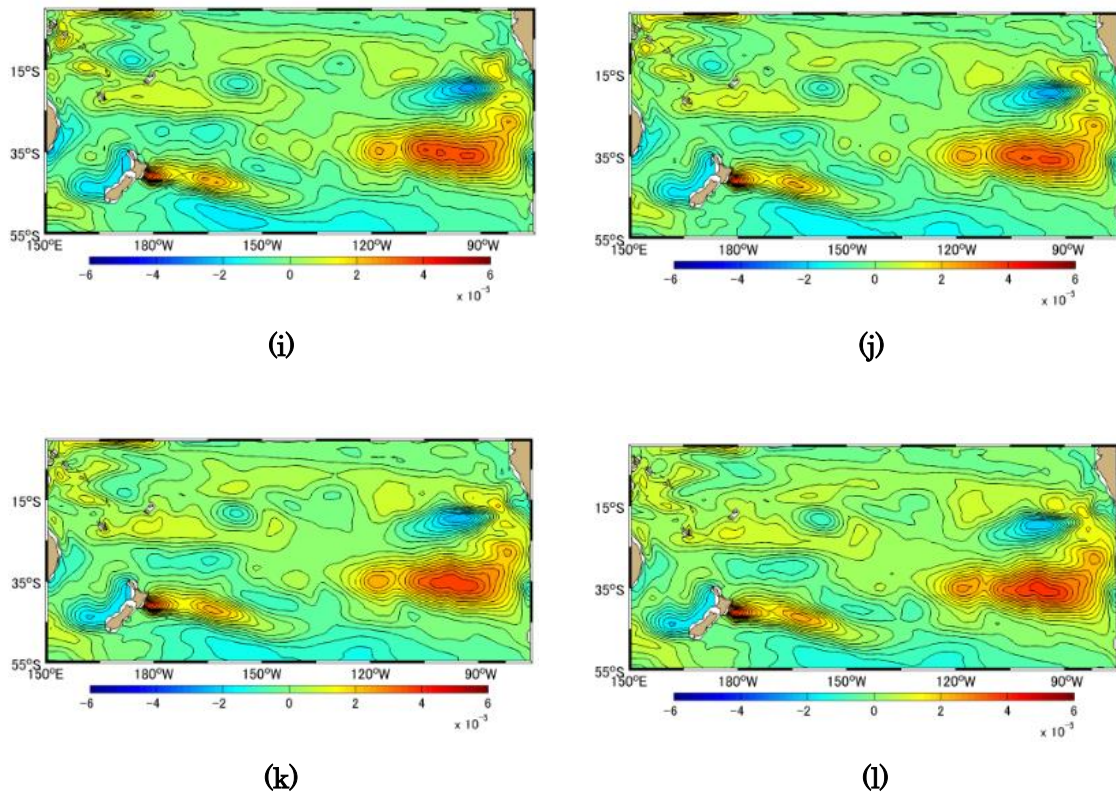
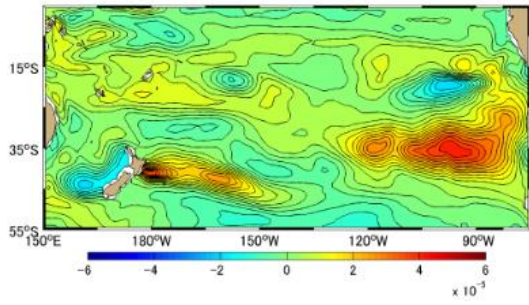
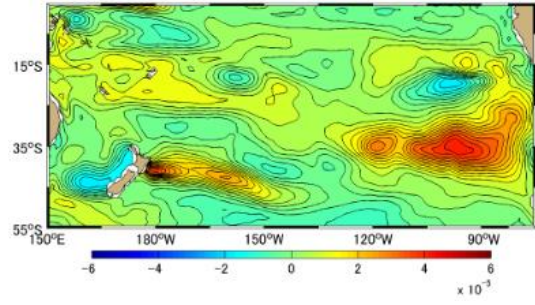


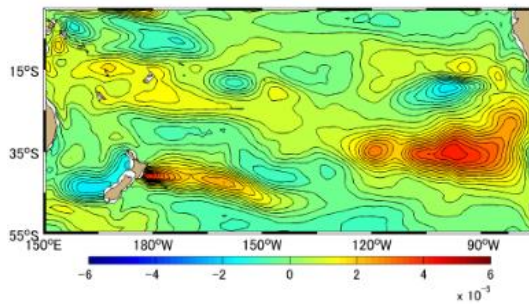
**Figure A-3.11 Difference [PgC] between Approximation Method and Simulation Method Monthly Mean in 2001, the South Pacific Ocean based on January 1991. (a)-(l) represents January-December**



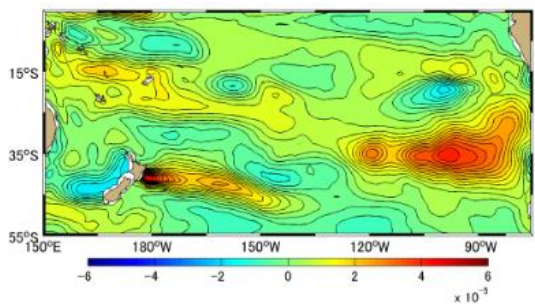
(a)



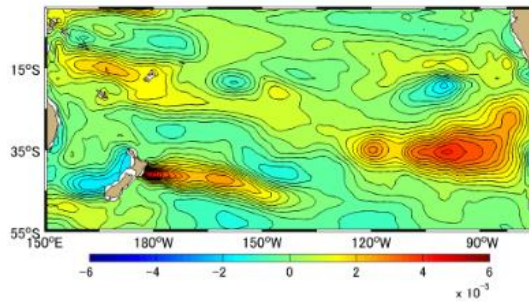
(b)



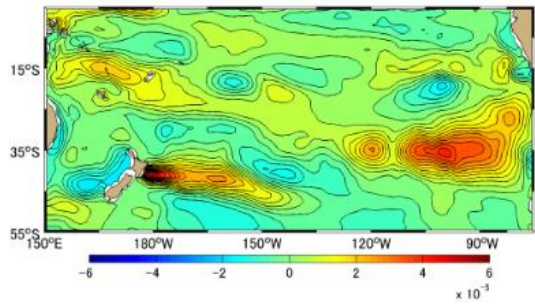
(c)



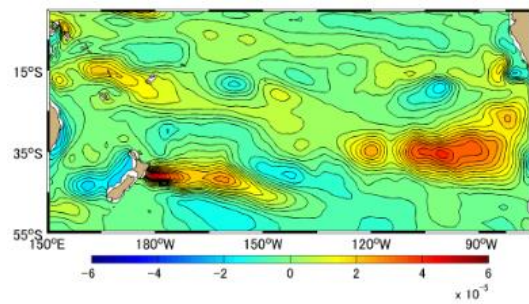
(d)



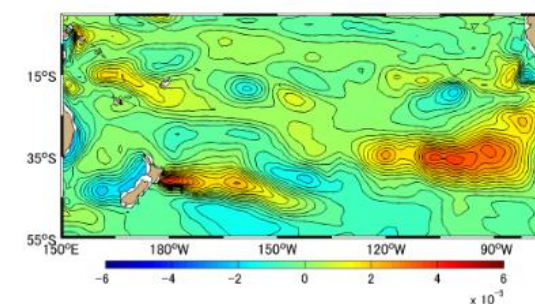
(e)



(f)



(g)



(h)

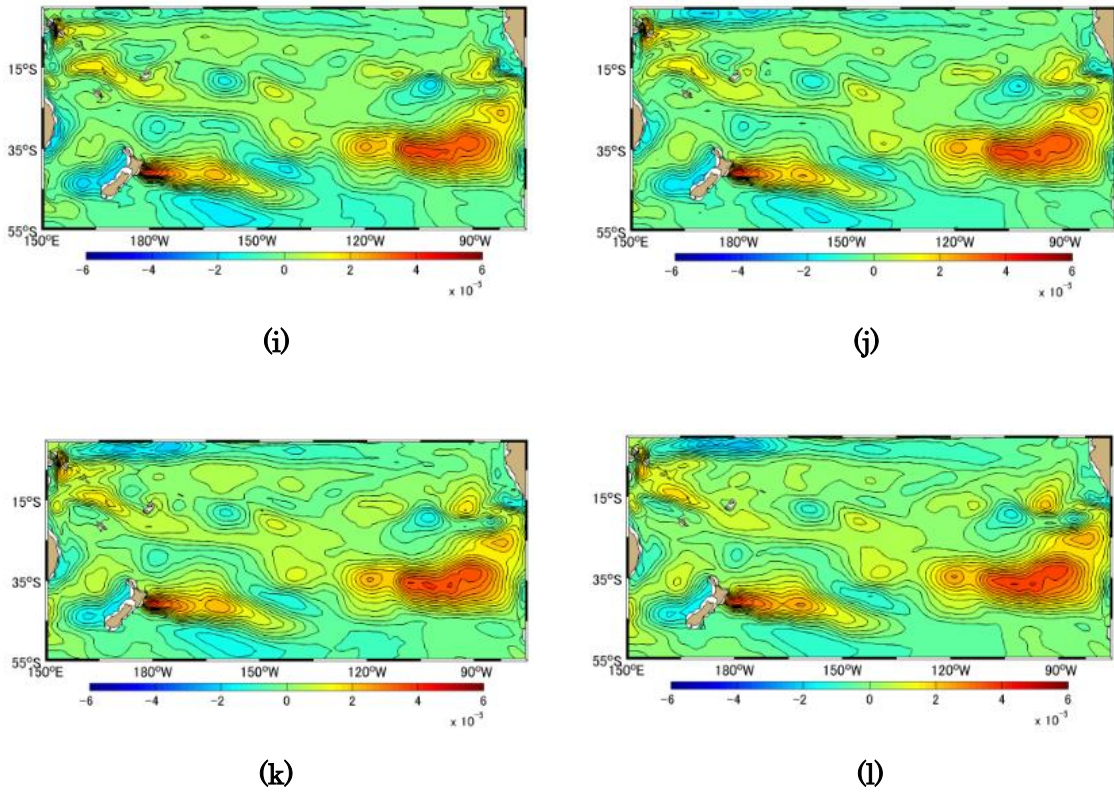
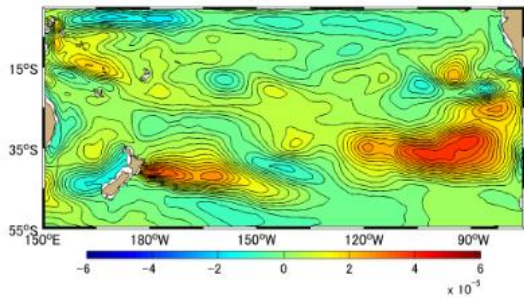
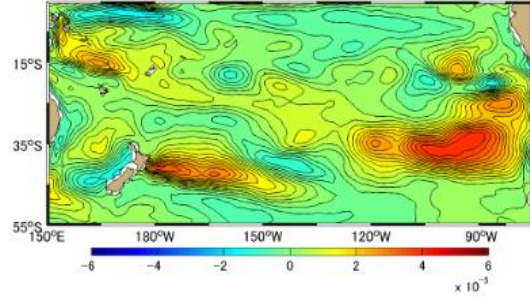


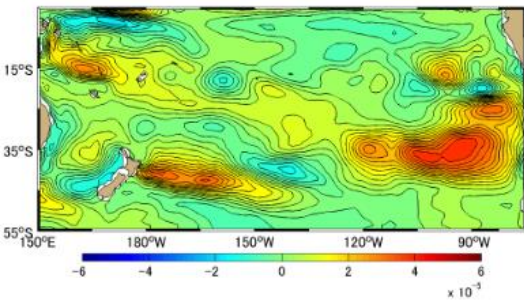
**Figure A-3.12 Difference [PgC] between Approximation Method and Simulation Method Monthly Mean in 2002, the South Pacific Ocean based on January 1991. (a)-(l) represents January-December**



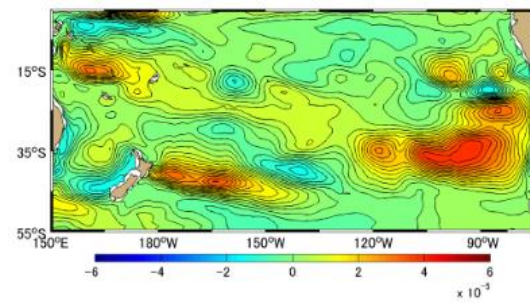
(a)



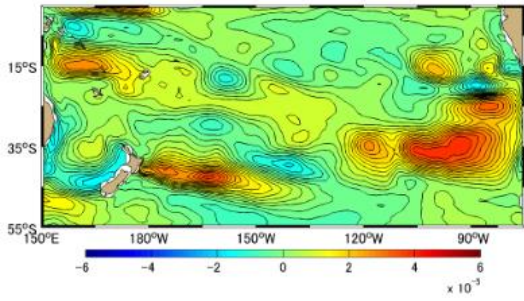
(b)



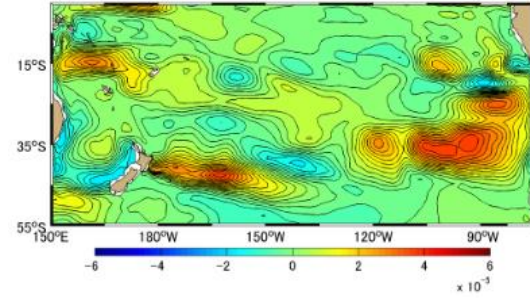
(c)



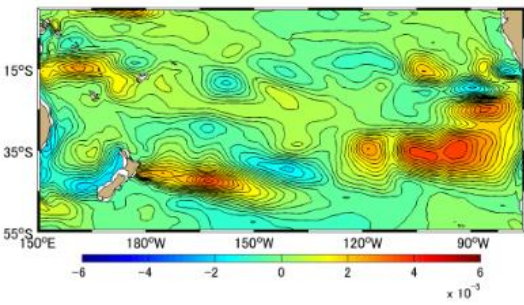
(d)



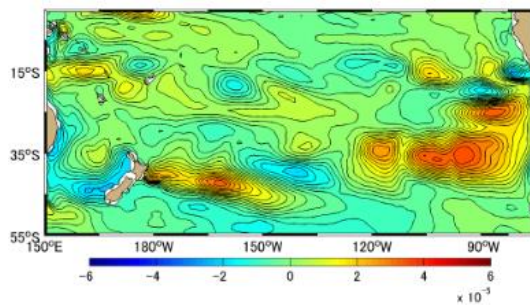
(e)



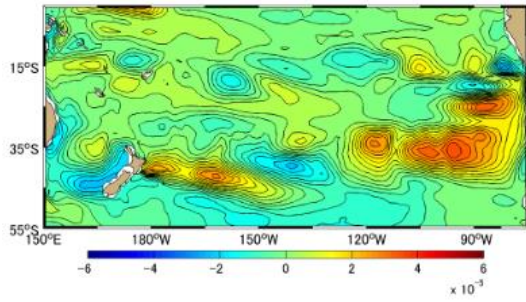
(f)



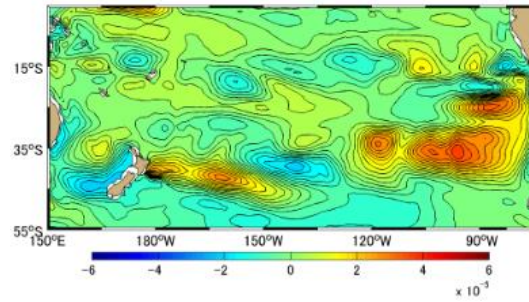
(g)



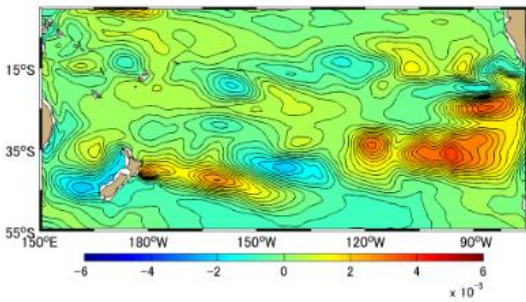
(h)



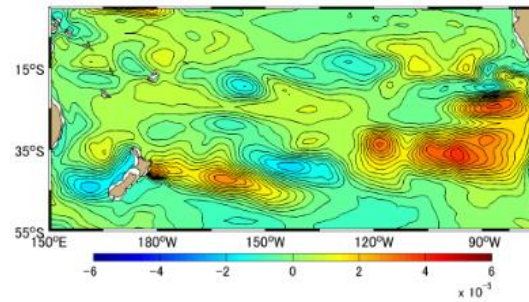
(i)



(j)

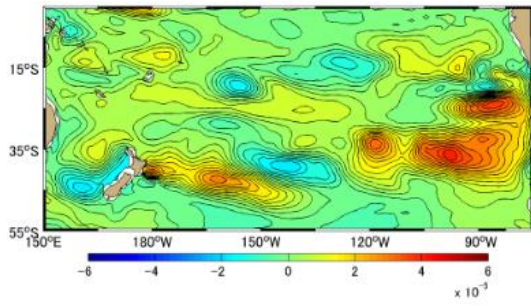


(k)

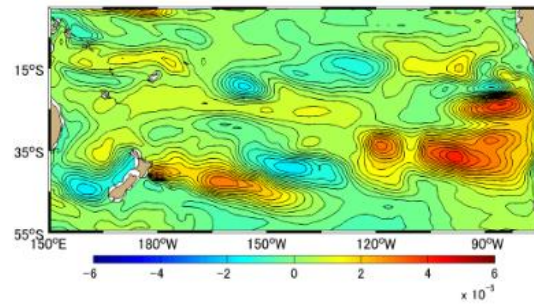


(l)

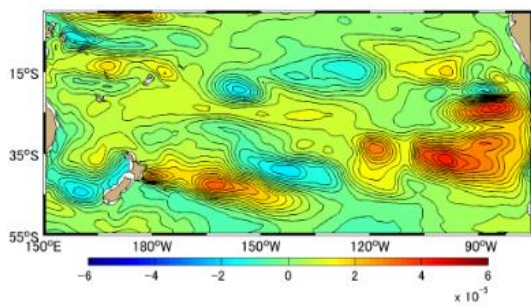
**Figure A-3.13 Difference [PgC] between Approximation Method and Simulation Method Monthly Mean in 2003, the South Pacific Ocean based on January 1991. (a)-(l) represents January-December**



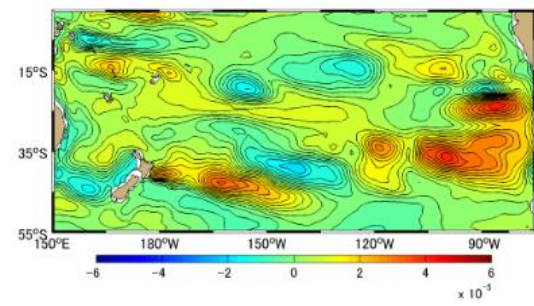
(a)



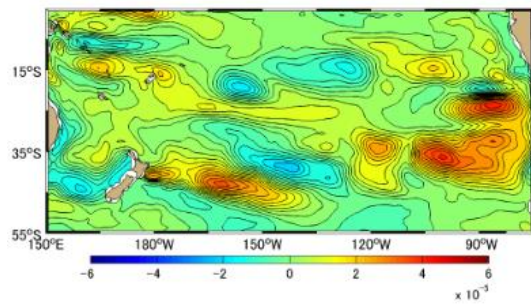
(b)



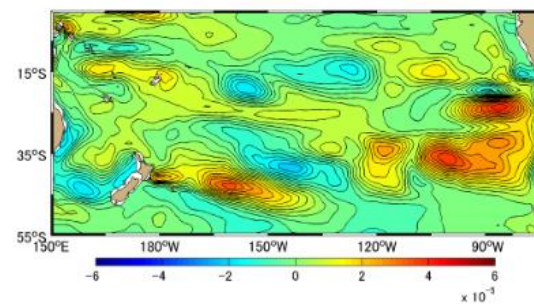
(c)



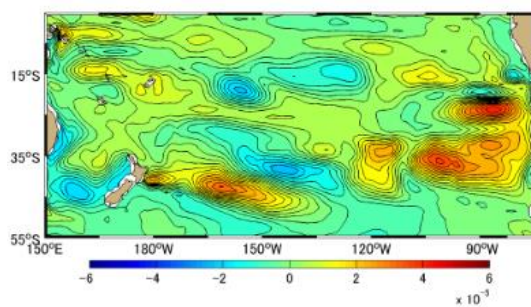
(d)



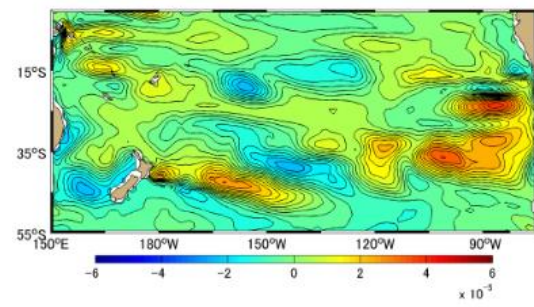
(e)



(f)



(g)



(h)

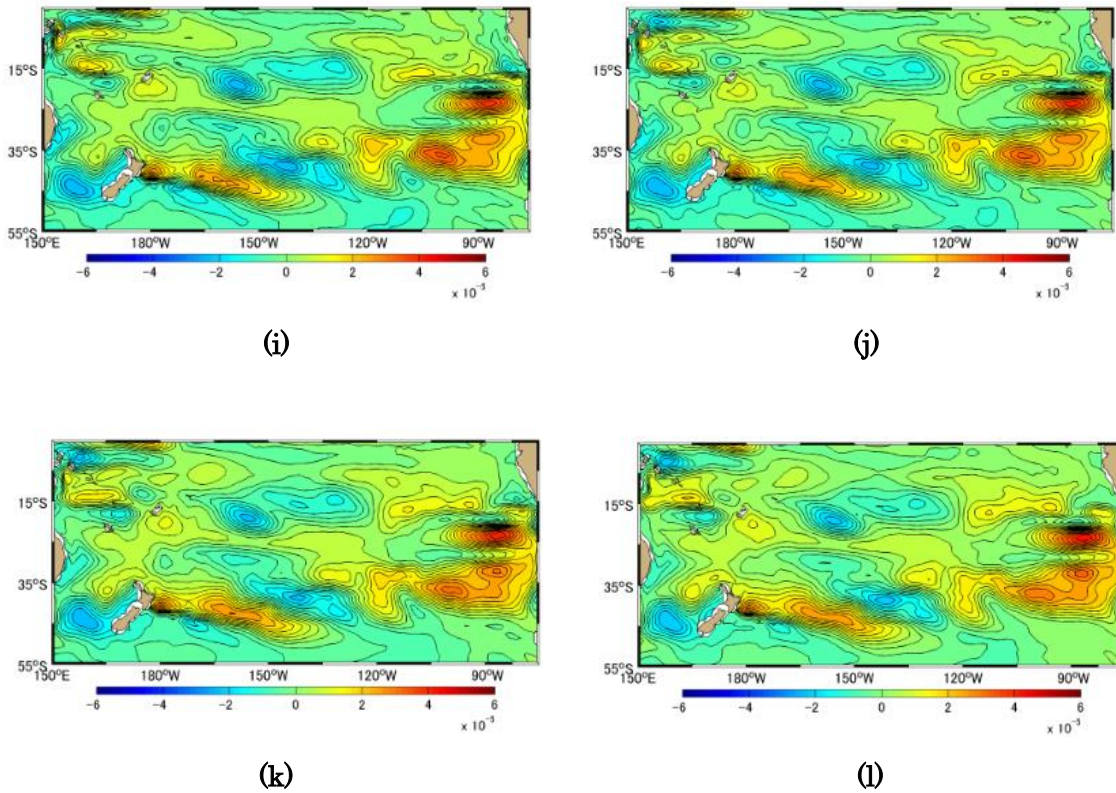
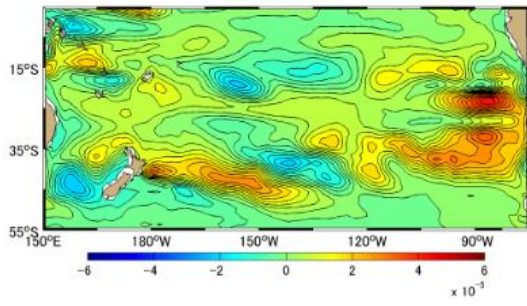
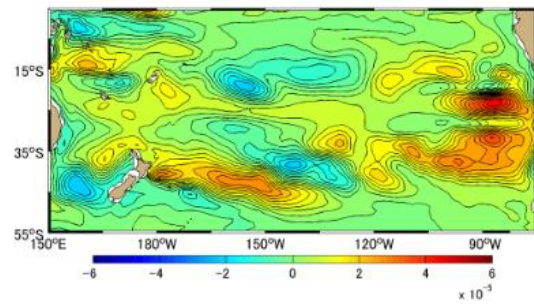


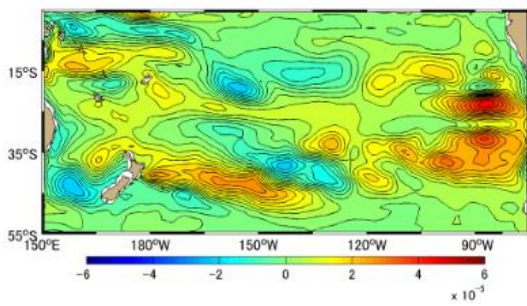
Figure A-3.14 Difference [PgC] between Approximation Method and Simulation Method Monthly Mean in 2004, the South Pacific Ocean based on January 1991. (a)-(l) represents January-December



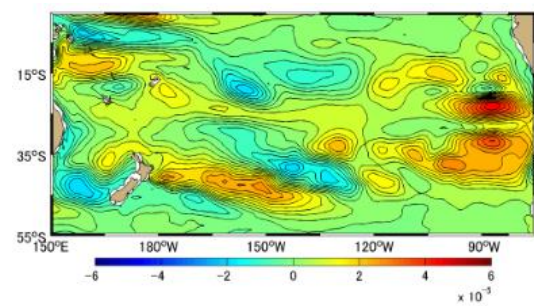
(a)



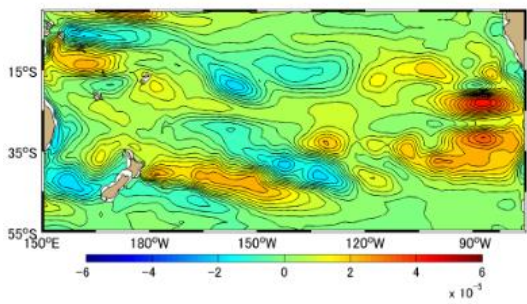
(b)



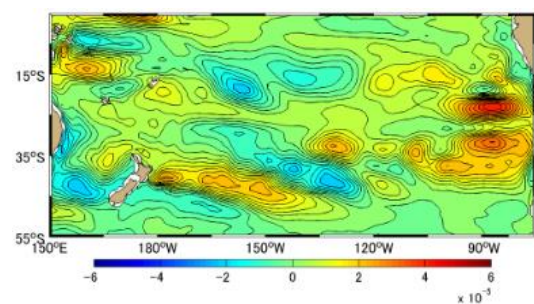
(c)



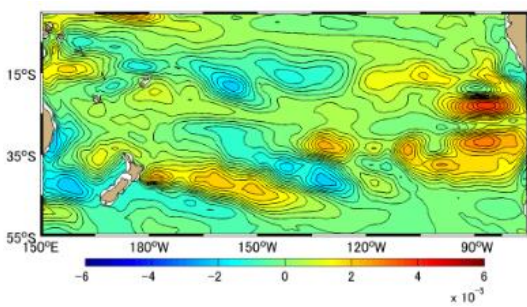
(d)



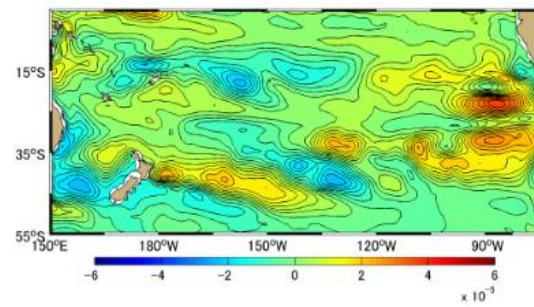
(e)



(f)



(g)



(h)



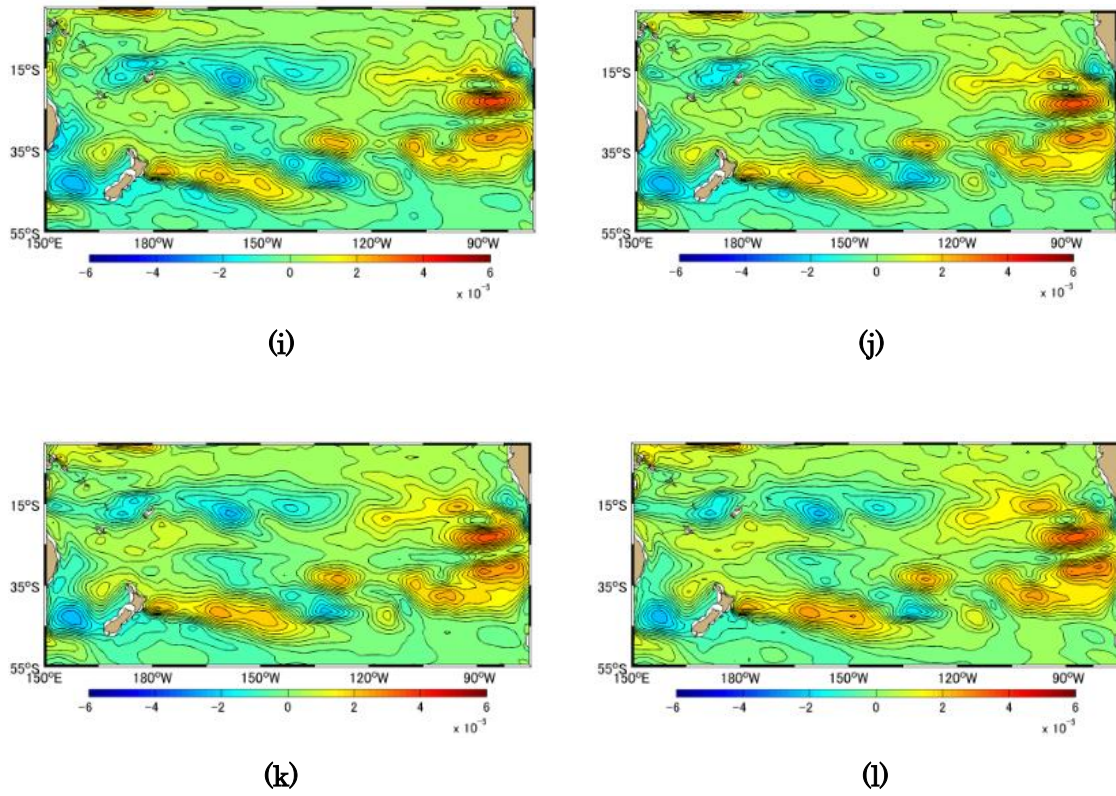
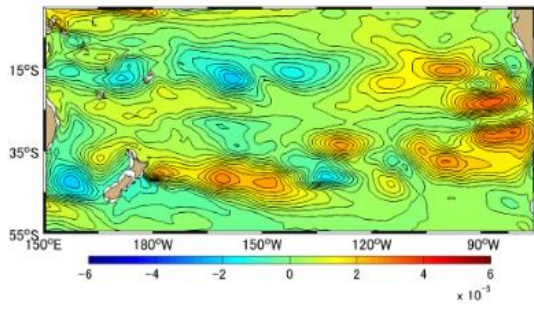
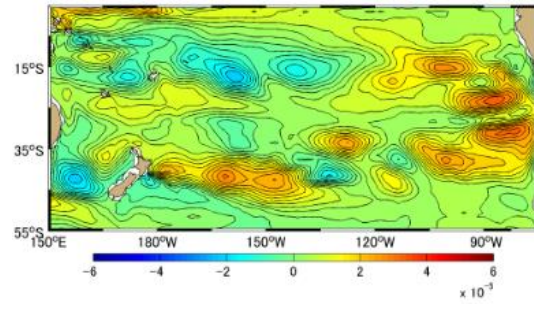


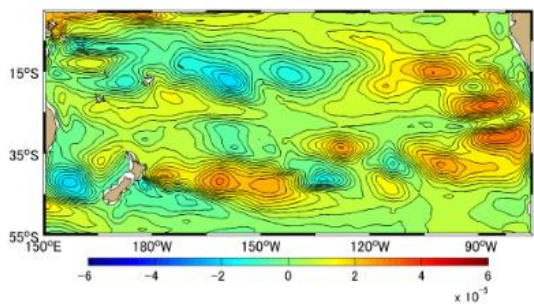
**Figure A-3.15** Difference [PgC] between Approximation Method and Simulation Method Monthly Mean in 2005, the South Pacific Ocean based on January 1991. (a)-(l) represents January-December



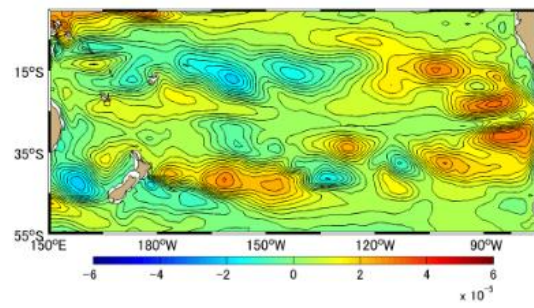
(a)



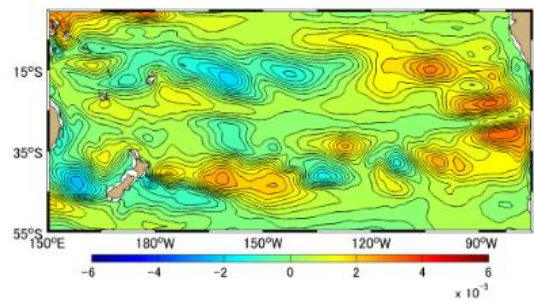
(b)



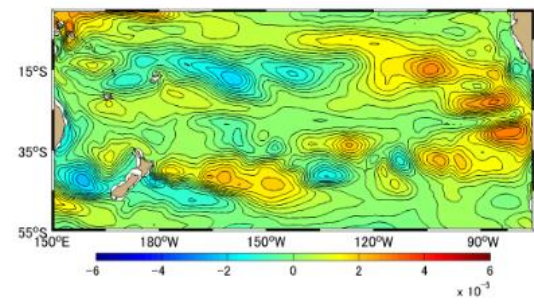
(c)



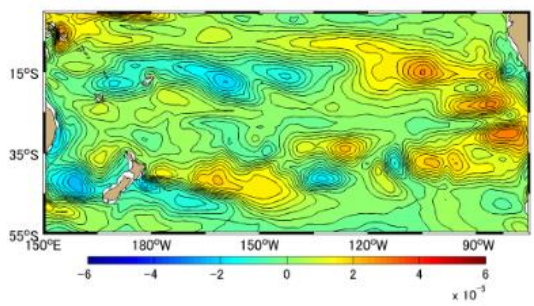
(d)



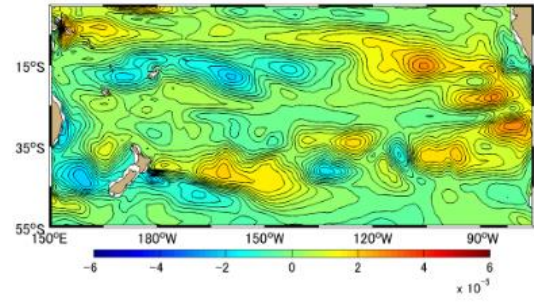
(e)



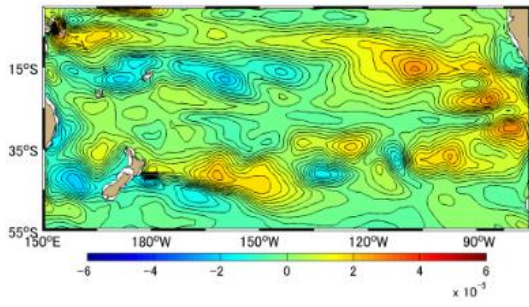
(f)



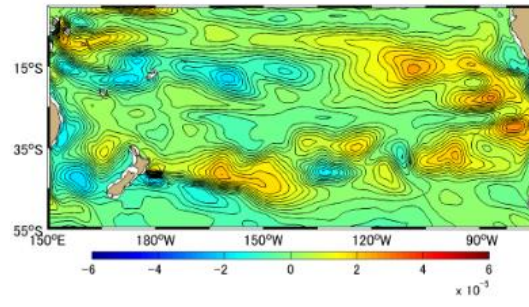
(g)



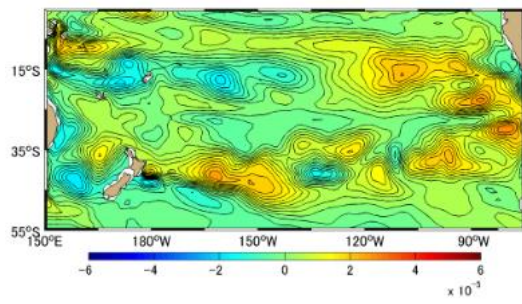
(h)



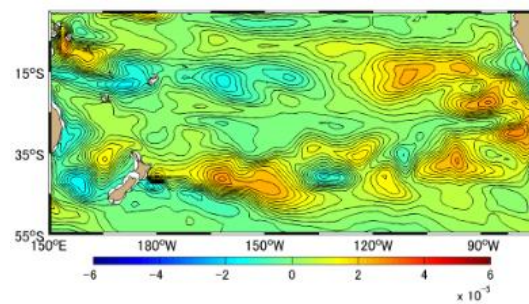
(i)



(j)

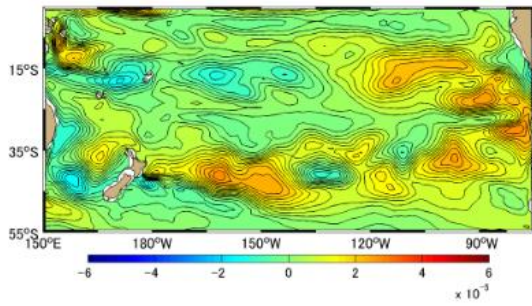


(k)

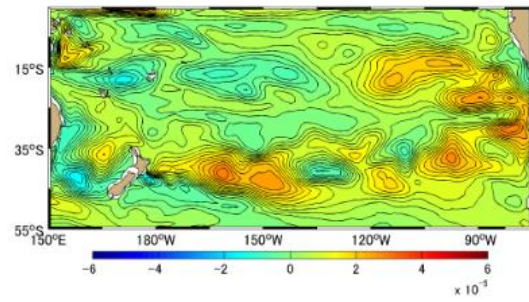


(l)

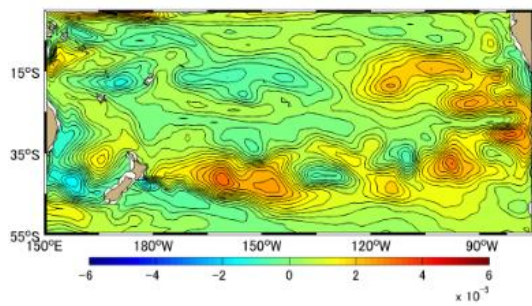
**Figure A-3.16 Difference [PgC] between Approximation Method and Simulation Method Monthly Mean in 2006, the South Pacific Ocean based on January 1991. (a)-(l) represents January-December**



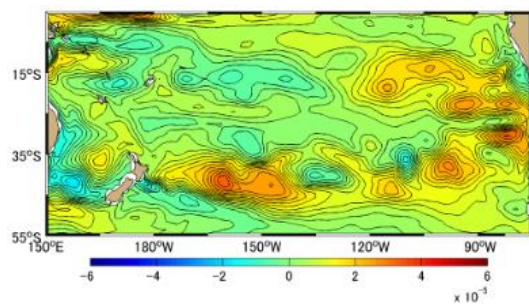
(a)



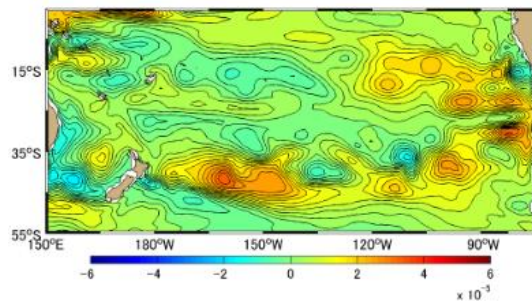
(b)



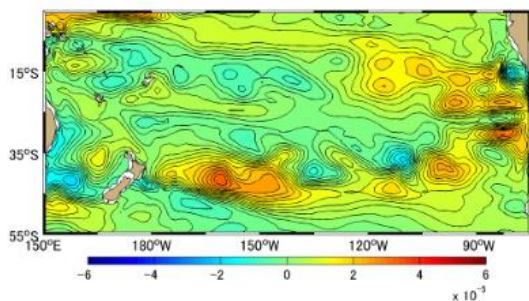
(c)



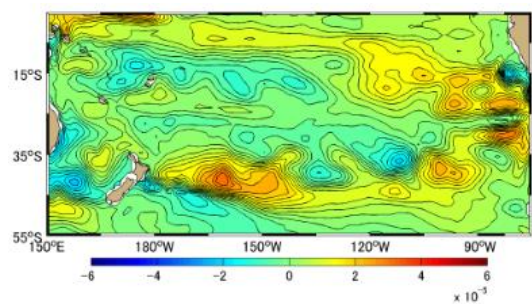
(d)



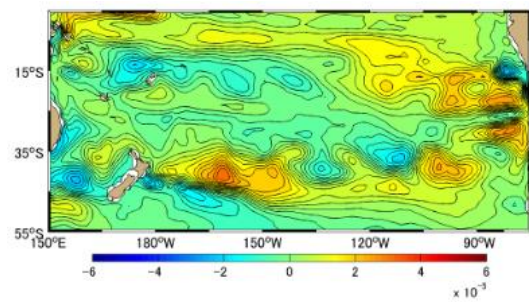
(e)



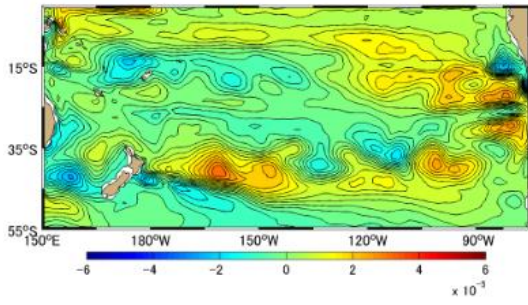
(f)



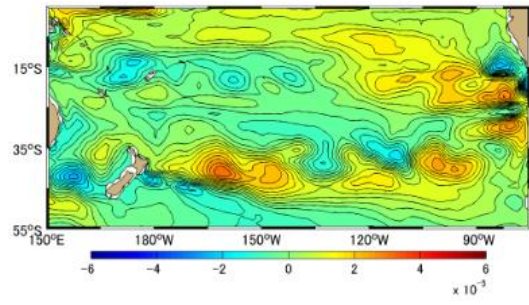
(g)



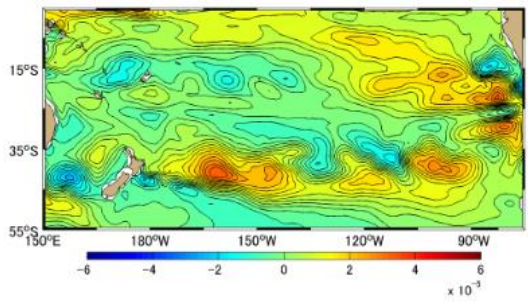
(h)



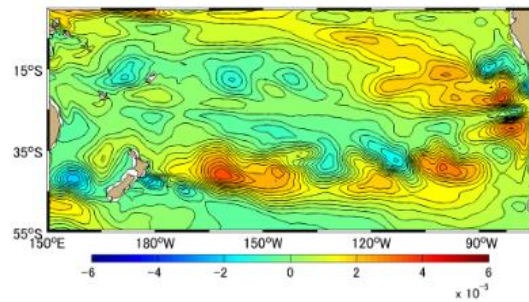
(i)



(j)

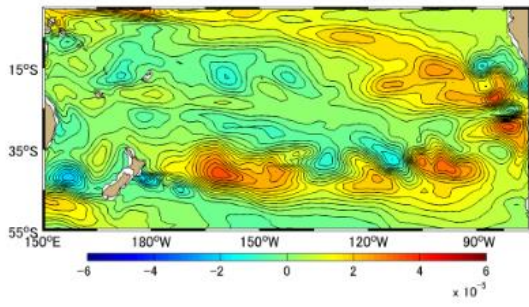


(k)

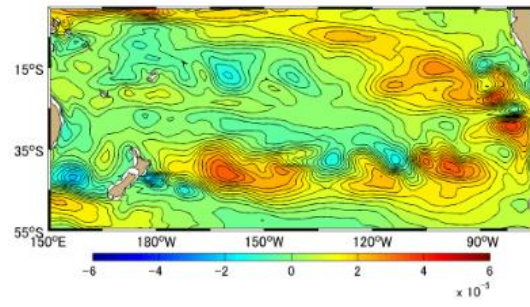


(l)

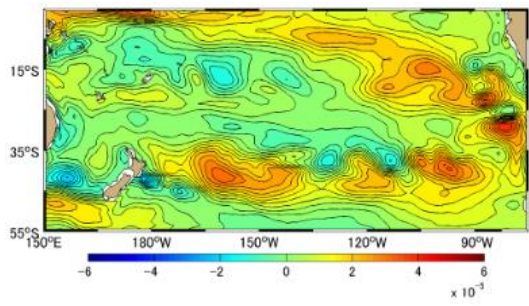
**Figure A-3.17 Difference [PgC] between Approximation Method and Simulation Method Monthly Mean in 2007, the South Pacific Ocean based on January 1991. (a)-(l) represents January-December**



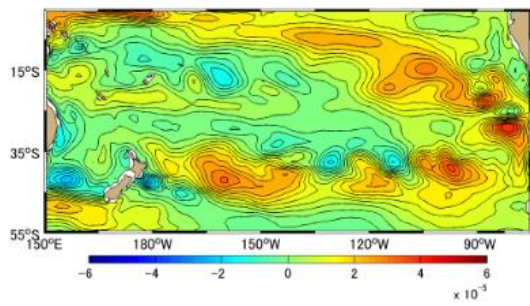
(a)



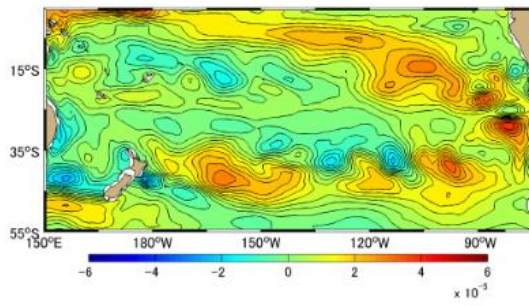
(b)



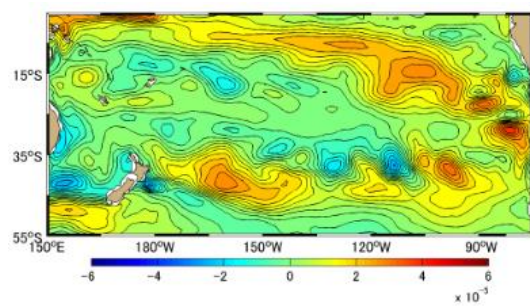
(c)



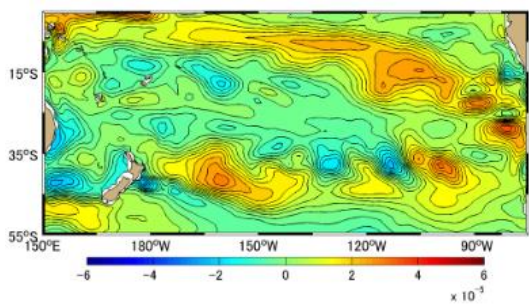
(d)



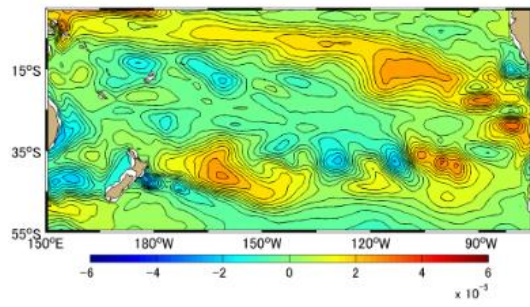
(e)



(f)



(g)



(h)

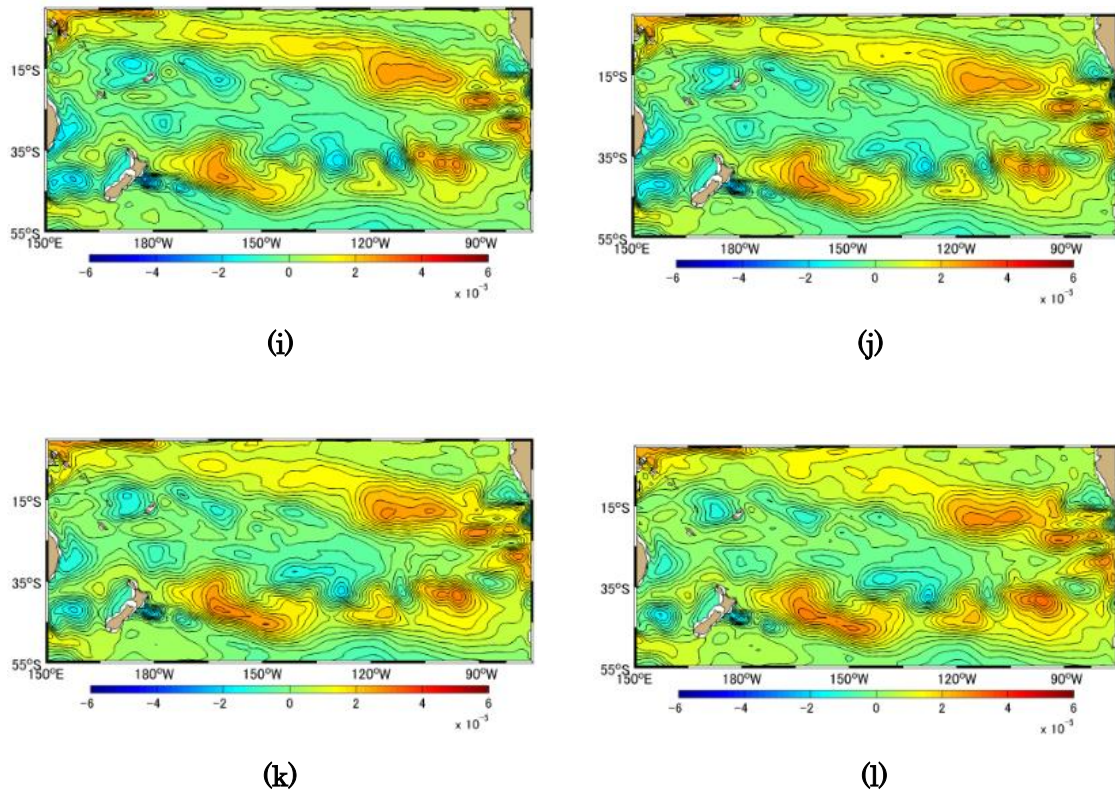
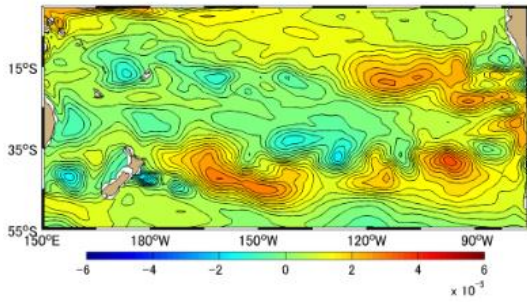
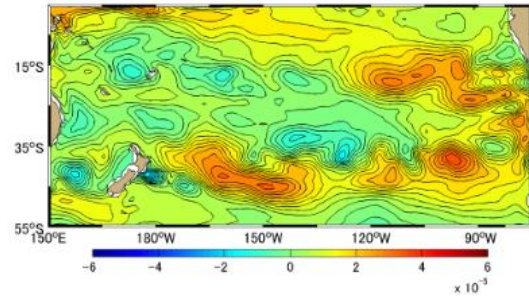


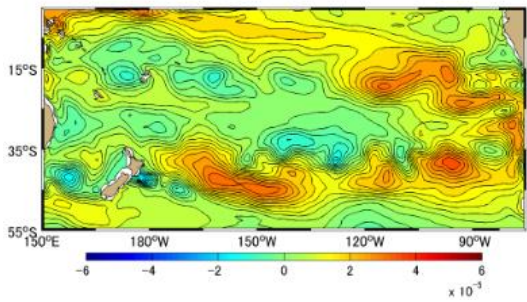
Figure A-3.18 Difference [PgC] between Approximation Method and Simulation Method Monthly Mean in 2008, the South Pacific Ocean based on January 1991. (a)-(l) represents January-December



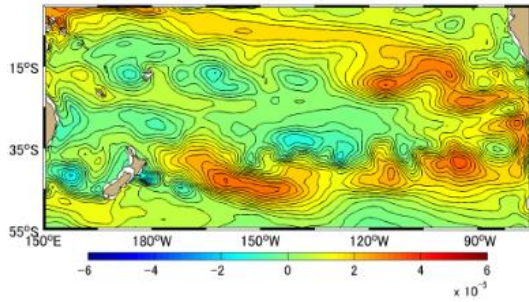
(a)



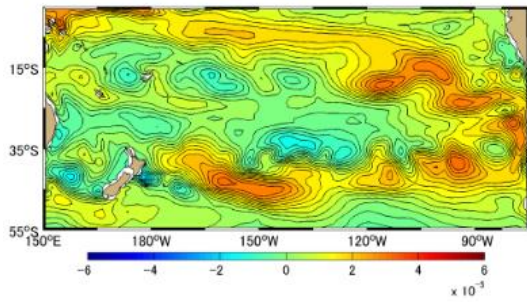
(b)



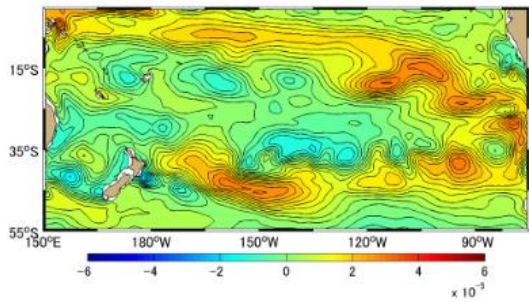
(c)



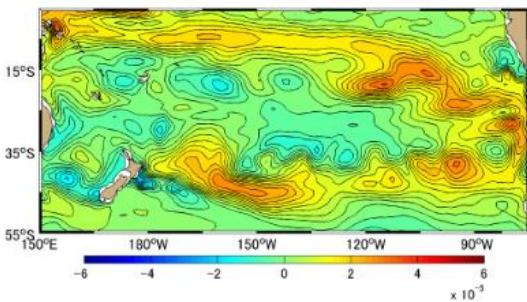
(d)



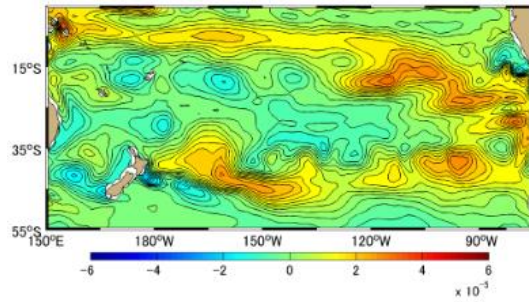
(e)



(f)



(g)



(h)



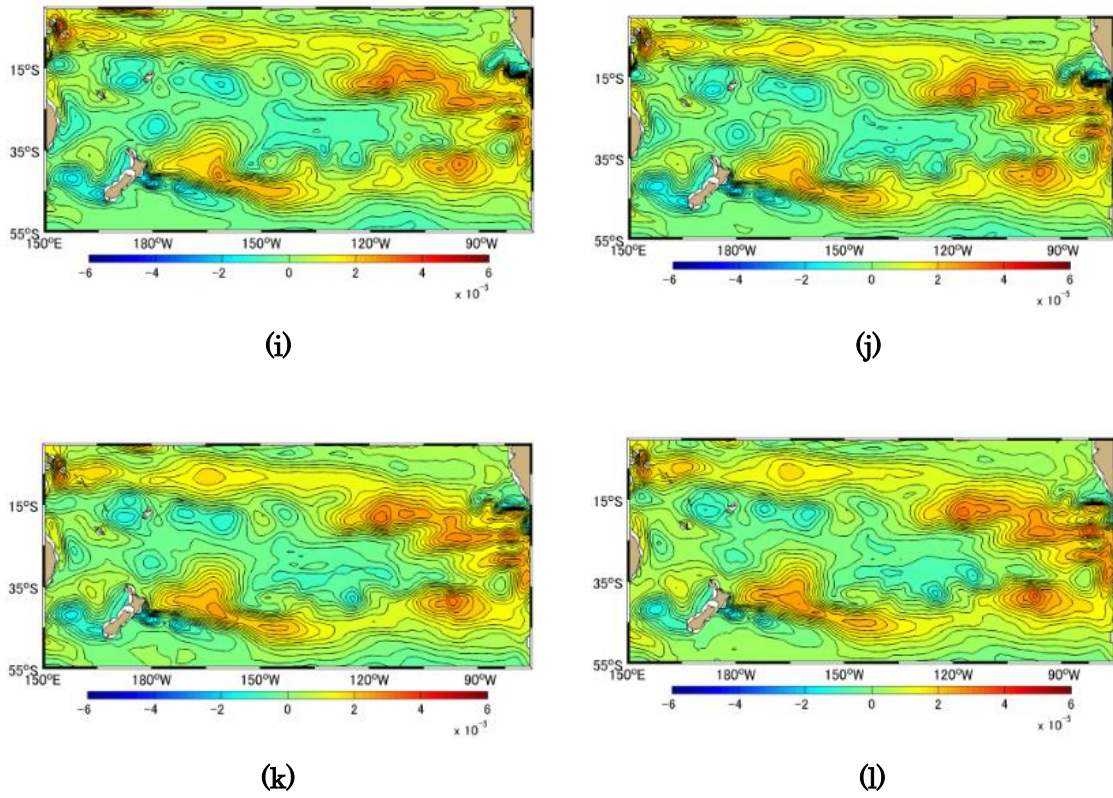
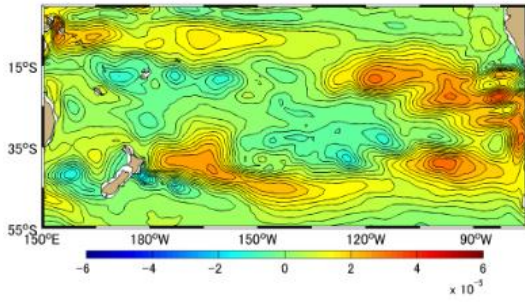
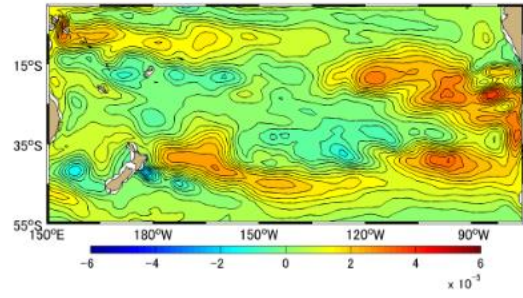


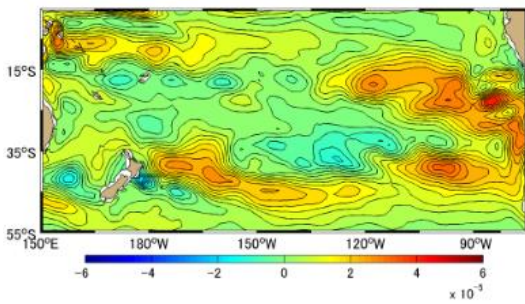
Figure A-3.19 Difference [PgC] between Approximation Method and Simulation Method Monthly Mean in 2009, the South Pacific Ocean based on January 1991. (a)-(l) represents January-December



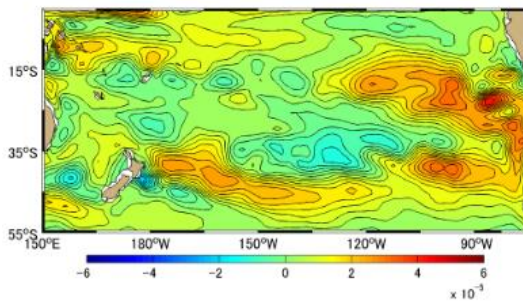
(a)



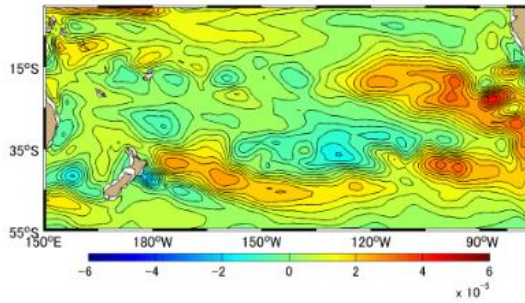
(b)



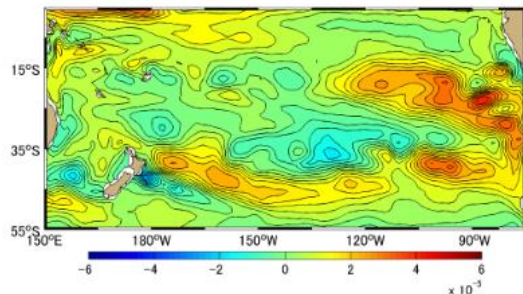
(c)



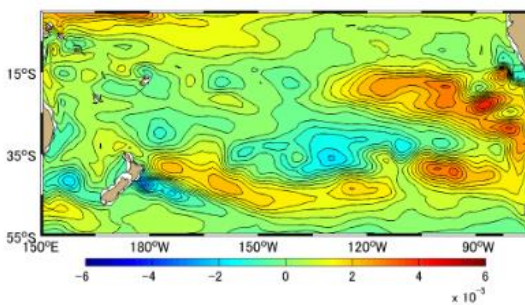
(d)



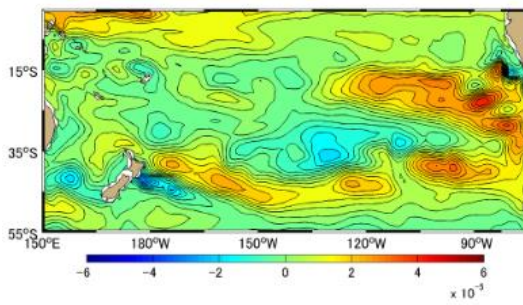
(e)



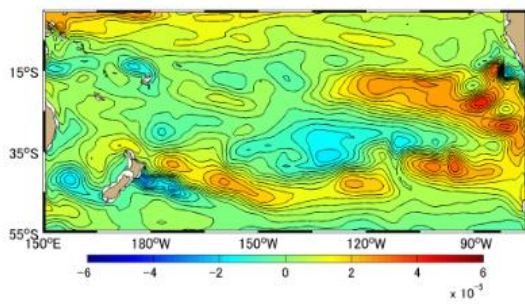
(f)



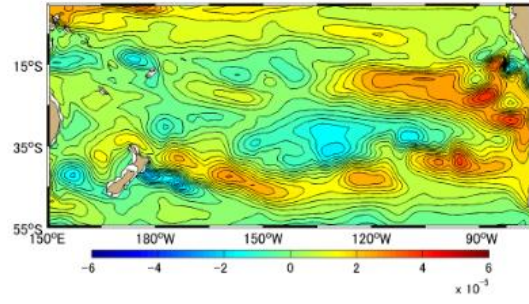
(g)



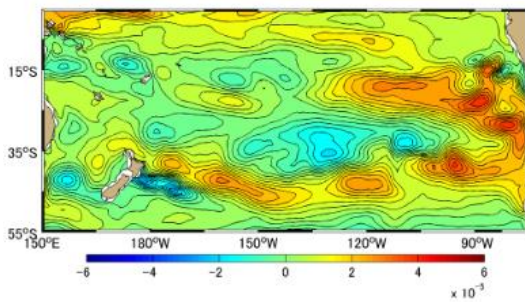
(h)



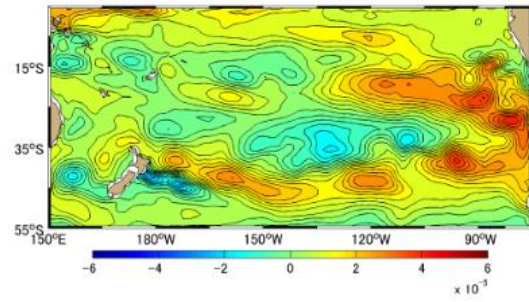
(i)



(j)

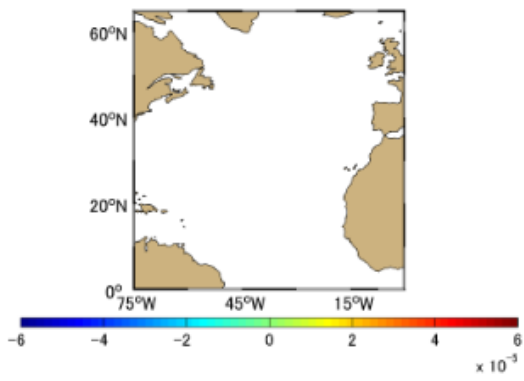


(k)

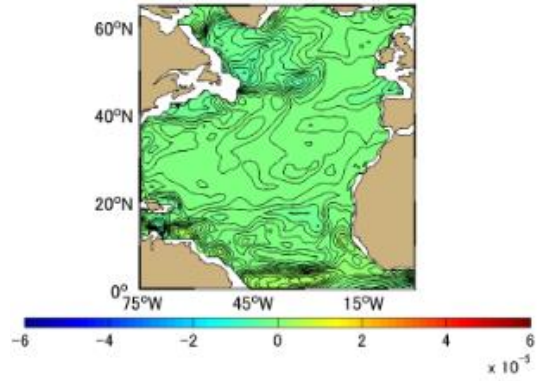


(l)

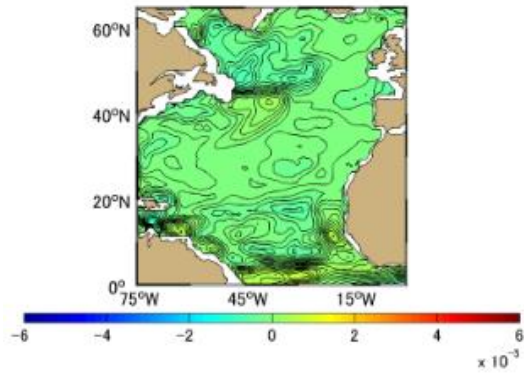
**Figure A-3.20 Difference [PgC] between Approximation Method and Simulation Method Monthly Mean in 2010, the South Pacific Ocean based on January 1991. (a)-(l) represents January-December**



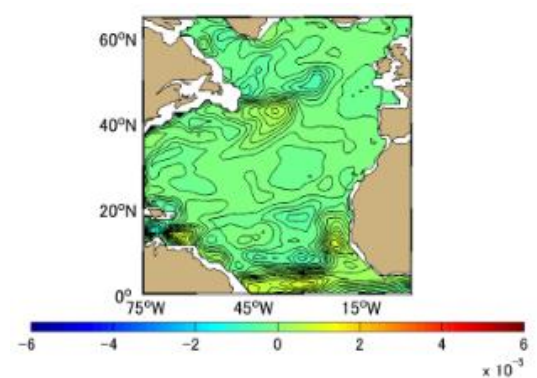
(a)



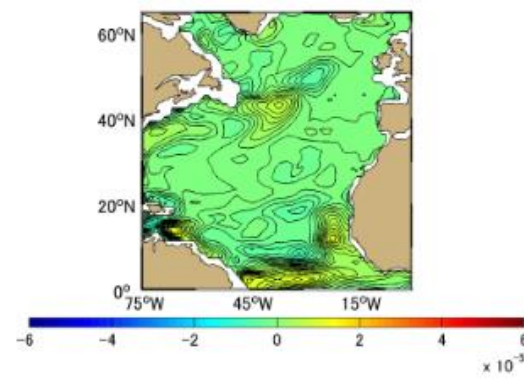
(b)



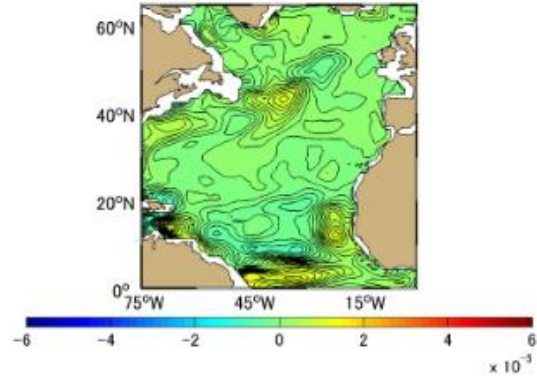
(c)



(d)



(e)



(f)

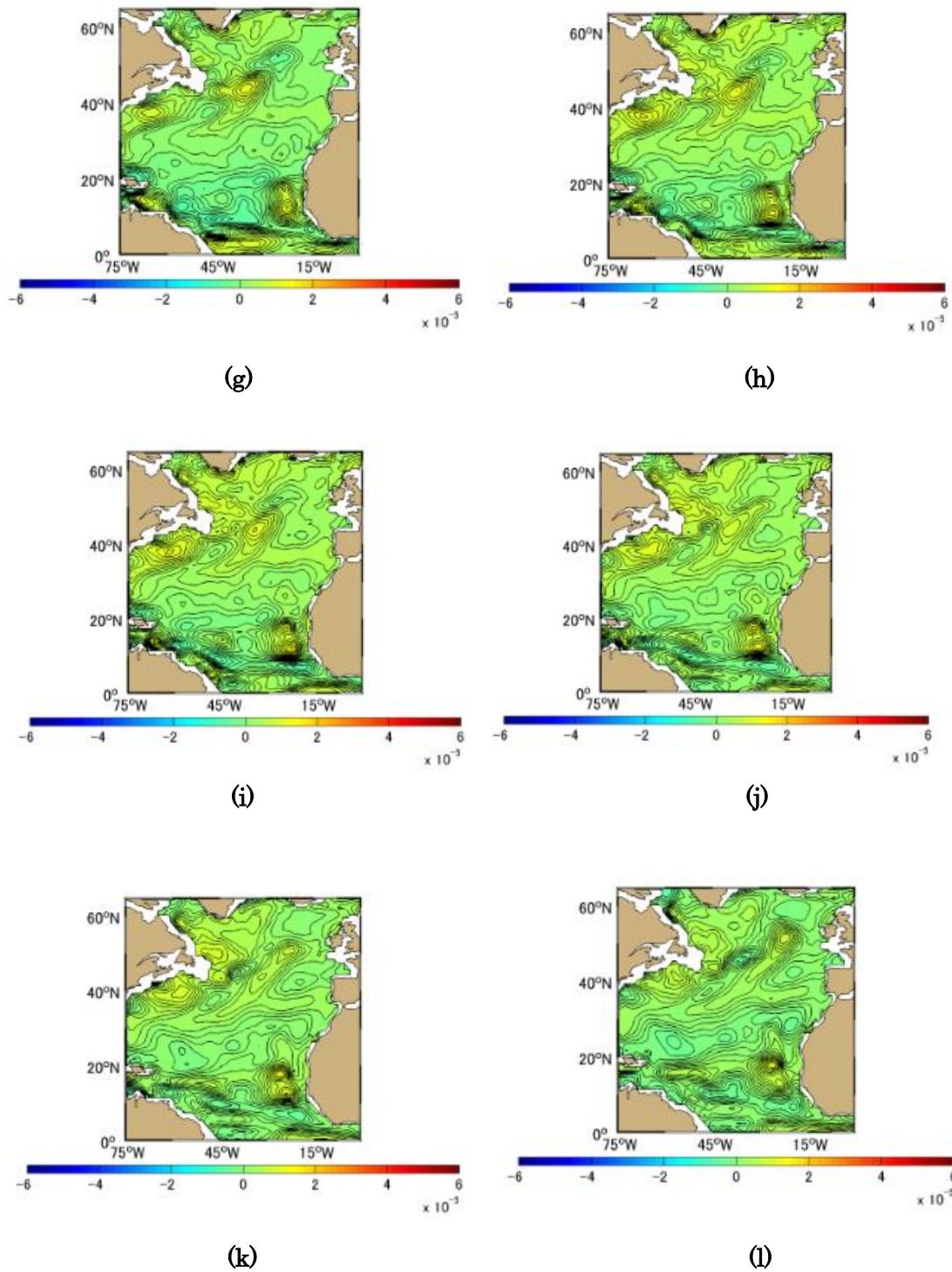
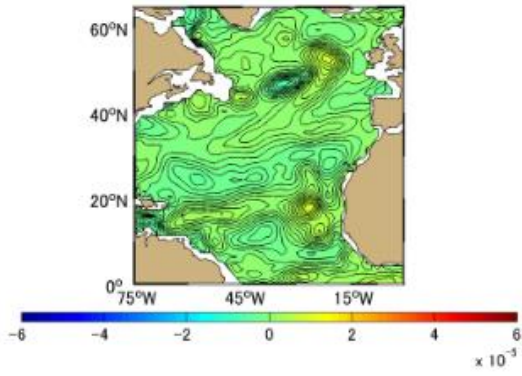
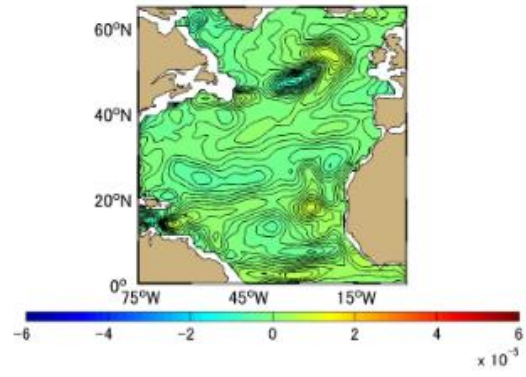


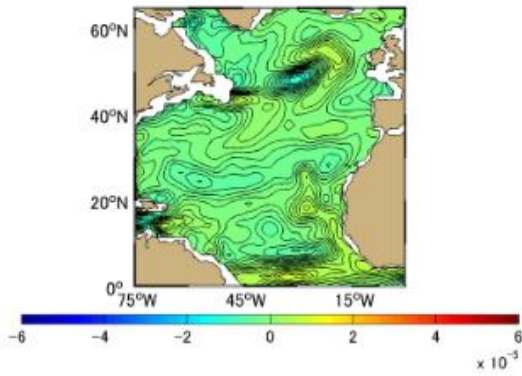
Figure A-4.1 Difference [PgC] between Approximation Method and Simulation Method Monthly Mean in 1991, the North Atlantic based on January 1991. (a)-(l) represents January-December



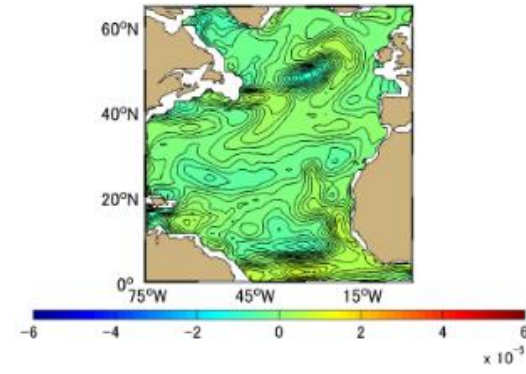
(a)



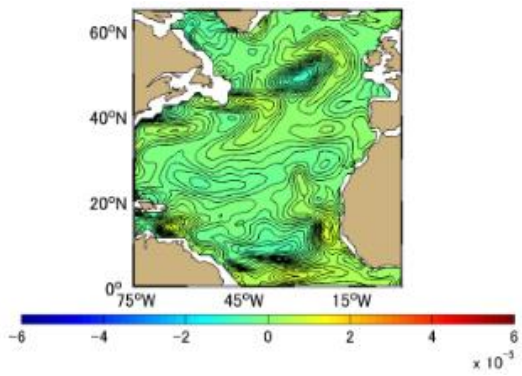
(b)



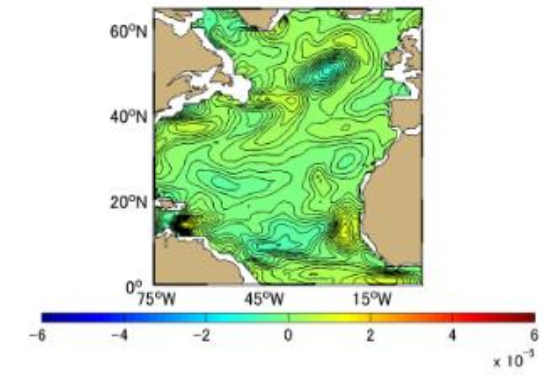
(c)



(d)



(e)



(f)

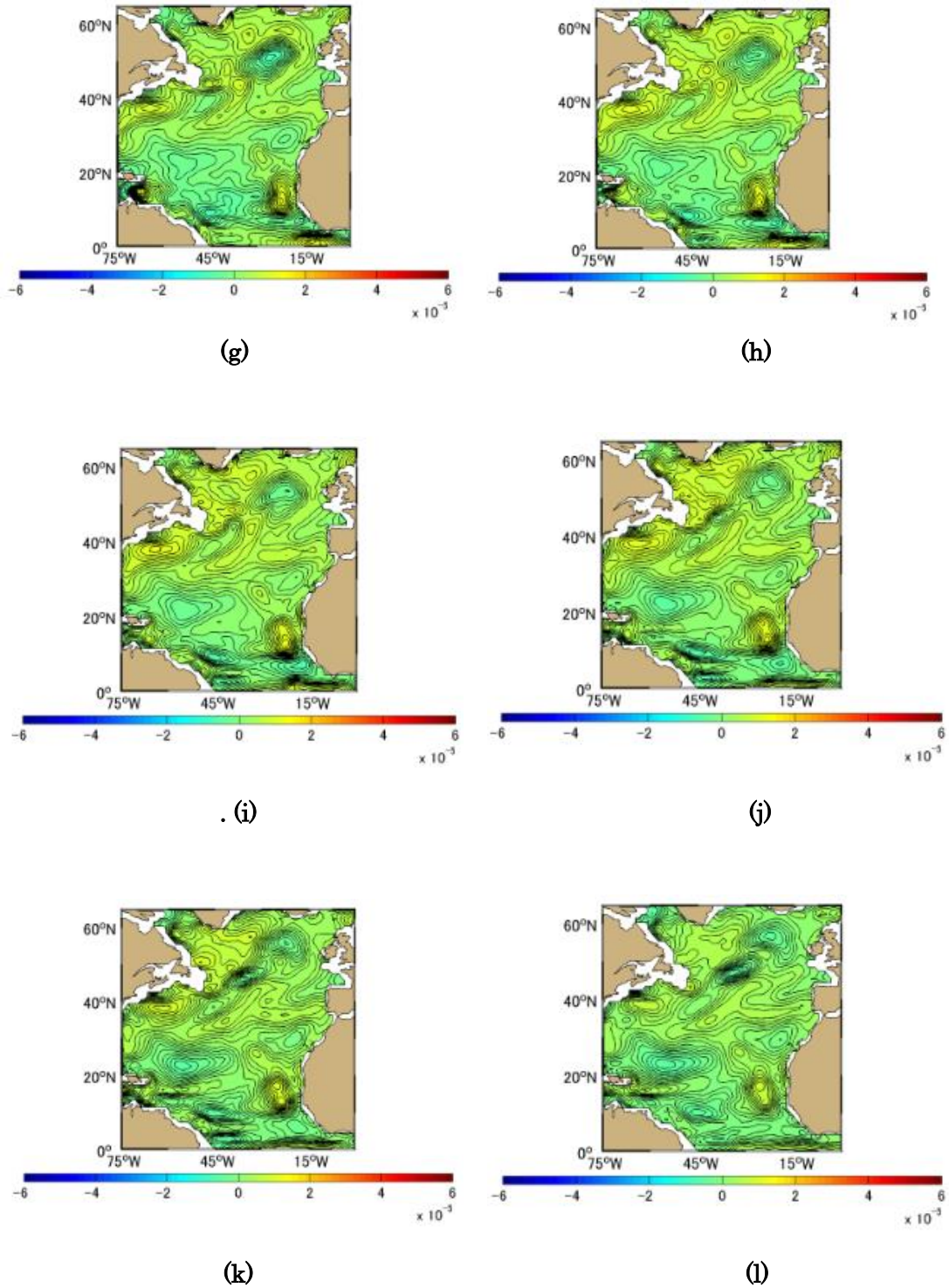
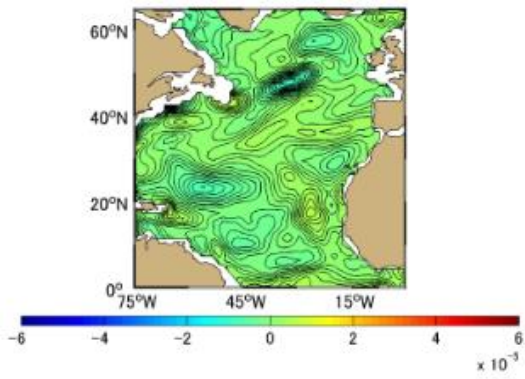
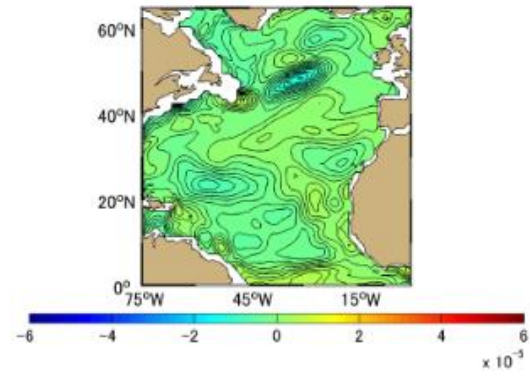


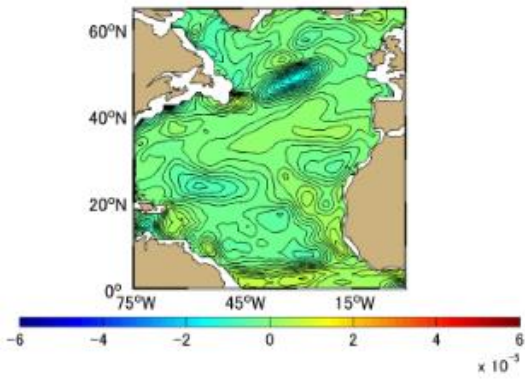
Figure A-4.2 Difference [PgC] between Approximation Method and Simulation Method Monthly Mean in 1992, the North Atlantic based on January 1991. (a)-(l) represents January-December



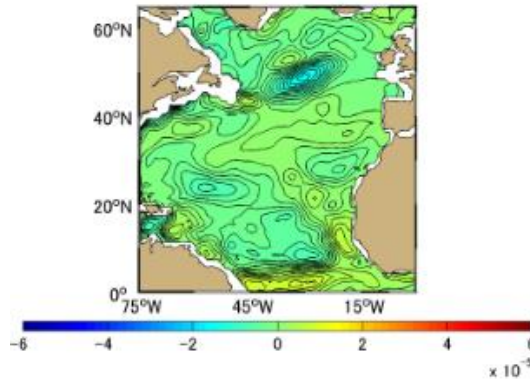
(a)



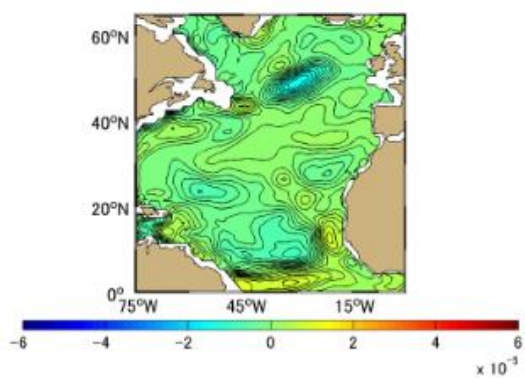
(b)



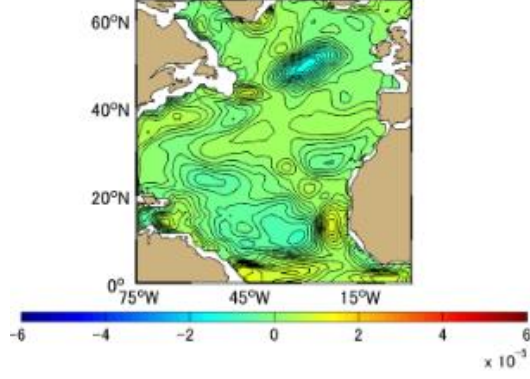
(c)



(d)



(e)



(f)



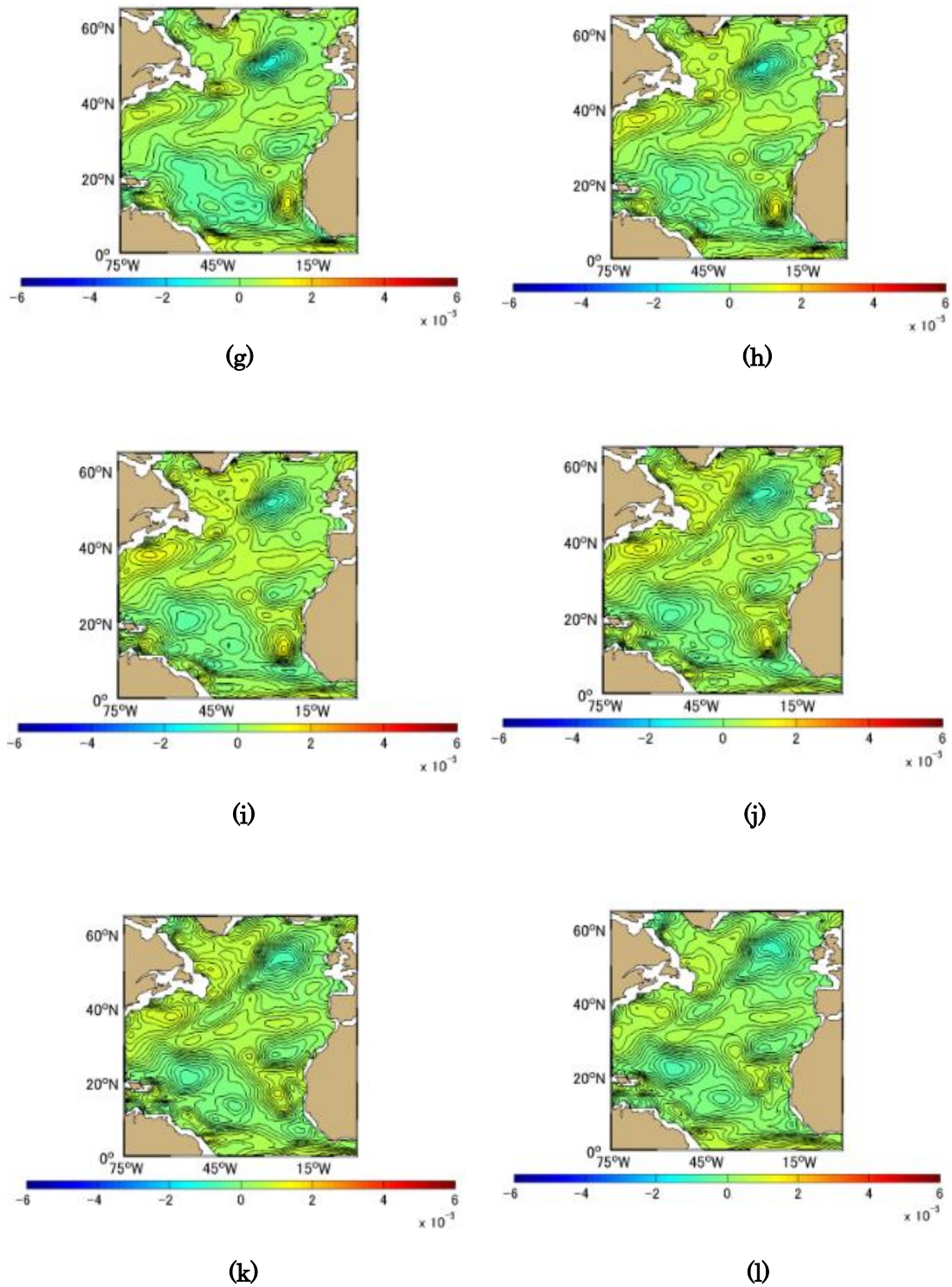
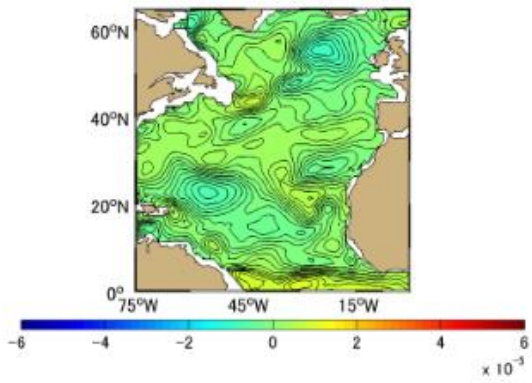
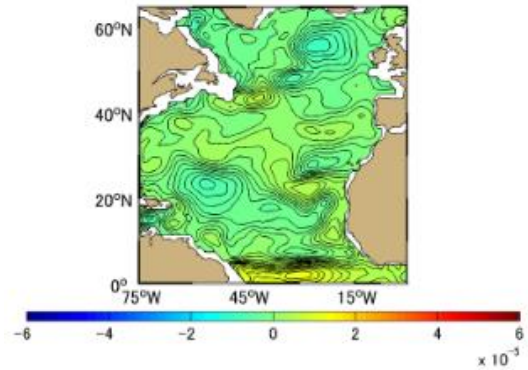


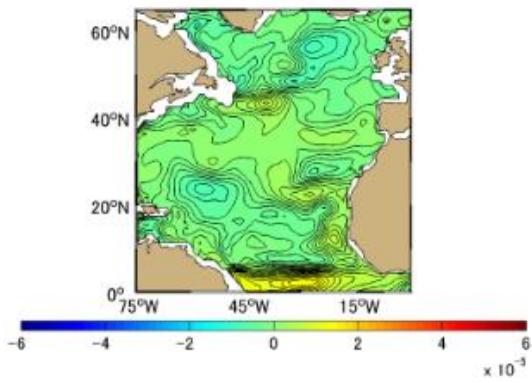
Figure A-4.3 Difference [PgC] between Approximation Method and Simulation Method Monthly Mean in 1993, the North Atlantic based on January 1991. (a)-(l) represents January-December



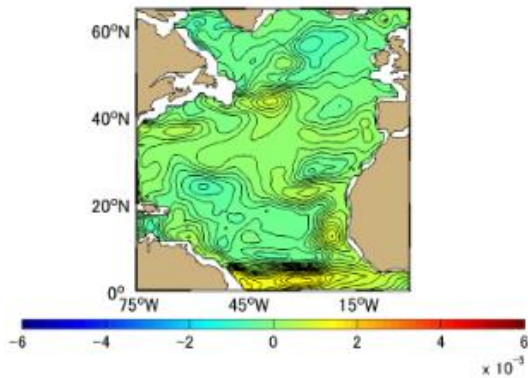
(a)



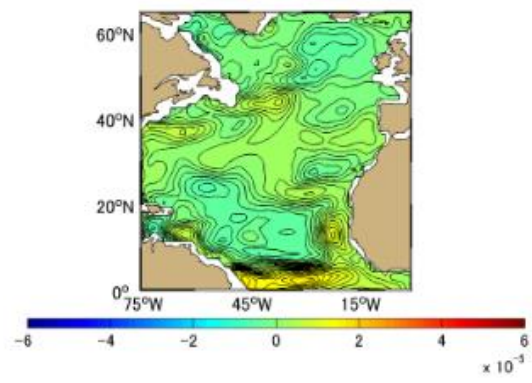
(b)



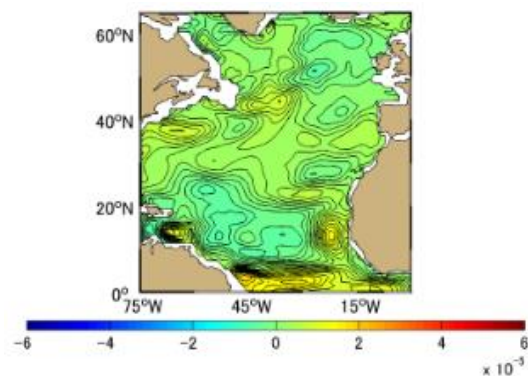
(c)



(d)



(e)



(f)

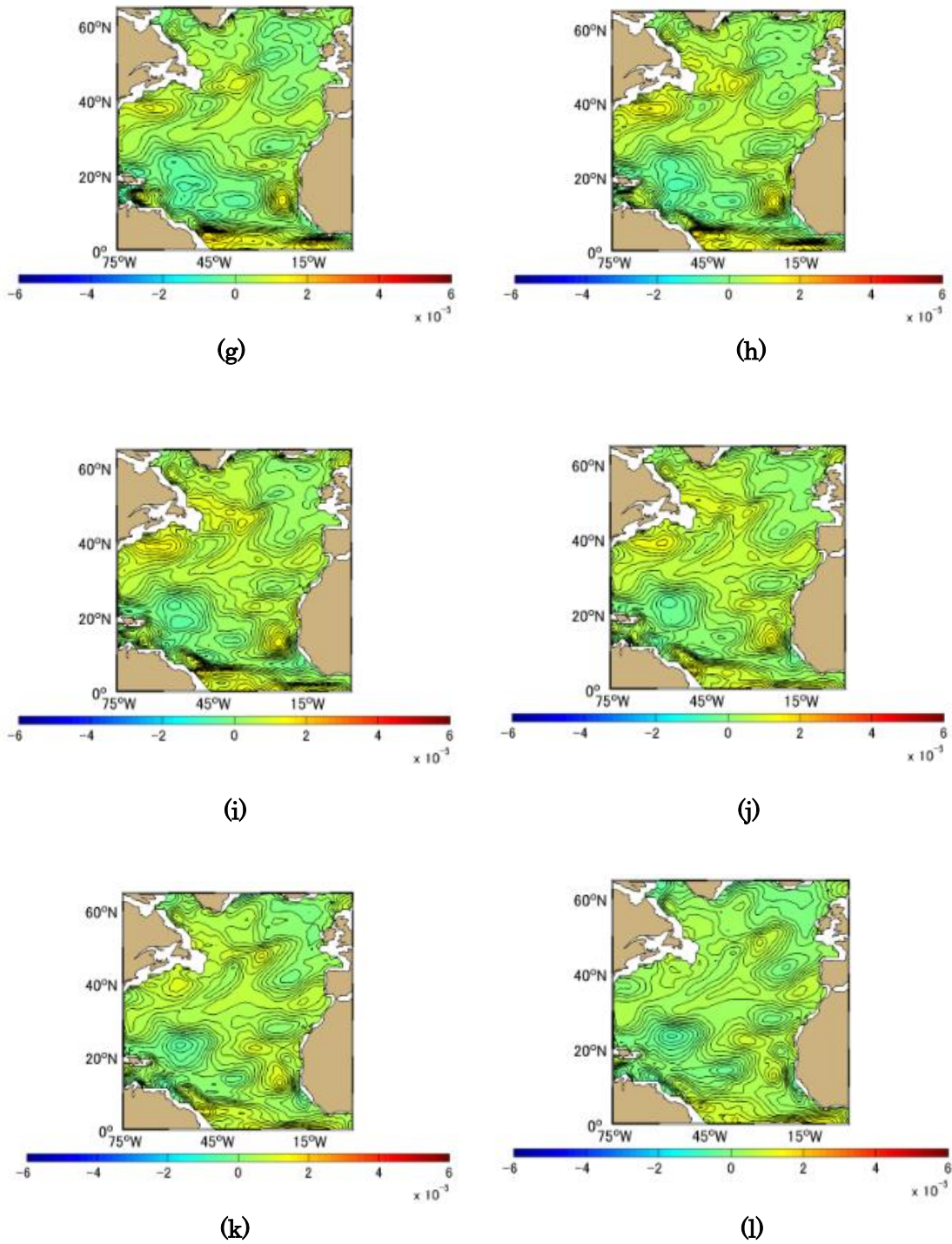
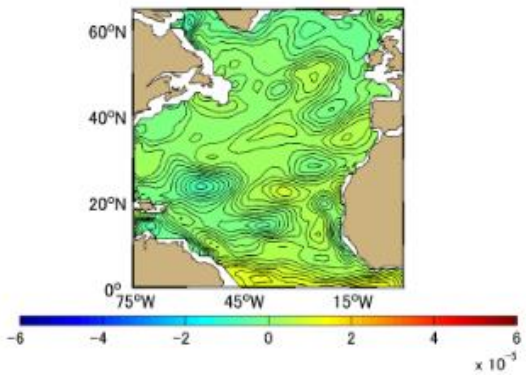
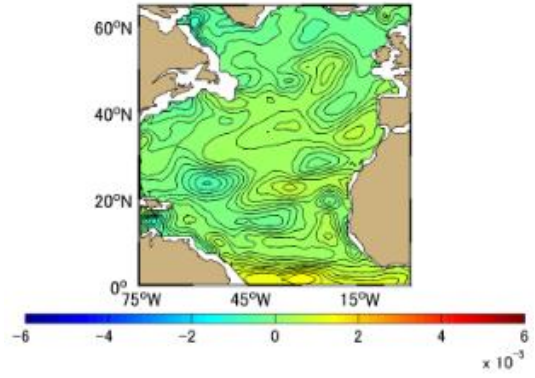


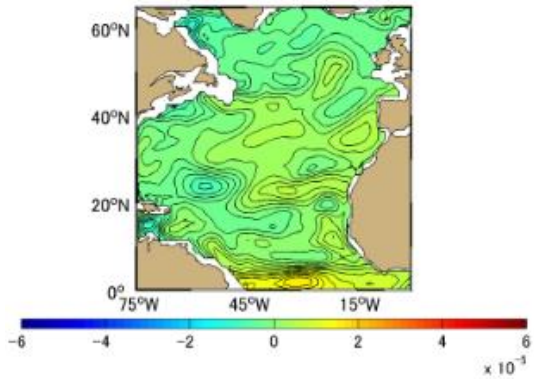
Figure A-4.4 Difference [PgC] between Approximation Method and Simulation Method Monthly Mean in 1994, the North Atlantic based on January 1991. (a)-(l) represents January-December



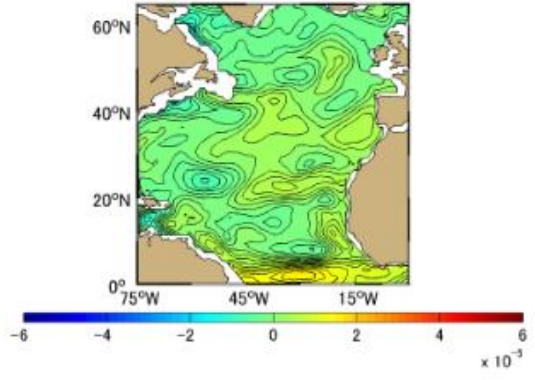
(a)



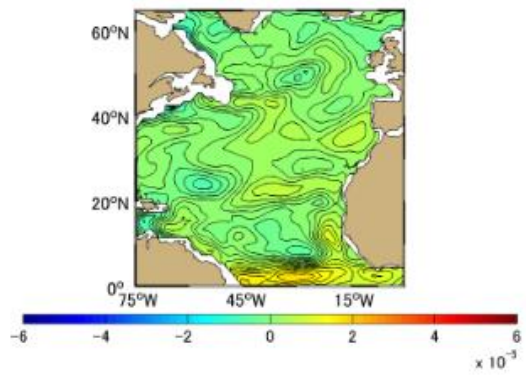
(b)



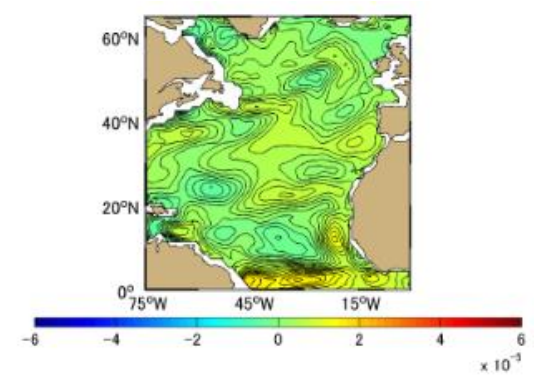
(c)



(d)



(e)



(f)

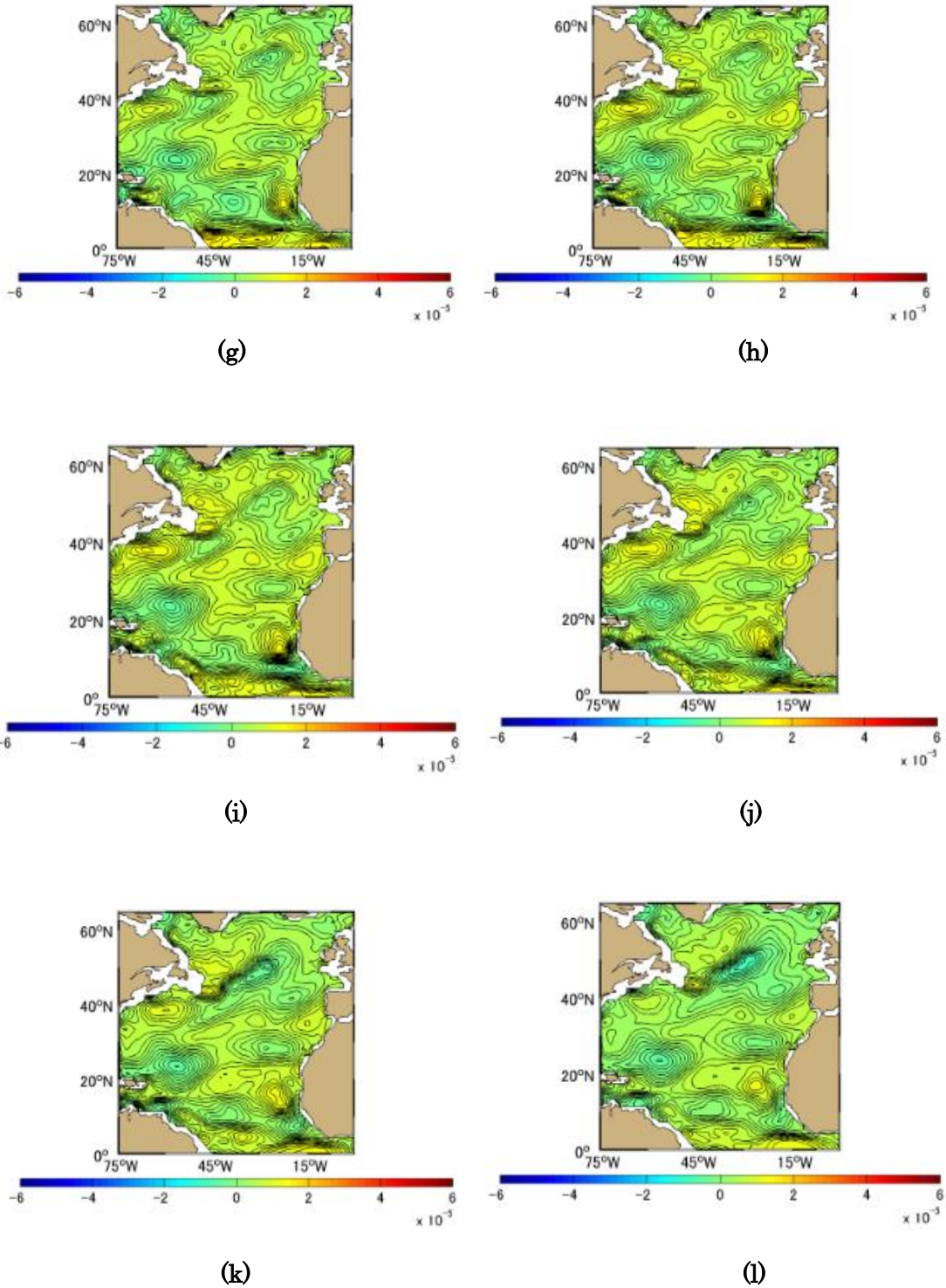
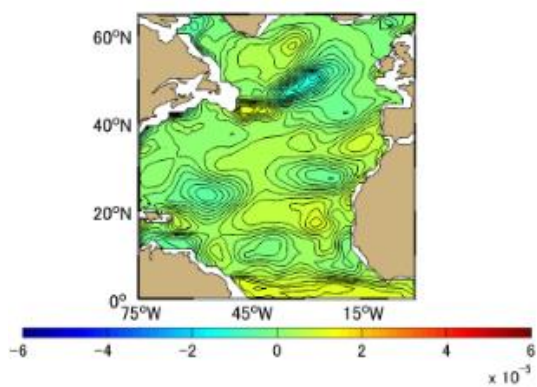
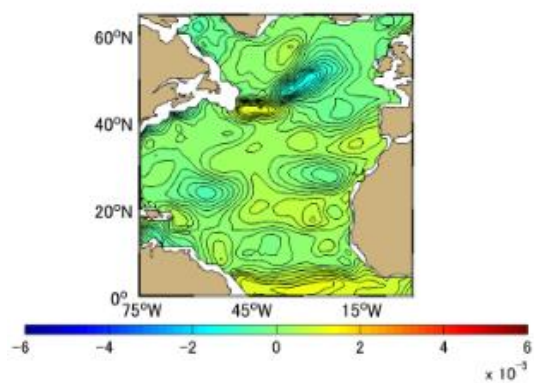


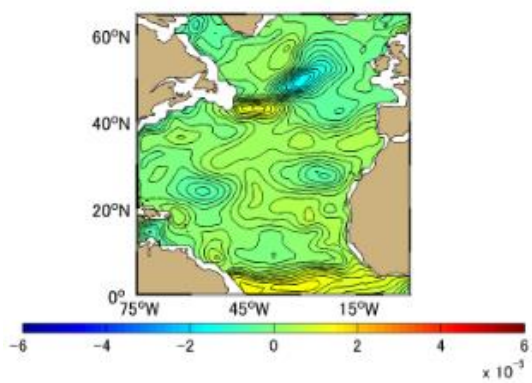
Figure A-4.5 Difference [PgC] between Approximation Method and Simulation Method Monthly Mean in 1995, the North Atlantic based on January 1991. (a)-(l) represents January-December



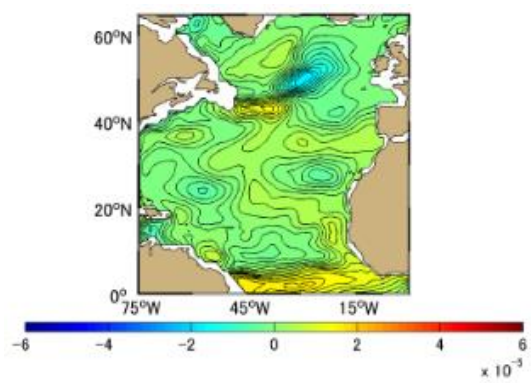
(a)



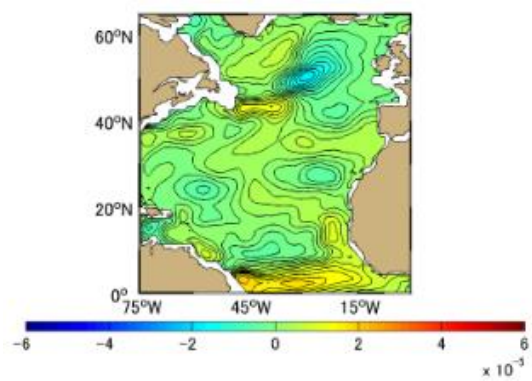
(b)



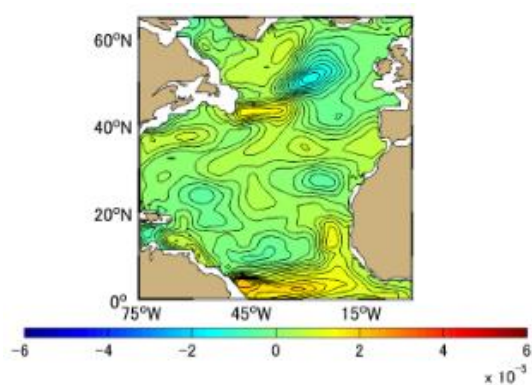
(c)



(d)



(e)



(f)

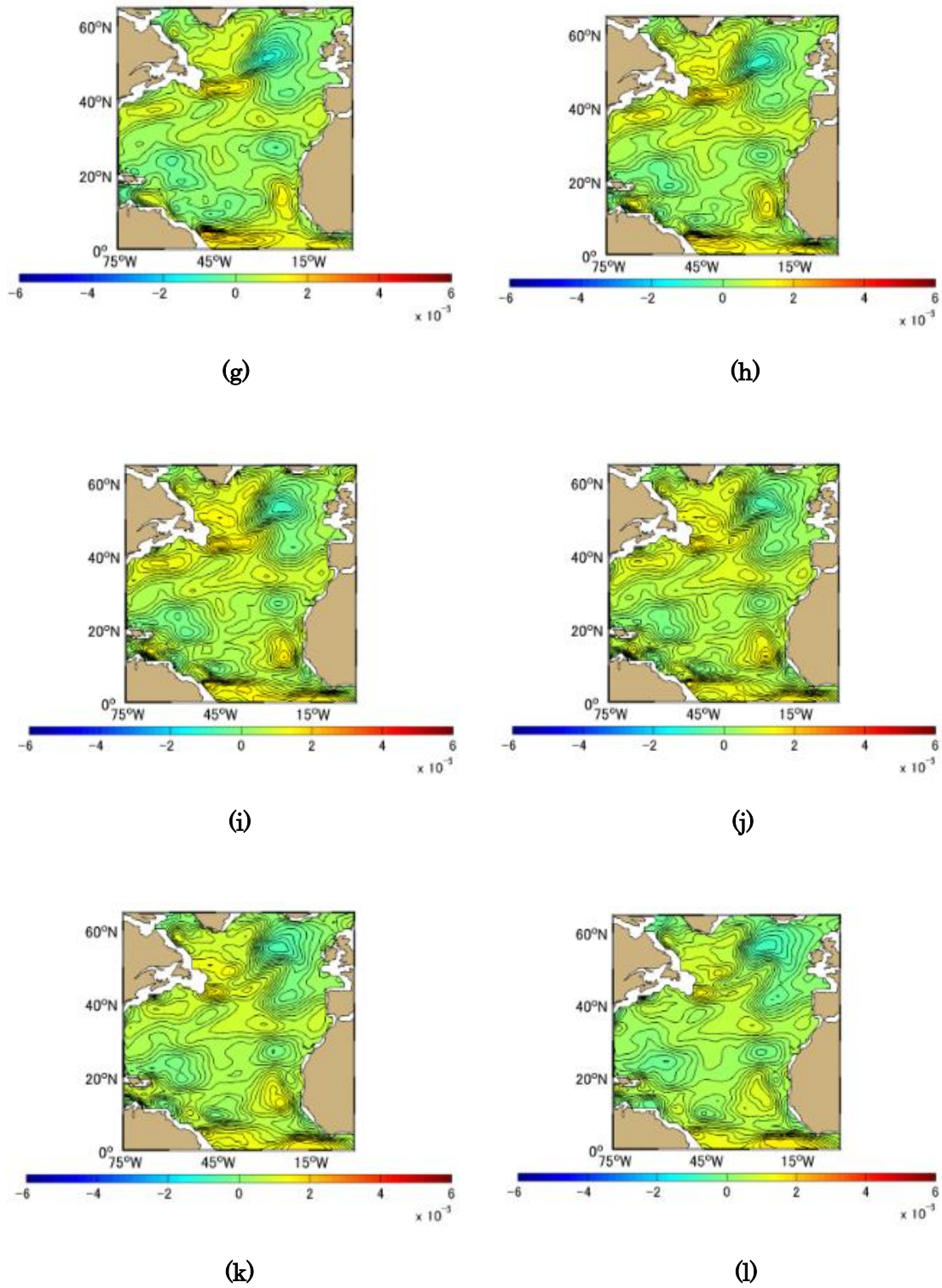
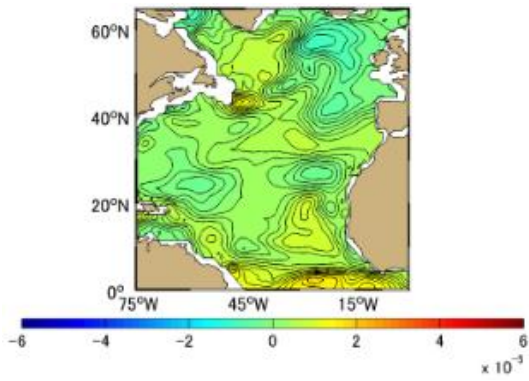
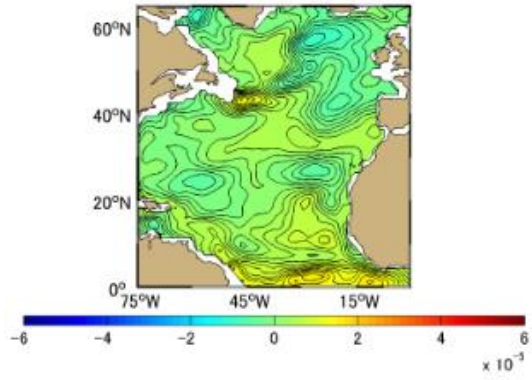


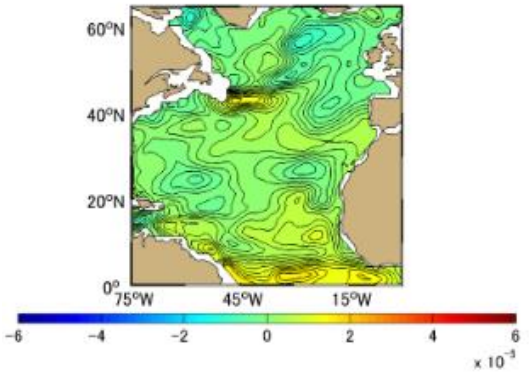
Figure A-4.6 Difference [PgC] between Approximation Method and Simulation Method Monthly Mean in 1996, the North Atlantic based on January 1991. (a)-(l) represents January-December



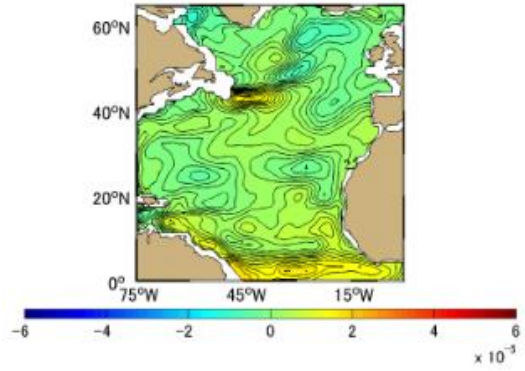
(a)



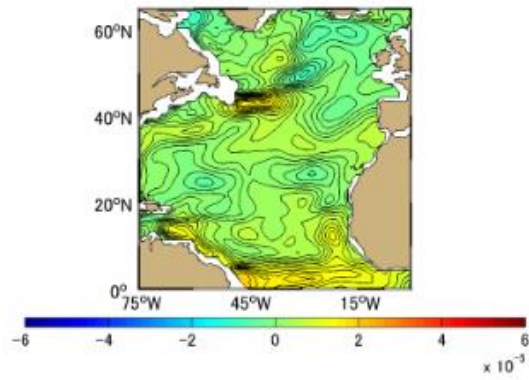
(b)



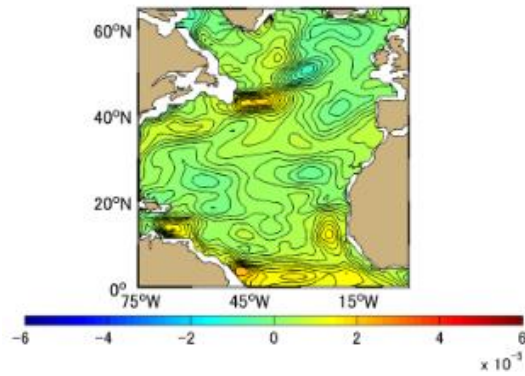
(c)



(d)

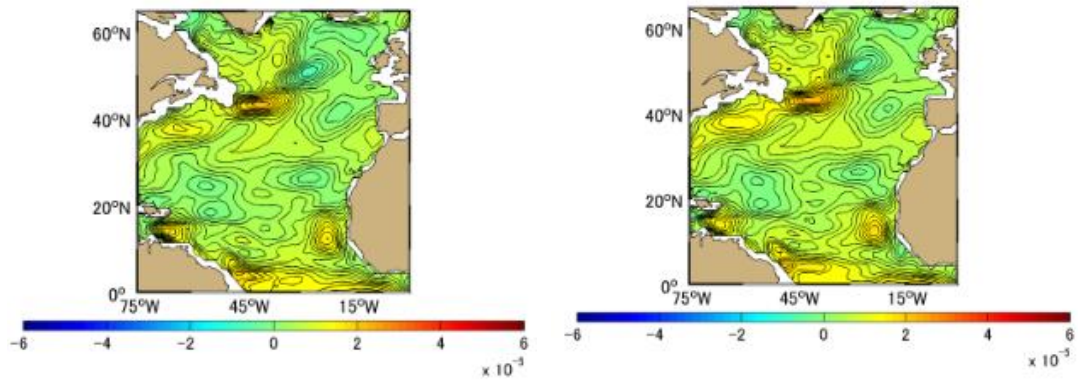


(e)



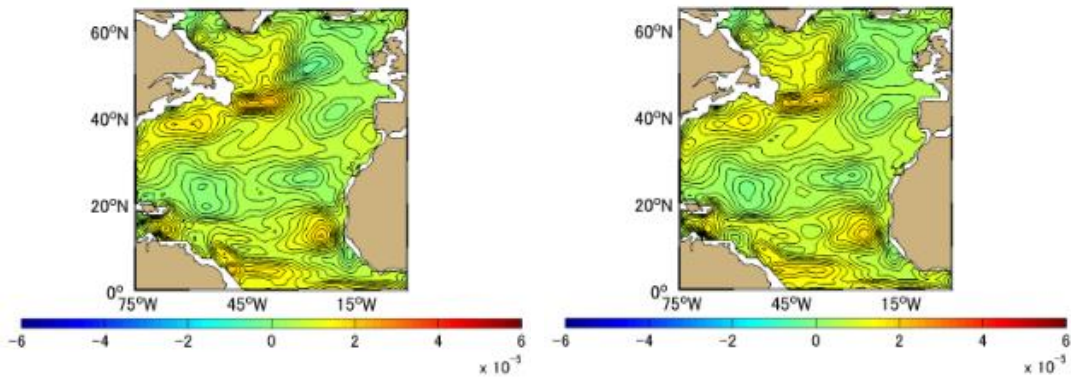
(f)





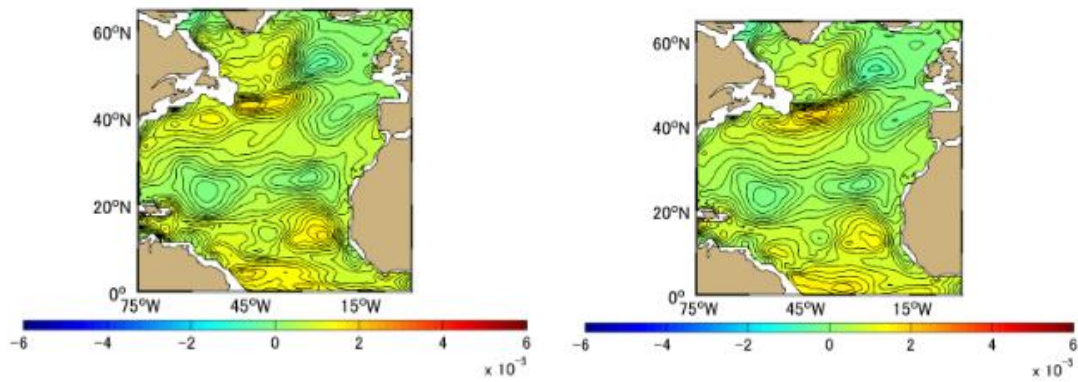
(g)

(h)



(i)

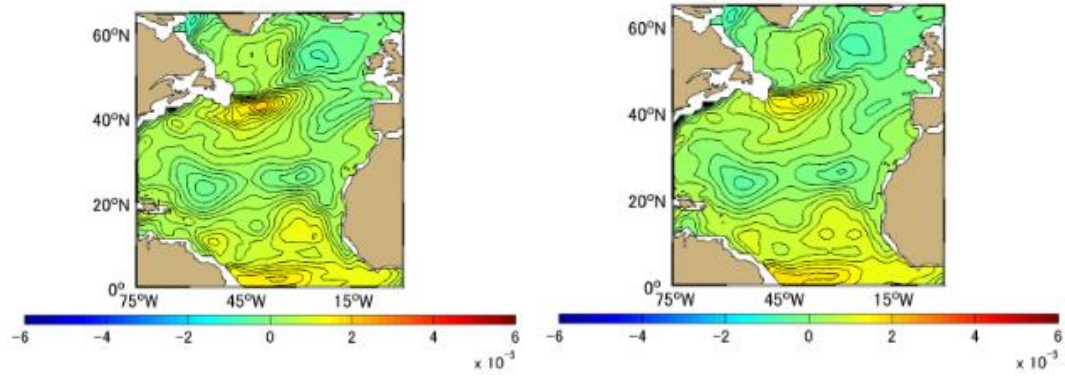
(j)



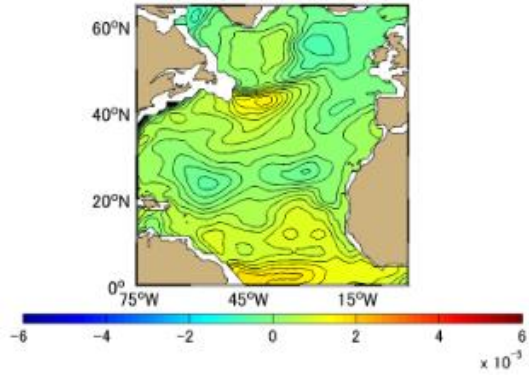
(k)

(l)

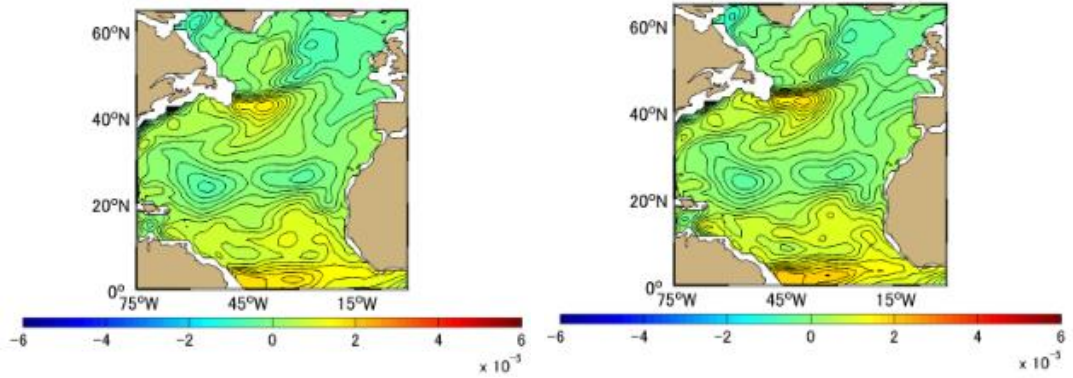
Figure A-4.7 Difference [PgC] between Approximation Method and Simulation Method Monthly Mean in 1997, the North Atlantic based on January 1991. (a)-(l) represents January-December



(a)

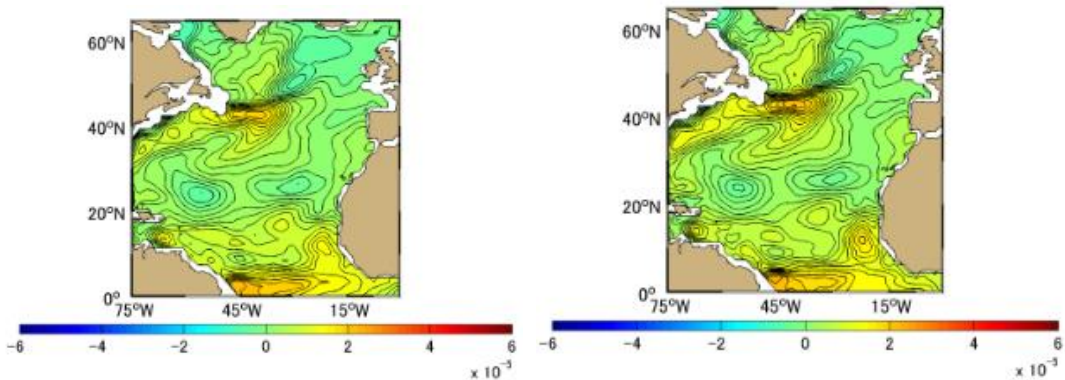


(b)



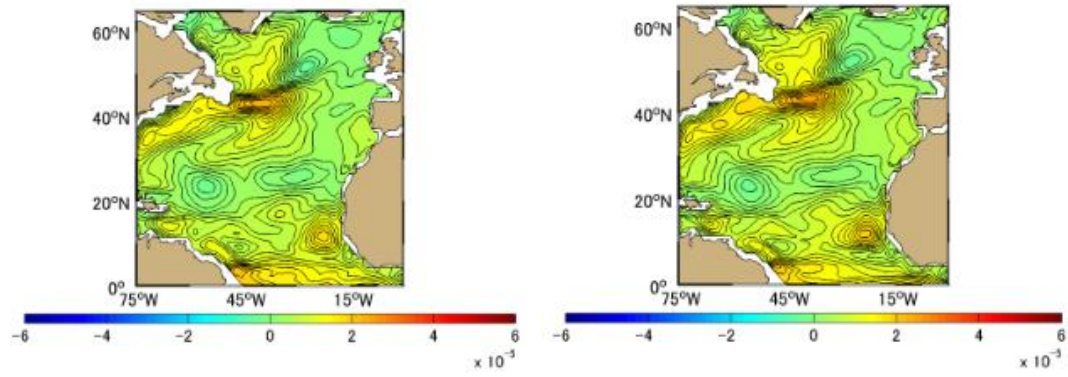
(c)

(d)



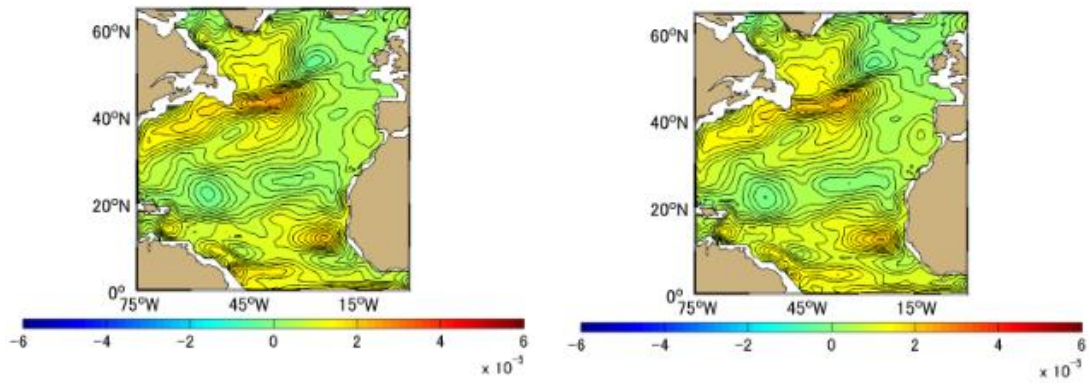
(e)

(f)



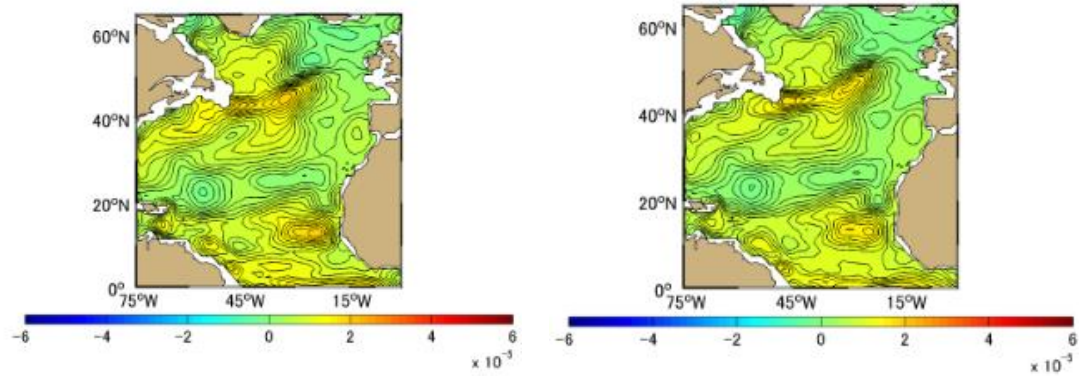
(g)

(h)



(i)

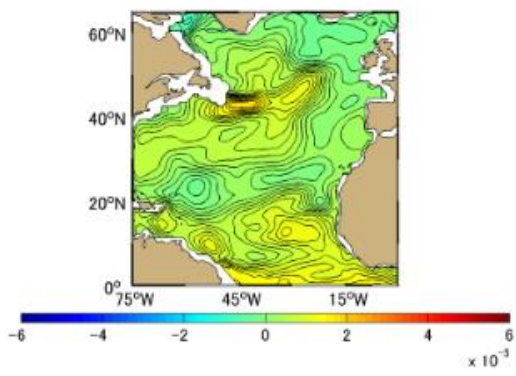
(j)



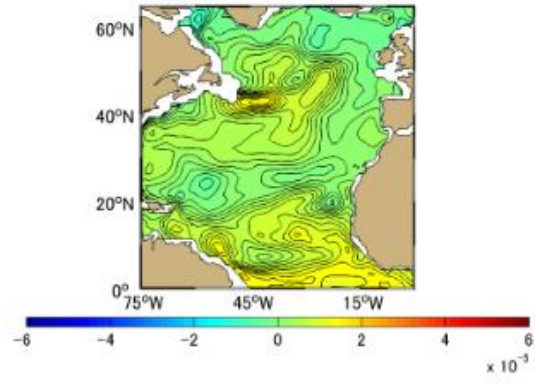
(k)

(l)

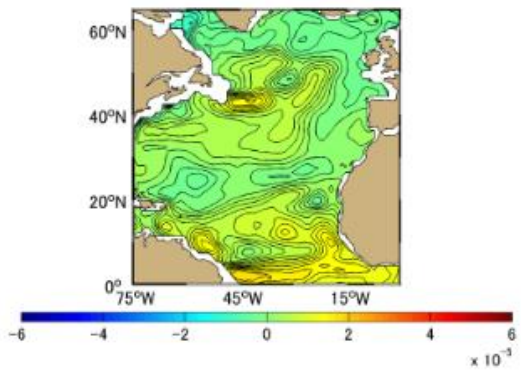
Figure A-4.8 Difference [PgC] between Approximation Method and Simulation Method Monthly Mean in 1998, the North Atlantic based on January 1991. (a)-(l) represents January-December



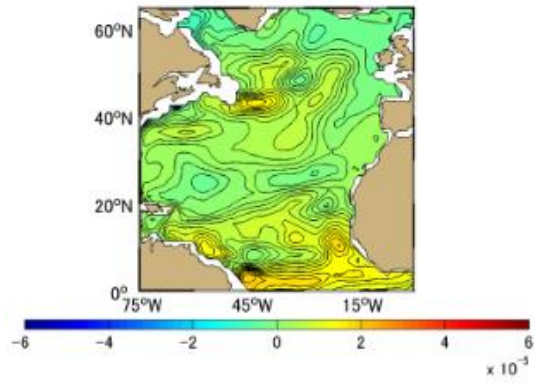
(a)



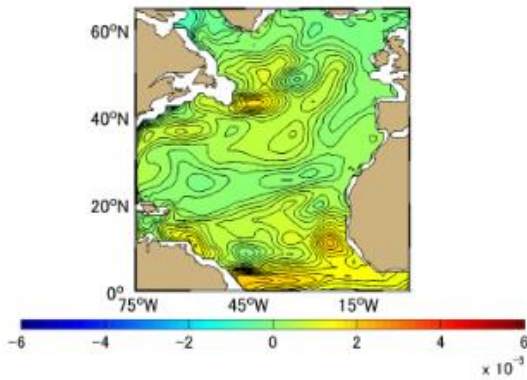
(b)



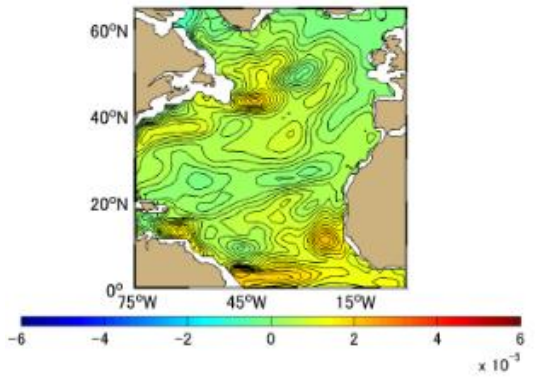
(c)



(d)



(e)



(f)

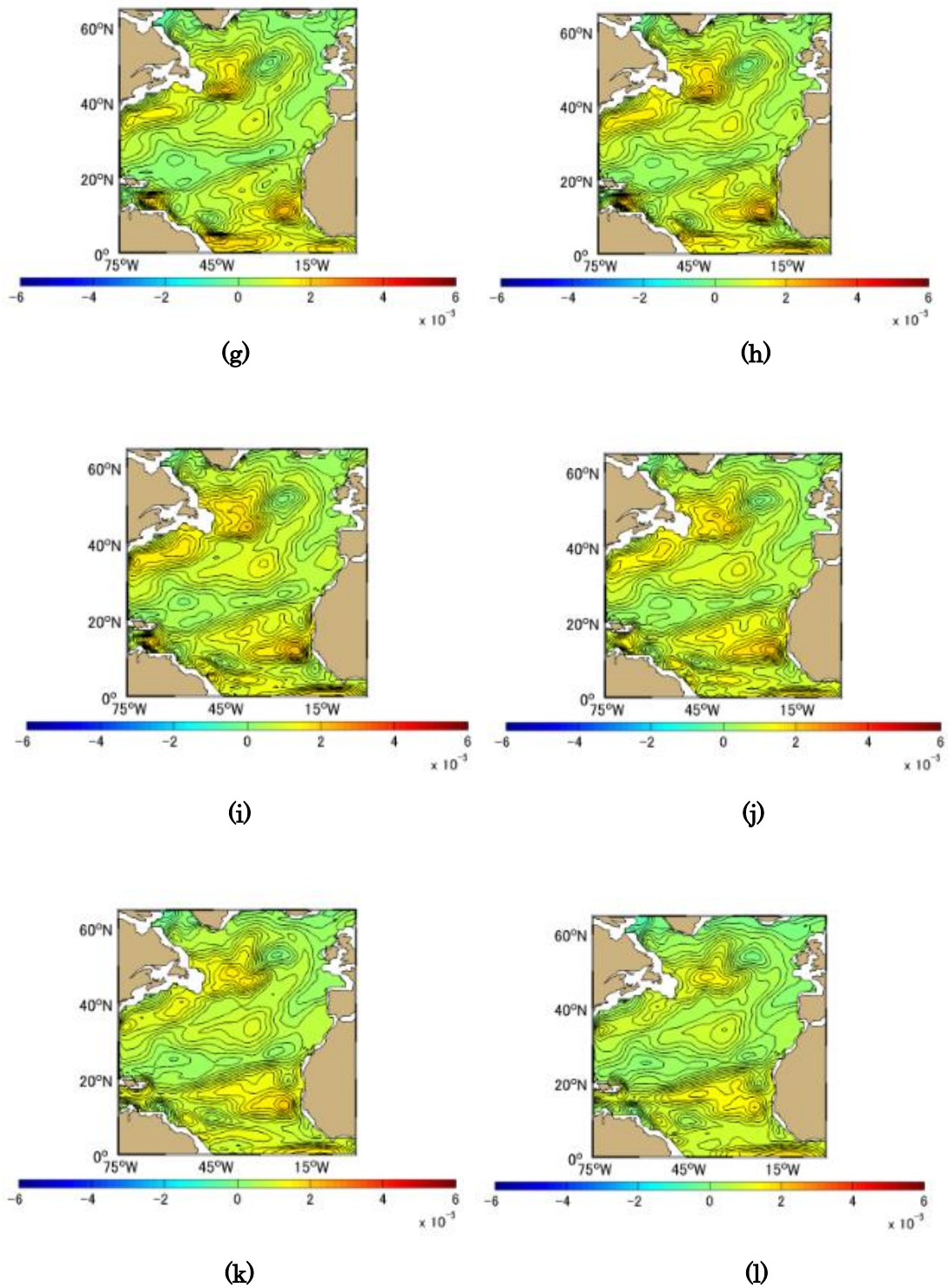
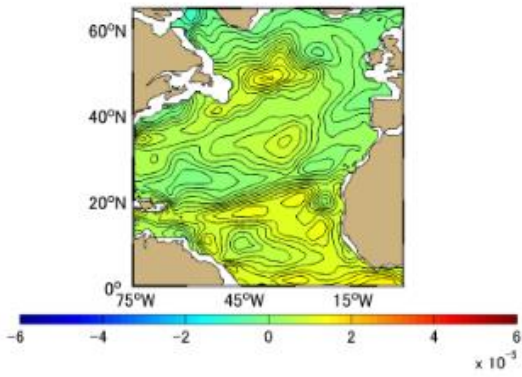
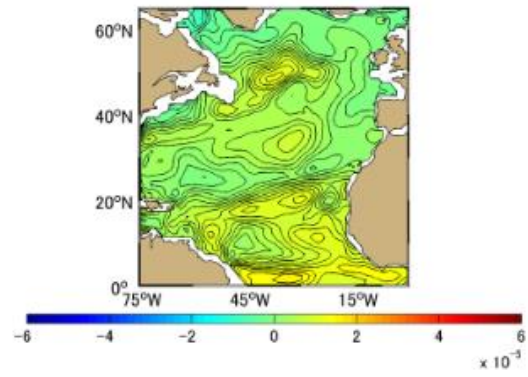


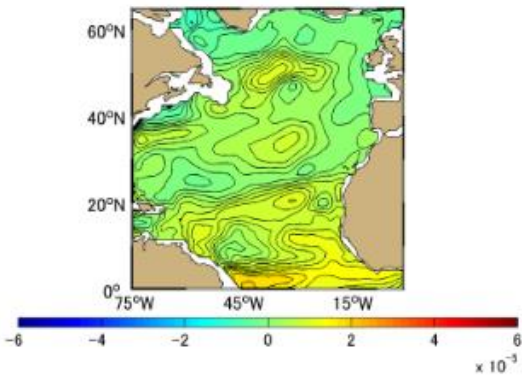
Figure A-4.9 Difference [PgC] between Approximation Method and Simulation Method Monthly Mean in 1999, the North Atlantic based on January 1991. (a)-(l) represents January-December



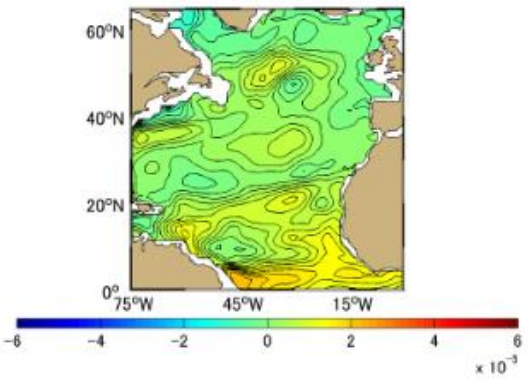
(a)



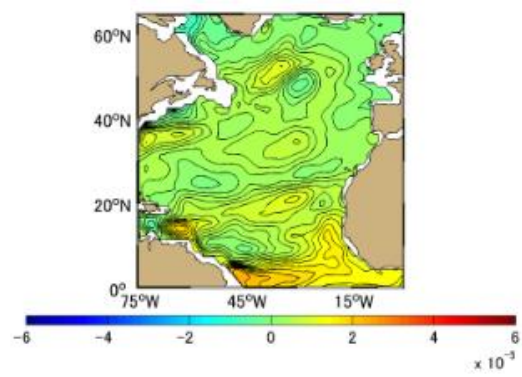
(b)



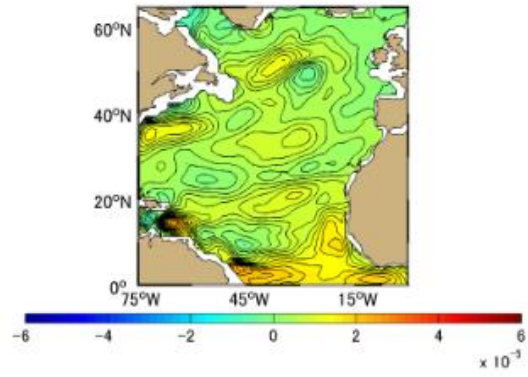
(c)



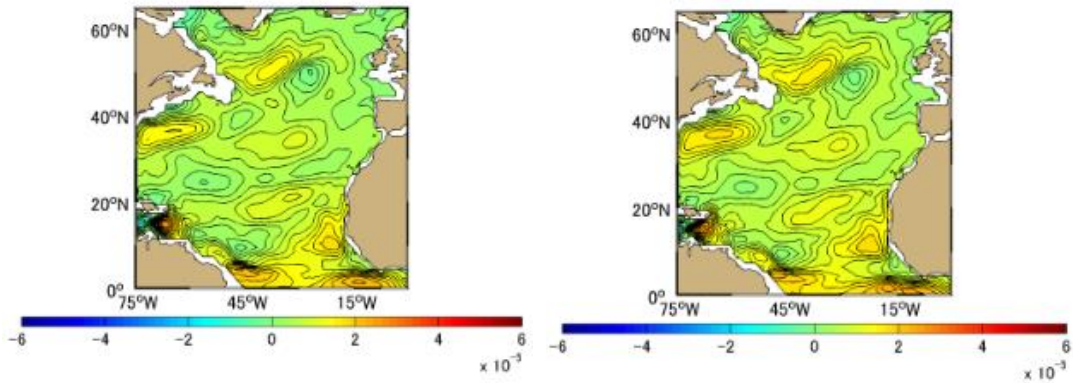
(d)



(e)

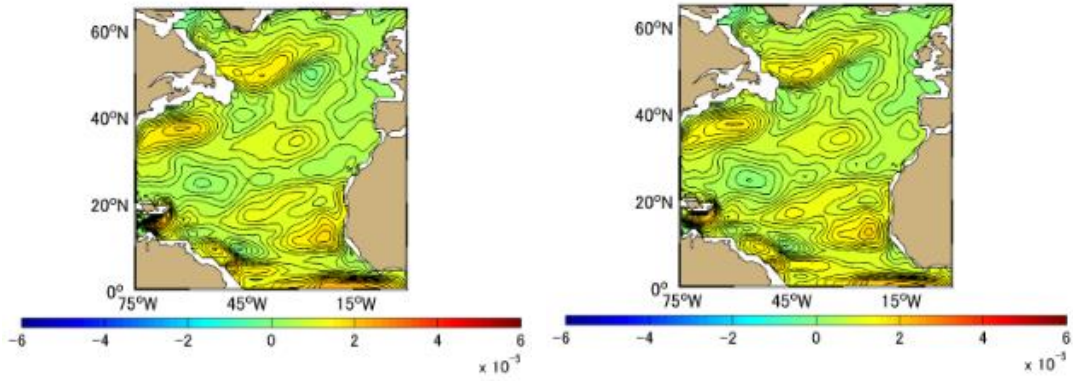


(f)



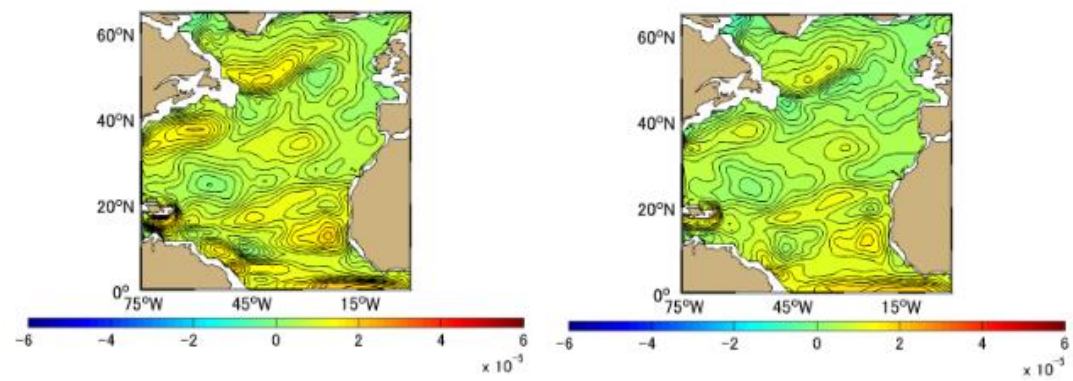
(g)

(h)



(i)

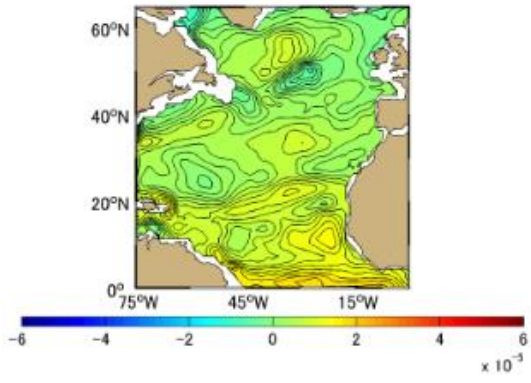
(j)



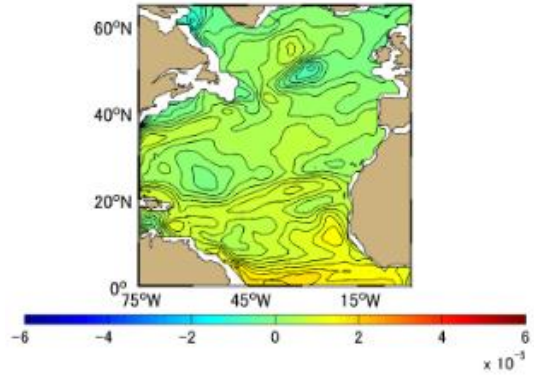
(k)

(l)

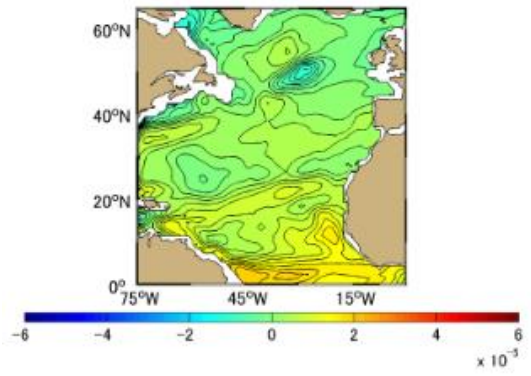
Figure A-4.10 Difference [PgC] between Approximation Method and Simulation Method Monthly Mean in 2000, the North Atlantic based on January 1991. (a)-(l) represents January-December



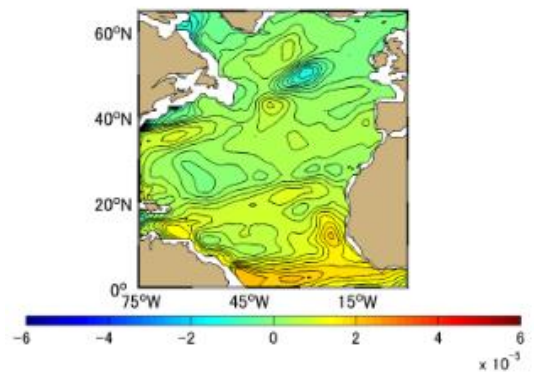
(a)



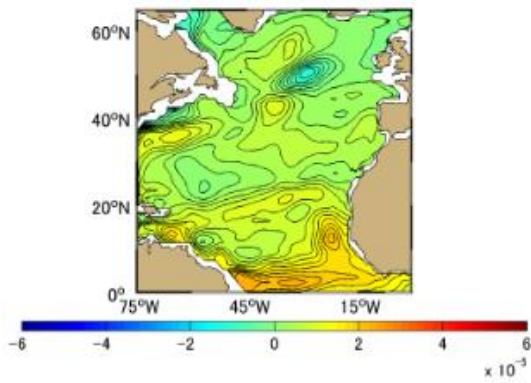
(b)



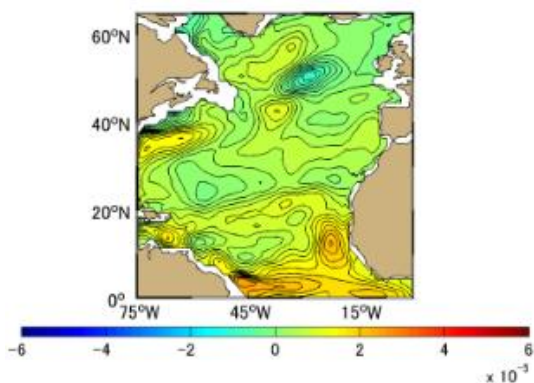
(c)



(d)



(e)



(f)



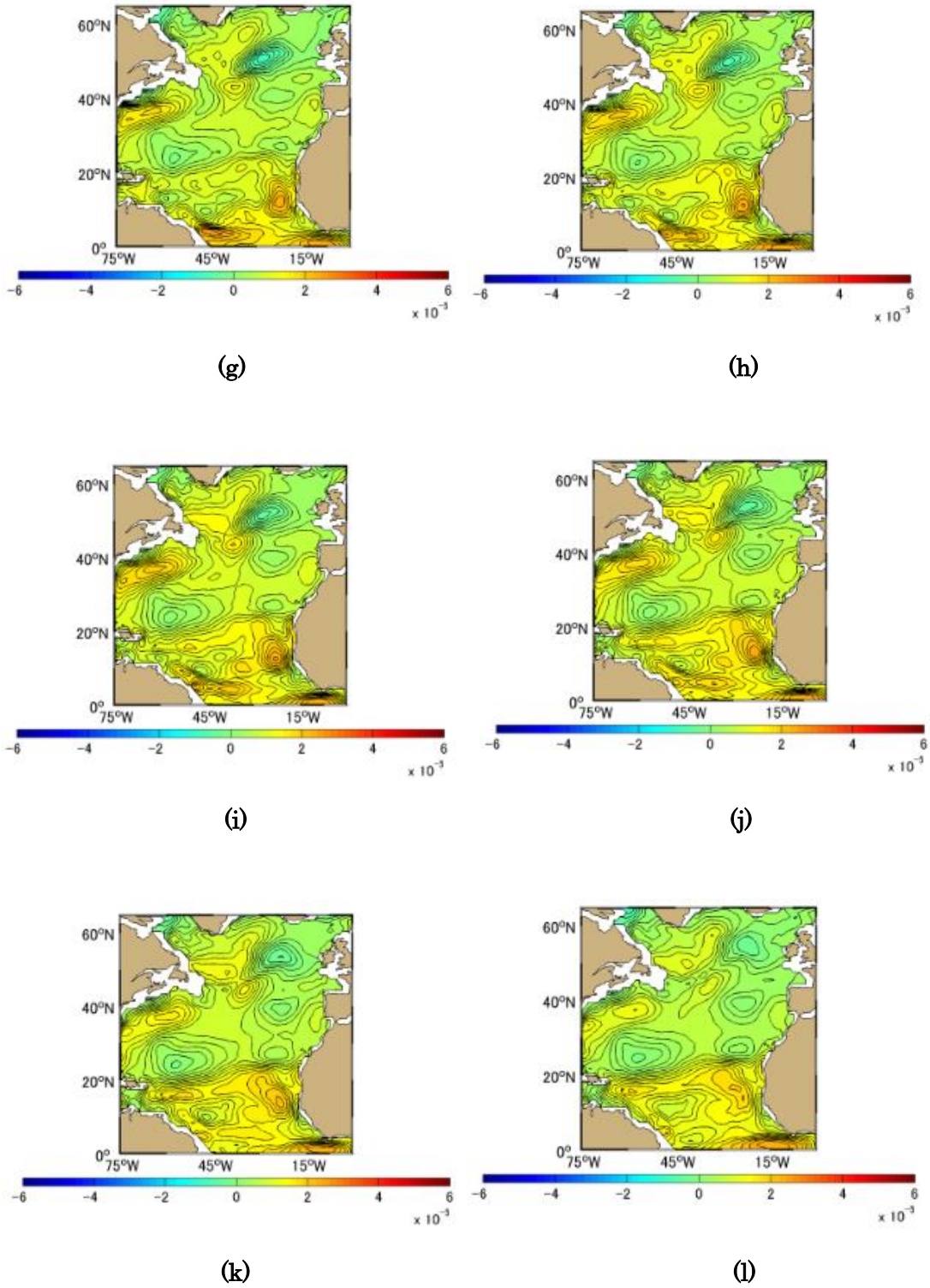
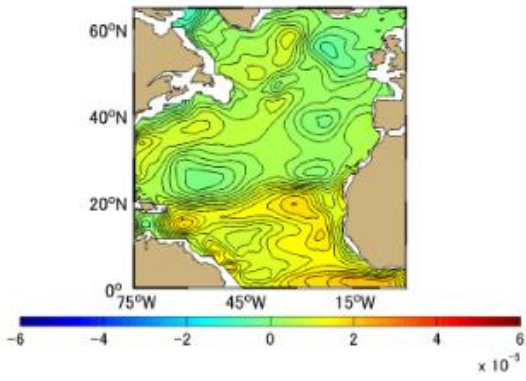
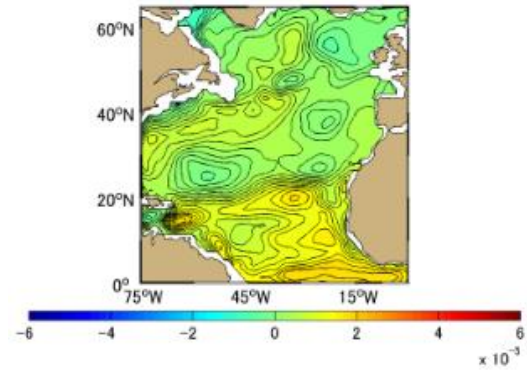


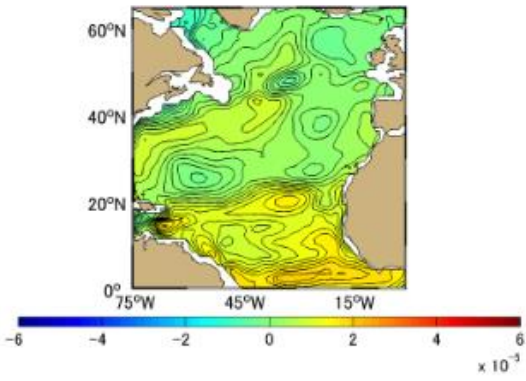
Figure A-4.11 Difference [PgC] between Approximation Method and Simulation Method Monthly Mean in 2001, the North Atlantic based on January 1991. (a)-(l) represents January-December



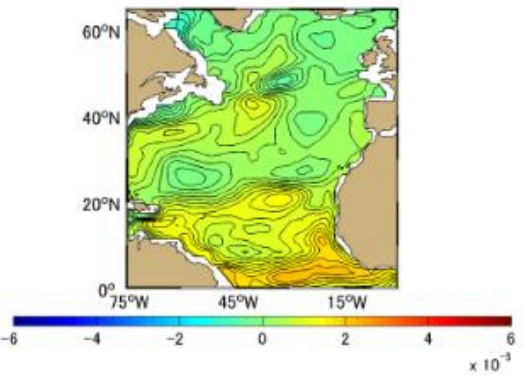
(a)



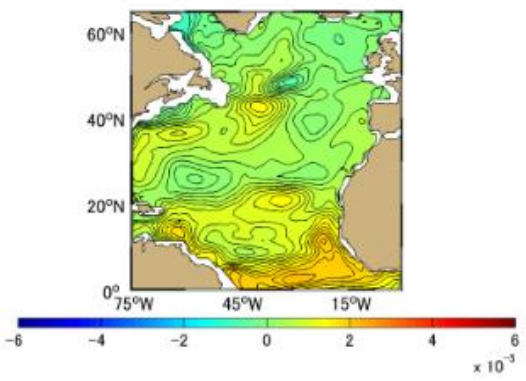
(b)



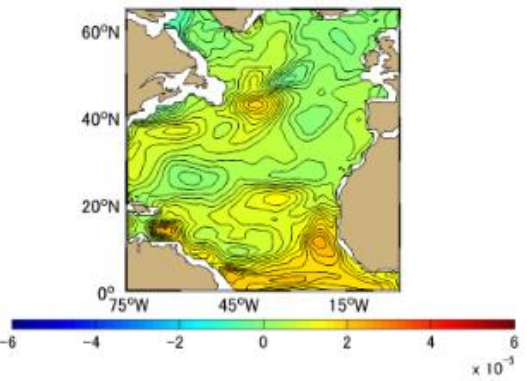
(c)



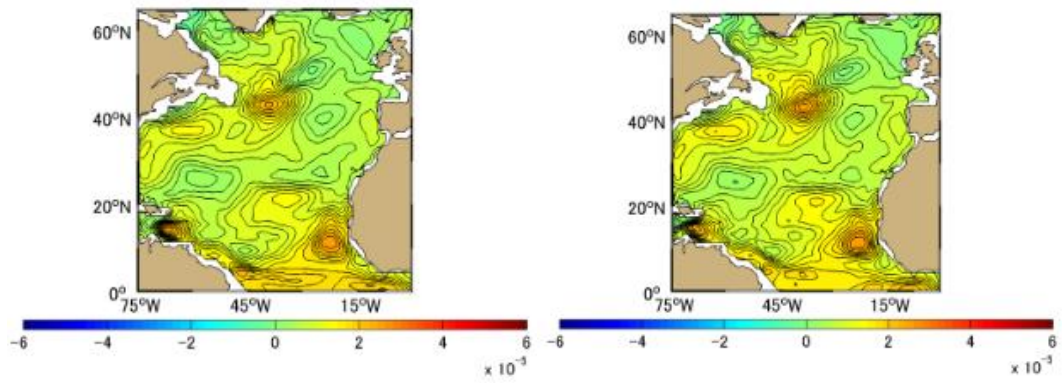
(d)



(e)

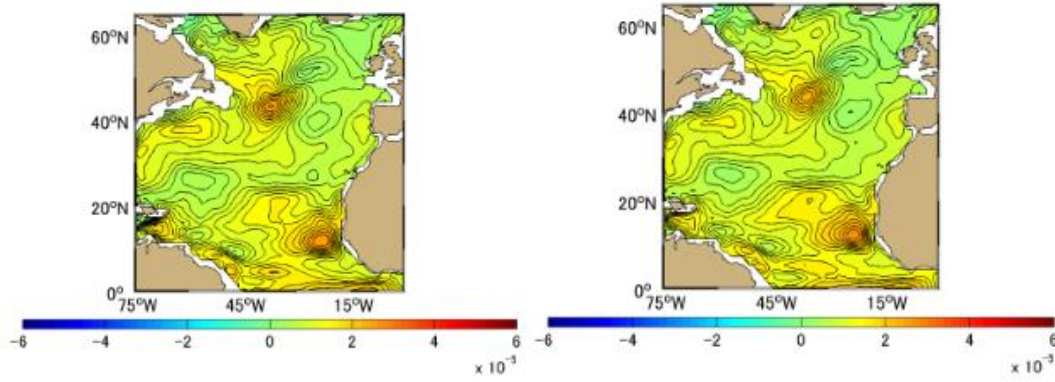


(f)



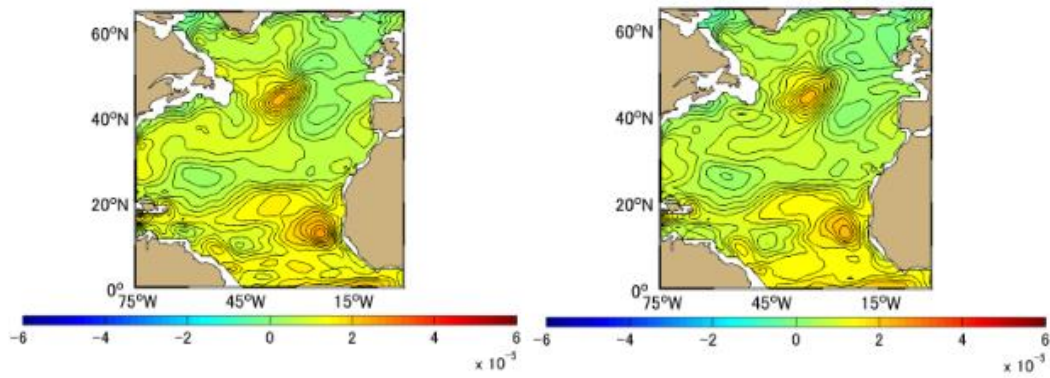
(g)

(h)



(i)

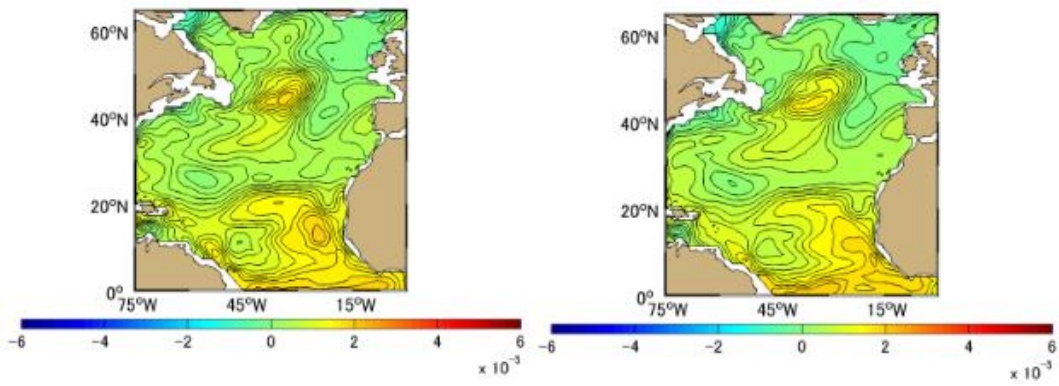
(j)



(k)

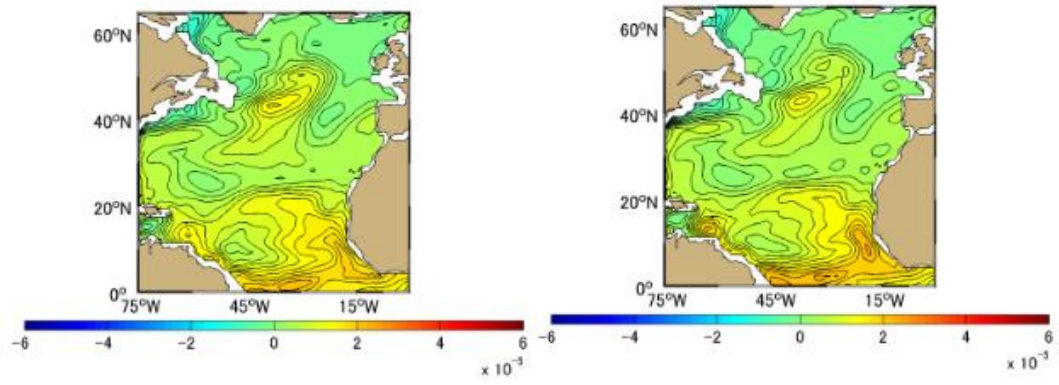
(l)

Figure A-4.12 Difference [PgC] between Approximation Method and Simulation Method Monthly Mean in 2002, the North Atlantic based on January 1991. (a)-(l) represents January-December



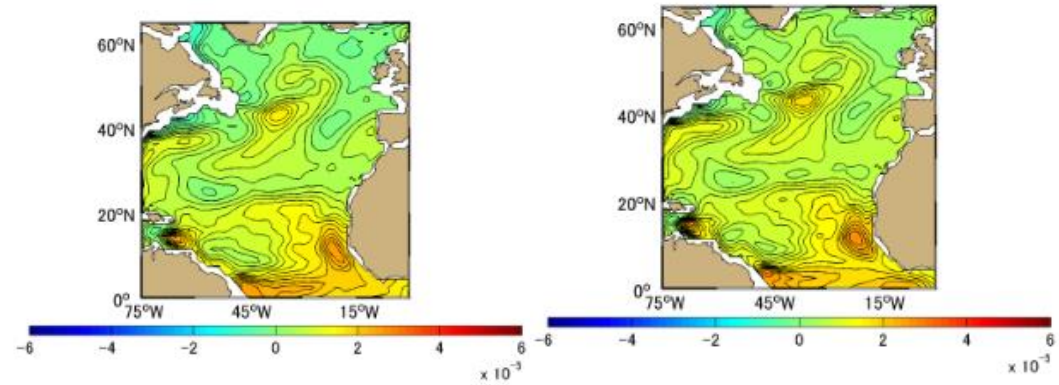
(a)

(b)



(c)

(d)



(e)

(f)

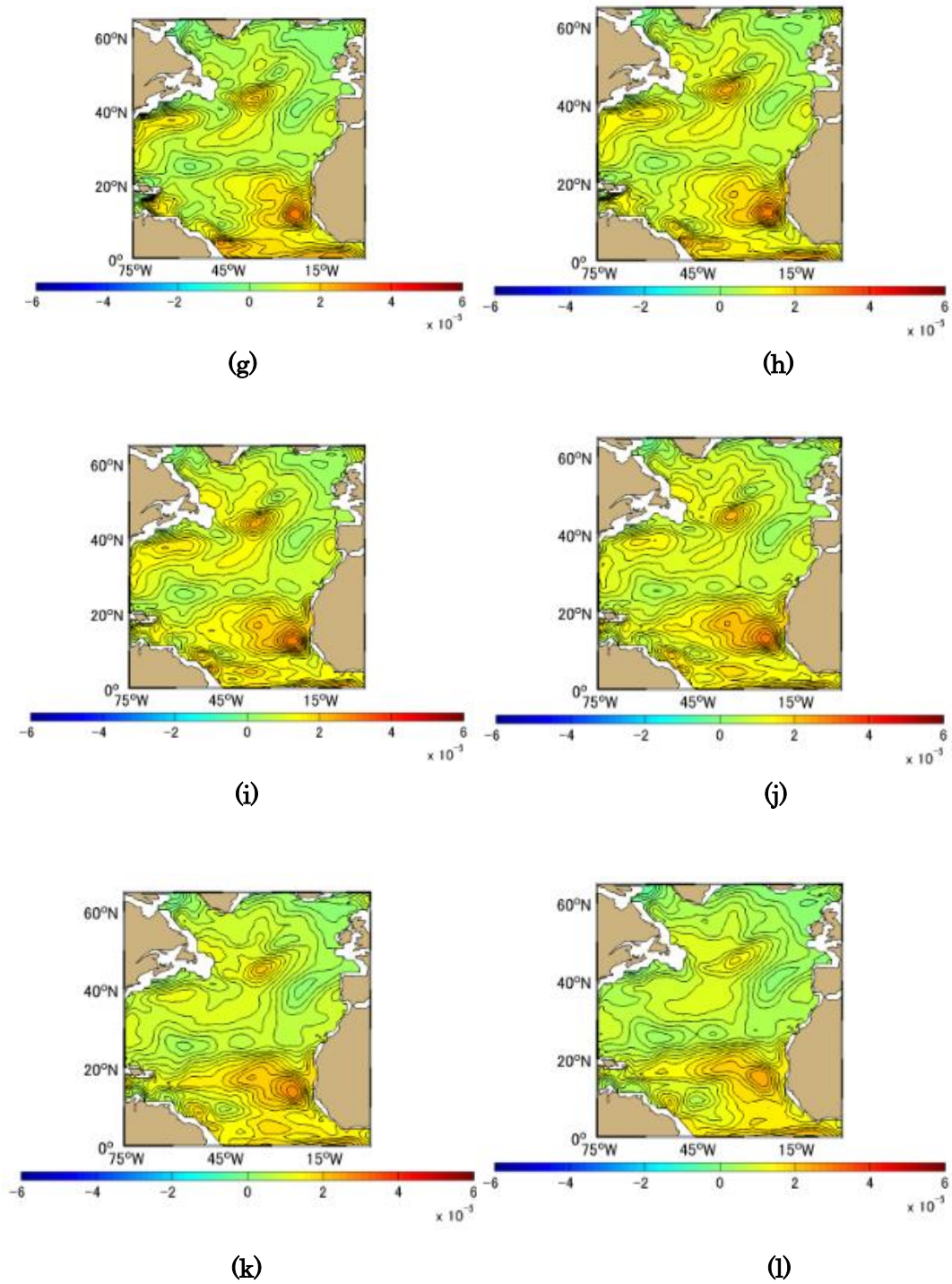
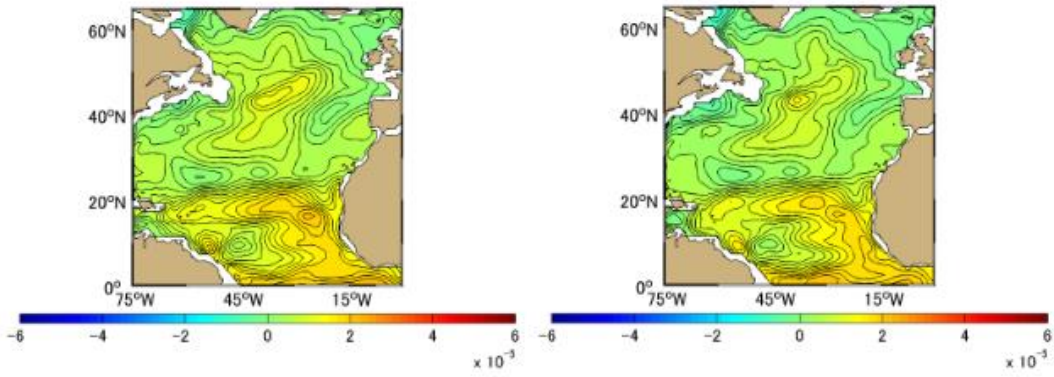
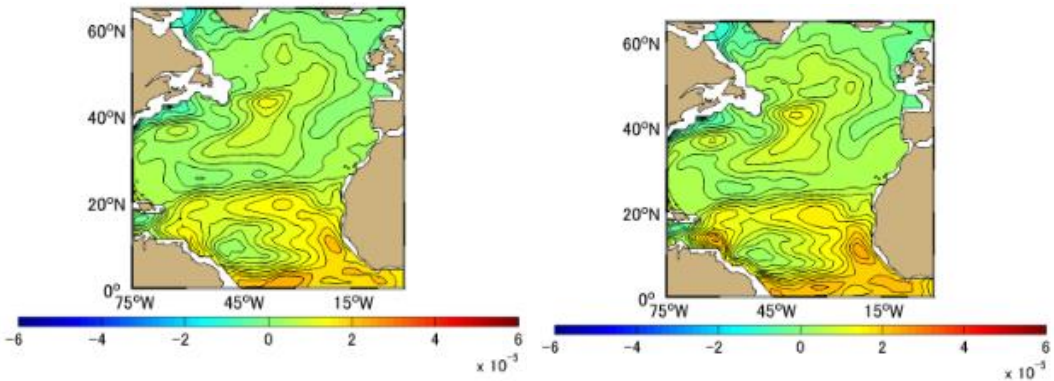


Figure A-4.13 Difference [PgC] between Approximation Method and Simulation Method Monthly Mean in 2003, the North Atlantic based on January 1991. (a)-(l) represents January-December



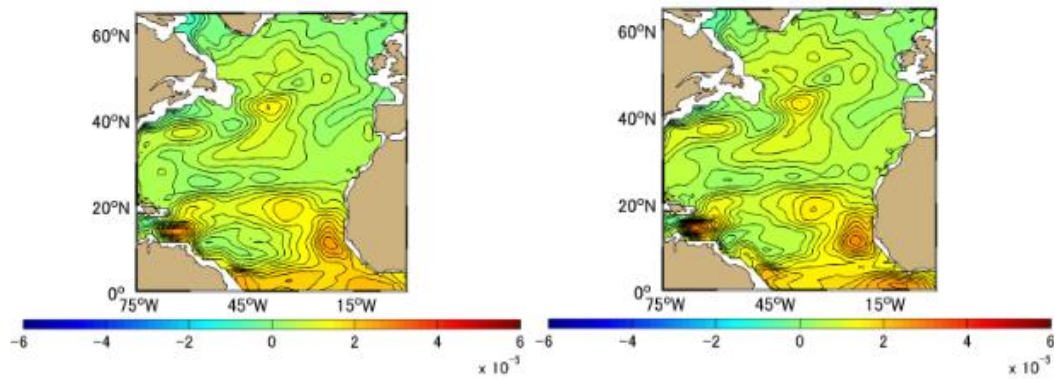
(a)

(b)



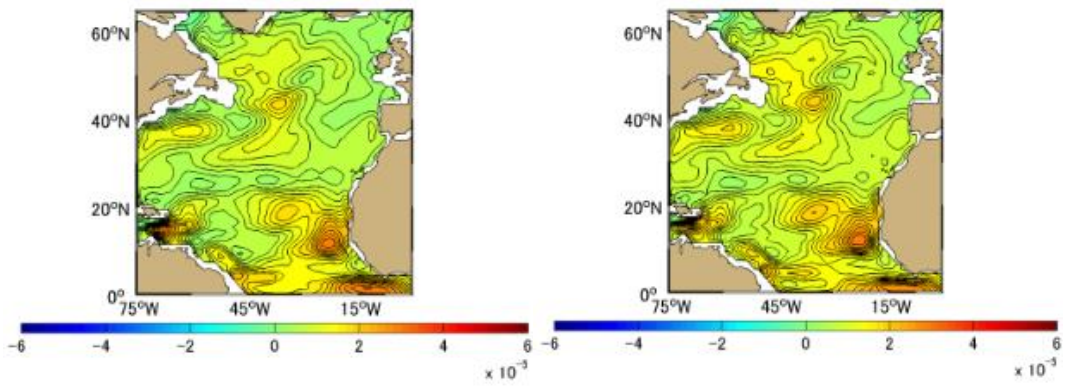
(c)

(d)



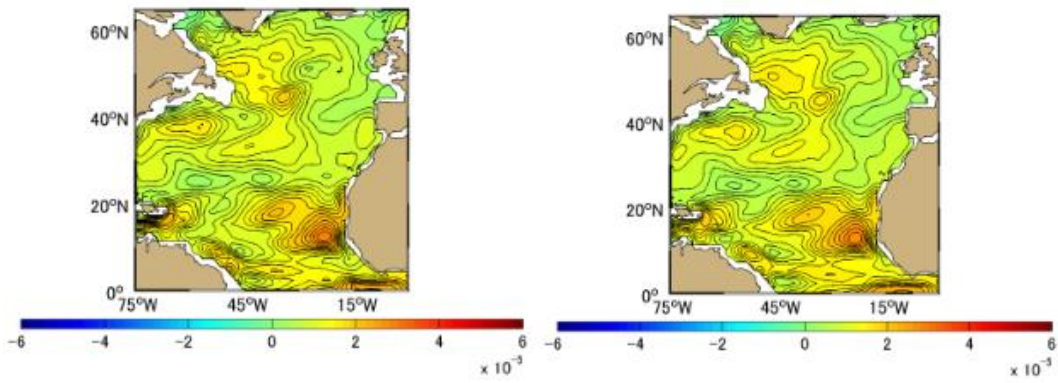
(e)

(f)



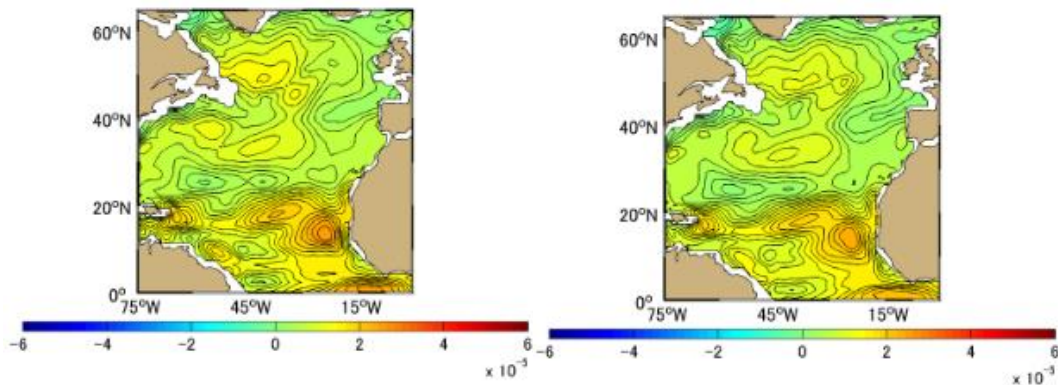
(g)

(h)



(i)

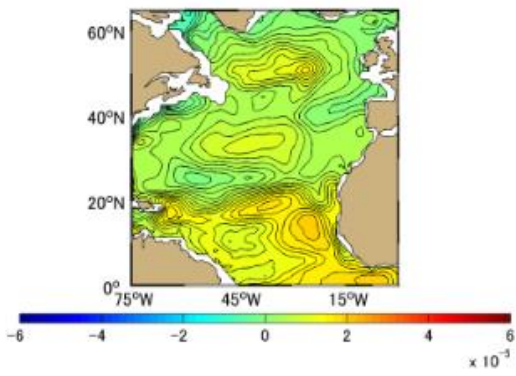
(j)



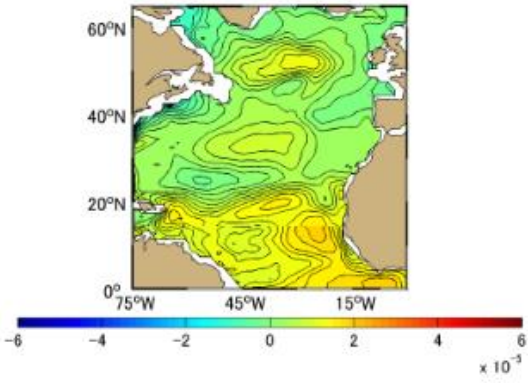
(k)

(l)

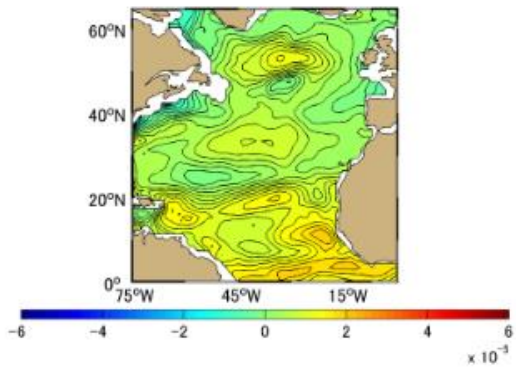
Figure A-4.14 Difference [PgC] between Approximation Method and Simulation Method Monthly Mean in 2004, the North Atlantic based on January 1991. (a)-(l) represents January-December



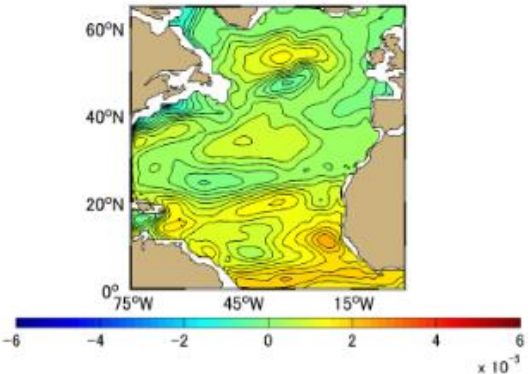
(a)



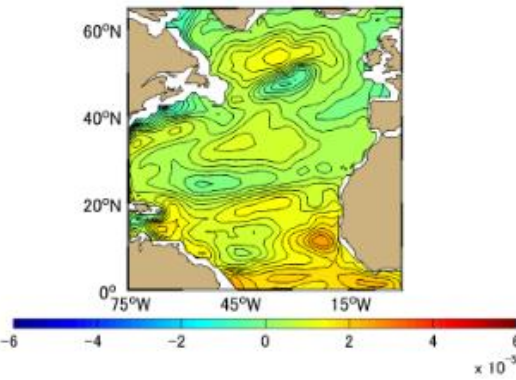
(b)



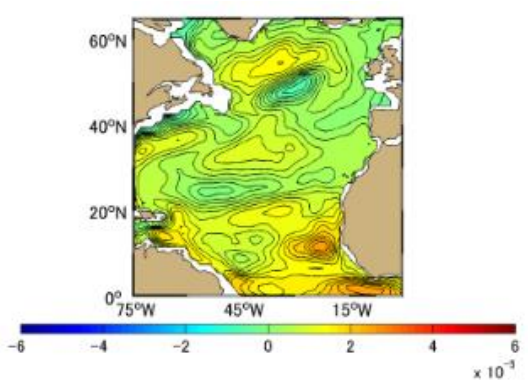
(c)



(d)

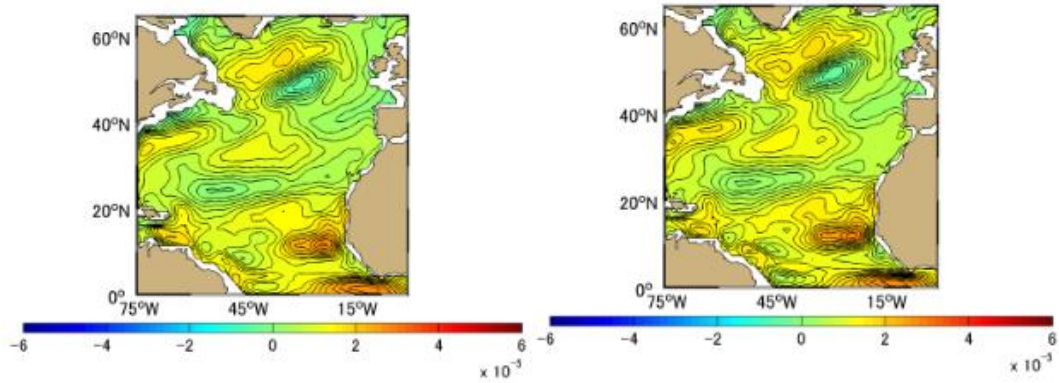


(e)



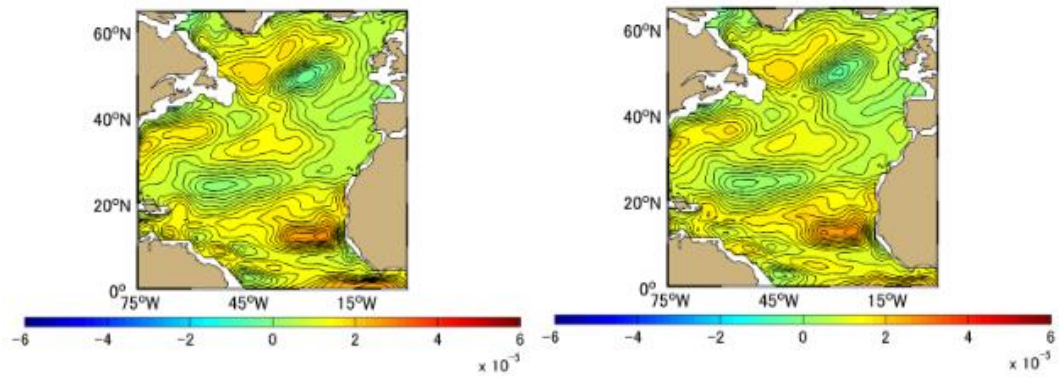
(f)





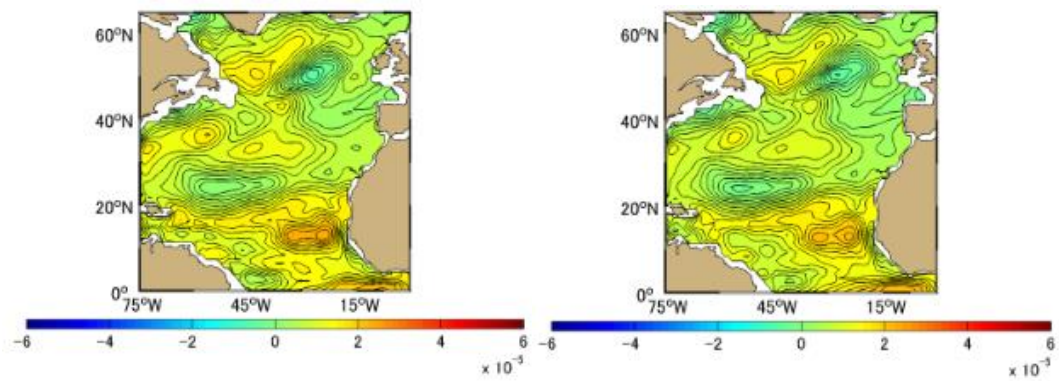
(g)

(h)



(i)

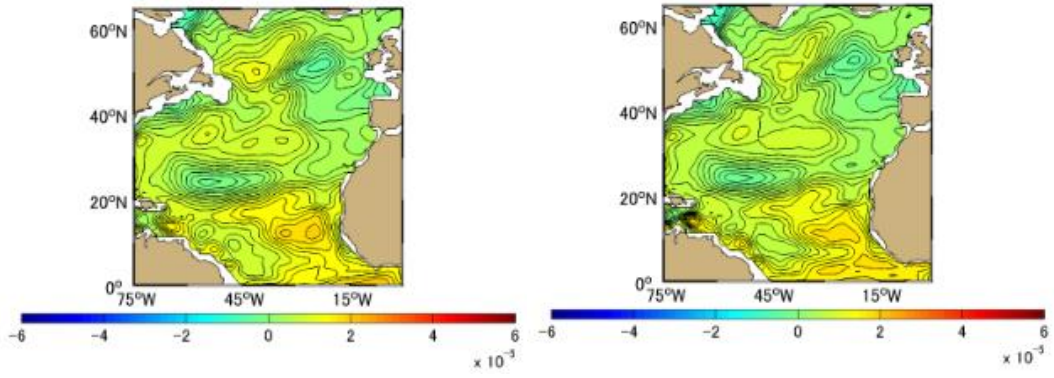
(j)



(k)

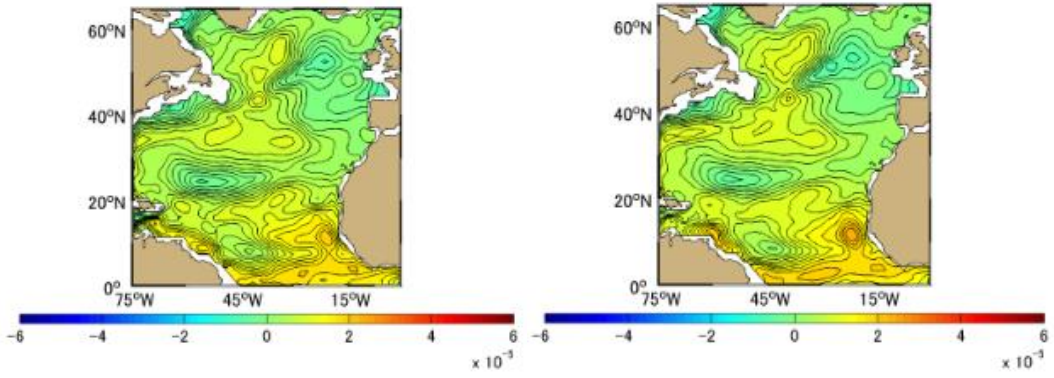
(l)

Figure A-4.15 Difference [PgC] between Approximation Method and Simulation Method Monthly Mean in 2005, the North Atlantic based on January 1991. (a)-(l) represents January-December



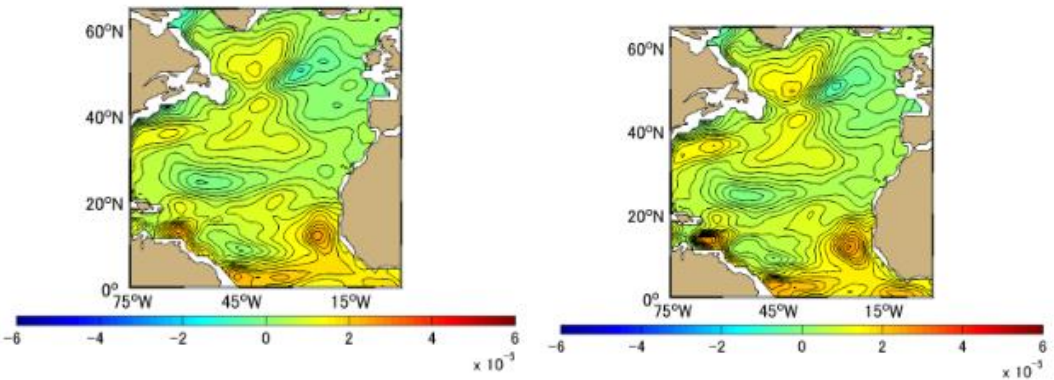
(a)

(b)



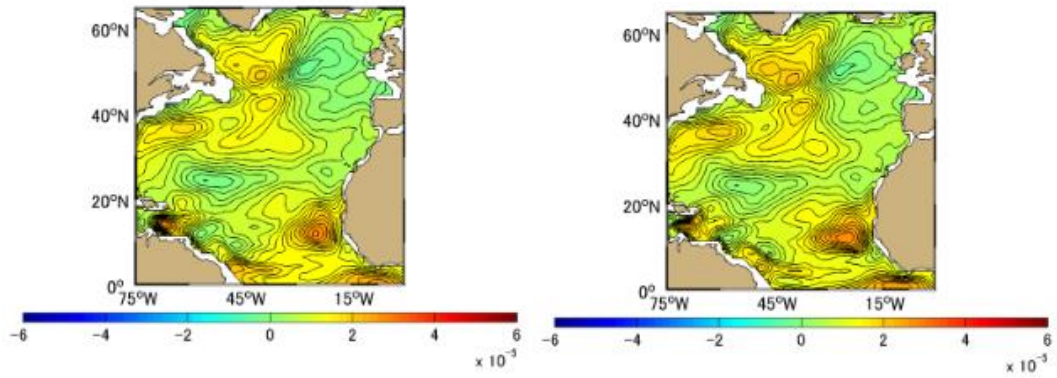
(c)

(d)



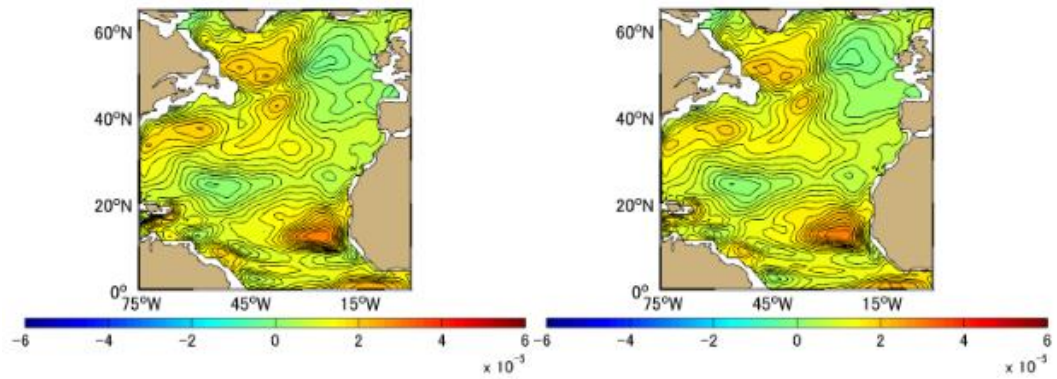
(e)

(f)



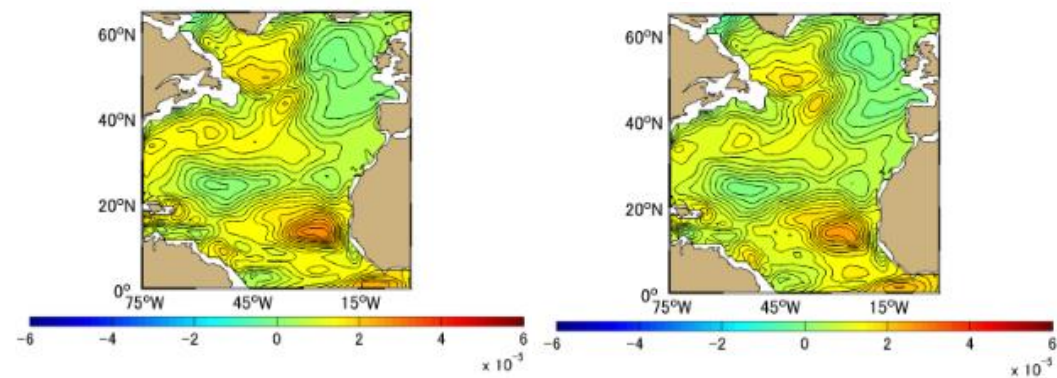
(g)

(h)



(i)

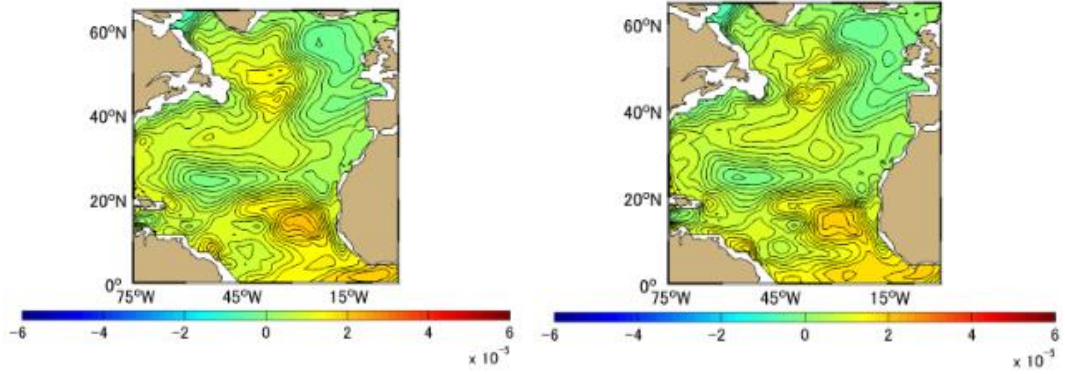
(j)



(k)

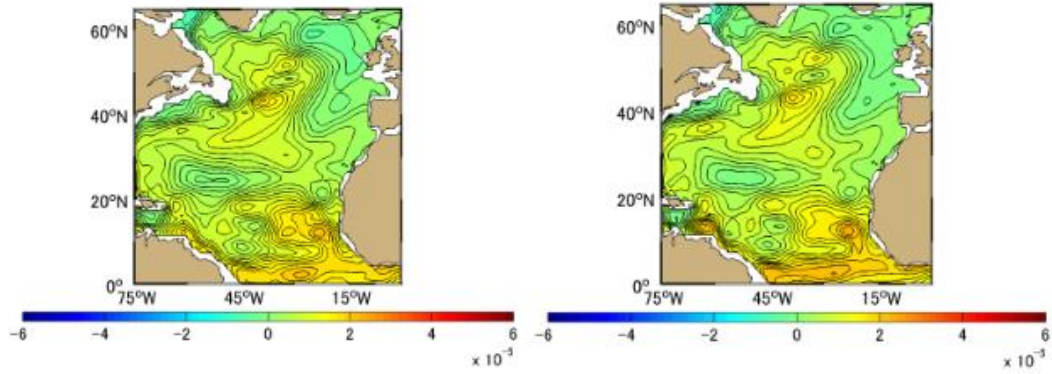
(l)

Figure A-4.16 Difference [PgC] between Approximation Method and Simulation Method Monthly Mean in 2006, the North Atlantic based on January 1991. (a)-(l) represents January-December



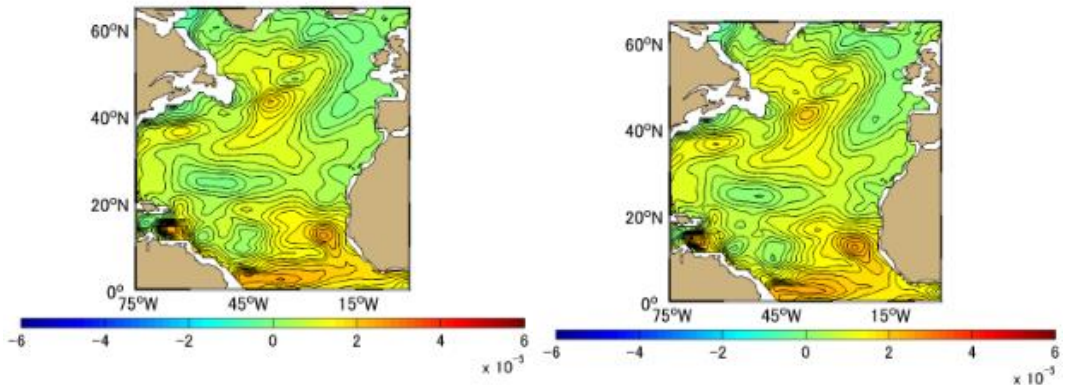
(a)

(b)



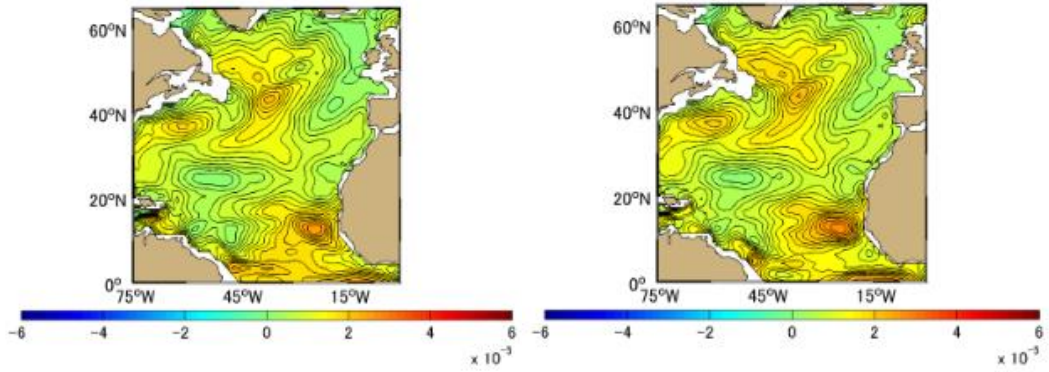
(c)

(d)



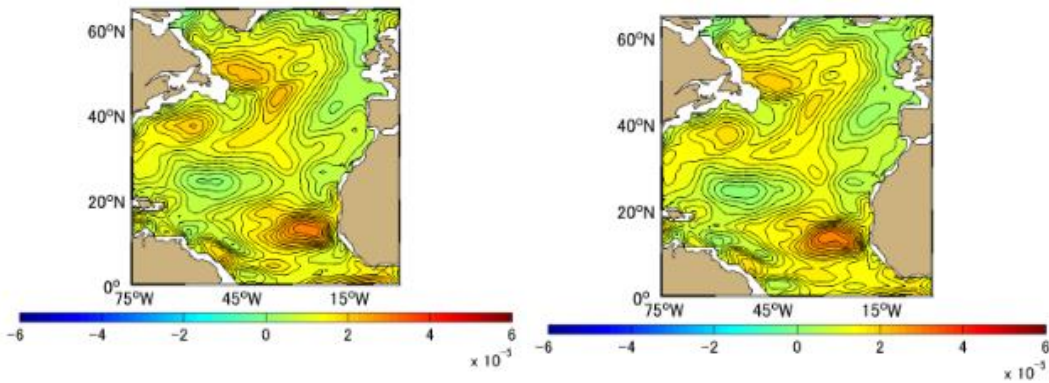
(e)

(f)



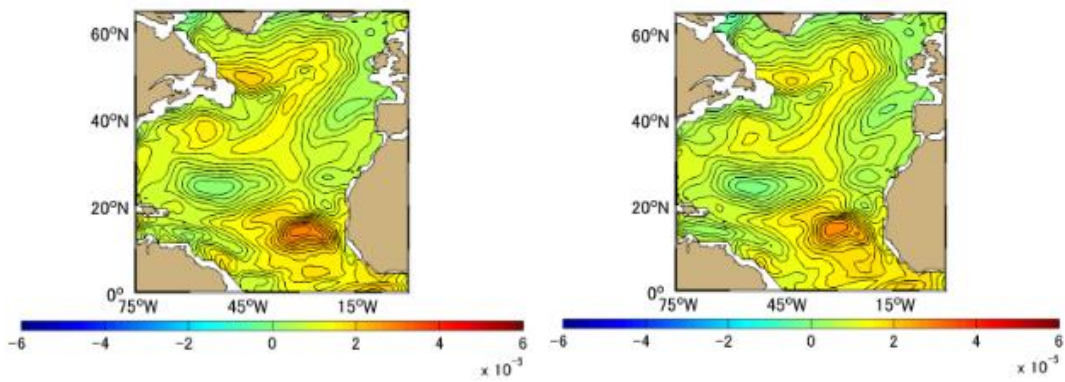
(g)

(h)



(i)

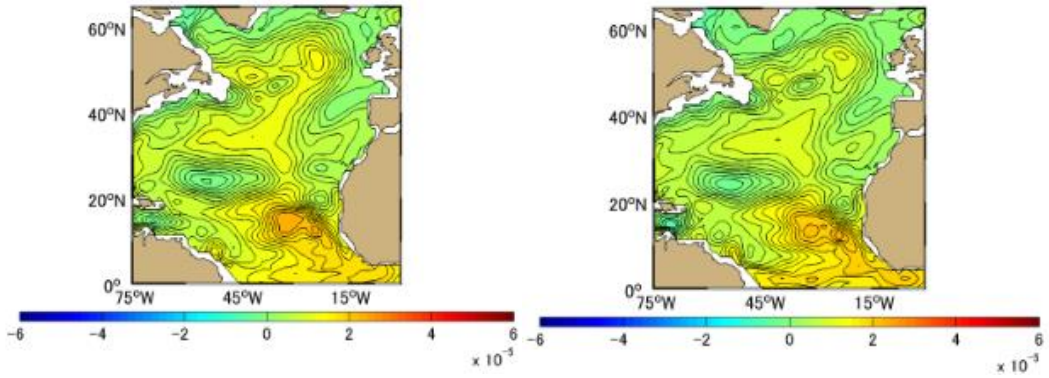
(j)



(k)

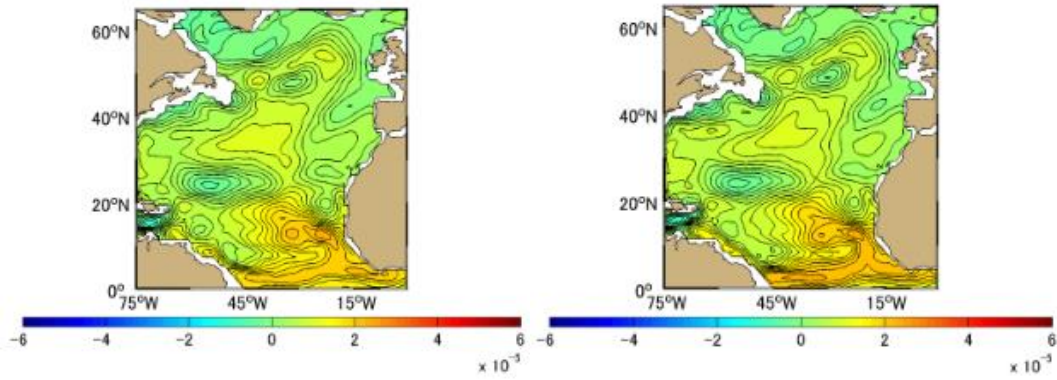
(l)

Figure A-4.17 Difference [PgC] between Approximation Method and Simulation Method Monthly Mean in 2007, the North Atlantic based on January 1991. (a)-(l) represents January-December



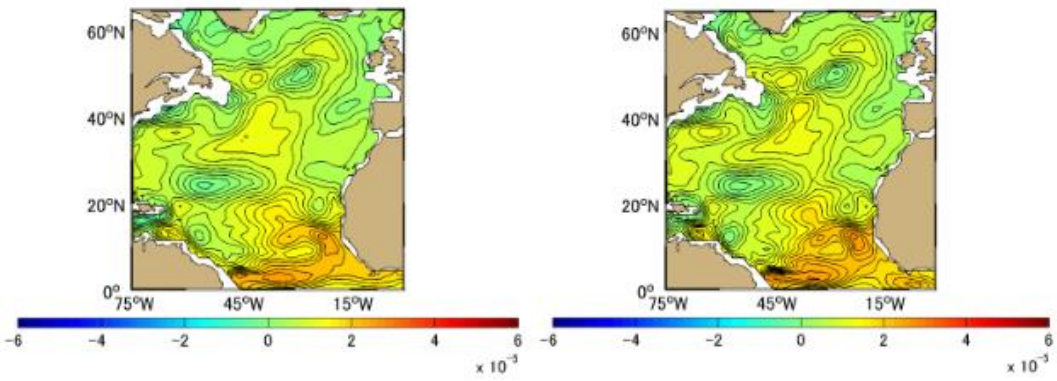
(a)

(b)



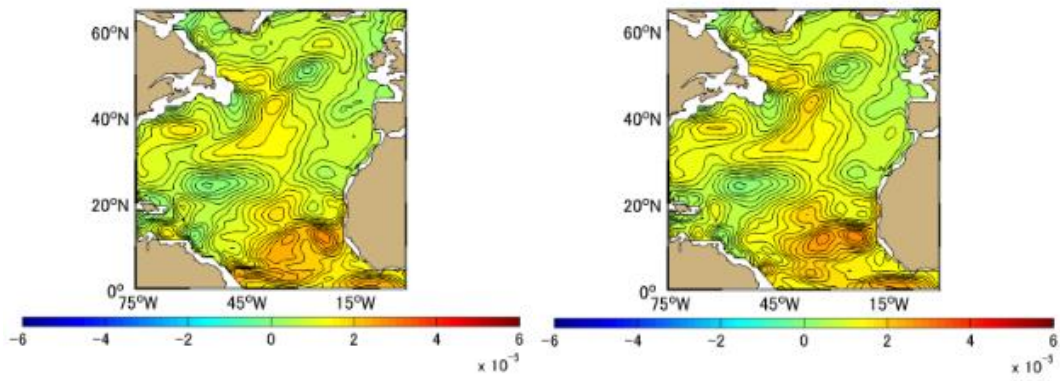
(c)

(d)



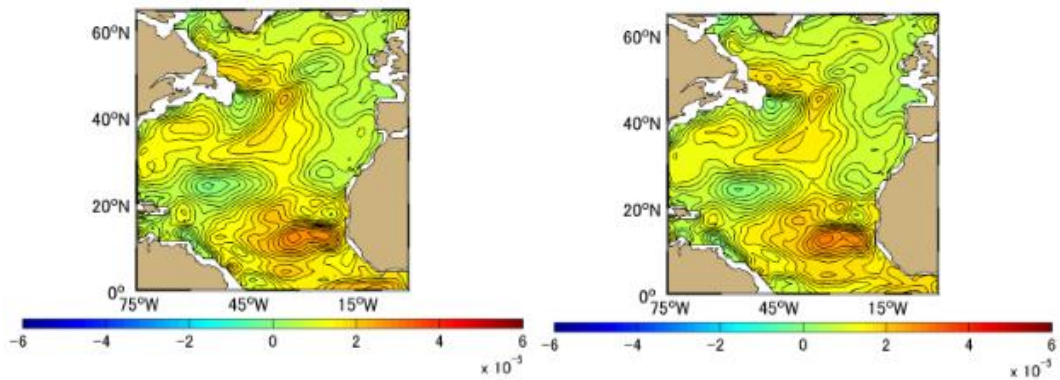
(e)

(f)



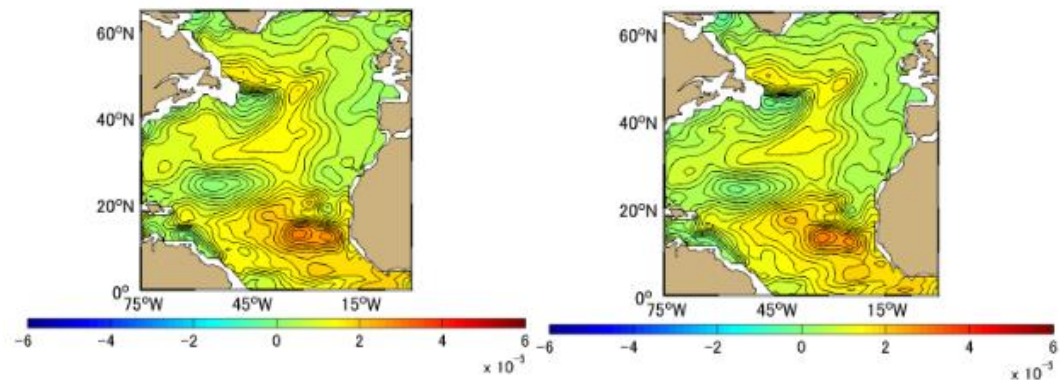
(g)

(h)



(i)

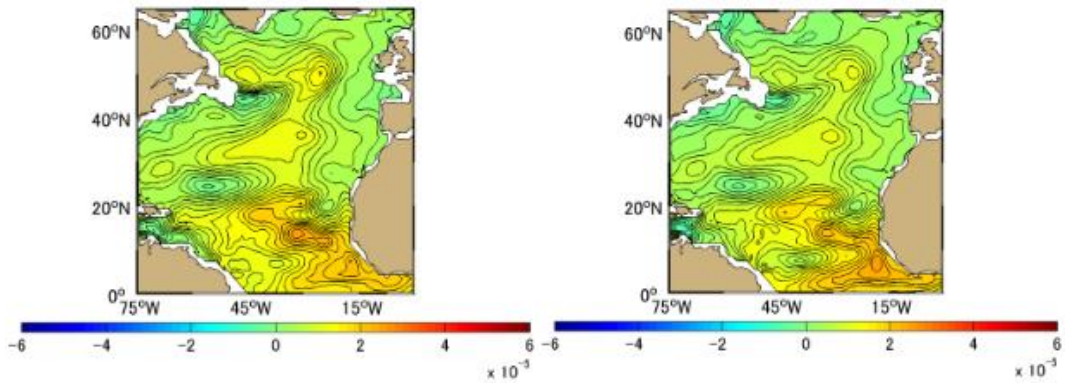
(j)



(k)

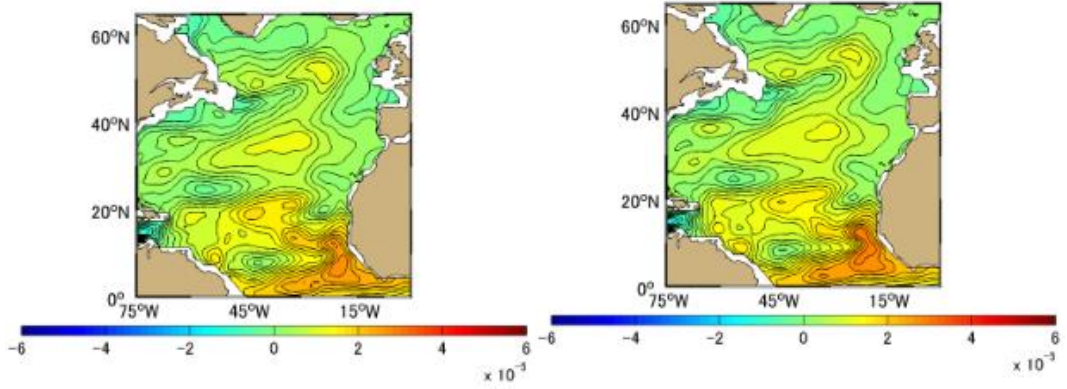
(l)

Figure A-4.18 Difference [PgC] between Approximation Method and Simulation Method Monthly Mean in 2008, the North Atlantic based on January 1991. (a)-(l) represents January-December



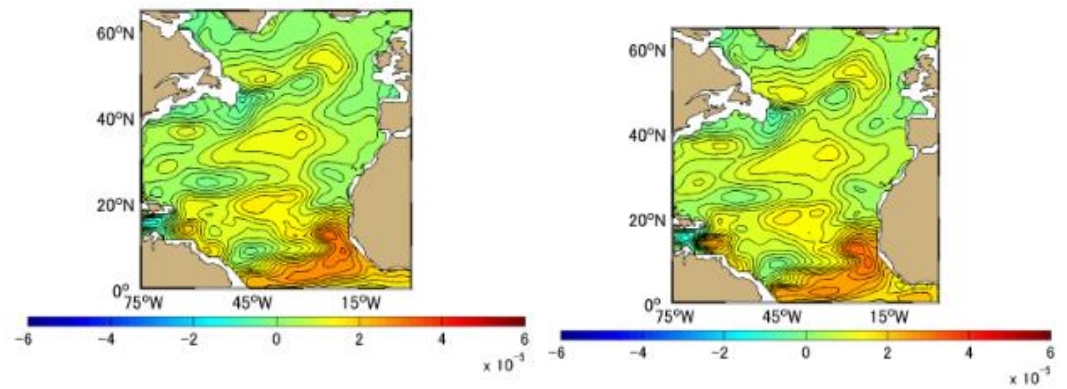
(a)

(b)



(c)

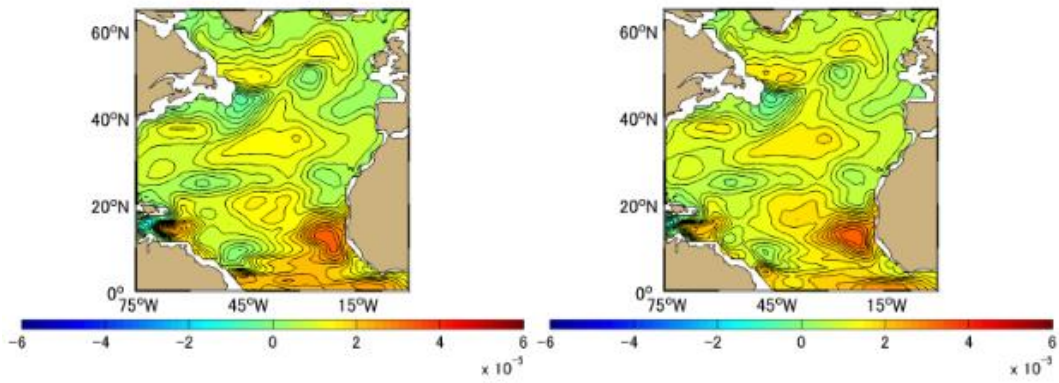
(d)



(e)

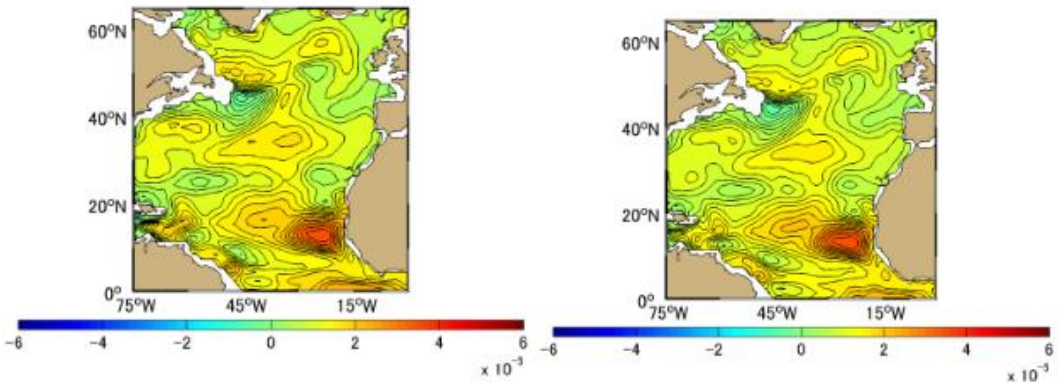
(f)





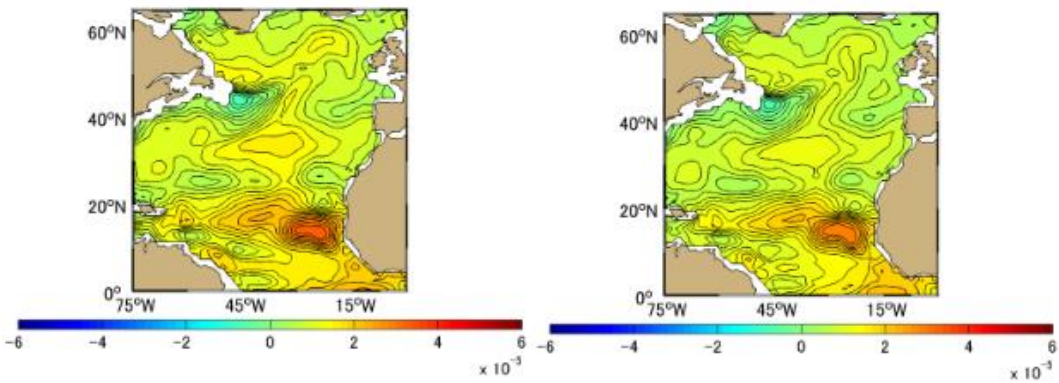
(g)

(h)



(i)

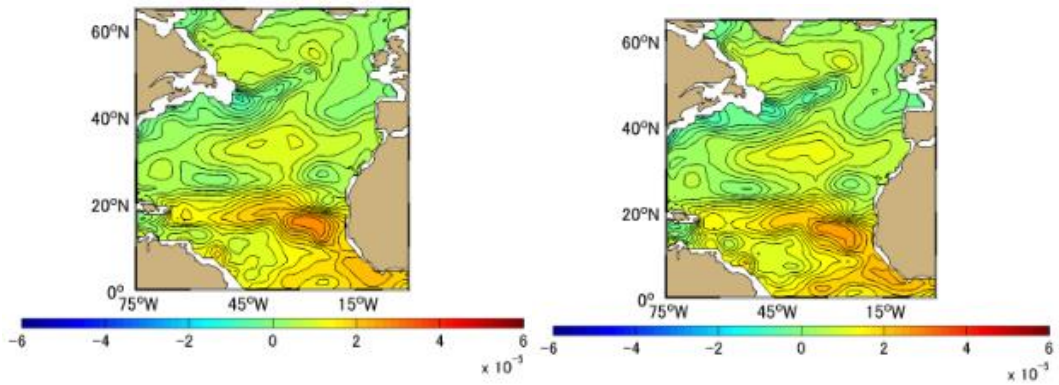
(j)



(k)

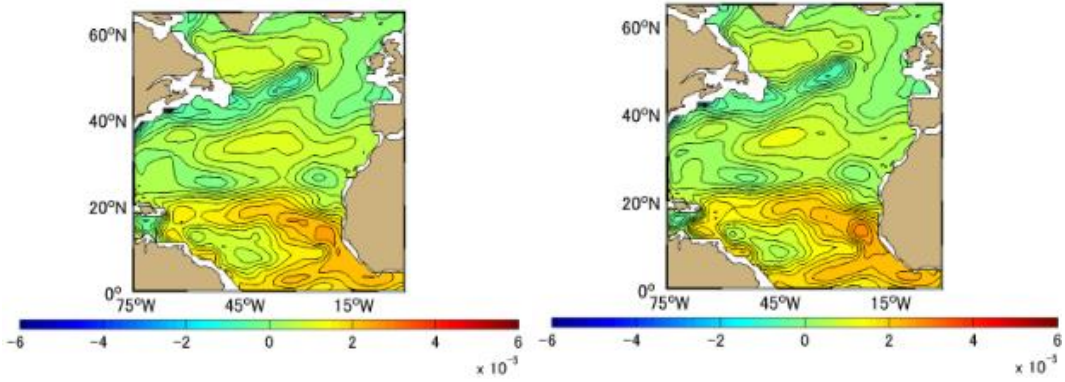
(l)

Figure A-4.19 Difference [PgC] between Approximation Method and Simulation Method Monthly Mean in 2009, the North Atlantic based on January 1991. (a)-(l) represents January-December



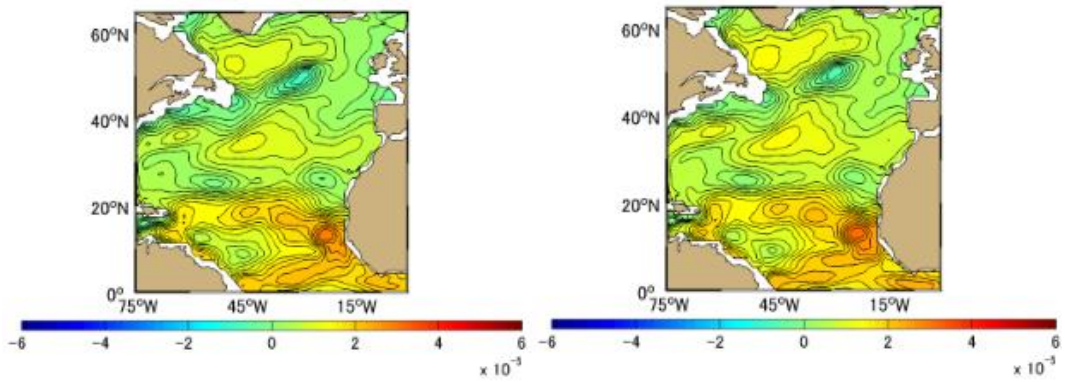
(a)

(b)



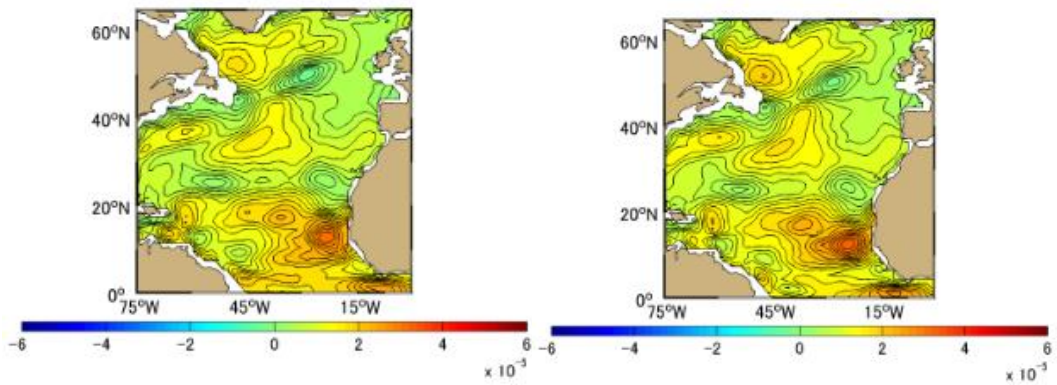
(c)

(d)



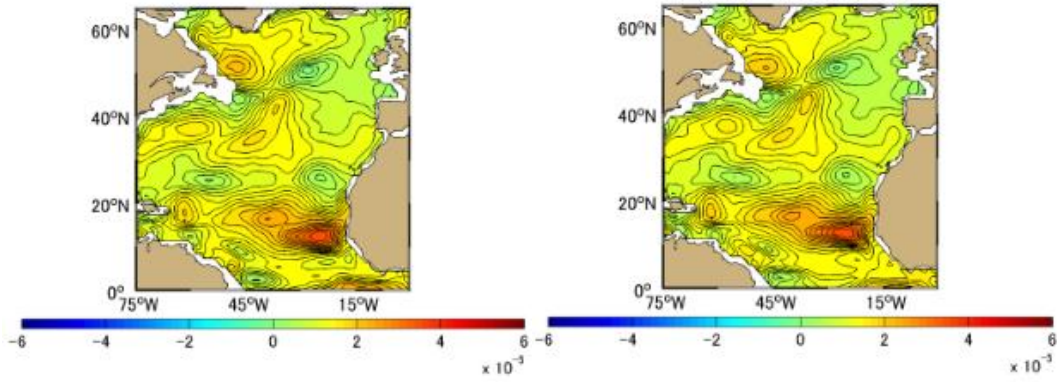
(e)

(f)



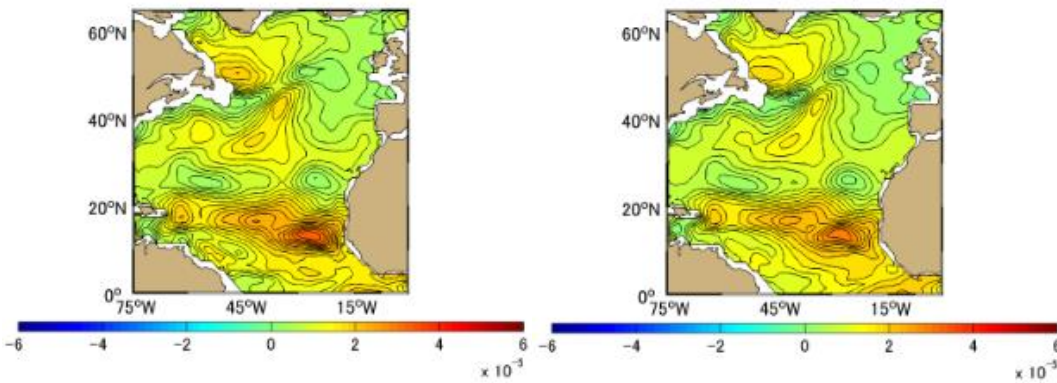
(g)

(h)



(i)

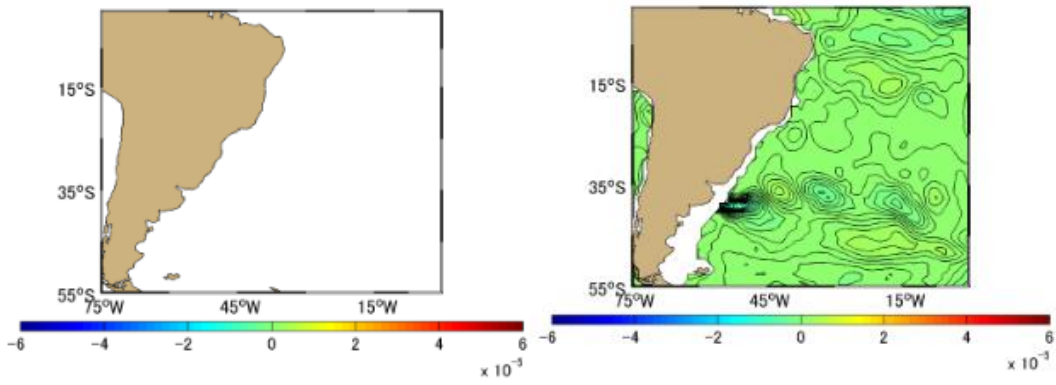
(j)



(k)

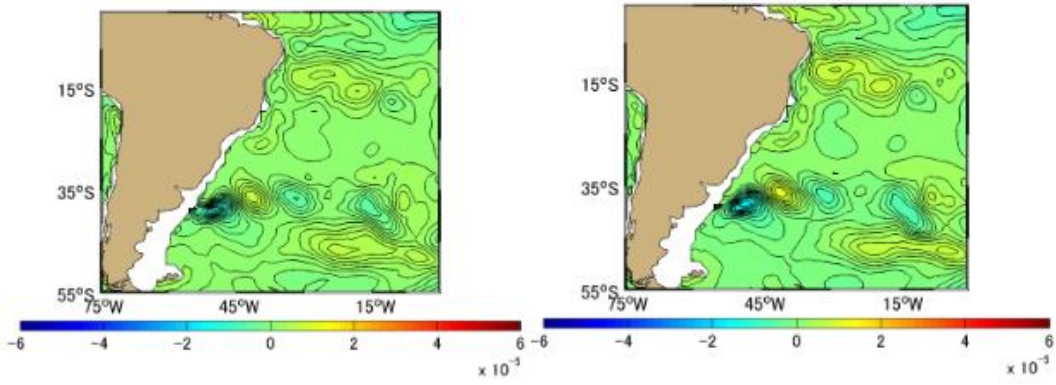
(l)

Figure A-4.20 Difference [PgC] between Approximation Method and Simulation Method Monthly Mean in 2010, the North Atlantic based on January 1991. (a)-(l) represents January-December



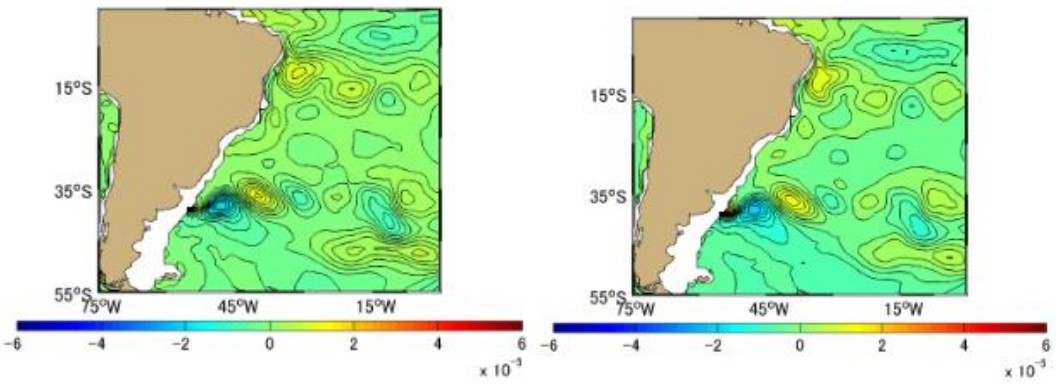
(a)

(b)



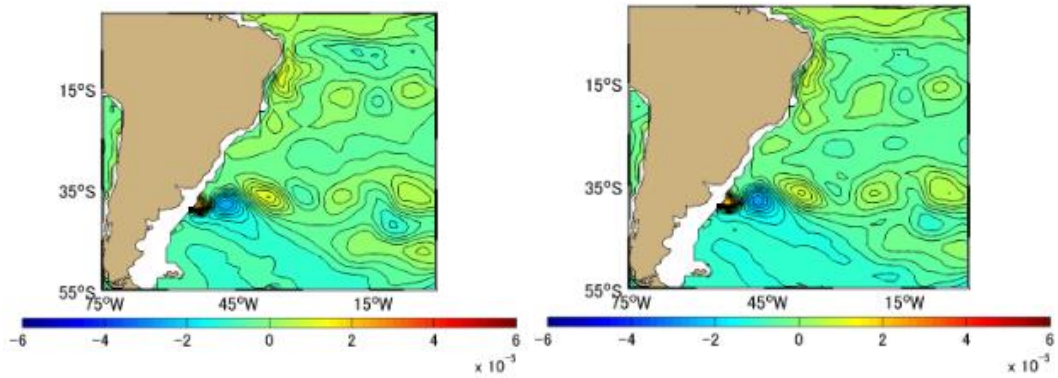
(c)

(d)



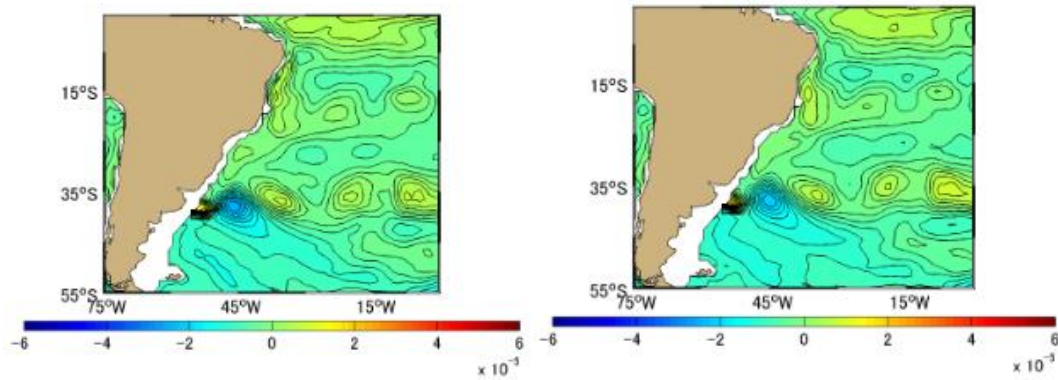
(e)

(f)



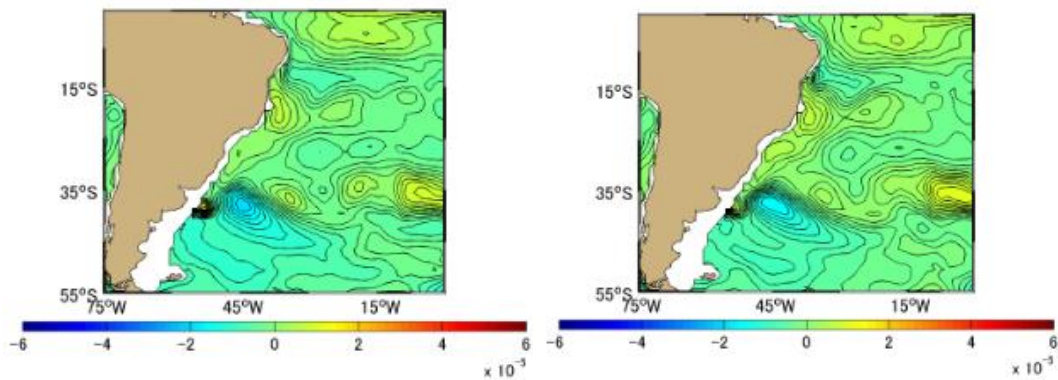
(g)

(h)



(i)

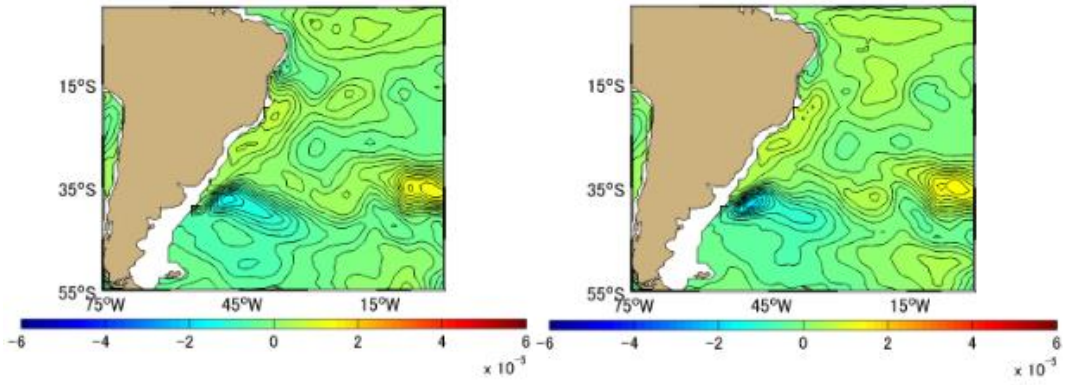
(j)



(k)

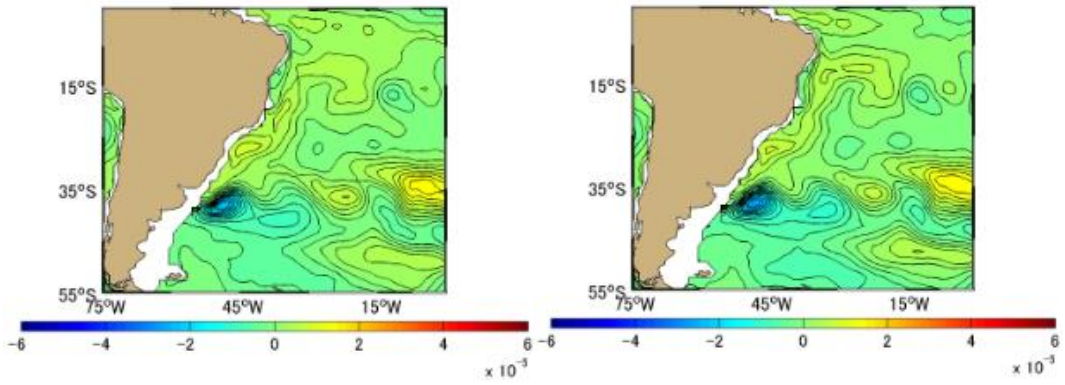
(l)

Figure A-5.1 Difference [PgC] between Approximation Method and Simulation Method Monthly Mean in 1991, the South Atlantic based on January 1991. (a)-(l) represents January-December



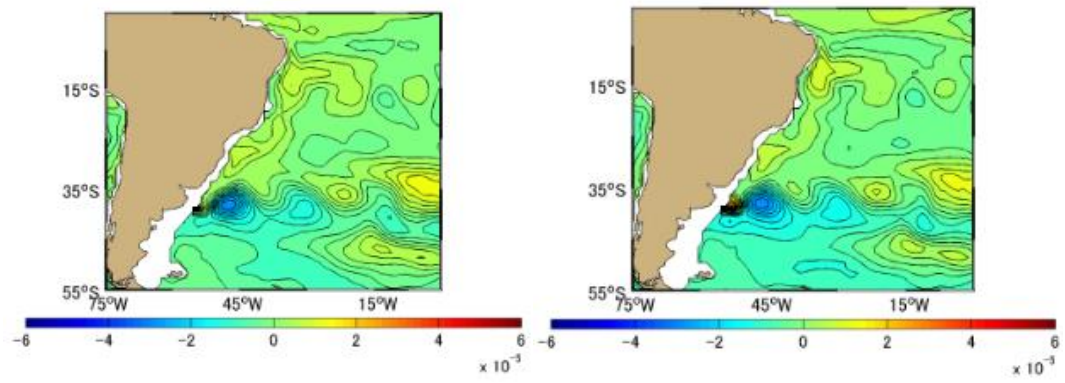
(a)

(b)



(c)

(d)



(e)

(f)

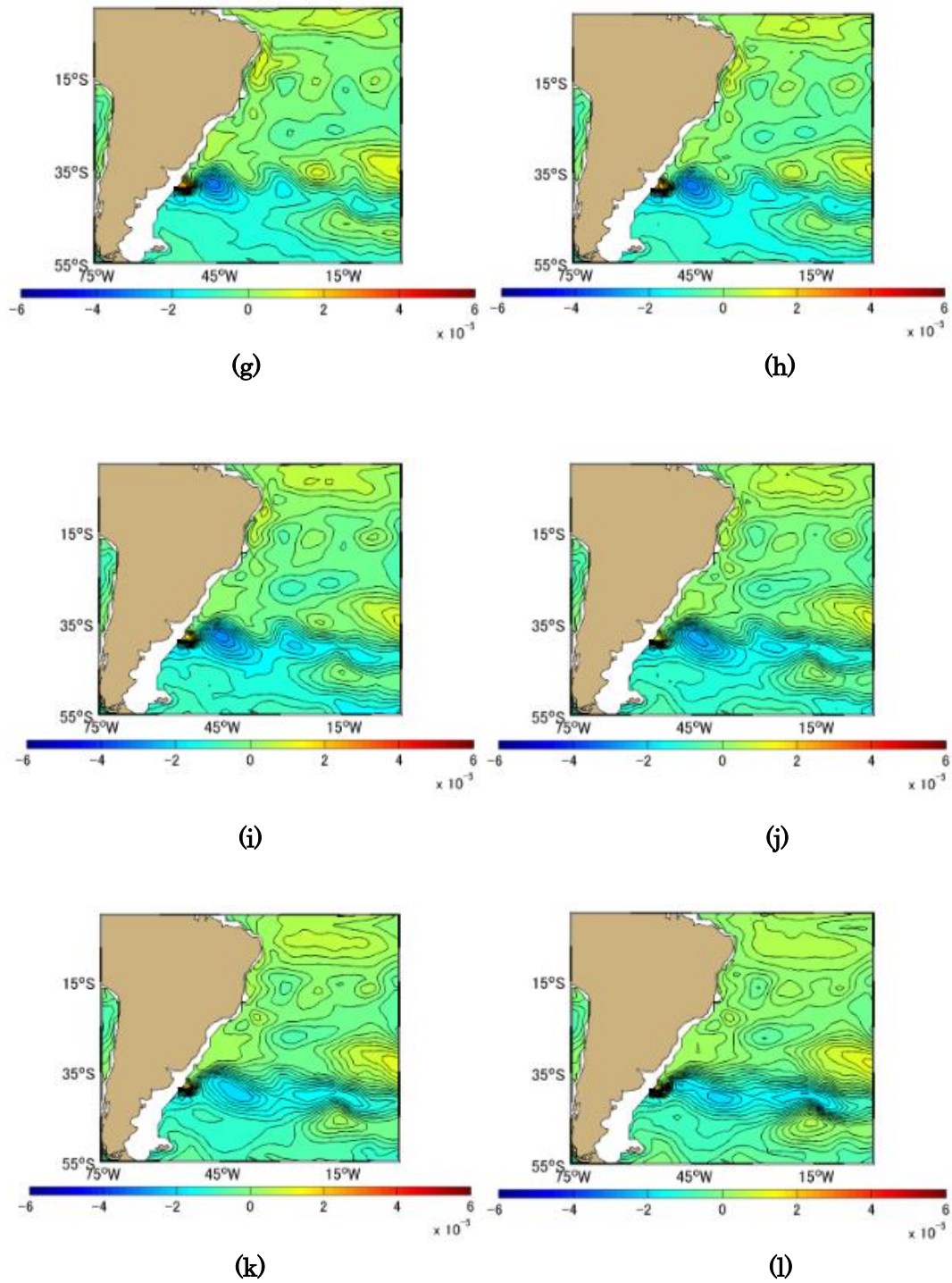
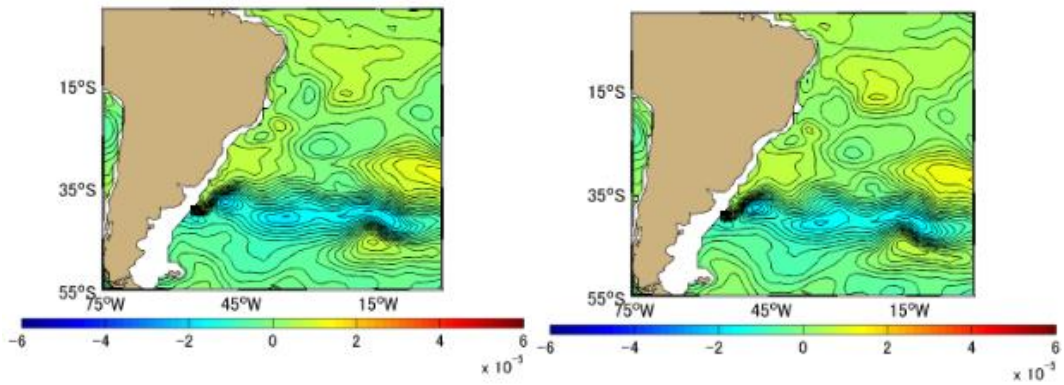
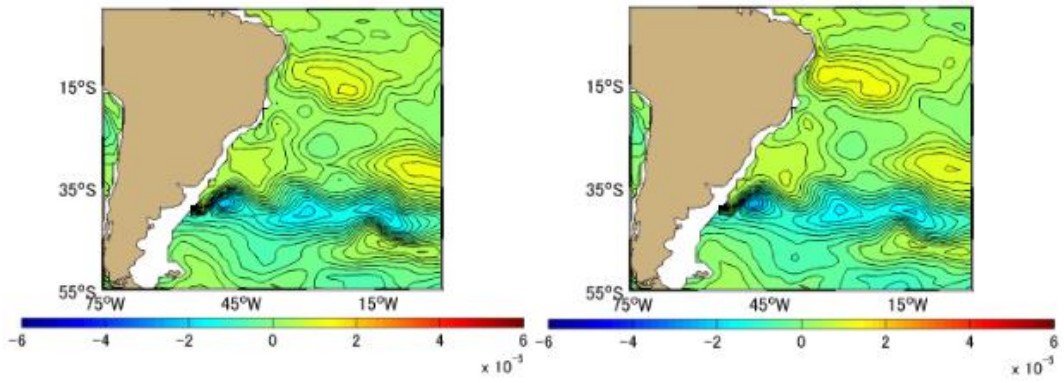


Figure A-5.2 Difference [PgC] between Approximation Method and Simulation Method Monthly Mean in 1992, the South Atlantic based on January 1991. (a)-(l) represents January-December



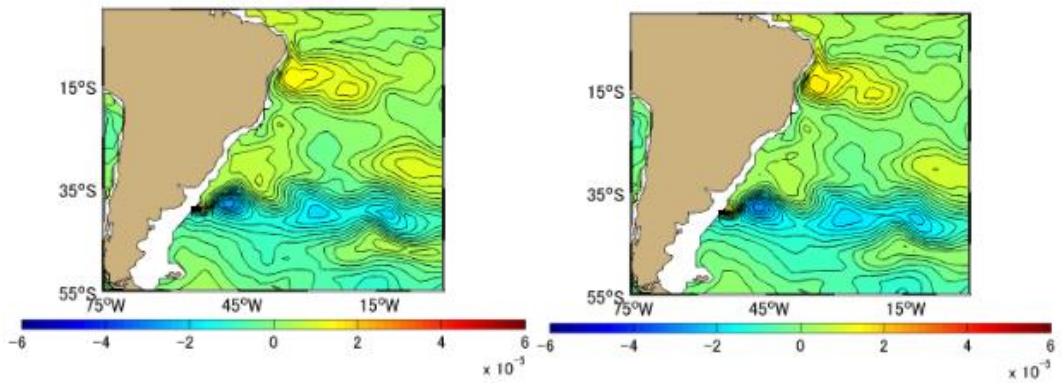
(a)

(b)



(c)

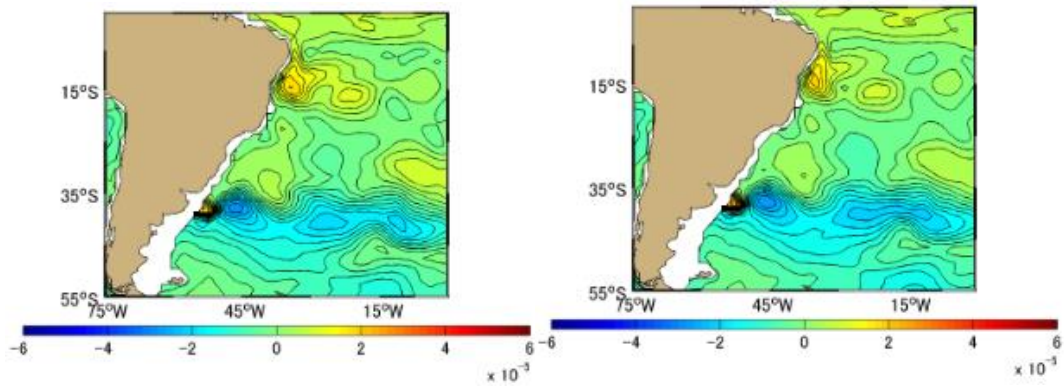
(d)



(e)

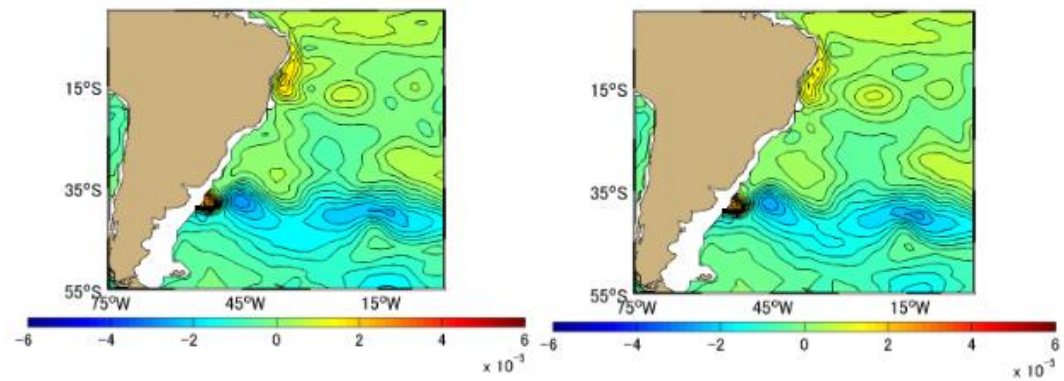
(f)





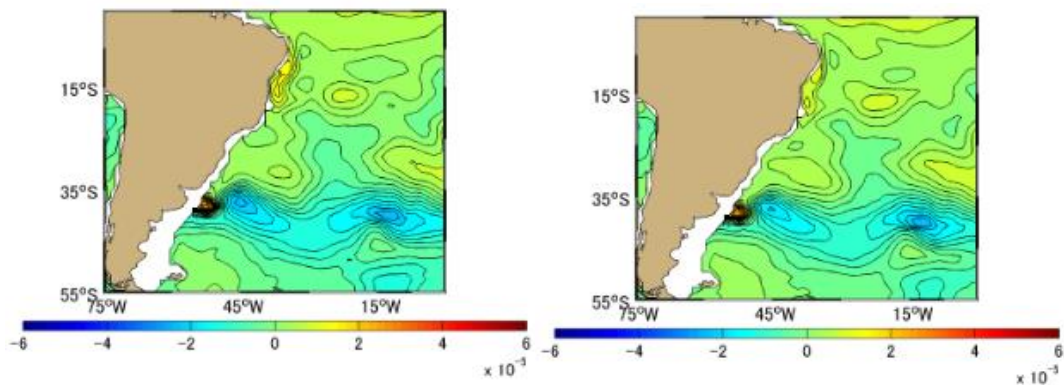
(g)

(h)



(i)

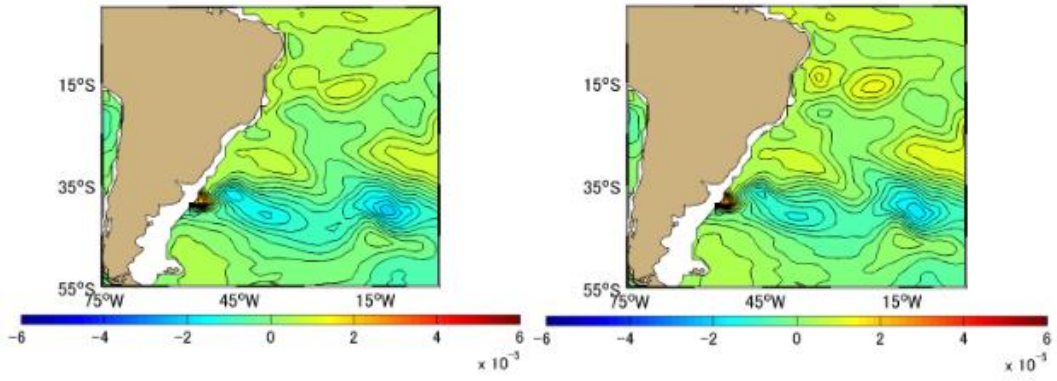
(j)



(k)

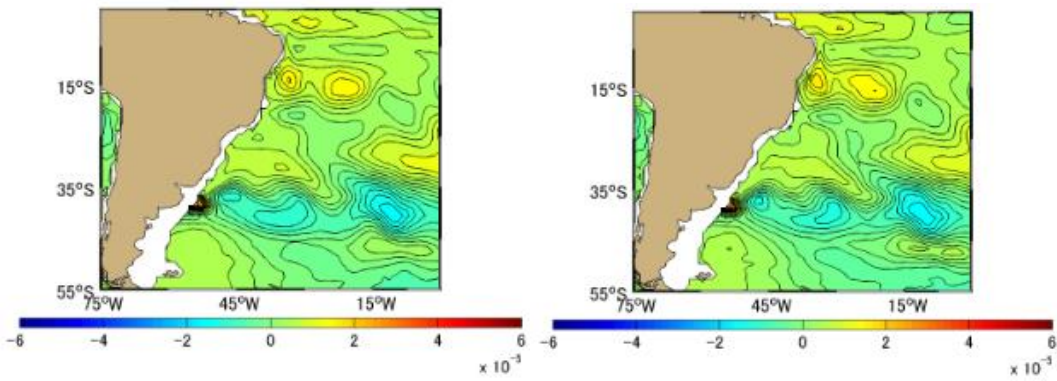
(l)

Figure A-5.3 Difference [PgC] between Approximation Method and Simulation Method Monthly Mean in 1993, the South Atlantic based on January 1991. (a)-(l) represents January-December



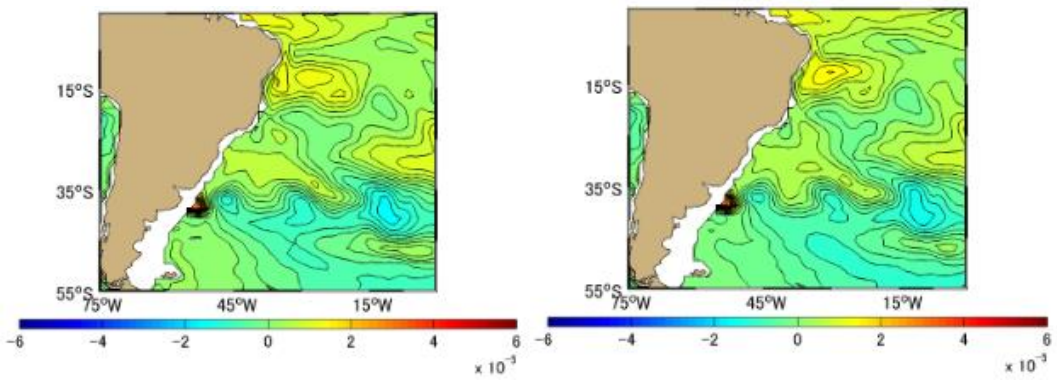
(a)

(b)



(c)

(d)



(e)

(f)

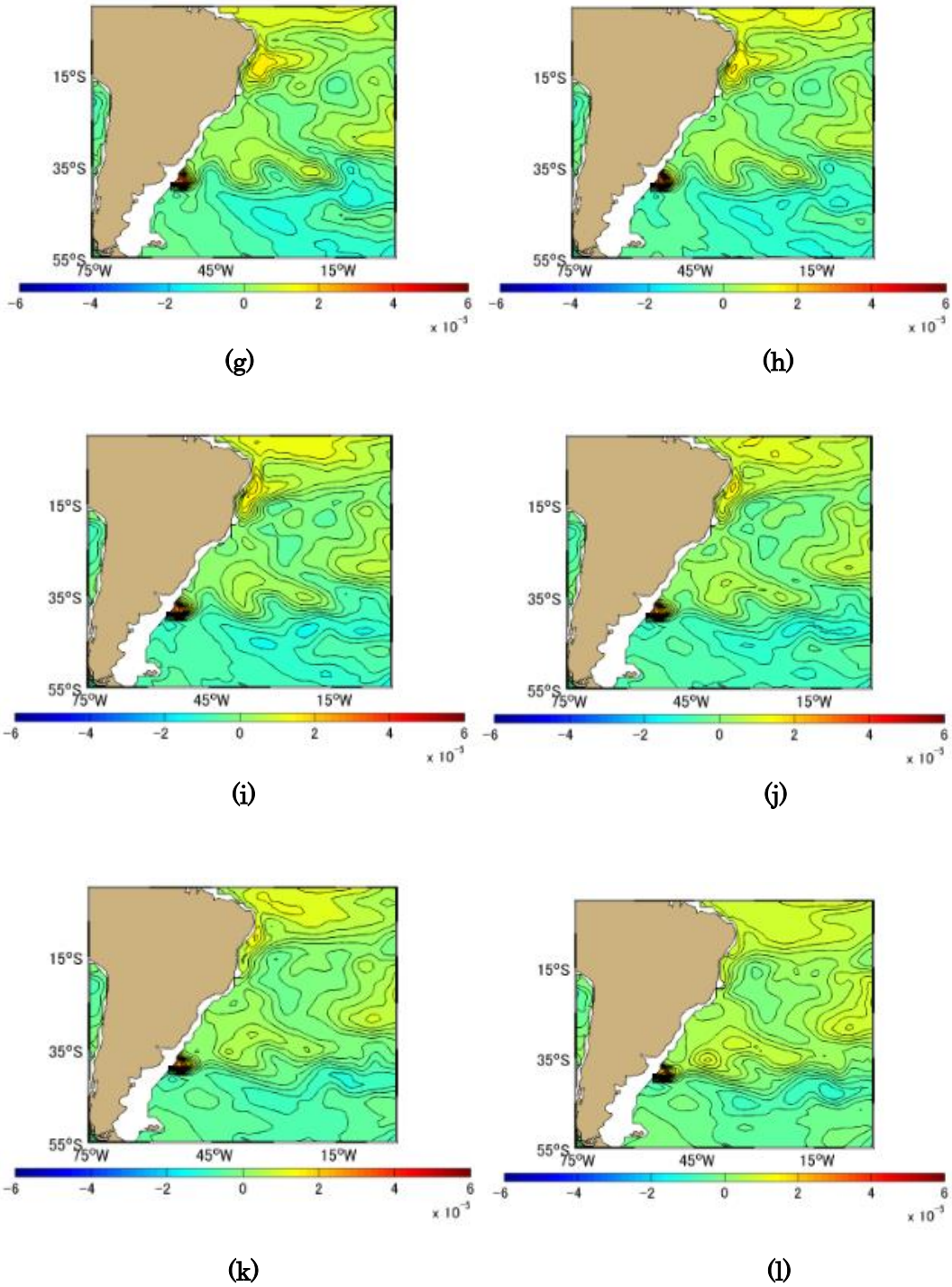
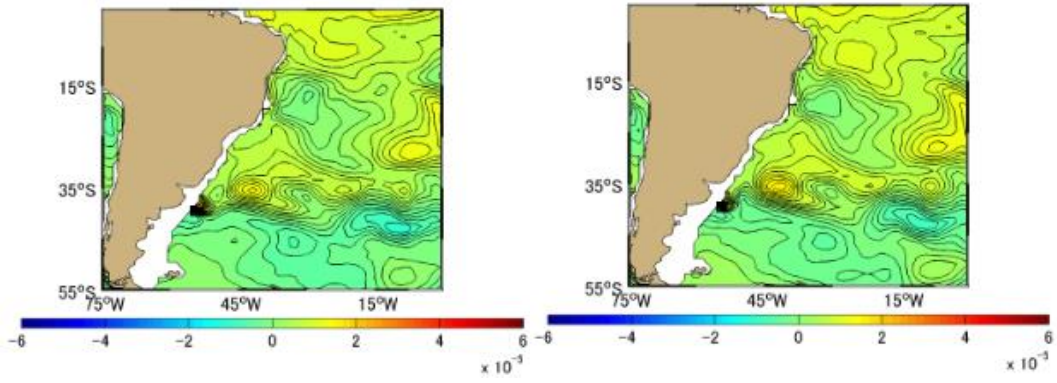
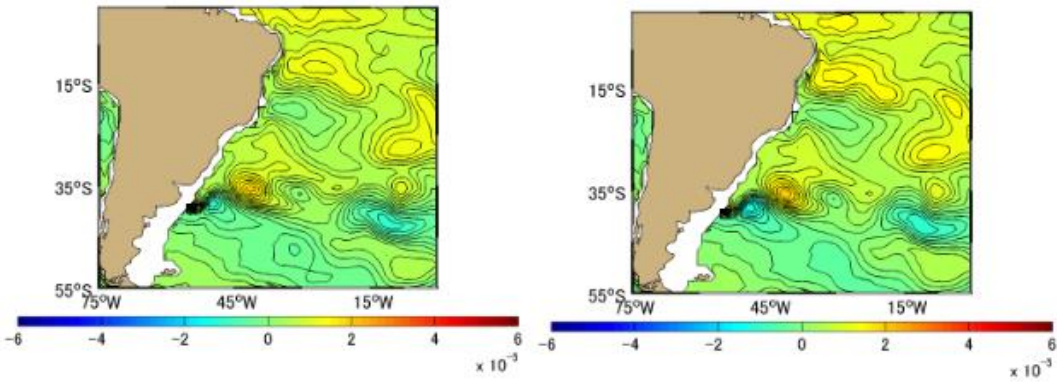


Figure A-5.4 Difference [PgC] between Approximation Method and Simulation Method Monthly Mean in 1994, the South Atlantic based on January 1991. (a)-(l) represents January-December



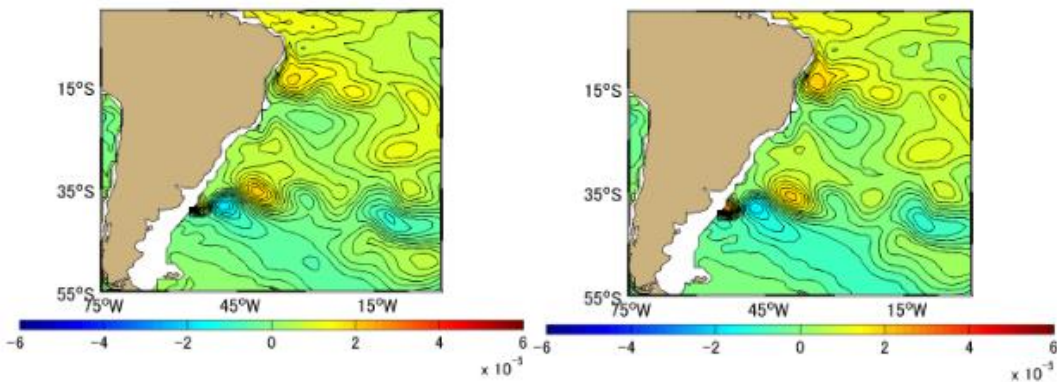
(a)

(b)



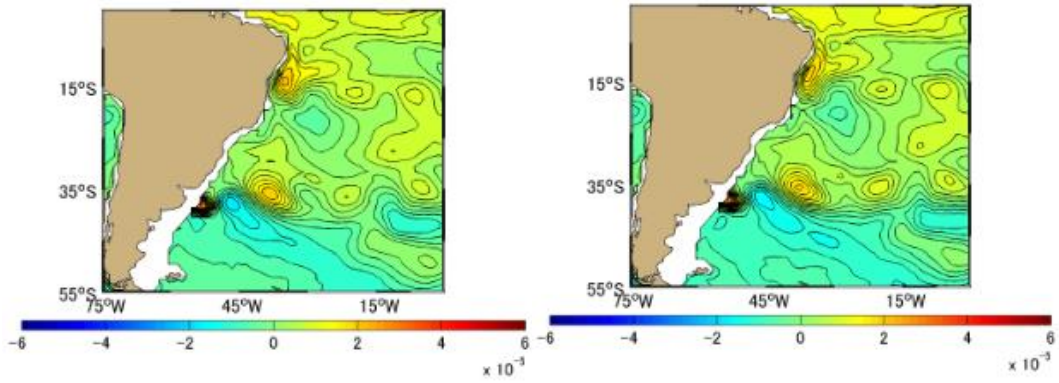
(c)

(d)



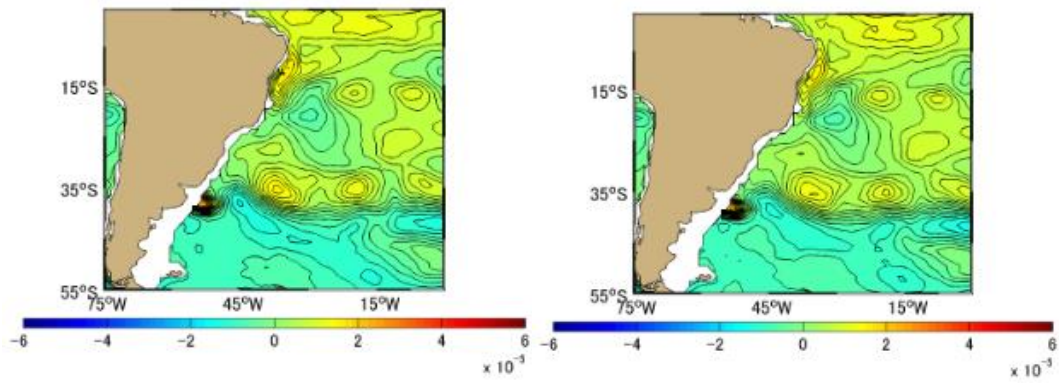
(e)

(f)



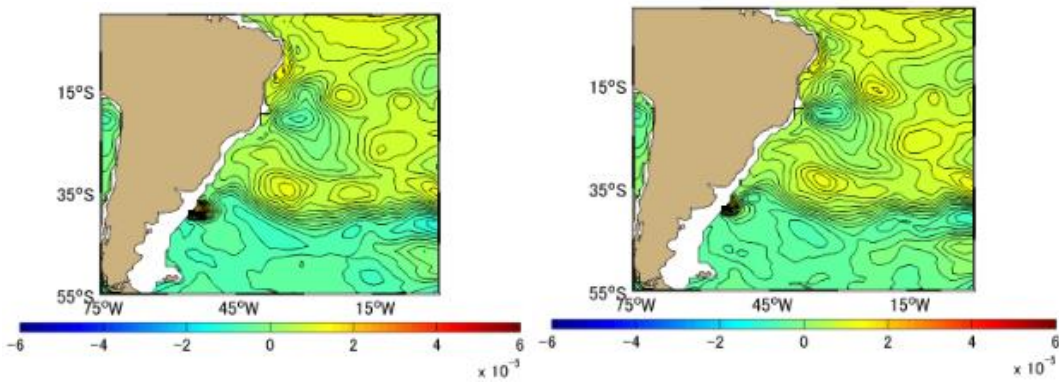
(g)

(h)



(i)

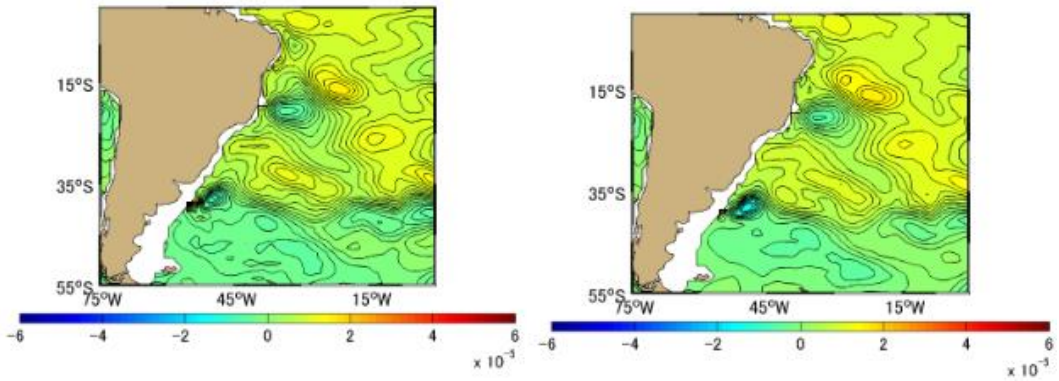
(j)



(k)

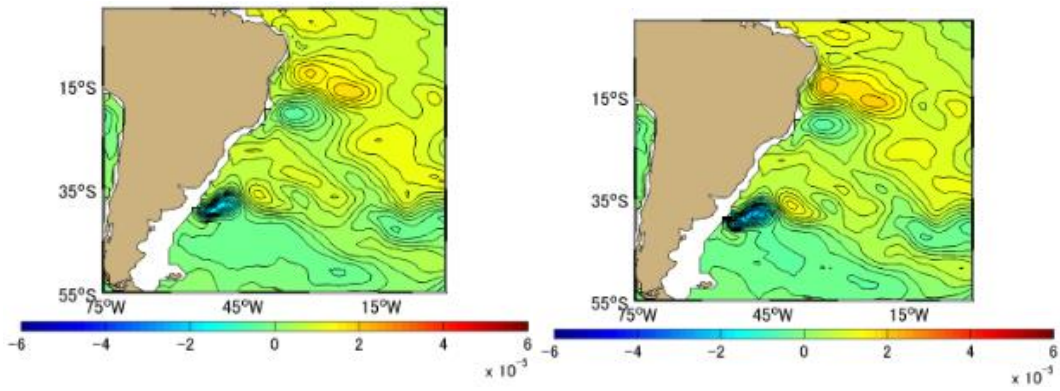
(l)

Figure A-5.5 Difference [PgC] between Approximation Method and Simulation Method Monthly Mean in 1995, the South Atlantic based on January 1991. (a)-(l) represents January-December



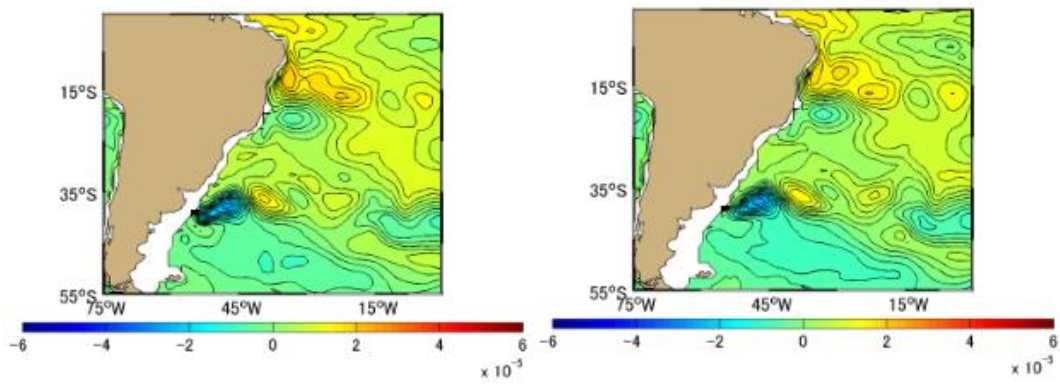
(a)

(b)



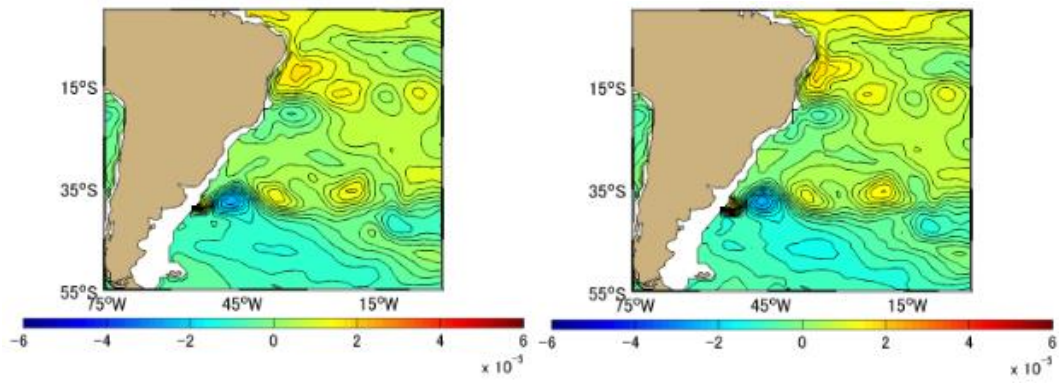
(c)

(d)



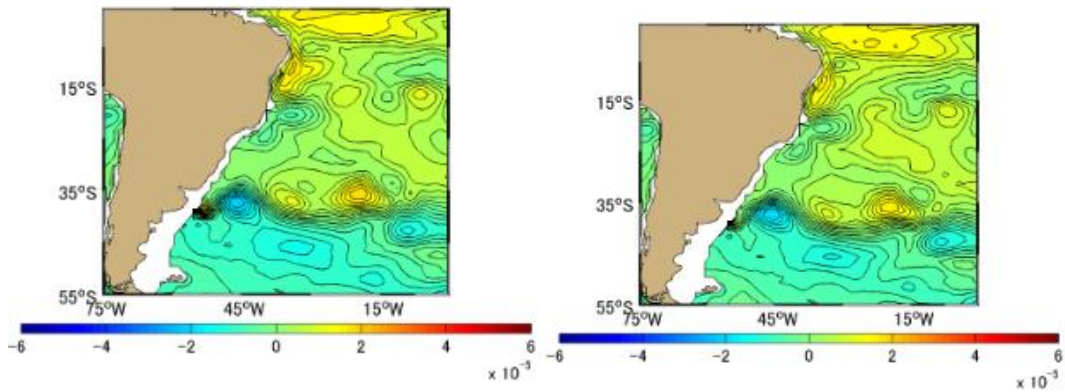
(e)

(f)



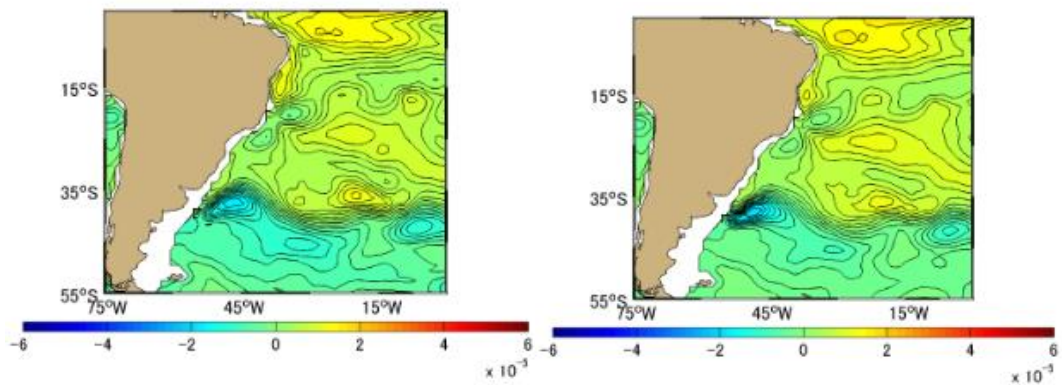
(g)

(h)



(i)

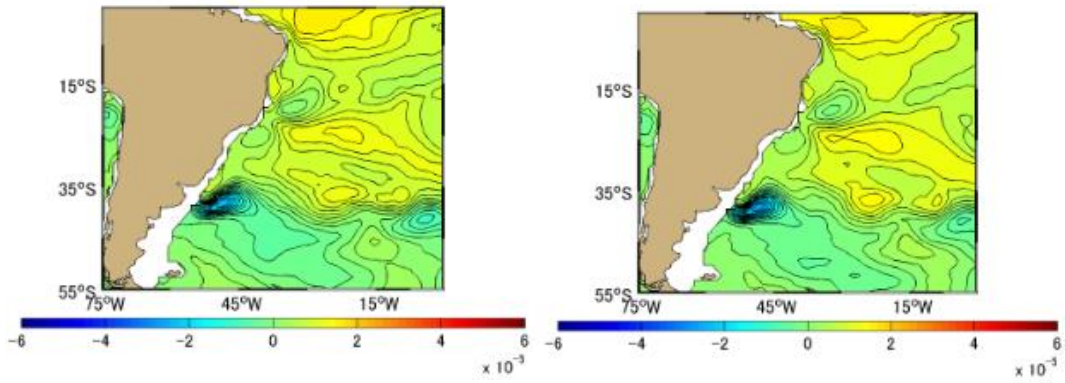
(j)



(k)

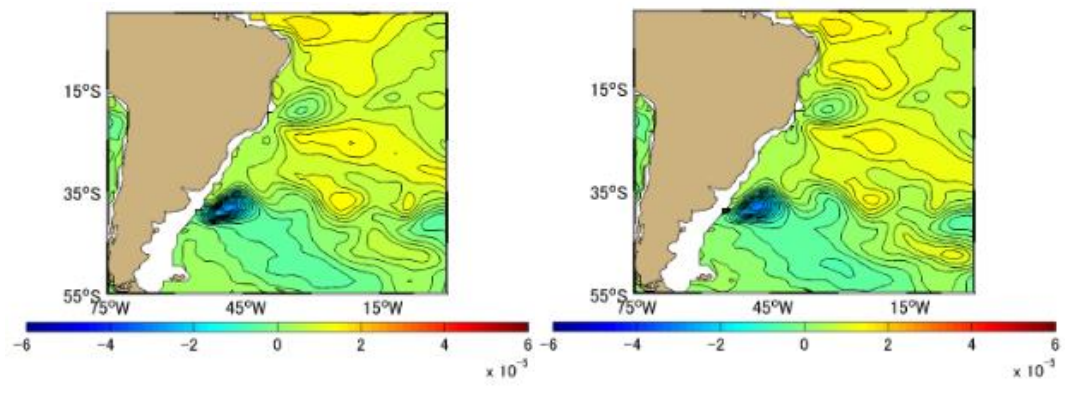
(l)

Figure A-5.6 Difference [PgC] between Approximation Method and Simulation Method Monthly Mean in 1996, the South Atlantic based on January 1991. (a)-(l) represents January-December



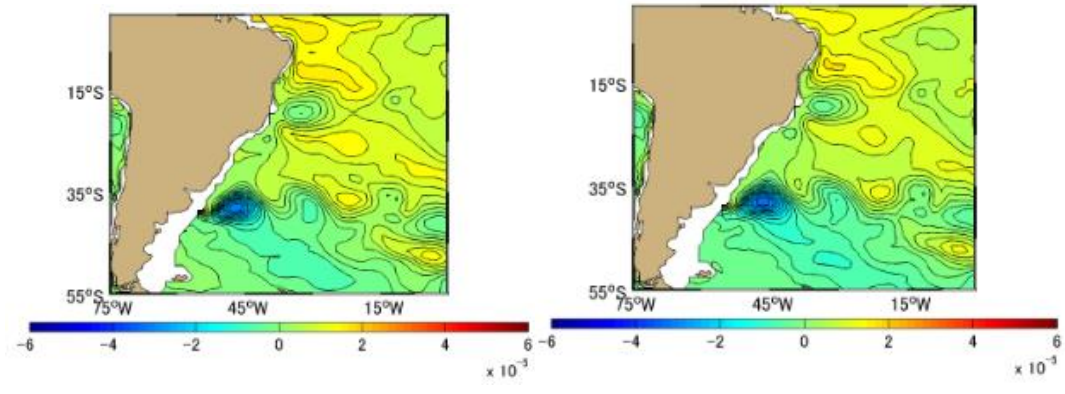
(a)

(b)



(c)

(d)



(e)

(f)



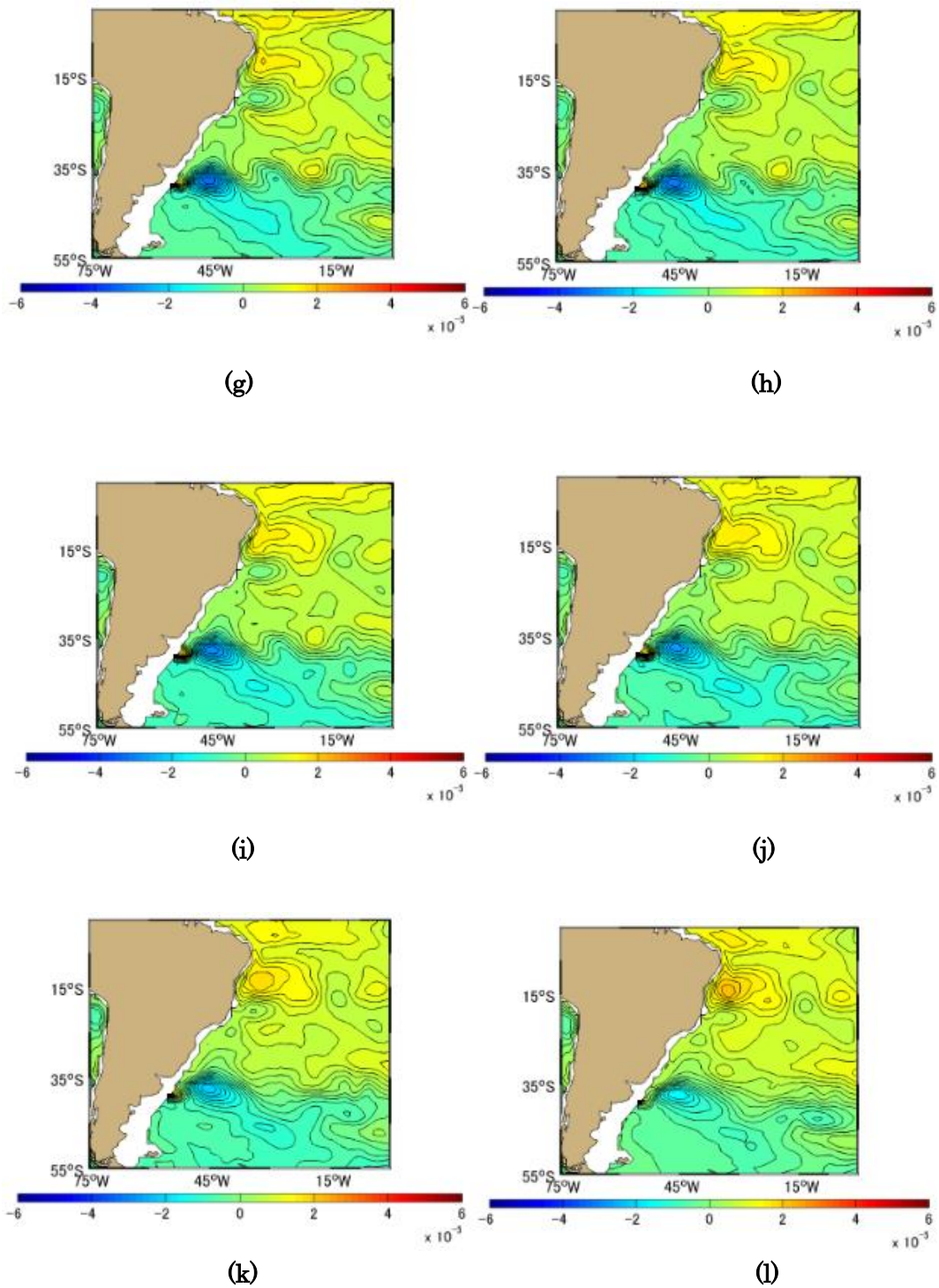
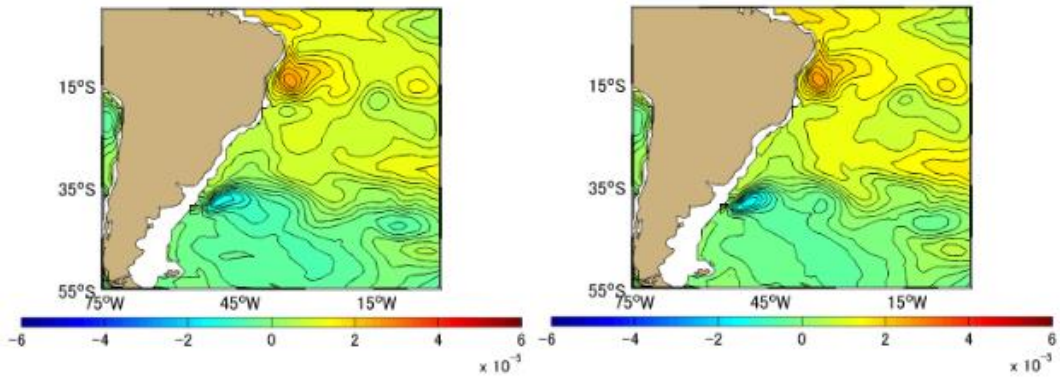
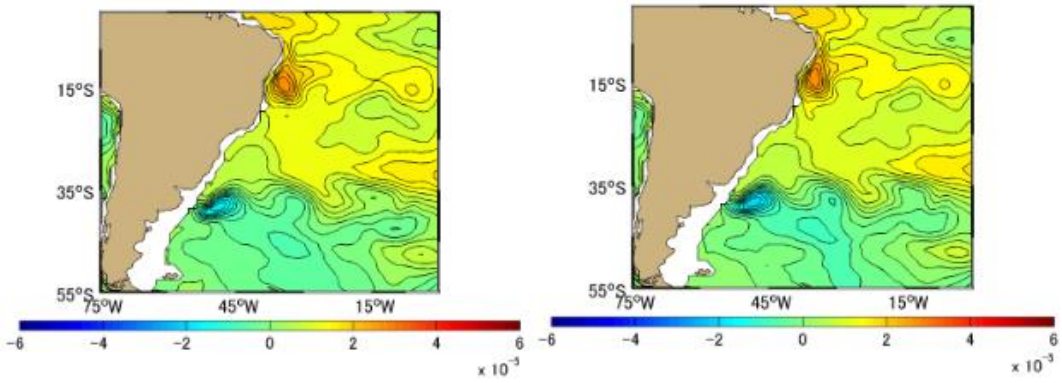


Figure A-5.7 Difference [PgC] between Approximation Method and Simulation Method Monthly Mean in 1997, the South Atlantic based on January 1991. (a)-(l) represents January-December



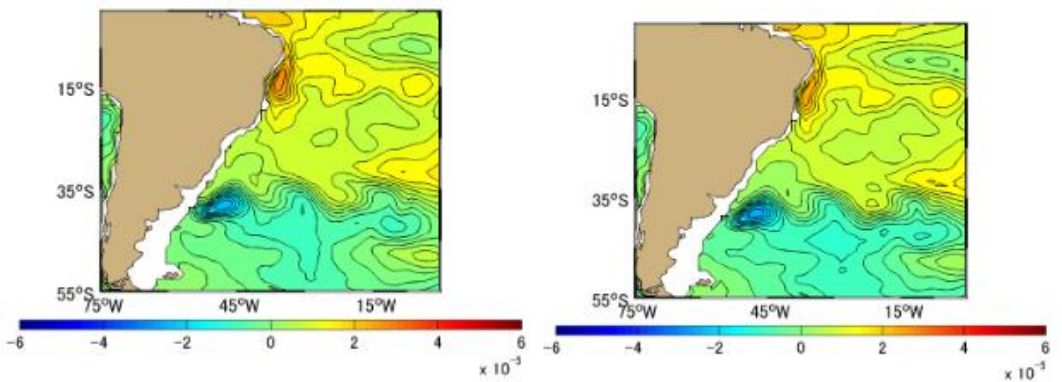
(a)

(b)



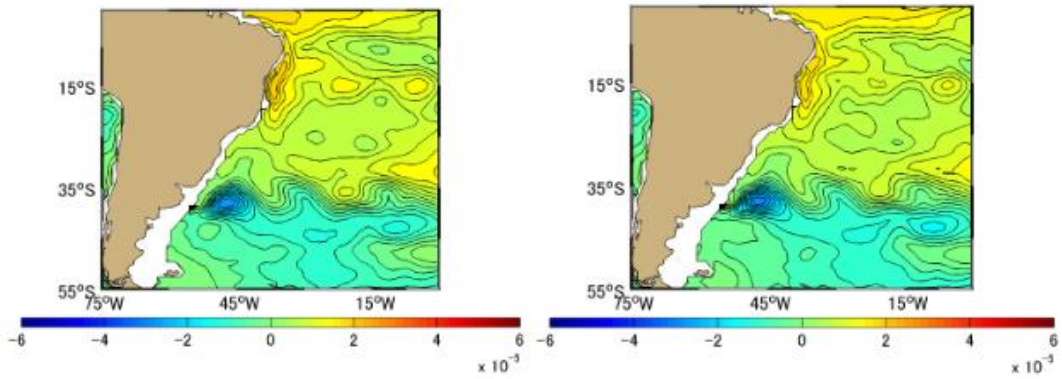
(c)

(d)



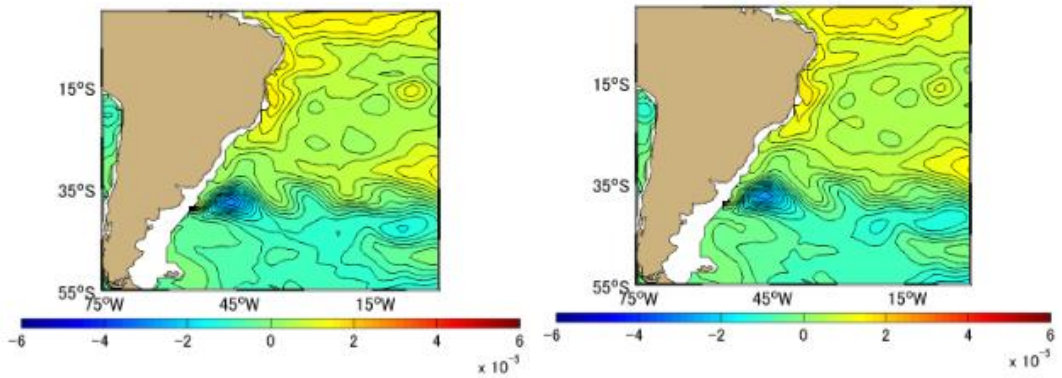
(e)

(f)



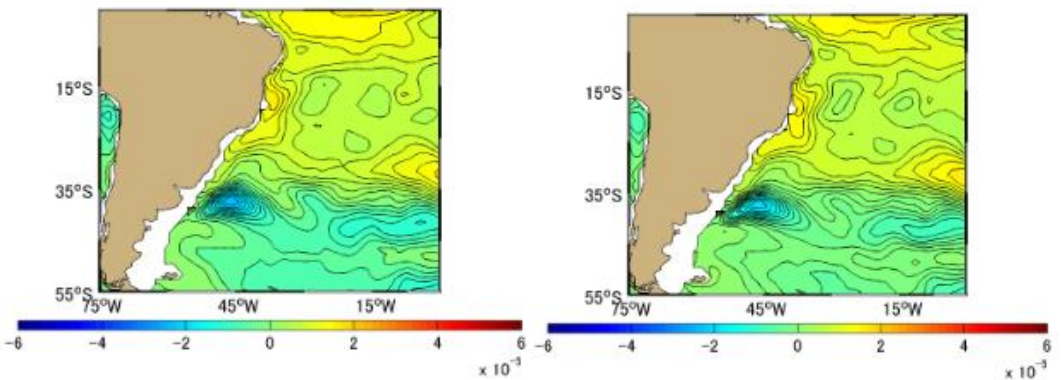
(g)

(h)



(i)

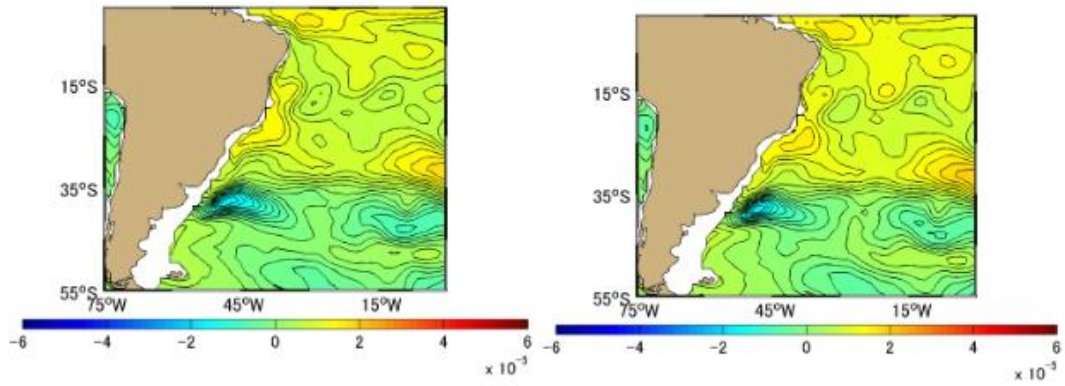
(j)



(k)

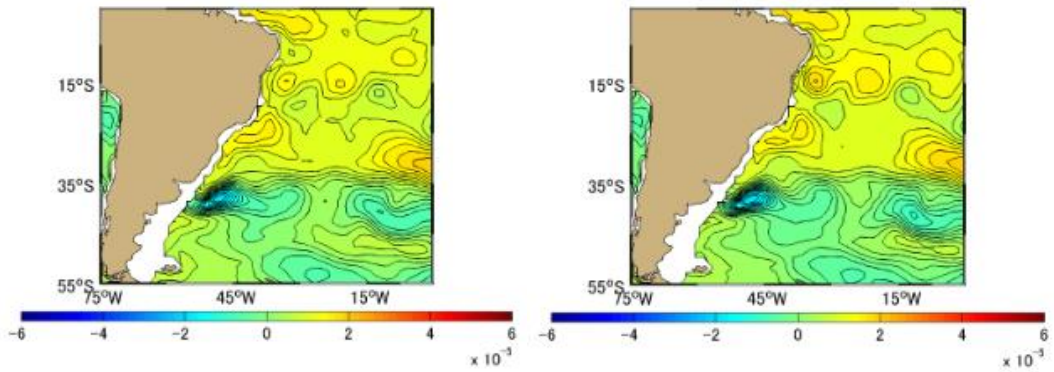
(l)

Figure A-5.8 Difference [PgC] between Approximation Method and Simulation Method Monthly Mean in 1998, the South Atlantic based on January 1991. (a)-(l) represents January-December



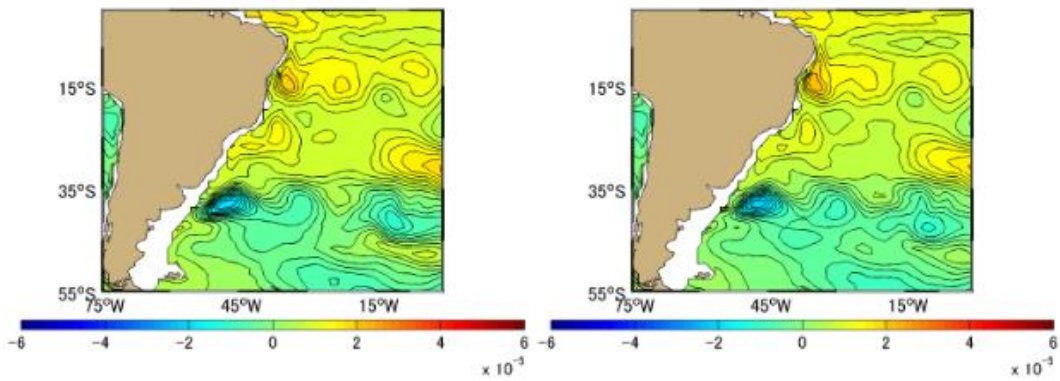
(a)

(b)



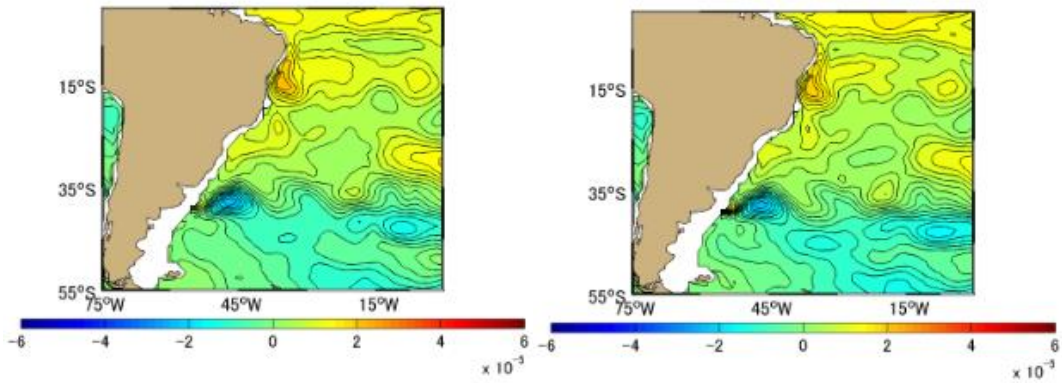
(c)

(d)



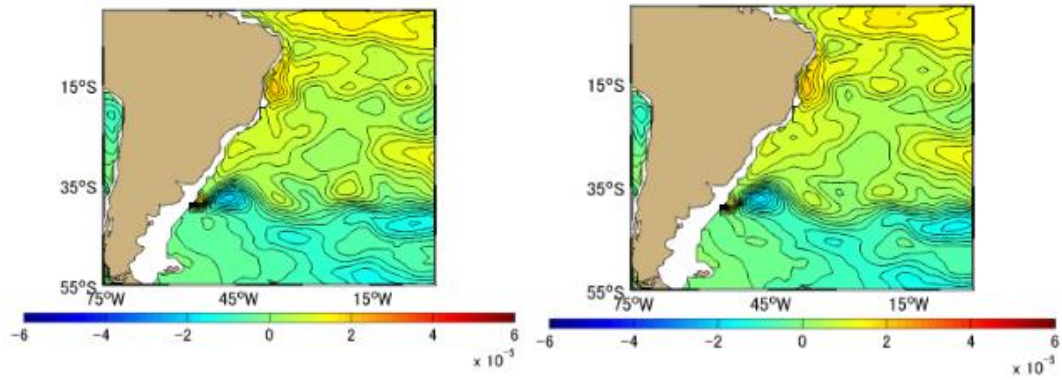
(e)

(f)



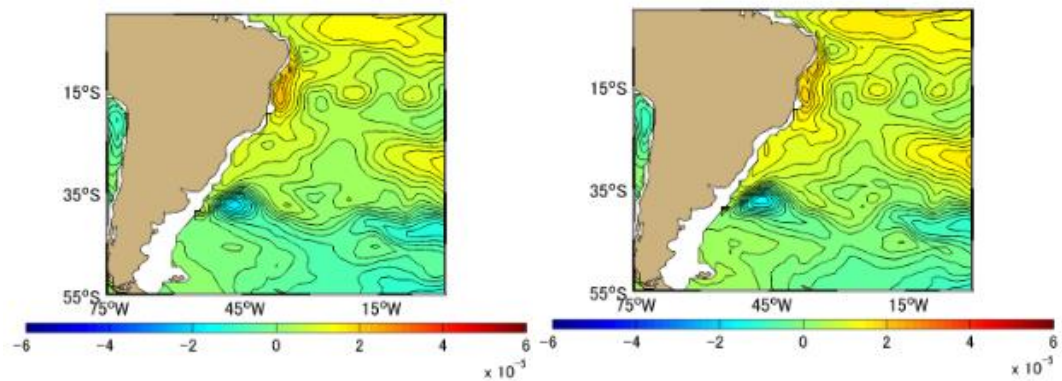
(g)

(h)



(i)

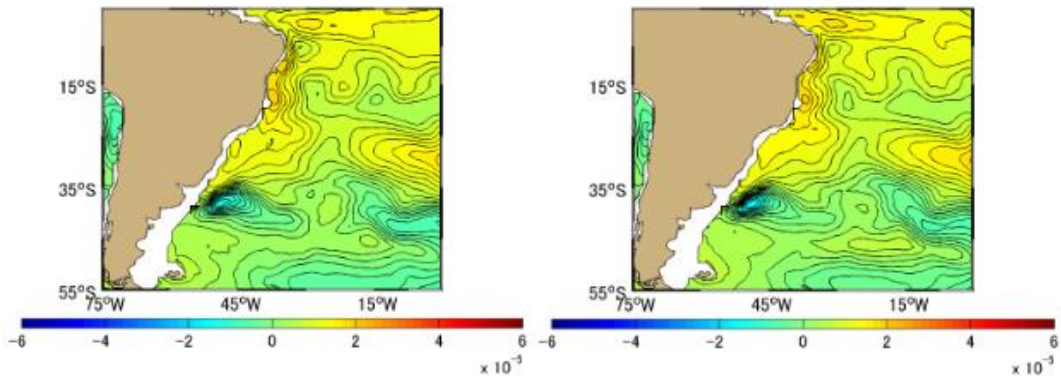
(j)



(k)

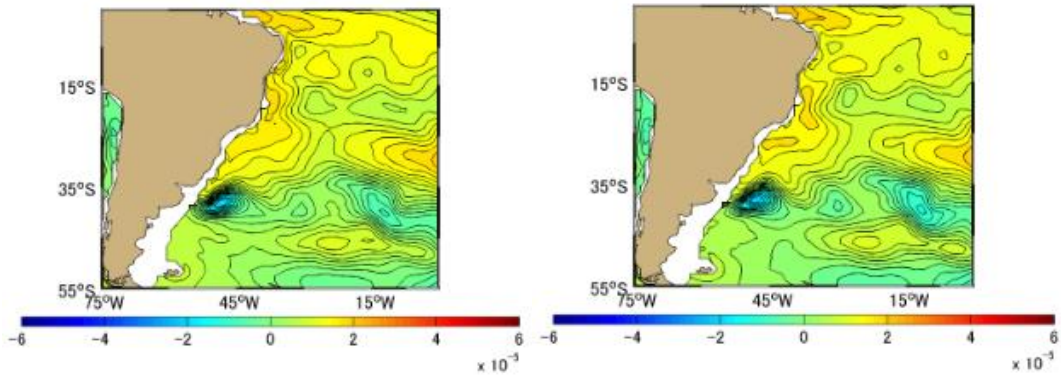
(l)

Figure A-5.9 Difference [PgC] between Approximation Method and Simulation Method Monthly Mean in 1999, the South Atlantic based on January 1991. (a)-(l) represents January-December



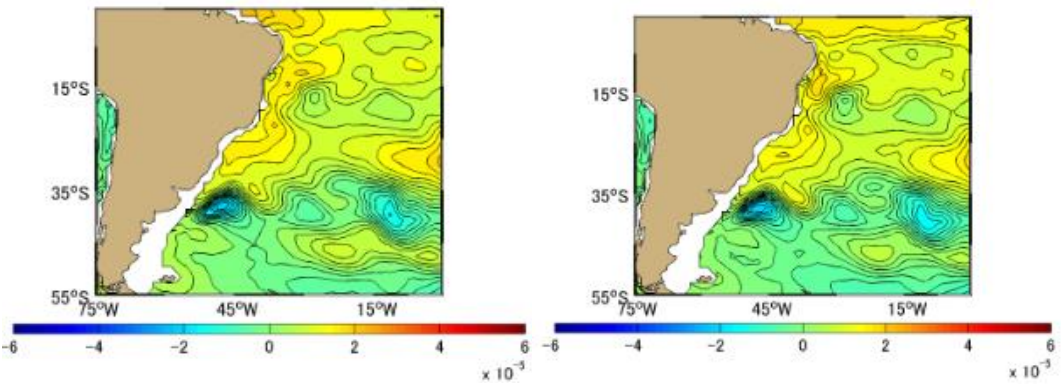
(a)

(b)



(c)

(d)



(e)

(f)

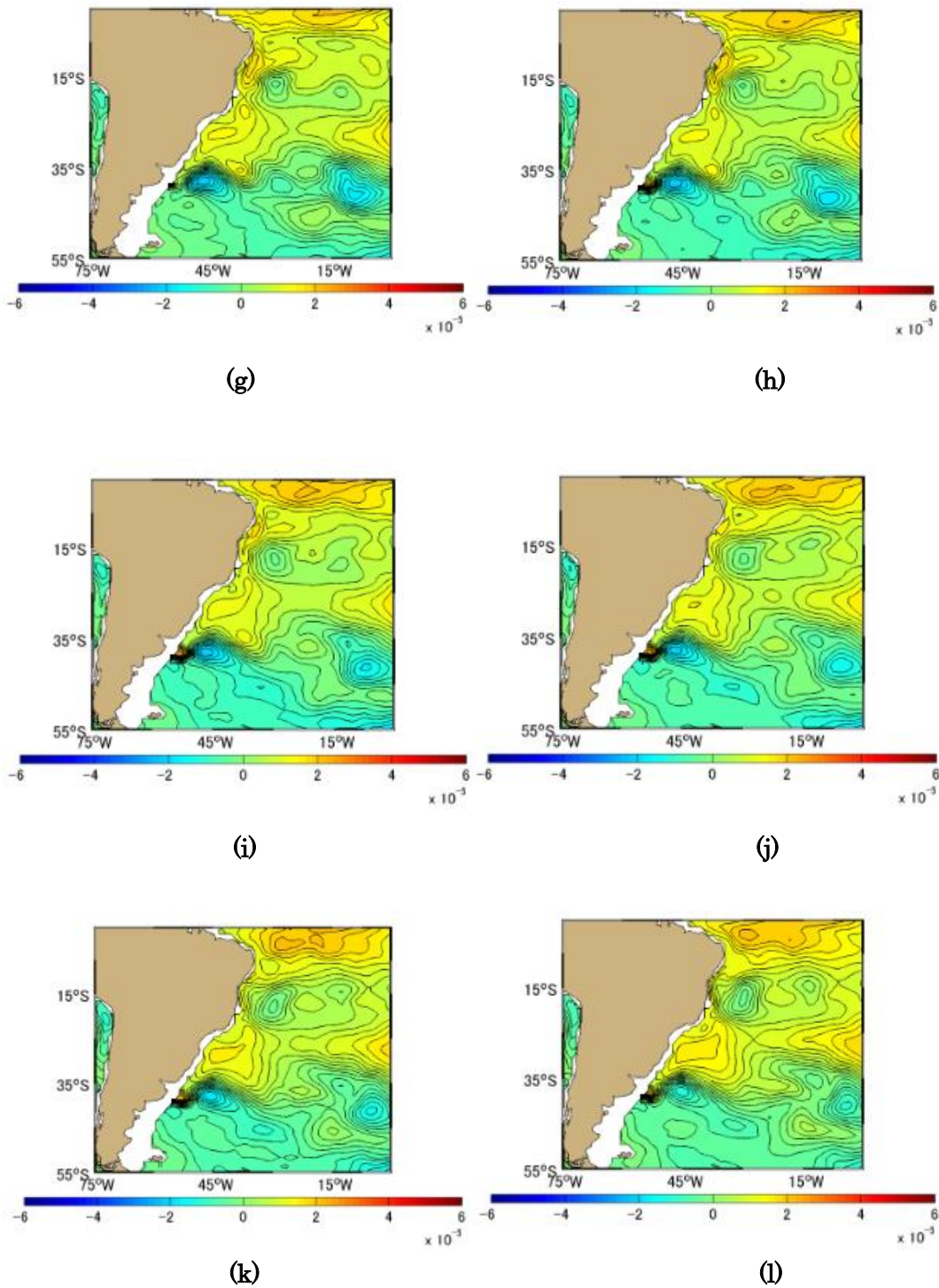
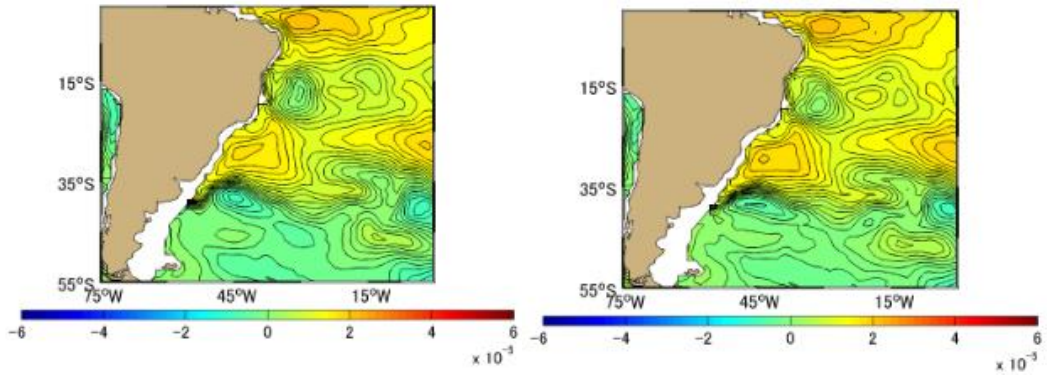
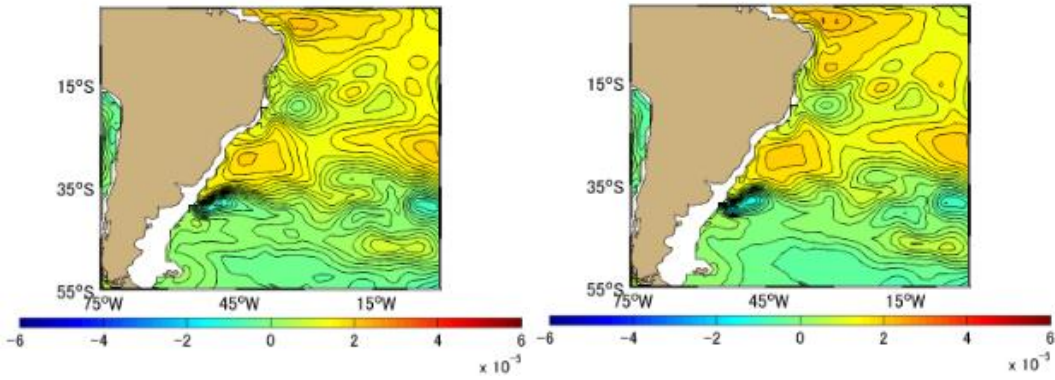


Figure A-5.10 Difference [PgC] between Approximation Method and Simulation Method Monthly Mean in 2000, the South Atlantic based on January 1991. (a)-(l) represents January-December



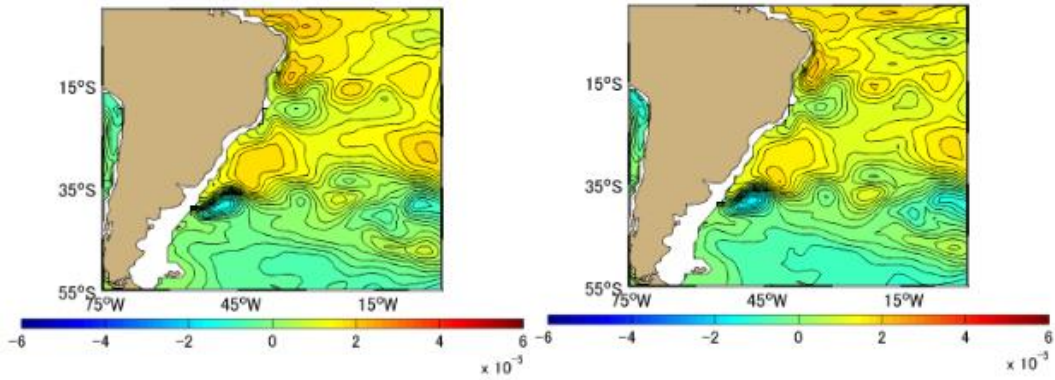
(a)

(b)



(c)

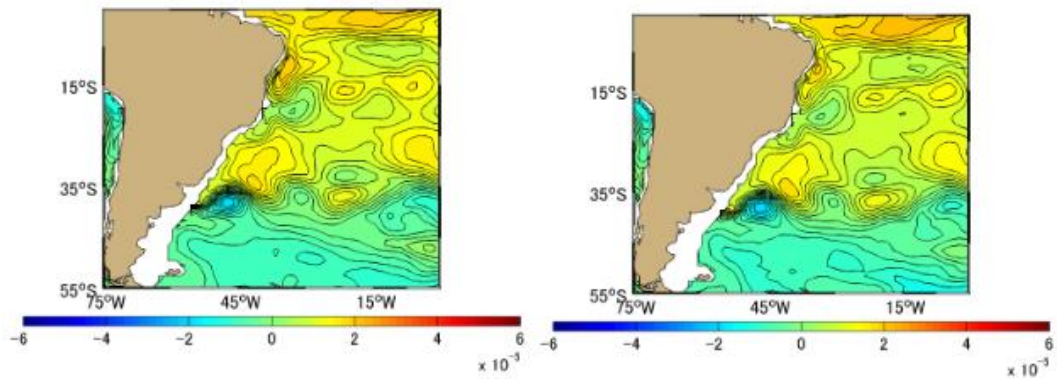
(d)



(e)

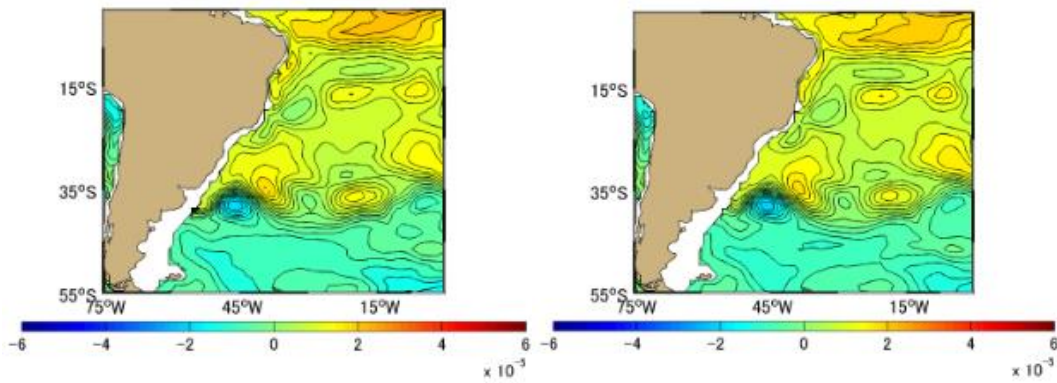
(f)





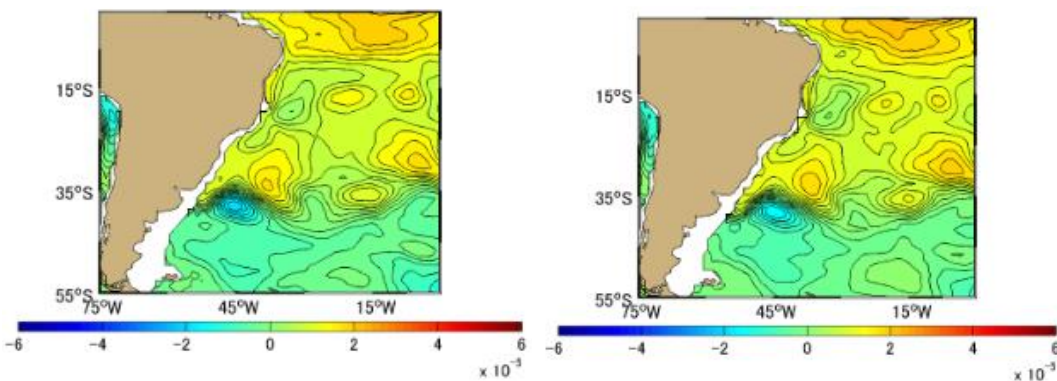
(g)

(h)



(i)

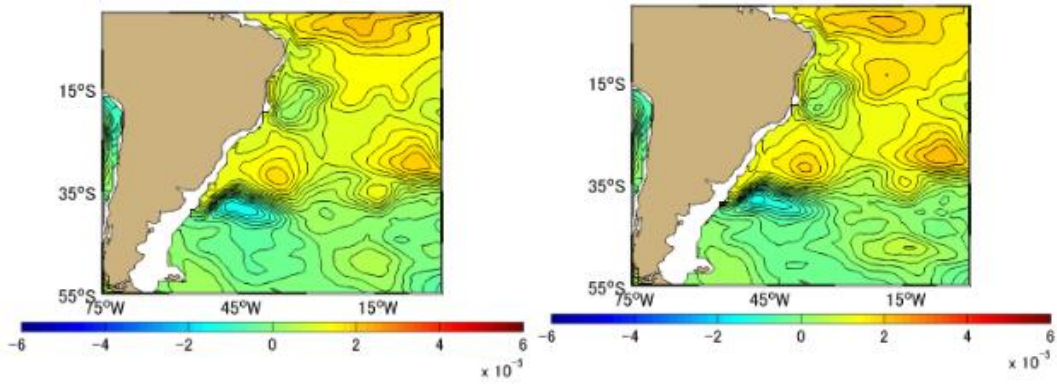
(j)



(k)

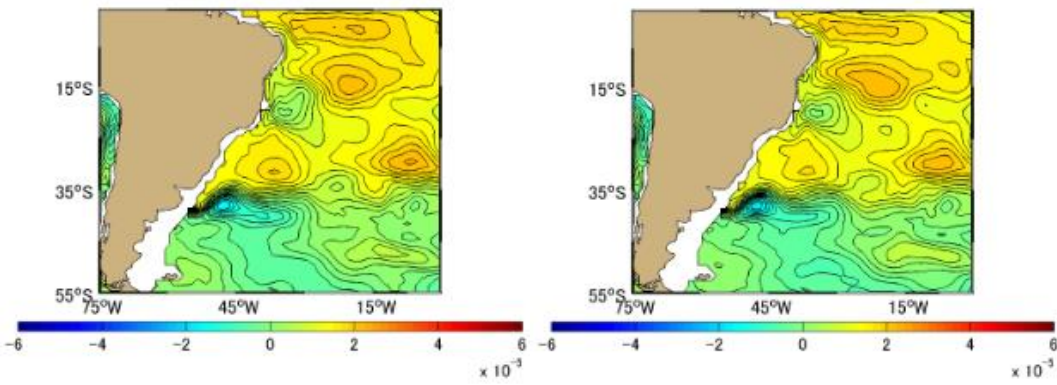
(l)

Figure A-5.11 Difference [PgC] between Approximation Method and Simulation Method Monthly Mean in 2001, the South Atlantic based on January 1991. (a)-(l) represents January-December



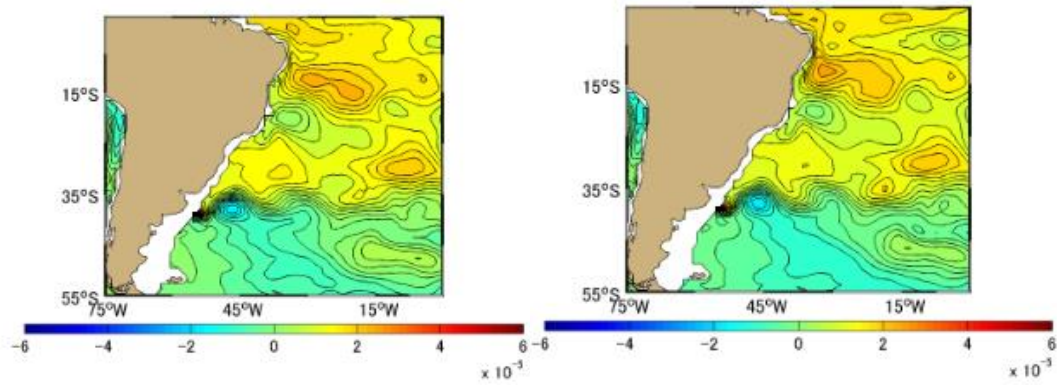
(a)

(b)



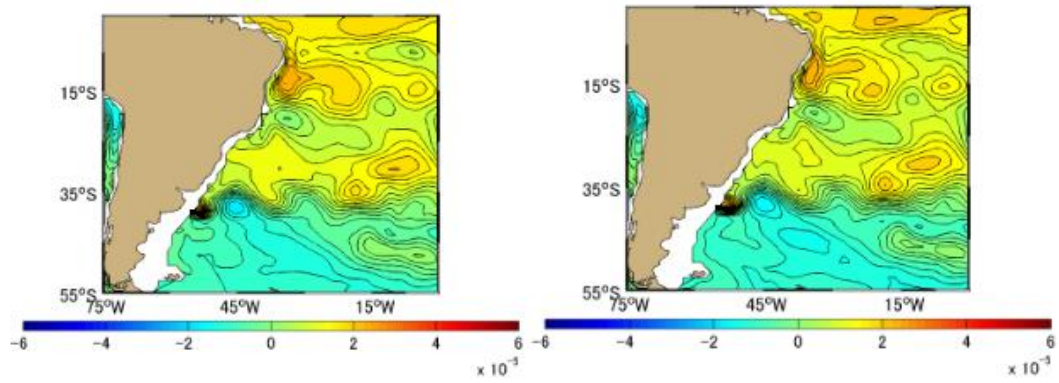
(c)

(d)



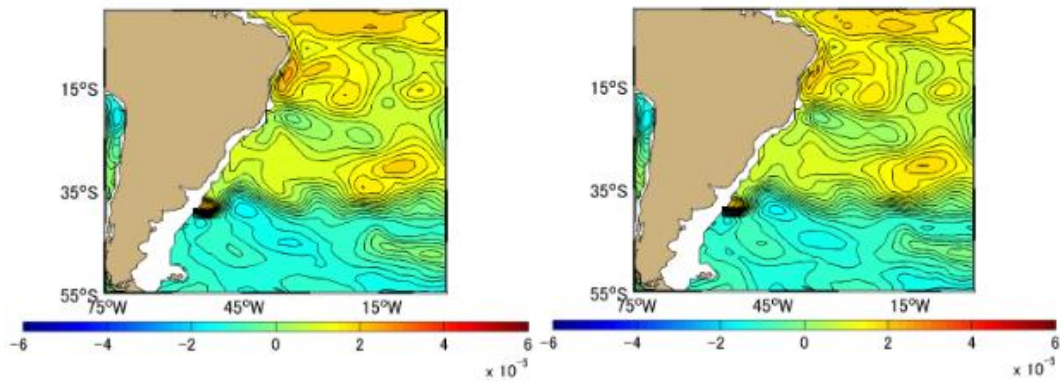
(e)

(f)



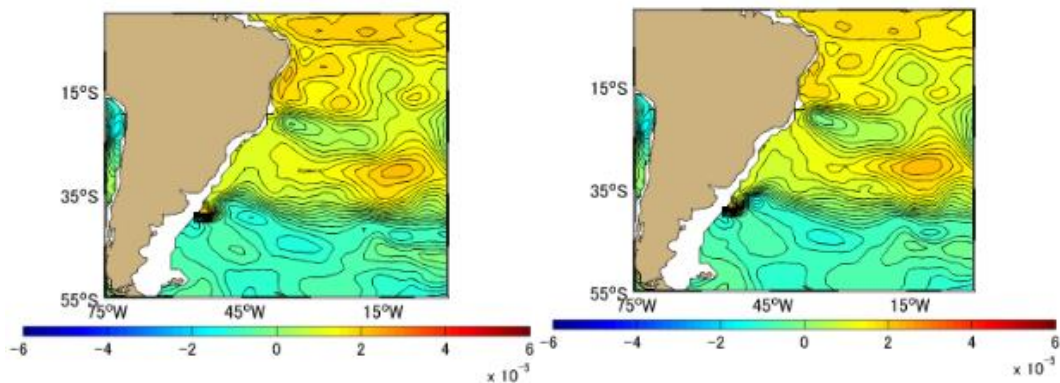
(g)

(h)



(i)

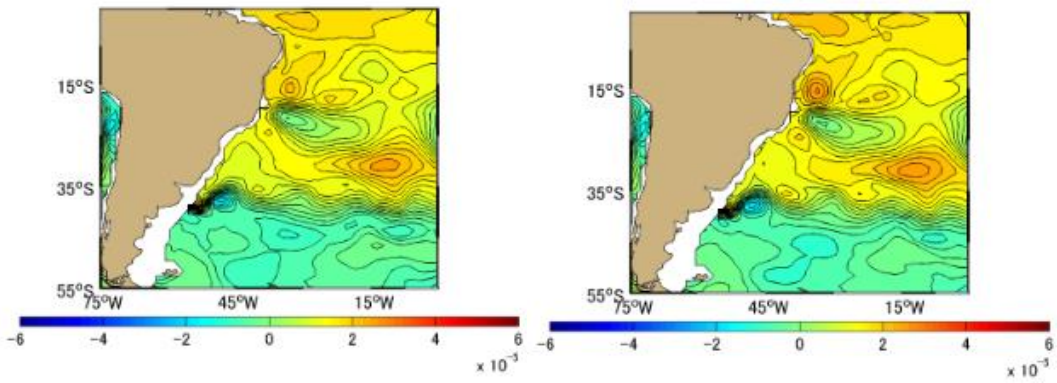
(j)



(k)

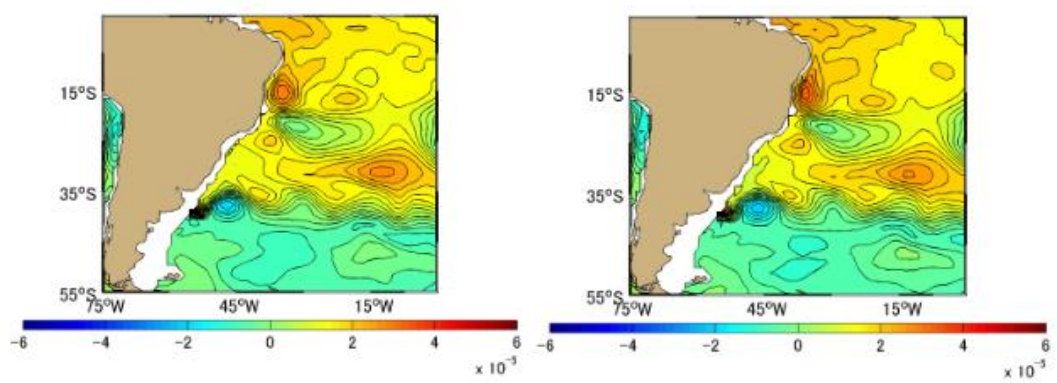
(l)

Figure A-5.12 Difference [PgC] between Approximation Method and Simulation Method Monthly Mean in 2002, the South Atlantic based on January 1991. (a)-(l) represents January-December



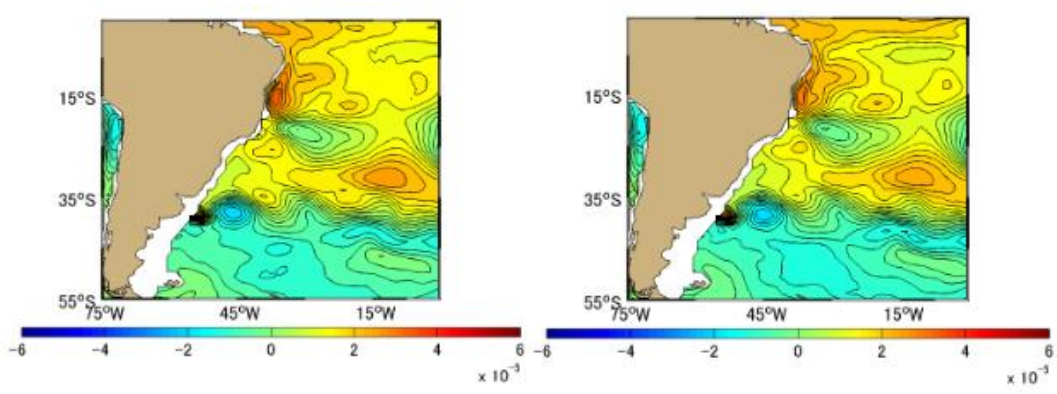
(a)

(b)



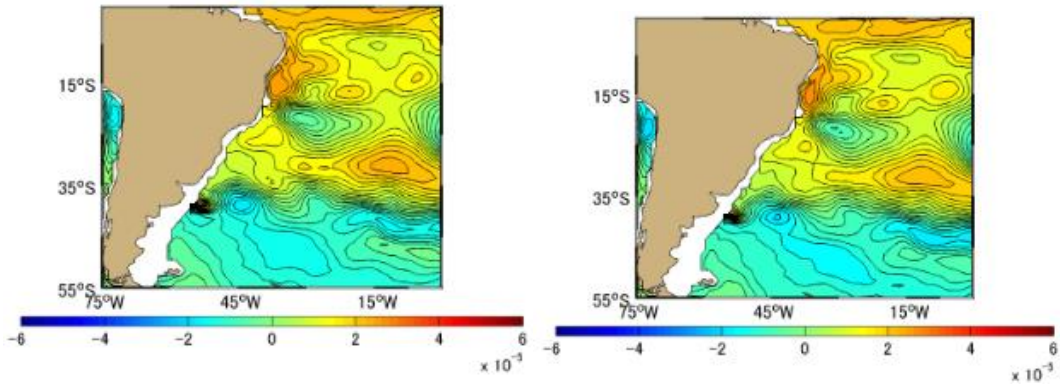
(c)

(d)



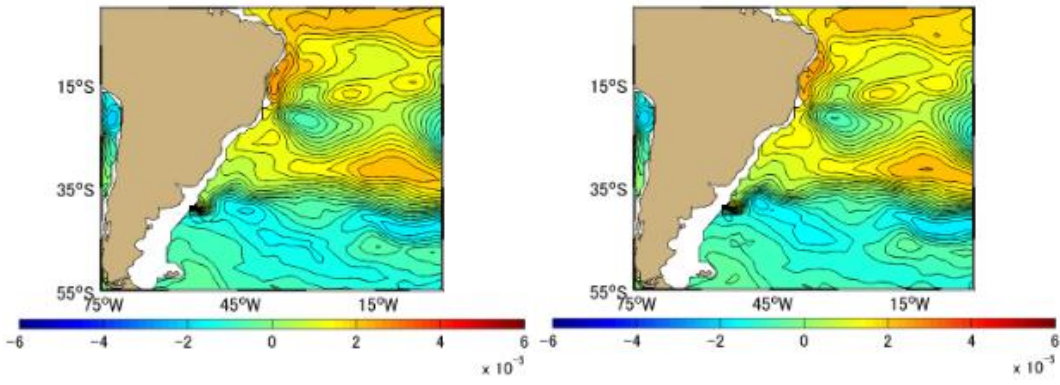
(e)

(f)



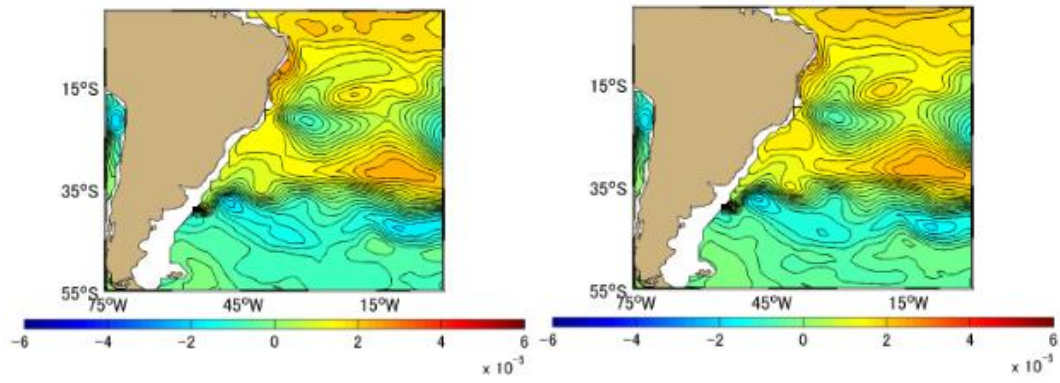
(g)

(h)



(i)

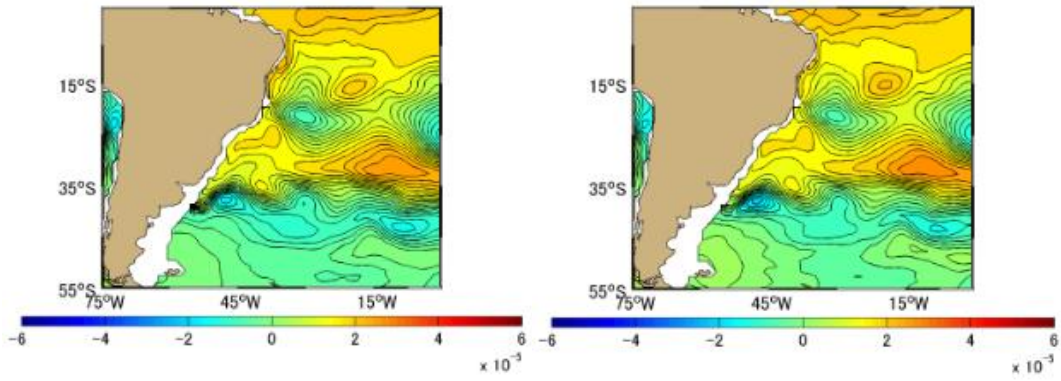
(j)



(k)

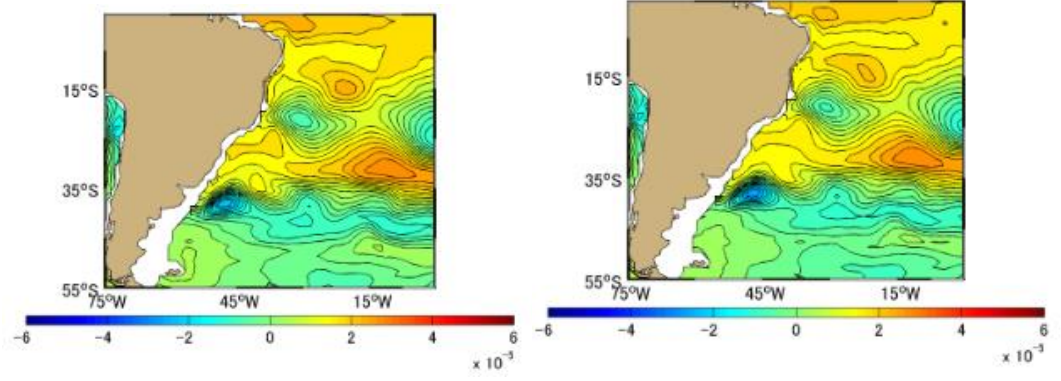
(l)

Figure A-5.13 Difference [PgC] between Approximation Method and Simulation Method Monthly Mean in 2003, the South Atlantic based on January 1991. (a)-(l) represents January-December



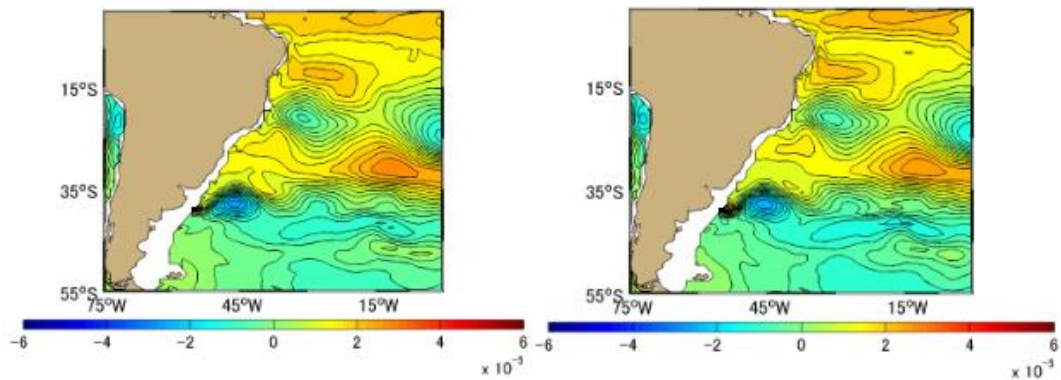
(a)

(b)



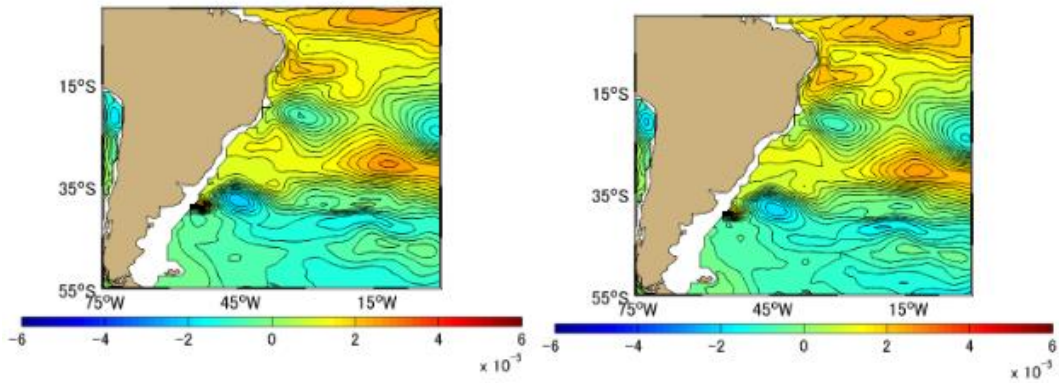
(c)

(d)



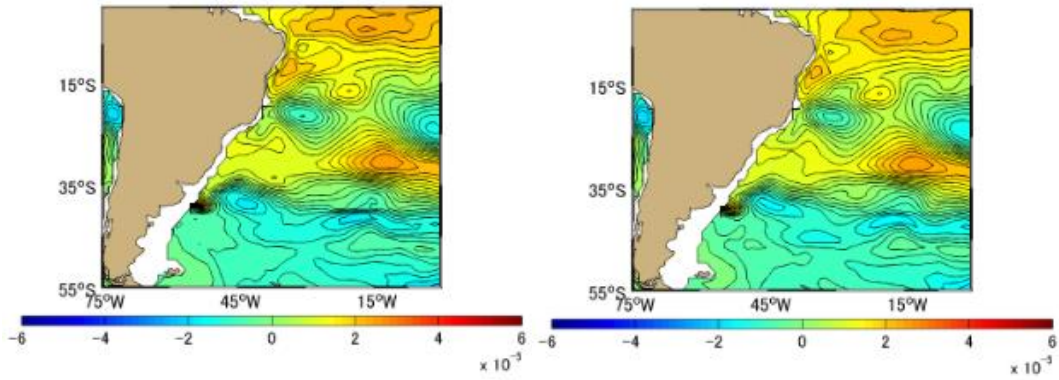
(e)

(f)



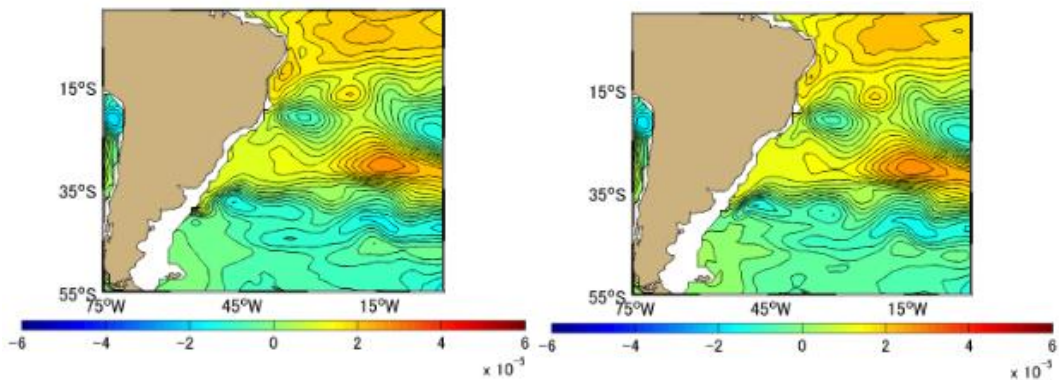
(g)

(h)



(i)

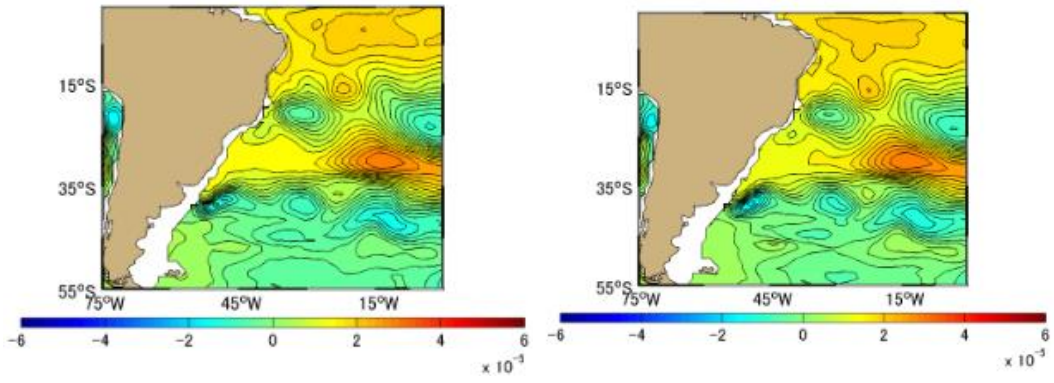
(j)



(k)

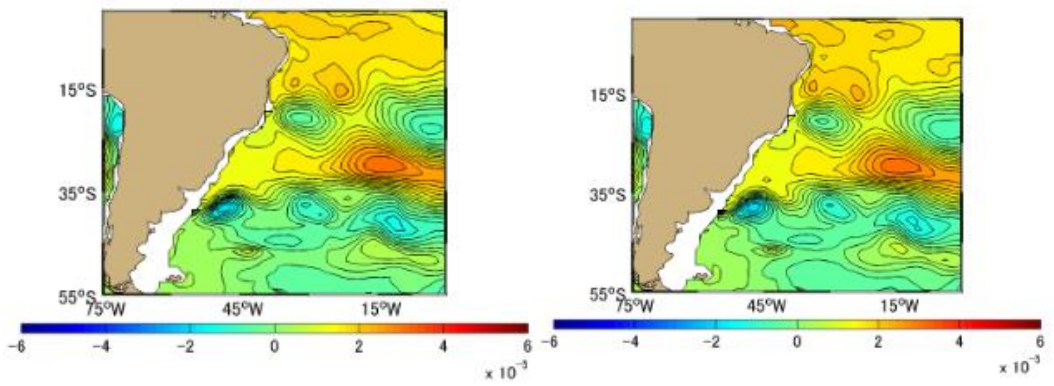
(l)

Figure A-5.14 Difference [PgC] between Approximation Method and Simulation Method Monthly Mean in 2004, the South Atlantic based on January 1991. (a)-(l) represents January-December



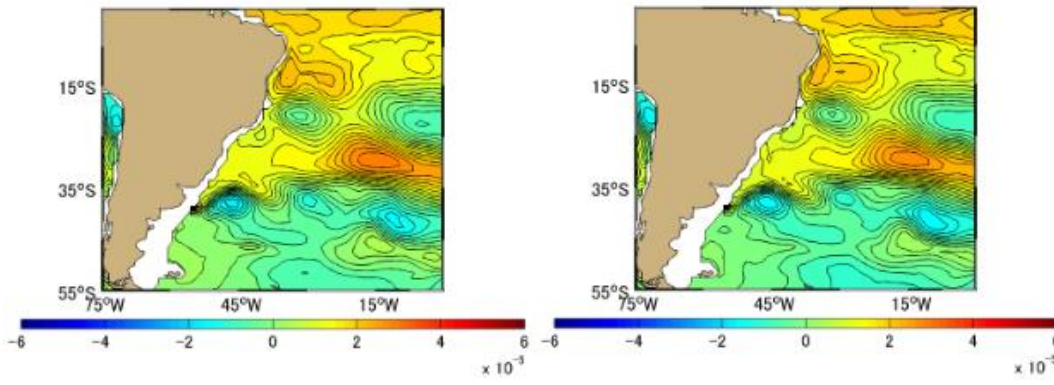
(a)

(b)



(c)

(d)



(e)

(f)



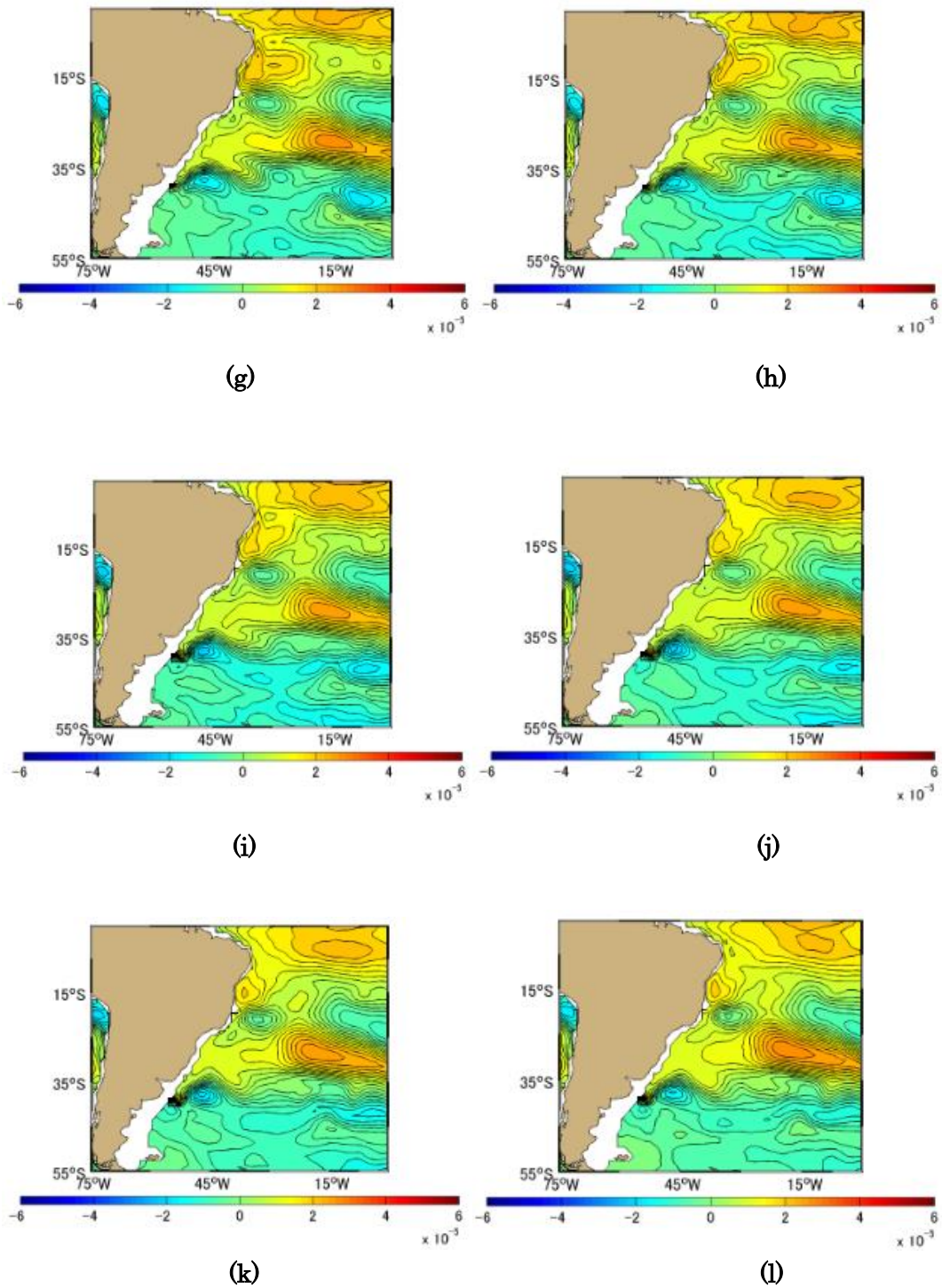
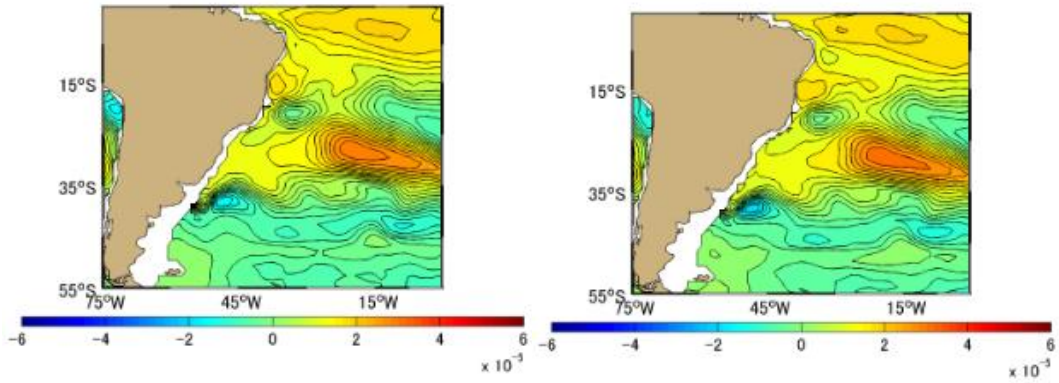
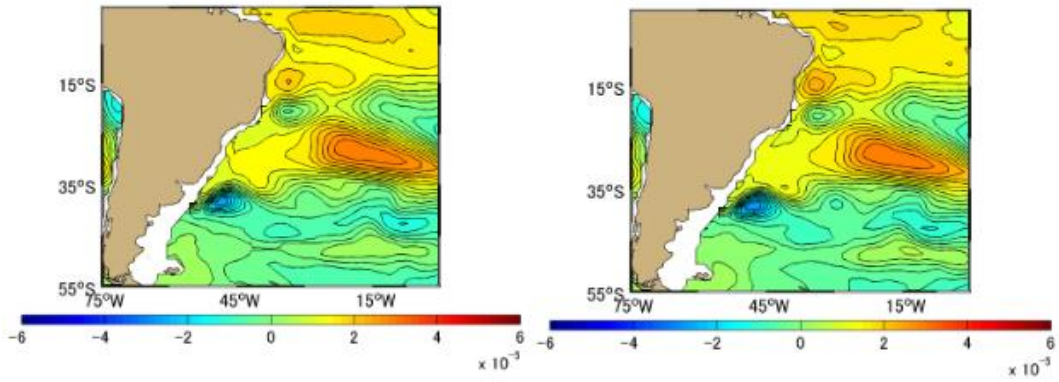


Figure A-5.15 Difference [PgC] between Approximation Method and Simulation Method Monthly Mean in 2005, the South Atlantic based on January 1991. (a)-(l) represents January-December



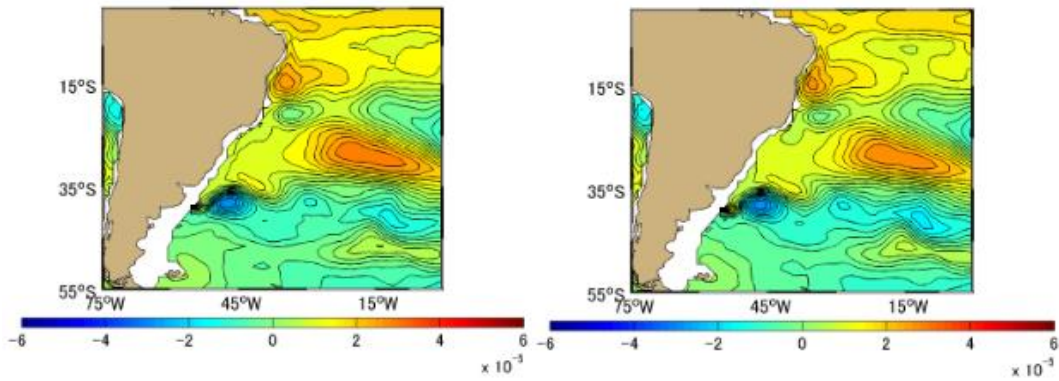
(a)

(b)



(c)

(d)



(e)

(f)

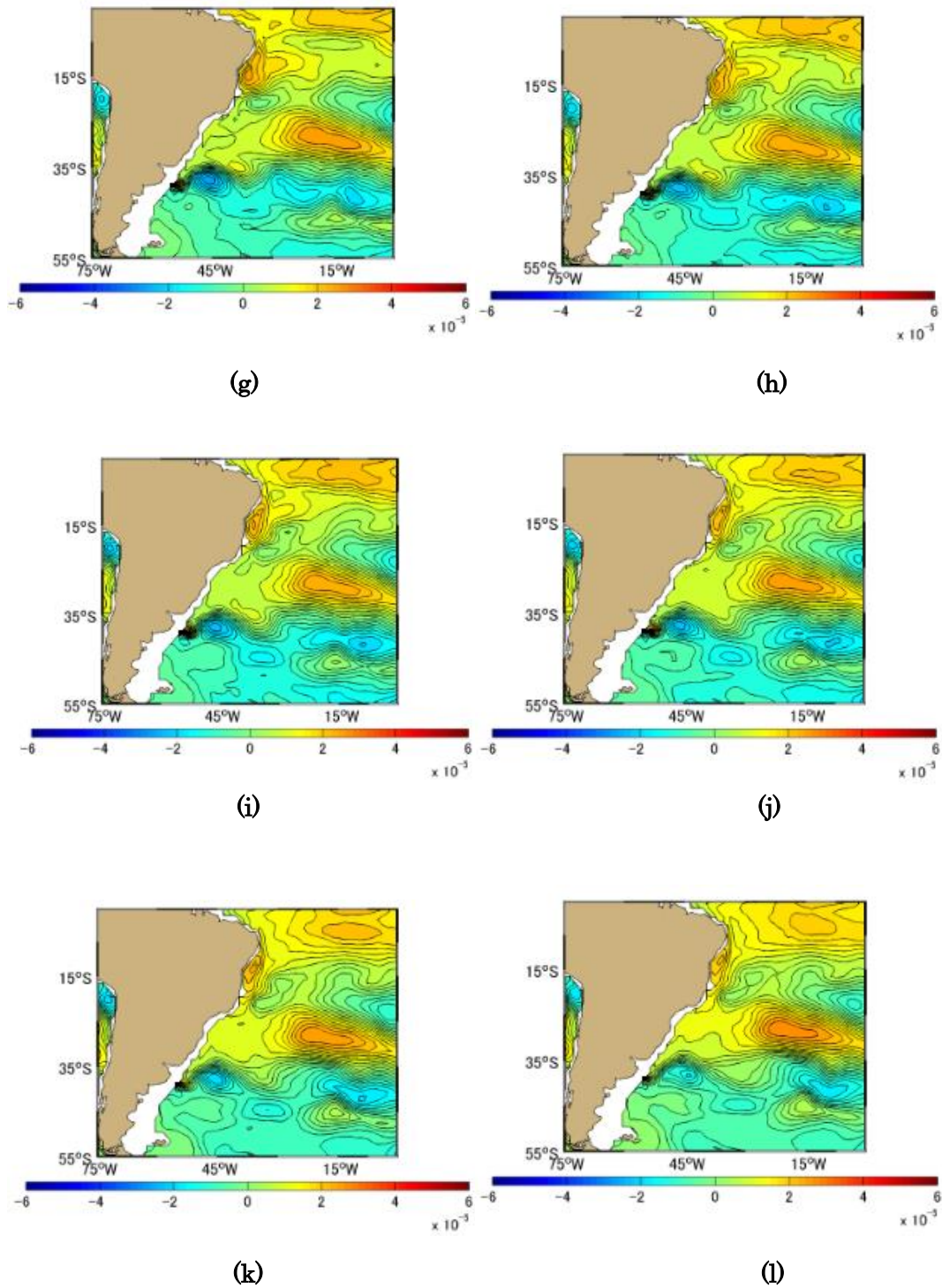
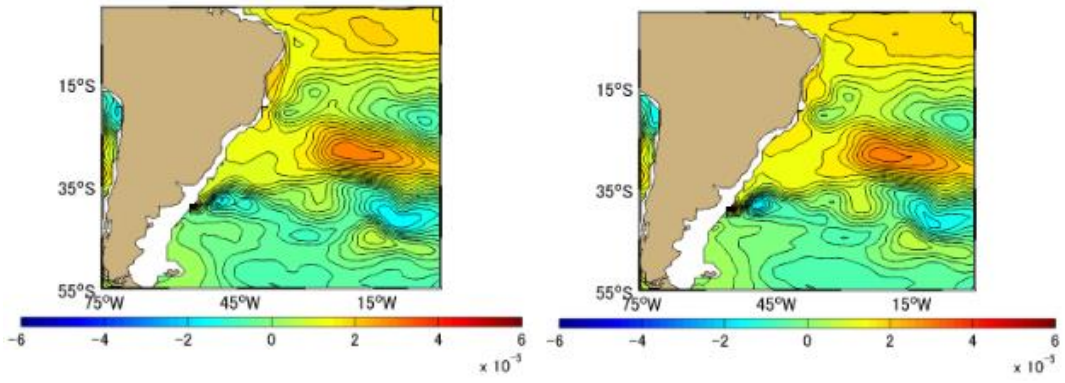
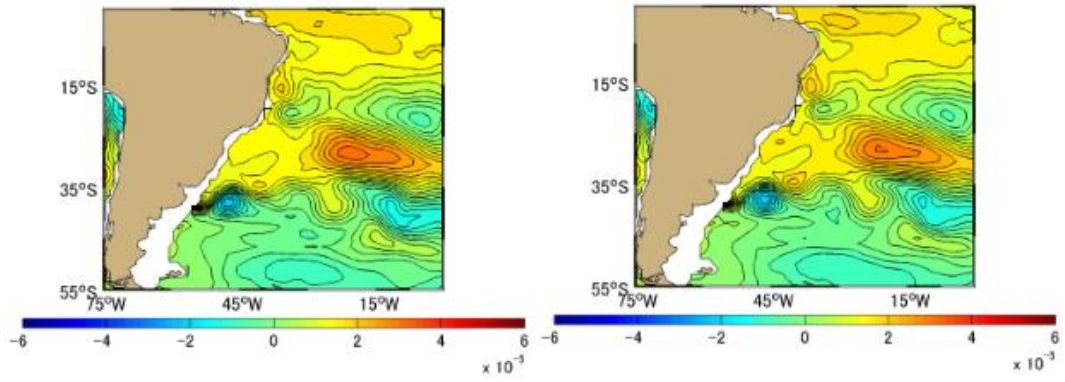


Figure A-5.16 Difference [PgC] between Approximation Method and Simulation Method Monthly Mean in 2006, the South Atlantic based on January 1991. (a)-(l) represents January-December



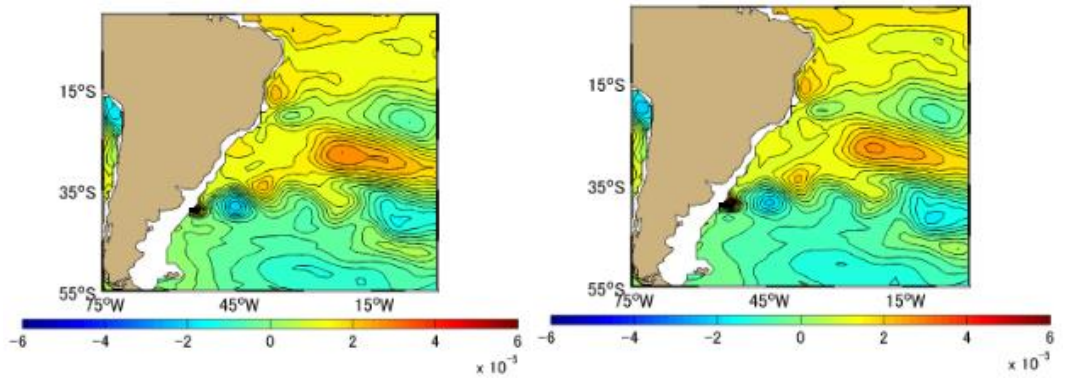
(a)

(b)



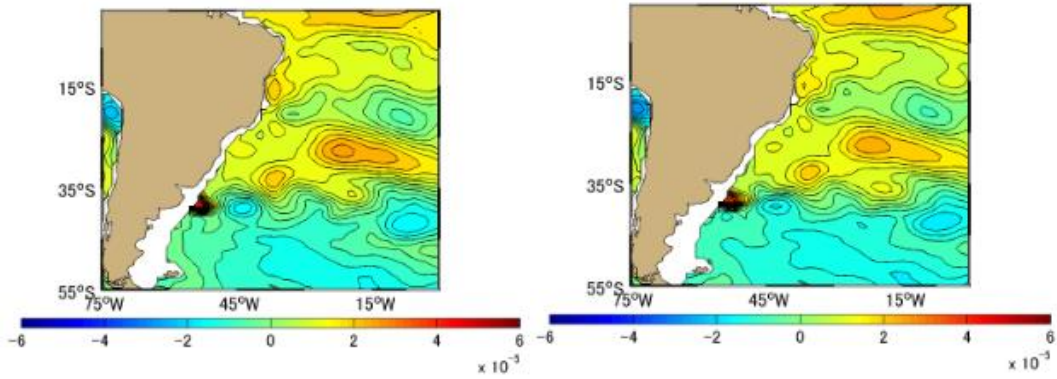
(c)

(d)



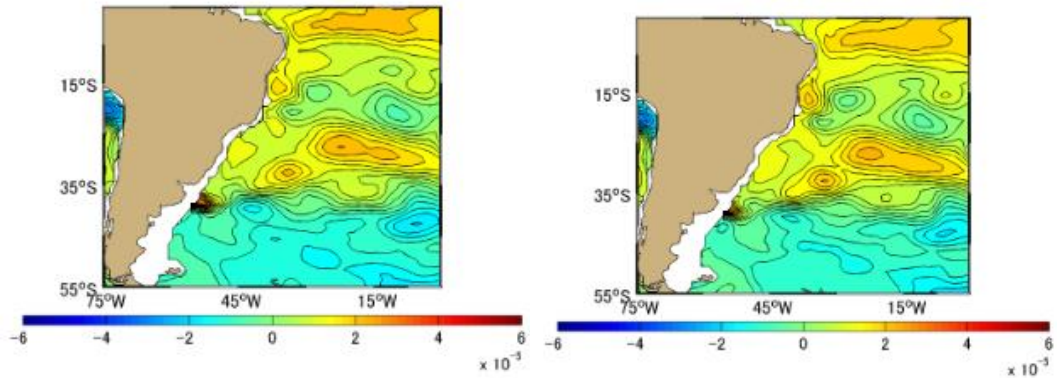
(e)

(f)



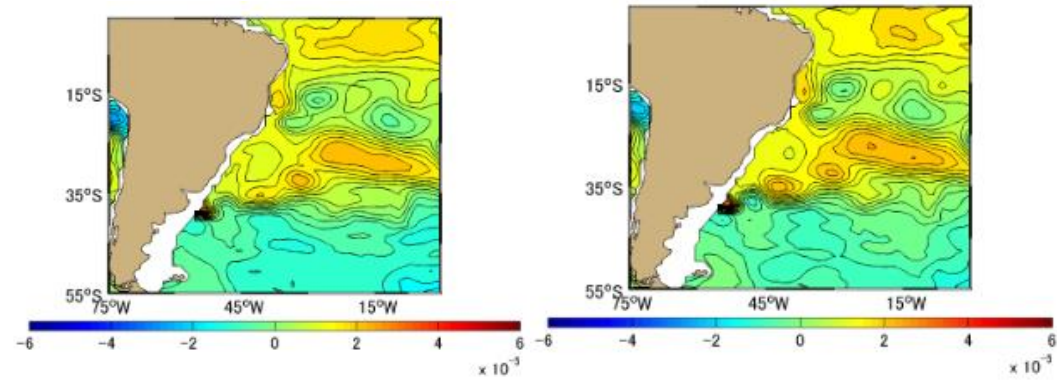
(g)

(h)



(i)

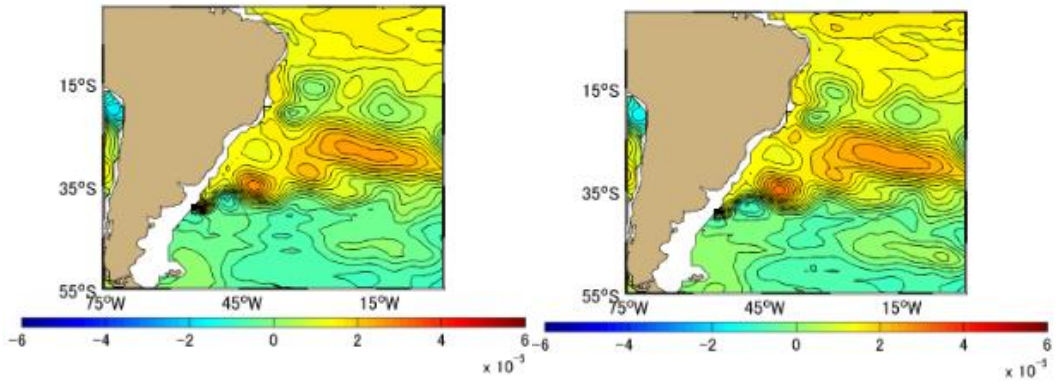
(j)



(k)

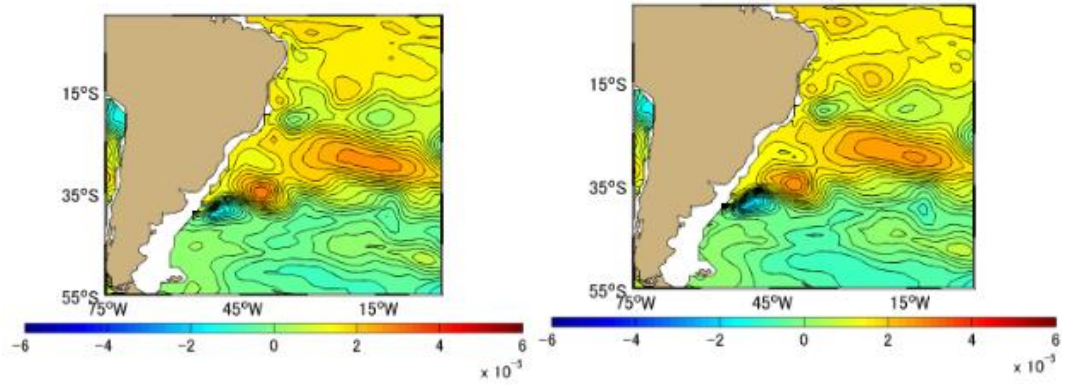
(l)

Figure A-5.17 Difference [PgC] between Approximation Method and Simulation Method Monthly Mean in 2007, the South Atlantic based on January 1991. (a)-(l) represents January-December



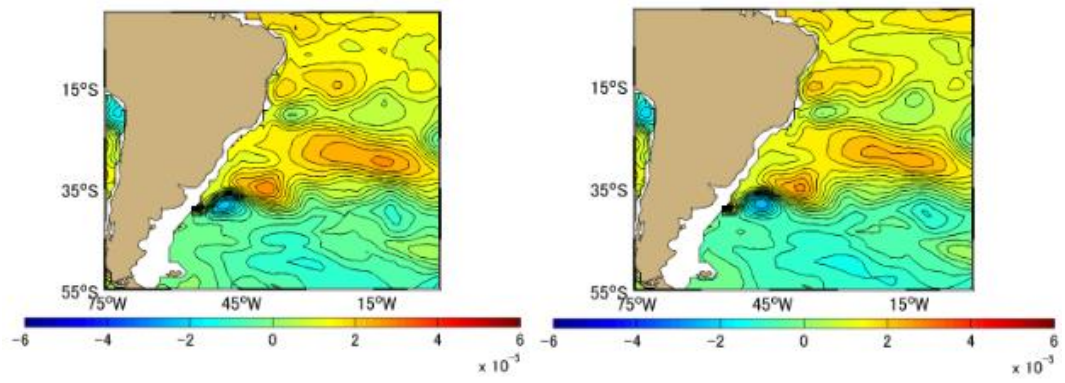
(a)

(b)



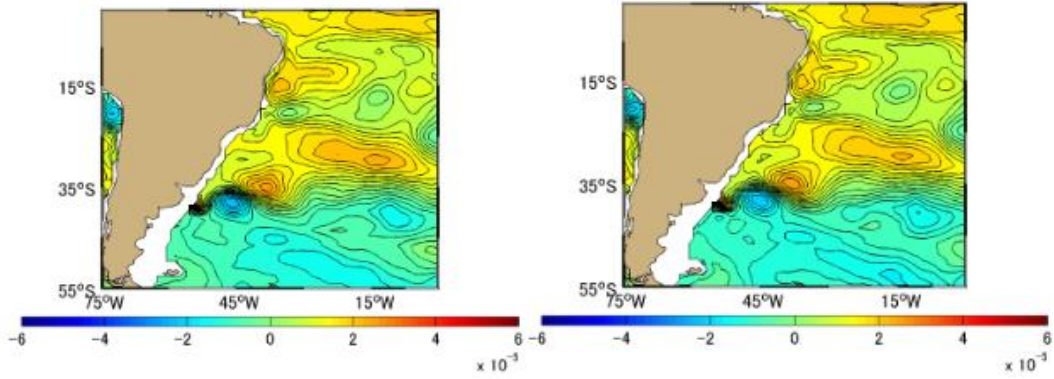
(c)

(d)



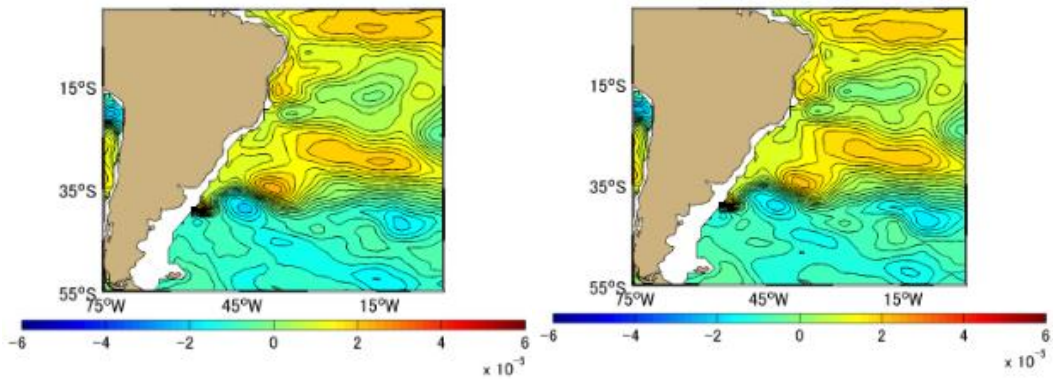
(e)

(f)



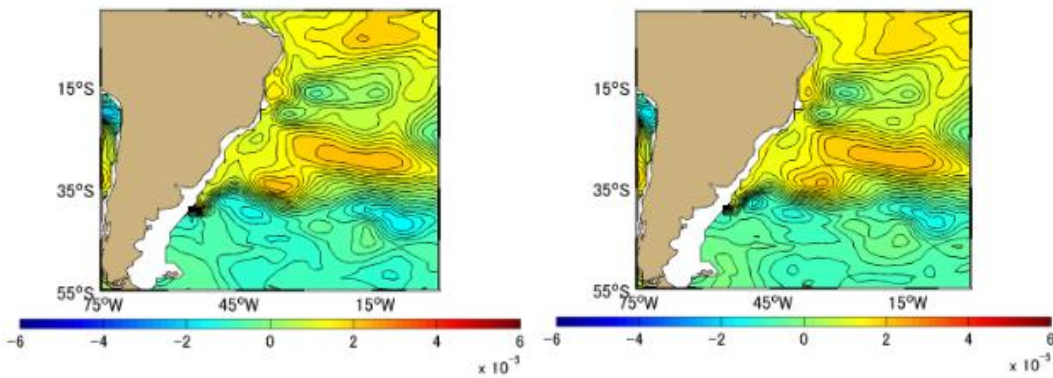
(g)

(h)



(i)

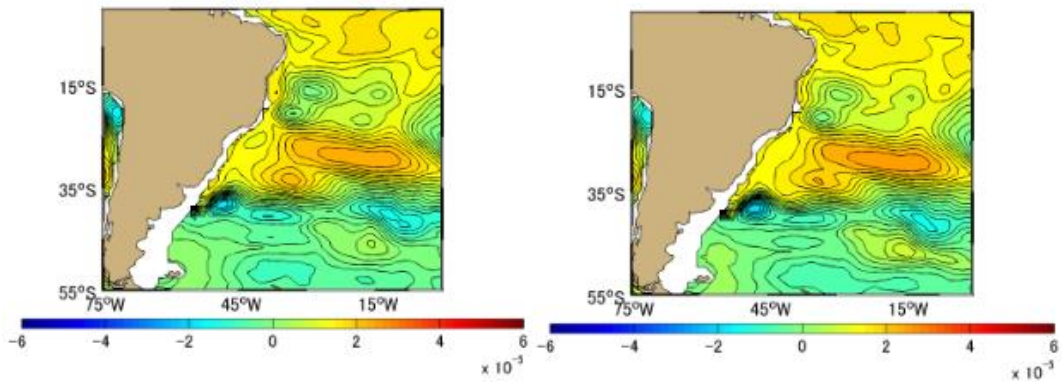
(j)



(k)

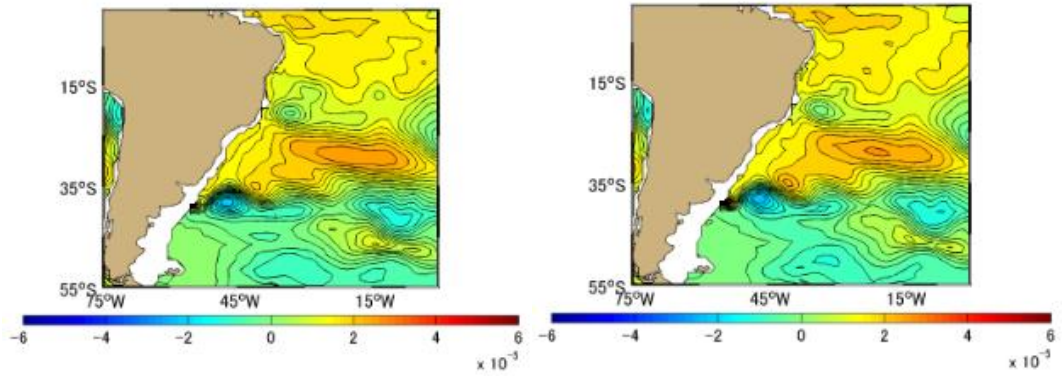
(l)

Figure A-5.18 Difference [PgC] between Approximation Method and Simulation Method Monthly Mean in 2008, the South Atlantic based on January 1991. (a)-(l) represents January-December



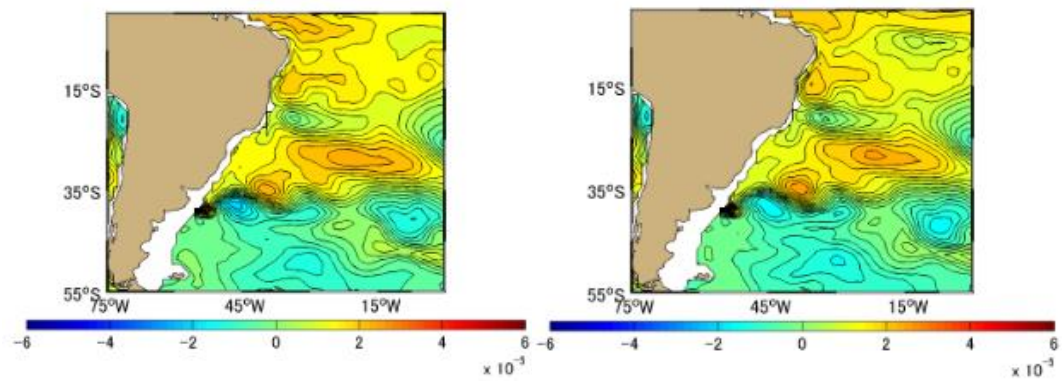
(a)

(b)



(c)

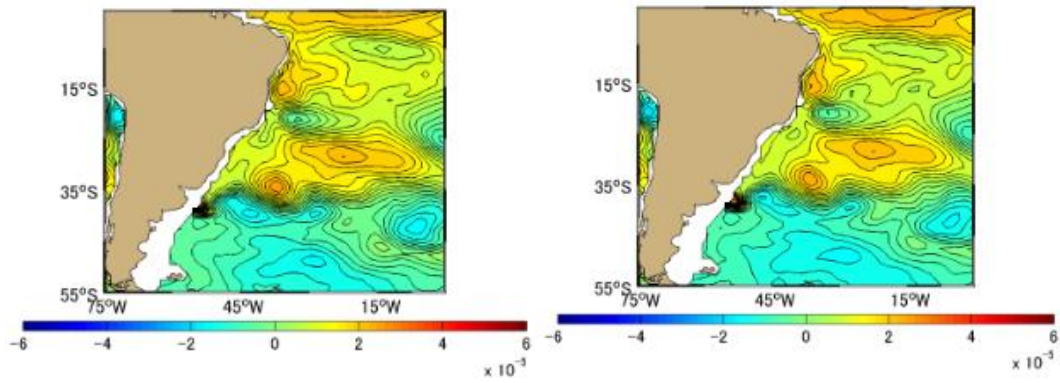
(d)



(e)

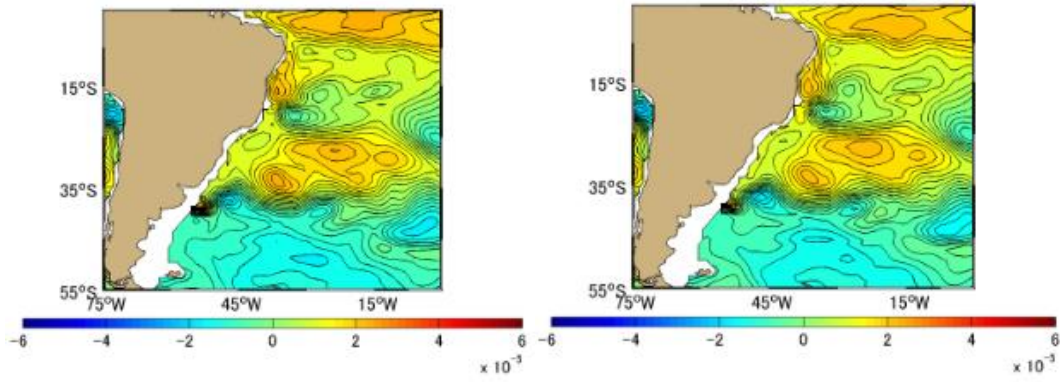
(f)





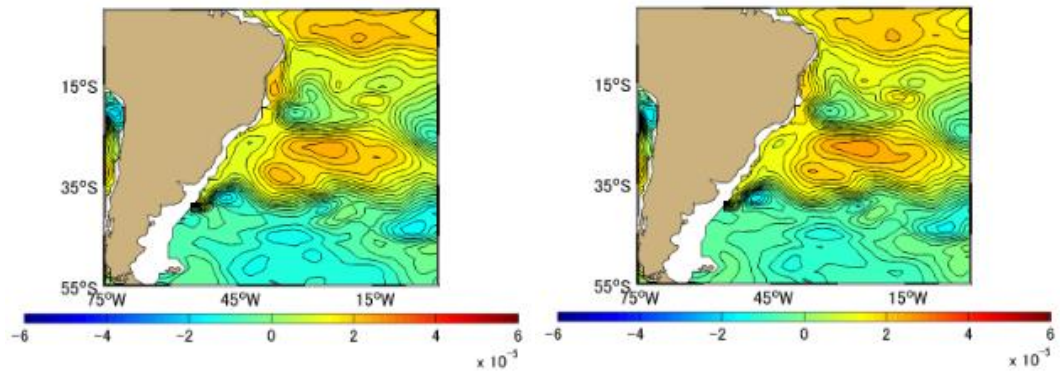
(g)

(h)



(i)

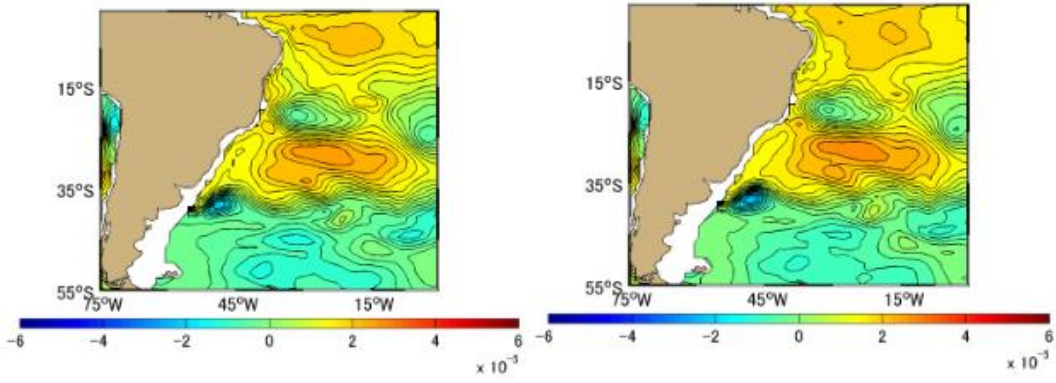
(j)



(k)

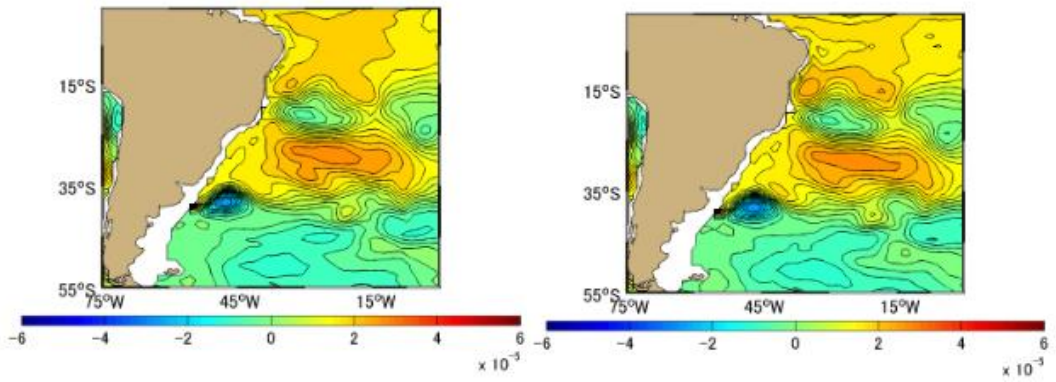
(l)

Figure A-5.19 Difference [PgC] between Approximation Method and Simulation Method Monthly Mean in 2009, the South Atlantic based on January 1991. (a)-(l) represents January-December



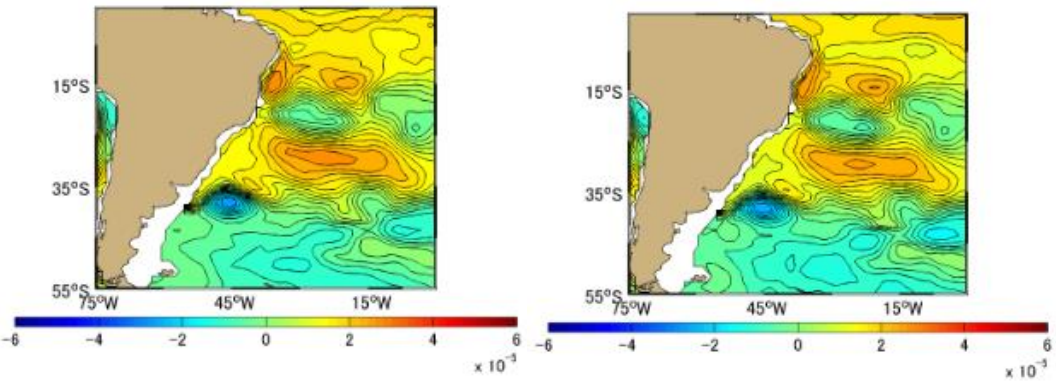
(a)

(b)



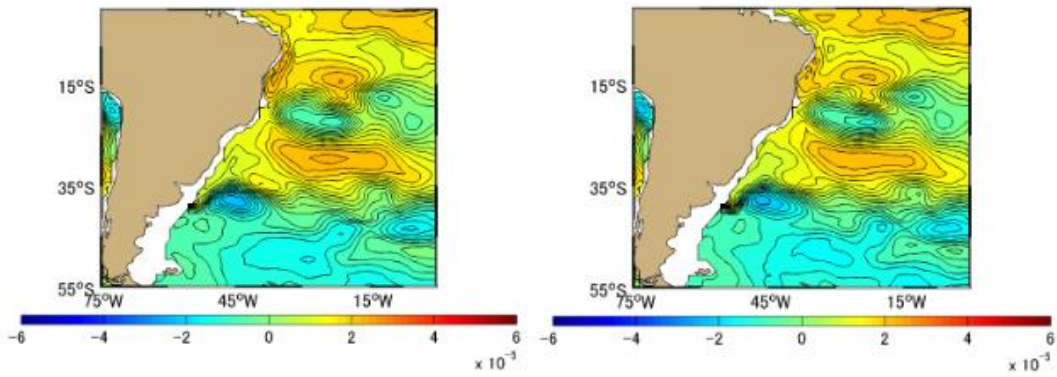
(c)

(d)



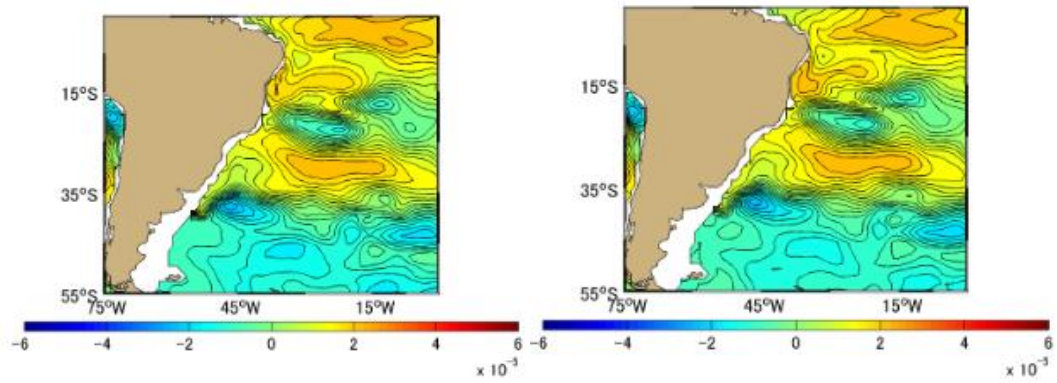
(e)

(f)



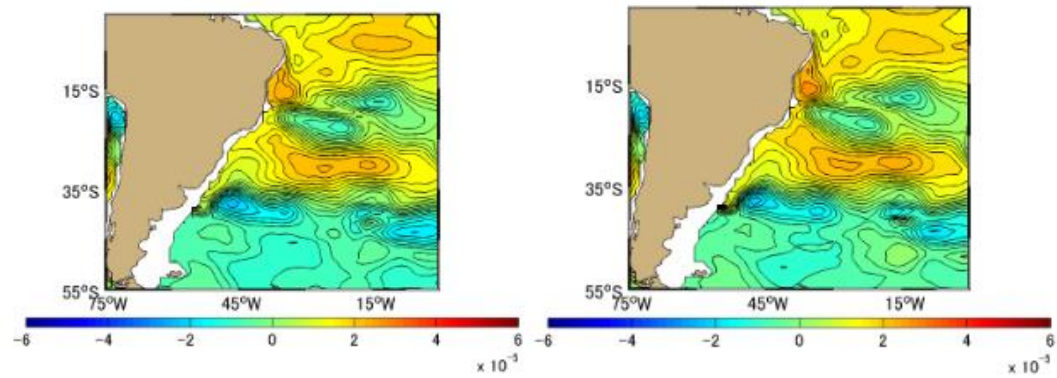
(g)

(h)



(i)

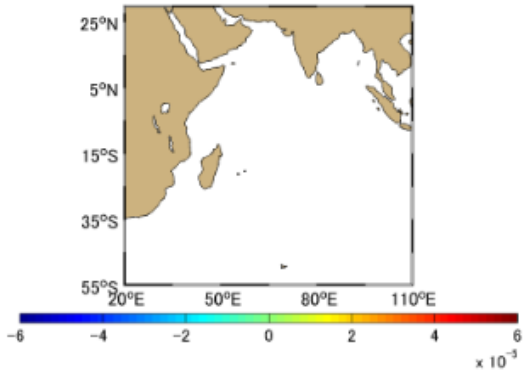
(j)



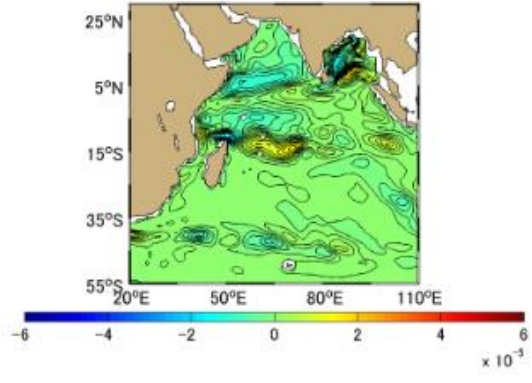
(k)

(l)

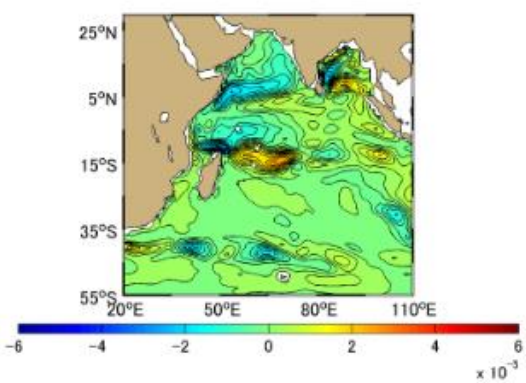
Figure A-5.20 Difference [PgC] between Approximation Method and Simulation Method Monthly Mean in 2010, the South Atlantic based on January 1991. (a)-(l) represents January-December



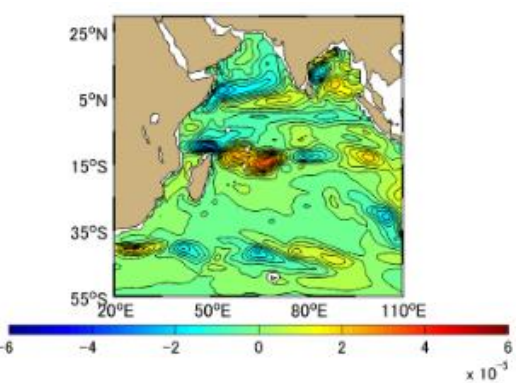
(a)



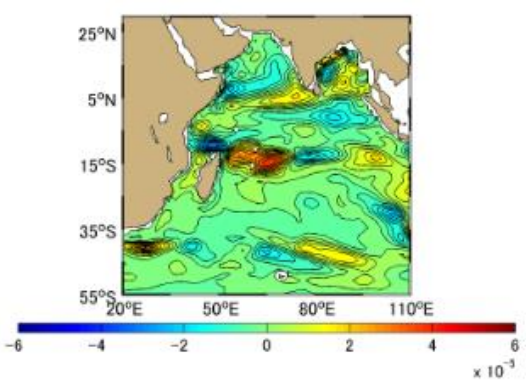
(b)



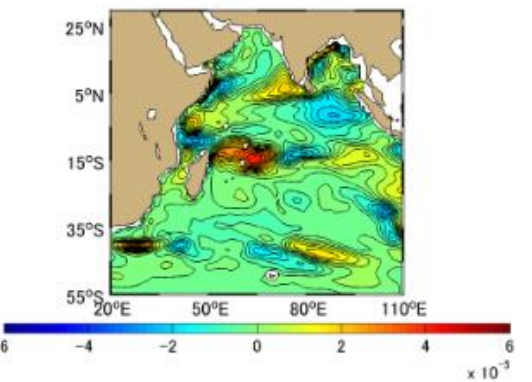
(c)



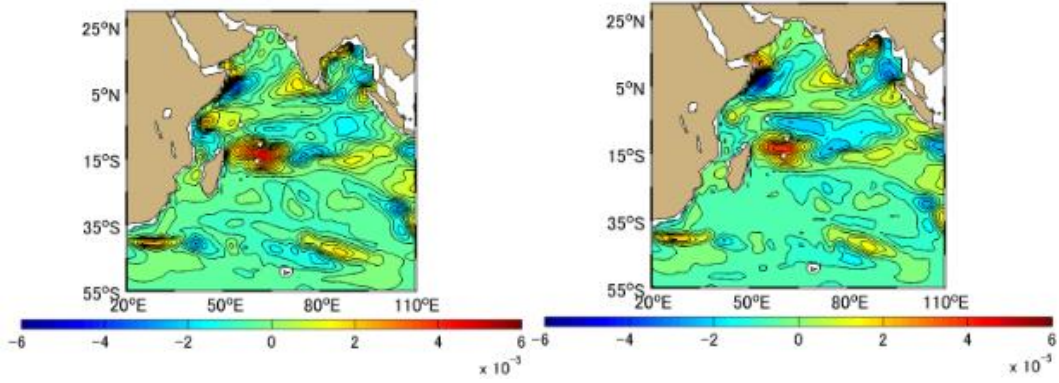
(d)



(e)

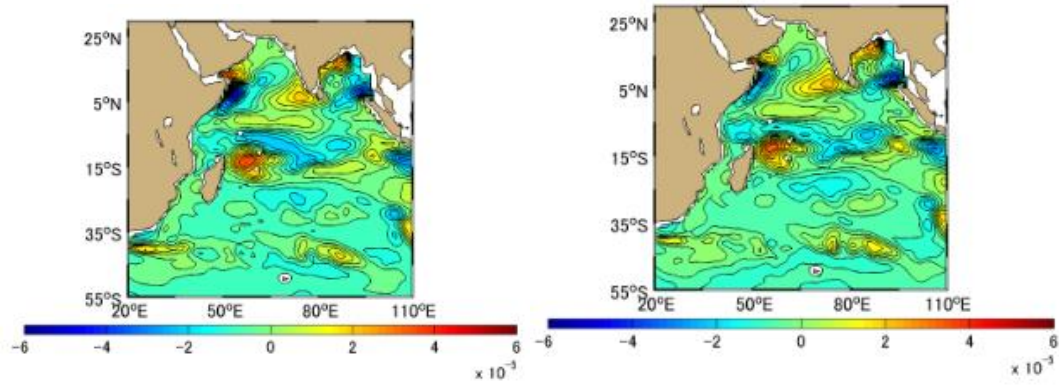


(f)



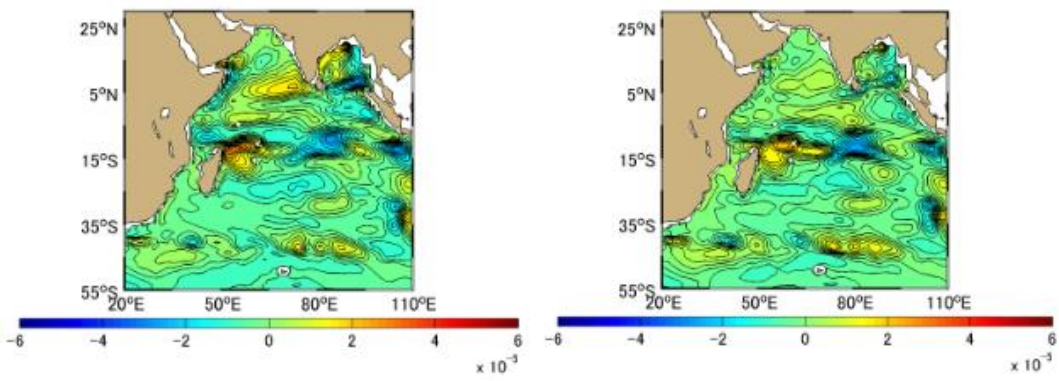
(g)

(h)



(i)

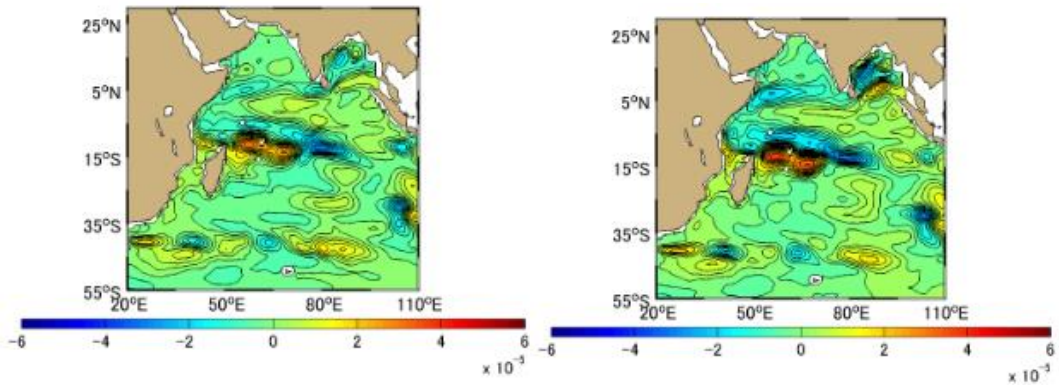
(j)



(k)

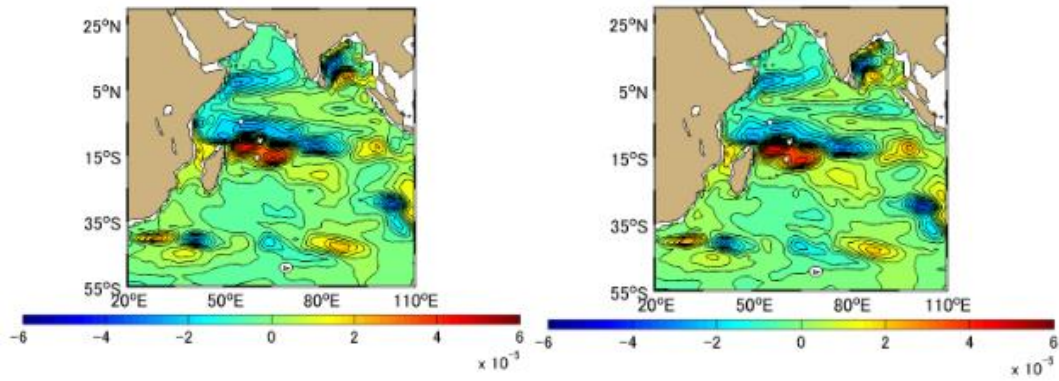
(l)

Figure A-6.1 Difference [PgC] between Approximation Method and Simulation Method Monthly Mean in 1991, the Indian Ocean based on January 1991. (a)-(l) represents January-December



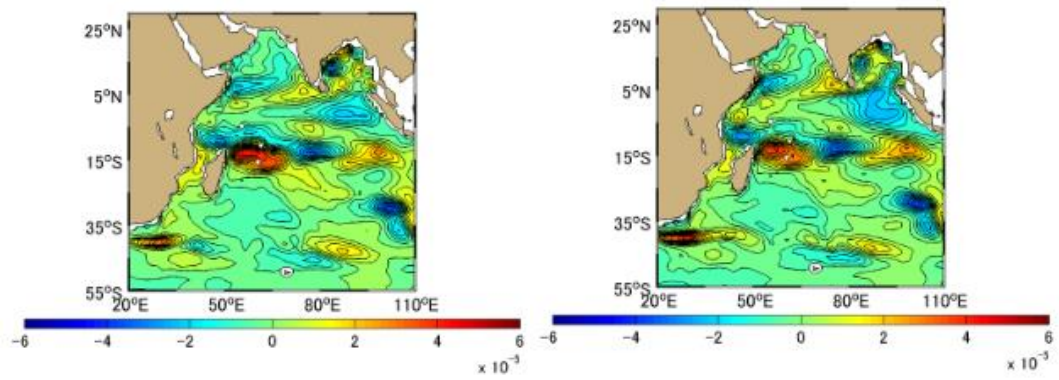
(a)

(b)



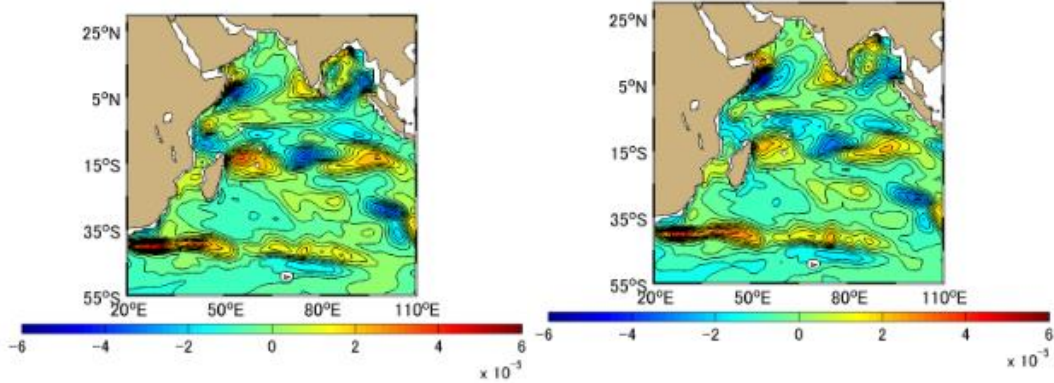
(c)

(d)



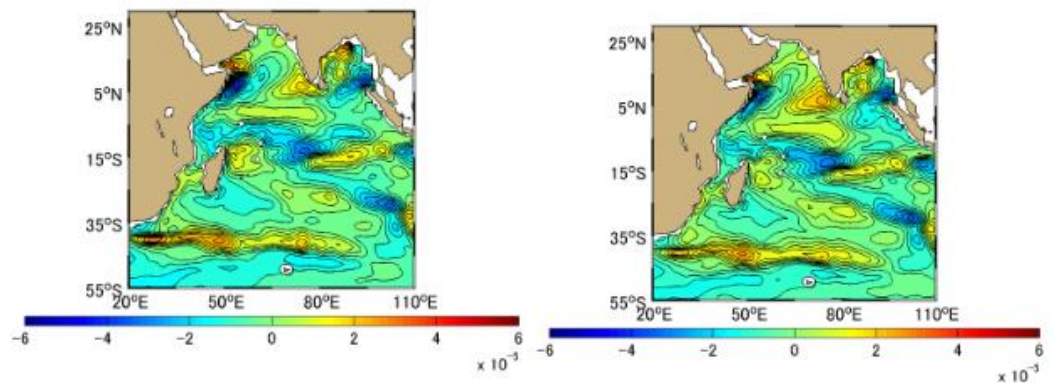
(e)

(f)



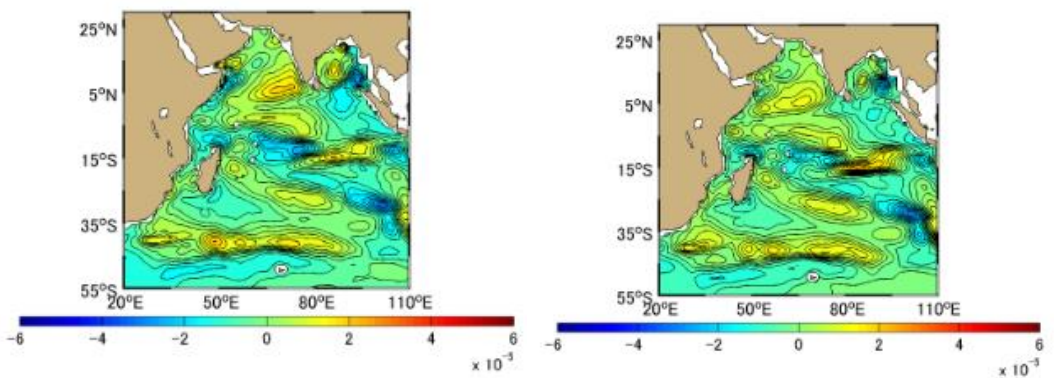
(g)

(h)



(i)

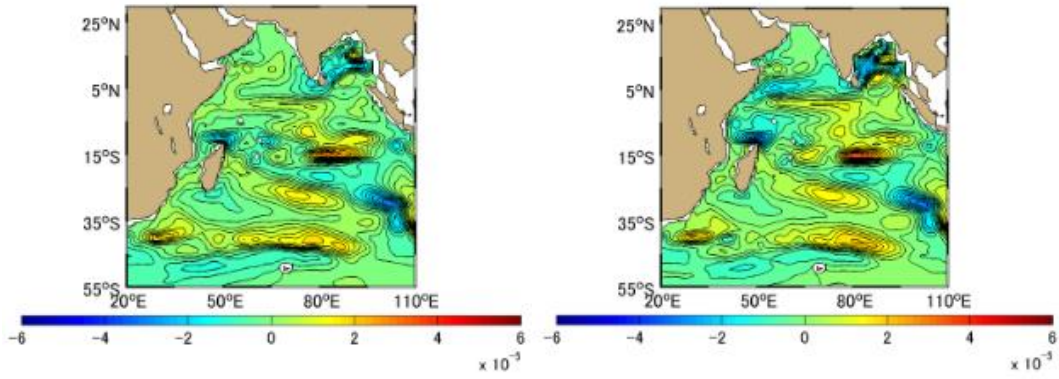
(j)



(k)

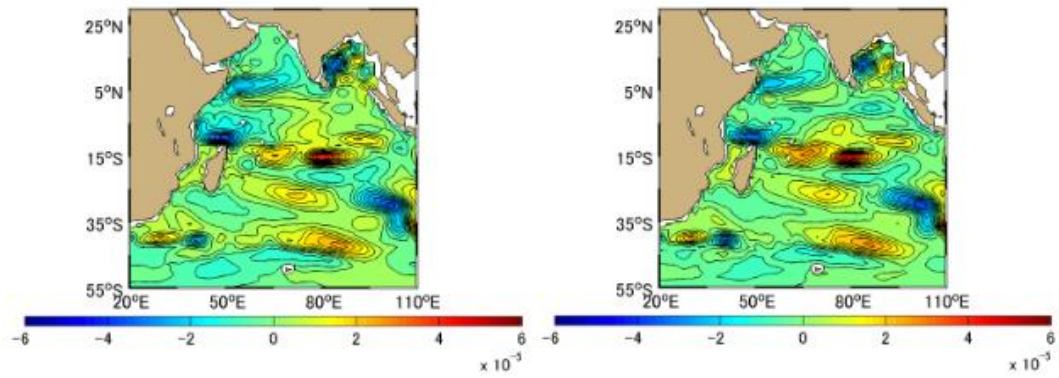
(l)

Figure A-6.2 Difference [PgC] between Approximation Method and Simulation Method Monthly Mean in 1992, the Indian Ocean based on January 1991. (a)-(l) represents January-December



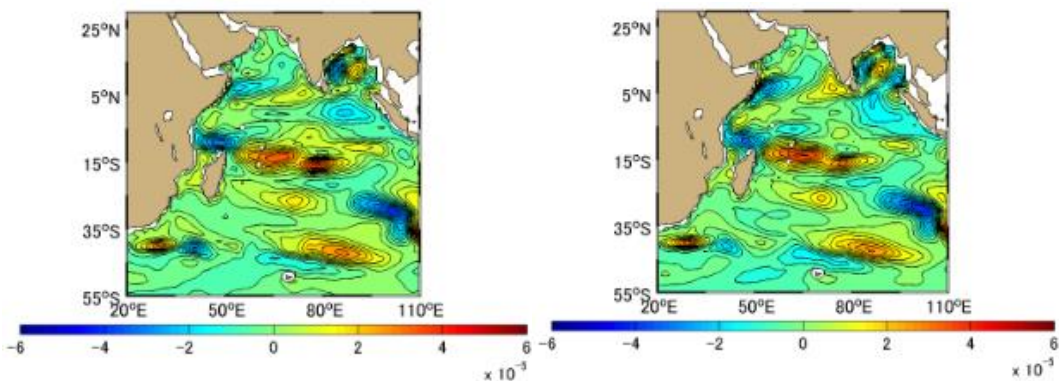
(a)

(b)



(c)

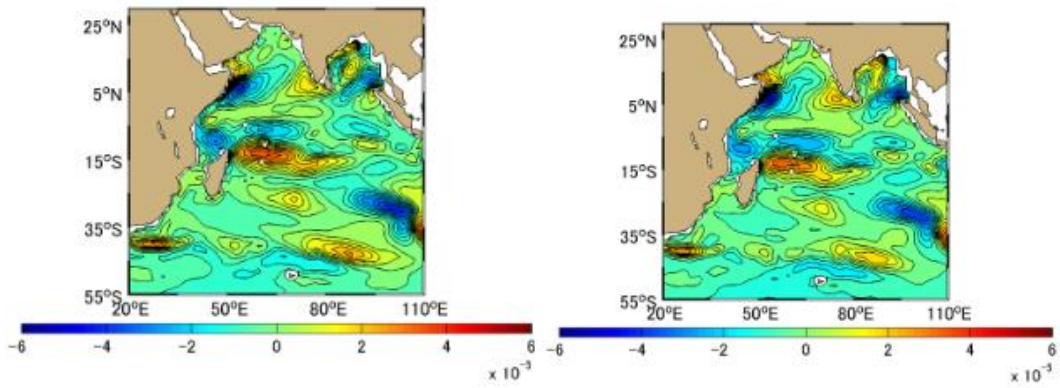
(d)



(e)

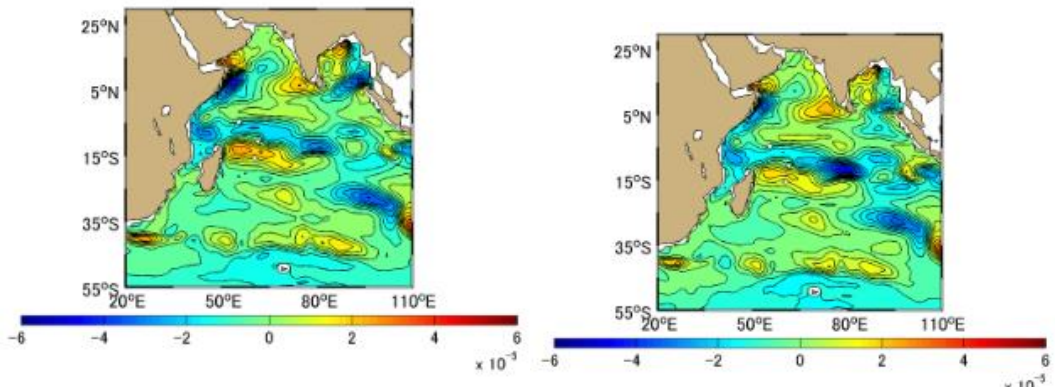
(f)





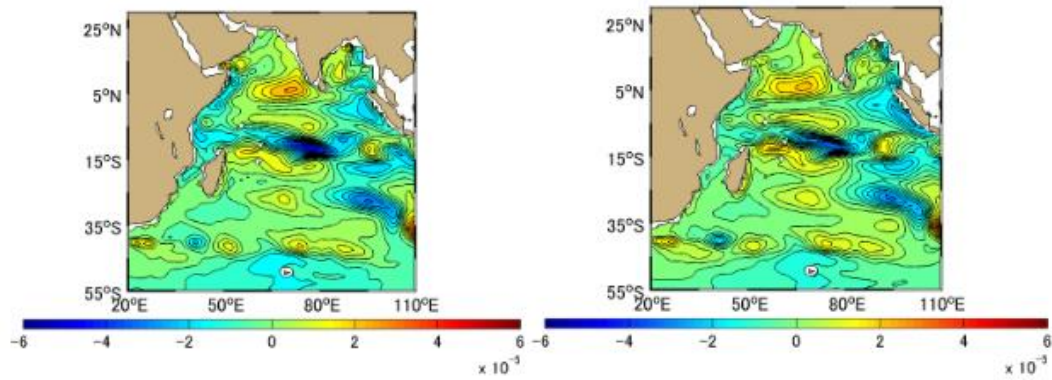
(g)

(h)



(i)

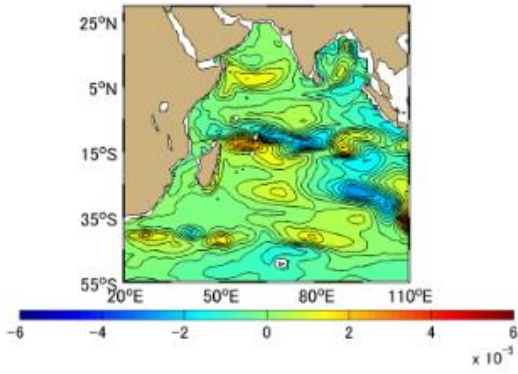
(j)



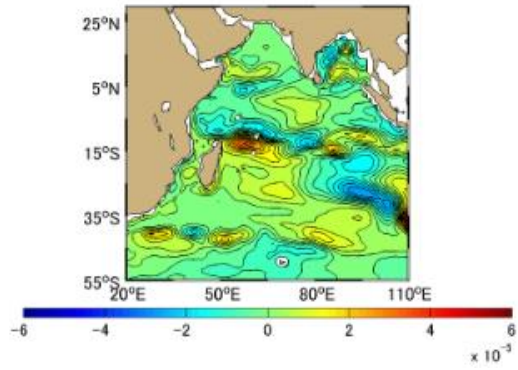
(k)

(l)

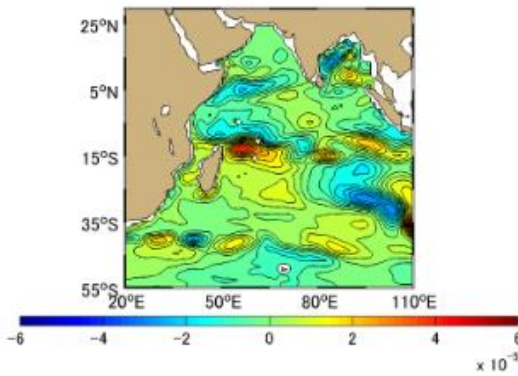
Figure A-6.3 Difference [PgC] between Approximation Method and Simulation Method Monthly Mean in 1993, the Indian Ocean based on January 1991. (a)-(l) represents January-December



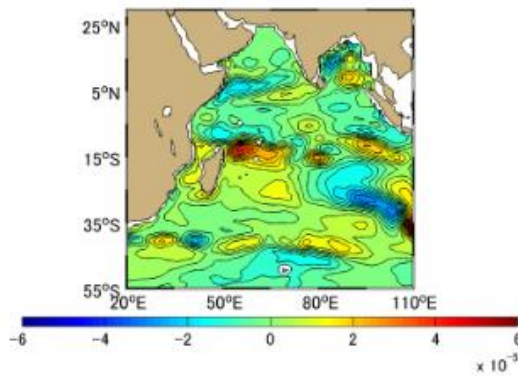
(a)



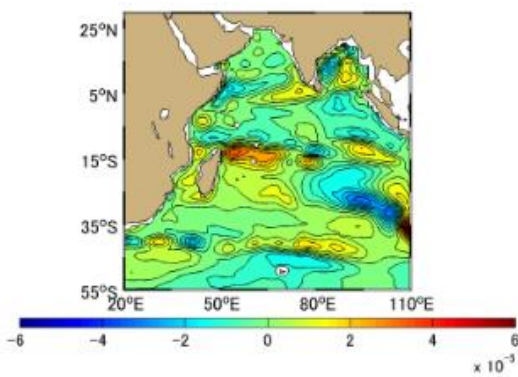
(b)



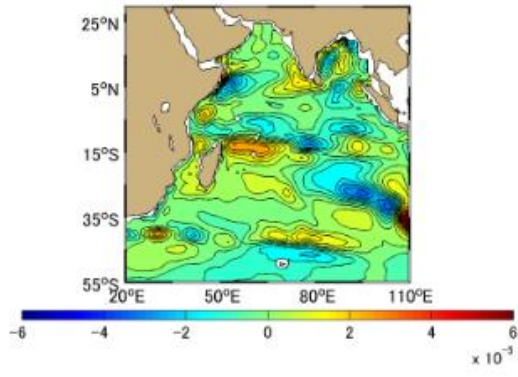
(c)



(d)



(e)



(f)

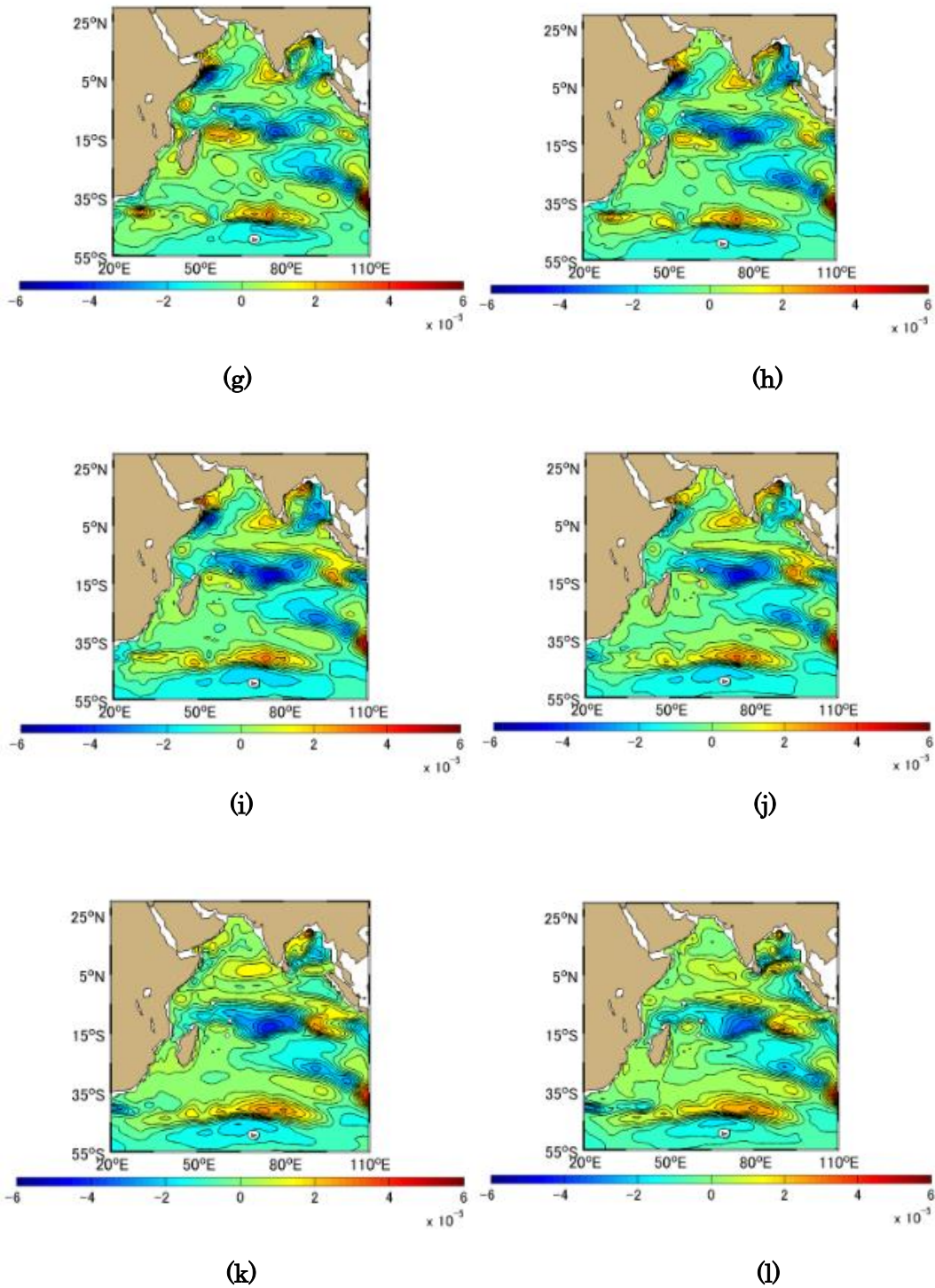
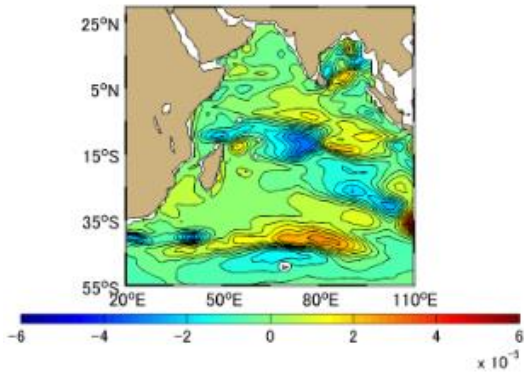
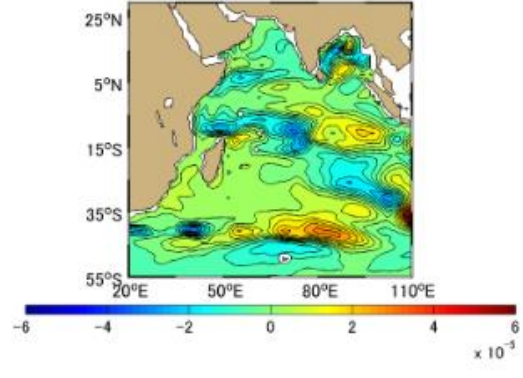


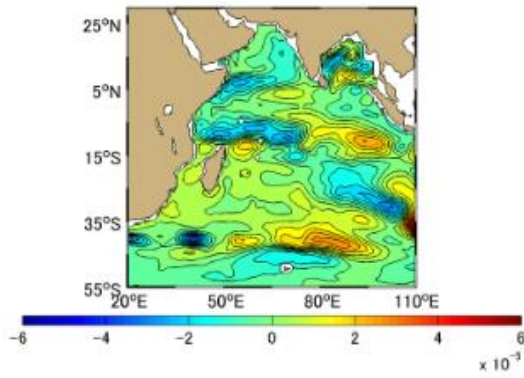
Figure A-6.4 Difference [PgC] between Approximation Method and Simulation Method Monthly Mean in 1994, the Indian Ocean based on January 1991. (a)-(l) represents January-December



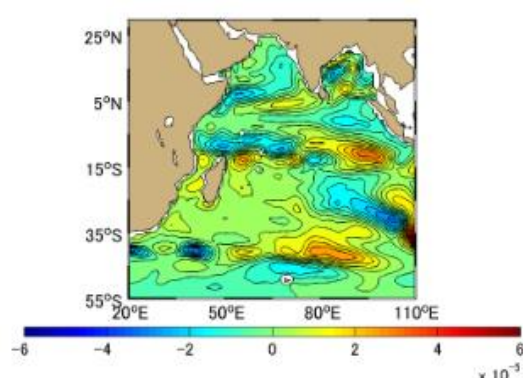
(a)



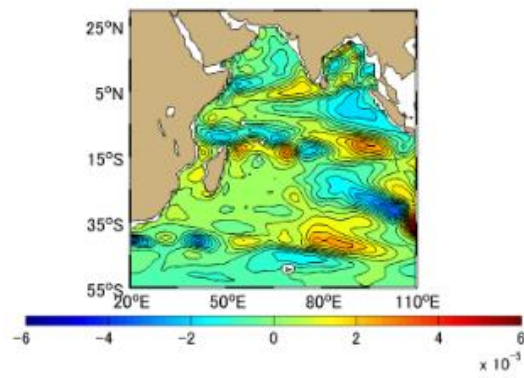
(b)



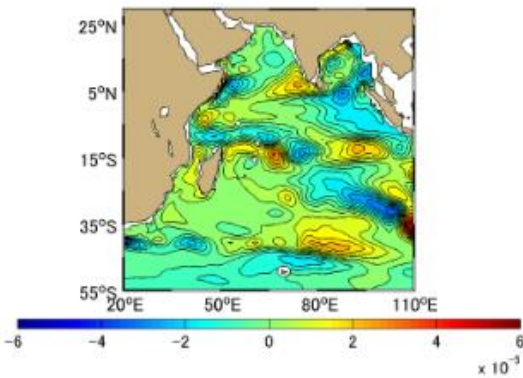
(c)



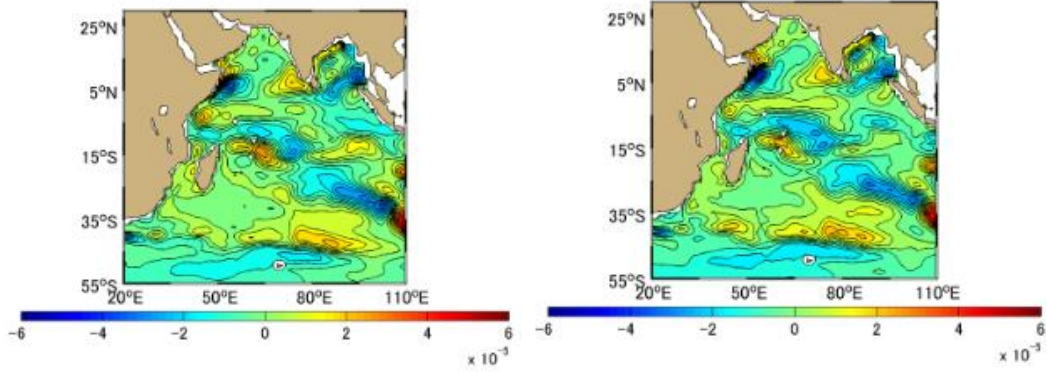
(d)



(e)

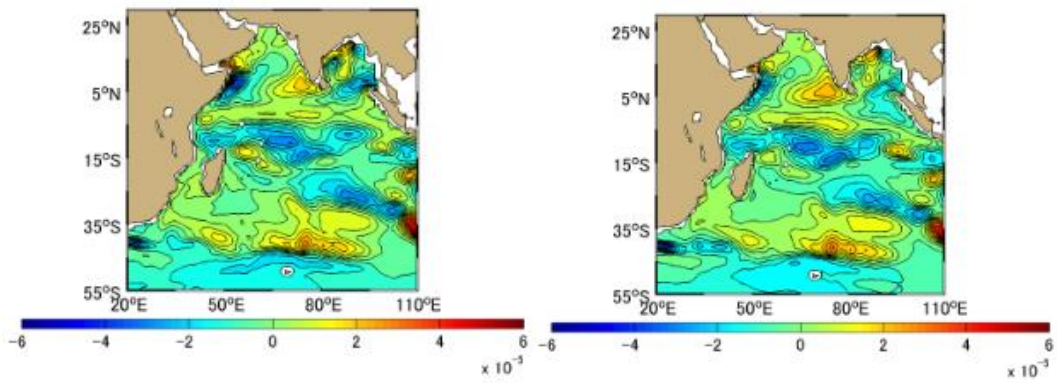


(f)



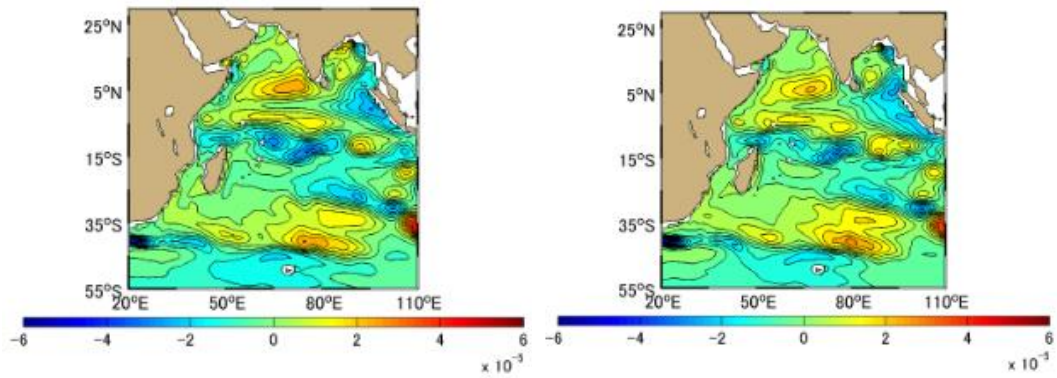
(g)

(h)



(i)

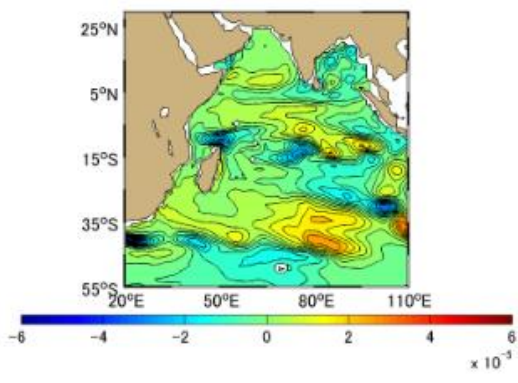
(j)



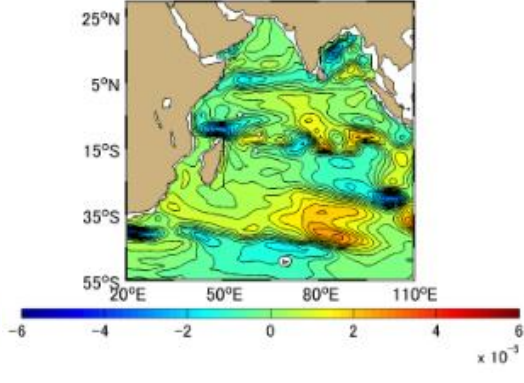
(k)

(l)

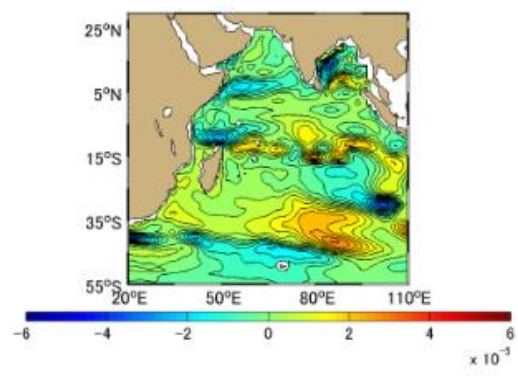
Figure A-6.5 Difference [PgC] between Approximation Method and Simulation Method Monthly Mean in 1995, the Indian Ocean based on January 1991. (a)-(l) represents January-December



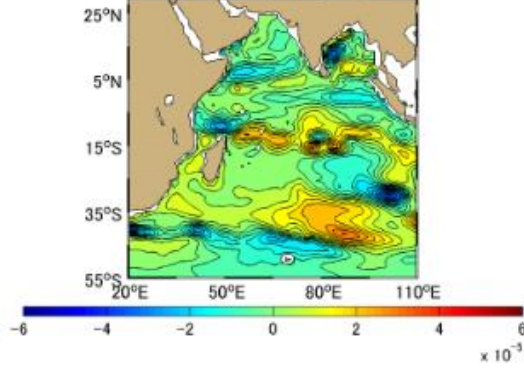
(a)



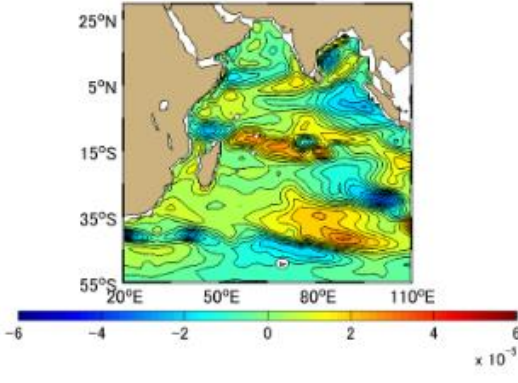
(b)



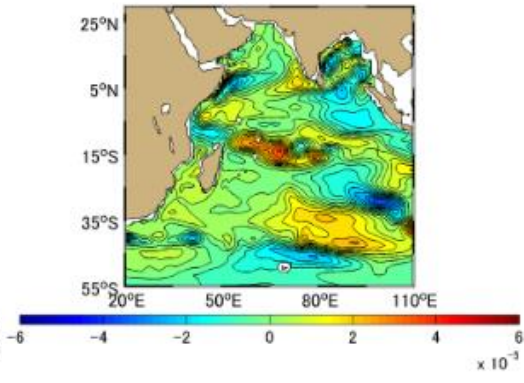
(c)



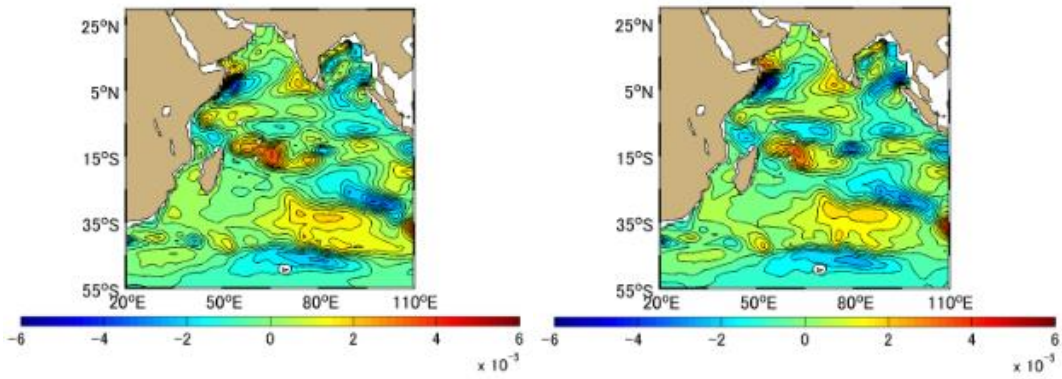
(d)



(e)

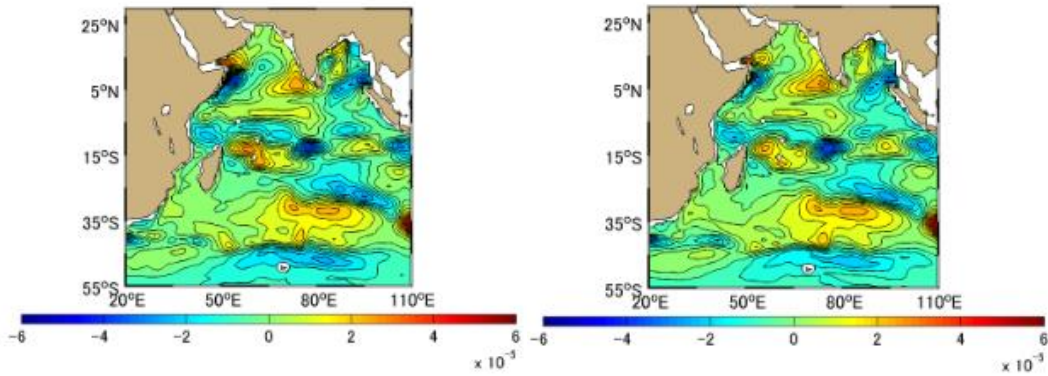


(f)



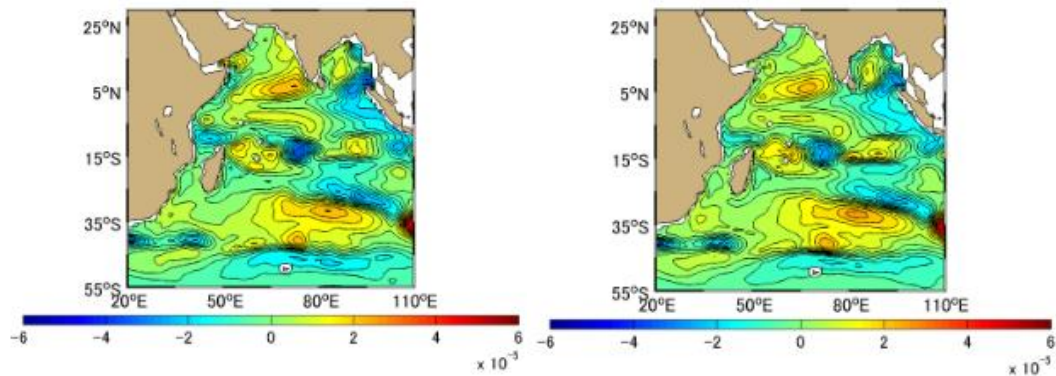
(g)

(h)



(i)

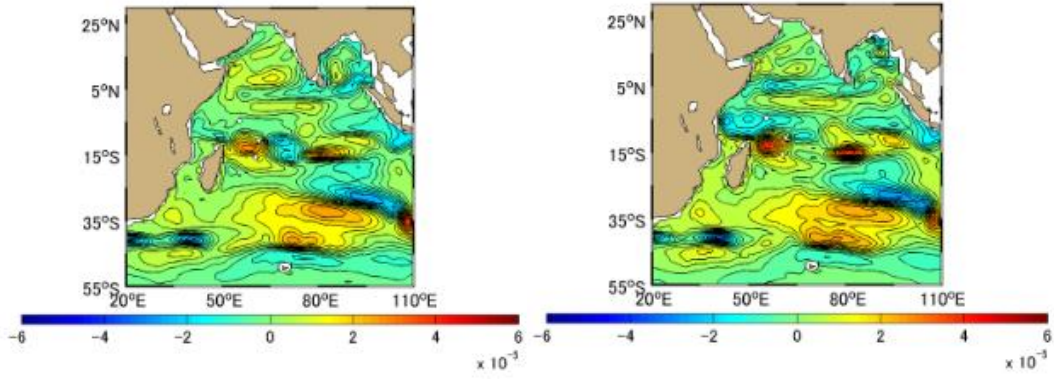
(j)



(k)

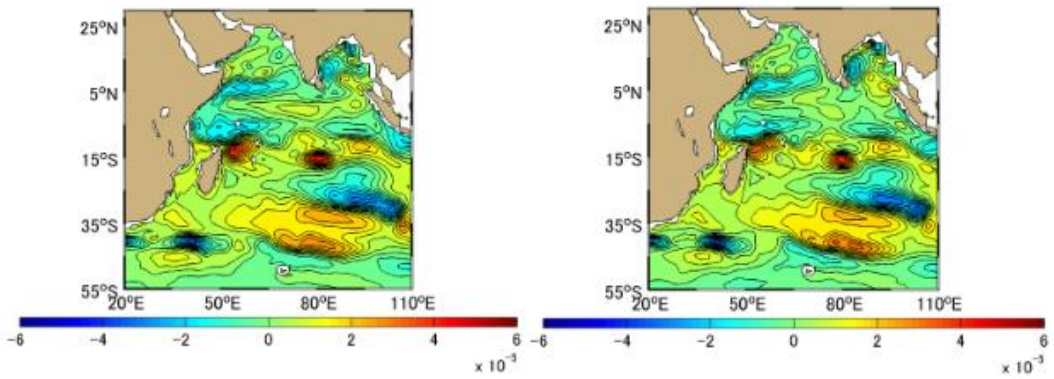
(l)

Figure A-6.6 Difference [PgC] between Approximation Method and Simulation Method Monthly Mean in 1996, the Indian Ocean based on January 1991. (a)-(l) represents January-December



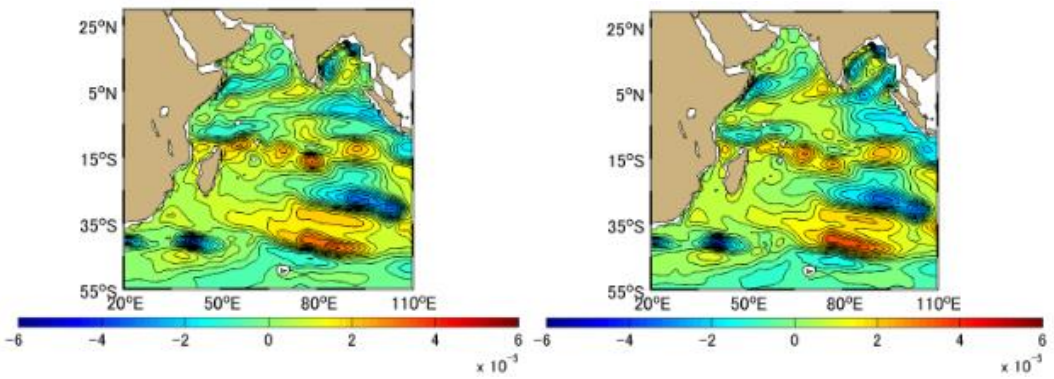
(a)

(b)



(c)

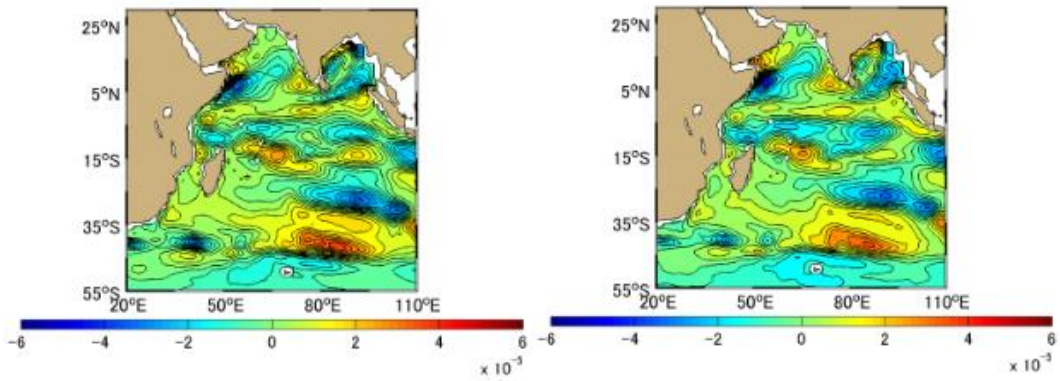
(d)



(e)

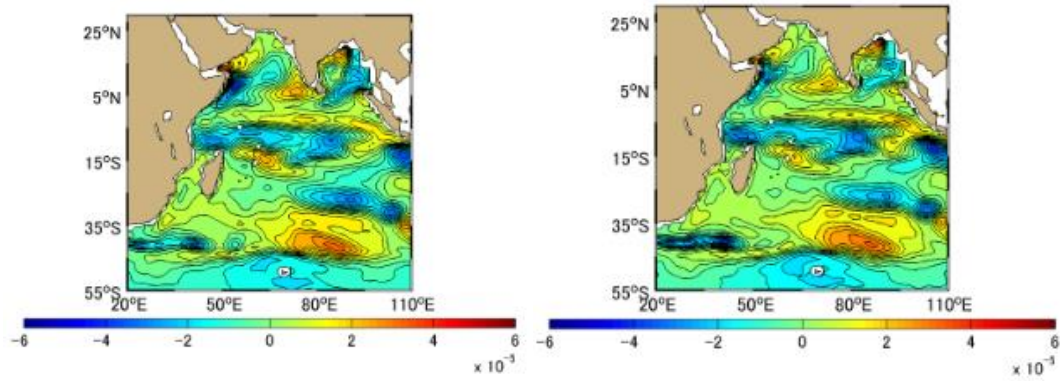
(f)





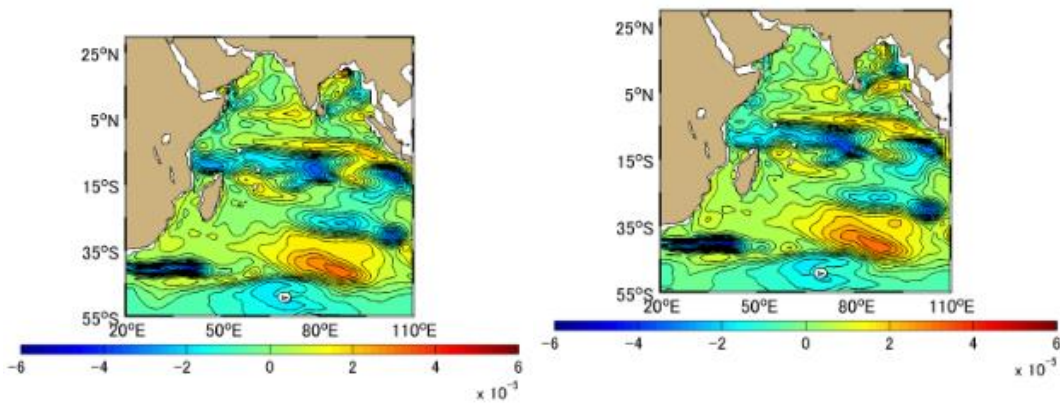
(g)

(h)



(i)

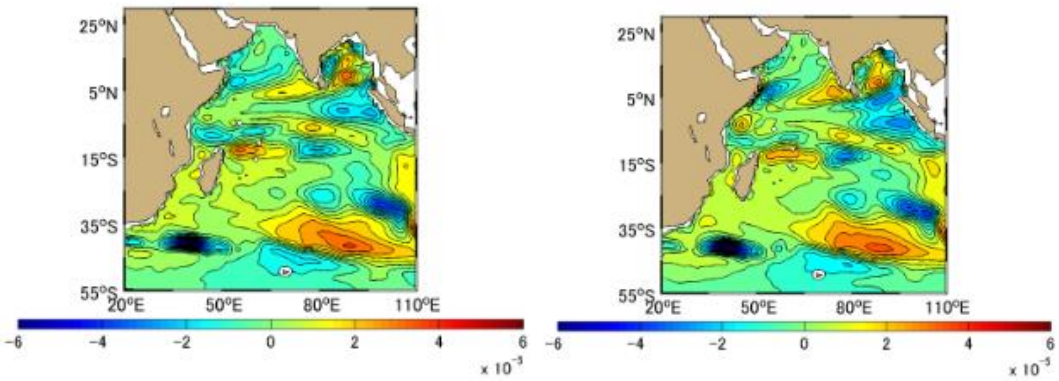
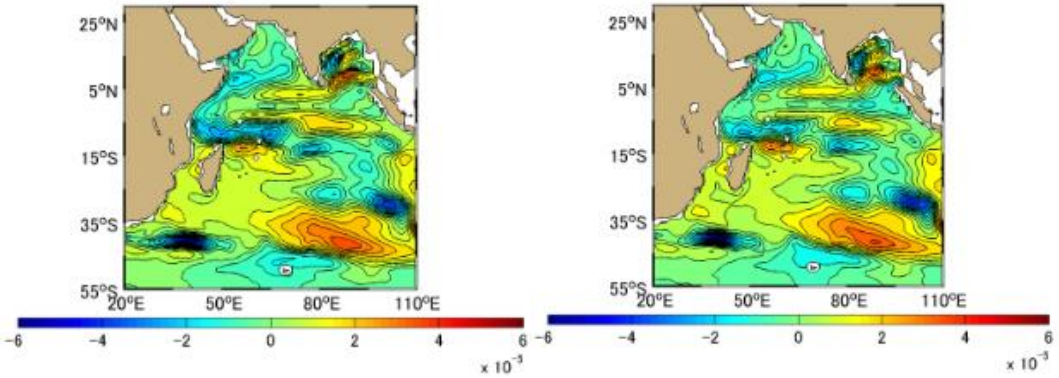
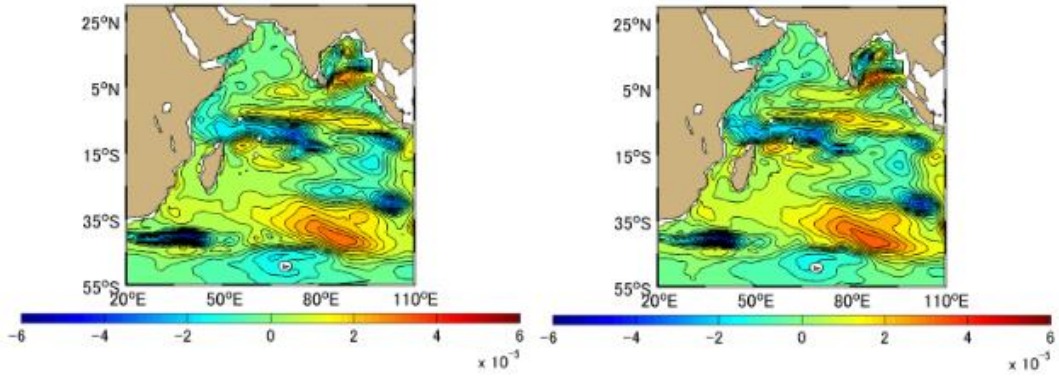
(j)

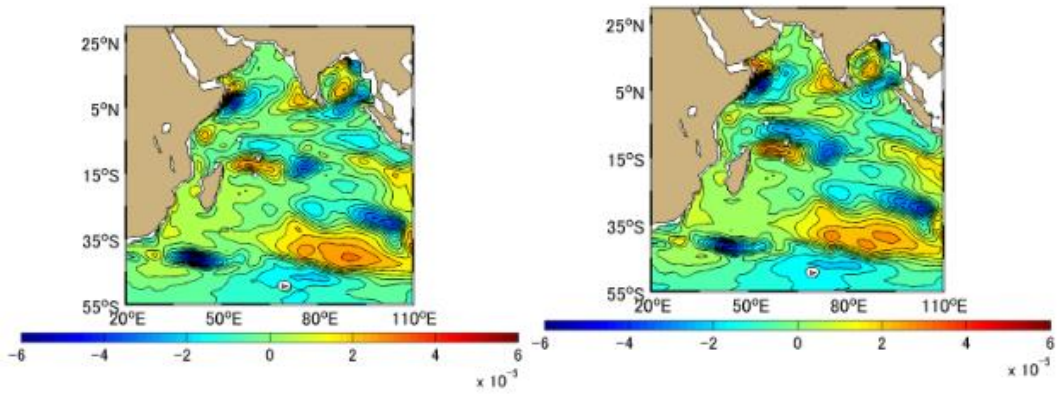


(k)

(l)

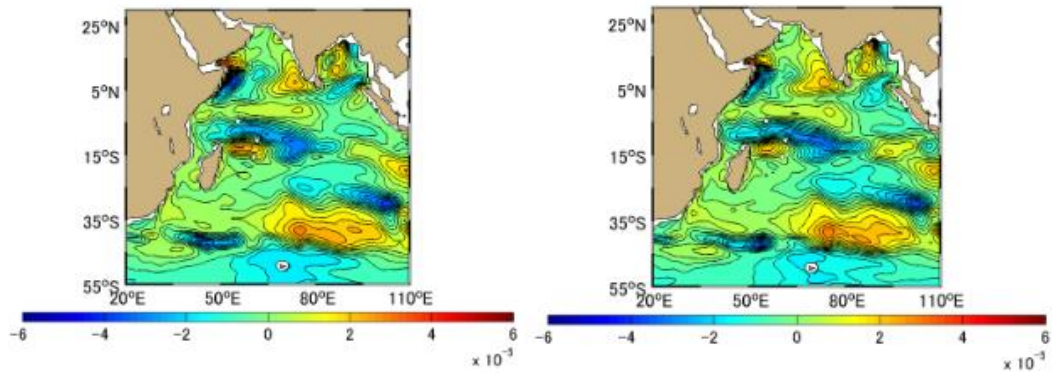
Figure A-6.7 Difference [PgC] between Approximation Method and Simulation Method Monthly Mean in 1997, the Indian Ocean based on January 1991. (a)-(l) represents January-December





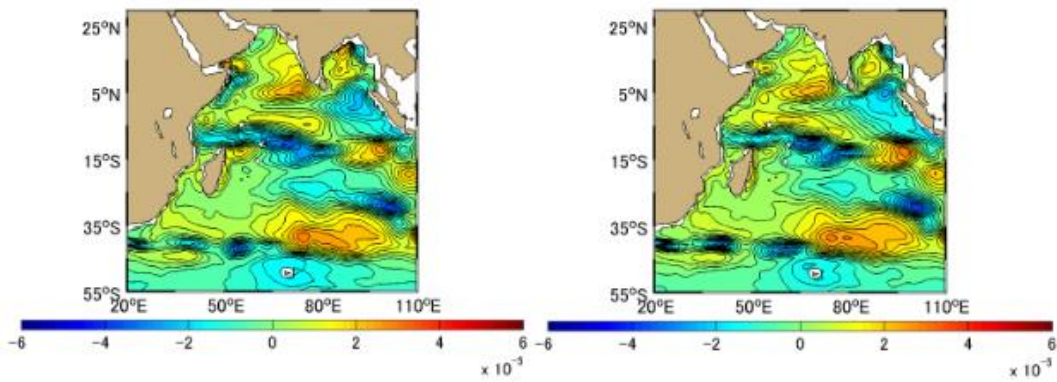
(g)

(h)



(i)

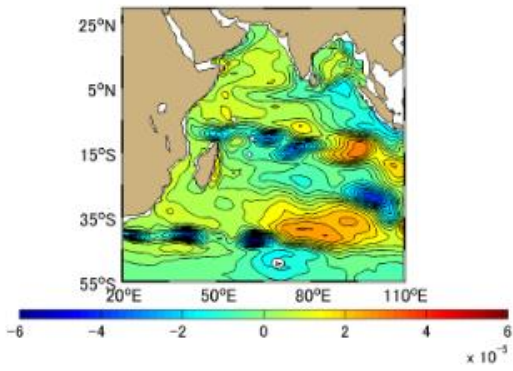
(j)



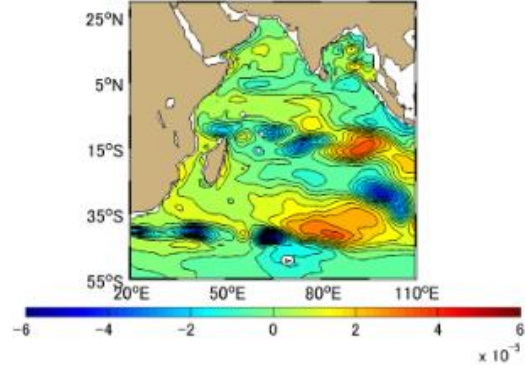
(k)

(l)

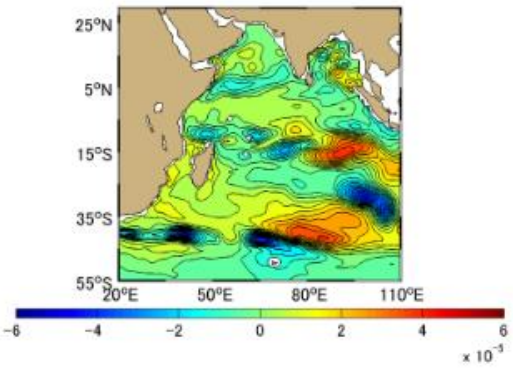
Figure A-6.8 Difference [PgC] between Approximation Method and Simulation Method Monthly Mean in 1998, the Indian Ocean based on January 1991. (a)-(l) represents January-December



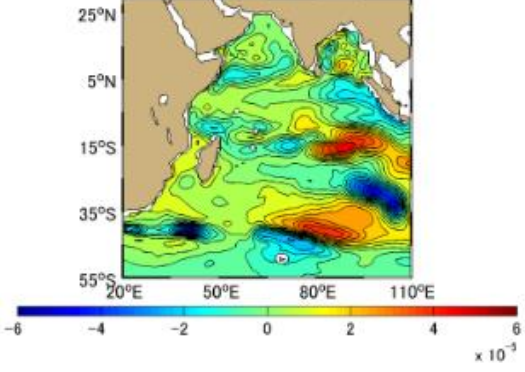
(a)



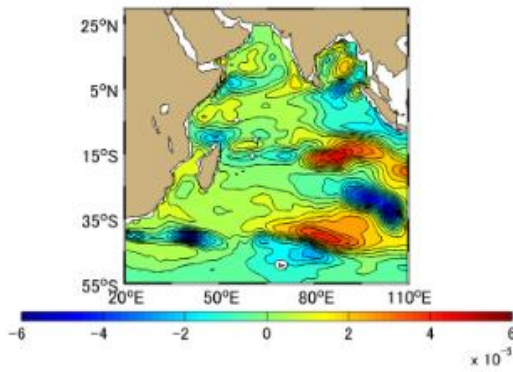
(b)



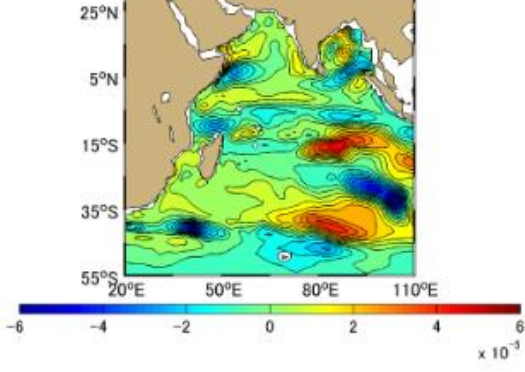
(c)



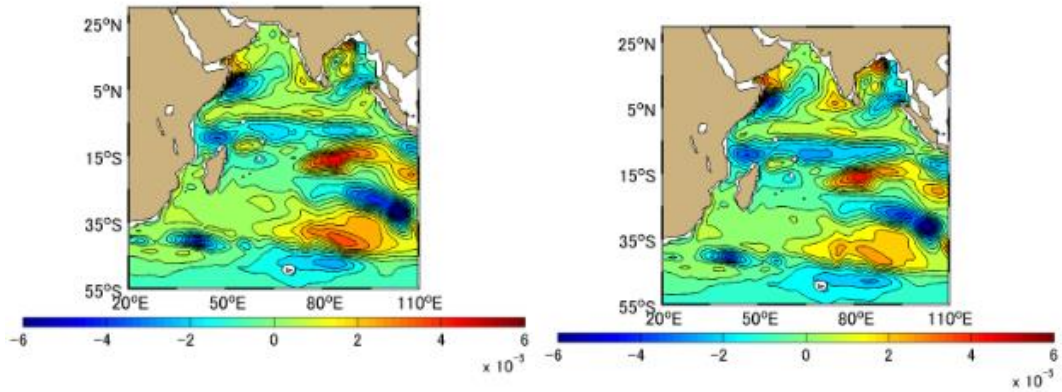
(d)



(e)

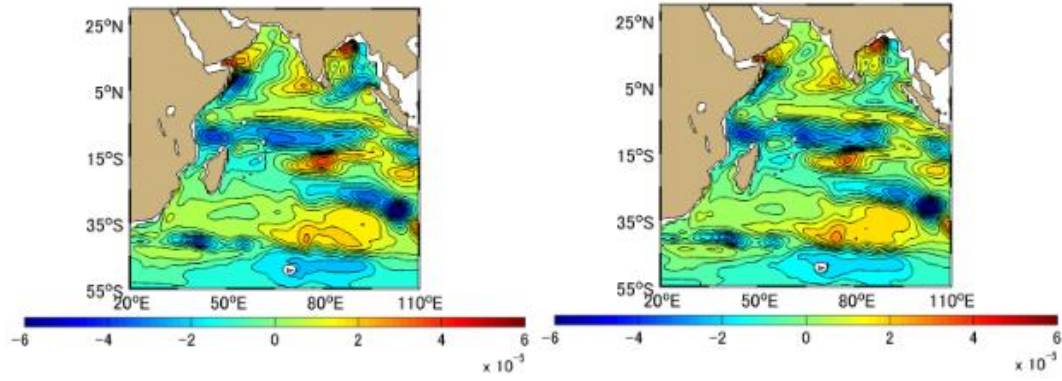


(f)



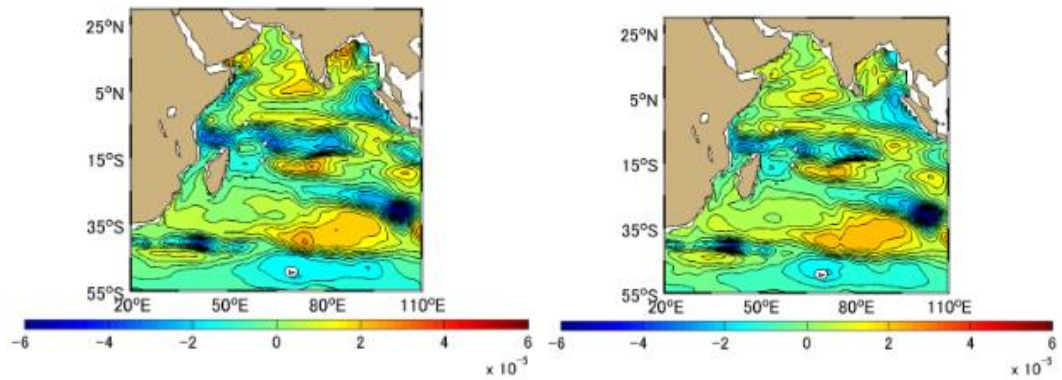
(g)

(h)



(i)

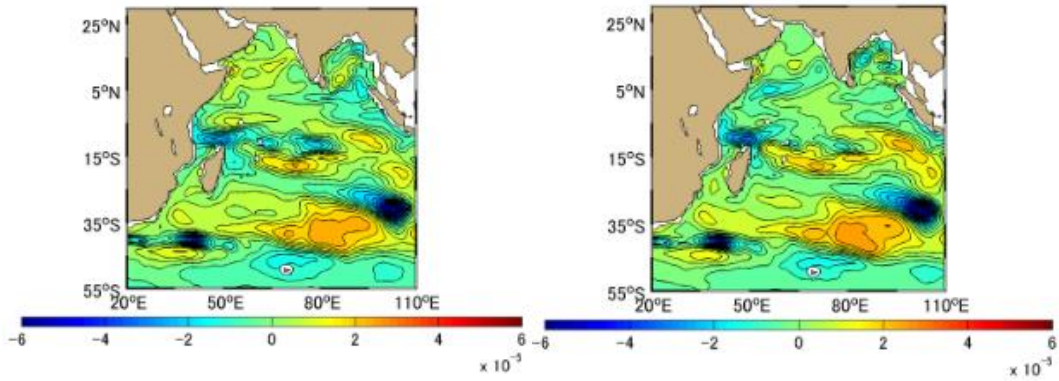
(j)



(k)

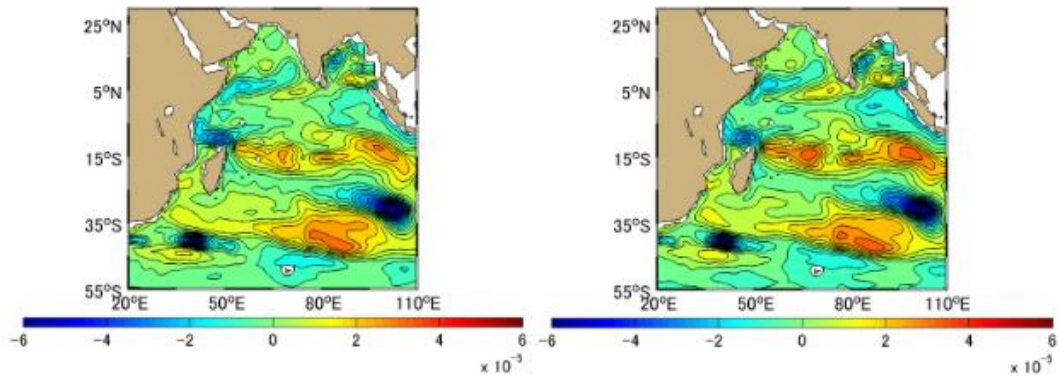
(l)

Figure A-6.9 Difference [PgC] between Approximation Method and Simulation Method Monthly Mean in 1999, the Indian Ocean based on January 1991. (a)-(l) represents January-December



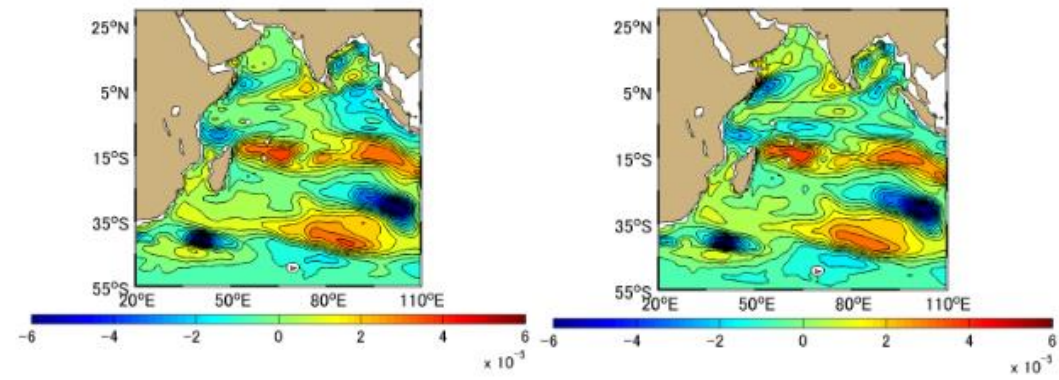
(a)

(b)



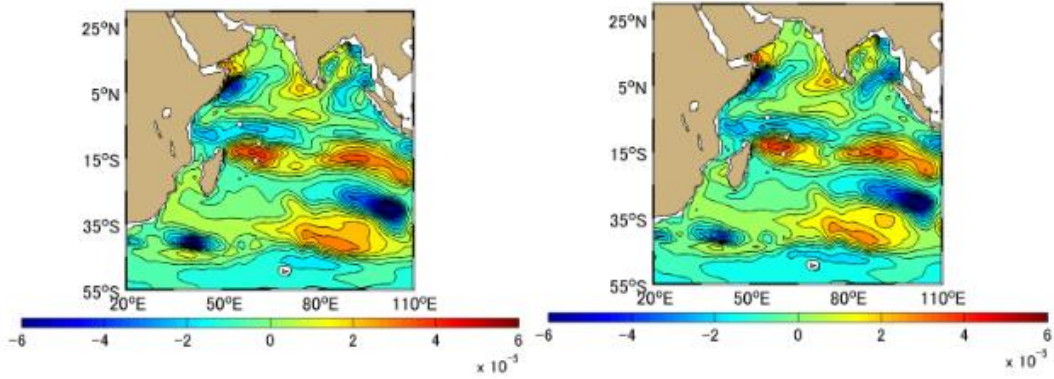
(c)

(d)



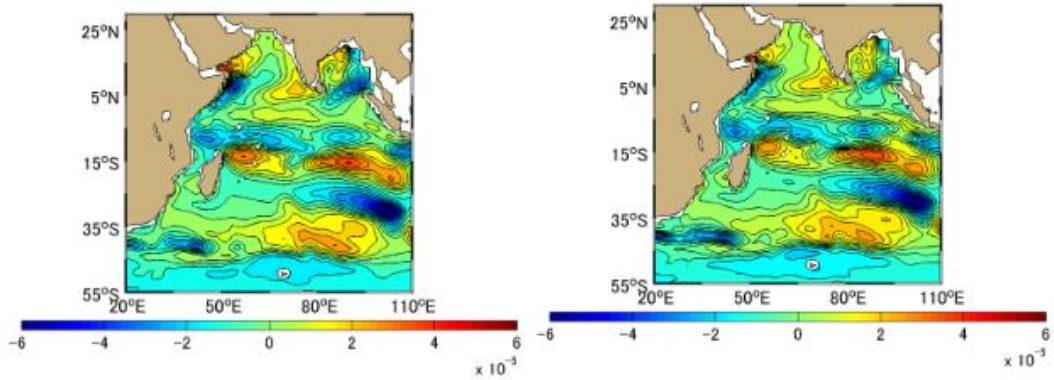
(e)

(f)



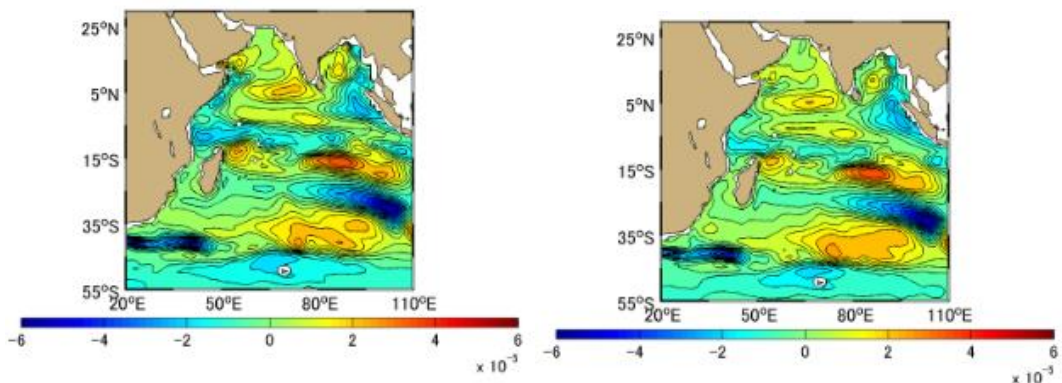
(g)

(h)



(i)

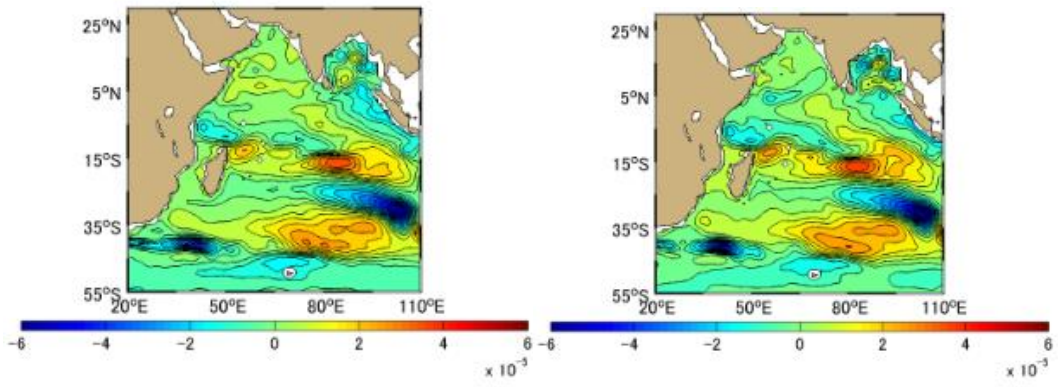
(j)



(k)

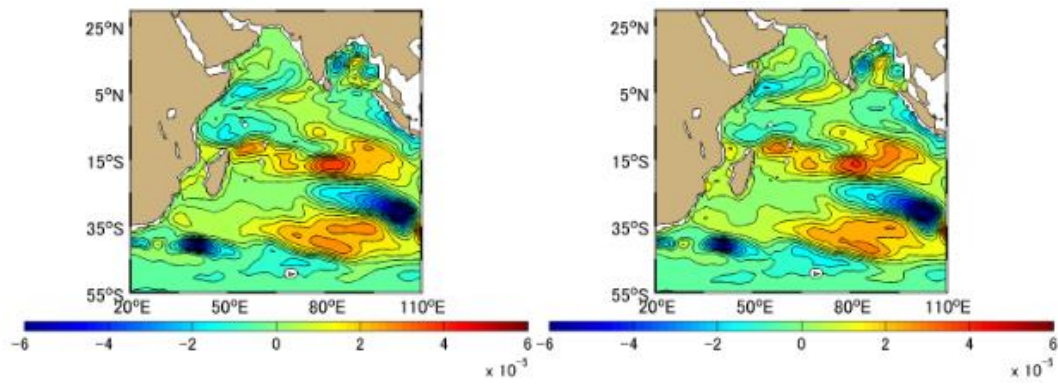
(l)

Figure A-6.10 Difference [PgC] between Approximation Method and Simulation Method Monthly Mean in 2000, the Indian Ocean based on January 1991. (a)-(l) represents January-December



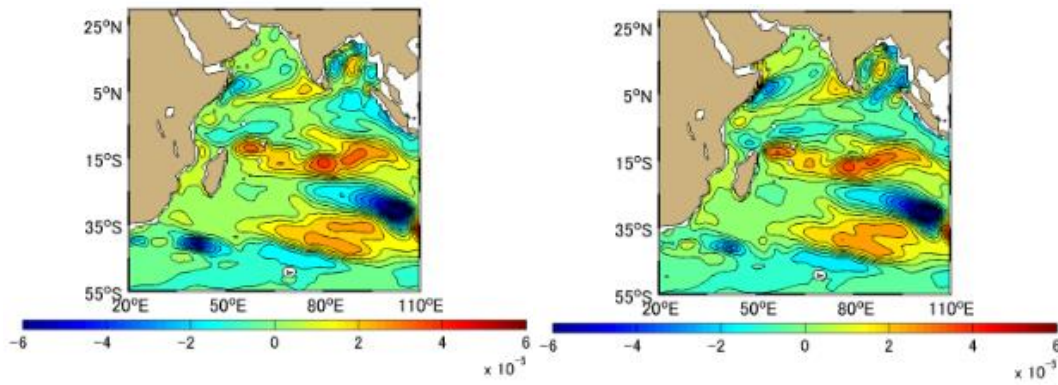
(a)

(b)



(c)

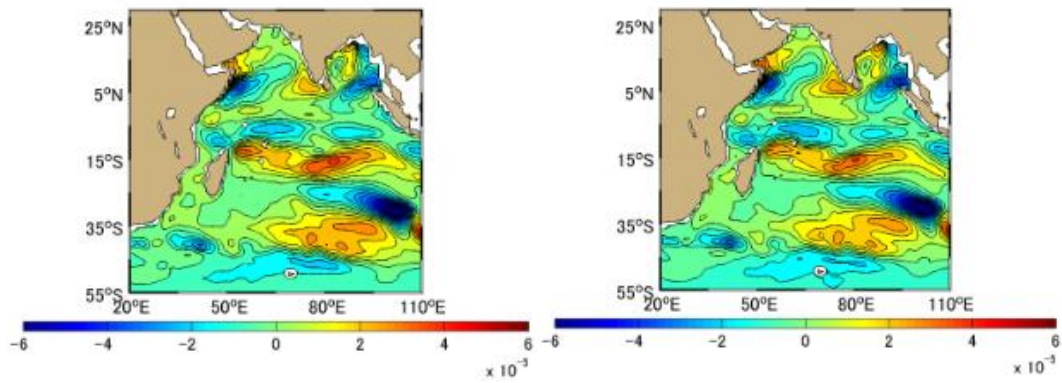
(d)



(e)

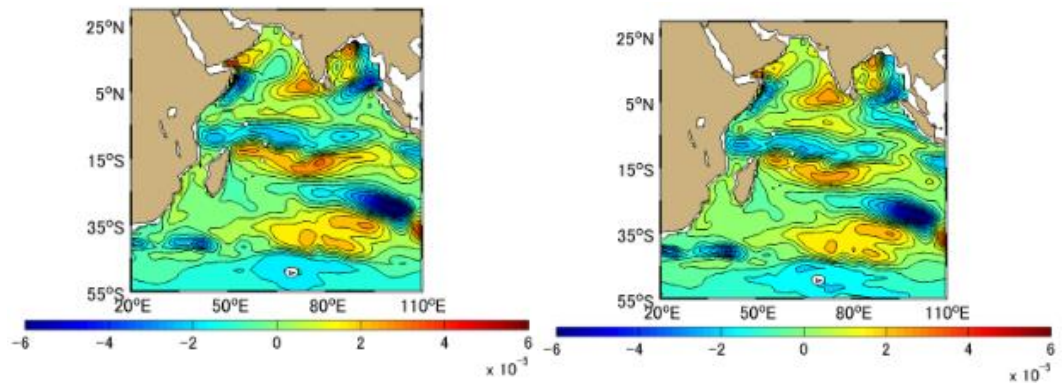
(f)





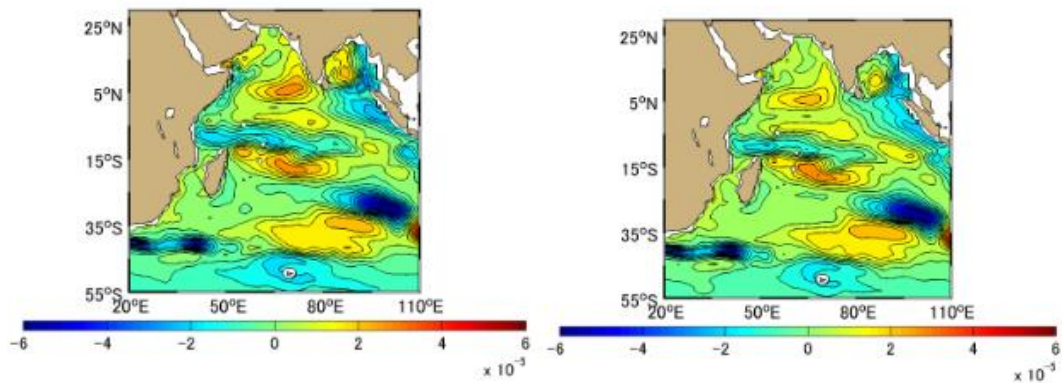
(g)

(h)



(i)

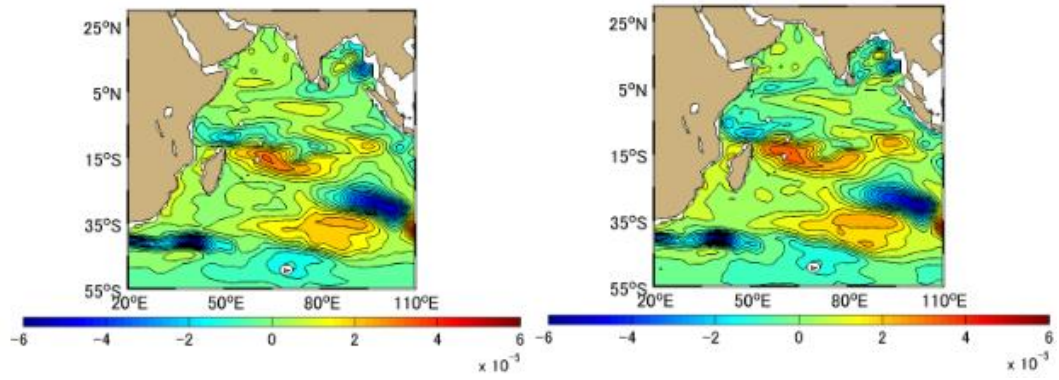
(j)



(k)

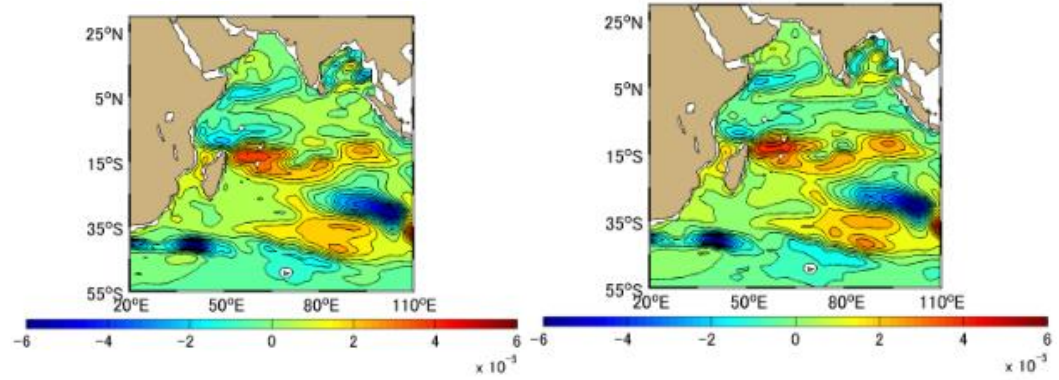
(l)

Figure A-6.11 Difference [PgC] between Approximation Method and Simulation Method Monthly Mean in 2001, the Indian Ocean based on January 1991. (a)-(l) represents January-December



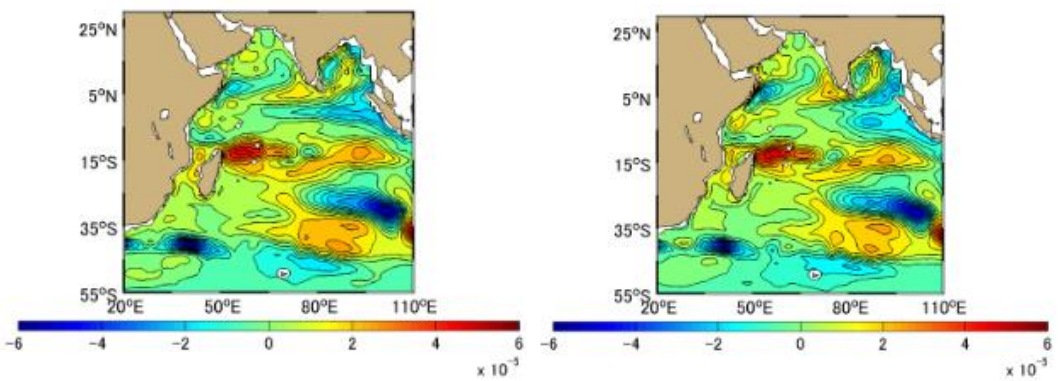
(a)

(b)



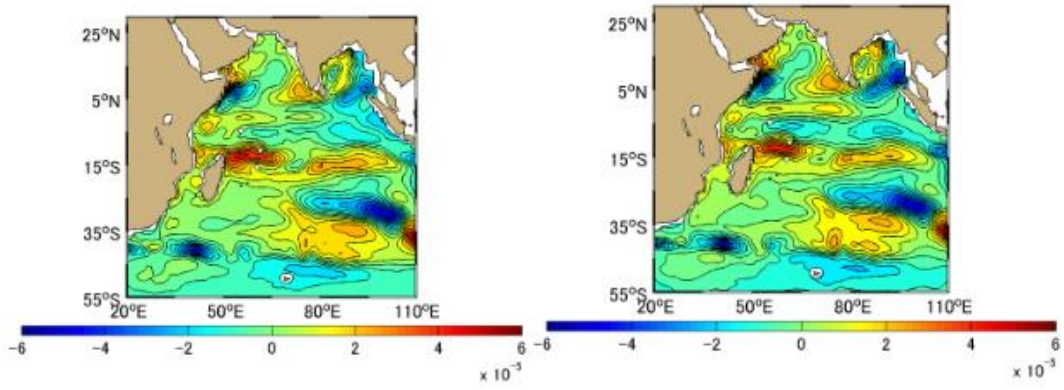
(c)

(d)



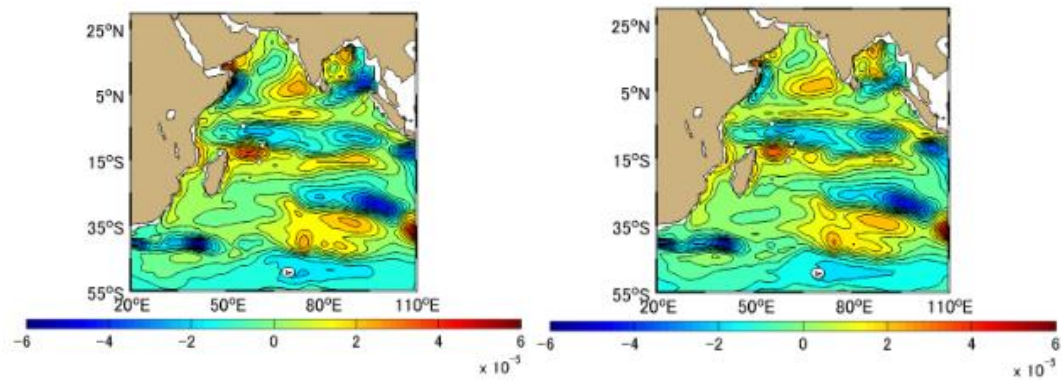
(e)

(f)



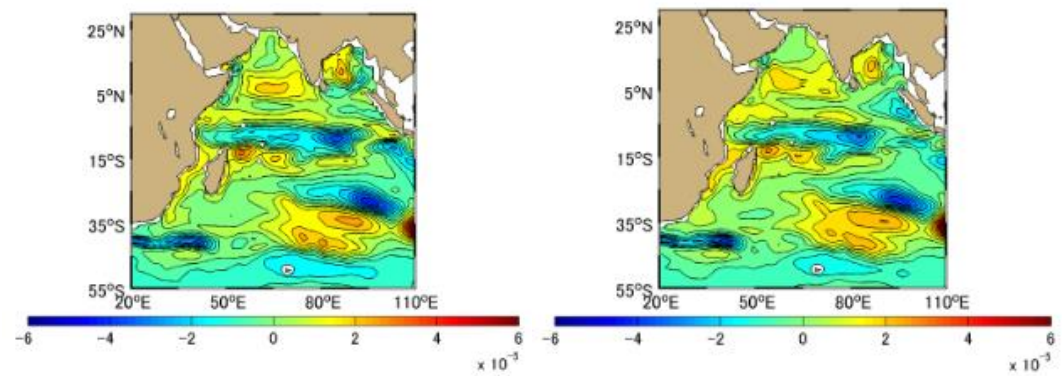
(g)

(h)



(i)

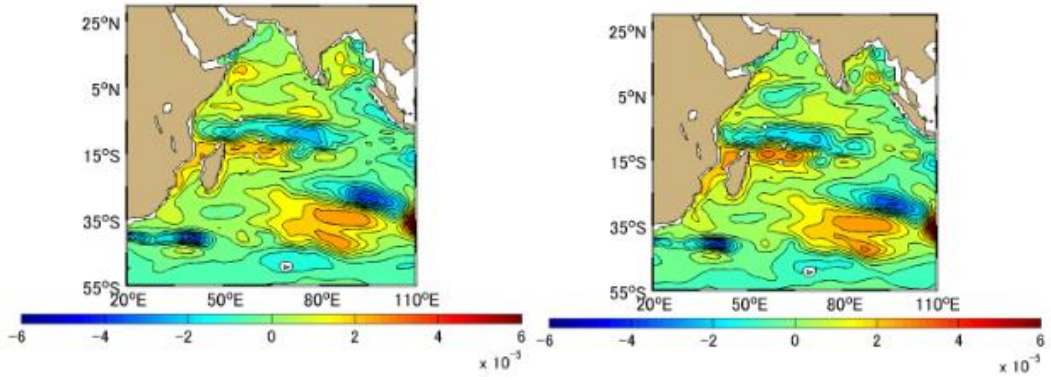
(j)



(k)

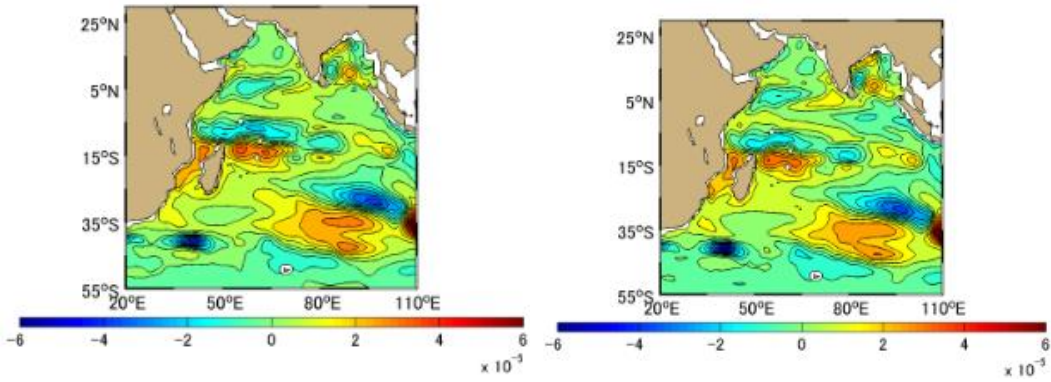
(l)

Figure A-6.12 Difference [PgC] between Approximation Method and Simulation Method Monthly Mean in 2002, the Indian Ocean based on January 1991. (a)-(l) represents January-December



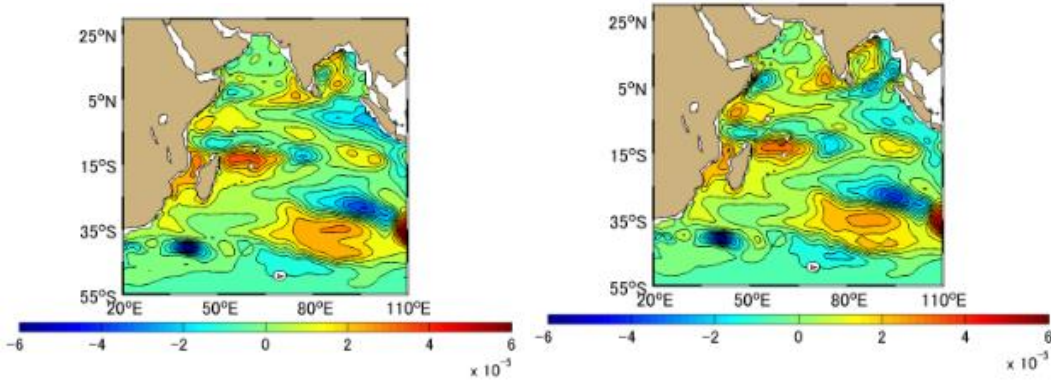
(a)

(b)



(c)

(d)



(e)

(f)

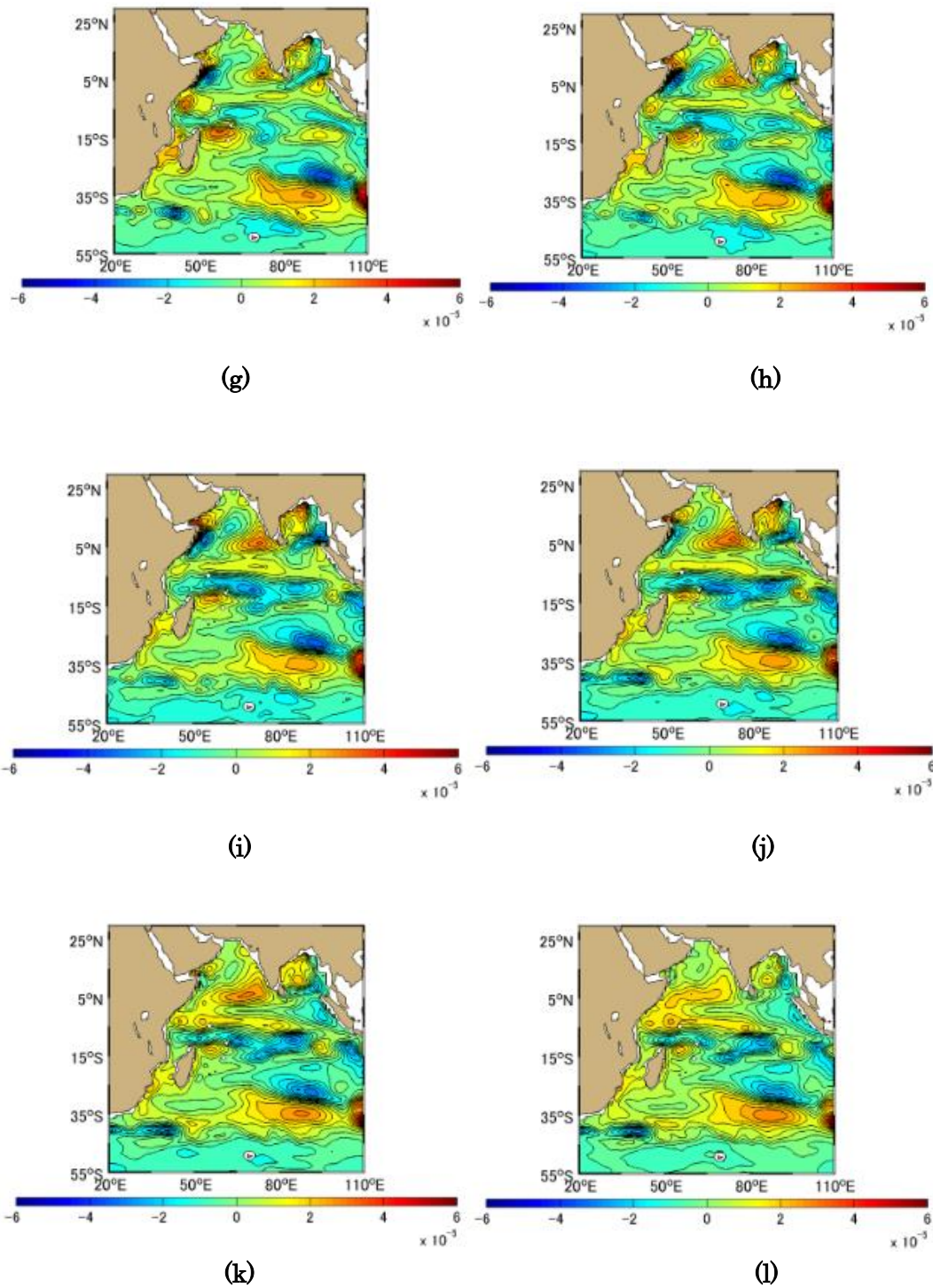
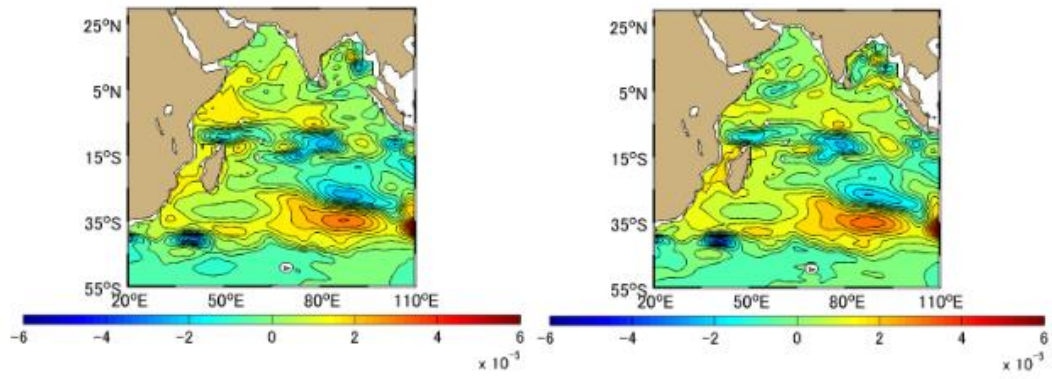
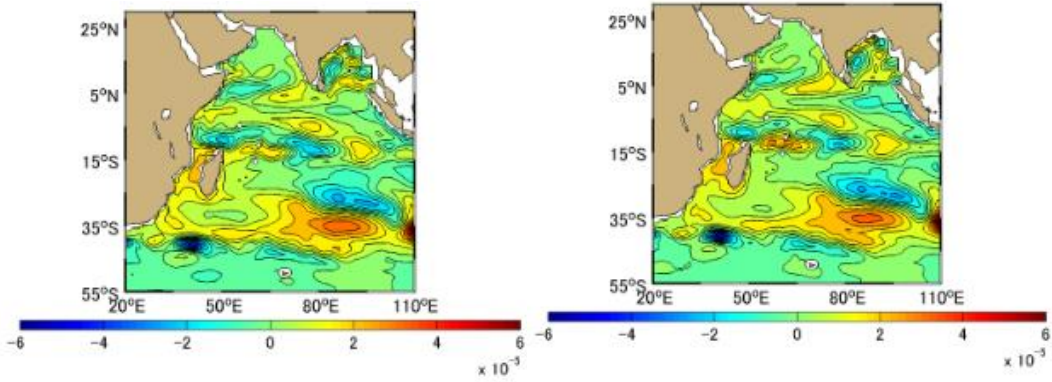


Figure A-6.13 Difference [PgC] between Approximation Method and Simulation Method Monthly Mean in 2003, the Indian Ocean based on January 1991. (a)-(l) represents January-December



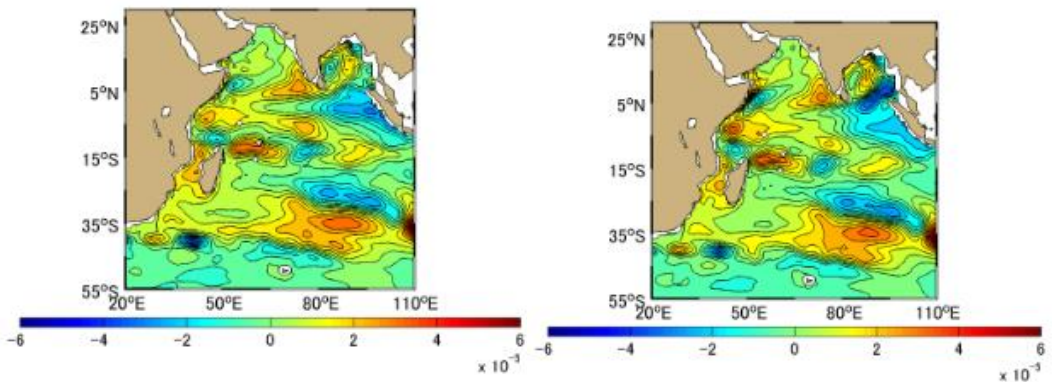
(a)

(b)



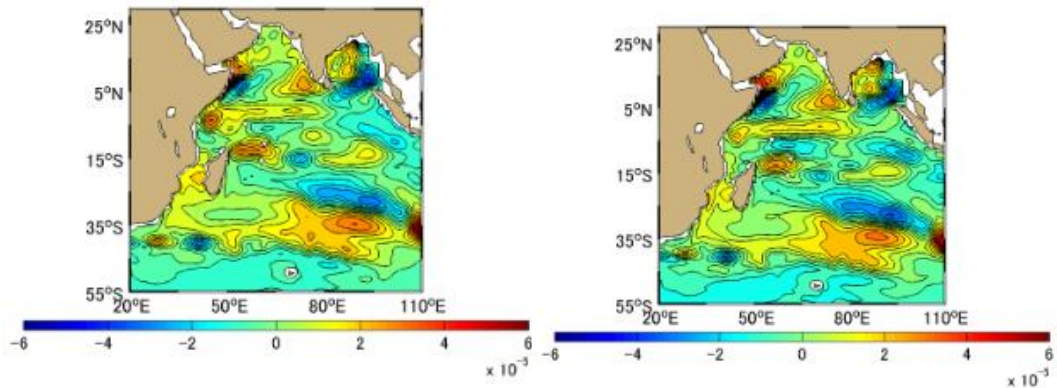
(c)

(d)



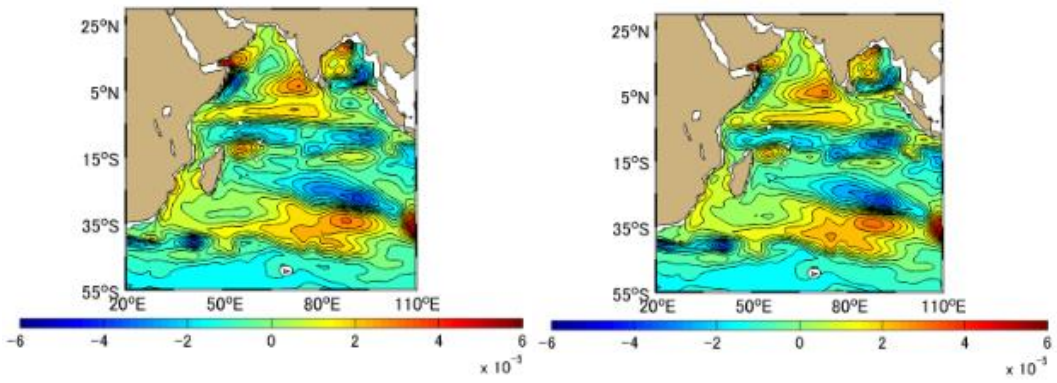
(e)

(f)



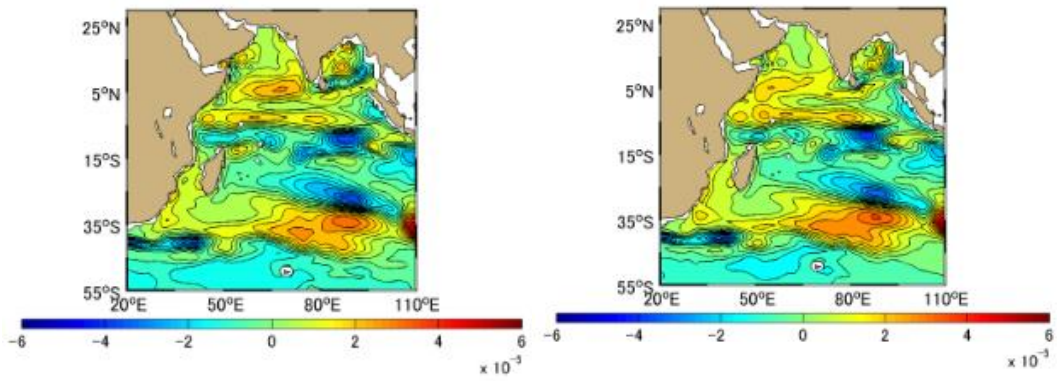
(g)

(h)



(i)

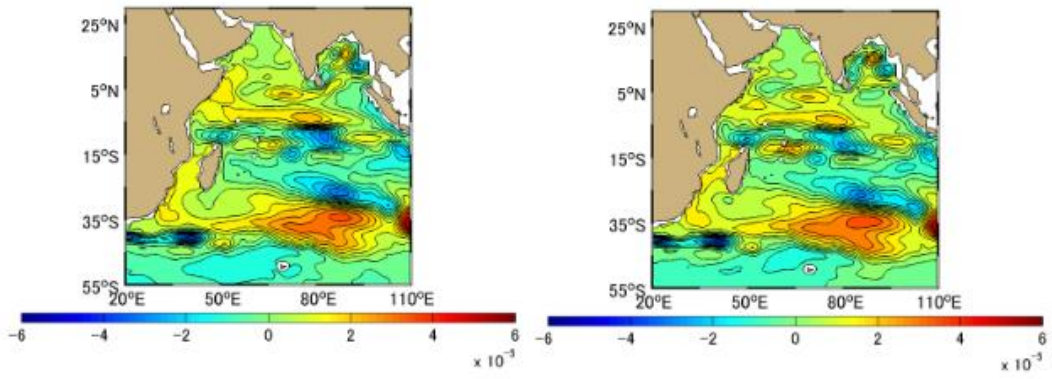
(j)



(k)

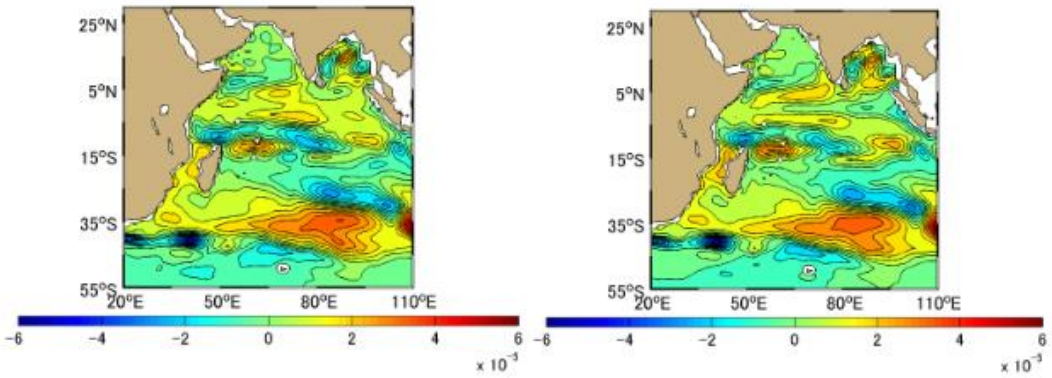
(l)

Figure A-6.14 Difference [PgC] between Approximation Method and Simulation Method Monthly Mean in 2004, the Indian Ocean based on January 1991. (a)-(l) represents January-December



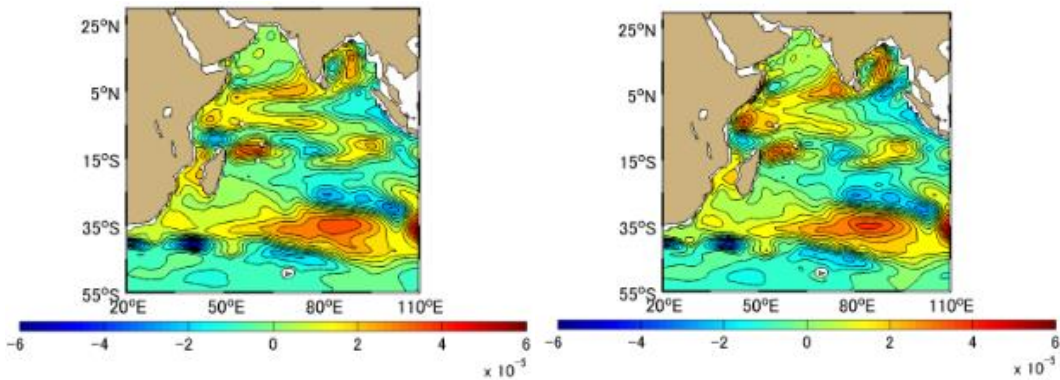
(a)

(b)



(c)

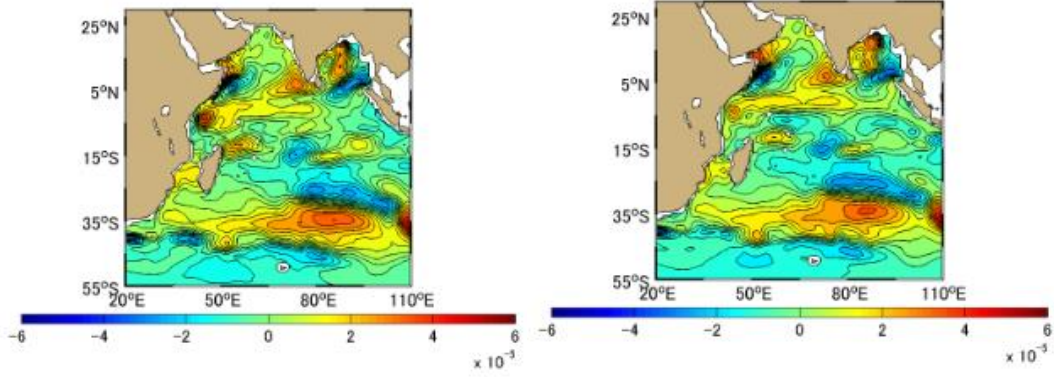
(d)



(e)

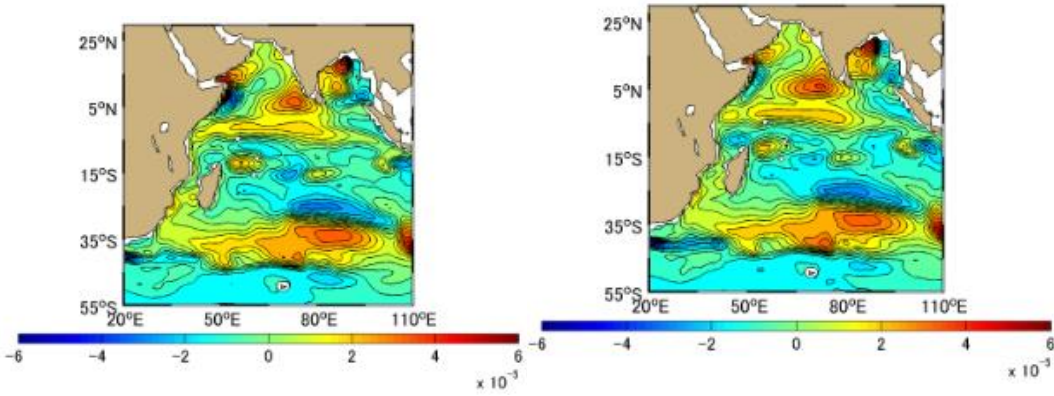
(f)





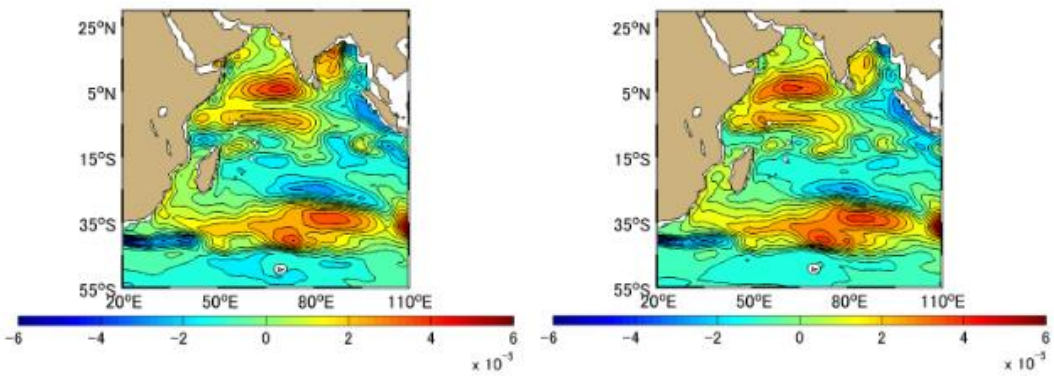
(g)

(h)



(i)

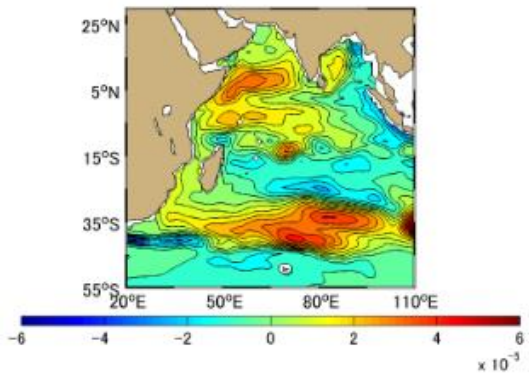
(j)



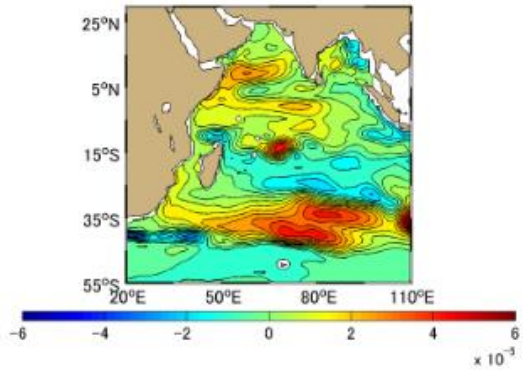
(k)

(l)

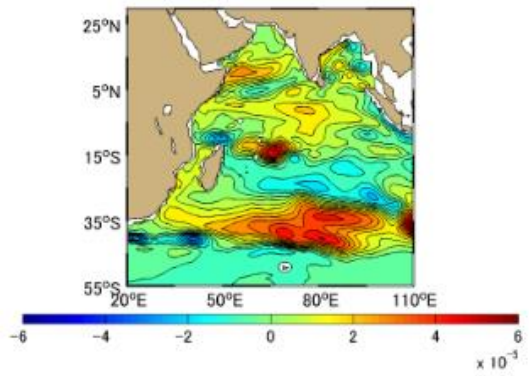
Figure A-6.15 Difference [PgC] between Approximation Method and Simulation Method Monthly Mean in 2005, the Indian Ocean based on January 1991. (a)-(l) represents January-December



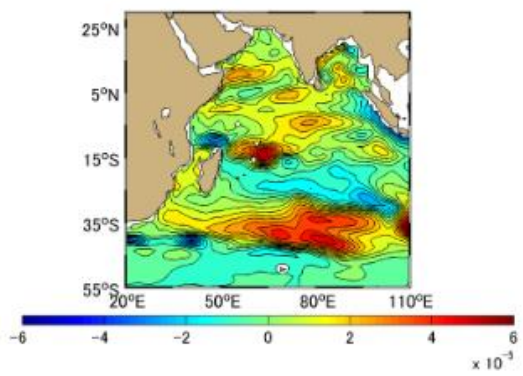
(a)



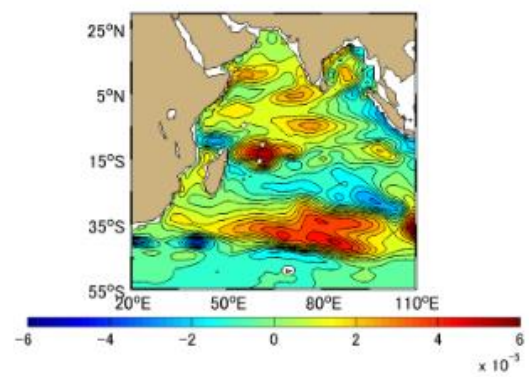
(b)



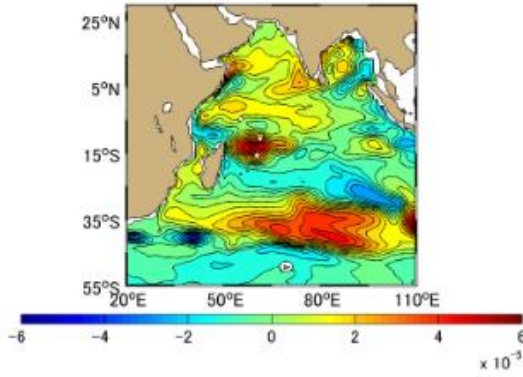
(c)



(d)



(e)



(f)

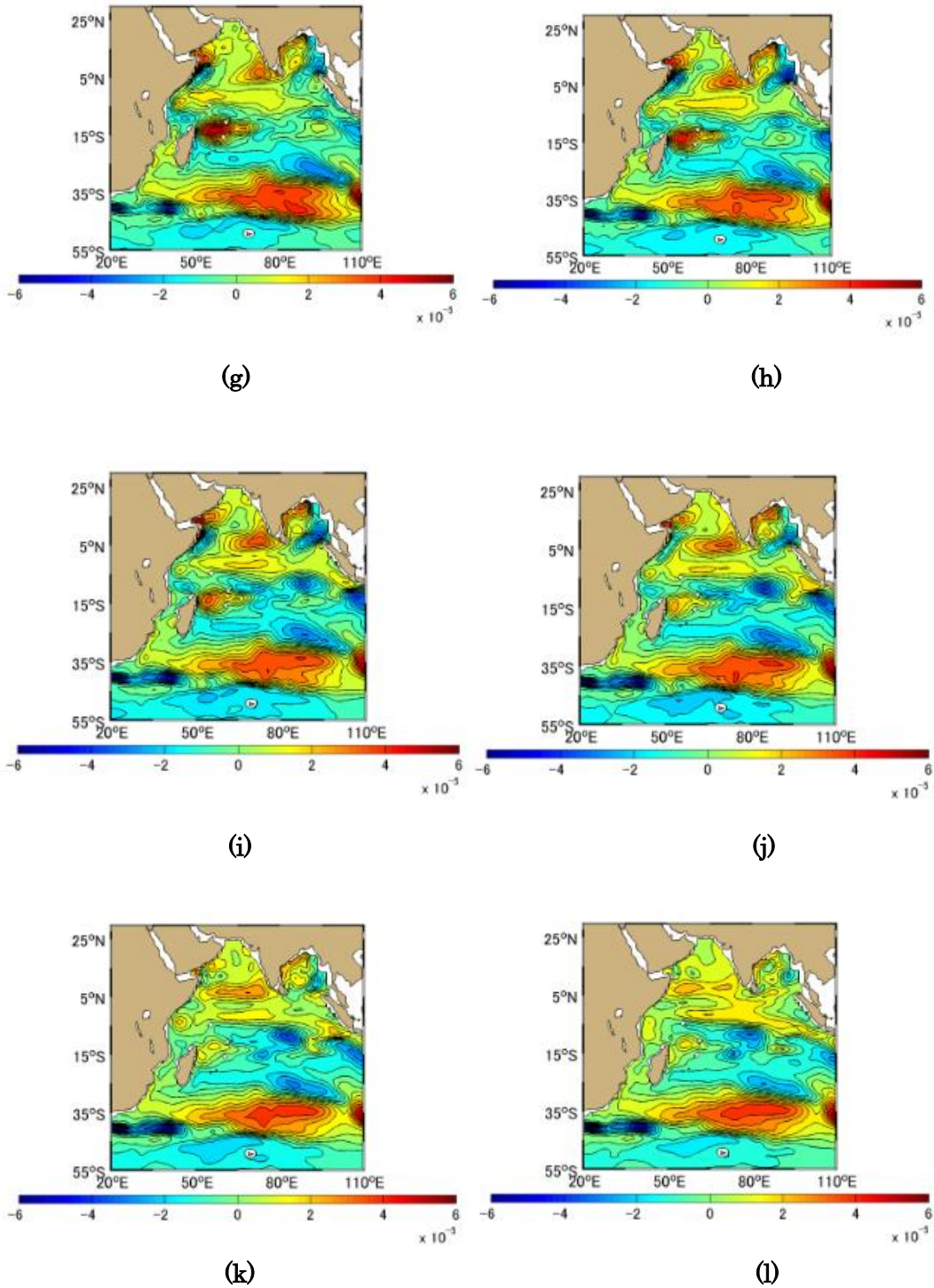
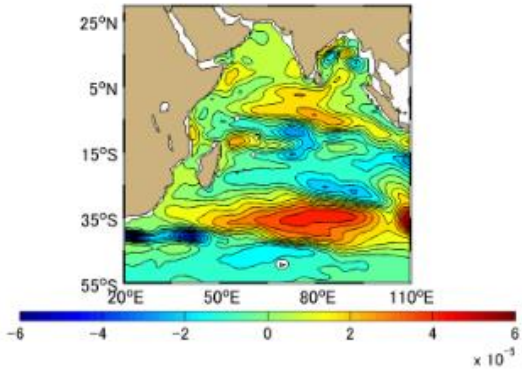
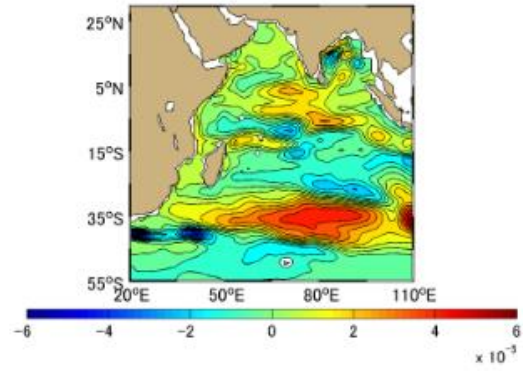


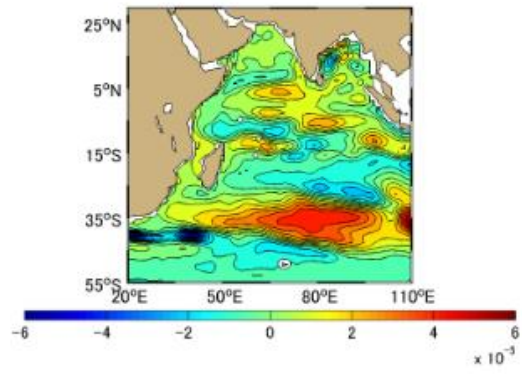
Figure A-6.16 Difference [PgC] between Approximation Method and Simulation Method Monthly Mean in 2006, the Indian Ocean based on January 1991. (a)-(l) represents January-December



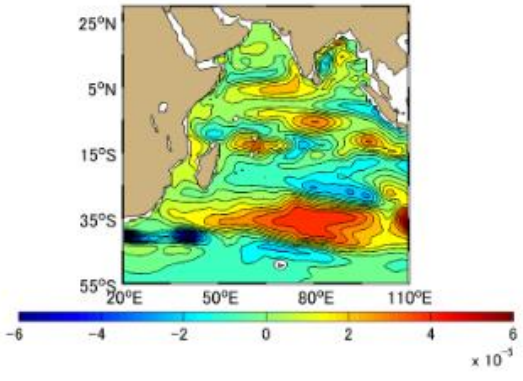
(a)



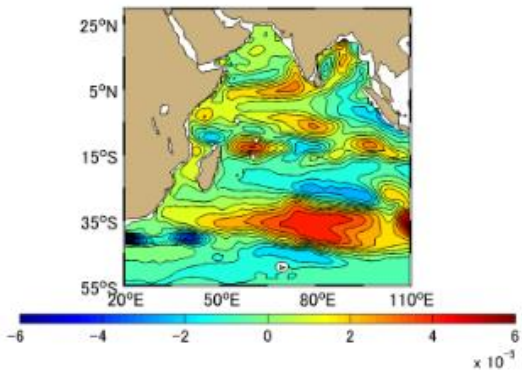
(b)



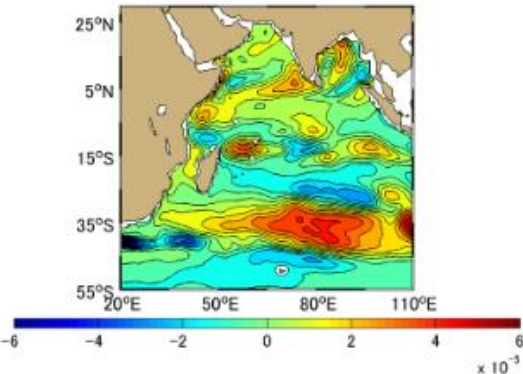
(c)



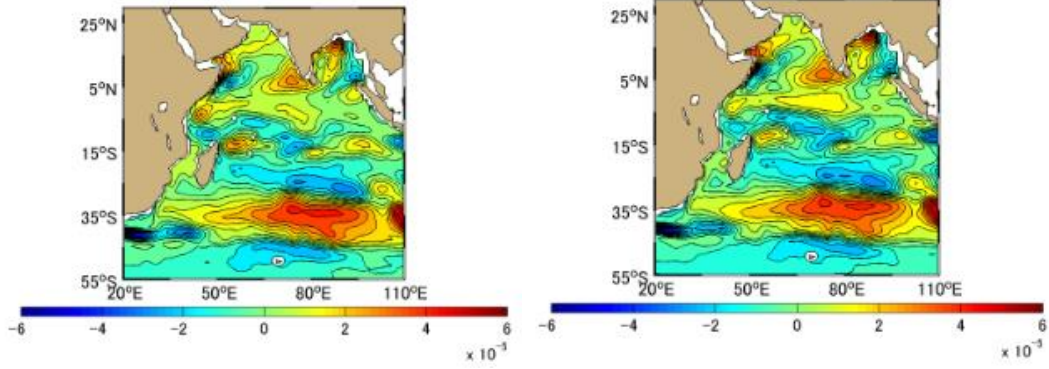
(d)



(e)

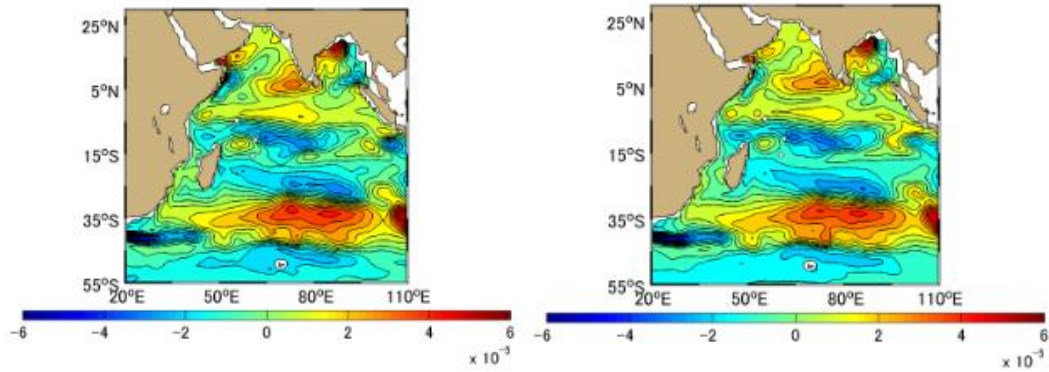


(f)



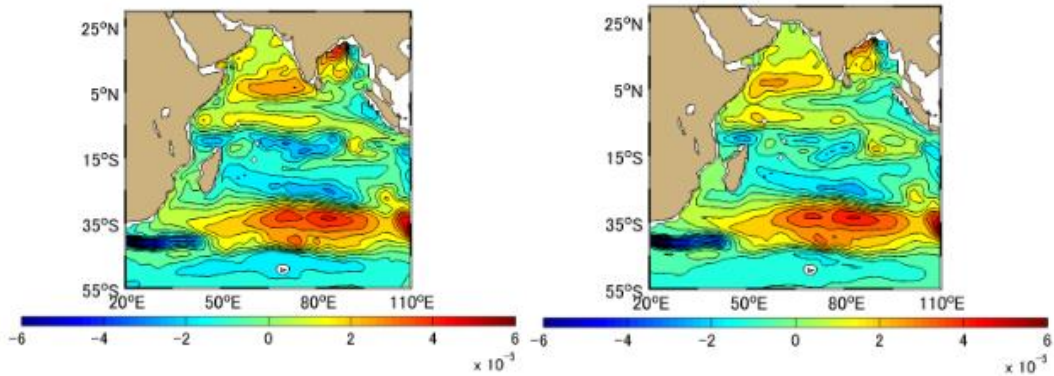
(g)

(h)



(i)

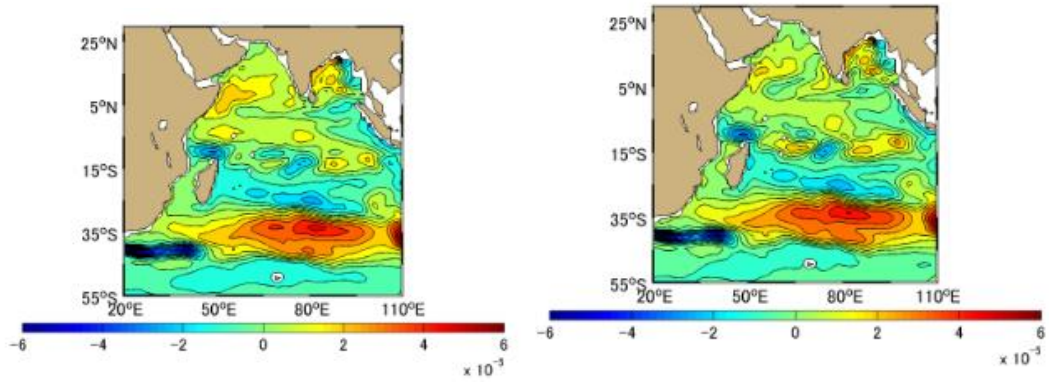
(j)



(k)

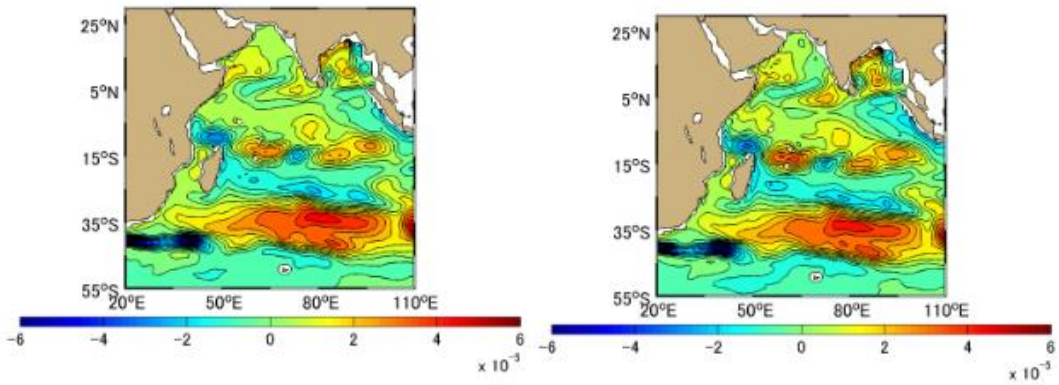
(l)

Figure A-6.17 Difference [PgC] between Approximation Method and Simulation Method Monthly Mean in 2007, the Indian Ocean based on January 1991. (a)-(l) represents January-December



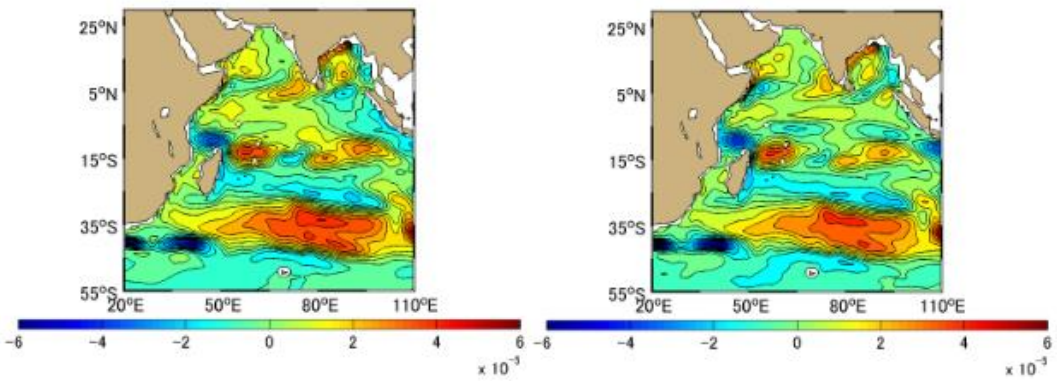
(a)

(b)



(c)

(d)



(e)

(f)

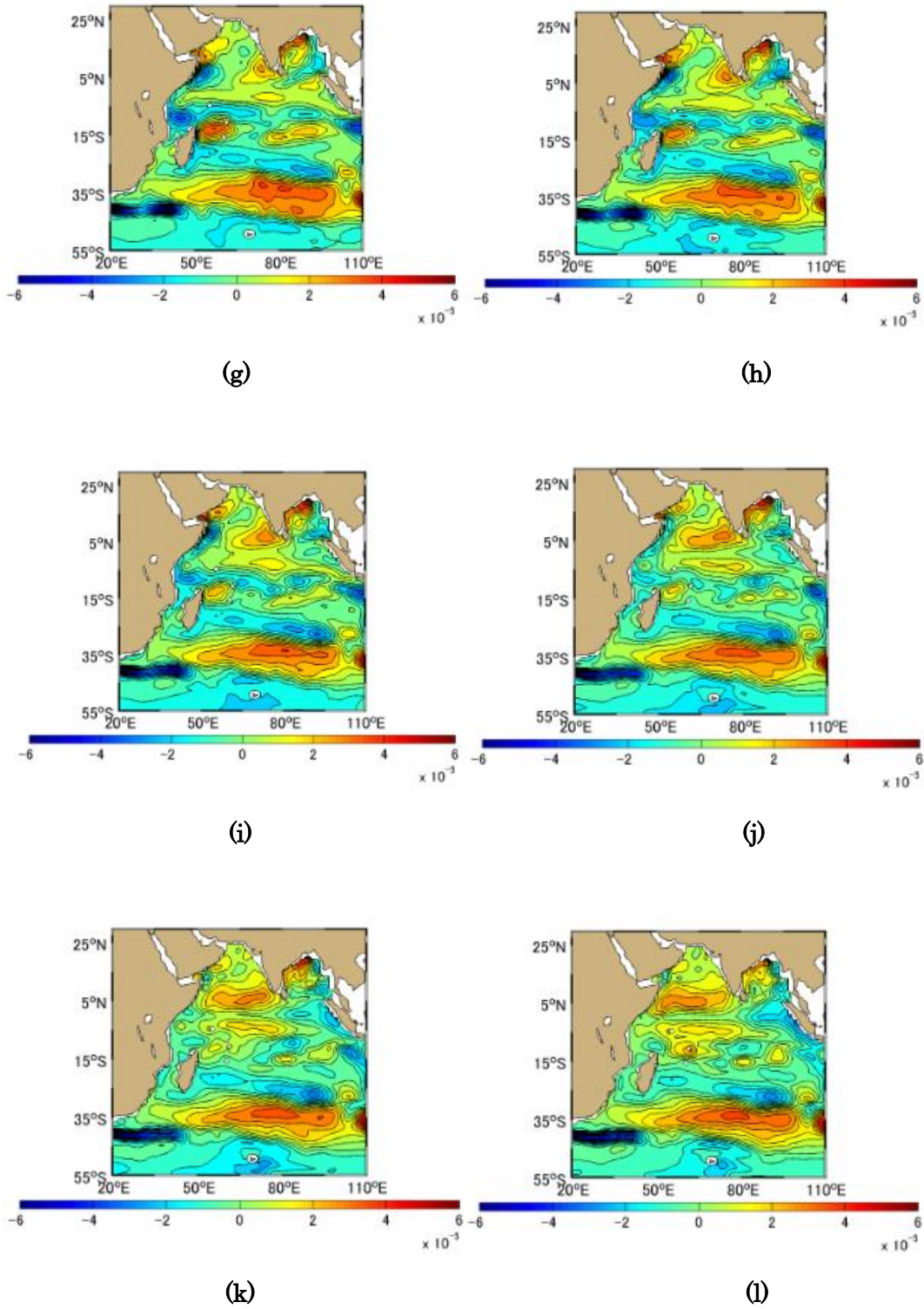
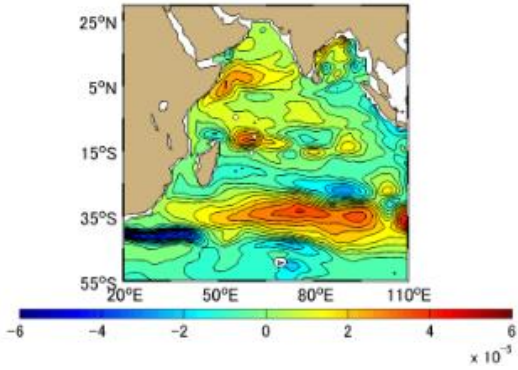
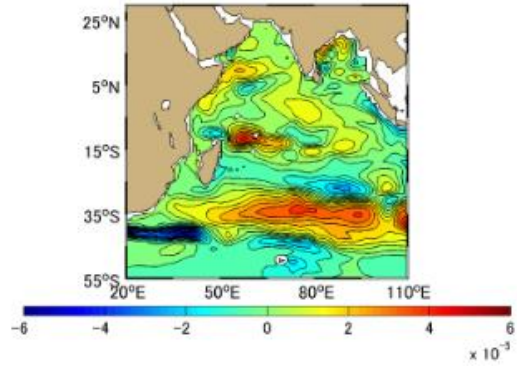


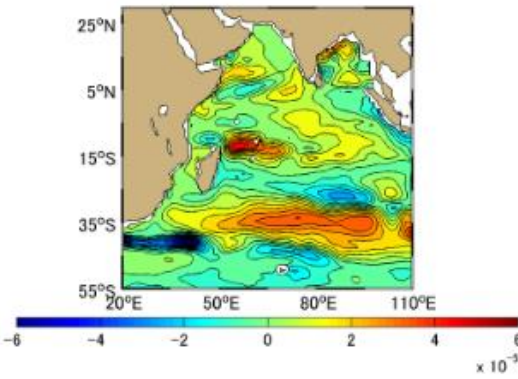
Figure A-6.18 Difference [PgC] between Approximation Method and Simulation Method Monthly Mean in 2008, the Indian Ocean based on January 1991. (a)-(l) represents January-December



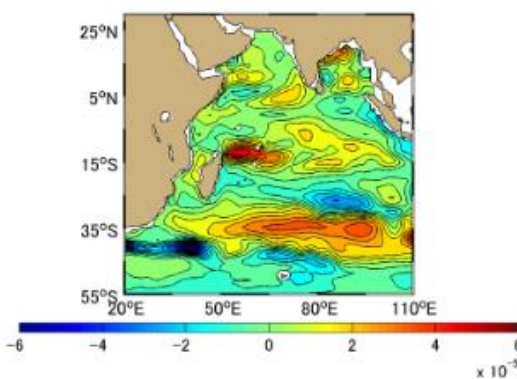
(a)



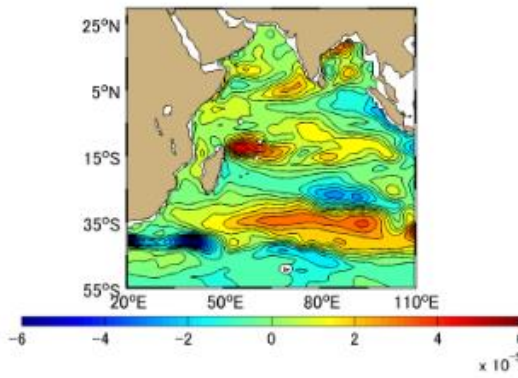
(b)



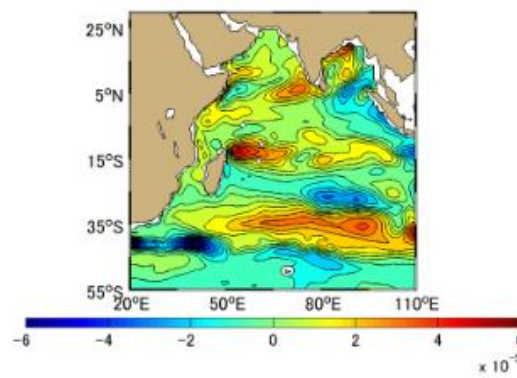
(c)



(d)

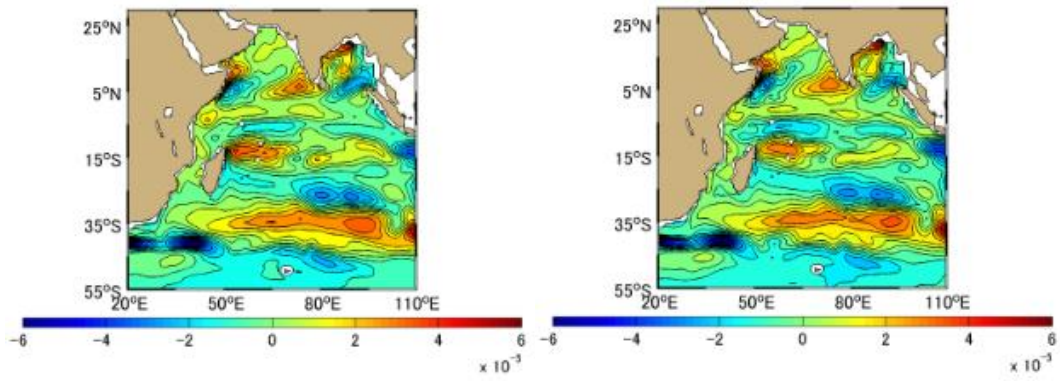


(e)



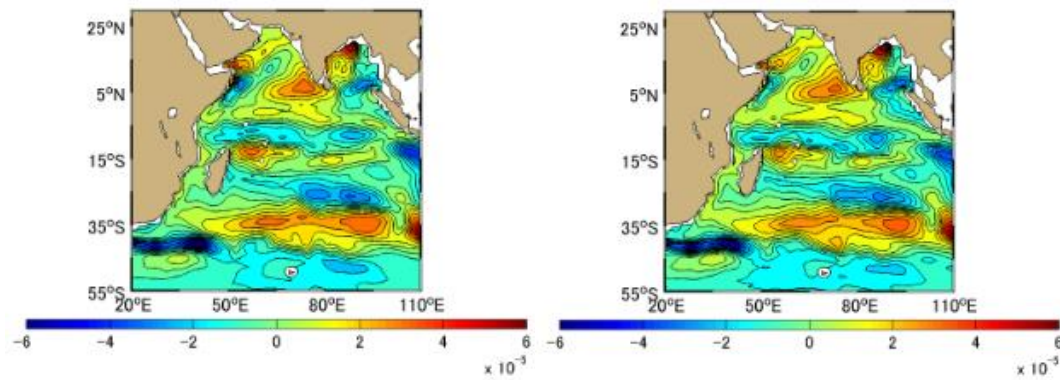
(f)





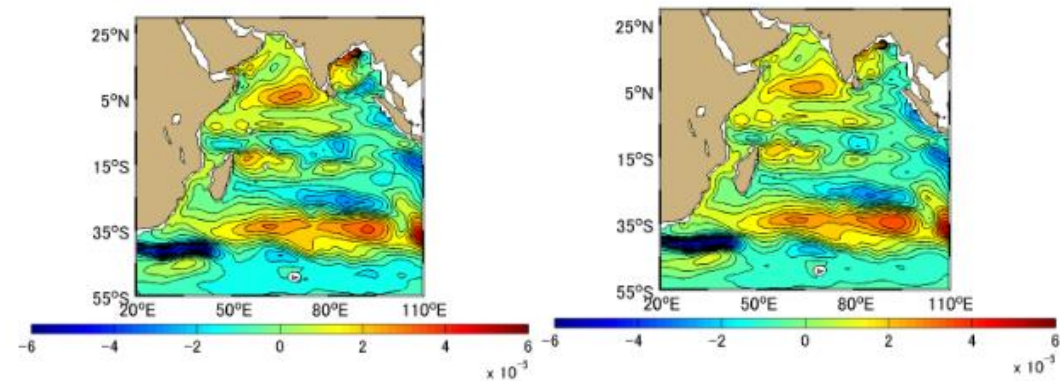
(g)

(h)



(i)

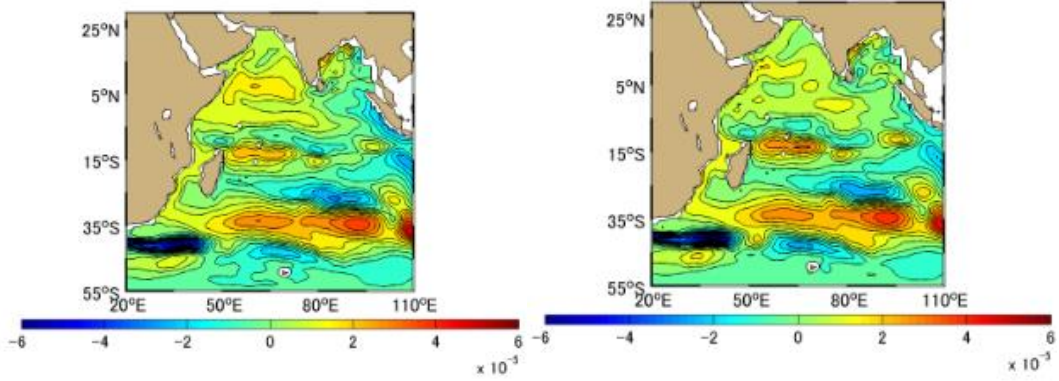
(j)



(k)

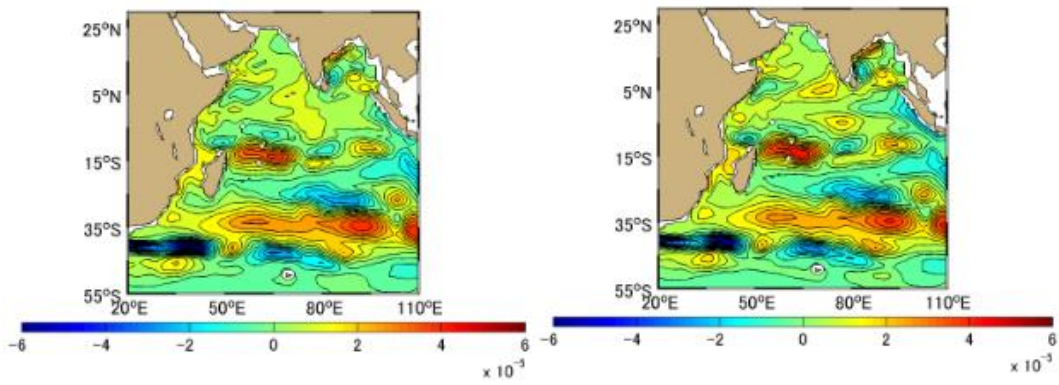
(l)

Figure A-6.19 Difference [PgC] between Approximation Method and Simulation Method Monthly Mean in 2009, the Indian Ocean based on January 1991. (a)-(l) represents January-December



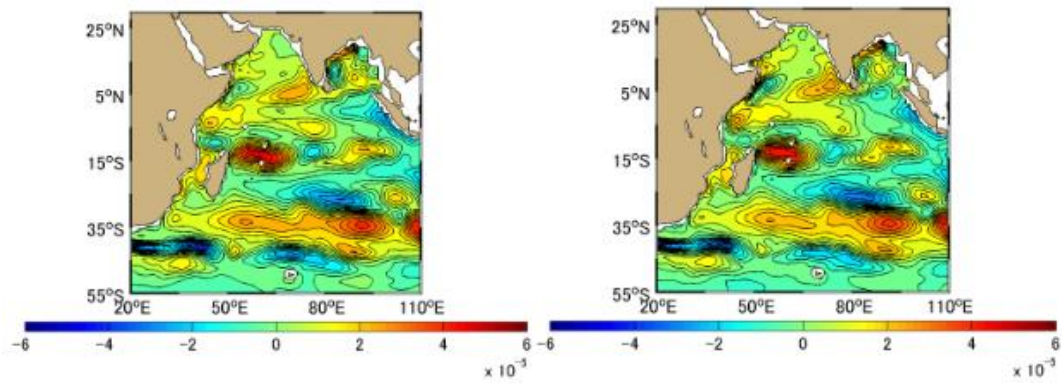
(a)

(b)



(c)

(d)



(e)

(f)

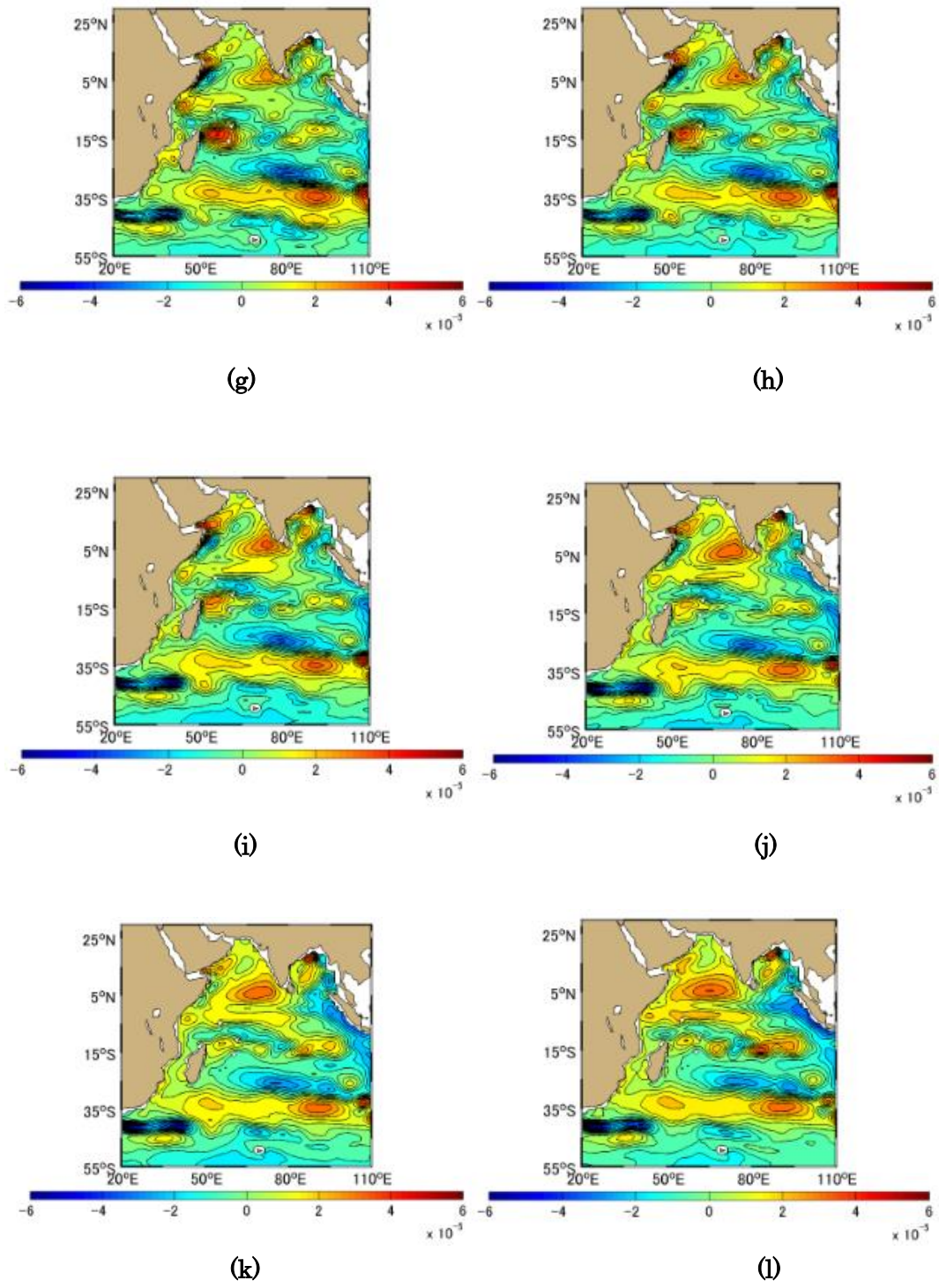
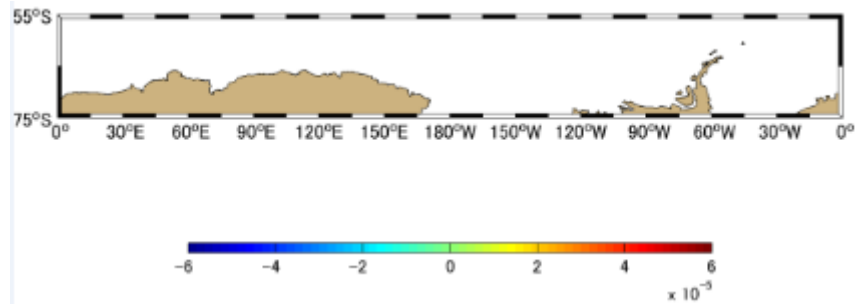
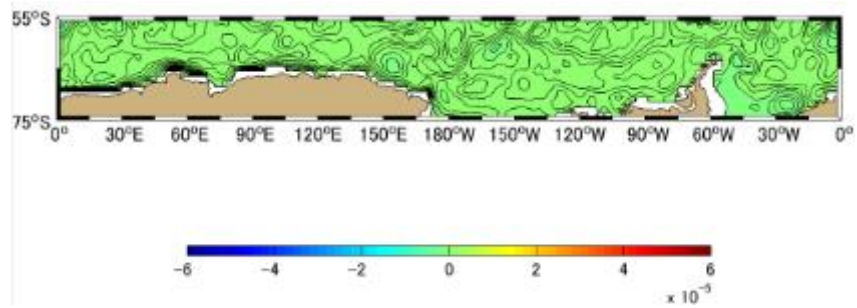


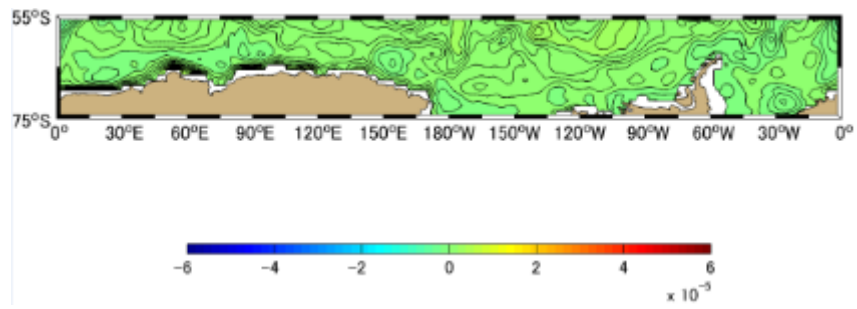
Figure A-6.20 Difference [PgC] between Approximation Method and Simulation Method Monthly Mean in 2010, the Indian Ocean based on January 1991. (a)-(l) represents January-December



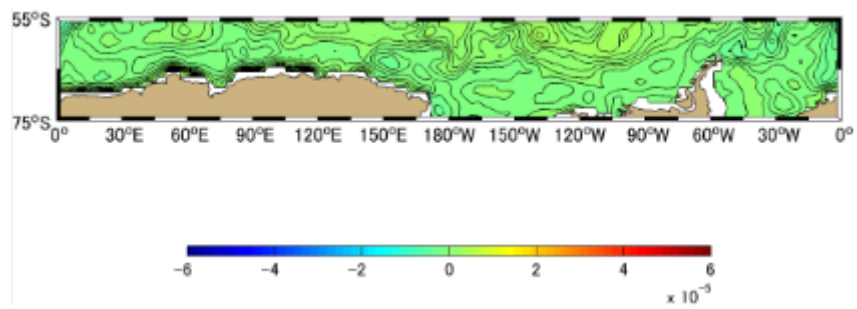
(a)



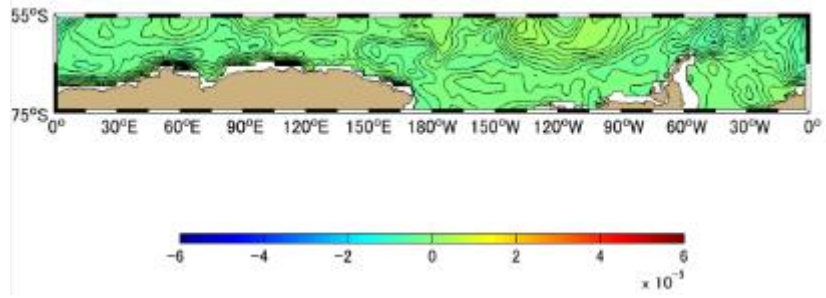
(b)



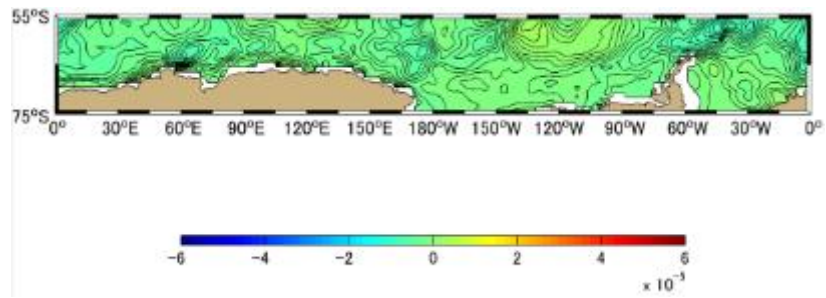
(c)



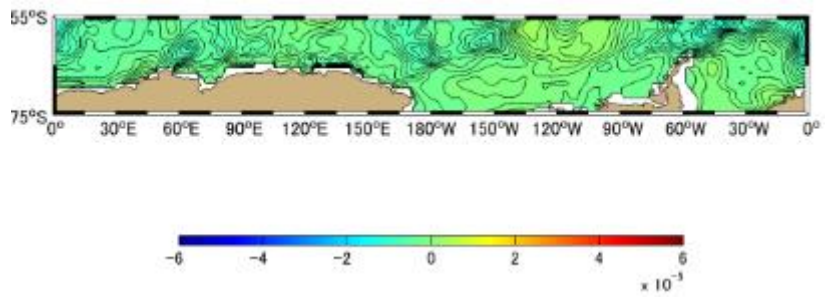
(d)



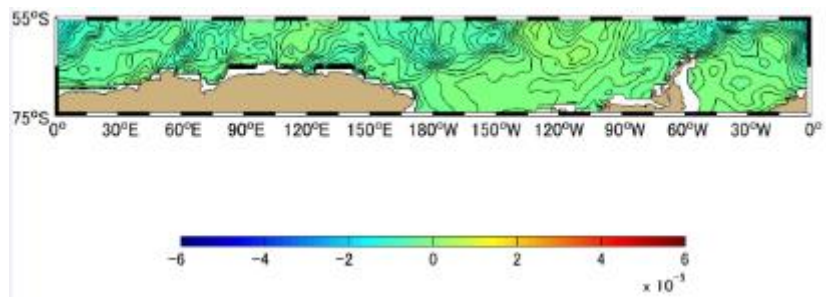
(e)



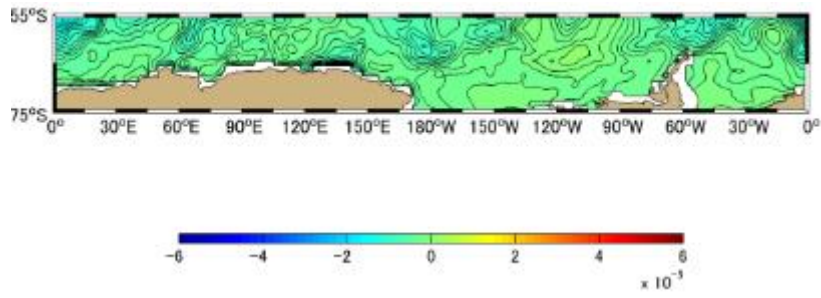
(f)



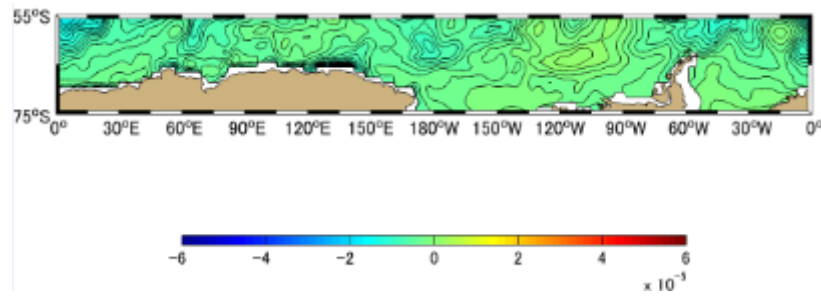
(g)



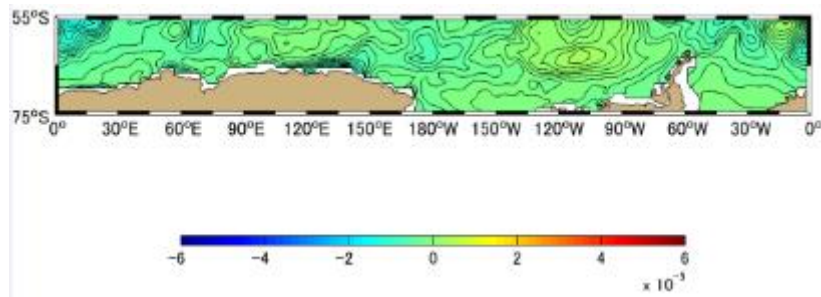
(h)



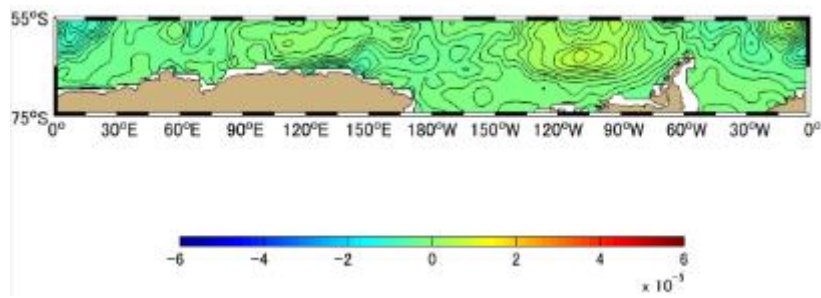
(i)



(j)

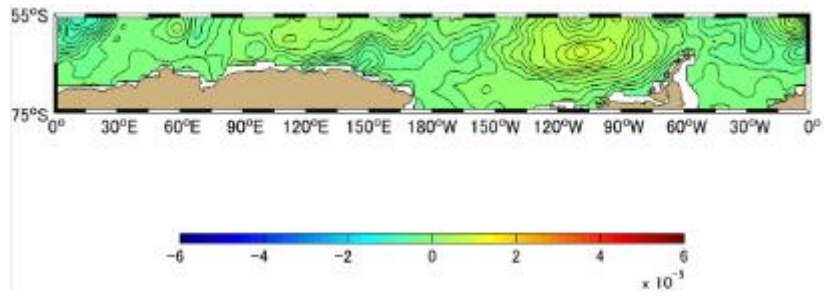


(k)

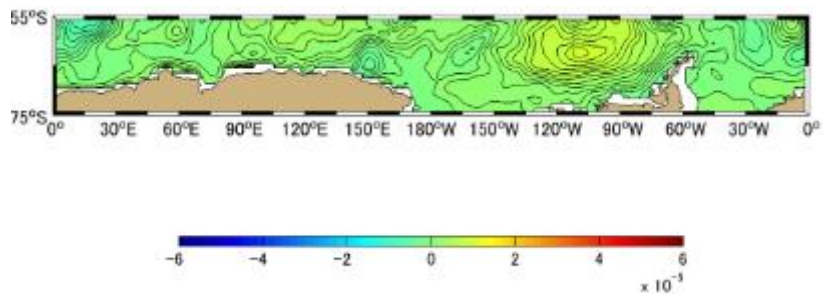


(l)

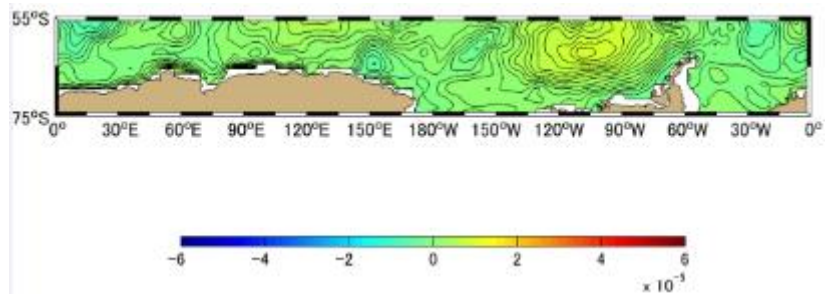
Figure A-5.1 Difference [PgC] between Approximation Method and Simulation Method Monthly Mean in 1991, the Southern Oceans based on January 1991. (a)-(l) represents January-December



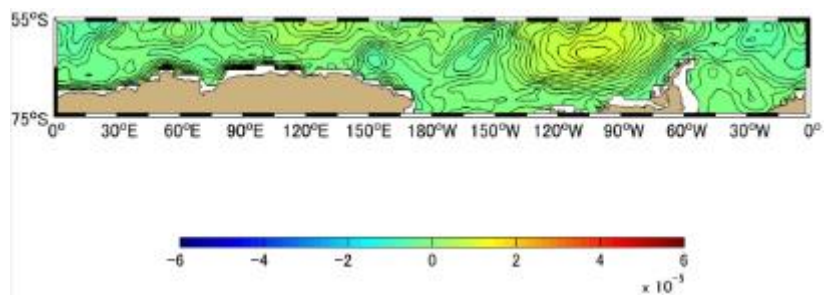
(a)



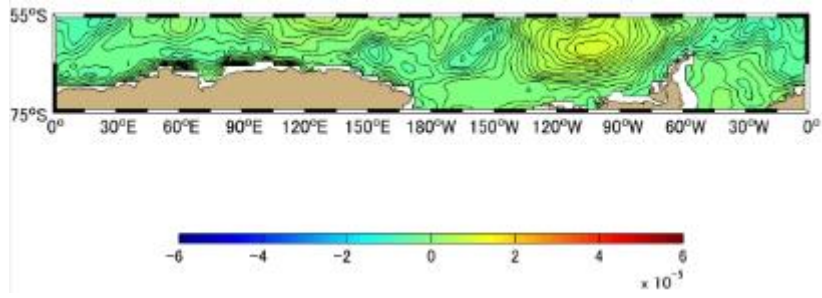
(b)



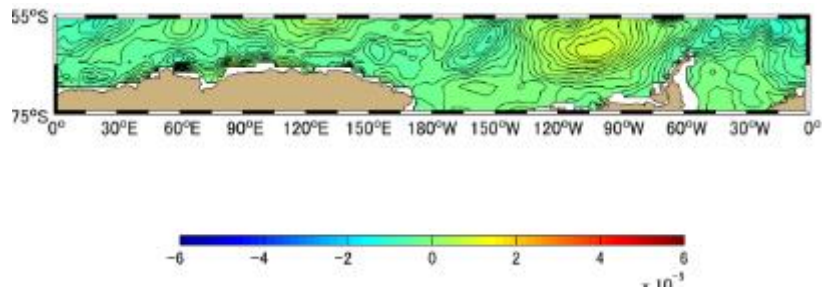
(c)



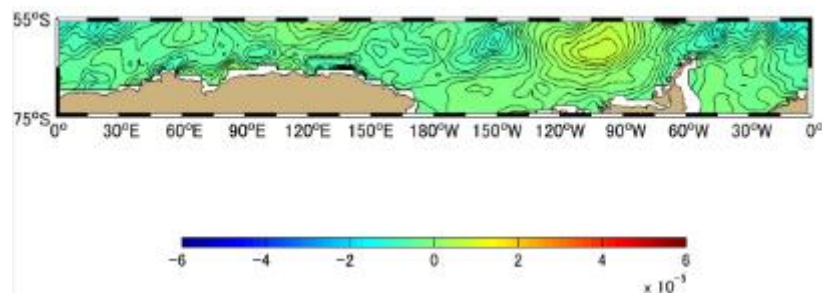
(d)



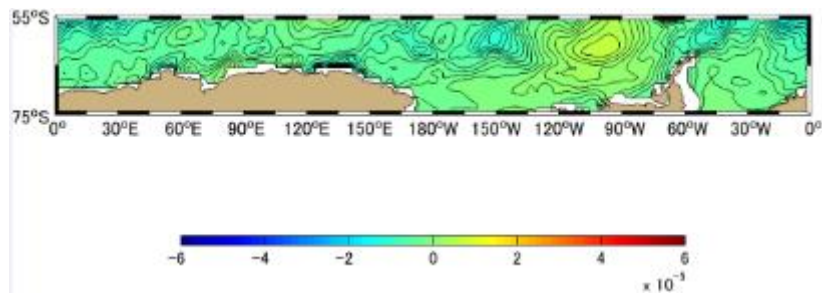
(e)



(f)



(g)



(h)



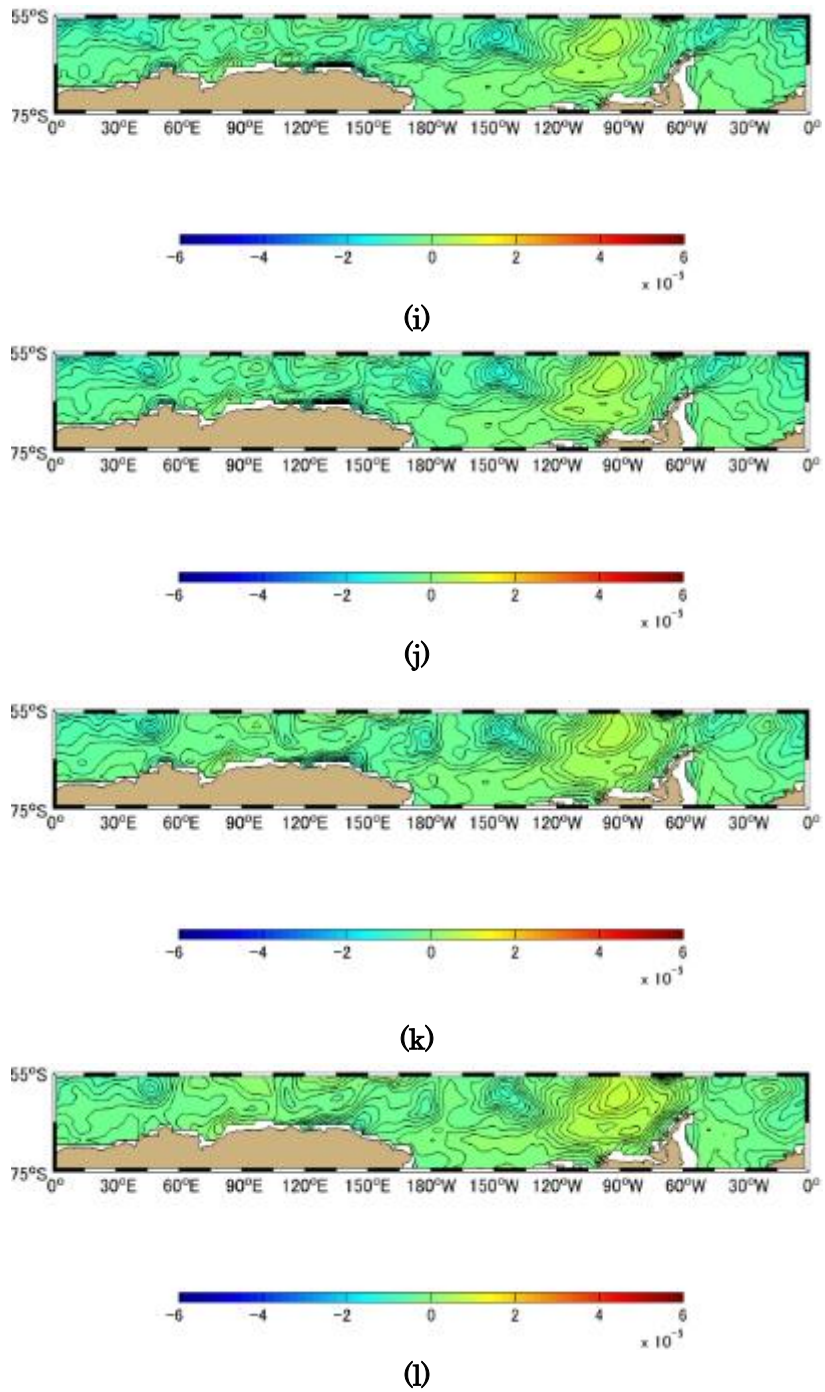
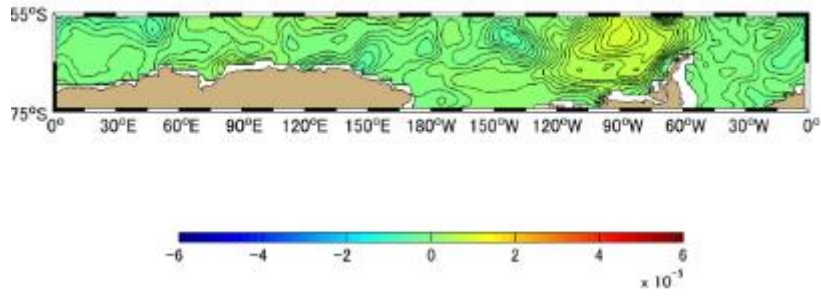
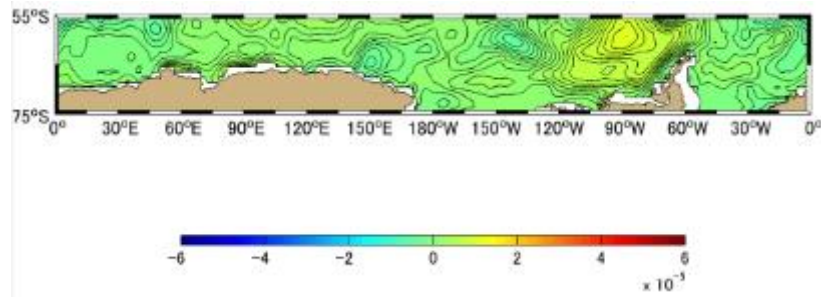


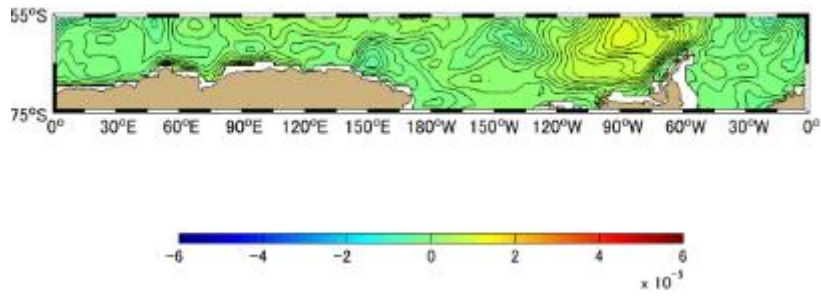
Figure A-5.2, Difference [PgC] between Approximation Method and Simulation Method Monthly Mean in 1992, the Southern Oceans based on January 1991. (a)-(l) represents January-December



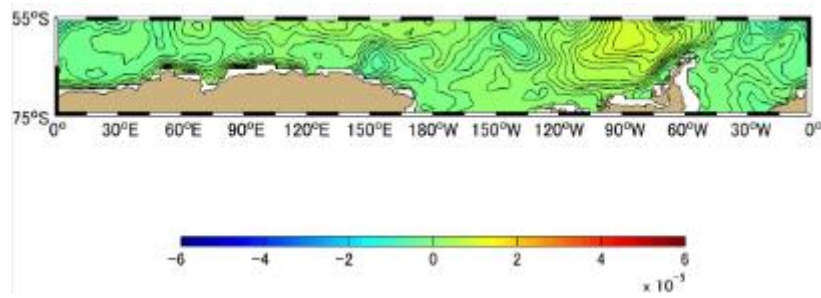
(a)



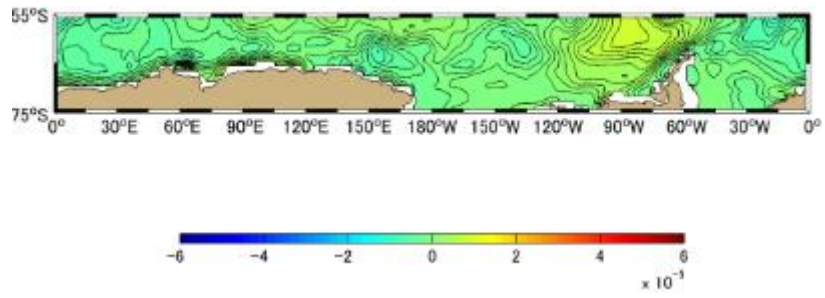
(b)



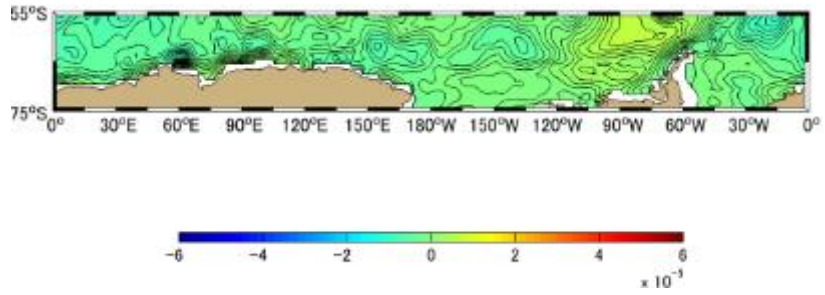
(c)



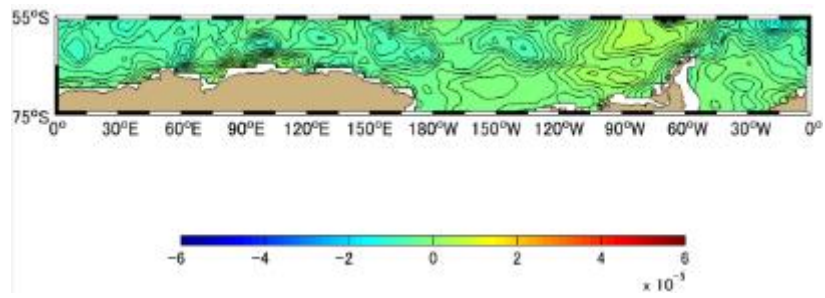
(d)



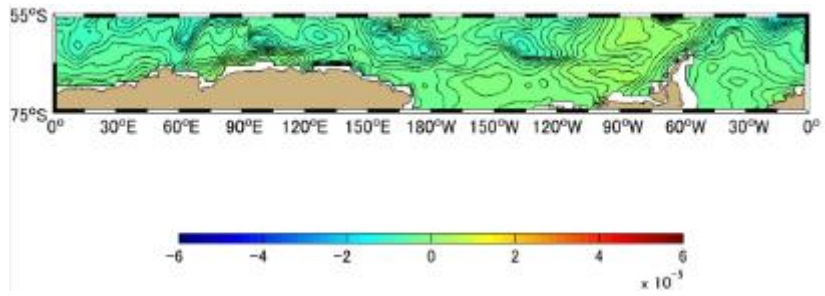
(e)



(f)



(g)



(h)

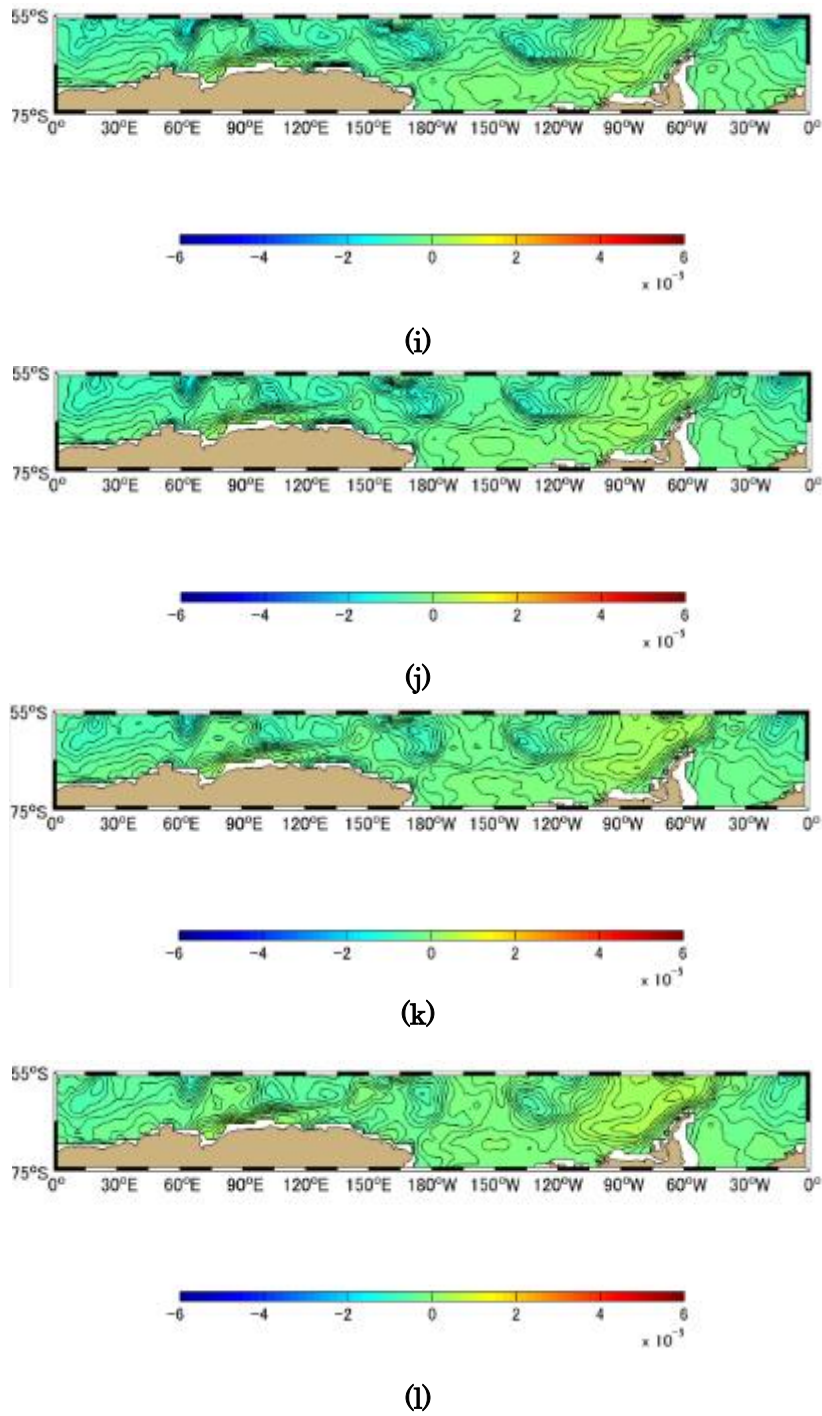
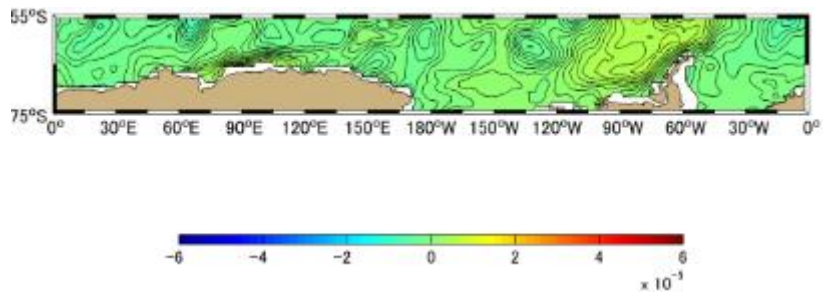
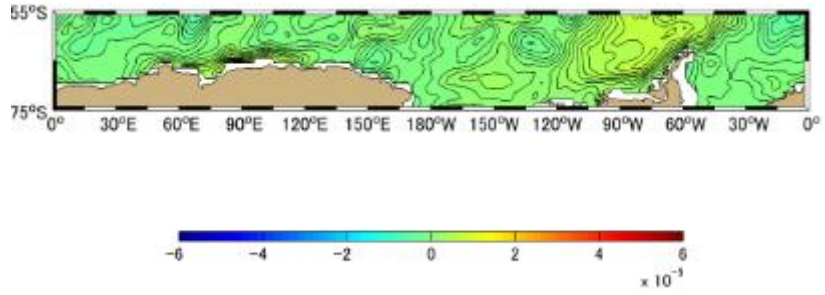


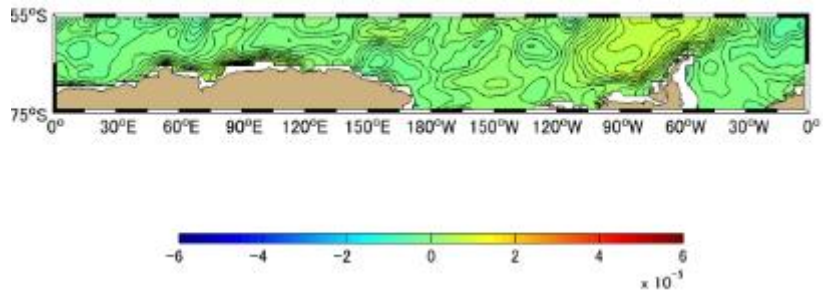
Figure A-5.3 Difference [PgC] between Approximation Method and Simulation Method Monthly Mean in 1993, the Southern Oceans based on January 1991. (a)-(l) represents January-December



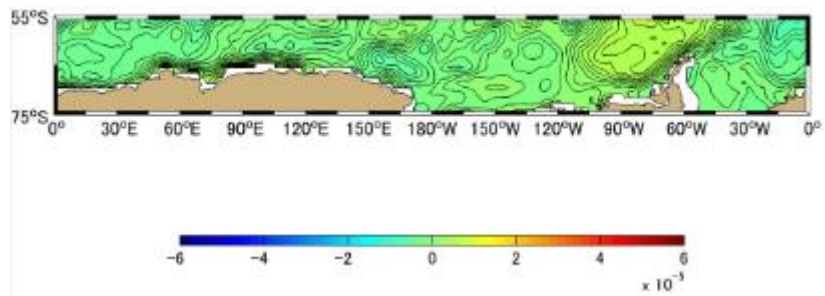
(a)



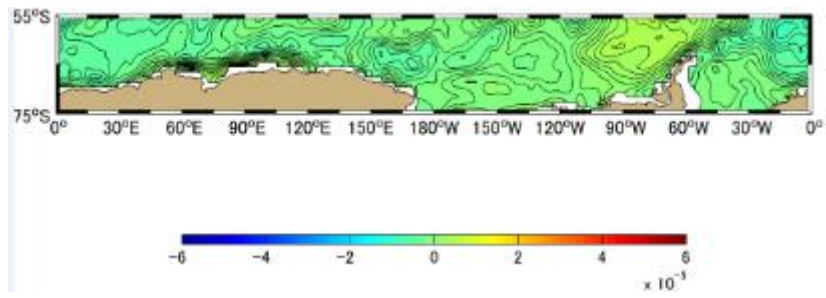
(b)



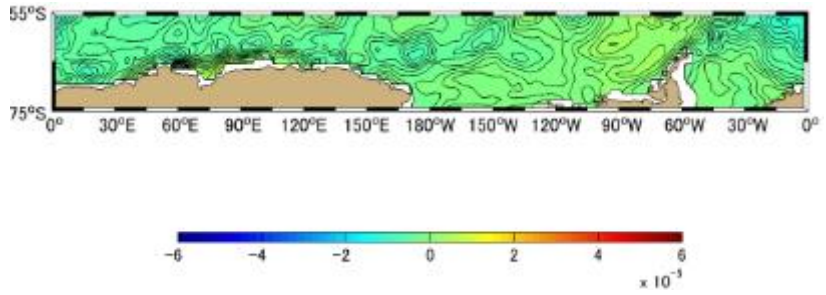
(c)



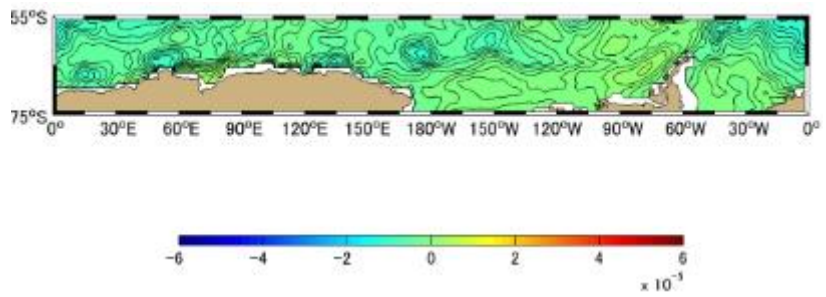
(d)



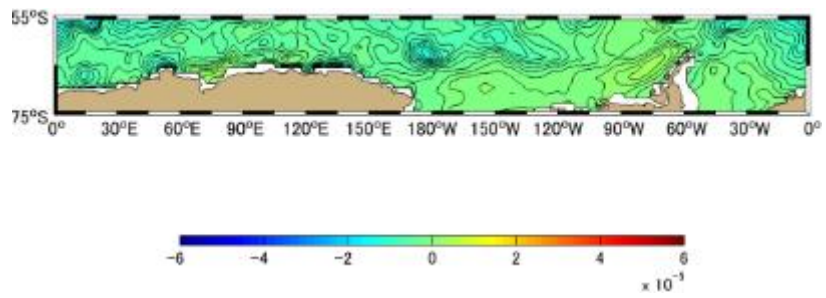
(e)



(f)



(g)



(h)

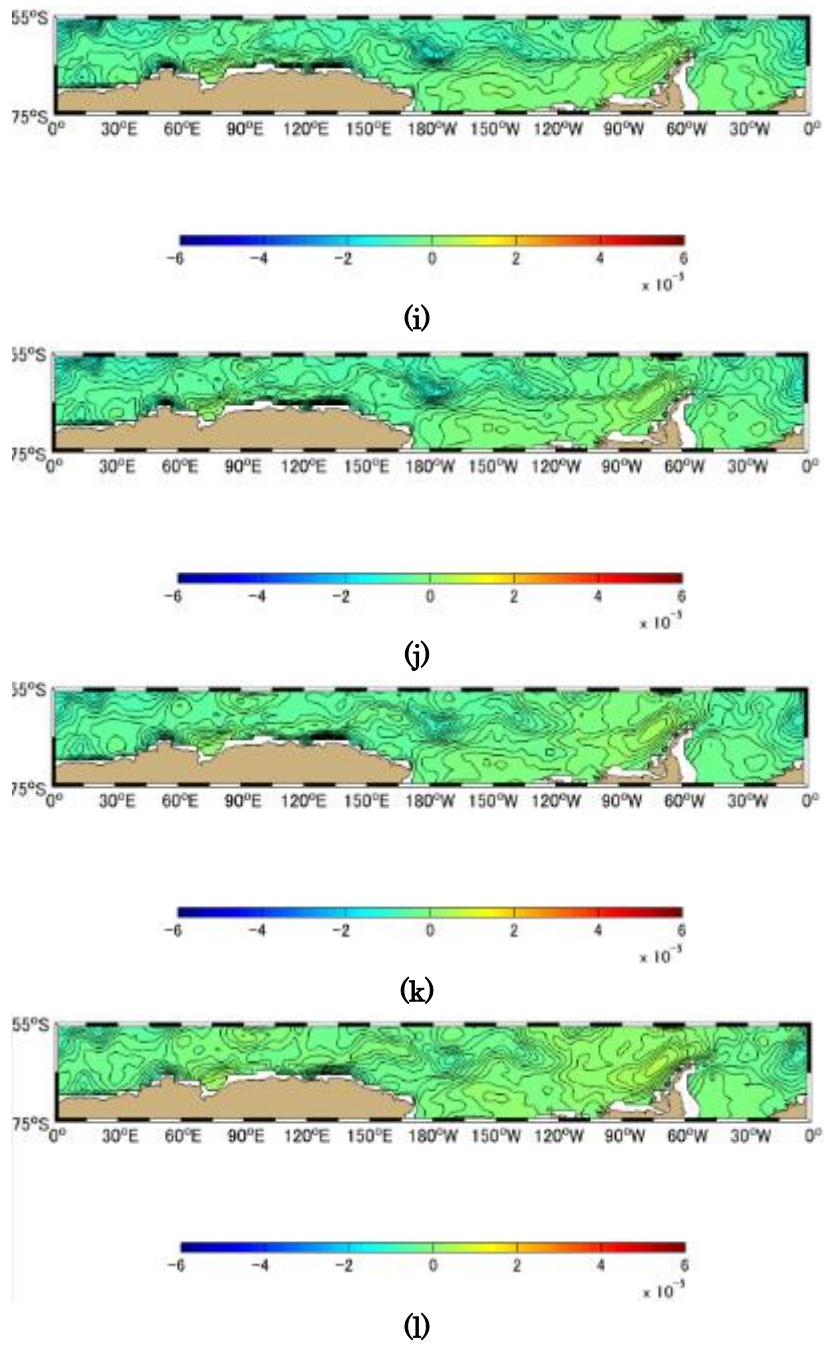
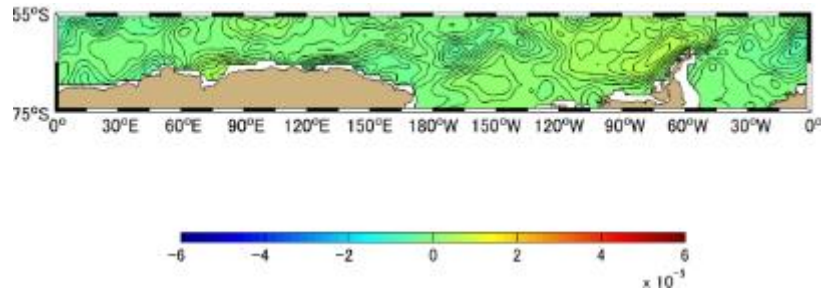
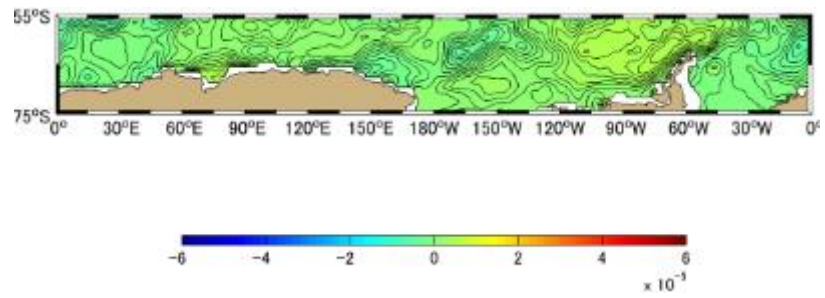


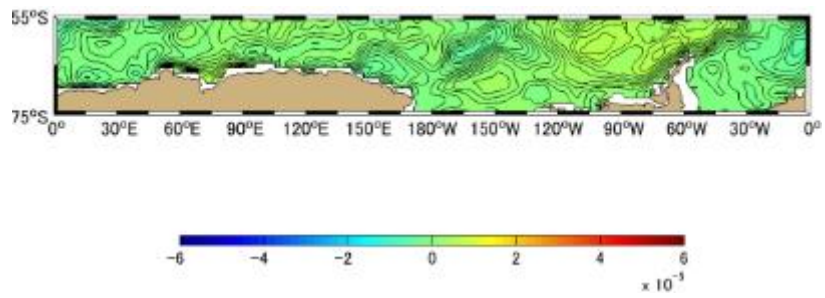
Figure A-5.4 Difference [PgC] between Approximation Method and Simulation Method Monthly Mean in 1994, the Southern Oceans based on January 1991. (a)-(l) represents January-December



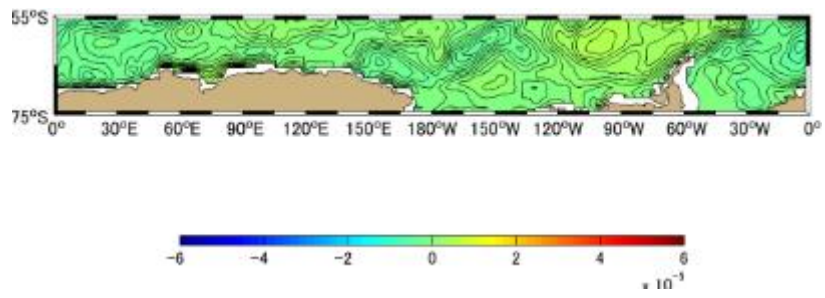
(a)



(b)

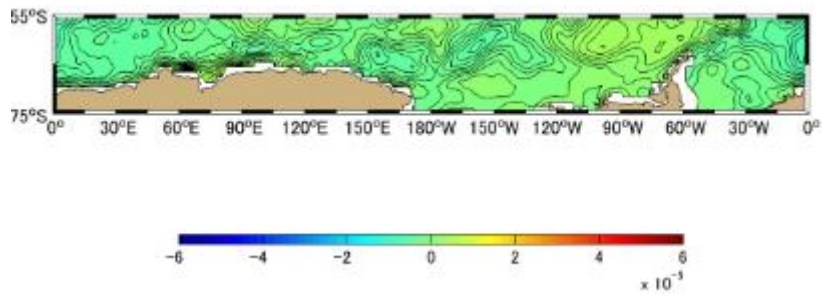


(c)

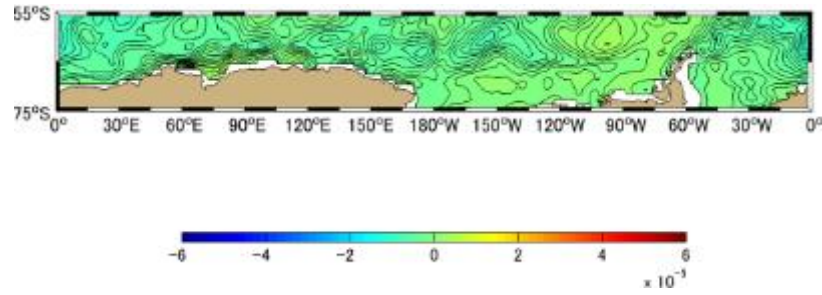


(d)

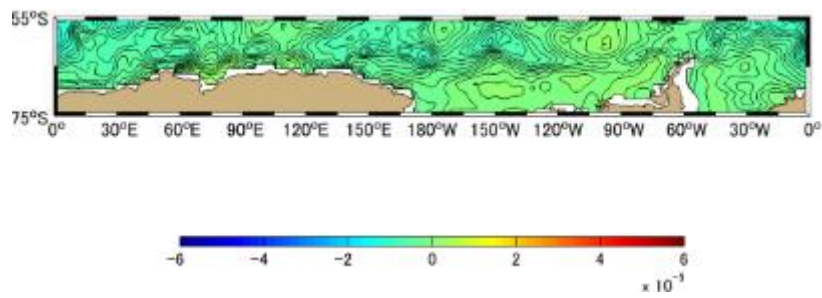




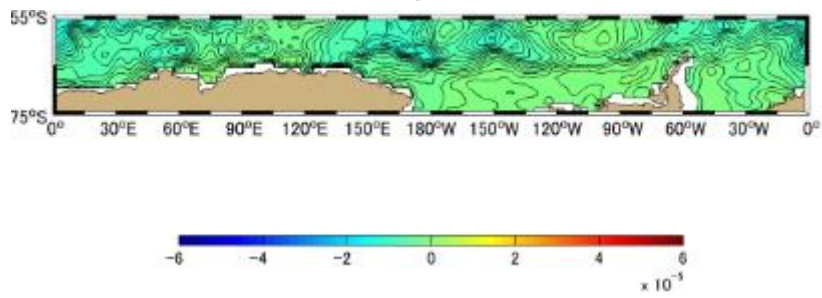
(e)



(f)



(g)



(h)

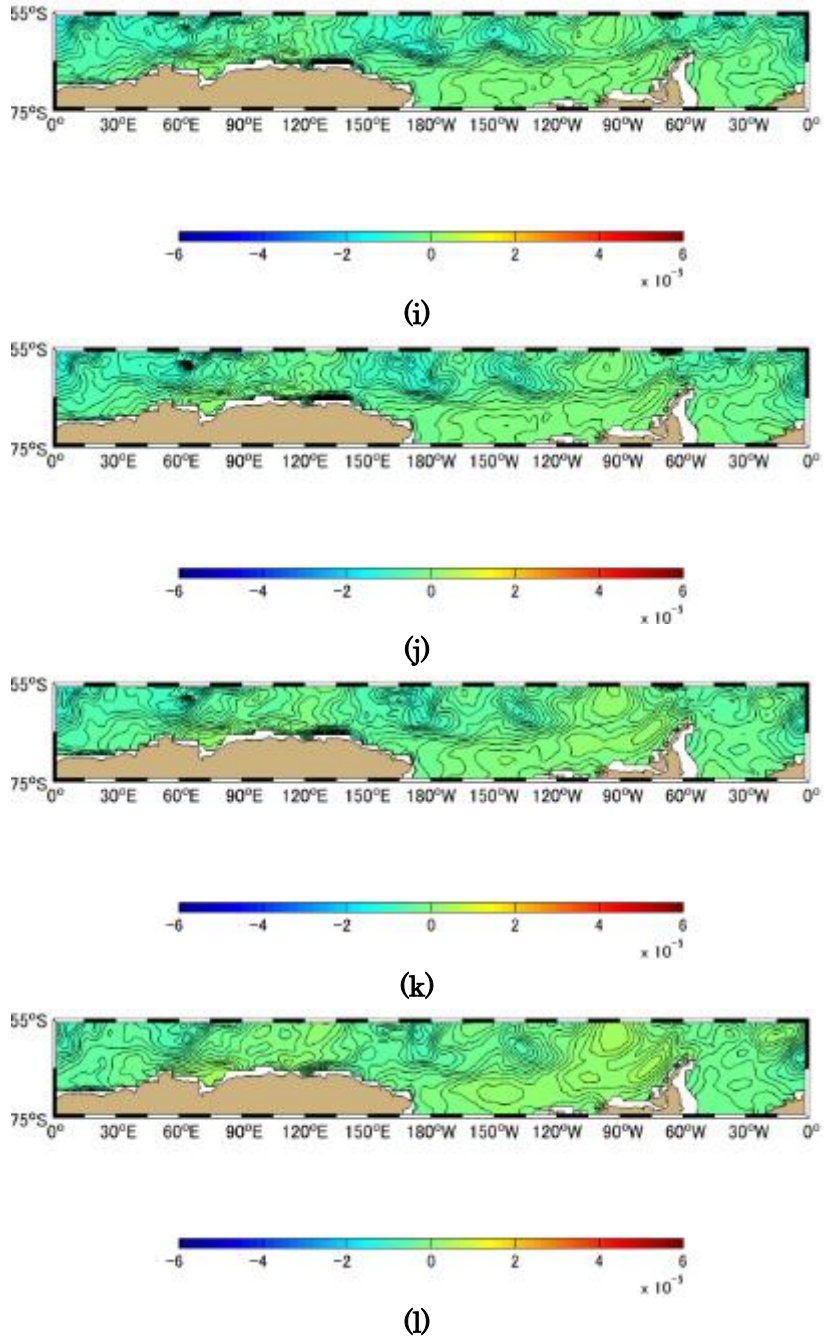
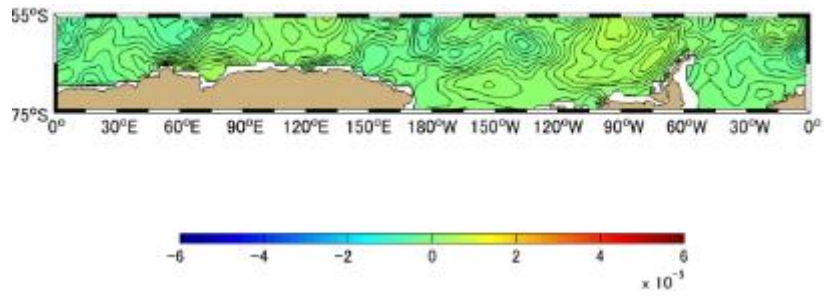
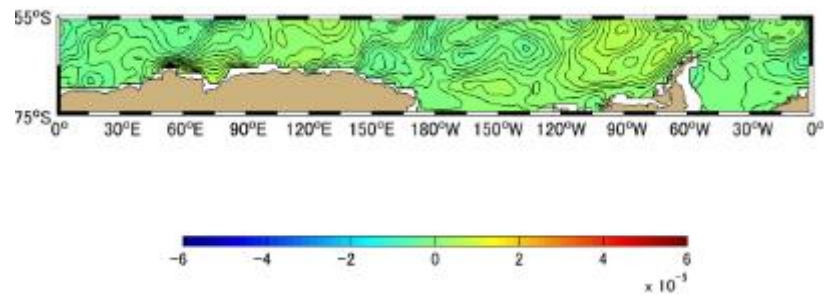


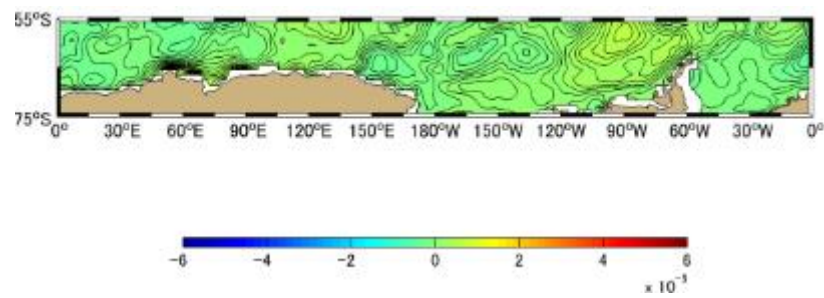
Figure A-5.5 Difference [PgC] between Approximation Method and Simulation Method Monthly Mean in 1995, the Southern Oceans based on January 1991. (a)-(l) represents January-December



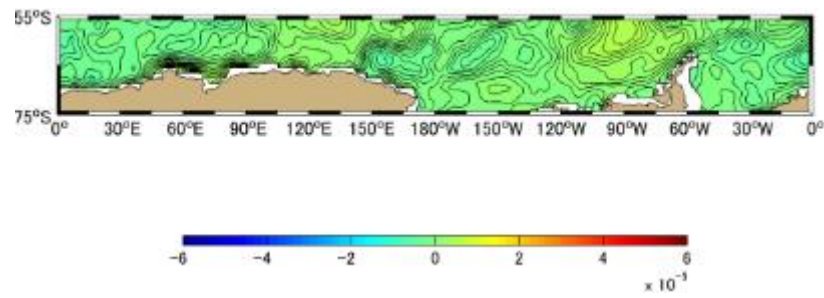
(a)



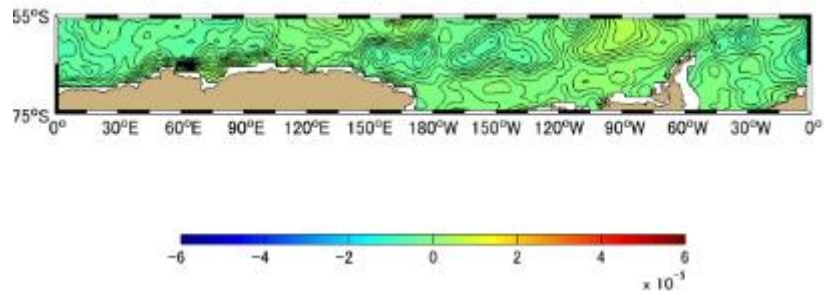
(b)



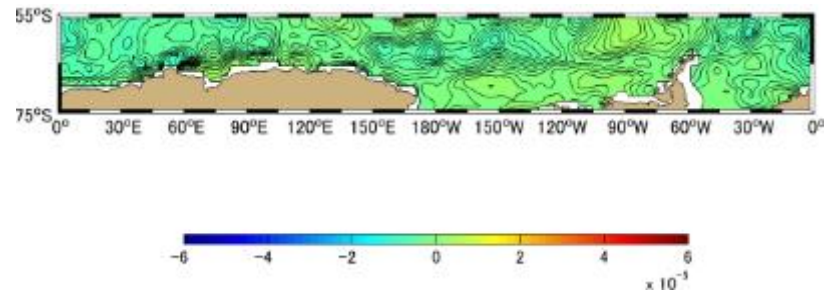
(c)



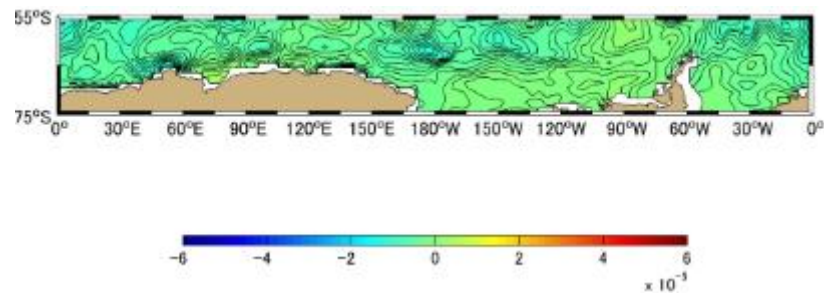
(d)



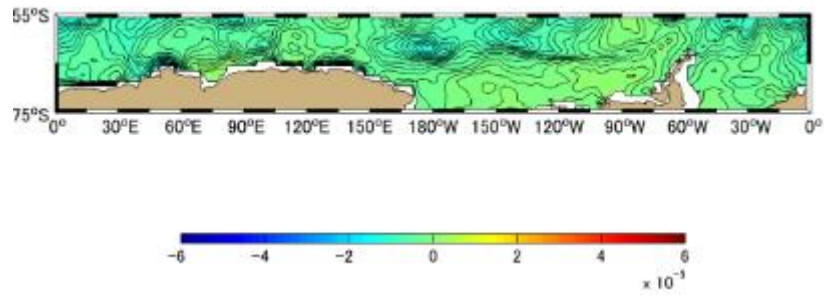
(e)



(f)



(g)



(h)

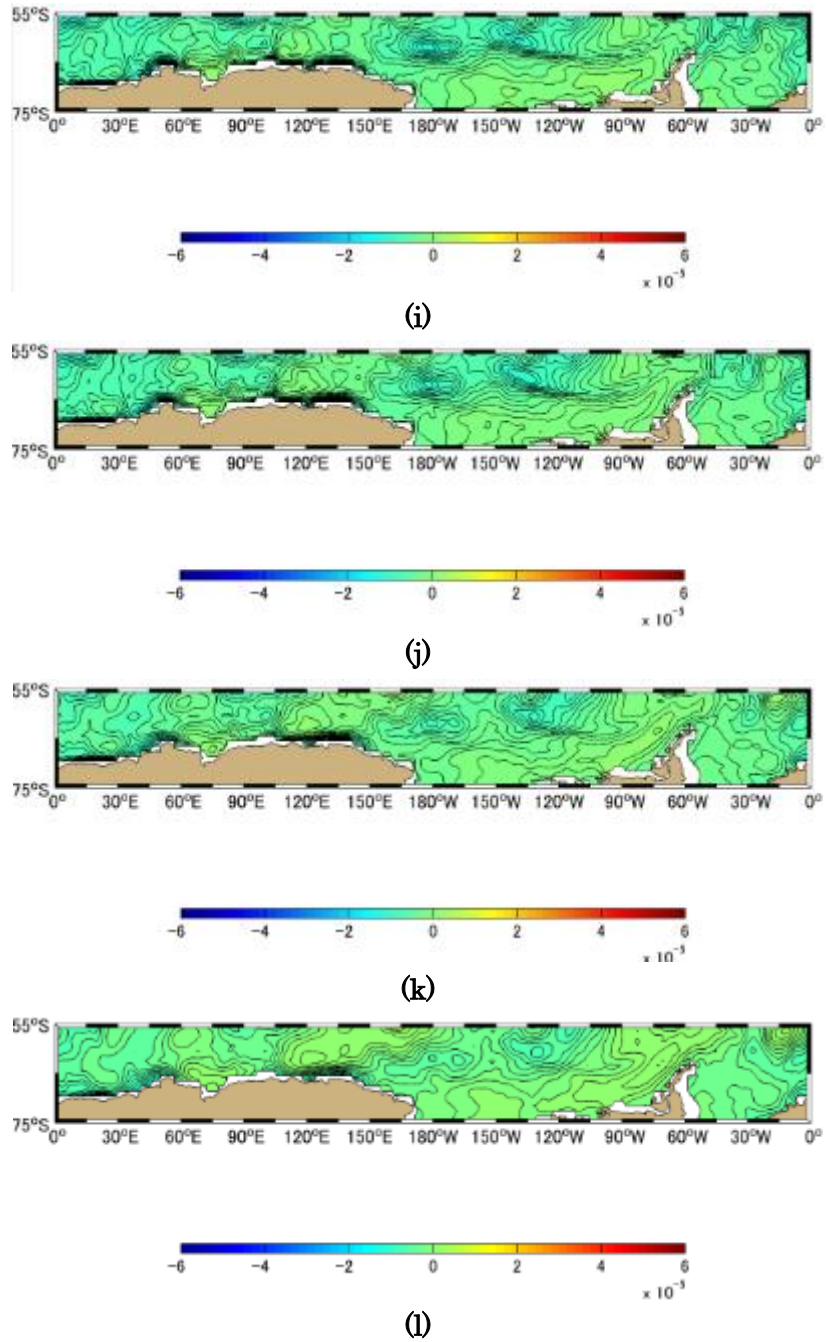
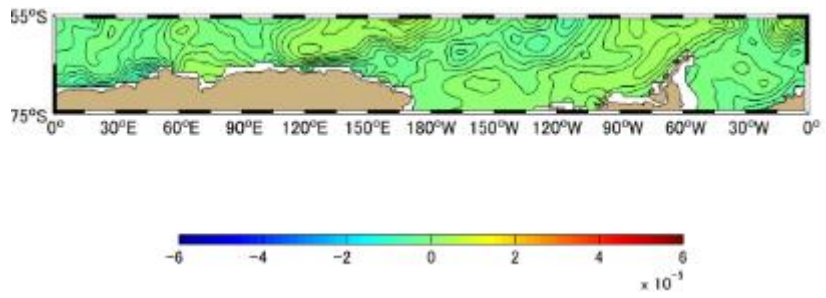
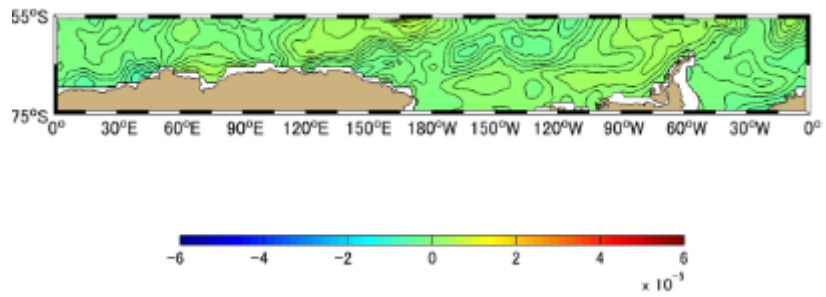


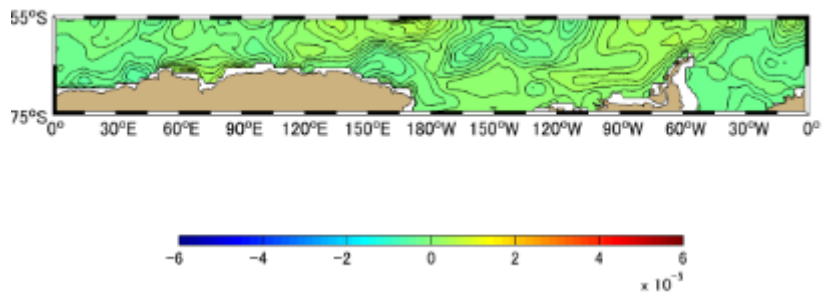
Figure A-5.6 Difference [PgC] between Approximation Method and Simulation Method Monthly Mean in 1996, the Southern Oceans based on January 1991. (a)-(l) represents January-December



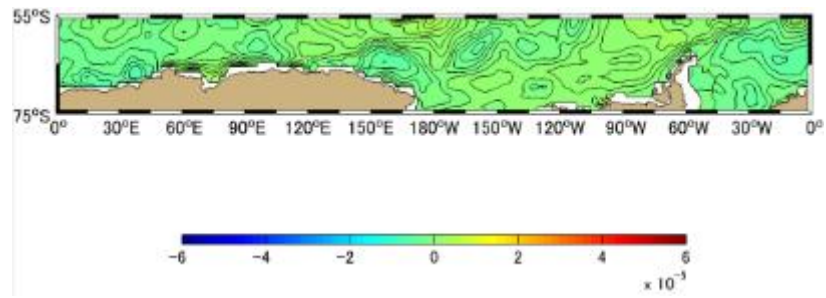
(a)



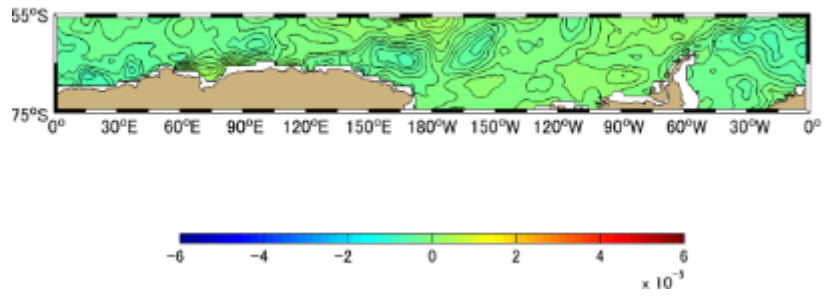
(b)



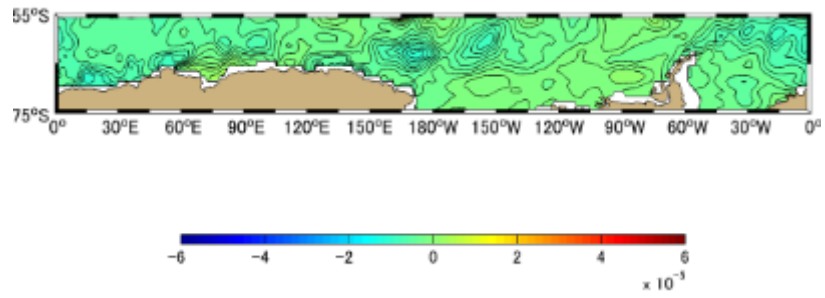
(c)



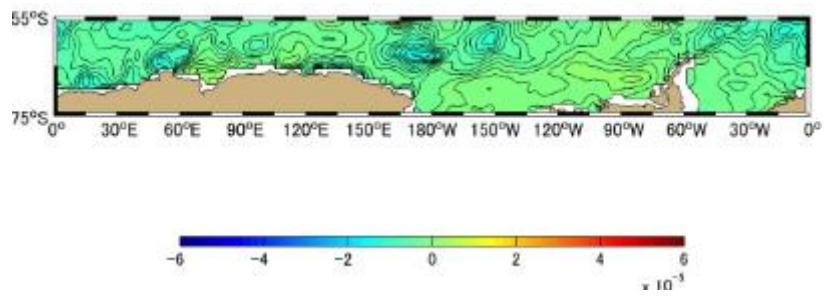
(d)



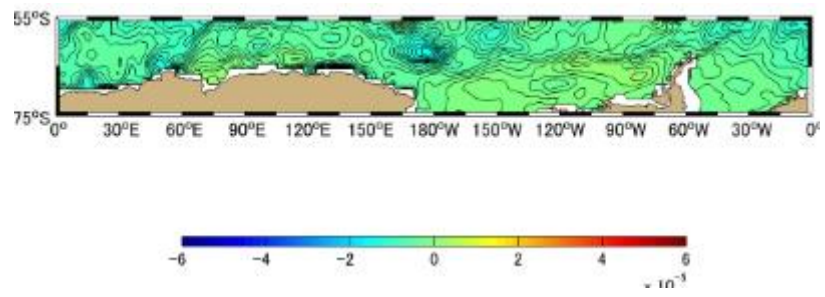
(e)



(f)



(g)



(h)

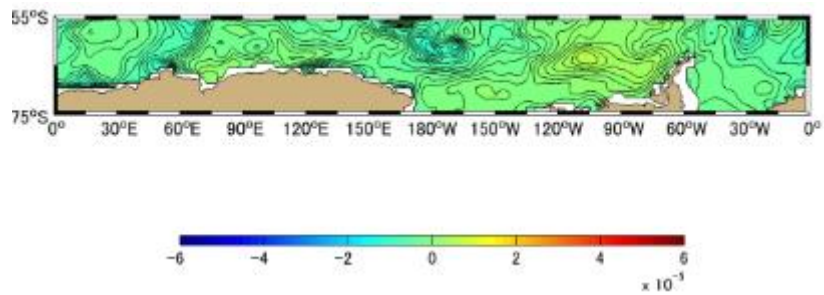
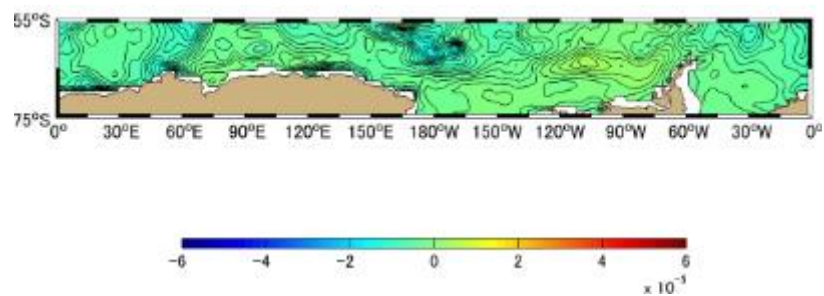
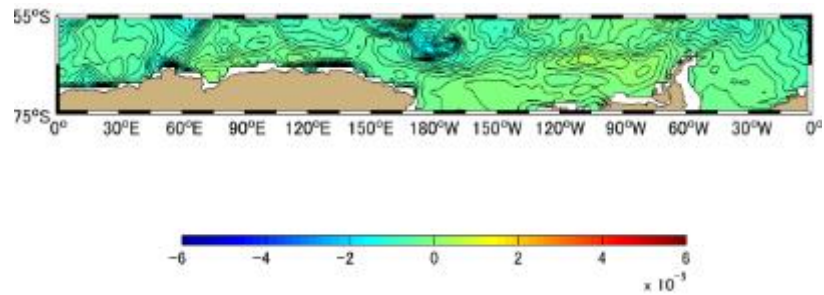
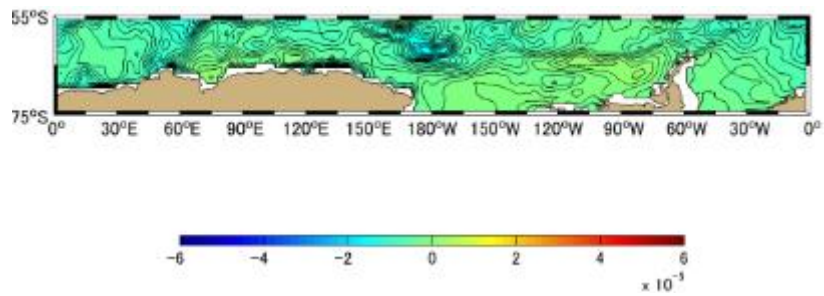
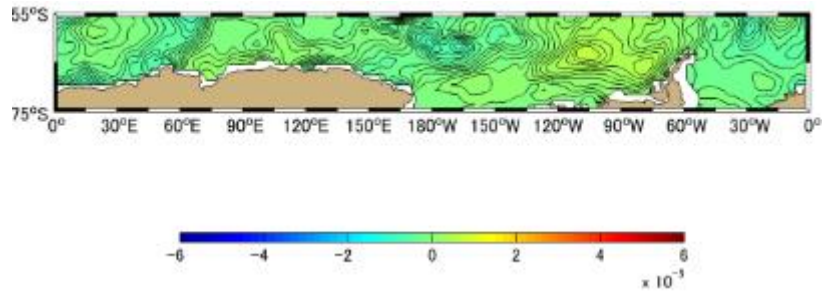
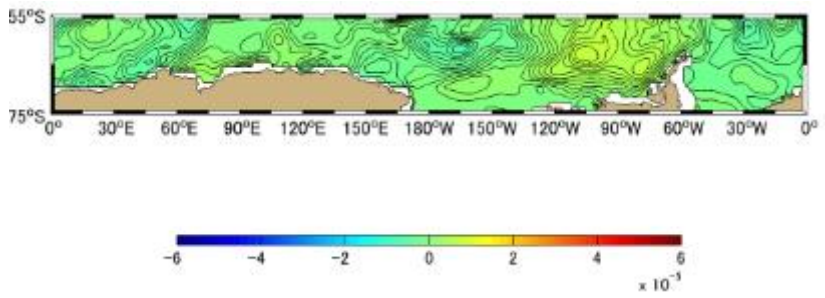


Figure A-5.7 Difference [PgC] between Approximation Method and Simulation Method Monthly Mean in 1997, the Southern Oceans based on January 1991. (a)-(l) represents January-December

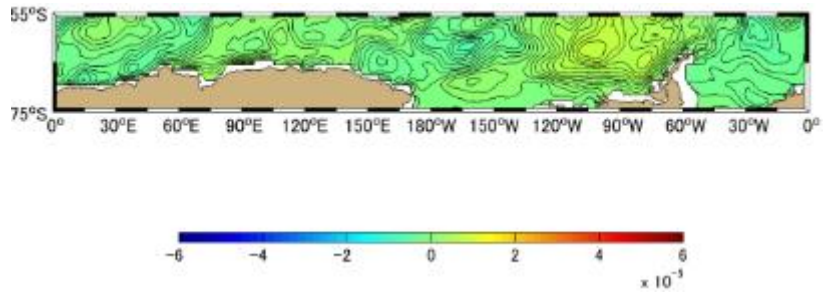




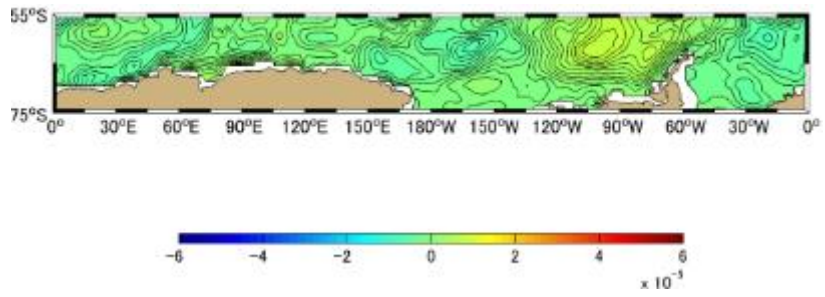
(a)



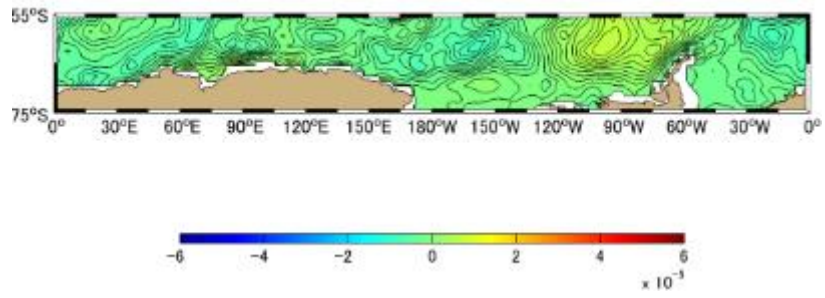
(b)



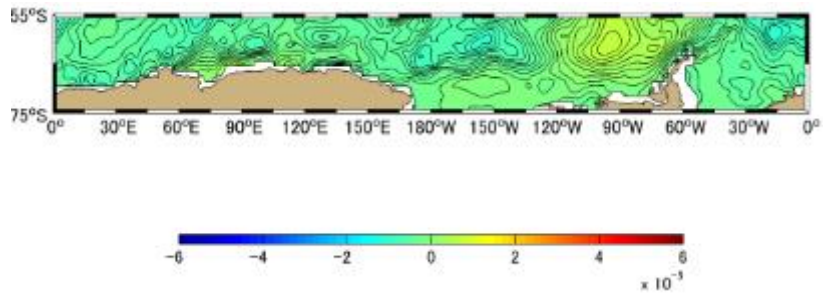
(c)



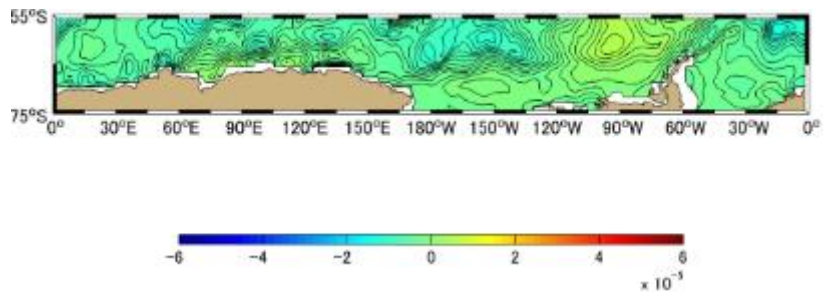
(d)



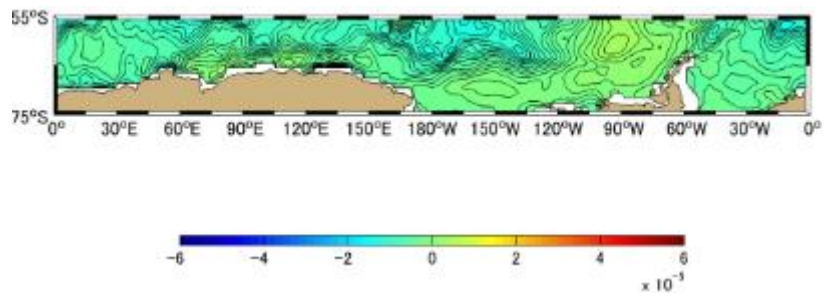
(e)



(f)



(g)



(h)

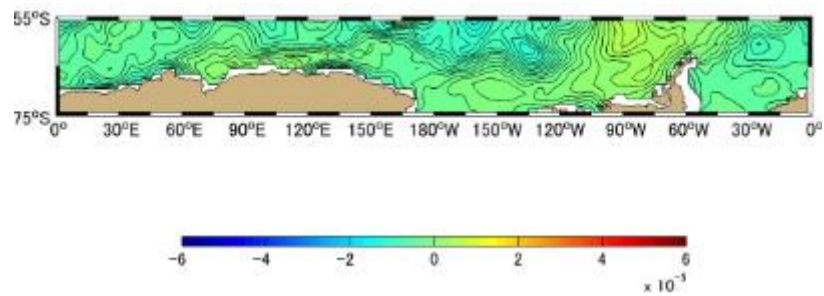
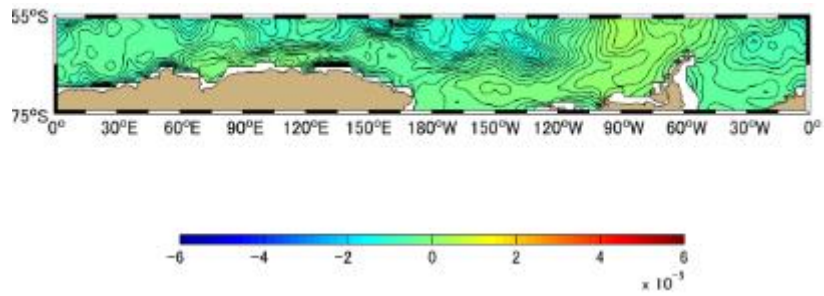
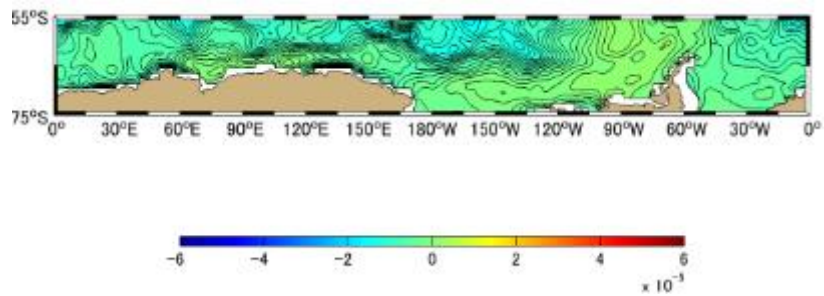
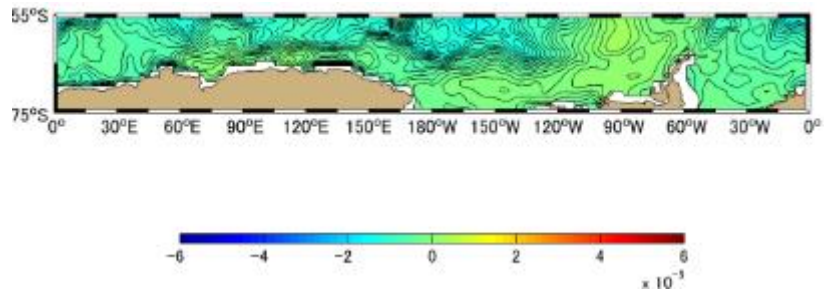
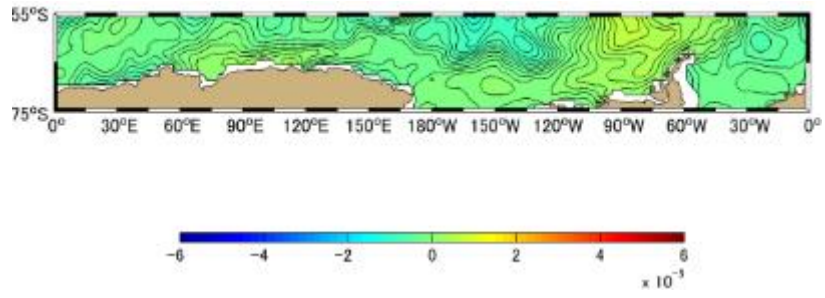
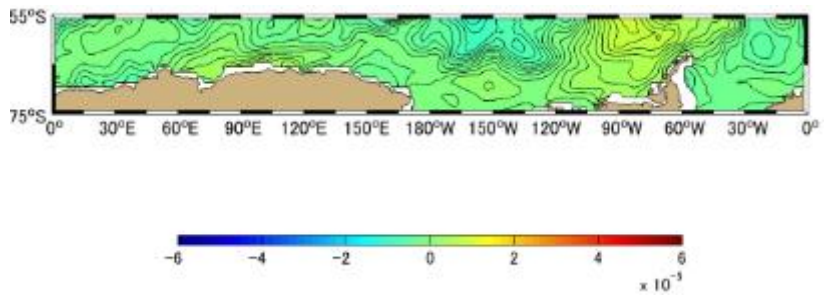


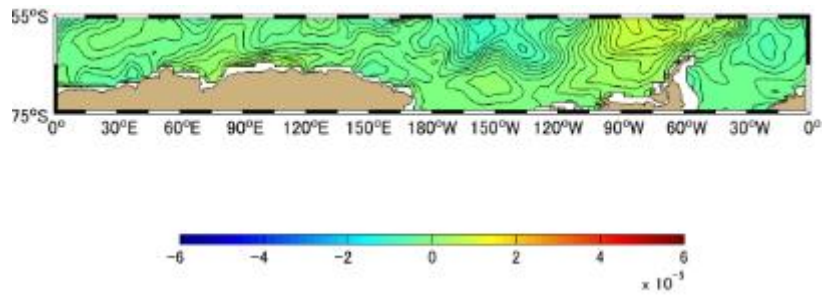
Figure A-5.8 Difference [PgC] between Approximation Method and Simulation Method Monthly Mean in 1998, the Southern Oceans based on January 1991. (a)-(l) represents January-December



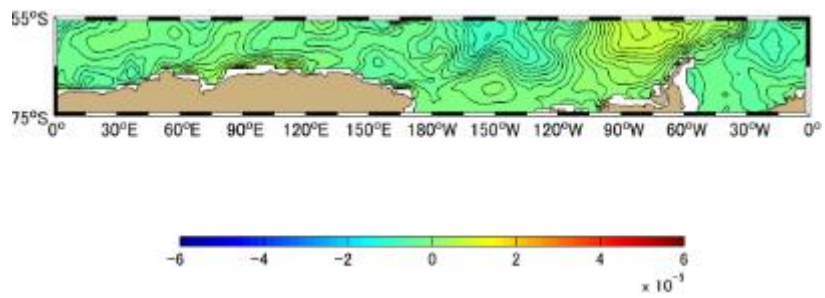
(a)



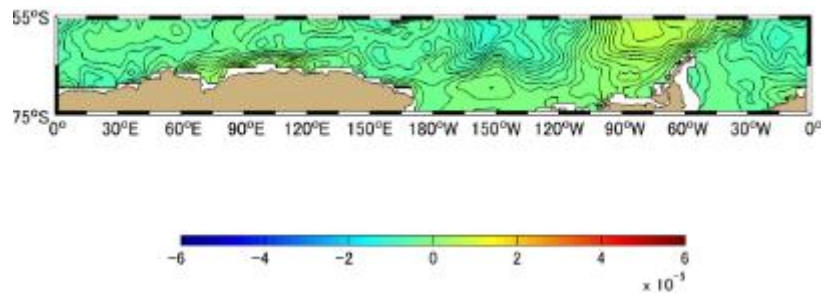
(b)



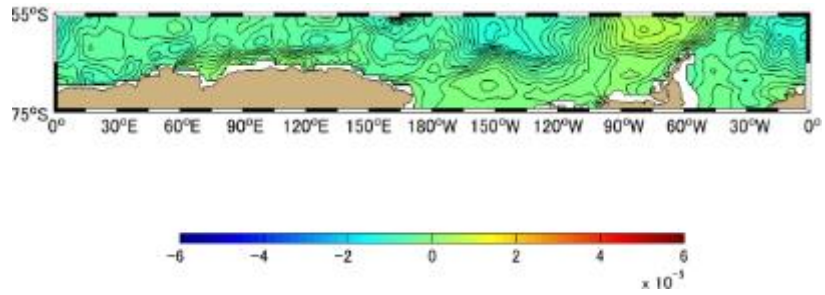
(c)



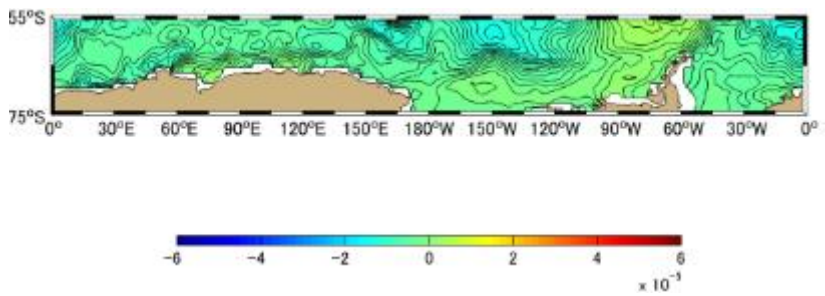
(d)



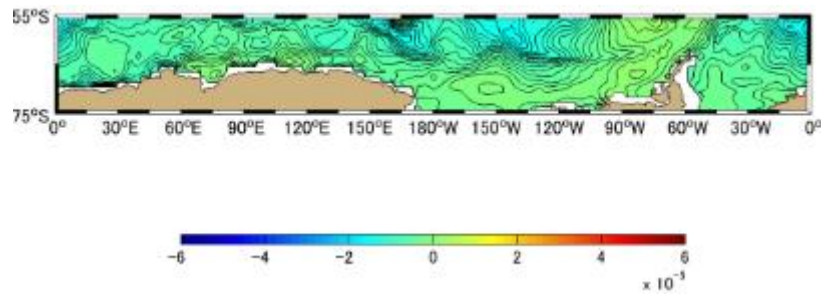
(e)



(f)



(g)



(h)

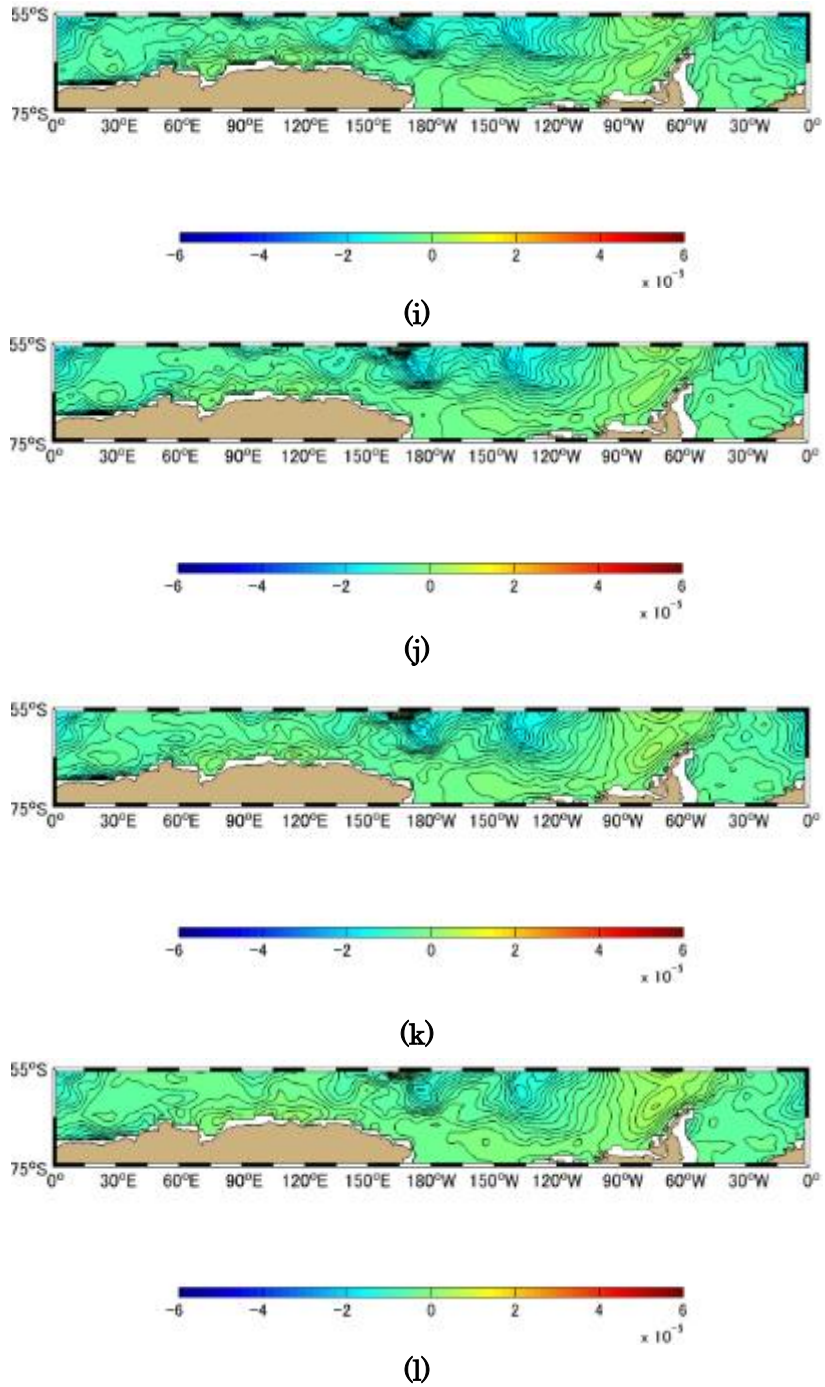
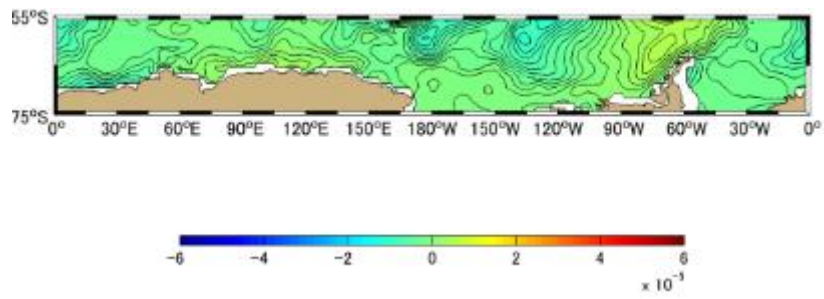
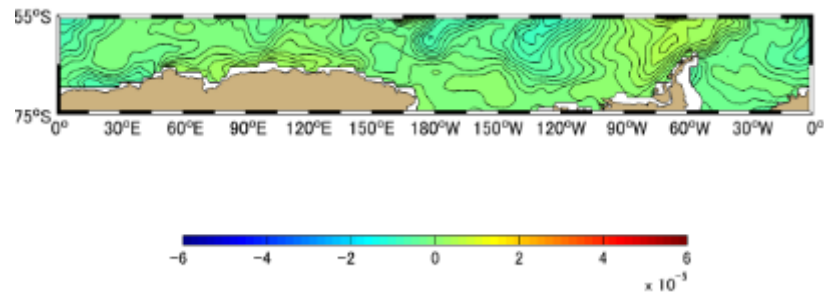


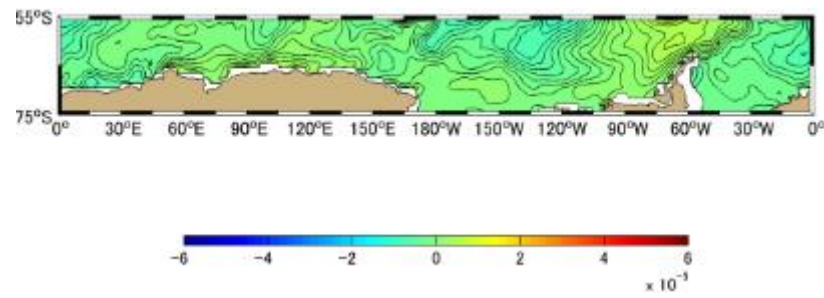
Figure A-5.9 Difference [PgC] between Approximation Method and Simulation Method Monthly Mean in 1999, the Southern Oceans based on January 1991. (a)-(l) represents January-December



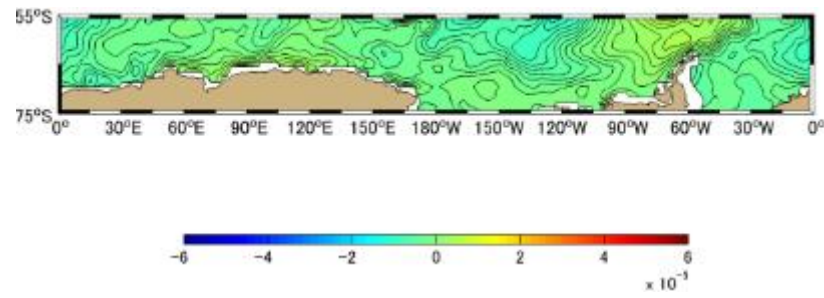
(a)



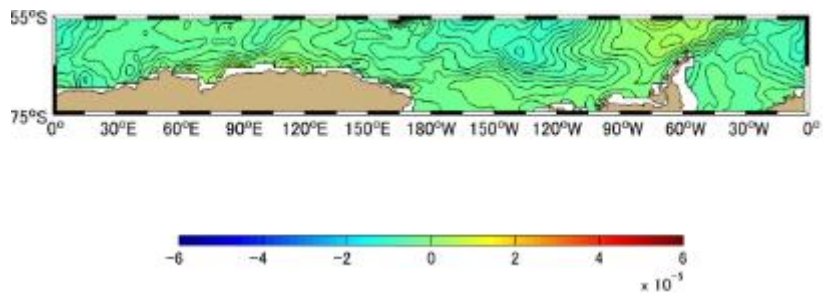
(b)



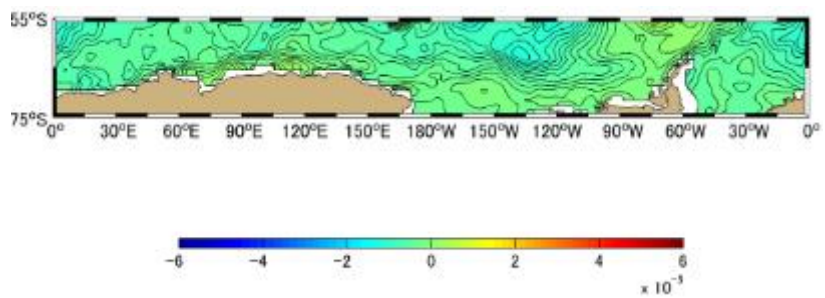
(c)



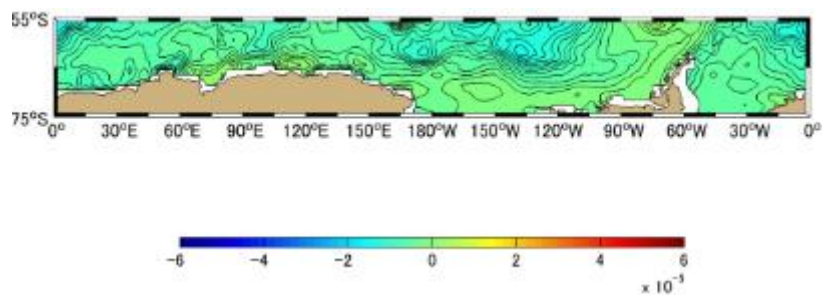
(d)



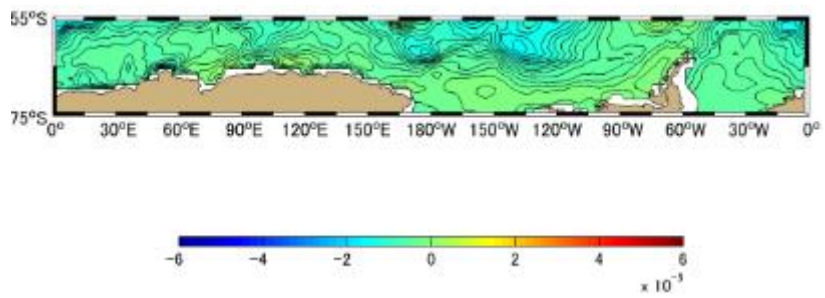
(e)



(f)



(g)



(h)



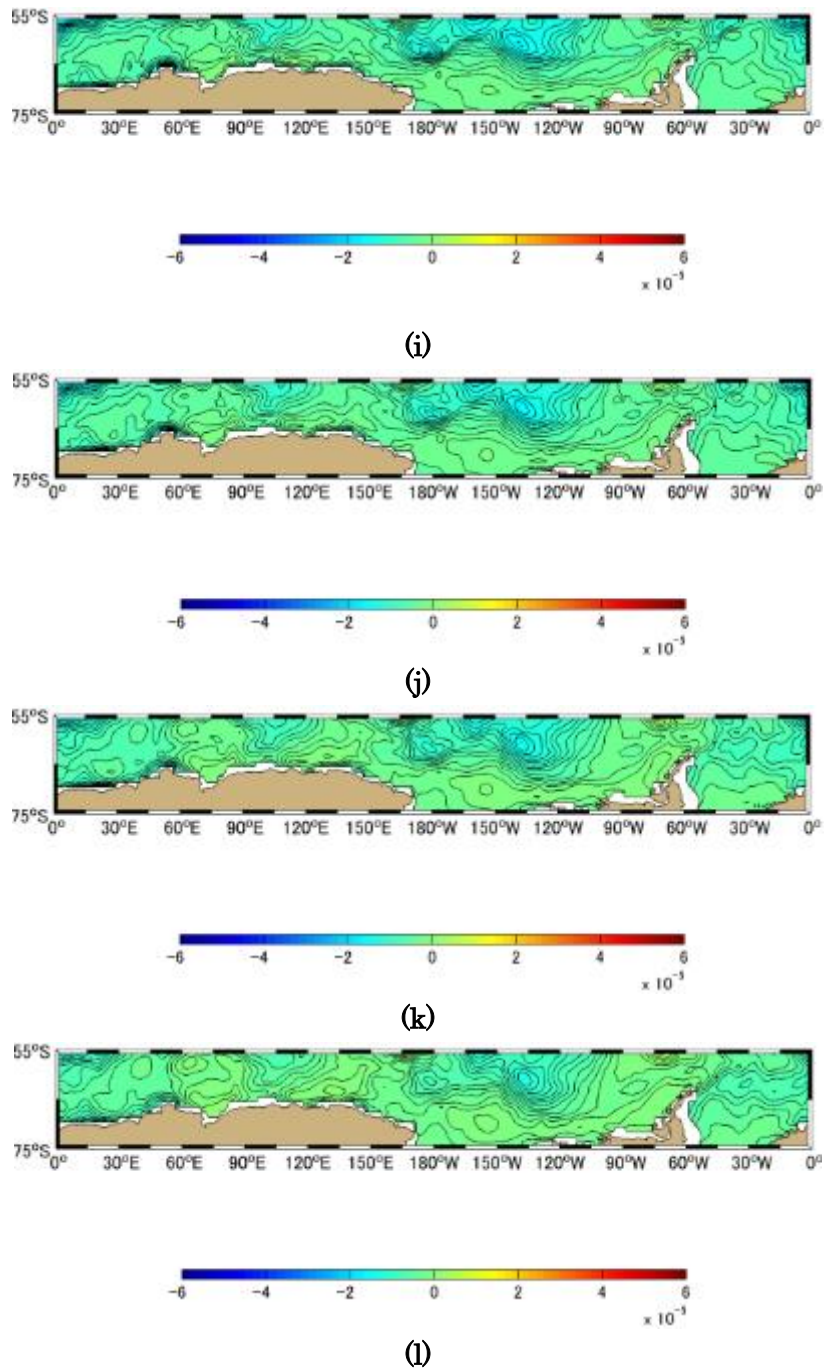
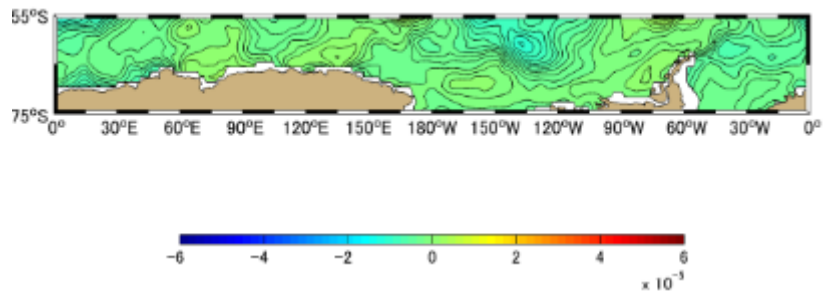
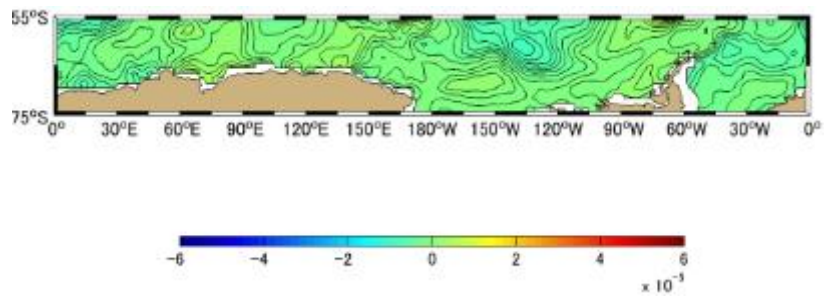


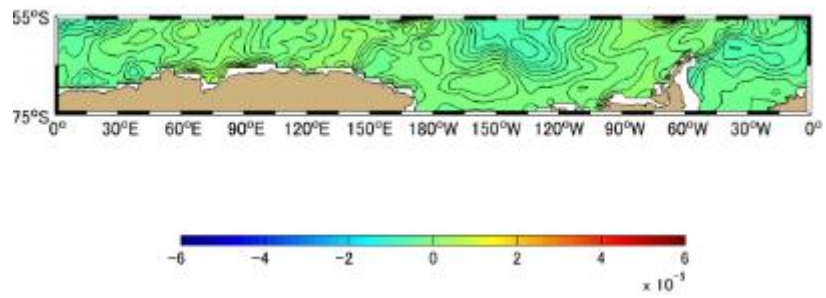
Figure A-5.10 Difference [PgC] between Approximation Method and Simulation Method Monthly Mean in 2000, the Southern Oceans based on January 1991. (a)-(l) represents January-December



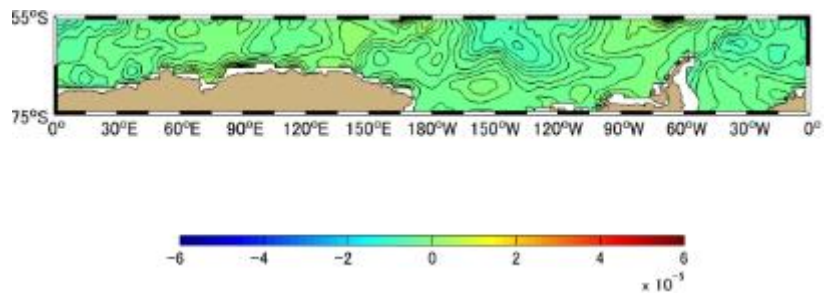
(a)



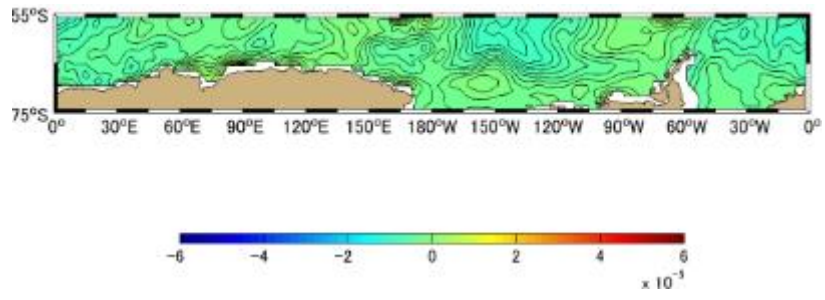
(b)



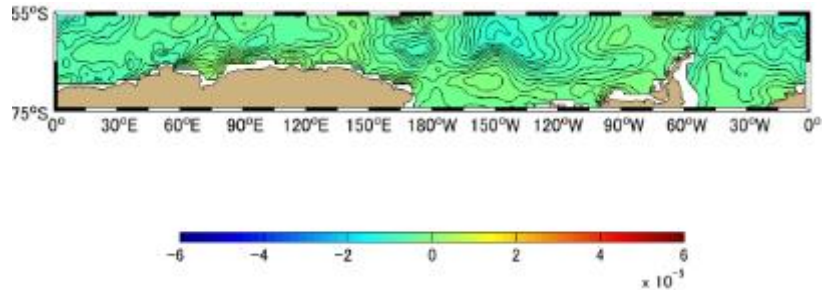
(c)



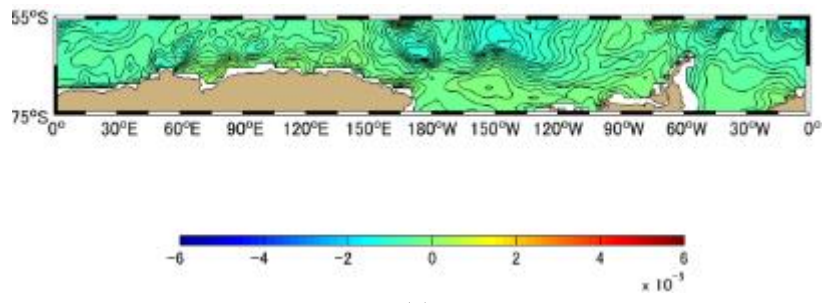
(d)



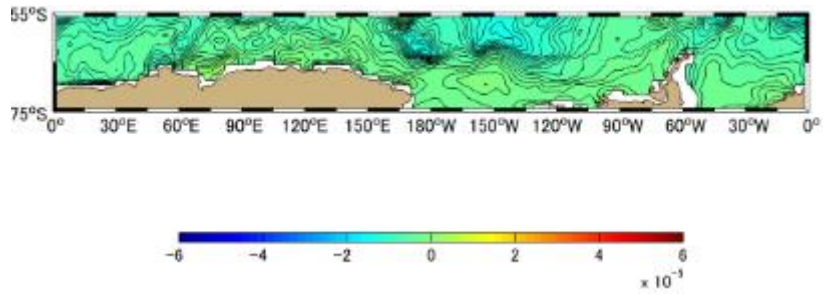
(e)



(f)



(g)



(h)

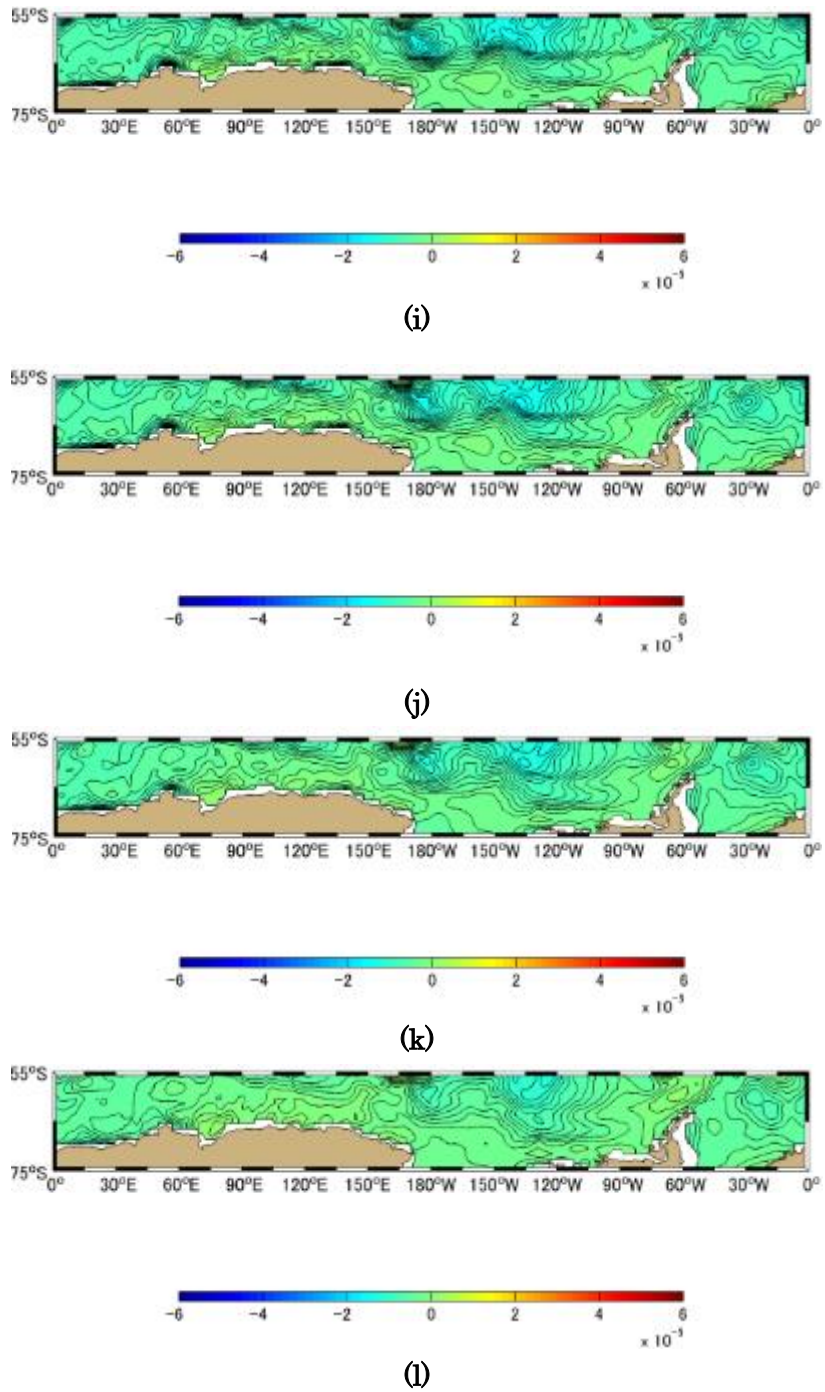
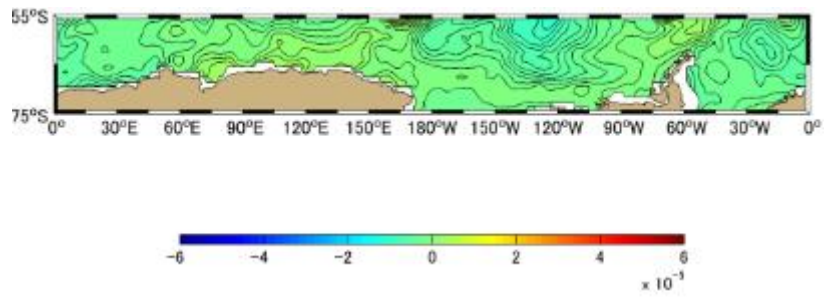
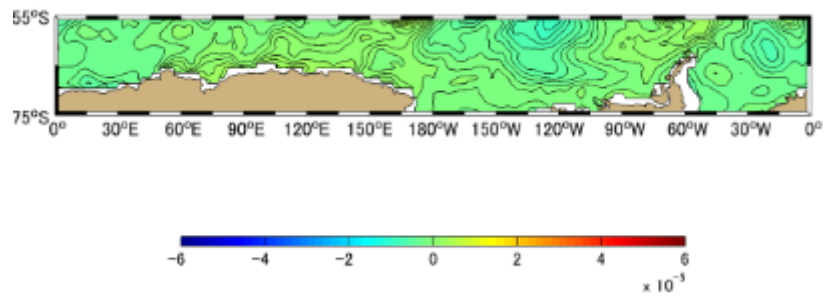


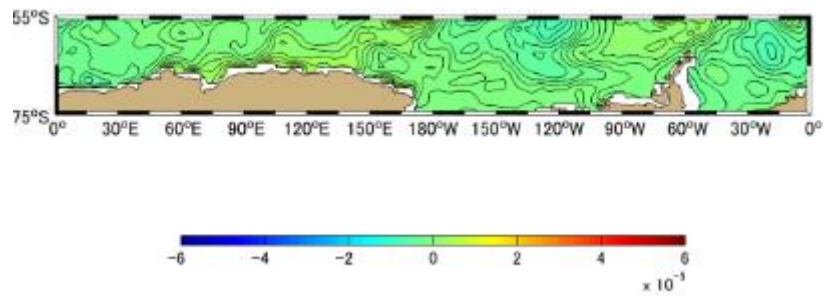
Figure A-5.11 Difference [PgC] between Approximation Method and Simulation Method Monthly Mean in 2001, the Southern Oceans based on January 1991. (a)-(l) represents January-December



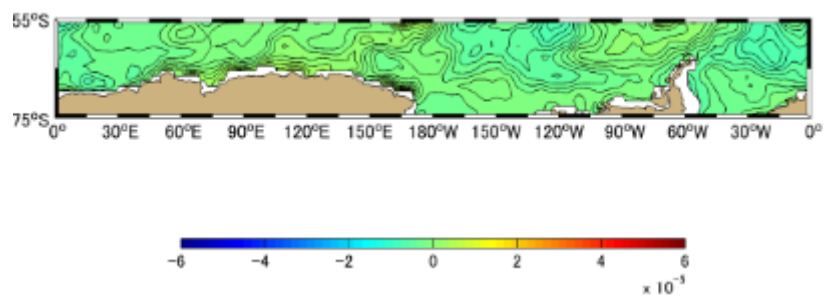
(a)



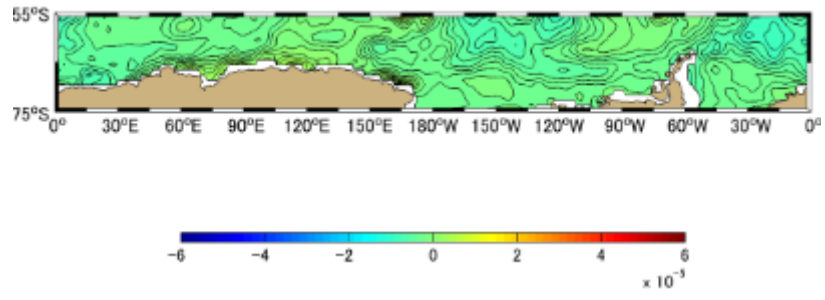
(b)



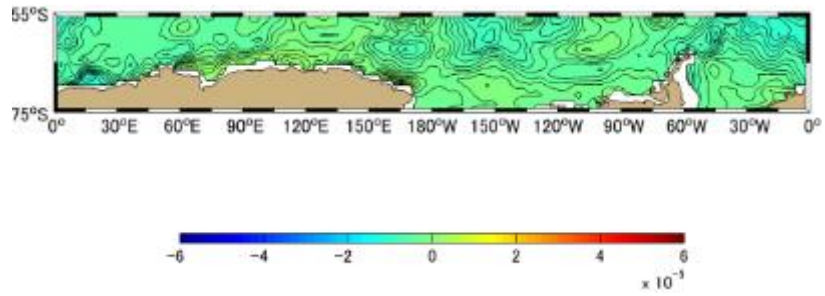
(c)



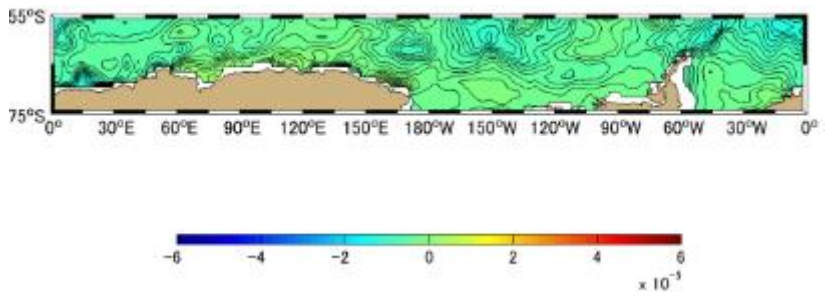
(d)



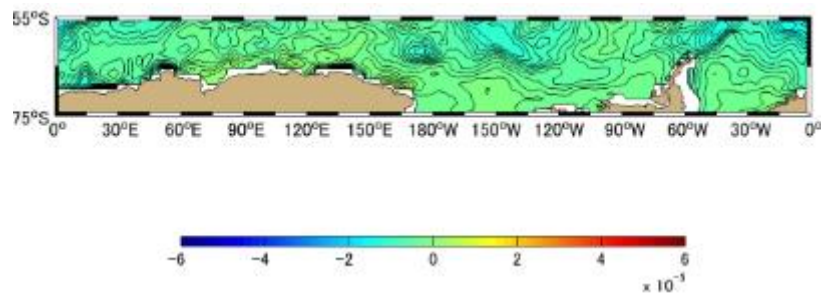
(e)



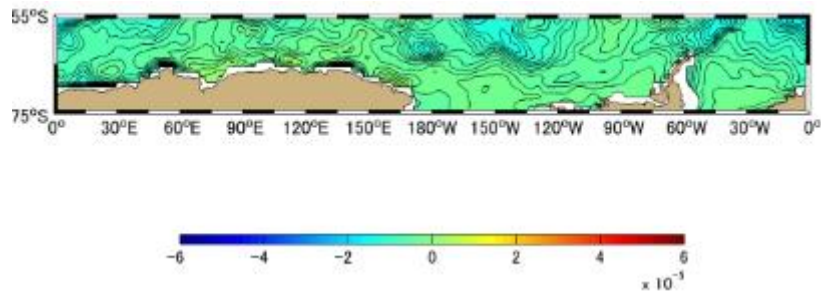
(f)



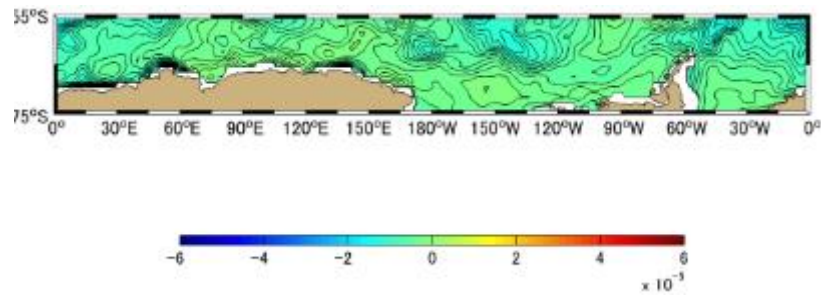
(g)



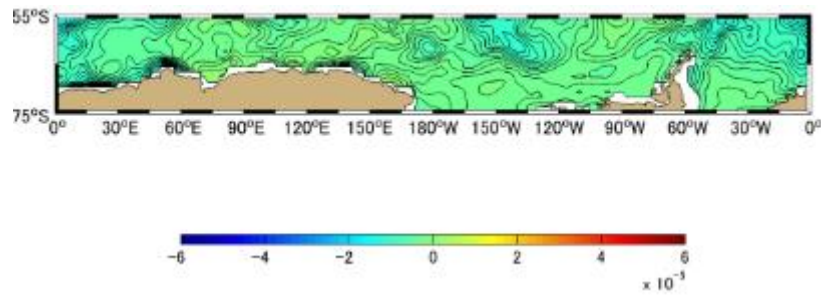
(h)



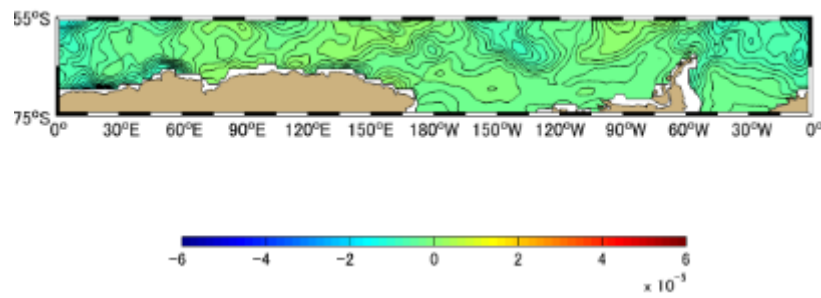
(i)



(j)

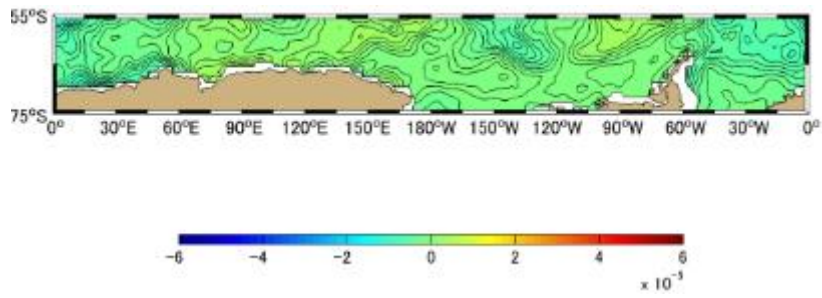


(k)

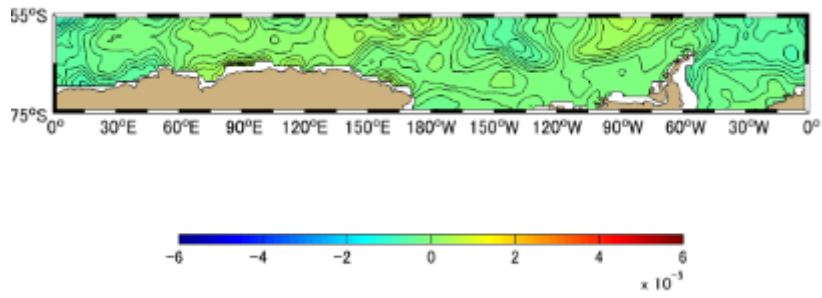


(l)

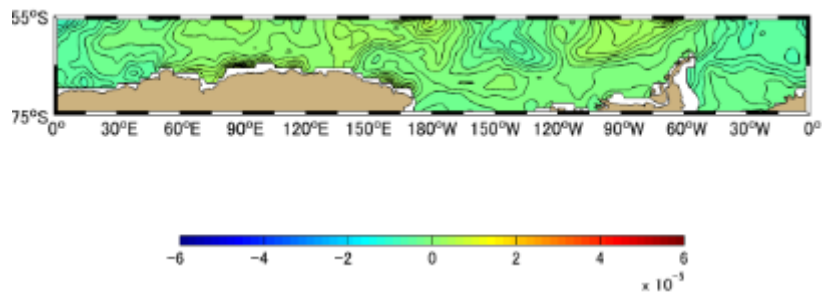
Figure A-5.12 Difference [PgC] between Approximation Method and Simulation Method Monthly Mean in 2002, the Southern Oceans based on January 1991. (a)-(l) represents January-December



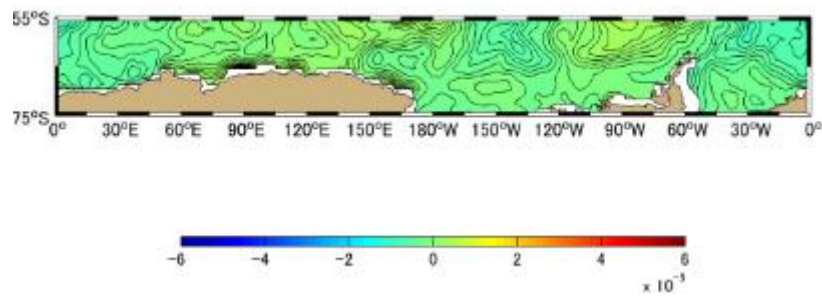
(a)



(b)

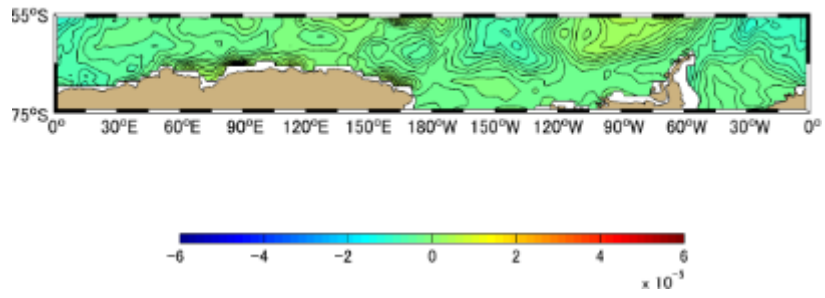


(c)

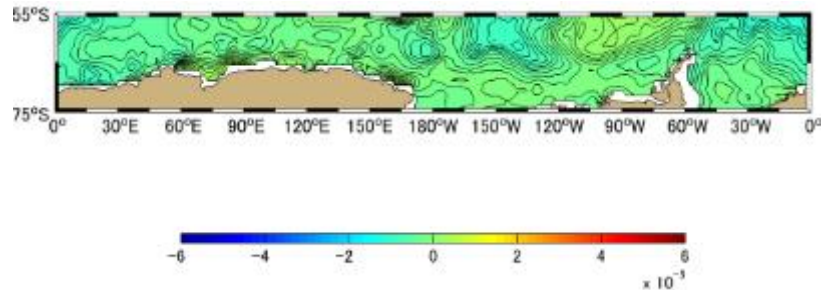


(d)

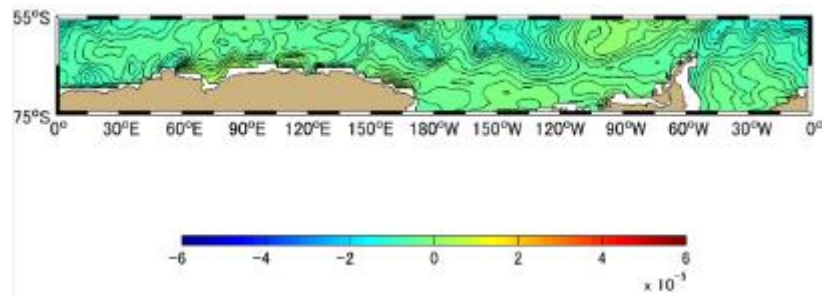




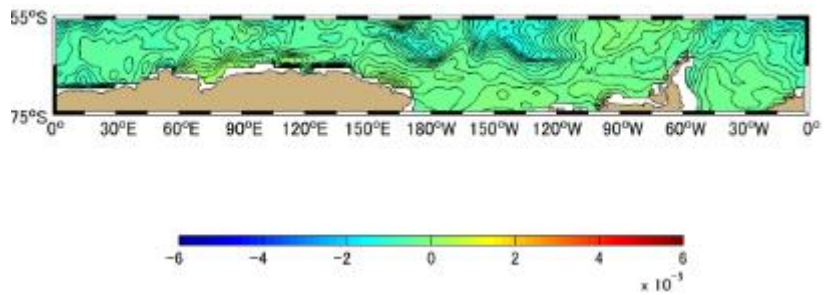
(e)



(f)



(g)



(h)

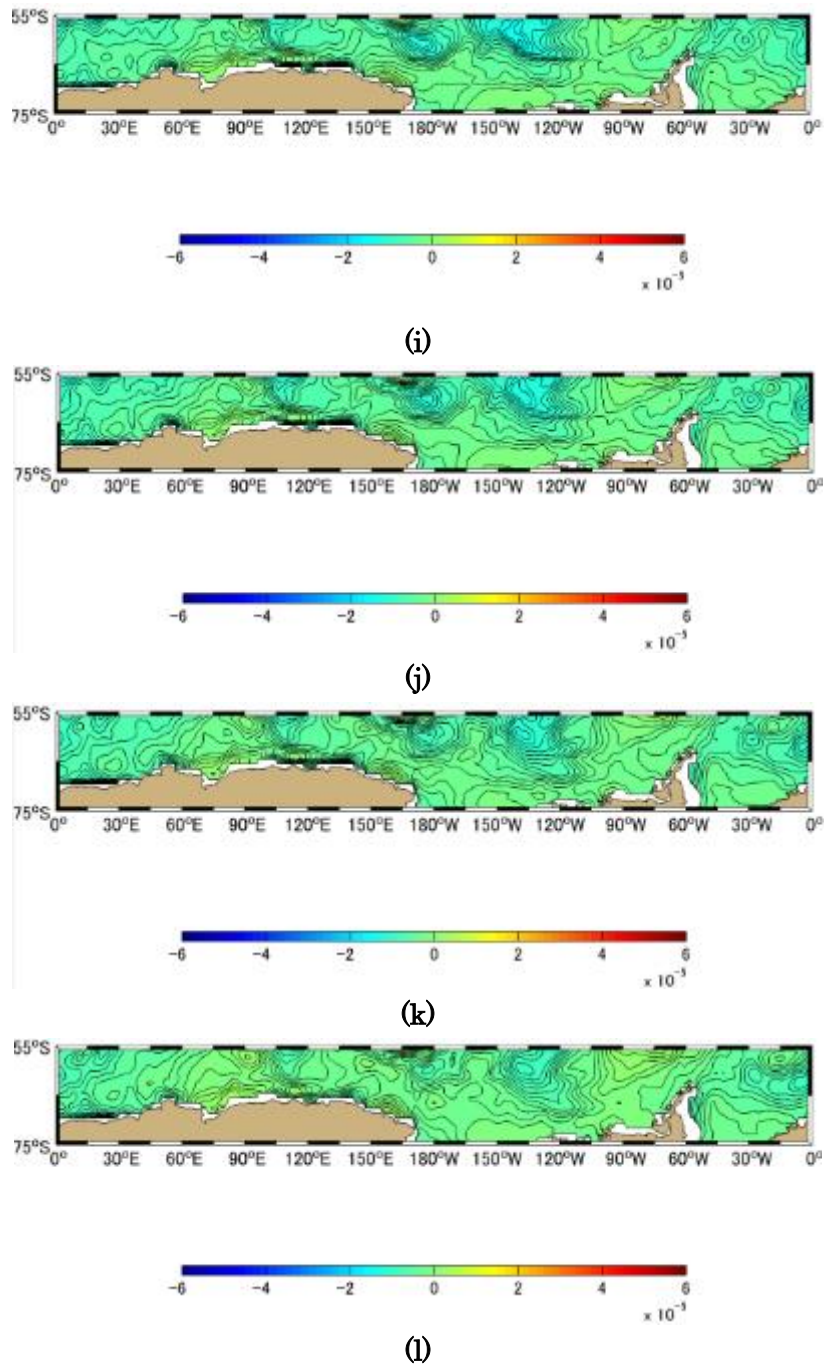
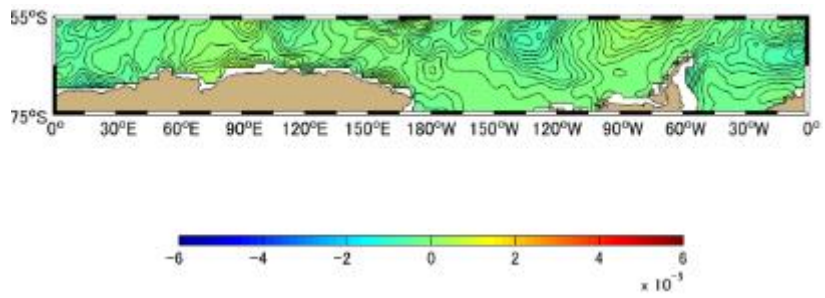
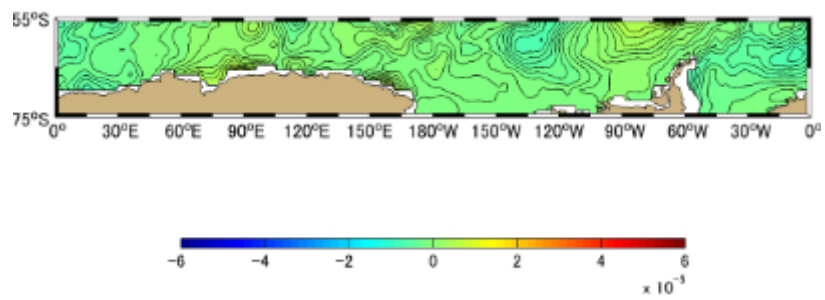


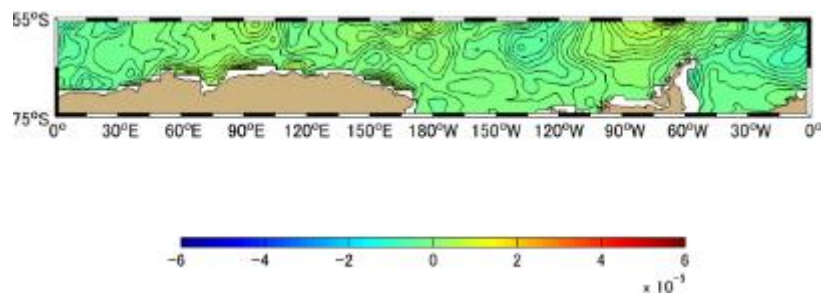
Figure A-5.13 Difference [PgC] between Approximation Method and Simulation Method Monthly Mean in 2003, the Southern Oceans based on January 1991. (a)-(l) represents January-December



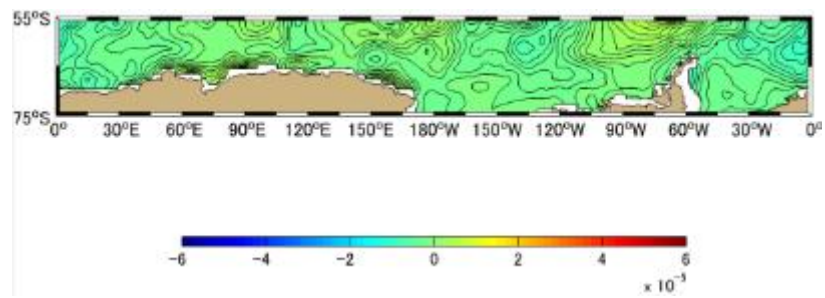
(a)



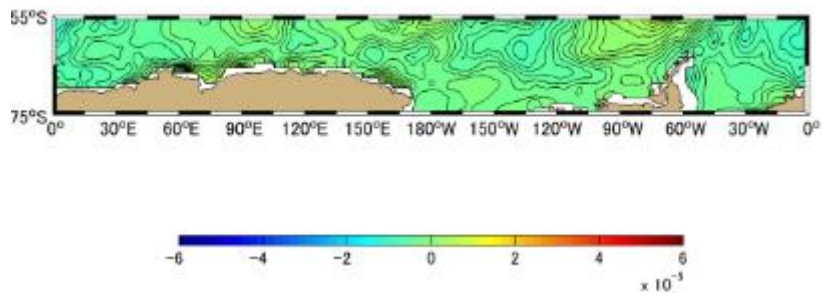
(b)



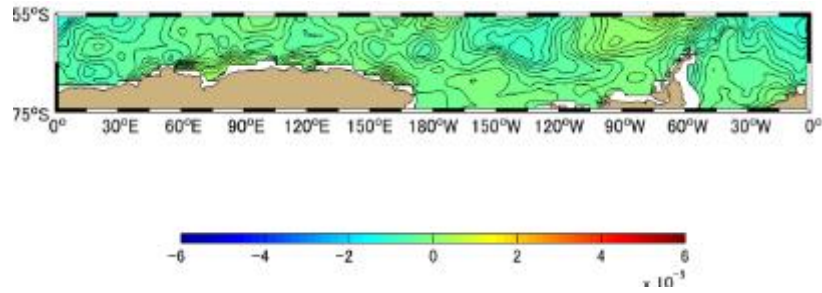
(c)



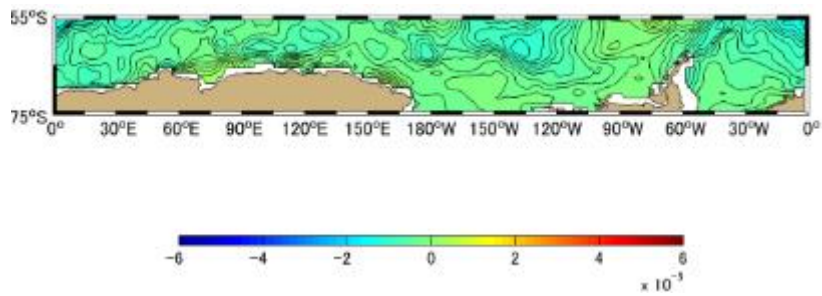
(d)



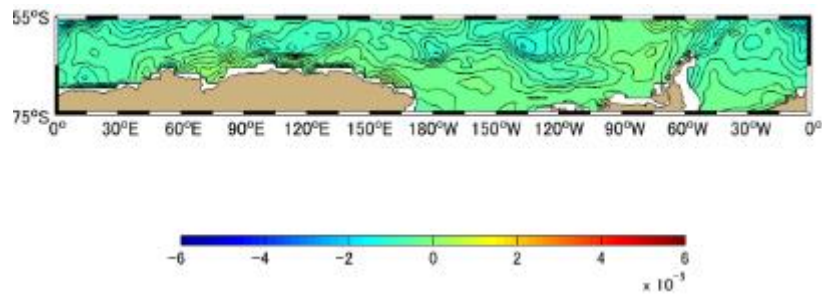
(e)



(f)



(g)



(h)

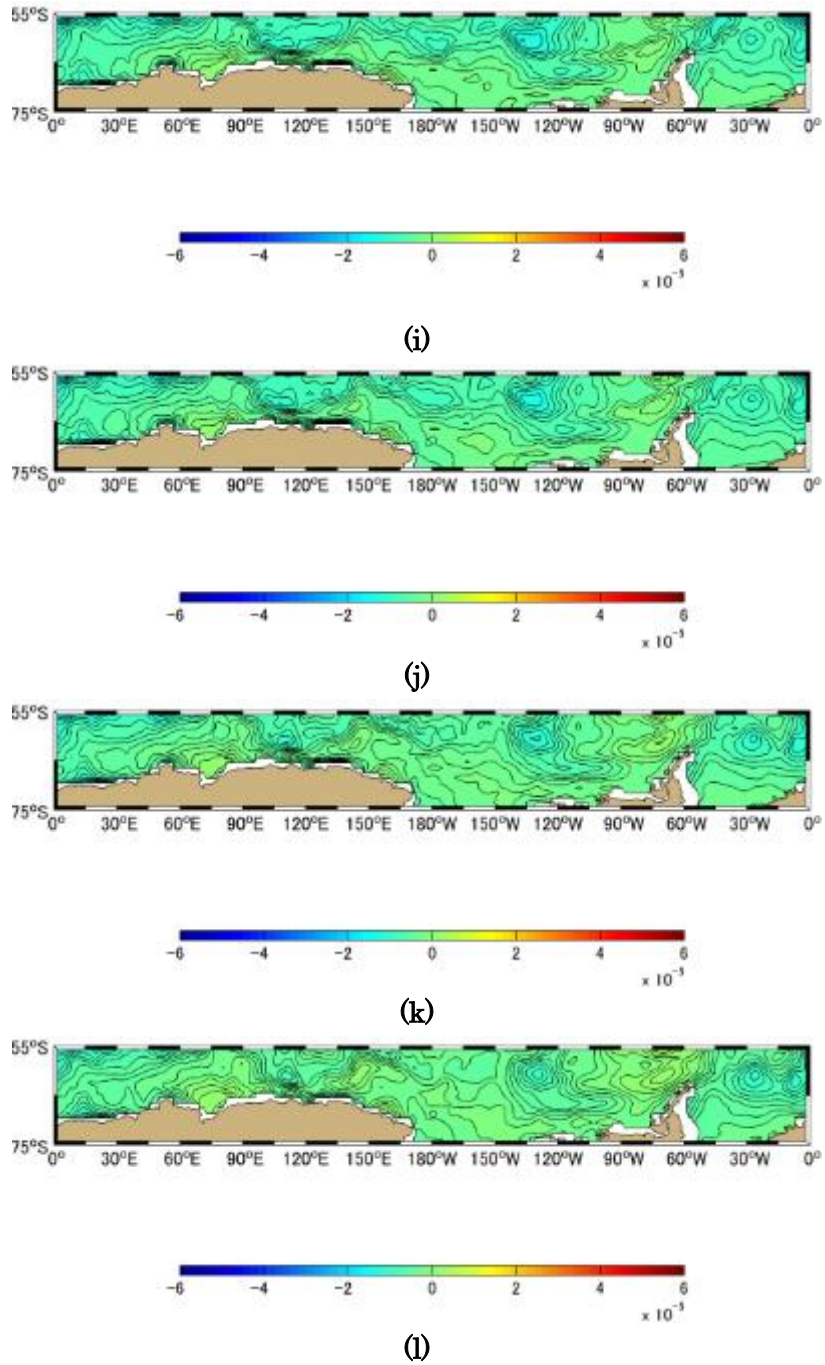
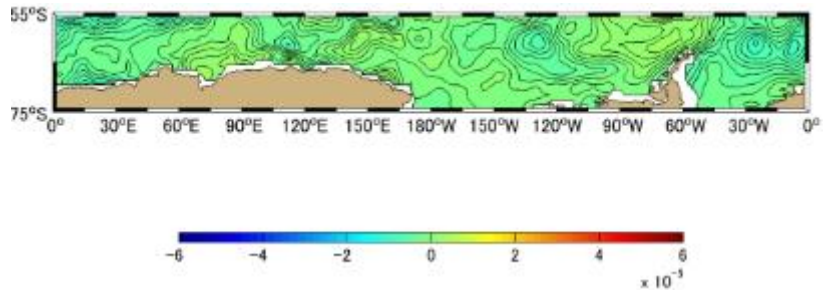
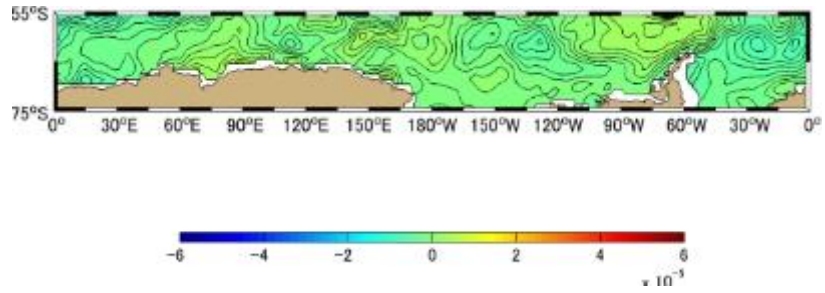


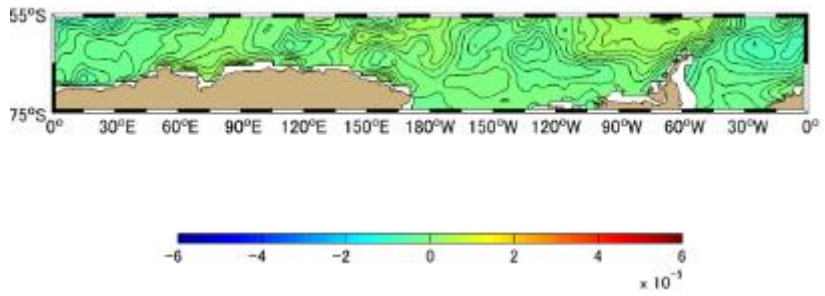
Figure A-5.14 Difference [PgC] between Approximation Method and Simulation Method Monthly Mean in 2004, the Southern Oceans based on January 1991. (a)-(l) represents January-December



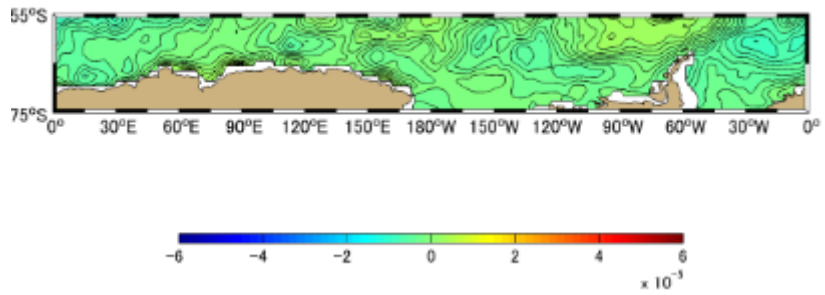
(a)



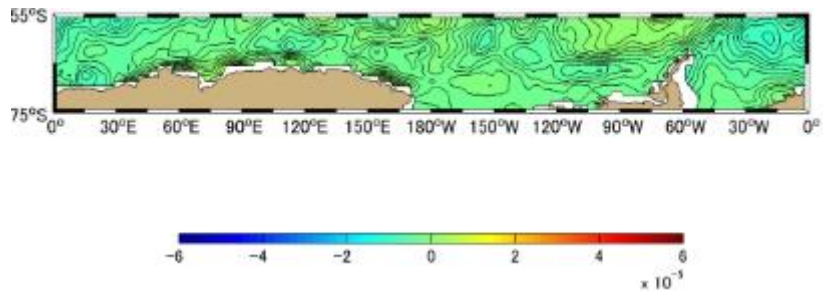
(b)



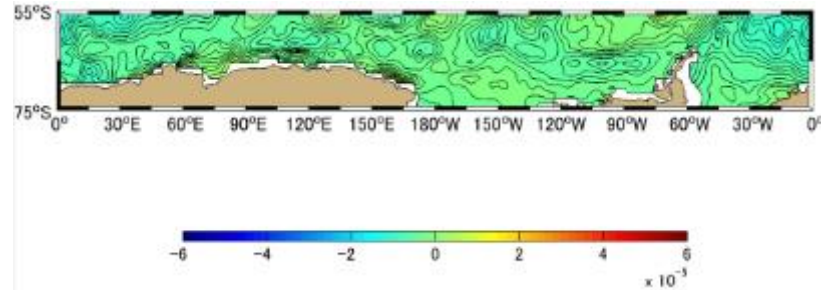
(c)



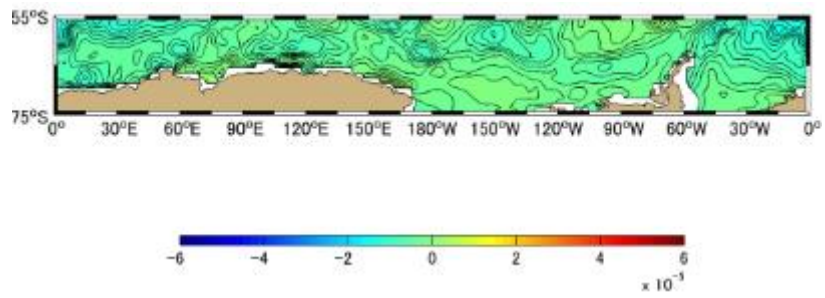
(d)



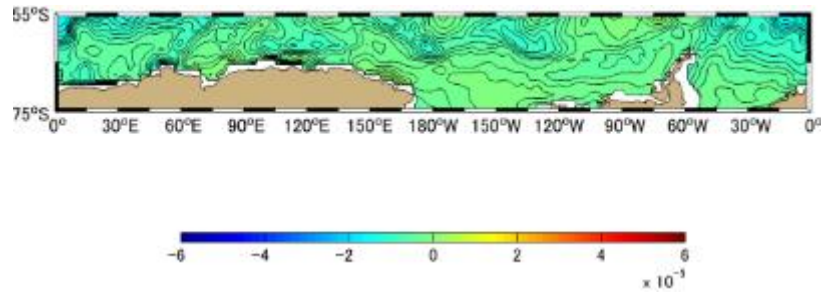
(e)



(f)



(g)



(h)

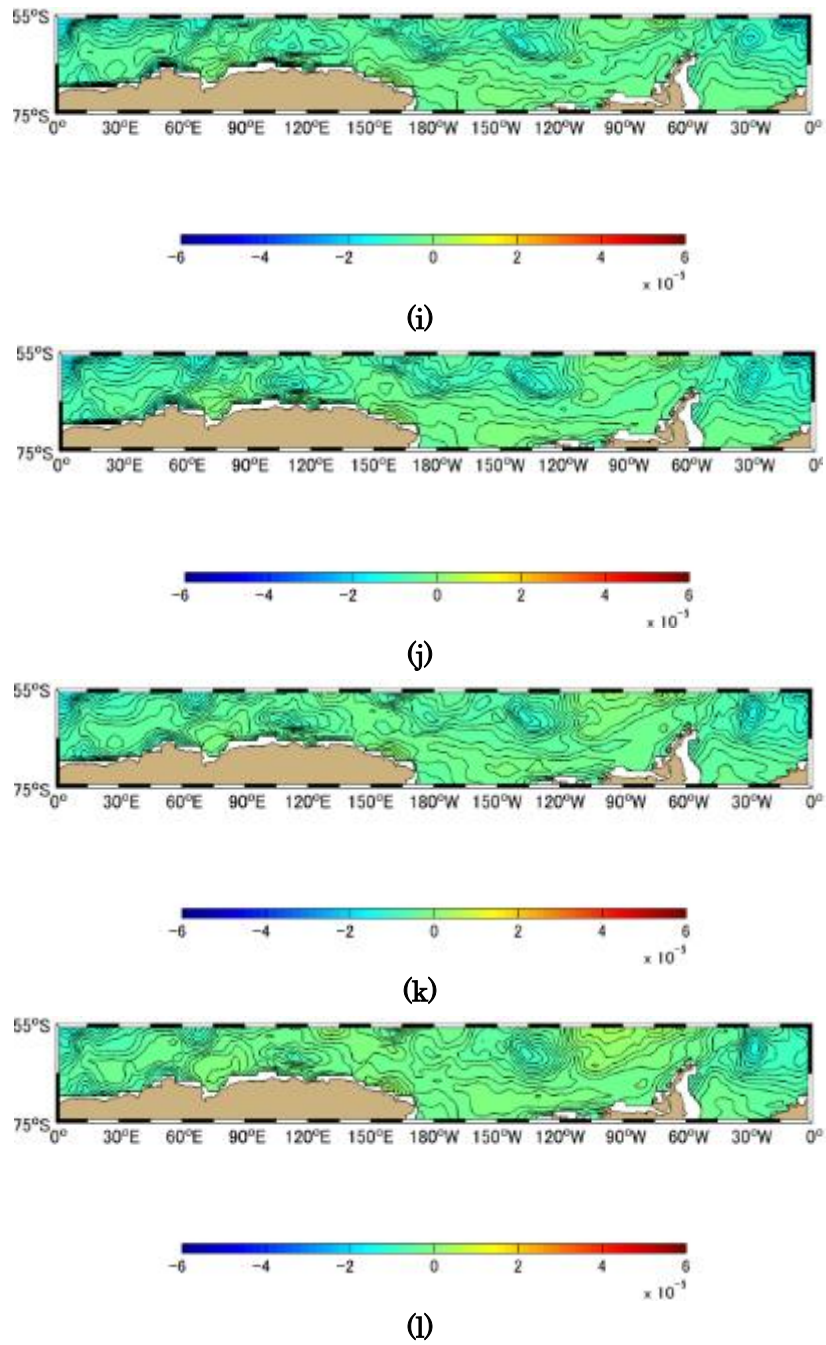
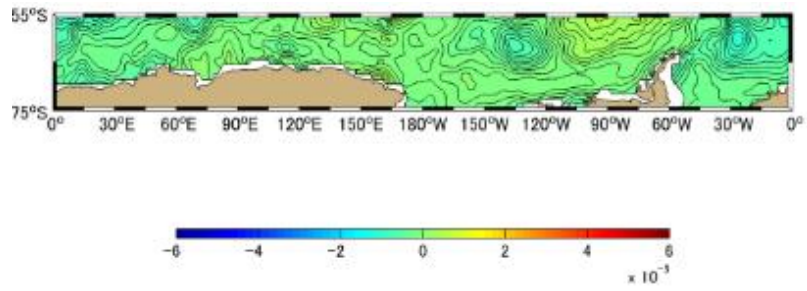
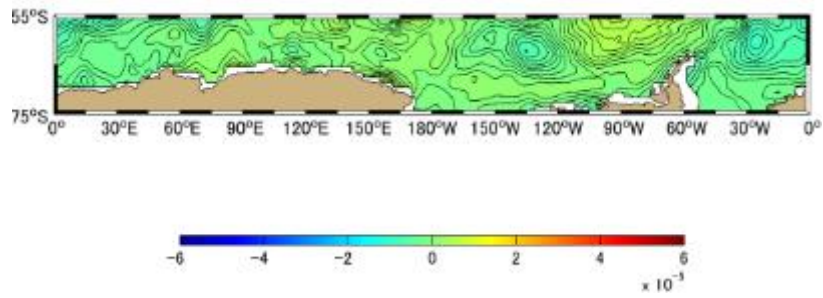


Figure A-5.15 Difference [PgC] between Approximation Method and Simulation Method Monthly Mean in 2005, the Southern Oceans based on January 1991. (a)-(l) represents January-December

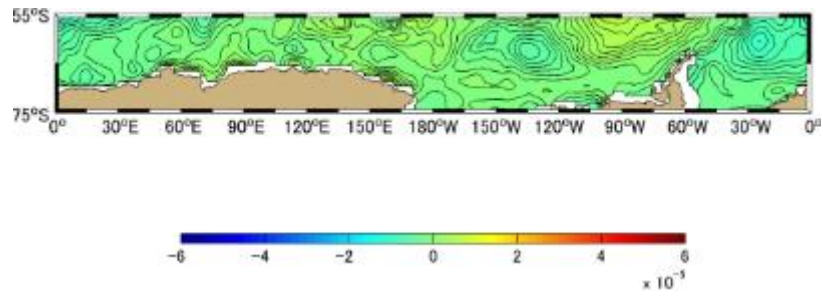




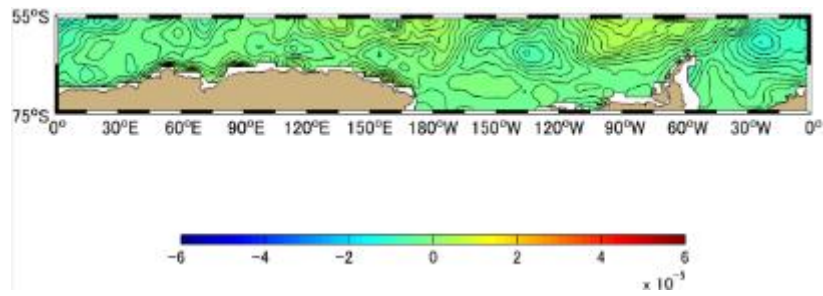
(a)



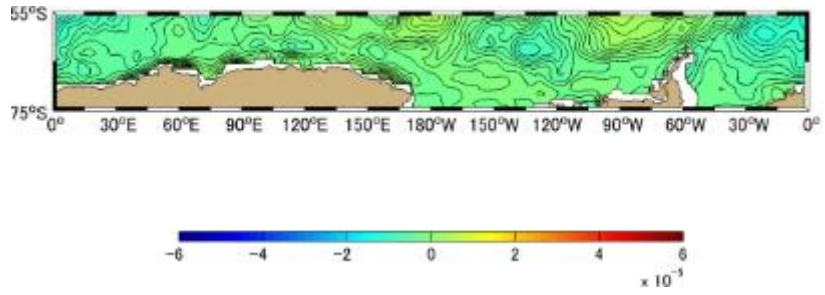
(b)



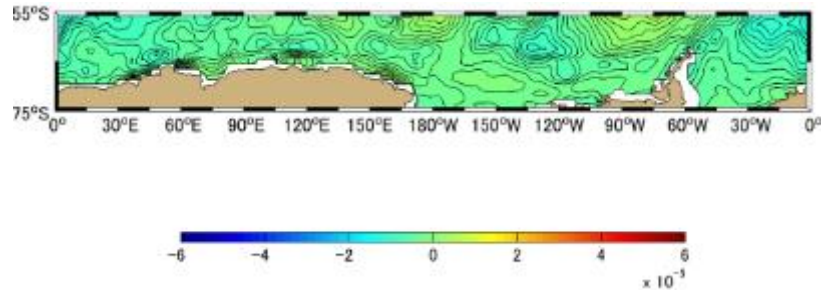
(c)



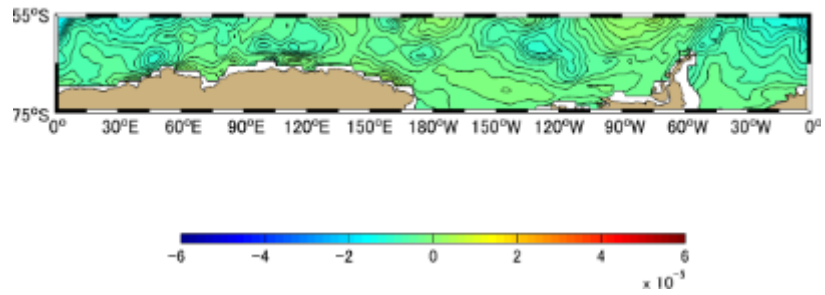
(d)



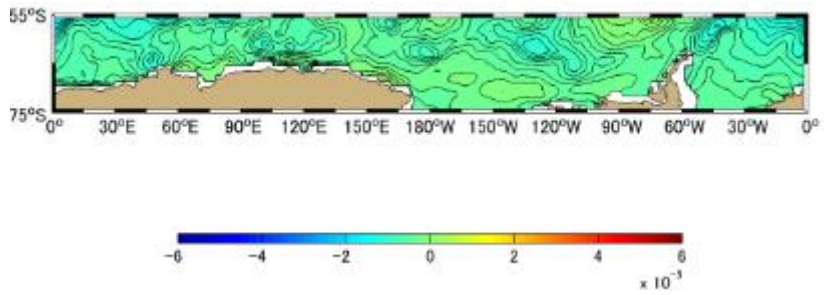
(e)



(f)



(g)



(h)

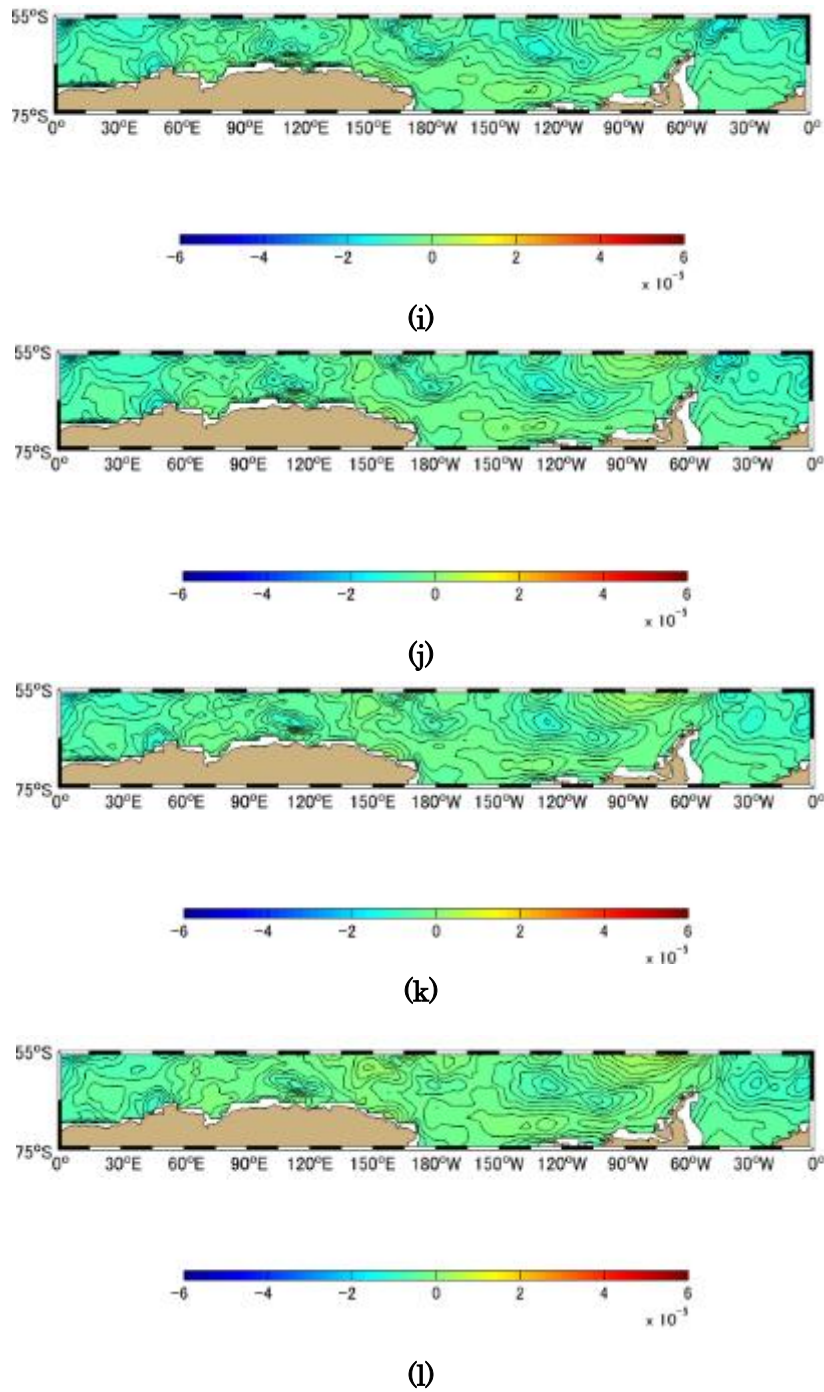
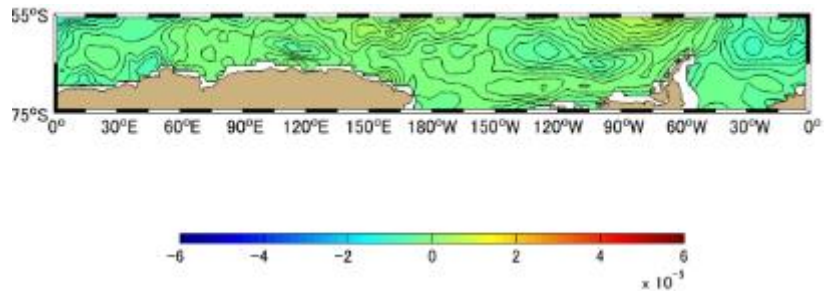
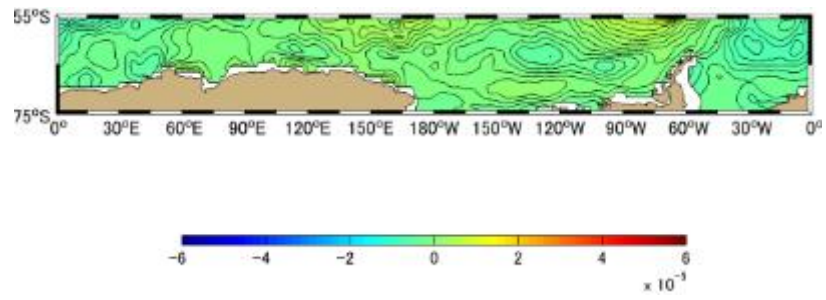


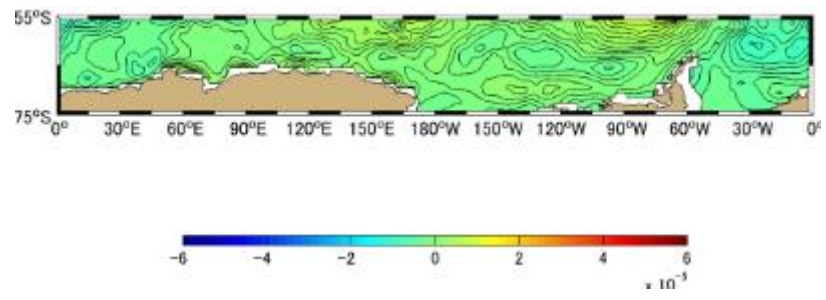
Figure A-5.16 Difference [PgC] between Approximation Method and Simulation Method Monthly Mean in 2006, the Southern Oceans based on January 1991. (a)-(l) represents January-December



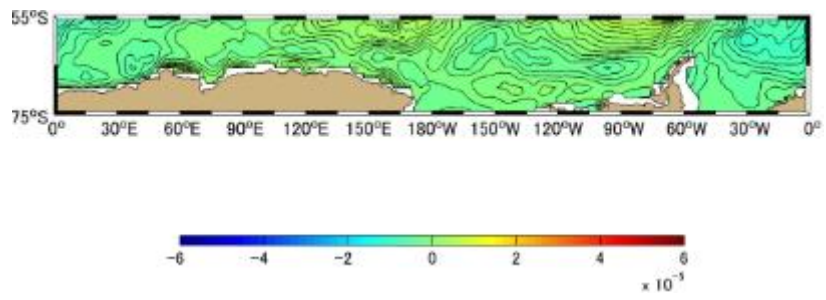
(a)



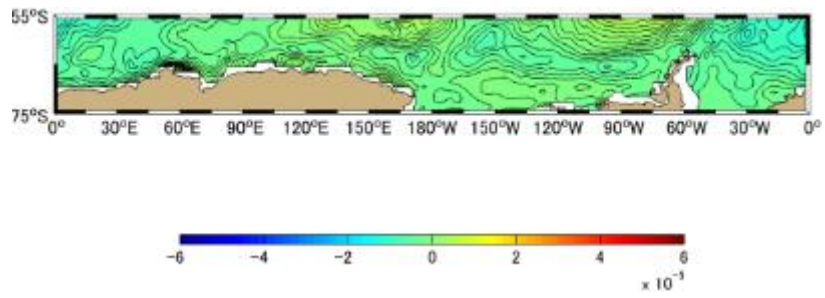
(b)



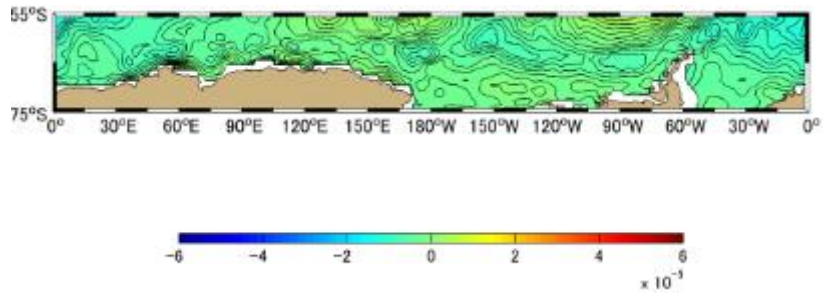
(c)



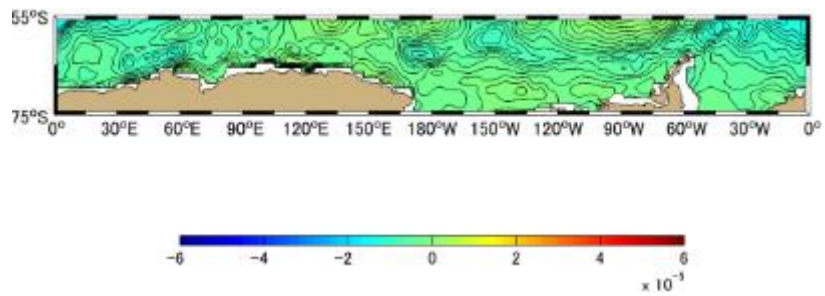
(d)



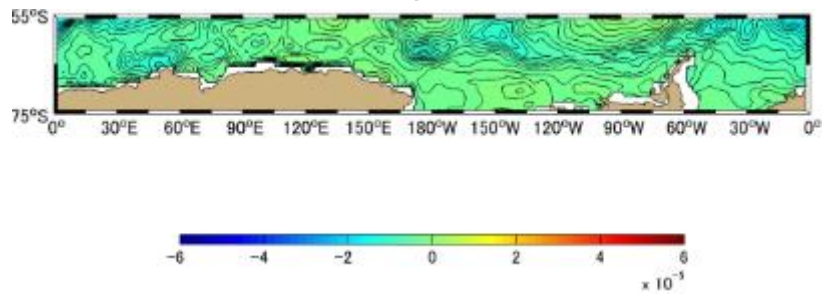
(e)



(f)



(g)



(h)

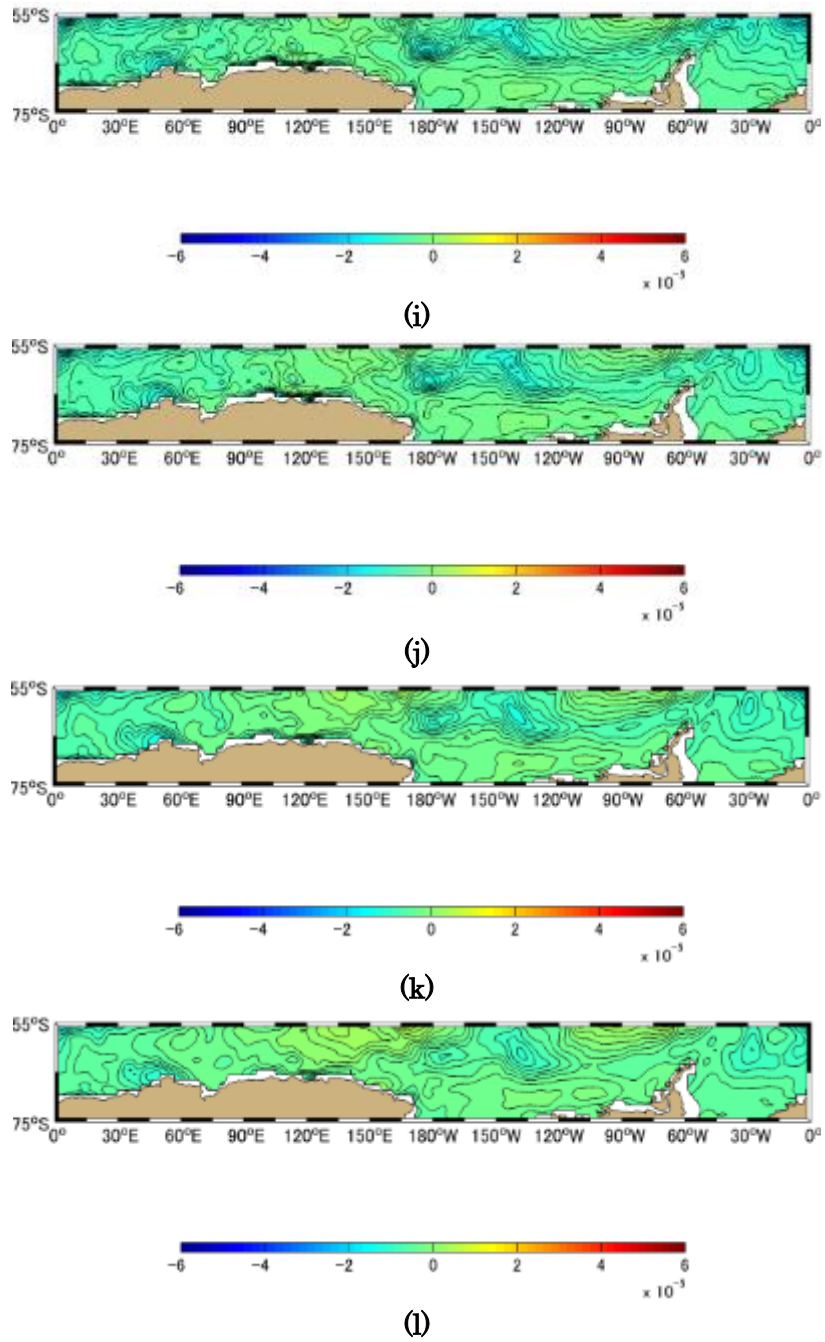
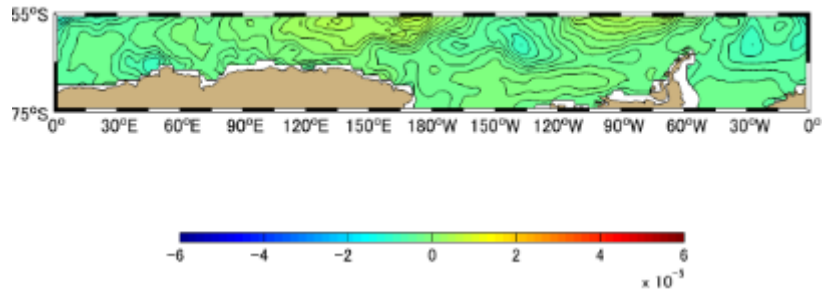
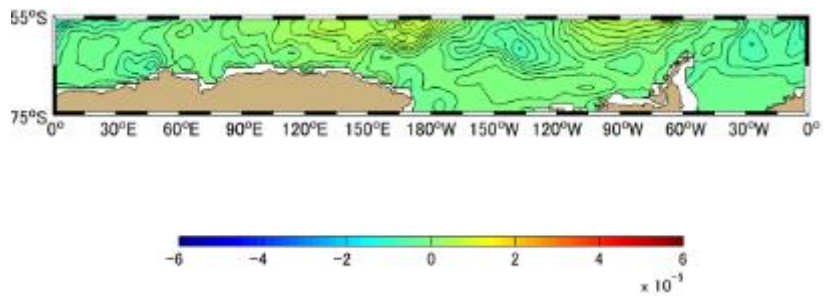


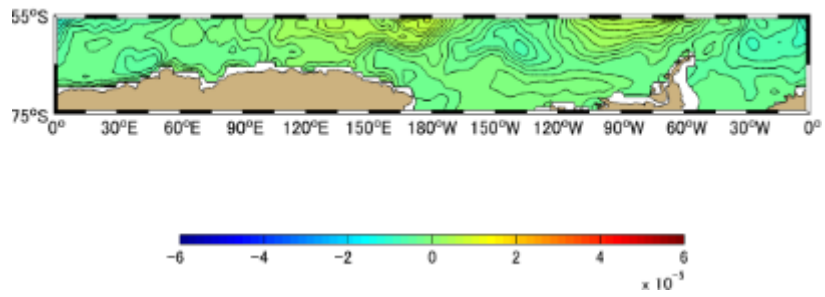
Figure A-5.17 Difference [PgC] between Approximation Method and Simulation Method Monthly Mean in 2007, the Southern Oceans based on January 1991. (a)-(l) represents January-December



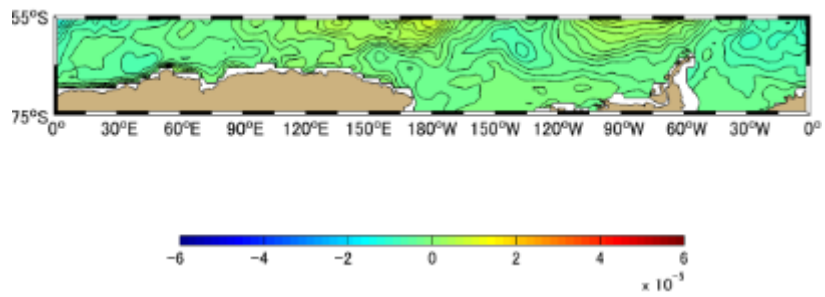
(a)



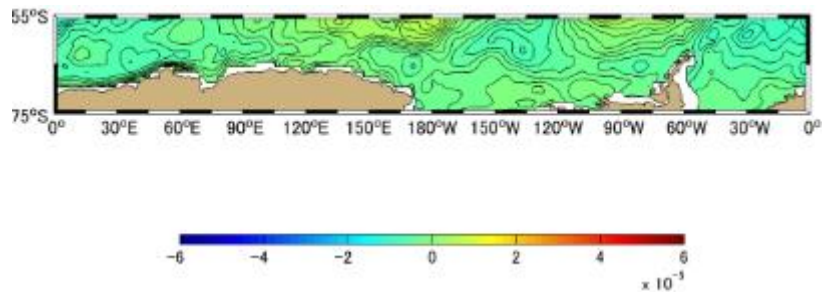
(b)



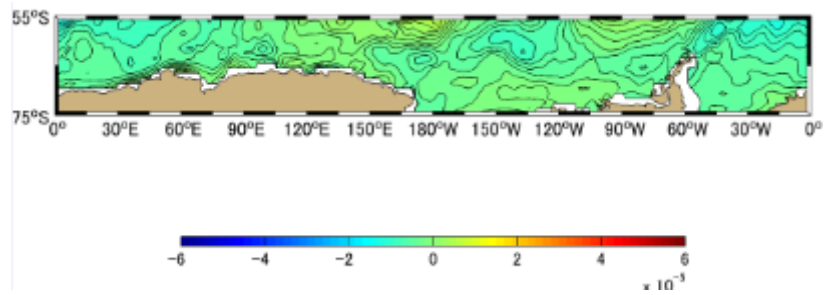
(c)



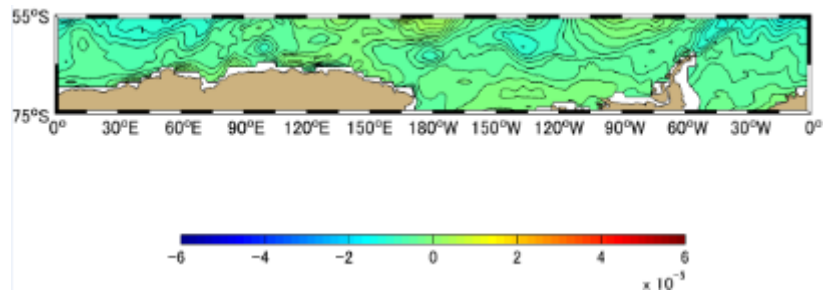
(d)



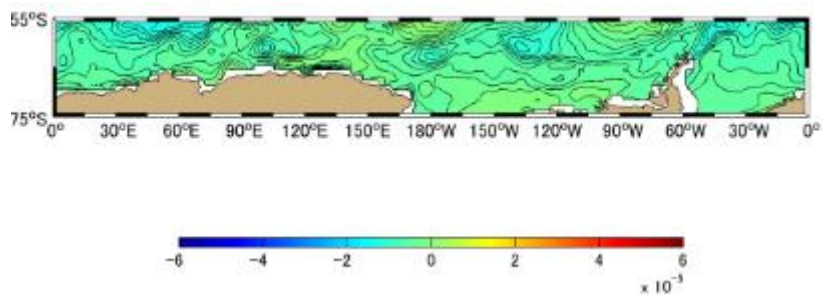
(e)



(f)



(g)



(h)



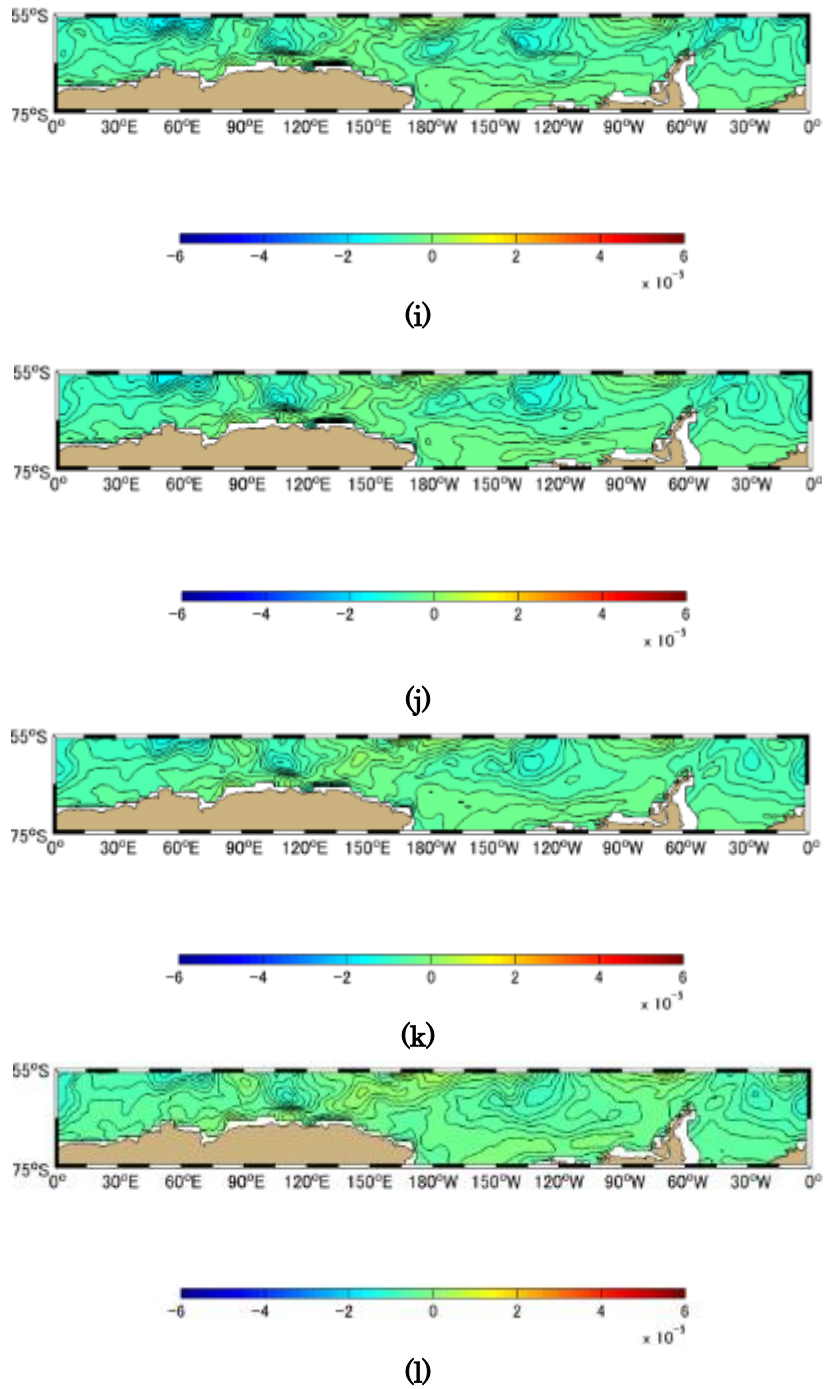
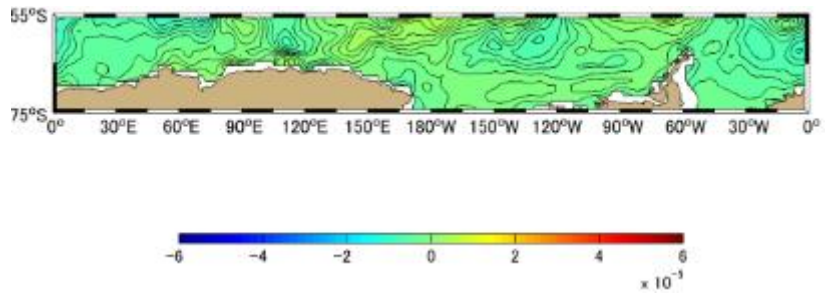
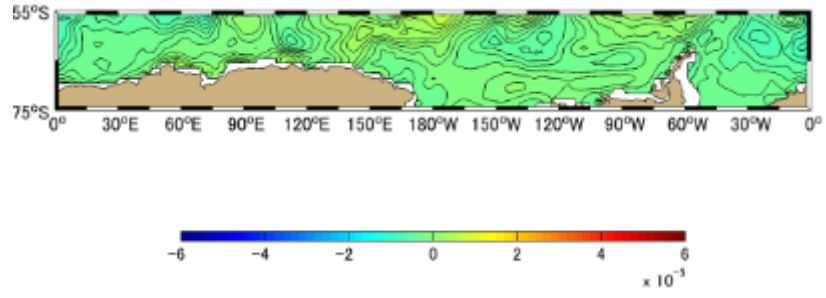


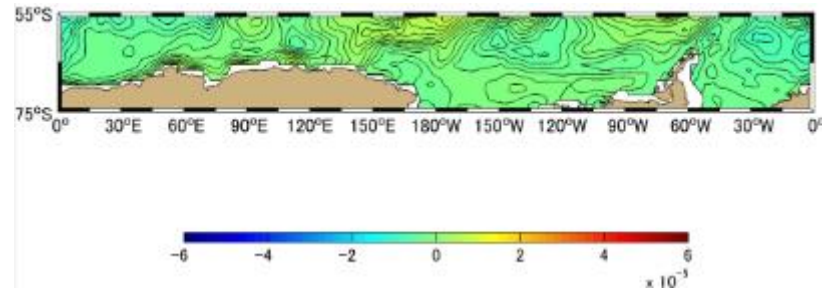
Figure A-5.18 Difference [PgC] between Approximation Method and Simulation Method Monthly Mean in 2008, the Southern Oceans based on January 1991. (a)-(l) represents January-December



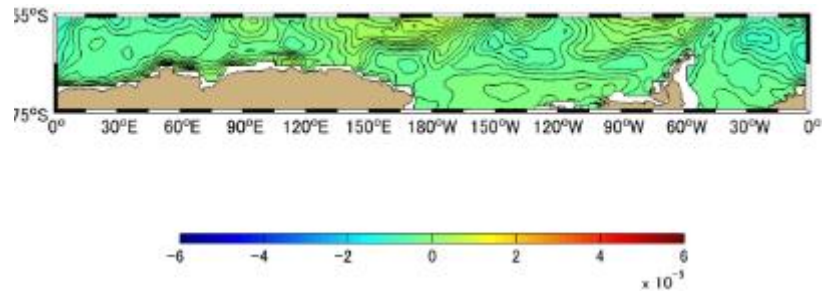
(a)



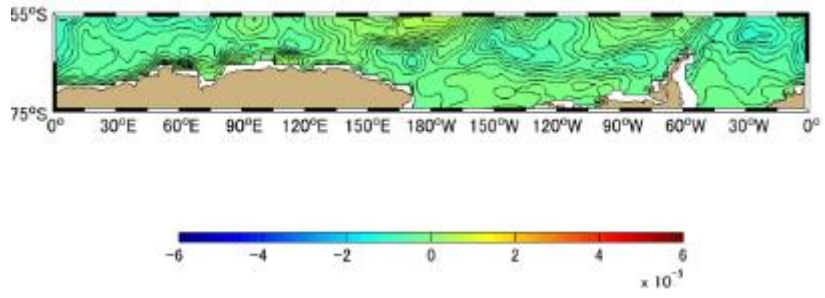
(b)



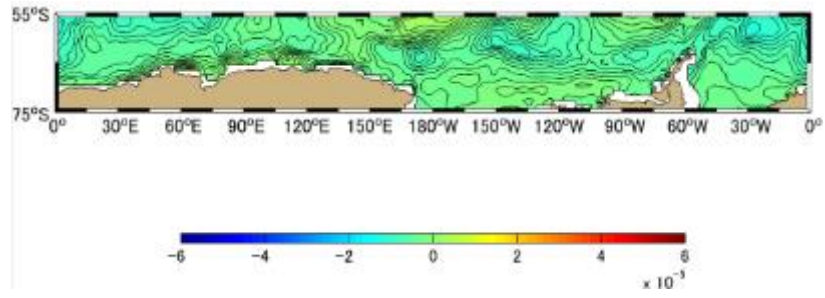
(c)



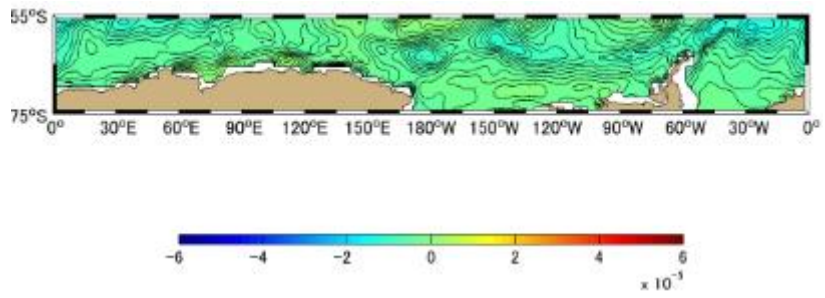
(d)



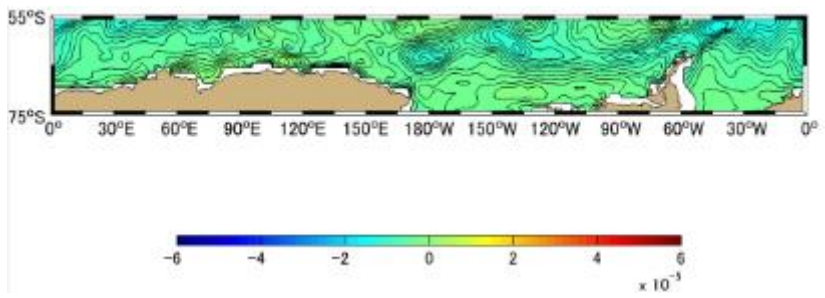
(e)



(f)



(g)



(h)

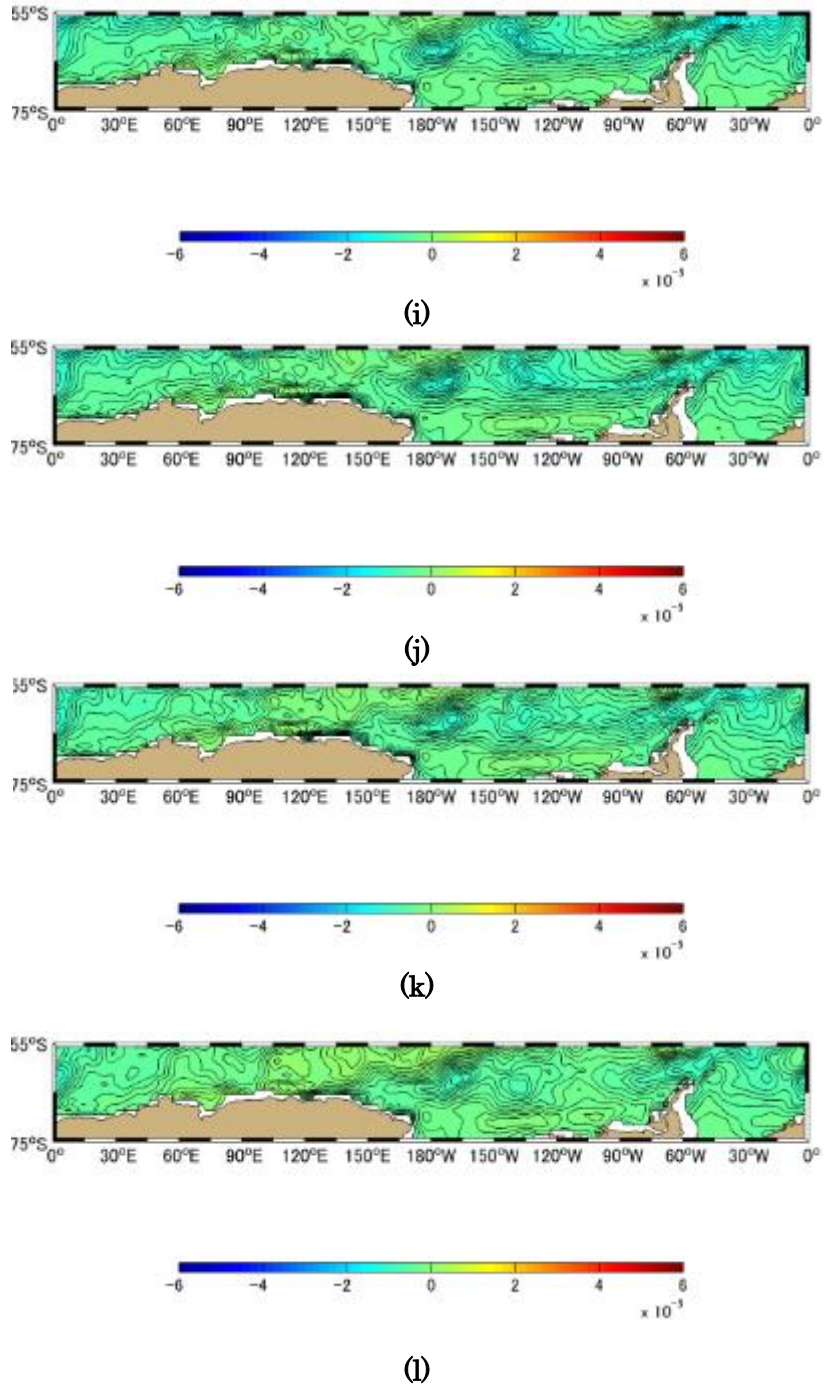
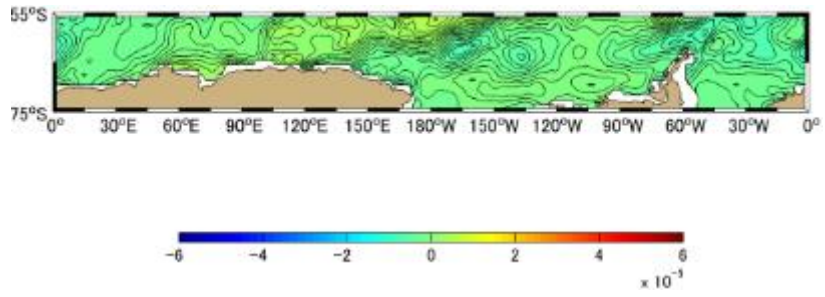
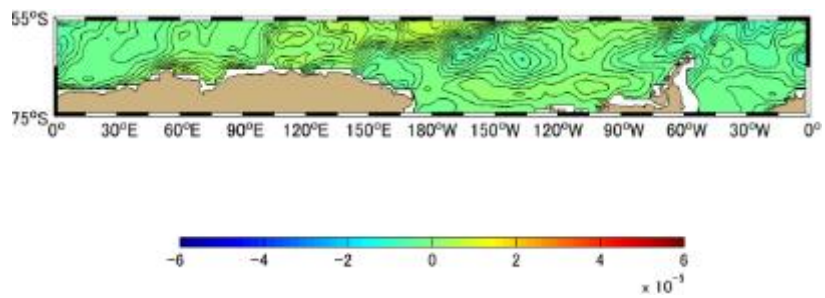


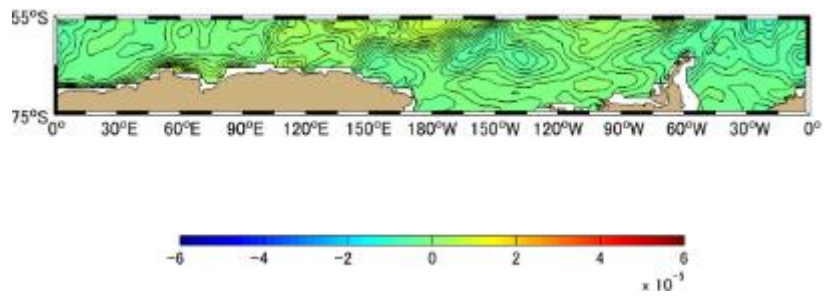
Figure A-5.19 Difference [PgC] between Approximation Method and Simulation Method Monthly Mean in 2009 the Southern Oceans based on January 1991. (a)-(l) represents January-December



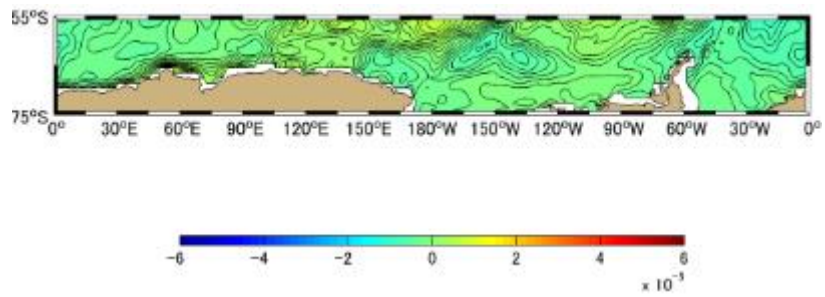
(a)



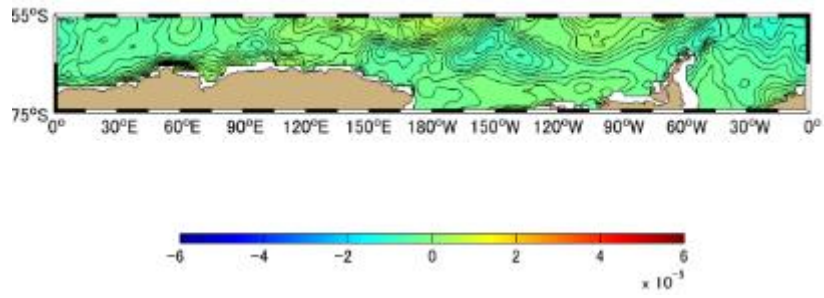
(b)



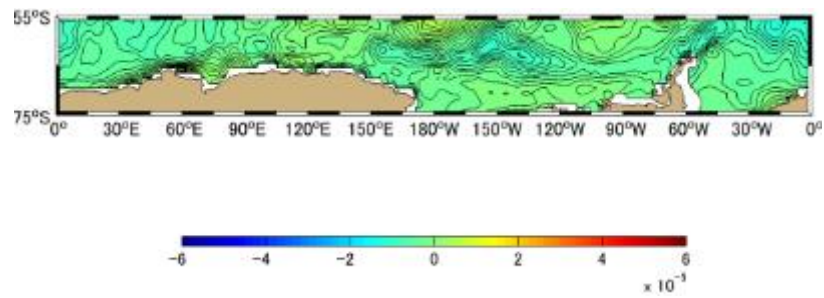
(c)



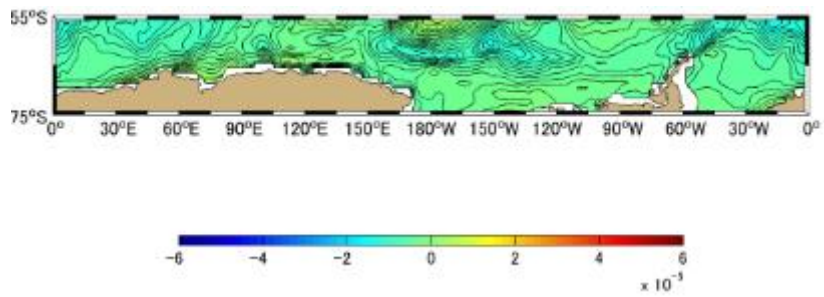
(d)



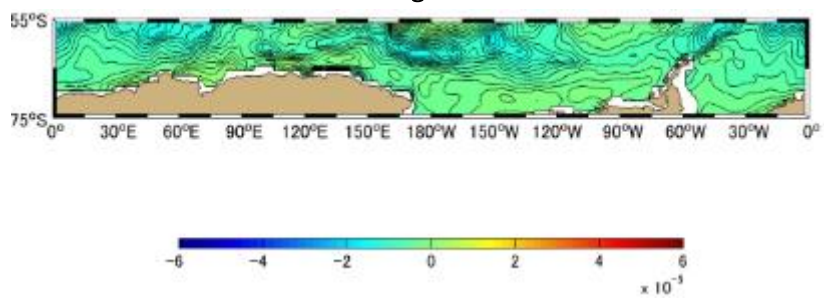
(e)



(f)



(g)



(h)

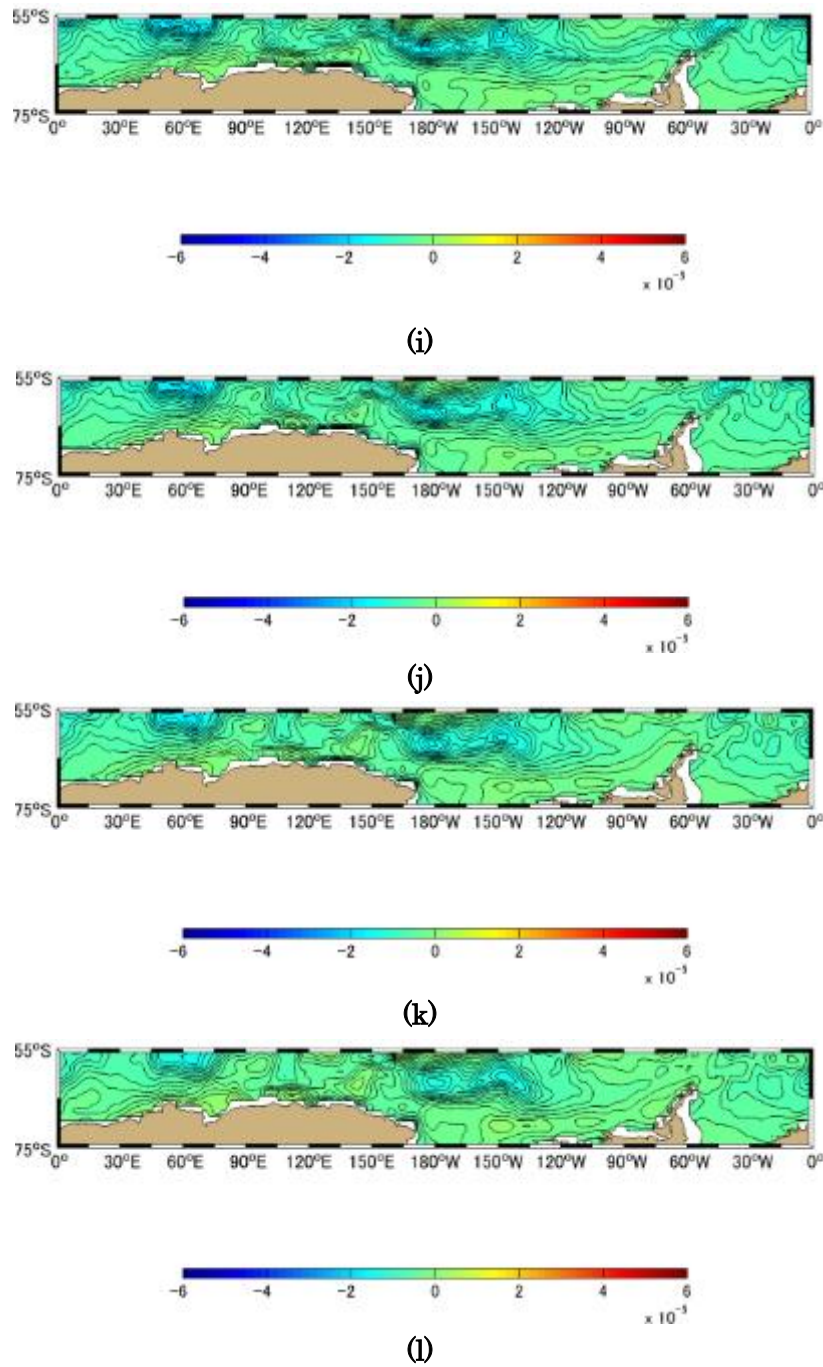


Figure A-7.20 Difference [PgC] between Approximation Method and Simulation Method Monthly Mean in 2010, the Southern Oceans based on January 1991. (a)-(l) represents January-December